Regulation of cardiogenesis by putative WNT signalling pathways

Tania Papoutsi

Doctor of Philosophy

Institute of Genetic Medicine
Faculty of Medical Sciences
Newcastle University

2011

Abstract

The Wnt/β-catenin and the Wnt/planar cell polarity (Wnt/PCP) signalling pathways have been shown to play important roles in cardiogenesis and their disruption has been shown to cause severe disturbances in heart development. Spatially and temporally complex interplays between the two pathways have been described. One component of the PCP pathway is Jnk, a member of the highly conserved mitogen-activated protein kinase (MAPK) family. This stress responsive mitogen is known to control a variety of cellular behaviours such as proliferation, apoptosis and cell migratory behaviour and as such, is likely to be of pivotal importance in cardiac development.

The aim of this study was to investigate the role played by Jnk in vertebrate heart formation and the relationships between Jnk signalling and canonical Wnt signalling, using *in silico* and *in vivo* approaches in zebrafish and an *in vitro* approach on a mouse embryonic stem (ES) cell model of cardiogenesis.

Firstly, using a range of bioinformatic methods, an analysis of *jnk* genes, splice variants and proteins, and an investigation of their phylogenetic relation with other species was undertaken. This suggested conservation of Jnk family members, but suggested that there were additional orthologues of *jnk1* present in the zebrafish transcriptome. The spatial and temporal expression profiles of these genes were then examined by semi-quantitative PCR and *in situ* hybridisation. The functional role of Jnk proteins during zebrafish development was subsequently investigated using a specific chemical inhibitor, SP600125. Inhibition of Jnk signalling during gastrulation and somitogenesis caused a convergence extension-like phenotype and severe cardiac defects, including looping anomalies and alterations in atrial versus ventricular cell numbers.

ES cells have the capacity to differentiate *in vitro* and give rise to cells of many different lineages, including cardiomyocytes. Canonical Wnt and Jnk components were manipulated during specific windows of differentiation as ES cells formed beating embryoid bodies. Examination of the spontaneous contractile behaviour of differentiating ES cells as they entered the cardiogenic lineage, and analysis of their developmental gene expression profiles, showed the beating behaviour of ES cell-derived cardiac cells was enhanced in a temporally specific manner after inhibition of the non-canonical Wnt/Jnk pathway, while there was marked alteration of canonical Wnt signalling. To investigate whether there were reciprocal interactions between the

two pathways, analysis of the system after activation of the canonical pathway was also undertaken.

These studies indicated that the beating behaviour of ES cell-derived cardiac cells was enhanced in a temporally specific manner after inhibition of Jnk, while after activation of canonical Wnt/β-catenin signalling, the cardiogenic potential of differentiating ES cells was severely suppressed.

The findings of this study extend our understanding of the role played by canonical and non-canonical Wnt signalling pathways in heart morphogenesis and highlight the interacting effects of related signalling pathways activity in cardiogenesis.

Acknowledgments

This thesis took a bit less than 4 years to be completed (although it felt like much more!). It had good and bad times, achievements and disappointments, it followed smooth paths (hardly any!) and rough paths, and it has definitely been an amazing experience and a huge task.

This thesis could not have been realized without the help, guidance and support of my supervisors Professor Deborah Henderson and Dr. Bill Chaudhry. I owe them a big thanks not only for advising me, guiding me and keeping me in track, but also for pushing me, challenging me and 'forcing' me to become better and to achieve more.

Also, a big thanks goes to my lab mates for their continuous support, understanding and help. But, even more I want to thank them for the good times we spent together, both in the lab and in the streets of the toon, the concerns we shared, the 'team' feeling we had! I would, especially, like to thank Helen Phillips, Hong Jun Rhee, Nic Child, Dave Burns, Mike Baker, Veronika Bozconadi, Vipul Sharma, Victoria Hildreth, Jon Peat, Darren Hoyland, Nicola Hunt and Iain Keenan. Also, part of the gang, although not in our lab, Amy-Leigh Johnson, Divya Venkatesh and Gavin Richardson. Not to forget all the people that have passed through our lab all these years and many other members of the Institute of Genetic Medicine; a bit thanks to them too!

Last but definitely not least, I would like to say 'thank you' to my family and friends. Thanks for your presence, support and encouragement, that helped me make it through some rough times. Also, thanks for helping me to gain perspective when all I could see was problems, for bringing me back to earth when I was lost and for giving me a push when I was stuck! Although it is hard to explain to someone who is not going through a PhD process what this is actually about, I was lucky to be surrounded by people that did their best in understanding and helping me in their very special way! I cannot mention them all here… But my parents, Anna, Lena, Ino, Dimitris, Andreia and Pedro could not be missing! Oh and Tali (but just because she asked me to).

Table of contents

List of figures

List of tables

Chapter 1. Introduction

In this thesis, the c-Jun N-terminal kinase (JNK) signalling pathway, part of the non-canonical Wnt and Mitogen-activated protein kinase (MAPK) cascades, is discussed in the context of zebrafish embryogenesis and mouse embryonic stem (ES) cell differentiation. In particular, zebrafish cardiogenesis and ES cell-derived cardiac differentiation are of interest. This first chapter is a review of what is known to date about the main components of the thesis: zebrafish embryonic development, embryonic stem cells, heart induction, specification and differentiation as well as Wnt, JNK and MAPK signalling pathways.

1.1. Congenital heart disease

Congenital heart defects are cardiac malformations present at birth and they account for 6 to 19 per 1000 live births (Hoffman and Kaplan, 2002). Their etiology is multifactorial, possibly both genetic and environmental, although the genetic components have only recently started to become understood and identified (Nora, 1968, Jenkins et al., 2007). Septation and alignment defects are among the most common heart anomalies observed in newborns or infants and they include ventricular and atrial septal defects, common arterial trunk, double outlet right ventricle and tetralogy of Fallot. Many cardiovascular defects are associated with known syndromes or with other defects. Commonly, cardiovascular anomalies are coupled with craniofacial defects, as in CHARGE (Coloboma in the iris, Heart defects, Atresia of nasal passages, Retardation of mental and somatic development, Genital anomalies, Ear abnormalities) (Pagon et al., 1981), diGeorge (Funke et al., 1999, Kirkpatrick and DiGeorge, 1968, Yagi et al., 2003) and Noonan syndromes (Noonan et al., 1968, Tartaglia et al., 2004a, Tartaglia et al., 2004b), but it is not unusual to occur in association with limb, as in the Holt-Oram syndrome (Basson et al., 1997), or kidney abnormalities, as in the Smith-Lemli-Opitz syndrome (Smith et al., 1964). Despite our comprehensive knowledge of genes associated with the formation of the heart during embryogenesis, little is still known about the morphological processes that underlie this highly complex procedure and only a few genes have been directly linked to specific cardiac defects in humans (Schott et al., 1998). Therefore, our complete understanding

of the genetic networks and the morphogenetic movements that govern the formation of the heart is of primary importance for any future therapeutical applications.

1.2. Early vertebrate embryonic development

Laboratory models are used to investigate cardiac development and malformation. Cardiomyocytes are specified at the time of gastrulation and differentiate during somitogenesis. A description of relevent early vertebrate embryogenesis will be presented in order to understand the events of cardiogenesis. Mouse, chick and zebrafish are the organisms of interest. Most of the processes are firstly described in zebrafish and then, any striking differences in the mouse are highlighted.

1.2.1. From formation of the zygote to the blastula period

In zebrafish, at approximately 40 minutes after fertilization the first cell division (cleavage) takes place (Figure 1.1). At this stage, the cells (blastomeres) remain connected to each other and to the underlying yolk cell. The vegetal and animal poles appear at this time, with the first being the one with the highest yolk concentration and the latter being the opposite pole, where the blastoderm is and from which the embryo will form. Only maternal mRNA is present in the zygote (Kimmel and Law, 1985a). The cleavage period is followed by the blastula period (2.25 hours post ferilization, hpf, until 5.25 hpf). Essential processes take place throughout this phase, with mid-blastula transition (MBT), formation of the yolk syncytial layer (YSL) and the enveloping layer (EVL) and initiation of epiboly, being the most important. MBT begins at cycle 10 (512-cell stage) and is mainly characterized by activation of the zygotic genome (Kane and Kimmel, 1993, Lindeman and Pelegri, 2010). The YSL, an extraembryonic structure that forms at the margin of the blastoderm (Kimmel and Law, 1985b), is known to function as a signalling centre, important, among others, for mesoderm induction and dorsoventral patterning (Chen and Kimelman, 2000, Sakaguchi et al., 2006, Sakaguchi et al., 2002). Between the YSL and the EVL (the most superficial layer of the blastoderm) lie the cells that will give rise to the embryo (Kimmel and Law, 1985b) (Figure 1.1.).

These very early stages of embryonic development, described so far in zebrafish, are quite similar in mammals, although differences are also observed. After fertilization

and early cell divisions in mice, a cavity, called blastocoel, forms in the centre of the cell mass of 16 cell-stage embryos (approximately 2.5 days post coitum, E2.5). Embryos of this stage are called blastocysts (E3.5-E4.5) and they consist of the inner cell mass (ICM) cells that will give rise to the embryo proper and to the amnion, and of trophoblasts cells that will give rise to the chorion (Fleming, 1987, Pedersen et al., 1986, Wiley, 1984, Gilbert, 2003).

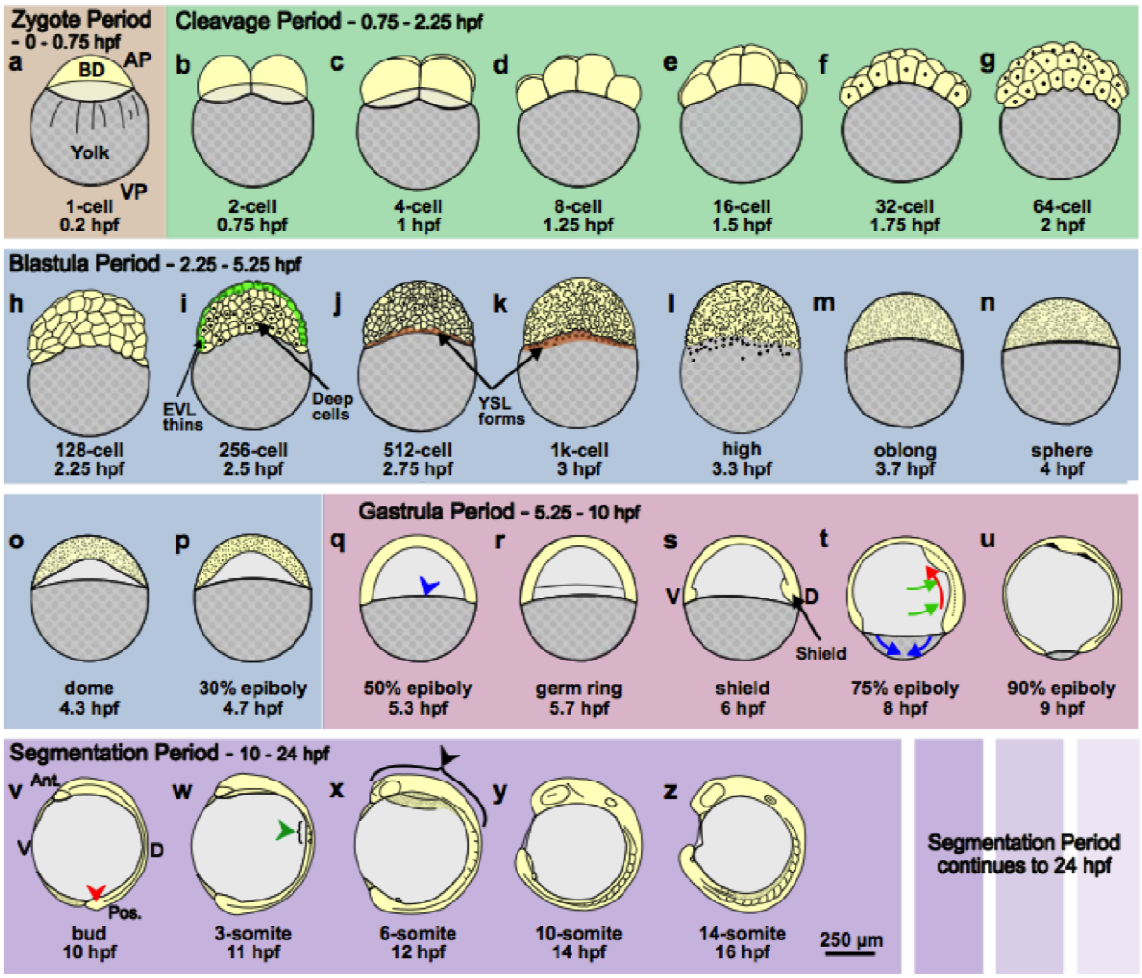

Figure 1. 1: Schematic representation of zebrafish embryonic development. Stages from the zygote period until the mid-segmentation period are shown. (a) The zygote period, when the embryo is at the single-cell level, is brief (0-0.75 hpf). The blastodisc (BD) shown here at the one-cell stage, will develop into the blastoderm during subsequent stages of development. (b)-(g) The cleavage period starts at the two-cell stage and lasts until the 64-cell stage (0.75-2.25 hpf). (h)-(p) The blastula period runs from the 128-cell stage until the 50% epiboly stage (2.25-5.25 hpf). Formation of the enveloping layer (EVL) and the yolk syncytial layer (YSL) is shown in (i), (j) and (k). (q)-(u) The gastrulation period starts at the end of the blastula period and ends at the bud stage (5.25-10 hpf). The blue arrowhead in (q) indicates the leading edge of the blastoderm. The dorso-ventral axis is first morphologically visible at the shield stage (6 hpf, s). Simultaneous epiboly (blue arrows), convergence (green arrows) and extension (red arrows) movements are shown in (t). (v)-(z) The segmentation period starts at 10 hpf and lasts until 24 hpf. Only the early stages of this last period are shown in this schematic, from 10 hpf until 16 hpf (14-somite stage). The tail bud is shown by the red arrowhead (v), somites by the green arrowhead (w) and the brain anlage by the black arrowhead (x). AP/VP: animal/vegetal pole, Ant/Pos: anterior/posterior, hpf: hours post fertilization (figure taken from Webb and Miller, 2007).

1.2.2. Gastrulation and the formation of the germ layers

Gastrulation is a highly conserved process across the animal kingdom and is responsible for establishment of the embryonic germ layers, from which all organs and structures of the embryo will arise. It is characterized by extensive cell movements (Figure 1.2) and ends with the formation of the embryonic germ layers (ectoderm, mesoderm and endoderm). During zebrafish gastrulation (5.25-10 hpf), epiboly (the thinning and spreading of the blastodisc and the YSL over the yolk), involution (inwards migration of marginal cells) and convergence-extension (CE) participate in the formation of the primary germ layers and define the embryonic axis. At the onset of gastrulation, when about half of the yolk cell has been covered by blastoderm cells (50% epiboly), a cell fate map is already established; this ascertains what regions and what organs the cells migrate into and what types of cells they differentiate to. At this stage, the superficial layer of the involuting blastoderm forms the epiblast (that will give rise to ectoderm and its derivatives), while the underlying layer is now called the hypoblast (which will give rise to mesendodermal derivatives) (Thisse et al., 1993). A local thickening, termed the embryonic shield, marks the future dorsal side of the embryo. Migration of cells and convergence-extension through the shield establishes the germ layers. The end of gastrulation is defined by completion of epiboly (100% yolk coverage) and formation of the tail bud.

Mammalian gastrulation shares many similarities but also diverges from that of the fish. The epiblast, which will, as in the zebrafish, give rise to the embryo proper, is part of the blastocyst ICM. A defining structure of mammalian (avian and reptilian as well) gastrulation, absent in fish, is the primitive streak. This is a local thickening of the epiblast starting posteriorly and progressing anteriorly. Convergence and extension movements are responsible for increasing the length of the streak and narrowing its width. Gastrulation begins at the node, a regional thickening of cells in the primitive streak. Epiblast cells migrate (ingress) through the primitive streak. Mouse embryonic development presents a peculiarity: the epiblast is cup-shaped rather than disc-shaped as in chick and human. As a result of that, at the end of gastrulation, presumptive ectodermal cells lie on the inside and endodermal cells on the outside of the ‘cup’. Subsequent embryonic turning of the body brings the endoderm to the inside, the mesoderm in the middle and the ectoderm outside.

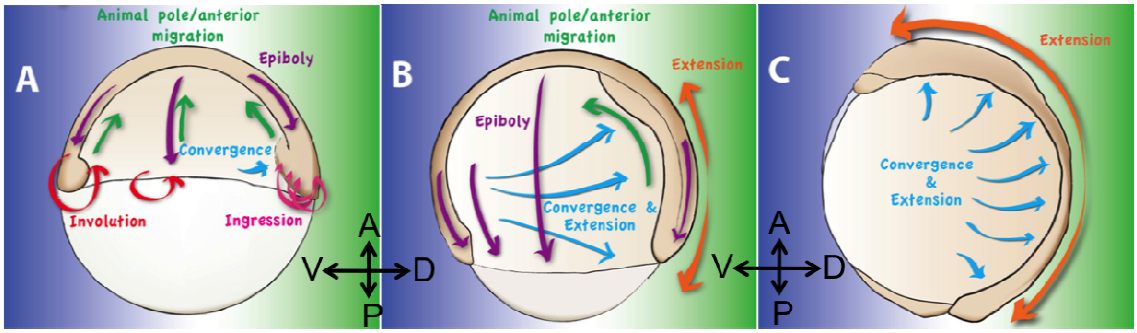

Figure 1. 2: Illustration of epiboly, involution and convergence-extension movements during zebrafish gastrulation. (A) At the beginning of gastrulation the blastoderm has engulfed half of the yolk cell by epiboly movements (purple arrows) and the shield thickening is visible (dorsally). Involution takes place at this stage, with cells from the overlying epiblast feeding cells into the underlying hypoblast (red arrows). (B) At mid-gastrulation stage, epiboly movements continue (75% epiboly has been achieved by this stage). These will stop when the blastoderm has engulfed the entire yolk by approximately 9.5 hpf. Convergence movements towards the future dorsal side of the embryo have started (blue arrows). Concomitantly, extension is taking place along the anterior-posterior axis (orange arrows). (C) At the tail-bud stage, when the entire yolk cell has been covered by the blastoderm, convergence of lateral and dorsal cell populations towards the dorsal side of the embryo is still underway (blue arrows). Concomitantly, extension along the anterior-posterior axis is taking place (orange arrows). V: ventral, D: dorsal, A: anterior, P: posterior (figure taken and adapted from Roszko et al., 2009).

At the end of the fish, avian and mammalian gastrulation, the three germ layers have formed and the embryos look similar: ectoderm surrounds the embryo, endoderm lines the inside of the embryo and mesoderm lies in between. Subsequently, cells interact with one another, rearrange and form tissues and organs. Cells from the ectoderm will give rise to the neural tube, the surface ectoderm and neural crests. Mesodermal cells will give rise to chordamesoderm, lateral plate mesoderm, paraxial mesoderm and intermediate mesoderm. Lastly, endoderm will give rise to the gastrointestinal tract and to the respiratory tube.

1.2.3. Dorsal-ventral and anterior-posterior patterning of the body

The establishment of the body axes during development is crucial for proper morphogenesis of the organs and of the embryo itself. In particular, cardiac development occurs simultaneously to, and relies on, body plan patterning along the anterior-posterior, ventral-dorsal and left-right axis. Anterior-posterior and dorsal-ventral axes are established early in development and are defined mainly by signalling gradients, including Bone Morphogenetic Protein (BMP), retinoic acid and WNT

gradients (Nguyen et al., 1998, Schier, 2001), the position of the node (shield in zebrafish, Hensen's node in chick and node in mammals) (Bachiller et al., 2000, Koshida et al., 1998) and the embryonic-extraembryonic axis (Brennan et al., 2001, Episkopou et al., 2001). The establishment of left-right patterning, which is of most interest in this study, is further discussed below.

1.2.4. Left-right patterning of the body

Left-right asymmetry, although not always visible externally, is essential for proper morphogenesis and positioning of internal organs. The onset of body symmetry breaking is postulated to occur at either cleavage stages or during gastrulation. Cilia, long and thin microtubule-based projections found in most mammalian cells (Poole et al., 1985), have been shown to be essential contributors to early left-right patterning events at the node (Nonaka et al., 1998). Recently, posterior positioning of the cilia within cells of the node was shown to be determined by Wnt/planar cell polarity (PCP) proteins Vangl1 and Vangl2 (for more details on this pathway see Section 1.4.2, page 31) and to be essential for proper establishment of left-right identities in mouse (Borovina et al., 2010, Guirao et al., 2010, Okada et al., 2005, Song et al., 2010). Each cell within the node has a unique motile cilium that can rotate in a clockwise manner (Nonaka et al., 2005, Okada et al., 2005). The posterior cellular localization of the cilium enables its posterior tilting and determines its rotational axis (Nonaka et al., 2005, Okada et al., 2005, Song et al., 2010). The leftward fluid flow that is generated by the rotation of the nodal cilia is thought to be a determining factor in establishing the left and the right sides of the embryo, possibly through an asymmetric calcium flux (McGrath et al., 2003, Tabin and Vogan, 2003, Yost, 2003).

'Transmission' of the asymmetric signal(s) from the node to the lateral plate mesoderm (LPM) dictates the directionality of many downstream processes, such as looping of the heart and the gut (Aw and Levin, 2008, Capdevila et al., 2000, Collignon et al., 1996, Ibanes and Izpisua Belmonte, 2009, Kawasumi et al., 2011). Signalling by Nodal, a member of the TGFβ family, is thought to be a major regulator of the establishment of left-restricted expression of genes and to play a key role in transferring the asymmetric signal from the node to the LPM (Ahmad et al., 2004, Baker et al., 2008, Duboc et al., 2005, Hamada et al., 2002, Kawasumi et al., 2011, Saijoh et al., 2003). It is initially symmetrically expressed in nodal cells, but becomes asymmetrically

expressed at the LPM and establishes a left-restricted gene expression cascade, involving *Lefty-1, Lefty-2* and *Pitx-2* (Brennan et al., 2002, Saijoh et al., 2003).

In zebrafish, the embryonic structure homologous to the murine node is the embryonic shield. After gastrulation, a group of cells within the shield give rise to a transient epithelial structure (appears at 10.33 hpf and is evident until 24-30 hpf) that is called the Kupffer's vesicle. Kupffer's vesicle cells were shown to contain a single cilium each (Essner et al., 2002) and to participate in left-right patterning, through a similar rotational ciliary movement and leftward fluid flow as in the mouse node (Amack and Yost, 2004, Essner et al., 2005). Nodal signalling genes in zebrafish, *cyclops, squint* and *southpaw* (Erter et al., 1998, Feldman et al., 1998, Long et al., 2003, Schier, 2009), are shown to be involved in establishing left-right asymmetrical gene expression in zebrafish embryos as well. The canonical Wnt pathway has, recently, been shown to be important for promoting normal development of the Kupffer's vesicle and for regulating asymmetric signals in the LPM (Lin and Xu, 2009). Thus, the basic mechanisms dictating embryonic development in terms of dorsal-ventral, anterior-posterior and left-right identities are conserved between vertebrate animal models. This common paterning will be extended to the patterning and development of the heart.

1.3. Mesoderm and the origin of the heart

The early events of vertebrate embryonic development, starting at fertilization and ending with the formation of the three germ layers and the patterning of the embryonic axes have been shown to be conserved between species. This section focuses on one of the germ layers, the mesoderm, and one of its main descendants, the heart. Here, zebrafish, chick and mouse heart formation is discussed. First, induction, specification, determination and differentiation of cardiac cells are presented (Sections 1.3.1-1.3.5), followed by an overview of heart development, morphogenesis and patterning (Sections 1.6-1.10).

A timeline of cardiogenesis in zebrafish, mouse and embryonic stem (ES) cells is shown in Figure 1.3. The main cardiogenesis-associated events are shown, along with the main transcriptional regulators and other cardiac genes involved in them. This figure will be used as a reference for comparison between the different aspects of this thesis. The correlation between ES cell differentiation and animal embryogenesis is not absolutely accurate because it depends to some extent on the properties of the cell line used, but provides a useful approximation.

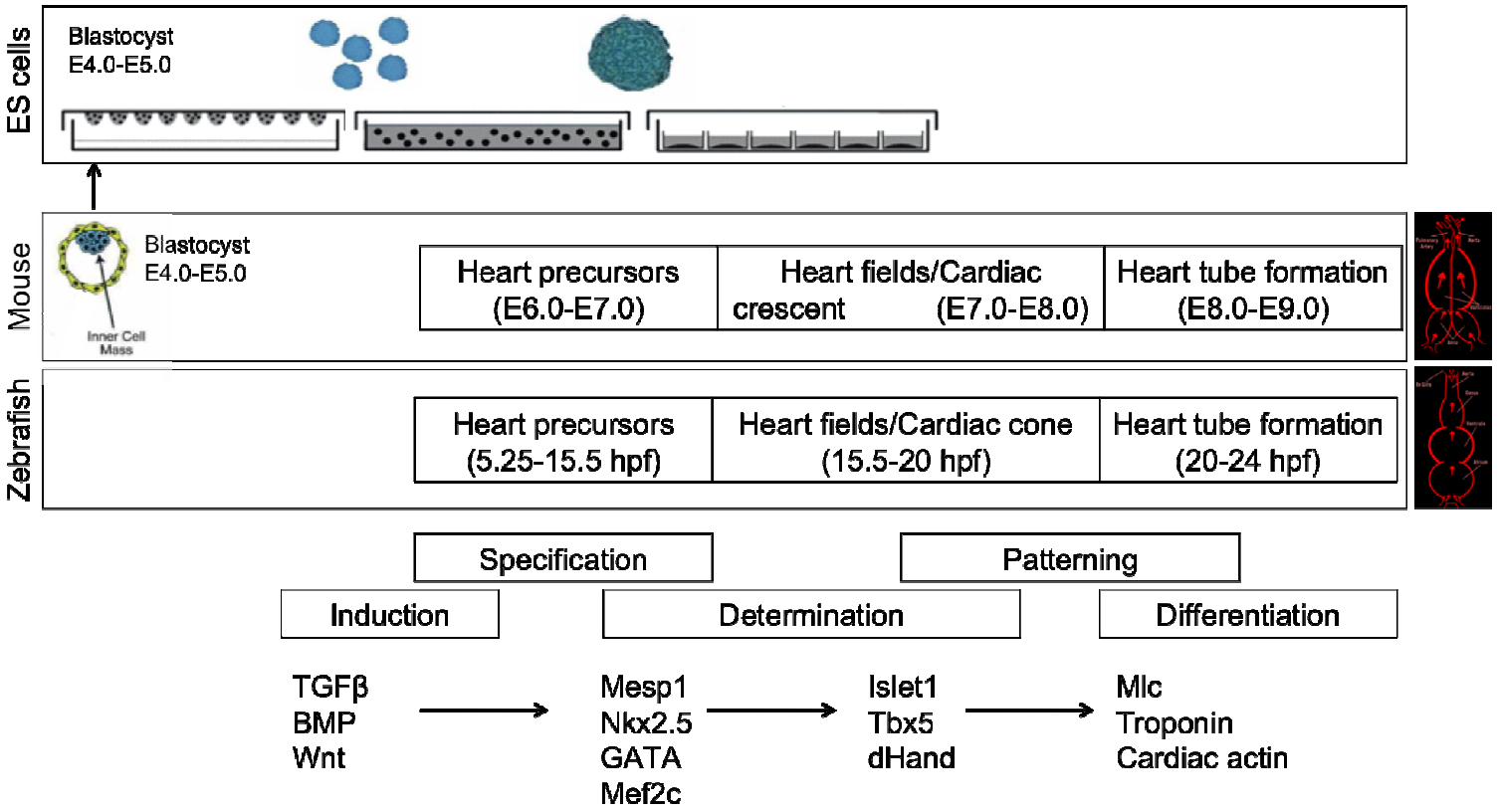

Figure 1. 3: Schematic representation showing the timeline of cardiac specification. Differentiation of mouse embryonic stem (ES) cells into cardiomyocytes is shown along with some of the early events of zebrafish and mouse embryogenesis. The time intervals during which induction, specification and determination of cardiac cells, as well as heart patterning and differentiation, are shown in boxes at the bottom of the figure. Some of the cardiac regulators are, also, shown at the bottom. Arrows do not indicate direct relationship, but rather highlight the sequence of events.

1.3.1. Induction of cardiac fate

An initial step in cardiogenesis is the induction of mesodermal cells to acquire a cardiogenic potential. This induction appears to be regulated by numerous complex, positive and negative signalling and transcriptional networks, involving members of the Wnt, BMP, sonic hedgehog (Shh), fibroblast growth factor (FGF) and Notch families. Recently, epigenetic events (Lickert et al., 2004) and micro-RNA translational regulation (Zhao et al., 2005, Ladd et al., 1998) have also been shown to play essential roles in fine-tuning cardiac gene and protein regulation.

Ingression of the presumptive cardiac cells through the rostral and middle segments of the primitive streak (in mouse and chick) during gastrulation follows, as described in previous sections. Absence of the hypoblast does not allow for cardiogenesis to occur, suggesting that the hypoblast is an essential inducer of myocardial specification, possibly secreting activin and transforming growth factor (TGF) (Ladd et al., 1998). Similarly, in mouse the anterior visceral endoderm (the mouse homolog of the chick hypoblast) has been shown to be essential for cardiomyocyte specification (Arai et al., 1997, Nijmeijer et al., 2009). Migration of myocardial progenitors from the epiblast through the primitive streak to the LPM brings them close to instructive signals from the underlying endoderm that are essential for further cardiac specification (Schlange et al., 2000, Tam et al., 1997). The two bilateral fields within the LPM, where heart progenitors are now located are designated as the cardiogenic fields and will be discussed in following sections. In zebrafish, the extraembryonic YSL and the endoderm adjacent to the blastoderm margin have been shown to secrete signals (mainly *gata-4, gata-5* and *gata-6*) that are essential for proper migration of cardiac precursors (Peterkin et al., 2009). Once in the anterior LPM, cardiac progenitors become further specified by receiving *gata-5* (Peterkin et al., 2009, Reiter et al., 1999)*, fgf8* (Reifers et al., 2000) and *bmp2* (Kishimoto et al., 1997, Reiter et al., 2001, Wang et al., 2007) signals, among others, originating mainly from the LPM itself.

In amniotes (including mammals and avians), inducing signals from the underlying endoderm are thought to be modulated by inhibitory signals that arise from the overlying ectoderm and the neighbouring notochord. BMP (Ladd et al., 1998, Schneider and Mercola, 2001), FGF (Abu-Issa et al., 2002, Frank et al., 2002), Shh (Gianakopoulos and Skerjanc, 2005) and non-canonical Wnt (Garriock et al., 2005, Pandur et al., 2002, Terami et al., 2004) are commonly thought to be among the

inducing factors, whereas Notch (Rones et al., 2000), Noggin (inhibitor of BMP) (Jamali et al., 2001), and canonical Wnt (Marvin et al., 2001, Schneider and Mercola, 2001) are thought to suppress cardiogenesis (Figure 1.4). Similarly, in zebrafish notochord cells are thought to play repressive roles in myocardial differentiation by restricting expression of *nkx2.5* in cells of the anterior LPM (Goldstein and Fishman, 1998, Serbedzija et al., 1998, Yelon and Stainier, 1999). The role of Wnts during cardiomyocyte differentiation and heart development will be discussed in more detail in Section 1.4 (page 25).

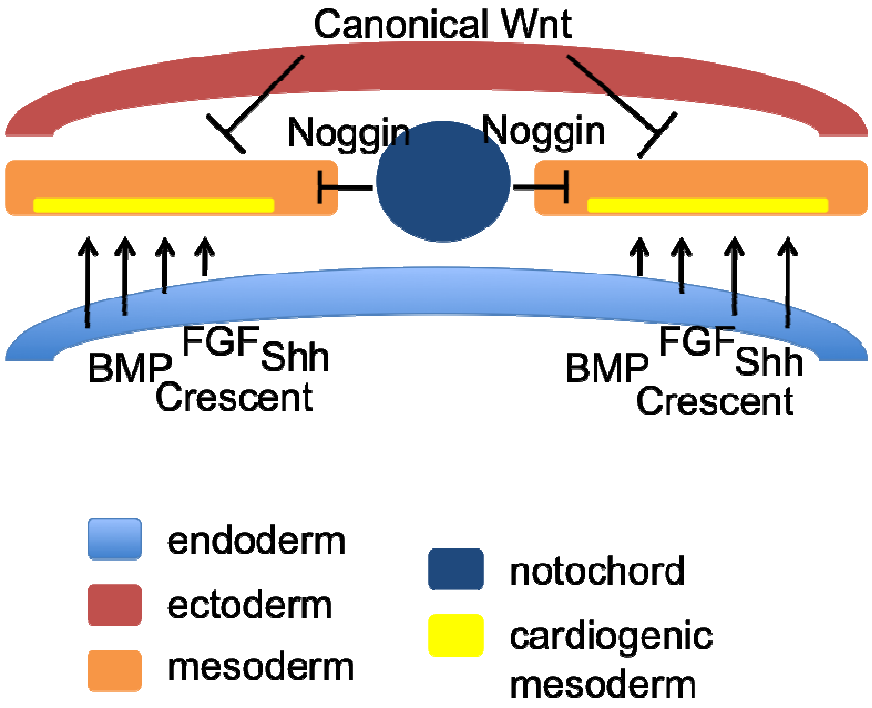

Figure 1. 4: Vertebrate myocardial induction. Cardiac-inducing signals from the endoderm and cardiac-inhibitory signals from the notochord and the ectoderm define the cardiogenic region of the mesoderm. Some representative signals are shown in the figure (BMP, FGF, Shh, Crescent, Noggin, canonical Wnt).

Taken together, extraembryonic tissues seem to be important for initial induction of mesoderm; mesodermal cells gain the potential to acquire a cardiac fate or, more accurately, to respond to cardiogenic signals. After migration and positioning of induced mesodermal cells to their future anterior LPM bilateral positions, the underlying endoderm specifies their cardiac signature by sending inductive signals, while the overlying ectoderm restricts cardiac fate by secreting inhibitory factors. An overview of cardiac specification at the single-cell level follows, with a description of the sequence of gene activation and cardiac progression.

1.3.2. Specification of cardiac progenitors

The absence of cell surface markers specific for heart progenitors has hampered a clear definition of a unique cardiac progenitor population. Nevertheless, the specification process of early mesodermal cells towards their cardiogenic fate is well described.

Mesodermal cells initially express *Brachyury* (*Bry*), a T-box transcription factor. Transient expression of Mesoderm Posterior-1 (*Mesp1*) marks mesodermal cells of cardiogenic potential. Expression of *Mesp1* encompasses all cardiac progenitors, when they are still located in the primitive streak in the mouse embryo, and marks cells that will contribute to all four main types of cells in the heart (cardiomyocytes, endothelial cells, vascular smooth muscle cells and cardiac fibroblasts). Expression of *Mesp1* is switched off when progenitor cells migrate away from the primitive streak and expand towards the LPM (Bondue et al., 2008, Wu, 2008, Ema et al., 2006, Garry and Olson, 2006, Huber et al., 2004, Kattman et al., 2006).

A first wave of *Flk1* expression (Vascular endothelial growth factor receptor-2) differentiates Bry^+ cells to haemangioblast precursors. After another wave of *Flk1* expression (E7.75 at the cardiac crescent stage), Bry^+ cells will differentiate to mesodermal cardiac precursors. These, often referred to as cardiovascular colony-forming cells, are common progenitors for cardiac myocytes of the primary (PHF) and secondary (SHF) heart field (Section 1.3.7, page 21), vascular smooth muscle and endothelial cells (Ema et al., 2006, Garry and Olson, 2006, Huber et al., 2004, Kattman et al., 2006, Moretti et al., 2006). Expression of *Flk1* precedes the onset of expression of cardiac transcription factors, such as *Gata-4, Nkx2.5* and *Mef-2c,* described in Section 1.3.5 (page 14). Within the SHF at approximately E8-E8.5 *Islet1* (*Isl1*), with *Nkx2.5* and *Flk1,* defines a population of cells, called multipotential $Isl1^+$ cardiovascular progenitor cells, which can give rise to cardiomyocytes, smooth muscle and endothelial cells (Moretti et al., 2006). In the PHF at approximately E9.5 *Nkx2.5* bipotent progenitors were shown to give rise to cardiomyocytes and smooth muscle cells (Garry and Olson, 2006, Wu et al., 2006).

In summary, mesodermal cells that are induced by signals from surrounding tissues to attain a cardiac fate, initiate a transcriptional cascade that will result in acquisition of a specific cardiac identity. The differential specification process for atrial and ventricular cells is discussed in the next section.

1.3.3. Atrial and ventricular cell fate specification

Myocardial induction and specification events promote the cardiogenic fate in mesodermal cells and set the scene for further differentiation. However, not all cells that are induced to attain a cardiac fate follow the same path. Cardiac cells that are destined to contribute to different compartments of the presumptive heart are thought to be distinctly located early in development and may, thus, be differentially regulated.

In zebrafish, myocardial progenitors just prior to gastrulation (40% epiboly, approximately 5 hpf) are found within the first four tiers of blastomeres, next to the embryonic margin on both the left and right sides of the forming embryo (Warga and Nusslein-Volhard, 1999), as shown in Figure 1.5. Labelling of single cardiogenic blastomeres at this stage showed that labelled progeny resulted in either the ventricle or the atrium, but never in both chambers (Stainier et al., 1993). Ventricular progenitors are located closer to the embryonic margin and towards the dorsal midline compared to atrial precursors (Keegan et al., 2004) (Figure 1.5).

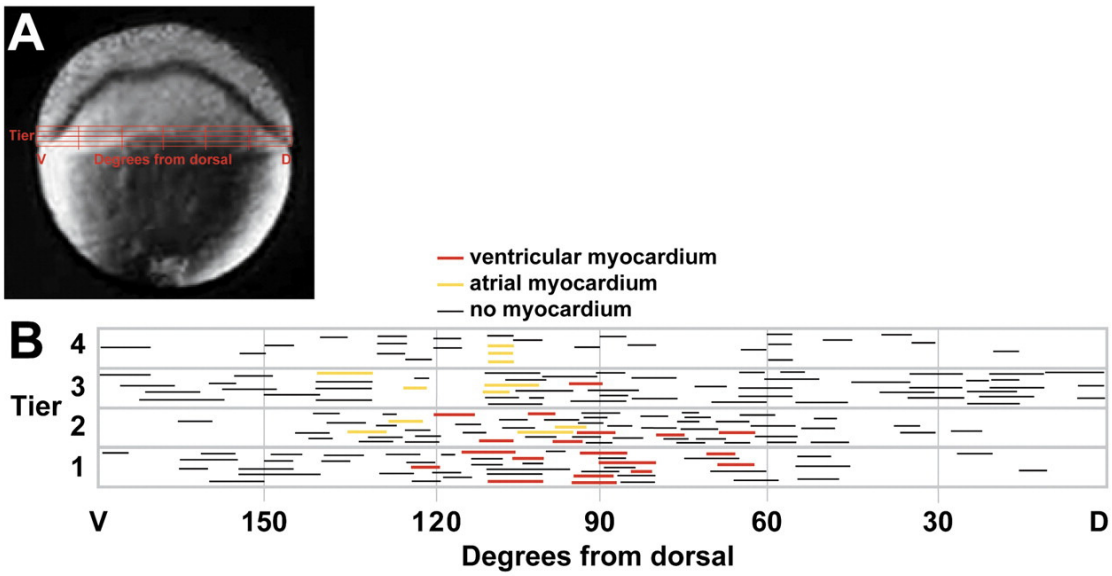

Figure 1. 5: Fate map of myocardial chamber progenitors. Ventricular and atrial myocardial progenitors are spatially differentiated already at 40% epiboly. A) The coordinates of the fate map are projected onto a 40% epiboly-stage zebrafish embryo (lateral view shown). The latitude (vertical axis) is expressed in tiers from the margin. Each tier represents one cell diameter. The longitude (horizontal axis) is expressed in degrees around the circumference of the embryo. B) Fate map of the distribution of atrial and ventricular progenitors. The position of each bar (representing an individual experimental embryo) corresponds to the location of labeled blastomeres. Red bars show ventricular progenitors, yellow bars show atrial progenitors and black bars indicate non-myocardial progeny. Data from both the left and right side of the embryo are summarized on this fate map. Ventricular progenitors are found 60-125^{o} from dorsal in tiers 1, 2 and 3, while atrial progenitors are found 90-140^{o} from dorsal in tiers 2, 3 and 4 (Keegan et al., 2004).

Cardiogenic blastomeres are among the first to involute at the beginning of gastrulation at 5.25 hpf (Warga and Kimmel, 1990). Blastomeres from different regions of the lateral marginal zone were shown to migrate and form distinct regions of the LPM: ventricular progenitors become located medially and rostrally in relation to atrial progenitors (Keegan et al., 2004, Yelon and Stainier, 1999). Relative orientation of atrial and ventricular progenitors within the LPM is maintained as heart tube assembly is underway, as will be discussed in following sections (Yelon and Stainier, 1999). The expression patterns of *atrial myosin heavy chain* (*amhc*) and *ventricular myosin heavy chain-2* (*vmhc-2*) subdivide the myocardial precursors into two cell populations that will give rise to the presumptive atrial and ventricular precursors, respectively. Expression of *amhc* starts at approximately the 19-somite stage (around 18.5 hpf), slightly later than the onset of *vmhc* expression at the 13-somite stage (around 15.5 hpf) (Yelon and Stainier, 1999).

Nkx (*nkx2.5* and *nkx2.7*) genes have been shown to differentially affect ventricular and atrial cell fates (Targoff et al., 2008). Specifically, it was shown that injection of anti-*nkx2.5* and anti-*nkx2.7* morpholinos in zebrafish embryos had differential effects on the forming ventricle and atrium: the ventricle appeared smaller and abnormal and contained less cells, while the atrium was stretched and enlarged (Targoff et al., 2008).

FGF signals have, also, been suggested to affect chamber proportions. Specifically, zebrafish *fgf8* mutants have small hearts with particularly small ventricles (Reifers et al., 2000), while mouse *Fgf8* hypomorphs ($Fgf8^{neo/-}$) exhibit hypoplastic right ventricles, along with other cardiovascular abnormalities (Abu-Issa et al., 2002). In chick, administration of exogenous *Fgf2* or *Fgf4* was shown to promote ventricular gene expression and to decrease atrial gene expression (Lopez-Sanchez et al., 2002). Lastly, after timely inhibition of *fgf* signalling in zebrafish embryos, greater sensitivity to the treatment was observed in ventricular cells compared to atrial cells (Marques et al., 2008). Additional factors, shown to affect atrial-ventricular cell fate in mouse and chick are, among others, the basic Helix-Loop-Helix transcription factors *Hand1* and *Hand2* (Firulli et al., 1998, Riley et al., 2000, Srivastava and Olson, 1997), *Tbx5* (Bruneau et al., 2001) and *Irx4* (Iroquois family of homeobox genes) (Bao et al., 1999).

1.3.4. Cardiac determination and differentiation

After initial specification of the cardiac fate in the LPM, cardiac progenitors will start expressing late cardiac genes, such as *aMhc*, *vMhc*, atrial myosin light chain-2 *(Mlc-*

2a), ventricular myosin light chain-2 (*Mlc-2v*), *Irx4,* cardiac Troponin-I (*cTnI),* cardiac Troponin-C *(cTnC)* and Troponin Type-2 *(Tnnt2)*, and become irreversibly committed and differentiated towards the cardiac lineage. When the murine linear tubular heart is formed (at approximately E8), *Mlc2v* and *Irx4* are expressed in a large part of the tube {O'Brien, 1993 #81} and even after looping, they extend in areas outside the ventricles (atrioventricular canal, ventricles, proximal outflow tract etc) (Bruneau et al., 2000, Christoffels et al., 2000, O'Brien et al., 1993). As development proceeds, they become more and more ventricle-confined (Small and Krieg, 2004). *Mlc-2a* is an important component of the atrial myofibrillar apparatus and its genetic deletion in mice has been shown to diminish atrial contraction (Huang et al., 2003). However, *Mlc-2a* is not atrial-specific throughout development; initially, its expression is ubiquitous in the linear heart tube and it becomes restricted to the atrial appendages between E10-E12 (Kubalak et al., 1994, O'Brien et al., 1993, Small and Krieg, 2004). Atrial Natriuretic Peptide (ANF) is another atrial-specific marker. It is a hormone that is specifically produced in and secreted by the atria and is thought to be involved in blood pressure regulation. Its upregulation in the ventricles has been shown to be correlated with hypertrophy (Chien et al., 1991). *cTntI* is a regulatory protein controlling the interaction between actin and myosin in the contractile apparatus (Sharma et al., 2004). This gene has been uniquely identified within the myocardium in mouse (Bodor et al., 1995). *Tnnt2*, another component of the contractile machinery of cardiac cells, is a tropomyosin-binding subunit of the troponin complex and is responsible for the regulation of muscle contraction (Ahmad et al., 2008, Nishii et al., 2008, Sumandea et al., 2009).

Cardiac progenitors become differentiated cardiomyocytes after cardiac specification, determination and differentiation, as described in previous sections. Depending upon their position within the developing embryo and upon interactions with surrounding structures cardiac cells acquire their specific cardiac fate. Some essential transcription factors, already briefly mentioned, are discussed in more detail in the next section.

1.3.5. Transcriptional regulation of cardiac cell differentiation

This section provides an overview of the cardiac transcriptional network, encompassing specification, determination and differentiation of cardiac progenitors. A master regulator gene that can trigger the myocardial program probably does not exist. It is rather thought that the regulation of the myocardial program is achieved by the

synergistic action of multimeric complexes of transcription factors. Probably, the most important cardiogenic network, at least in mouse, is that of *Gata-4, Tbx5* and *Baf60c*, suggested by Takeuchi and Bruneau in 2009 (Takeuchi and Bruneau, 2009). *Gata-4* and *Tbx5* are transcription factors essential for cardiogenesis, further explained in Sections 1.3.5.2 and 1.3.5.3. *Baf60c* is a subunit of the Swi/Snf-like BAF chromatin-remodelling complex and was recently identified as a potential cardiogenic factor (Lickert et al., 2004). The *Gata-4*, *Tbx5* and *Baf60c* triad was shown to be sufficient for differentiation of non-cardiogenic mesoderm to cardiomyocytes. *Nxk2.5*, another essential cardiac transcription factor (Section 1.3.5.1), although not part of the minimal set of factors required for cardiac differentiation, it was subsequently induced by the combinatorial activity of *Gata-4* and *Baf60c* (Takeuchi and Bruneau, 2009). Absence of *Tbx5* in this context did not allow beating foci to appear (Takeuchi and Bruneau, 2009). More recently, another critical triad was suggested as the minimum transcriptional requirement for cardiogenic differentiation in mouse: *Gata-4, Mef2c* and *Tbx5*, selected among 14 cardiomyocyte-inducing candidates (Ieda et al., 2010). Ieda and colleagues (2010) showed that trans-differentiation of postnatal mouse cardiac and dermal fibroblasts into functional, beating cardiomyocytes was achieved by the combined activation of these three factors (Ieda et al., 2010). Although the minimal requirements for cardiogenesis suggested by the two groups (Takeuchi and Bruneau, 2009, Ieda et al., 2010) do not fully agree, a discrepancy possibly due to the different target cells (mesodermal cells versus fibroblasts, respectively), the necessity for expression of *Gata-4* and *Tbx5* is common ground. Below, individual contributions of four master regulators of cardiogenesis (*Nkx2.5, Gata-4, Tbx5* and *Islet1*) are discussed.

1.3.5.1. Nkx2.5

Nkx2.5 is one of the earliest markers of cardiac cells and plays a fundamental role in promoting the myocardial phenotype and in defining the cardiogenic fields across species (Evans et al., 1995, Harvey, 1999, Olson, 2006, Terada et al., 2011). In avian development it has been shown to be one of the earliest markers of mesoderm induced to attain a cardiac fate (Schultheiss et al., 1995). It is an important transcriptional regulator of a wide range of genes required for normal heart development, such as *Mlc-2v*, Natriuretic peptide precursor type-a (*Nppa*), Natriuretic peptide precursor type-b (*Nppb*), Myocyte-specific enhancer factor 2c (*Mef-2c*) and others (Akazawa and Komuro, 2005, Bruneau et al., 2000). Surprisingly, commitment towards the cardiac

lineage occurs even in the absence of *Nkx2.5*; beating but small hearts develop in *Nkx2.5* null mouse mutants but the embryos eventually die of heart failure (Lyons et al., 1995). In zebrafish, *nkx2.5* over-expression expands the cardiac fields and promotes expression of other cardiac genes, but fails to develop beating cardiomyocytes (Chen and Fishman, 2000a, Chen and Fishman, 2000b), suggesting that this gene is necessary but not sufficient for cardiogenesis. In humans, NKX2.5 mutations have been associated with Tetralogy of Fallot, atrial septal defects and atrioventricular conduction block (Goldmuntz et al., 2002, Schott et al., 1998). Although commonly used as an early cardiac marker, its expression is not restricted to the cardiogenic fields, it is also present in other tissues such as the pharyngeal endoderm, pharyngeal arches, gut and spleen (Eisenberg, 2002).

1.3.5.2. Gata family transcription factors

The GATA family of transcription factors has been shown to have important contributions to heart development. Three members of the GATA family are expressed in precardiac cells: *Gata-4*, *Gata-5* and *Gata-6* (Peterkin et al., 2009, Reifers et al., 2000, Reiter et al., 2001). Members of this family are so called because they can bind to the consensus DNA sequence GATA and activate transcription of cardiac-specific genes. This occurs via the interaction of the GATA proteins with co-factors, such as *Nkx2.5* and *Mef-2C* (Charron and Nemer, 1999, Charron et al., 1999, Molkentin et al., 2000, Morin et al., 2000). Among their targets are genes that code for important components of cardiac cells, such as *cTnC*, *cTnI* and α-cardiac actin. *Gata-4*, specifically, has been shown to be an important activator of cardiac-specific genes, such as *Nppa*, *Nppb*, Myosin Heavy polypeptide 6 (*Myh6*, previously called α-myosin heavy chain), *β-mhc* (β-myosin heavy chain) and others (Molkentin et al., 2000, Pikkarainen et al., 2004) that are essential for cardiomyocyte maturation. Its deletion blocks formation of the primitive heart tube and inhibits terminal differentiation of cardiomyocytes (Garg et al., 2003, Kuo et al., 1997, Molkentin et al., 1997, Zeisberg et al., 2005). It has also been shown to contribute to cardiomyocyte differentiation, proliferation and survival (Peterkin et al., 2005) and to the development of the valves in the heart (Rivera-Feliciano et al., 2006). *Gata4* null mouse embryos exhibit formation of normal amounts of myocardial tissue, although the embryos go on to develop cardia bifida (Holtzinger and Evans, 2005, Kuo et al., 1997, Molkentin et al., 1997, Narita et al., 1996). It is, therefore, possible that there is significant redundancy with other GATA factors, such

as *Gata-5* and *Gata-6* (Holtzinger and Evans, 2005, Molkentin et al., 1997, Peterkin et al., 2007). This is also suggested by a study in zebrafish embryos, where loss of *gata-4* had little effect on specification and differentiation of cardiomyocytes (Serbedzija et al., 1998), when *gata-5* and *gata-6* expression was not altered. Similarly to *Nkx2.5*, *Gata-4* is not uniquely expressed in cardiac progenitors and in the heart but also in pharyngeal endoderm, in the liver and in other endodermal and mesodermal derivatives (Burch, 2005, Molkentin et al., 2000, Patient and McGhee, 2002).

1.3.5.3. Tbx5

Tbx5 (T-Box 5) is a T-box-containing transcription factor that plays an essential role in regulating many developmental processes. It is initially expressed throughout the cardiac crescent but later becomes restricted to the inflow compartment of the heart (Bruneau et al., 2001). Mutations of this gene have been mainly associated with the Holt-Oram syndrome, which affects the development of the heart and the upper limbs (Basson et al., 1997, Fan et al., 2003, Terrett et al., 1994). Although it has been shown to be essential for normal cardiac morphogenesis in Xenopus (Horb and Thomsen, 1999) and for chamber specification in mouse (Liberatore et al., 2000) its specific cellular activities have not been defined. According to a recent publication, as described above, *Tbx5* was suggested to be an essential contributor to initiation of spontaneous contraction, since its absence prevented beating foci to appear (Takeuchi and Bruneau, 2009). In zebrafish, *tbx5a* (one of the *tbx5* orthologs) is expressed in cardiac progenitor cells throughout development and, as in other vertebrates, it is an important regulator of fin (limb) development (Begemann and Ingham, 2000). It is thought to be mainly involved in late cardiomyocyte differentiation, rather than early progenitor specification, despite its early expression in the heart fields (Garrity et al., 2002). *Tbx5b* (the other zebrafish *tbx5* gene) has lost the characteristic fin expression but has retained the eye and heart expression, partially overlapping with *tbx5a* (Albalat et al., 2010).

1.3.5.4. Islet1

Islet1 (*Isl1*) is another important regulator of cardiogenesis. It is a LIM-homeodomain containing transcription factor, transiently expressed in cardiac progenitors, mainly of the SHF, as discussed in Section 1.3.7 (page 21), before their migration into the heart tube and silenced as development proceeds (Cai et al., 2003). *Isl1* is also expressed,

among others, in embryonic neurons (Thaler et al., 2004, Thor et al., 1999). Study of *Isl1* knockout mice revealed moto-neuron defects, pancreatic development anomalies and premature death at E10.5-E11 (Ahlgren et al., 1997, Pfaff et al., 1996). In subsequent experiments, it was revealed that *Isl1* knockout mice carried severe cardiac defects at E9.0 and E9.5 (Cai et al., 2003). Specifically, the hearts of *Isl1* mutant embryos failed to undergo looping and had a common atrium and one ventricular chamber with left ventricular identity, while the right ventricle and the outflow tract were missing (Cai et al., 2003). Lineage tracing experiments showed that *Isl1*-expressing cells colonize the outflow tract, the right ventricle, part of the atria and a minor portion of the left ventricle. *Isl1* has also been shown to be required for the survival, proliferation and migration of SHF cells into the heart tube (Cai et al., 2003). However, subsequent investigations have shown that the expression of *Isl1* is not restricted to the SHF, but may potentially also be expressed in the PHF. Isl1 protein, in contrast to *Isl1* mRNA, was shown to be expressed at E7.5 in mouse embryos in regions that encompass both PHF and SHF (Prall et al., 2007). Similarly, as discussed in Section 1.3.7 (page 21), *Isl1* has been found to be transiently co-expressed with *Nkx2.5* in the cardiac crescent (first heart field) in Xenopus embryos (Brade et al., 2007). These and similar data have suggested that *Isl1* may in fact be a pan-cardiac progenitor marker. In zebrafish, *islet1* has been shown to be expressed in ganglia, vascular endothelium and endoderm lying dorsal to the cardiac fields (Trinh and Stainier, 2004). Its ablation caused motility defects, cardiac contraction irregularity and reduced contractile frequency (de Pater et al., 2009).

1.3.5.5. Summary of cardiac transcriptional regulation

Although the major cardiac transcriptional regulators were described individually in the previous sections, they in fact do not work in isolation but interact extensively with each other. For example, as shown earlier, *Gata-4* and *Tbx5* work together (along with Baf60c) to promote cardiogenic differentiation of mouse mesodermal cells (Takeuchi and Bruneau, 2009). In Xenopus, the combination of *gata4* and *nkx2.5* is crucial for normal expression of atrial-specific genes (Small and Krieg, 2003), while in zebrafish *gata-5* and *nkx2.5* have been shown to work in coordination for the regulation of normal cardiogenesis (Reiter et al., 1999, Reiter et al., 2001). It is, therefore, important to consider the cardiac transcriptional system as a highly interacting network of genes, the expression and function of which is tightly temporally and spatially regulated.

1.3.6. Heart fields in the LPM and heart tube formation

So far, the induction, specification, differentiation and transcriptional regulation of cardiogenic cells have been described. Next, the organization of these cells into early heart structures and their subsequent movement and morphogenesis, until the emergence of the chambered heart, are described. The development of the zebrafish heart is firstly described and any differences in the mouse and chick models are highlighted at the end.

In zebrafish embryos, differentiation of cardiac precursors initiates while these cells reside at bilateral regions within the anterior lateral plate mesoderm (LPM), at approximately 16 hpf (McFadden and Olson, 2002, Yelon and Stainier, 1999). The assembly of a single heart tube in the midline requires the coordinated migration of these cell populations: medially located ventricular precursors move first, followed by laterally located atrial precursors. Myocardial cells reach the midline at approximately 18 hpf and then cardiac fusion starts (Glickman and Yelon, 2002, Yelon and Stainier, 1999). First, the ventricular precursors come in contact at the posterior fusion point and form a V-shape structure. Second, both atrial and ventricular precursors meet at the anterior fusion point and create a ring-like structure with a central lumen (Figure 1.6). On a lateral view, this structure resembles a cone and is thus called the cardiac cone, with ventricular cells residing in its apex and atrial cells in its base (Stainier and Fishman, 1992, Trinh and Stainier, 2004). At 19 hpf, atrial myocardial cells within the cardiac cone start migrating towards the left and anterior, resulting in the relocation of the myocardium to the left of the midline. Clockwise rotation and leftward jogging of the cone results in conversion of the initial dorsal-ventral axis of the cone to the anterior-posterior axis of the forming linear heart tube (Baker et al., 2008, Kathiriya and Srivastava, 2000). As the head lifts and the yolk sac regresses, atrial cells become re-orientated caudally to the ventricular cells (Stainier and Fishman, 1992) (Figure 1.6). Formation of the mammalian and avian linear heart tube is similar to that of the fish (Figure 1.6). Cardiogenic cells residing bilaterally in the anterior LPM form the so-called PHF (approximately E6.5 in mouse and stage 5 in chick). Fusion in the midline gives rise to a horse-shoe-shaped structure, called the cardiac crescent at E7-E8 in the mouse and stage 8-9 in the chick (Tam et al., 1997, reviewed by Moorman and Christoffels, 2003). As the mouse embryo undergoes folding (or turning at approximately E8, described in Section 1.2.2, page 4), cells within the cardiac crescent migrate along the midline and give rise to the linear heart tube by E8.5-E9 (Figure 1.6).

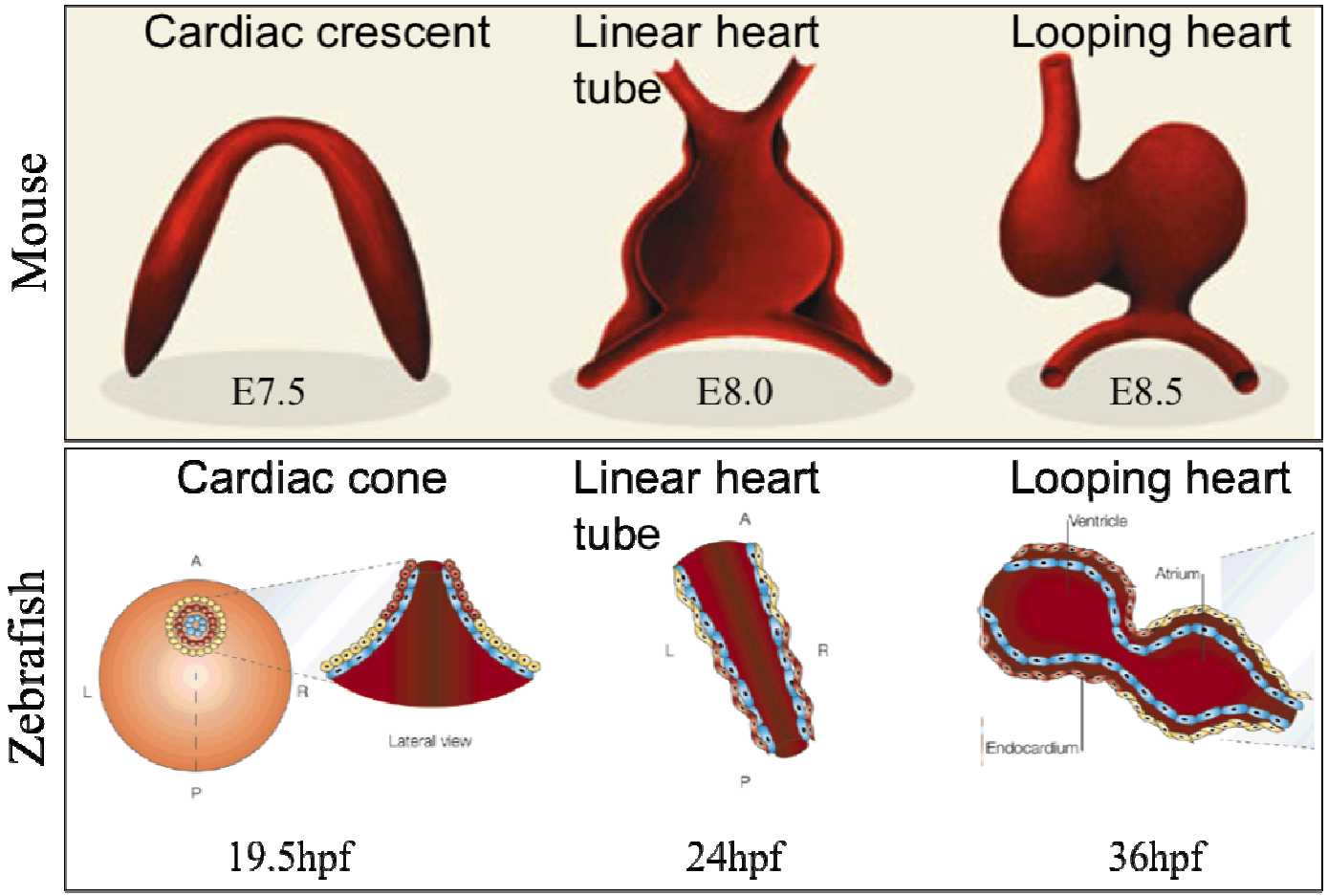

Figure 1. 6: Schematic of mouse and zebrafish heart development. In mouse the cardiac crescent forms at E7.5 after migration of the bilaterally located myocardial progenitors of the LPM to the midline. Closure of the foregut pocket brings cardiac progenitors of the PHF together in the midline to form the linear heart tube (E8). Further morphogenetic movements, including rightward looping, lead to the final conformation of the mammalian heart. In zebrafish at 19 hpf cardiac cells have migrated from their bilateral positions in the LPM to the midline and have formed a cone (the cardiac cone). Ventricular cells are found at the centre and apex of the cone, while atrial cells are found at its base. Then, the cone tilts and forms the linear heart tube by 24 hpf, along the anterior-posterior axis. The atrium is now found to the left of the midline. By 36 hpf, the heart has already started looping. A: anterior, P: posterior, L: left, R: right (Bruneau, 2005, Stainier, 2001).

Chick embryos do not undergo folding but similarly form a linear heart tube (stage 10-11) in the midline as the foregut pockets (deriving from endoderm and giving rise to the pharynx) fuse in the midline.

For years it was believed that the early chick and mouse heart tube was pre-patterned along its anterior-posterior axis (segmentation model) (Buckingham et al., 2005, Harvey, 1999). More recently, a new idea has emerged based on evidence from lineage tracing experiments in mouse, according to which the cardiac crescent contributes largely to the atria and the left ventricle while the outflow tract and the right ventricle originate from the SHF or anterior heart field (Buckingham et al., 2005, Cai et al., 2003, Kelly et al., 2001, Mjaatvedt et al., 2001, Waldo et al., 2001, Zaffran et al., 2004), described in detail in the next section.

1.3.7. Secondary heart field (SHF)

The discovery of the SHF in the chick (Mjaatvedt et al., 2001, Waldo et al., 2001) and in the mouse (Buckingham et al., 2005, Kelly et al., 2001) has shed more light in the complexity of the cardiogenic process. The SHF represents a cell population located medial and dorsal to the PHF and contributes myocardial, endocardial and smooth muscle cells to the arterial pole (Figure 1.7). It is part of the cardiogenic fields but it segregates and contributes to the heart (large part of the outflow tract, the presumptive right ventricle and the atria) only after looping has started (Buckingham et al., 2005, Cai et al., 2003, Kelly et al., 2001, Mjaatvedt et al., 2001, Waldo et al., 2001, Zaffran et al., 2004). This delay is thought to be due to the close proximity of the SHF to the midline, where inhibitory Wnt signals emanate from (Srivastava, 2006). The SHF is marked by the transcription factor *Islet1* (Cai et al., 2003), which was discussed in Section 1.3.5.4 (page 17).

Nowadays, there is a lot of discussion about whether the SHF represents a distinct cell population or whether it is actually only a subdivision of the PHF, of the same origin and expressing the same subset of cardiac genes but in a temporally distinct manner due to its position and its interactions with different combinations of transcription factors (Abu-Issa et al., 2004, Moorman et al., 2007). In recent studies, it has been suggested that the PHF-derived heart tube provides the scaffold upon which SHF-derived cells migrate and construct the cardiac chambers (Buckingham et al., 2005) (Figure 1.7).

Taken together, the PHF and SHF seem to be governed by shared genetic programs. However, the differences in the time course of myocardial differentiation and the distinct spatial contributions of the two heart fields in the embryonic heart support the idea that, despite the presence of some shared genetic components, the two lineages may have distinct transcriptional hierarchies, with *Nkx2.5* being a critical regulator in both lineages and *Isl1*, being a key regulator in the SHF (Laugwitz et al., 2008).

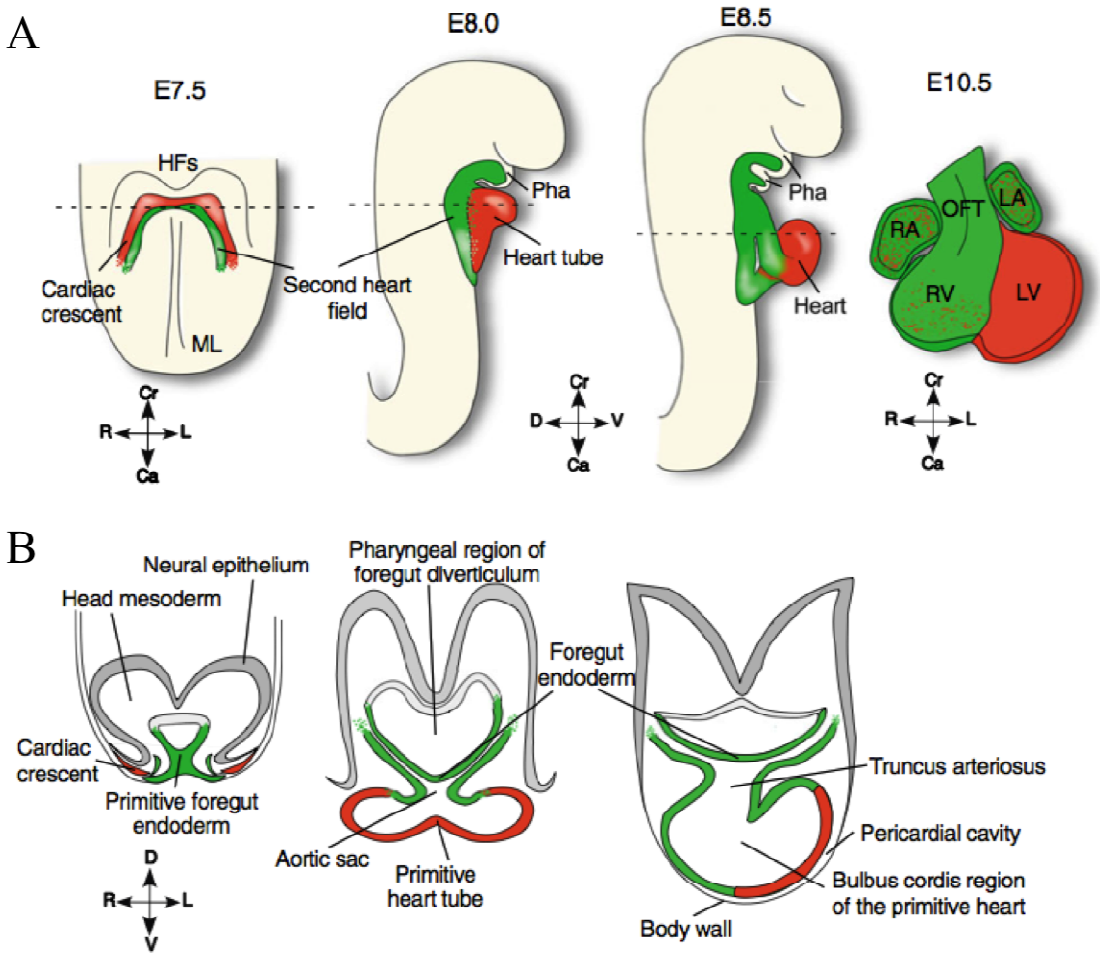

Figure 1. 7: Schematic representation of the contributions of the primary and secondary heart fields in the developing mouse heart. (A) This drawing shows the relative position and contribution of secondary heart field progenitors (shown in green) relative to the primary heart field cells (shown in red) from the cardiac crescent stage (E7.5) through to the looping stages of mouse heart development and to the final conformation of the four-chambered heart (E10.5). (B) Transverse sections of the hearts at corresponding developmental stages as in (A) are shown. The dashed lines in (A) indicate the position of the corresponding sections in (B). Secondary heart field is shown in green and primary heart field is shown in red. Cr/Ca: cranial/caudal, R/L: right/left, D/V: dorsal/ventral, DOFT: distal outflow tract, HFs: head folds, LA: left atrium, LV: left ventricle, ML: midline, PhA: pharyngeal arches, OFT: outflow tract, POFT: proximal outflow tract, RA: right atrium, RV: right ventricle (figure taken and adapted from Laugwitz et al., 2008).

In lower vertebrates the presence of a SHF is not well established. In zebrafish, a SHF has not been conclusively identified. However, two spatially and temporally distinct phases of cardiomyocyte differentiation that contribute to heart tube growth have been identified (de Pater et al., 2009, Lazic and Scott, 2011). The initial phase is characterized by a continuous wave of differentiation that starts in the ventricle, ends in the atrium and requires *isl1*. During the late phase, new cardiomyocytes are added to the arterial pole (by 36 hpf) (de Pater et al., 2009). More recently, it was shown that most of the cells of the second wave originate from the same pre-gastrula region as the cells of the first phase, suggesting a common progenitor (Lazic and Scott, 2011). The two waves of cell addition to the heart (de Pater et al., 2009, Lazic and Scott, 2011) were shown to be required for regulation and growth of the zebrafish heart (especially up to 48 hpf, when no cardiomyocyte proliferation is observed) and contribute to changes in the size and morphology of the heart. Their correlation with the presence of an additional heart field in zebrafish remains, however, elusive.

1.3.8. Heart looping and morphogenetic patterning

By 24 hpf, the zebrafish heart tube has formed in the midline, is functional and exhibits regular peristaltic contractions. Further morphogenetic movements, including looping and chamber formation, follow. Zebrafish heart looping takes place at approximately 30 hpf (Figure 1.6). This process (rightward heart looping) involves a gradual bending between the forming ventricle and atrium that creates an S-shaped structure, bringing the ventricle to lie to the right of the atrium (Chen et al., 1997, Chin et al., 2000, Glickman and Yelon, 2002). Although heart looping starts at approximately 36 hpf, its direction has been determined earlier in development, during cardiac jogging (see Section 1.3.6, page 19). The directionality of jogging is dictated by asymmetric Nodal signalling and subsequent asymmetric gene expression at the LPM (see Section 1.2.4, page 6) (Baker et al., 2008). Modifications in cell proliferation, migration, differentiation and death are, also, suggested to be involved in the jogging and looping processes (Kathiriya and Srivastava, 2000). Disturbances of the left-right asymmetry or failure to interpret left-right cues can cause reverse jogging, reverse looping, no jogging or no looping (Ahmad et al., 2004, Chin et al., 2000). Incomplete jogging or looping towards the correct direction can also be observed (Chin et al., 2000).

Similarly, the mouse and chick linear heart tubes start to elongate, beat and loop, soon after their formation in the midline. The elongation and simultaneous narrowing

take place both by expansion of the already existing tissue and addition of cells to the outflow and the inflow poles. The majority of the outflow tract is added during looping (stages 13-22 in chick, E8-E11 in mouse) and this happens by the addition of newly formed cells from the SHF (Kelly et al., 2001, Mjaatvedt et al., 2001, Waldo et al., 2001), as mentioned earlier. Abnormalities in the looping process have been associated with defective left-right patterning in the mouse as well. For example, *Pitx2*$^{-/-}$ and *Cited2*$^{-/-}$ (a transcriptional co-activator of TfAp2) embryos exhibit abnormal cardiac looping, right isomerism and hyposplenia, correlated with defective establishment of left-right identities (Bamforth et al., 2004, Gage et al., 1999, Kitamura et al., 1999, Liu et al., 2001).

1.3.9. Extra-cardiac additions to the heart

Two important extra-cardiac cell additions supplement the forming avian and mammalian heart and contribute to its proper morphogenesis: epicardially-derived cells and neural crest cells. Epicardially-derived cells arise from the epicardium, which originates from cells outside the heart. Epicardially-derived cells populate the forming myocardium (E11.5-E12.5 in mouse, stages 16-20 in chick), contributing to coronary smooth muscle cells, endothelial cells and fibroblasts and providing support and signalling cues to the developing heart (Kwee et al., 1995, Moore et al., 1999, Perez-Pomares et al., 2003). The existence of the epicardium has been confirmed in zebrafish as well, with its earliest progenitors firstly seen in the LPM (Serluca, 2008). It is thought to regulate myocardium maturation and establishment of the coronary vasculature, as in other vertebrates (Serluca, 2008).

Cardiac neural crest cells are essential for normal heart development; they provide the parasympathetic innervation to the heart (Kirby et al., 1983) and the smooth muscle tunics of the great arteries (Bockman and Kirby, 1984), they contribute to the aorticopulmonary septum, which divides the outflow tract into the systemic and the pulmonary vessels (Kirby et al., 1983) and they participate in aortic arch remodelling (Waldo et al., 1996). In zebrafish, cardiac neural crest cells have also been identified (Sato and Yost, 2003); they contribute to the myocardium of the outflow tract, atrium, atrio-ventricular junction and ventricle (Sato and Yost, 2003).

1.3.10. The mature heart

After initial morphogenetic movements and cell additions are complete in the heart, development of specialized conduction system, valve formation, ventricular wall thickening, trabeculae formation and further cardiac remodelling take place and form the mature heart (Glickman and Yelon, 2002, Hu et al., 2000, Hu et al., 2001). This, in mammals and birds, consists of a four-chambered structure through which two parallel blood circulations (pulmonary and systemic) are propelled around the body. In zebrafish, the mature heart consists of two chambers (an atrium and a ventricle) pumping in series, with no division between pulmonary and systemic circulation (Figure 1.6).

1.4. The Wnt signalling network

The Wnt pathway is an ancient and highly conserved cascade. Wnt are secreted glycoproteins, rich in cysteine and act in short-range as ligands for receptor-mediated signalling. In mammals, there are 19 members of the Wnt family, expressed in spatially restricted and dynamic patterns within the developing embryo and in adulthood (Kemp et al., 2005, Kemp et al., 2007). Therefore, it is not surprising that Wnt proteins are nowadays known to activate more than one signalling pathway. The best understood and most extensively studied of these pathways is the canonical, β-catenin-dependent, which plays crucial roles in a variety of early developmental processes such as cell proliferation and survival, cell fate specification, body axis formation and many more (thoroughly analysed in following sections, reviewed by Kemp et al., 2005, Kemp et al., 2007). However, there are two more Wnt pathways that are independent of β-catenin and are called non-canonical Wnt pathways; these are the planar cell polarity (PCP) and the calcium cascades. All of the Wnt pathways share some of their upstream components, such as Frizzled and Dishevelled, but they are activated by diverse upstream Wnt ligands and diverge downstream, eliciting different cellular responses (Figure 1.8). For example, Wnt5a and Wnt11 have been shown to act preferentially through non-canonical Wnt, while Wnt3a and Wnt8 are thought to mainly act through canonical Wnt (reviewed by Veeman et al., 2003). Divergent downstream components are further discussed in the next sections.

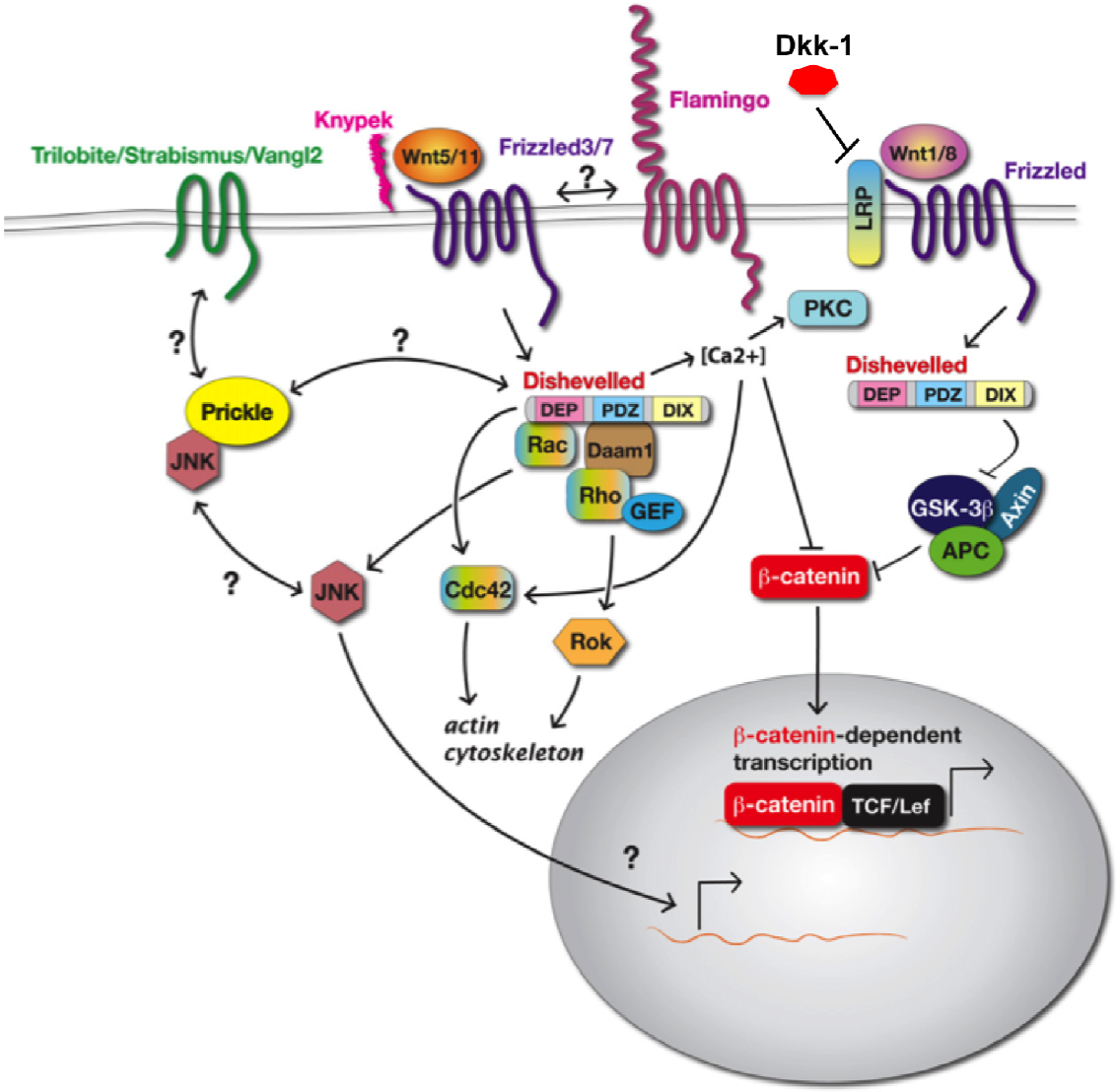

Figure 1. 8: Schematic illustration of the Wnt signalling network in vertebrates. Wnt signalling has been shown to activate multiple pathways, traditionally classified into either canonical or non-canonical. In the canonical Wnt/β-catenin pathway, binding of a Wnt ligand to Frizzled receptors activates the cytoplasmic protein Dishevelled, which in turn suppresses degradation of β-catenin. Accumulation of β-catenin in the cytoplasm and subsequent relocation into the nucleus leads to activation of downstream genes through TCF/Lef complex activation of transcription. The non-canonical Wnt/PCP pathway also involves Frizzled and Dischevelled. Upon Wnt stimulation (commonly Wnt5 and Wnt11), a multiprotein complex (Frizzled, Dishevelled, Prickle, Vangl2, Flamingo) forms in the cell membrane. Further transduction of the Wnt signal involves small GTPases of the Rho and Rac families, which activate downstream kinase effectors, like Jnk and ROCK. Although the canonical and non-canonical Wnt pathways are described in isolation, they in fact work as a network (figure taken and adapted from Roszko et al., 2009).

Interestingly, although Frizzled receptors act both in canonical and non-canonical Wnt signal transduction, different family members have been shown to be preferentially involved in each pathway, depending mainly upon their binding affinity for proteins that contain PDZ (Postsynaptic density 95, Discs Large, Zonula occludens-1) domains (Kay

and Kehoe, 2004) and upon their association with co-receptors (He et al., 1997, Mikels and Nusse, 2006). Similarly, Dishevelled proteins are known to interact with proteins of each pathway through different domains: their amino-terminal Dishevelled-Axin (DIX) domain binds to Axin and activates Wnt/β-catenin signalling (Fagotto et al., 1999, Schwarz-Romond et al., 2007a, Schwarz-Romond et al., 2007b), while their carboxyl-terminal Dishevelled/Egl-10/Pleckstrin (DEP) domain binds to other proteins, involved, among others, in transduction of non-canonical Wnt signals (Gao and Chen, 2010, Wong et al., 2000) (Figure 1.8). Details about each pathway are discussed below.

In summary, the Wnt signalling pathway consists of both shared and divergent components that form a network but also participate individually in one of the three Wnt branches (canonical Wnt, PCP and calcium pathways), dependent upon their interaction with other molecules and upon the cellular and timely context. These three pathways are individually presented below.

1.4.1. The canonical Wnt/ β-catenin pathway

The canonical Wnt cascade is the best characterized among the Wnt pathways. In the absence of a Wnt ligand, β-catenin is recruited in an inhibitory complex, containing Adenomatosus Polyposis Coli (APC) and Axin, which enables its phosphorylation by Glycogen Synthase Kinase 3 (GSK3) and its subsequent proteolytic degradation. In this case, there are low levels of nuclear β-catenin, which is the form of the protein responsible for the propagation of the signal through gene expression activation. Upon binding of a Wnt ligand to members of the Frizzled family of receptors and low-density Lipoprotein Receptor-related Protein 5/6 (LRP5/6) co-receptors, Dishevelled is activated and recruited to the membrane, which in turn leads to degradation of Axin and inhibition of GSK3. The destruction of the Axin/APC/GSK3 complex results in the release of β-catenin, its accumulation in the cytoplasm and its translocation into the nucleus, where it can now interact with T-cell factor (TCF) and lymphoid enhancer-binding factor (LEF) family members and activate target gene transcription (Figure 1.8).

1.4.1.1. The canonical Wnt pathway during embryogenesis

The canonical Wnt signalling pathway has been shown to play crucial roles during the development of vertebrate embryos. Although genes associated with canonical Wnt signalling are present very early during embryogenesis, already at blastocyst-stage

mouse embryos (Chapman et al., 2004, Eisenberg and Eisenberg, 2006, Skromne and Stern, 2001, Yamaguchi et al., 1999), there is no evidence for active β-catenin signalling during pre-implantation development (up to E5.0) (Kemler et al., 2004, Kemp et al., 2005, Lloyd et al., 2003). In fact, the first evidence of active canonical Wnt signalling is at the peri-implantation stage, where its tight regulation is essential for molecular patterning (Huelsken et al., 2000) and morphological patterning (Chazaud and Rossant, 2006) of the visceral endoderm and epiblast and for correct migration of visceral endodermal cells (Kimura-Yoshida et al., 2005). Failure to do so leads to absence of anterior-posterior polarization in pre-gastrula mouse embryos (Huelsken et al., 2000). β-catenin is also important for mesoderm induction (Gadue et al., 2006, Lindsley et al., 2006). Also, its absence is pivotal for the development of anterior-most tissues, such as anterior neural development (Glinka et al., 1998, Mukhopadhyay et al., 2001, Tam and Steiner, 1999). As the embryo develops, the Wnts are found involved in many diverse processes, such as the regulation of proliferation in the central nervous system (Takada et al., 1994), axon remodelling and guidance and the proper formation of organs, such as the kidneys and the lungs (Parr et al., 2001, Stark et al., 1994). The involvement of the Wnt/β-catenin pathway in cardiac induction, specification and differentiation is presented below.

1.4.1.2. The canonical Wnt pathway during heart development and in vitro cardiac differentiation

The role of the canonical Wnt pathway in the induction, formation and morphogenesis of the heart has been much investigated. However, its precise role remains poorly defined. Initial studies in *Drosophila* embryos showed that the formation of the dorsal vessel, a primitive form of the vertebrate heart, is dependent on expression of the Wnt-1 ortholog (Park et al., 1996). More recently, enhanced cardiac differentiation was observed after activation of β-catenin signalling during differentiation of pluripotent mouse carcinoma P19CL6 cells (Nakamura et al., 2003). However, subsequent studies in chick and frog embryos showed that Dickkopf-1 (Dkk-1) and Crescent, potent canonical Wnt inhibitors, could promote cardiogenesis in many contexts (Foley and Mercola, 2005, Marvin et al., 2001, Schneider and Mercola, 2001). Also, activation of β-catenin was shown to inhibit cardiac differentiation *in vivo* (Klaus et al., 2007) and *in vitro* (Yamashita et al., 2005). These data, in contrast to the data shown before, showed

that inhibition of canonical Wnt signalling was an absolute requirement for the development of heart tissue.

Recent work has partially resolved this discrepancy by suggesting a biphasic and stage-specific role for the canonical Wnt/β-catenin signalling during cardiogenesis in differentiating mouse ES cells and during zebrafish development (Kwon et al., 2007, Naito et al., 2006, Ueno et al., 2007). It was shown that activation of the canonical Wnt pathway during *in vitro* ES cell differentiation (Naito et al., 2006, Ueno et al., 2007) and during early stages (before gastrulation) of zebrafish development (Ueno et al., 2007) promoted cardiogenesis, while later activation (after cardiac specification had taken place) had negative effects on cardiac differentiation (Kwon et al., 2007, Naito et al., 2006, Ueno et al., 2007). It is, thus, possible that early activation of β-catenin is essential for mesoderm specification (Gadue et al., 2006, Lindsley et al., 2006, Naito et al., 2006) and for the development and proliferative expansion of cardiac progenitors (Kwon et al., 2007, Ueno et al., 2007), while during later differentiation it has negative effects on cardiogenesis and sets the boundaries of the heart-forming field (Naito et al., 2006, Ueno et al., 2007). The early cardiogenic effect has been suggested to be a result of direct exposure to a high concentration of Wnt ligands in the primitive streak, which promote cardiac cell fate decisions (Kwon et al., 2007, Naito et al., 2006, Ueno et al., 2007). Subsequent migration of committed cells into the heart-forming region through gastrulation movements exposes them to Wnt inhibitors, which is essential for their maturation (Figure 1.4) (Naito et al., 2006, Ueno et al., 2007).

Although there is a lot of evidence to support the model presented above (early canonical Wnt promoting cardiogenesis and late canonical Wnt inhibiting it), two recent publications reinforced the traditional notion that β-catenin is inhibitory for cardiogenesis (Afouda et al., 2008, Wang et al., 2011). Afouda and colleagues (2008) showed that activation of the canonical Wnt pathway caused suppression of cardiogenesis, mediated by inhibition of *Gata-4*, in Xenopus explants (Afouda et al., 2008). In turn, Wang and colleagues (2011) used two mouse ES cell lines to show that timely (and throughout differentiation) administration of Dkk-1 (an antagonist of canonical Wnt) (Kawano and Kypta, 2003, Mao et al., 2001) and XAV939 (a small molecule inhibitor of Wnt/β-catenin) (Huang et al., 2009) induced cardiomyogenesis (Wang et al., 2011).

Of note, progenitors of the SHF have been shown to require Wnt/β-catenin signalling for their expansion (Ai et al., 2007, Cohen et al., 2007) This needs to take place at a time when PHF cells have already been specified and require suppression of

canonical Wnt signals for full differentiation and maturation. β-catenin was shown to downregulate *Isl1 in vivo* and *in vitro* and this decrease in *Isl1* expression was believed to be essential for β-catenin-mediated expansion of cardiovascular progenitors (Kwon et al., 2009). In *Isl1* knockdown ES cells, the appearance of beating foci was severely compromised as was the expression of cardiac sarcomeric genes (Kwon et al., 2009).

In summary, it is evident that the spatio-temporal coordination and complex regulation of cardiac induction, specification and differentiation is of primary importance. The data presented above, also, highlight the fact that although a lot of studies have focused on elucidating the canonical Wnt contribution in cardiogenesis, the conflict about when and how this pathway acts remains unresolved.

1.4.1.3. The canonical Wnt pathway in embryonic stem (ES) cell differentiation

Wnt proteins play important roles in stem cell biology, reflecting their roles in embryonic development (see above), such as mesoderm differentiation (Gadue et al., 2006, Lindsley et al., 2006, Wawrzak et al., 2007) and cardiac inhibition (Foley and Mercola, 2005, Marvin et al., 2001, Schneider and Mercola, 2001). Also, there is increasing evidence to suggest that the canonical Wnt pathway can contribute to the maintenance of mouse and human stem cells in their undifferentiated, pluripotent state, either independently of, or in conjunction with, LIF (discussed further in Section 1.6.1.1, page 45) (Cartwright et al., 2005, Dravid et al., 2005, Miyabayashi et al., 2007, Ogawa et al., 2006, Sato et al., 2004, Singla et al., 2006, Takao et al., 2007). Whether this pathway is absolutely necessary for stem cell pluripotency, or whether it acts redundantly with other signalling pathways, remains to be elucidated (Dravid et al., 2005, Huelsken et al., 2000).

1.4.1.4. Canonical Wnt pathway; a summary

The canonical Wnt pathway, one of the earliest signalling cascades established in embryogenesis, is involved in a variety of developmental processes, like mesoderm induction, body axis determination and cardiogenesis. However, its role in heart induction and development, although heavily investigated, remains poorly defined and highly contradictory.

1.4.2. The non-canonical Wnt/Planar cell polarity (PCP) pathway

Another branch of the Wnt signalling network is the non-canonical Wnt/PCP pathway. It has traditionally been thought to be involved in polarization of tissues, hence the name, as firstly shown in Drosophila and later in vertebrates (reviewed by Simons and Mlodzik, 2008, Wang and Nathans, 2007). Until recently in the literature, there was a common belief that the main genes, known to be involved in PCP, acted in a single pathway. Briefly, this pathway was thought to consist of an upper level of proteins, including Fat (Ft), Dachsous (Ds) and Four-jointed (Fj), which interpret the direction of body axis polarization and transmit patterning information to the lower level group (or core group) (Ma et al., 2003, Seifert and Mlodzik, 2007, Yang et al., 2002). The core group comprises the non-canonical Wnt proteins Frizzled, Dishevelled, Prickle, Vang Gogh-strabismus (Vang), Diego and Flamingo-Starry night (Fmi), in Drosophila. These proteins, through elaborate interactions and asymmetric localization within the cells, establish cell polarization and amplify the polarization signal within the tissue, through downstream effectors, such as RhoA, Rac, Rho-associated kinase (ROCK) and JNK (Ma et al., 2003, Seifert and Mlodzik, 2007, Strutt and Strutt, 2009, Yang et al., 2002). However, a new idea has recently emerged. There is evidence to suggest that the Ft/Ds/Fj pathway (involved in tissue polarization) is in fact a parallel system to the core Wnt group and that Wnt ligands, at least in flies, may not be necessary for its activation (reviewed by Casal et al., 2006, Goodrich and Strutt, 2011, Henderson and Chaudhry, 2011, Lawrence et al., 2007). In vertebrates, this scenario has not been elucidated. An overview of the so-called core Wnt/PCP group follows.

The PCP pathway is β-catenin-independent but still involves Frizzled receptors and Dishevelled proteins. The main ligands that trigger this pathway are Wnt5a and Wnt11. Upon Wnt stimulation, a multiprotein complex containing Frizzled, Dishevelled, Prickle, Vangl2, Celsr and Diego is formed at the cell membrane. Activation of Dishevelled through recruitment of this complex leads to Dishevelled-associated activator of morphogenesis-1 (Daam-1)-mediated interaction of Dishevelled with small GTPases of the Rho family (Figure 1.8). These further activate downstream kinase effectors, such as JNK and ROCK that bring about changes in the actin cytoskeleton and regulate migration, adhesion, elongation and polarity of the cell as well as gene transcription (reviewed by Barrow, 2006). Upon activation within a Dishevelled-Daam1-Rho complex, Rho stimulates the activity of ROCK, which along with Cdc42, participates in remodelling of the actin cytoskeleton (Ishizaki et al., 1997,

Leung et al., 1996, Marlow et al., 2002, Winter et al., 2001). Rac acts independently of Daam1 but also binds to Dishevelled and activates JNK (Boutros et al., 1998). In Drosophila and in cultured cells, JNK was shown to act downstream of Dishevelled and to mediate the PCP pathway (Boutros et al., 1998, Davis, 2000). In Drosophila, the JNK ortholog basket has been suggested to be involved in regulation of transcription of target genes during eye morphogenesis (Fanto et al., 2000, Weber et al., 2000). In Xenopus embryos, JNK was shown to be activated upon Wnt5a stimulation, to transduce the PCP signal and to mediate CE movement regulation (Yamanaka et al., 2002). JNK, although a downstream effector of the PCP pathway, has also been shown to activate transcription of Wnt11, one of the upstream ligands of the pathway in zebrafish (Seo et al., 2010). Of note, PCP effectors, often cell- or tissue- specific, exert their intracellular activities in response to PCP signals but cannot in turn affect the polarized localization of upstream PCP proteins (reviewed by Goodrich and Strutt, 2011).

Overall, the PCP pathway is most commonly related to tissue polarization in *Drosophila*, but it has also been shown to play fundamental roles in a variety of morphogenetic processes in vertebrates that require coordination of cell polarity, cell motility and cell cohesion. More recently, PCP was also associated with human disease (reviewed by Roszko et al., 2009, Simons and Mlodzik, 2008).

1.4.2.1. The non-canonical Wnt/PCP pathway during embryogenesis and convergence extension (CE)

Non-canonical Wnt/PCP signalling was initially described as an important regulator of the coordinated polarization of cells within the plane of an epithelium, as well as polarized cell behaviour and cell shape. In *Drosophila*, where the identification of the core PCP proteins was achieved, this form of polarity is involved in the organization of the wing hairs and the ommatidia of the compound eye (Baena-Lopez et al., 2005, Matakatsu and Blair, 2004, Strutt, 2001), while in vertebrates it is mainly associated with inner ear cell organization (Curtin et al., 2003, Montcouquiol et al., 2003, Wang et al., 2006), hair follicle orientation (Guo et al., 2004), CE movements during gastrulation (Barrow, 2006, Heisenberg et al., 2000, Roszko et al., 2009, Wallingford et al., 2002) and neural tube closure defects (Ciruna et al., 2006, Murdoch et al., 2003). Less well described but widely accepted are the roles of PCP during vertebrate neuronal migration (Ciruna et al., 2006, Wada and Okamoto, 2009), ciliogenesis (Ross et al., 2005) and heart development (Eisenberg and Eisenberg, 1999, Garriock et al., 2005, Hamblet et

al., 2002, Henderson et al., 2001, Montcouquiol et al., 2003, Pandur et al., 2002, Phillips et al., 2008, Phillips et al., 2007, Torban et al., 2004).

The regulation of CE during gastrulation is of most interest here, while the role of the PCP pathway in heart development is discussed in the next section. Gastrulation in vertebrates requires the coordinated migration of large amounts of cells around the forming body in order to establish the embryonic germ layers. CE movements are responsible for the narrowing of a tissue along one axis and its concomitant lengthening in the perpendicular axis, during which the body plan is defined. They have been extensively studied in frog and fish embryos, where movements of cells are easy to follow (Figure 1.2). The Wnt/PCP pathway is a key regulator of CE movements, as shown among others, in zebrafish embryos that carry mutations in PCP components. Trilobite, *vangl2* mutant (Jessen et al., 2002), knypek, *glypican-4* mutant (Topczewski et al., 2001), silberblick, *wnt11* mutant (Heisenberg et al., 2000) and pipetail, *wnta5/5b* mutant (Kilian et al., 2003, Rauch et al., 1997) embryos exhibit defective CE movements during gastrulation that result in shortened (in the anterior-posterior axis) and wider (in the medial-lateral axis) bodies. Intracellular mediators of the non-canonical Wnt pathway, such as rhoA, cdc42 and jnk, have also been shown to be important for regulation of CE movements in zebrafish and Xenopus embryos (Bakkers et al., 2004, Habas et al., 2003, Matsui et al., 2005, Yamanaka et al., 2002). Similarly, in mammals, mutations in PCP components impair CE during gastrulation and neurulation. *Vangl2*/Loop-tail (Kibar et al., 2001, Torban et al., 2004), *Scribble*/Circle-tail (Murdoch et al., 2003), *Celsr-Flamingo* (Curtin et al., 2003), *Dishevelled* (Hamblet et al., 2002) and *Sfrp* (Wnt antagonists that deregulate PCP signalling) (Satoh et al., 2008) mouse mutants display body shortening, notochord and somite widening and neurulation defects.

1.4.2.2. The non-canonical Wnt/PCP pathway during heart development and in vitro cardiogenesis

The non-canonical Wnt/PCP pathway has been shown to be an important player during cardiogenesis in several animal models. In quail embryos Wnt11, an upstream activator of the PCP cascade, was shown to promote ectopic formation of cardiomyocytes (Eisenberg and Eisenberg, 1999, Eisenberg et al., 1997) and in *Xenopus* explants it was shown to induce myocardial gene expression and to trigger contractile activity (Garriock et al., 2005, Pandur et al., 2002). Similarly, it has been shown to enhance

cardiogenesis *in vitro*: it increases the number of *Nkx2.5* positive cells in mouse ES cells (Terami et al., 2004), it promotes cardiomyocyte formation in P19 cells (Pandur et al., 2002) and it activates cardiac gene expression in mouse mesenchymal stem cells (Schulze et al., 2005) and bone marrow stem cells (Belema Bedada et al., 2005).

Disruption of downstream PCP components has also been shown to cause cardiac abnormalities. Severe heart malformations have been reported in *Dishevelled* (Hamblet et al., 2002), *Vangl2* (Henderson et al., 2001) and *Scribble* (Phillips et al., 2007) mouse mutants, mainly associated with cardiomyocyte organization, cardiac looping, aortic arch remodelling and outflow tract patterning. Also, ROCK-inhibited mouse and chick embryos were shown to exhibit cardia bifida (Wei et al., 2001). Similarly, in zebrafish embryos, selective deletion or downregulation of PCP members caused anomalies in the progression of cardiac morphogenesis. Zebrafish embryos expressing a dominant negative form of dishevelled (DvlΔDEP, specifically affecting the PCP pathway) or a combination of morpholinos against *wnt4a, wnt11* and *wnt11-R* (another *wnt11* gene) exhibited cardia bifida, along with CE defects, described before (Matsui et al., 2005).

1.4.2.3. The non-canonical Wnt/PCP pathway; a summary

The non-canonical Wnt pathway has, for years, been associated with planar cell polarization, but recent evidence suggests that the link between the two is not universal. In some contexts, however, it has been confirmed to be involved in polarization of tissues and coordination of directional cell migration; Drosophila wing hair and ommatidia polarization, mouse inner ear polarization and CE are among the most heavily investigated and best understood contributions of Wnt/PCP during embryonic development. Its involvement in heart induction and morphogenesis is also well established.

1.4.3. The non-canonical Wnt/Calcium pathway

The Wnt/calcium pathway is also stimulated by non-canonical Wnt ligands and Frizzled receptors and triggers the release of intracellular calcium and the activation of calcium-responsive enzymes like Protein kinase C (PKC), Calcium/calmodulin-dependent protein kinase II (CaMKII) and Calcineurin (Kuhl et al., 2000, Saneyoshi et al., 2002). Intracellular calcium release is mainly mediated through activation of the phosphatidylinositol (PI) cascade, which acts via a PI-specific phospholipase C

(Slusarski and Pelegri, 2007). This, in turn, hydrolyses phosphatidylinositol (4,5) bisphosphate (PIP_2) at the cell membrane and generates diacylglycerol (DAG) and inositol 1,4,5-trisphosphate (IP_3). Finally, IP3 stimulates release of calcium into the cytosol (Westfall et al. 2003). The role of the Wnt/calcium pathway in promoting ventral cell fate in *Xenopus*, in regulating gastrulation movements and orchestrating heart development has been well studied (Kuhl et al., 2000, Pandur et al., 2002) but will not be analysed further here.

1.4.4. Cross talk between the Wnt branches

The three branches of the Wnt pathway are usually described and studied independently. However, Wnt proteins are now thought to activate a complex signalling network within the cell, rather than individual pathways (Figure 1.8). The specific outcome of the activation of this network is time- and context- dependent. This idea is strongly supported by a series of evidence in the literature that show clear cross talk between the different Wnt branches.

Firstly, upstream Wnt components (ligands, receptors and co-receptors), although shown to preferentially act through either the canonical or non-canonical Wnt pathway (see beginning of this section), can in fact, under different conditions, participate in both pathways. For example, Wnt-11, which is a generally considered non-canonical Wnt ligand, was suggested to have the ability to repress the canonical Wnt pathway in carcinoma P19 cells (Maye et al., 2004). Similarly, Dkk-1, a common antagonist of the canonical Wnt pathway that acts through binding to and inactivating the LRP6 co-receptor (Davidson et al., 2005, Tamai et al., 2000, Zeng et al., 2005), was recently shown to activate the PCP pathway and regulate CE movements in zebrafish (Caneparo et al., 2007).

Downstream Wnt components and effectors have also been shown to allow considerable cross talk between the canonical and non-canonical pathways. For example, Rac-1, a downstream effector of the PCP pathway, has been suggested to participate in β-catenin signalling and to activate TCF, through JNK (Esufali and Bapat, 2004, Wu et al., 2008). Inhibition of JNK in this context decreased Lef-1 luciferase expression and inhibited nuclear accumulation of β-catenin (Wu et al., 2008). An important link between JNK and β-catenin has also been established. Inhibition of jnk signalling in Xenopus embryos was shown to induce β-catenin target gene expression, through a GSK3-independent mechanism (Liao et al., 2006). These effects were

associated with hyperdorsalization of the embryonic body and increased levels of nuclear and non membrane-bound β-catenin. Similarly, Jnk was shown to inhibit β-catenin-mediated gene transcription in mammalian cells and to favour export of β-catenin from the nucleus (Liao et al., 2006). In contrast, activation of Jnk suppressed transcription of β-catenin target genes and blocked β-catenin–induced axis duplication (Liao et al., 2006).

The list of examples that highlight the complex interactions governing the Wnt network is long and only a few of them are presented here. It is, however, evident that the combination of various ligands and intracellular components differentially orchestrates the Wnt signalling network depending on the cell type, the timing and the input from surrounding signalling centres (reviewed by Kestler and Kuhl, 2008). Therefore, the distinction between Wnt pathways is an arbitrary, albeit sometimes useful, convention and not a representation of the reality within the cell.

1.5. JNK signalling

JNK is a member of the evolutionarily conserved family of Mitogen-activated protein kinases (MAPK). As part of this family, JNK amplifies and integrates signals from a wide range of stimuli, giving rise to varied cellular responses (Figure 1.9). As mentioned before, JNK is also an important downstream member of the non-canonical Wnt signalling pathway, shown to be essential for PCP signal propagation (Boutros et al., 1998, Habas et al., 2003, Yamanaka et al., 2002).

The importance of JNK during development (Boutros et al., 1998, Davis, 2000, Fanto et al., 2000, Seo et al., 2010, Yamanaka et al., 2002) and in adulthood (reviewed by Bogoyevitch, 2006, Rose et al., 2010, Bogoyevitch and Kobe, 2006) has been known for years in both vertebrates and invertebrates. It is known to play crucial roles in regulating embryogenesis, proliferation, apoptosis, differentiation, gastrulation movements, CE and tissue polarization in vertebrates (Bogoyevitch and Kobe, 2006, Krens et al., 2008, Yamanaka et al., 2002). Also, its function during cardiac development and at many stages of heart disease progression is widely recognized (reviewed by Bogoyevitch and Kobe, 2006, Rose et al., 2010).

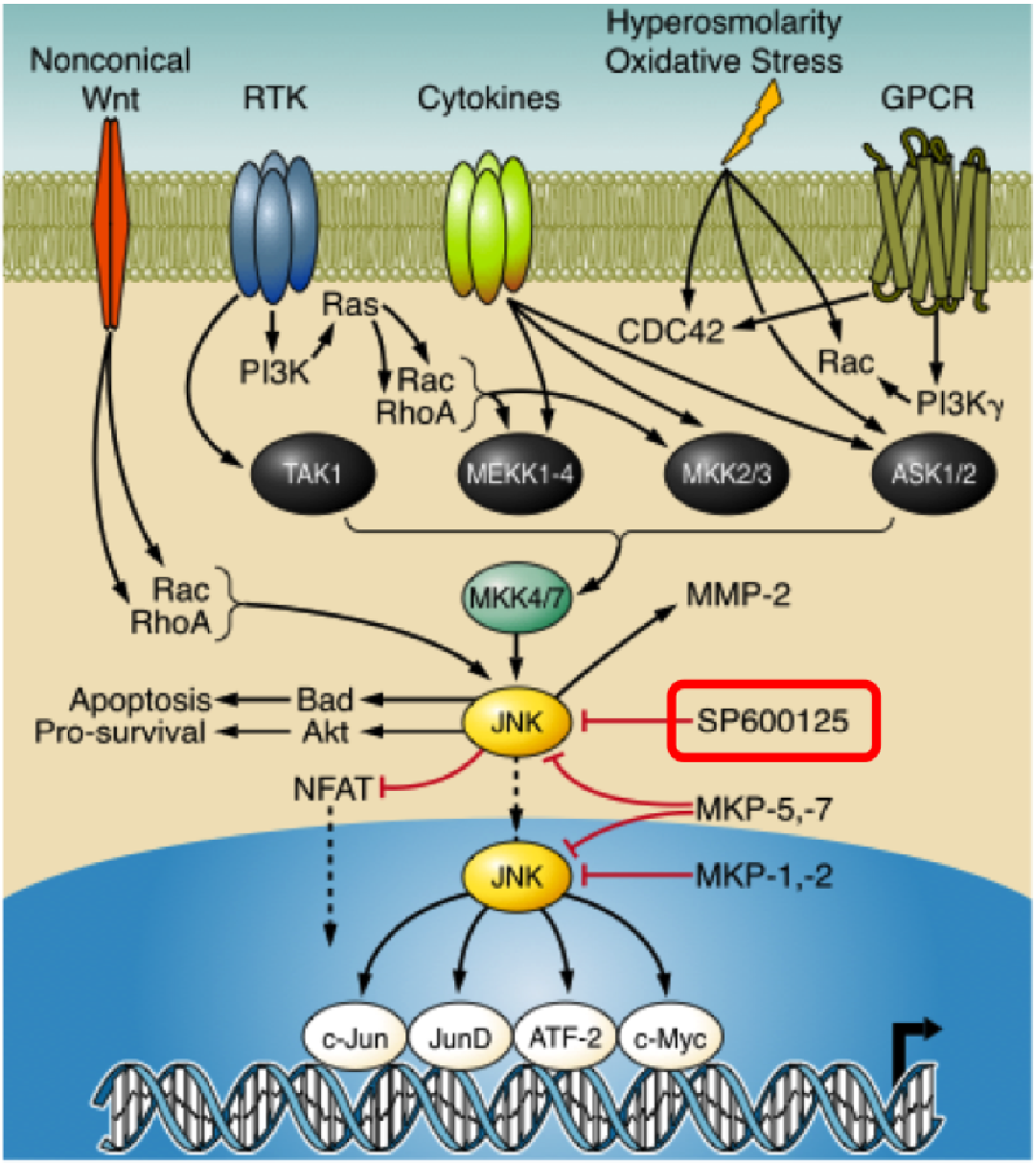

Figure 1. 9: MAPK and JNK signalling. Activation of JNK occurs in response to a number of different stimuli: cellular stresses (heat shock, hyperosmolarity etc), growth factors, G protein-coupled receptors and non-canonical Wnt signals. Upon stimulation JNK can become activated through phosphorylation by upstream kinases. Activated JNK has a vast array of downstream substrates, both cytoplasmic and nuclear. Depending on the stimulus, JNK has the ability to move between cytoplasm and nucleus to exert its effects. Not all connections represent direct interactions, but rather the end product of multiple steps, not all of which are defined. SP600125, a pharmacological inhibitor of JNK, further discussed in Chapter 4, is highlighted in a red box. GPCR: G-protein coupled receptor, RTK: receptor tyrosine kinase, MKP: MAPK phosphatase (Figure taken and adapted from Rose et al., 2010).

1.5.1. An overview of JNK signalling

JNK is a component of both the non-canonical Wnt/PCP and the MAPK pathways and is involved in crucial cellular processes associated with both these cascades. Members of the MAPK family are present in almost all eukaryotic organisms, including animals, fungi and plants, where they form complex signalling networks. MAPK are organized and act in a sequential manner: the top-most kinases called MAPK kinase kinases (MAPKKK, also known as MEKK) phosphorylate MAPK kinases (MAPKK, also called MAPK/Extracellular-signal-regulated kinases, ERK or MEK) that in turn phosphorylate MAPK. Finally, activated MAPK phosphorylate downstream targets, such as transcription factors (including c-Jun, AP-1, NFAT, c-Myc) and other proteins (including apoptosis-related proteins). The deactivation of these kinases occurs via dephosphorylation by specialised phosphatases.

JNK belong to the most downstream kinases of the cascade described above. They are mainly activated by cytokines and exposure to environmental stress, hence they are also known as Stress-Activated Protein Kinase or SAPK. Upon stimulation, they phosphorylate and either activate or inhibit downstream targets. A variety of molecules have been identified as phosphorylation targets of JNK, residing in the nucleus, the mitochondria or in other parts of the cell, revealing the vast range of processes these kinases are involved in. Their most recognized and firstly identified target is the transcription factor c-Jun (Derijard et al., 1994), but a variety of transcription factors, such as ATF-2 (Gupta et al., 1995), AP-1, Elk-1 (Yang et al., 1998), NFAT (Chow et al., 1997) and p53 (Das et al., 2007), populate the list of JNK targets. Additional and equally important targets of JNK are mitochondria-associated proteins, such as Bim-related members of the Bcl2 family, which through JNK activation lead to Bax-dependent apoptosis (Lei and Davis, 2003).

1.5.2. Jnk genes

Jnk orthologs have been identified in a variety of organisms and an astonishing evolutionary conservation is observed between different species. In *Drosophila* one single *jnk* gene has been identified, called *basket*, shown to be important for dorsal and thorax closure during mid-embryogenesis (Stronach and Perrimon, 1999). However, in other multicellular organisms, more than one *jnk* genes have been identified (see below).

In mammals there are three *Jnk* genes, *Jnk-1*, *Jnk-2* and *Jnk-3* (also known as *mapk8*, *mapk9* and *mapk10*, respectively), located on different chromosomes, which through alternative splicing encode at least ten different protein isoforms. Mouse *Jnk1* and *Jnk2* are ubiquitously expressed, while *Jnk3* is predominantly expressed in the brain and to a lesser extent in the testes and the heart (Martin et al., 1996, Mohit et al., 1995). Although the precise differences between the isoforms are not clearly defined, it is known that they differentially recognize, bind and phosphorylate their downstream effectors (Bogoyevitch et al., 2004, Gupta et al., 1996). For example, Jnk1 was found to selectively interact with Jamp (Kadoya et al., 2005), while Jnk3, but not Jnk1 or Jnk2, was found to bind to β-arrestin 2 (McDonald et al., 2000).

Zebrafish *jnk* genes have not been extensively studied. The first attempt to identify zebrafish orthologs revealed a single *jnk1* isoform that showed 87%, 77% and 80% identity to human, mouse and rat *Jnk1*, respectively, and 71% identity to human, mouse and rat *Jnk2* orthologs (Krens et al., 2006). Zebrafish *jnk1* was shown to be weakly expressed in early developmental stages, highly expressed from late gastrula stages to segmentation (10-24 hpf) and after a significant decrease between days 1 and 5, its expression reached highest levels in adulthood. Expression of *jnk1* at 24 hpf was localized in the brain. At 48 hpf its expression pattern became more defined and was found in the telencephalon, the cerebellum, the hindbrain, the hypothalamus, the pectoral fins and the presumptive gut (Krens et al., 2006). Recently, four *jnk* isoforms were reported: *jnk1a-1, jnk1a-2, jnk2* and *jnk3*, closely resembling their three mammalian orthologs (Seo et al., 2010).

The high conservation of JNK and its varied cellular targets and activators highlight the complexity and diversity of JNK signalling, even in simple organisms, and emphasizes its importance in biological processes in diverse eukaryotic species.

1.5.3. Mouse Jnk genes during development

In mammalian systems, the study of *Jnk* has been more intensive. *Jnk1* and *Jnk2* were initially thought to have redundant roles; however, it has recently been shown that they activate different substrates and thus participate in distinct cellular responses (reviewed by Bogoyevitch, 2006). For example, activation of Itch by Jnk1 caused excessive apoptotic death (Gao et al., 2004), while Jnk2 was shown to activate Tau (a microtubule-associated protein), not regulated by Jnk1 (Yoshida et al., 2004). All three genes (*Jnk1, Jnk2* and *Jnk3*) have been studied in transgenic mouse models by selective

disruption or deletion. Single *Jnk* mutant mice (*Jnk1*$^{-/-}$, *Jnk2*$^{-/-}$ or *Jnk3*$^{-/-}$) are born normally and thus, allow for a close examination of the defects that arise from deletion of each gene. However, putative redundancy effects between the highly similar *Jnk* genes and their products cannot be overlooked in these cases. Double mutants between *Jnk1* or *Jnk2* and *Jnk3* (*Jnk1*$^{-/-}$;*Jnk3*$^{-/-}$ and *Jnk2*$^{-/-}$;*Jnk3*$^{-/-}$) are also viable until birth and develop fairly normally (Aouadi et al., 2006, Gerits et al., 2007). In contrast, *Jnk1* and *Jnk2* double mutants (*Jnk1*$^{-/-}$;*Jnk2*$^{-/-}$) die early in gestation (E11-E12) due to abnormal levels of apoptosis in the brain (Kuan et al., 1999).

Selective disruption and targeted deletion of upstream activators and downstream targets of JNK have also been performed but their contribution to our understanding of JNK signalling has been limited (Derijard et al., 1994, Gerits et al., 2007). This is mainly due to the fact that JNK is not uniquely activated by one molecule and does not act on a single substrate. By the studies presented above, it becomes clear that JNK-regulated events cover a broad spectrum of conserved cellular and morphogenetic processes and although the potential for therapeutic applications is evident, the potential for unwanted side effects cannot be disregarded. A description of the phenotypes seen after deletion of each mouse *Jnk* gene or combinations of *Jnk* genes follows.

1.5.3.1. Jnk1 and Jnk2

Jnk1 and *Jnk2* have been shown to have essential roles in regulating and modulating the function of immune cells by mediating alternative T-cell lineages. Specifically, loss of either gene causes aberrant T-cell activation and proliferation and defective differentiation (Dong et al., 1998, Resnick and Fennell, 2004, Sabapathy et al., 1999, Yang et al., 1998). Increased levels of cell death in the forebrain and decreased levels in the lateral areas of the hindbrain in developing mouse *Jnk1*$^{-/-}$;*Jnk2*$^{-/-}$ mutant embryos (the reason for their *in utero* death) revealed the involvement of these two genes in regulation of apoptosis levels in the developing brain (Kuan et al., 1999). Recently, distinct roles for *Jnk1* and *Jnk2* have also been demonstrated. *Jnk1*$^{-/-}$ mice show microtubule assembly defects (Chang et al., 2003), activation of neovascularization by thrombospondin-1 (Jimenez et al., 2001), protection against obesity-induced insulin resistance (Hirosumi et al., 2002) and deregulation of intestinal homeostasis accompanied by spontaneous tumour formation (Tong et al., 2007). Only a small number of studies on *Jnk2*$^{-/-}$ mice are available to date. These have shown that Jnk2

mediates inflammatory and innate immune responses by inducing interferon and activating gene expression (Chu et al., 1999, Han et al., 2002).

The study of combined deletions of *Jnk1* and *Jnk2* has not been possible, as described before, due to embryonic lethality of compound mutants (*Jnk1*$^{-/-}$;*Jnk2*$^{-/-}$) (Kuan et al., 1999). Studies, in which at least one of the wild type alleles was retained, have allowed a deeper understanding of the combined roles of these two genes in mammals. *Jnk1*$^{-/-}$; *Jnk2*$^{+/-}$ mice revealed that Jnk proteins are essential for optic fissure closure (Weston et al., 2003). Mouse mutants with only one *Jnk1* allele (*Jnk1*$^{+/-}$;*Jnk2*$^{-/-}$) showed reduced obesity-induced insulin resistance and lower inflammatory cytokines (Tuncman et al., 2006). Overall, both *Jnk1* and *Jnk2* were shown to be important in the regulation of lipid and glucose metabolism in the whole organism, with each one involved in distinct processes; for example, *Jnk1* is suggested to be mainly involved in type II diabetes, while *Jnk2* in type I diabetes (Aouadi et al., 2006, Gerits et al., 2007, Jaeschke et al., 2005).

1.5.3.2. Jnk3

Loss of *Jnk3* has not been associated with an obvious abnormal phenotype. However, *Jnk3*$^{-/-}$ mice are shown to be protected from glutamate- and kainic acid-induced neurotoxicity that is commonly associated with elevated and/or sustained levels of activated Ap-1 and c-Jun (Aouadi et al., 2006, Yang et al., 1997). This finding made *Jnk3* an interesting potential target for the treatment of diseases such as stroke, Parkinson's or Alzheimer's disease, in which neuronal death is to be prevented (reviewed by Bogoyevitch et al., 2004).

1.5.4. Zebrafish jnk genes during embryonic development

The four newly identified *jnk* genes in zebrafish (Seo et al., 2010) were studied during gastrulation only (5.25-10 hpf) and were assessed on their ability to control and guide normal gastrulation. It was shown that during gastrulation *jnk1a-1, jnk1a-2* and *jnk2* were present, but it was mainly the expression and activity of *Jnk2* that was important for controlling convergence and extension (CE) movements, as shown by morpholino injections. However, a more detailed analysis of the temporal and spatial expression pattern of the genes, as well as a more in depth investigation of their potential roles during zebrafish development were not carried out.

Surprisingly, although zebrafish *jnk* genes and the corresponding proteins have not been examined in detail, a considerable number of publications that have used chemical inhibitors or morpholino injections against *jnk* are available. Rui and colleagues (2007) showed that jnk has a dorsalizing activity during zebrafish development and body axis formation (Rui et al., 2007) and Schwarz-Romond and colleagues (2002) suggested that either activation or inhibition of jnk leads to disturbed gastrulation movements (Schwarz-Romond et al., 2002), an idea supported by a more recent publication that showed body axis shortening and defective CE movements after jnk inhibition (Matsui et al., 2005). It has also been shown that inactivation of jnk can cause macrophage migration defects (Zhang et al., 2008), microcephaly and micropthalmia (Matsui et al., 2005).

1.5.5. JNK in embryonic stem (ES) cell culture and differentiation

The role of JNK has been studied in stem cell culture as well, either by using mouse ES cells isolated from *Jnk* knockout mice or by chemically inhibiting the proteins of interest. ES cells deficient for either *Jnk1* or *Jnk2* showed defective endoderm differentiation (Binetruy et al., 2007). Additionally, although Jnk was shown to be dispensable for renewal and proliferation of ES cells, it was shown to be involved in their differentiation. Defective cavitation (absence of cavity formation in differentiating embryoid bodies) has been associated in the past with abnormal differentiation (Hernandez-Garcia et al., 2008), suggesting a putative role for Jnk in cavity formation and differentiation progression. Also, cell proliferation seems to be defective in the absence of both *Jnk1* and *Jnk2*, while apoptosis levels are not significantly affected (Xu and Davis, 2010). *Jnk* deficiency was also shown to cause severe defects in mesodermal and mild defects in endodermal and ectodermal development *in vitro* (Xu and Davis, 2010). Interestingly, absence of *Jnk1*, but not *Jnk2* or *Jnk3*, in differentiating ES cell culture caused enhanced epithelial differentiation, marked by increased E-cadherin, in the expense of neurogenesis. It was shown that this shift in cell fate was accompanied by markedly increased expression of Wnt4, Wnt6 and Bmp4 (Amura et al., 2005), known players in lineage commitment during ES cell differentiation (Aubert et al., 2002, Munoz-Sanjuan and Brivanlou, 2002).

1.5.6. JNK in heart disease

Members of the MAPK cascade and the Wnt pathway (Section 1.4) have been shown to be important players in cardiac development, physiology and disease. The role of JNK in the heart, related mainly to hypertrophy, regulation of cell death and remodelling has been an area of great interest and intense controversy (reviewed in (Rose et al., 2010). It was initially shown that upon infection of cultured neonatal rat cardiac myocytes with vectors expressing a constitutively active form of MKK7 (upstream regulator of JNK), hypertrophy and cellular pathology developed: cell size was increased, expression of ANF was upregulated and sarcomere organization was disturbed (Wang et al., 1998). Subsequent *in vivo* experiments in adult mice, deficient for MEKK1 (another upstream activator of JNK), did not confirm this finding (Liang and Molkentin, 2003, Sadoshima et al., 2002). Conversely, adenovirus-mediated gene transfer of MKK4 (upstream regulator of JNK) in the adult rat heart caused loss of function of *Jnk* and blocked hypertrophy *in vivo* (Choukroun et al., 1999, Minamino et al., 2002). However, genetic inactivation of individual *Jnk* genes, combinations of them (Tachibana et al., 2006) or of individual downstream targets (Hilfiker-Kleiner et al., 2006, Liang and Molkentin, 2003, Shao et al., 2006) did not have the same effect.

Similarly, controversial roles for JNK have been reported in cardiomyocyte death regulation: JNK activity has been shown to play an important role in cardiac myocyte apoptosis after ischemia/reperfusion (Ferrandi et al., 2004, Hreniuk et al., 2001) and in cardiac myocyte survival and cardioprotection (Andreka et al., 2001, Dougherty et al., 2002, Kyoi et al., 2006, Sadoshima et al., 2002, Shao et al., 2006) Additionally, constitutive Jnk activation, by a Cre/loxP-mediated gene switch for targeted expression of an upstream activator of Jnk (MKK7D), in mouse ventricular myocytes caused contractile dysfunction, induction of the fetal gene programme and premature death (7 weeks after birth) with signs of heart failure (Petrich et al., 2004).

A connection between the structure of the cardiac cell gap junctions and JNK has also been established. Adenovirus-mediated activation of MKK7 in cultured myocytes caused prolonged activation of *Jnk* and was reported to cause reduction in Connexin-43 (Cx43) expression at both the mRNA and protein levels and impaired cell communication (Petrich et al., 2002). Similarly, using a Cre/loxP system for activation of MKK7 and thus Jnk in the myocardium of mouse embryos, downregulation of Cx43, loss of gap junctions and slowed conduction velocity in the heart were observed (Petrich et al., 2002, Ursitti et al., 2007).

Although significant progress has been made in understanding and unravelling the role of MAPK and JNK, in particular, in the heart, basic questions about the functional roles of these kinases in the regulation of major events during heart development and disease remain unanswered. Discovering additional interacting partners and their intricate contribution to MAPK signalling, and dissecting primary and secondary effects of their activity, will greatly improve our knowledge and will provide useful insight into potential therapeutic or preventative approaches.

1.5.7. JNK signalling; a summary

JNK is a kinase, member of the MAPK family and a downstream effector of the non-canonical Wnt/PCP pathway. Three *Jnk* genes have been identified in mammals and four in zebrafish. Their presence has been confirmed in early developmental stages and throughout embryogenesis. JNK is a pleiotropic molecule; it is regulated by a multitude of signals and, in turn, regulates the activity of a variety of downstream targets. Proliferation, cell death, migration and differentiation are only a few of the processes to which JNK has been shown to contribute. Its involvement in heart disease is well reported, although highly controversial. In contrast, its contribution to induction and differentiation of the embryonic heart remains elusive and is mainly correlated with the PCP pathway.

1.6. Experimental models of embryonic development

Embryonic development comprises an array of processes, from cell proliferation, migration and differentiation to tissue interactions and morphogenetic patterning. Popular models for studying these events are the mouse, chick, zebrafish and frog embryos for *in vivo* analyses and cell culture systems of either primary or pluripotent cells for *in vitro* analyses. In the next two sections, zebrafish embryos and mouse embryonic stem cells, which were used as models in the present study, are presented.

1.6.1. Mouse embryonic stem (ES) cells

Mouse ES cells were first isolated in 1981 (Evans and Kaufman, 1981, Martin, 1981) and have since become an important tool in biomedical research. At approximately E4,

some cells of the inner cell mass (ICM) of blastocyst-stage mouse embryos form the epiblast that will give rise to the embryo proper. These cells are undifferentiated and pluripotent, which means that they can differentiate towards all embryonic (but not extraembryonic) cell lineages and contribute to the formation of the presumptive tissues and organs. This population of undifferentiated, pluripotent ES cells can be isolated and grown in culture. They preserve their undifferentiated state and their pluripotency when grown under appropriate conditions *in vitro* and they can be induced to differentiate towards a multitude of cell lineages, recapitulating (to some extent) their *in vivo* differentiation potential, which would result in the formation of a whole embryo.

1.6.1.1. Mouse ES cell maintenance

The culture of mouse ES cells is demanding and requires supplementation of factors, normally provided by their *in vivo* environment in order to keep them undifferentiated and pluripotent. Leukemia inhibitory factor (LIF, also known as differentiation inhibitory activity, Dia) is one such supplement. LIF is a glycoprotein cytokine (Smith et al., 1988), expressed in the trophoectoderm surrounding the ICM, while its receptor (LIF-R) is expressed in the ICM. ES cells reside in the ICM, so removing them from that area also removes their source of LIF. Absence of LIF facilitates differentiation, so during mouse ES cell culture, when pluripotency and stemness need to be maintained, LIF needs to be added to the medium or supplied (secreted) by an underlying layer of feeder cells (mitotically inactivated fibroblasts, discussed in Section 5.1.2, page 173).

Briefly, LIF exerts its effect by binding to a receptor (LIF-R) on the cell membrane and activating downstream kinases, such as Janus tyrosine kinase (JAK) and antiphosphotyrosine immunoreactive kinase (TIK). These, in turn, activate downstream components, such as the signal transducer and activator of transcription-3 (STAT3), which then translocates to the nucleus. After transduction of the signal to the nucleus, transcription factors, such as *Oct4* and *Nanog,* cause changes in gene expression associated with phenotypic traits of ES cells (Boeuf et al., 1997, Matsuda et al., 1999, Niwa et al., 1998). *Oct4, Nanog* and *Sox2* are commonly used as pluripotency markers for ES cells *in vitro* and are further discussed in Section 6.1.1 (page 223).

Serum (usually foetal calf serum, FCS) is also commonly used as a supplement in cell culture media. It provides a variety of molecules, nutrients and other proteins (hormones, growth factors), necessary for *in vitro* growth of cells, but it also adds buffering capacity to the media and neutralizes toxic compounds (Gissel et al., 2006,

Goldman and Wurzel, 1992, Sachinidis et al., 2003). Its presence, thus, is important for proper growth and differentiation of cells. It is thought that serum also plays an important role during stem cell differentiation, likely providing a BMP signal that, in turn, is essential for Wnt signalling (ten Berge et al., 2008). However, the exact mixtures of growth factors and inhibitors that serum contains are mostly undefined. It is, therefore, preferable to omit serum during ES cell culture in order to avoid unknown confounding effects and to supplement, if necessary, with artificial, not animal-derived, combinations of growth factors, available commercially (serum replacement factors) (Sachinidis et al., 2003).

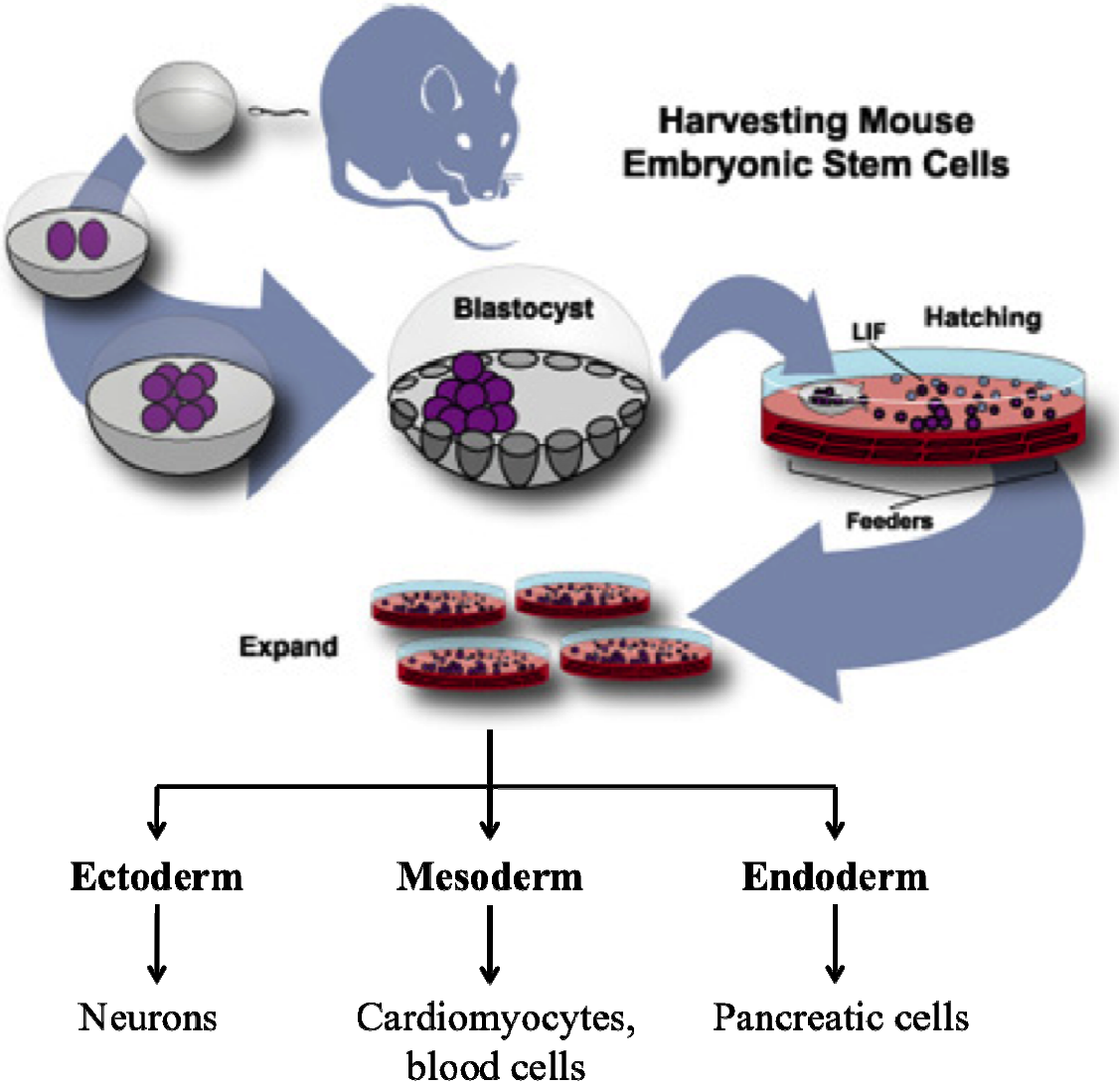

Figure 1. 10: The origin and differentiation potential of mouse embryonic stem (ES) cells. ES cells are derived from the inner cell mass (ICM) of pre-implantation stage mouse blastocysts and can be maintained indefinite in culture in an undifferentiated state. Upon stimulation, they can start differentiating and give rise to cells of all embryonic germ layers, ectoderm, endoderm and mesoderm. Cardiac progenitors are mesodermal derivatives and can be easily visualized because of their spontaneous contraction.

1.6.1.2. ES cell differentiation recapitulates aspects of early embryonic development

Differentiation of ES cells can be achieved by removal of LIF and of any other factors (such as the feeder cells) that keep cells in an undifferentiated state. Differentiation of ES cells in culture is commonly, but not uniquely, mediated by the formation of embryoid bodies (EB). These are three-dimensional, spherical cell aggregates resembling early peri-implantation embryos, hence the name. EB can form spontaneously and irreversibly from differentiating ES cells in the appropriate environment (Keller et al., 1993). They can form either by spontaneous aggregation of ES cells in suspension (in low attachment dishes or in the presence of methylcellulose) or by culture of ES cells in hanging drops. The latter culture method gives rise to uniform sized EB but it is not applicable for high throughput studies and is technically more challenging (Dang et al., 2002, Kurosawa et al., 2003). It is the preferred method in the current study.

Evidently, EB cannot develop into a real embryo as they lack the node (and primitive streak), extraembryonic structures and many other environmental factors that are essential for embryo patterning, but they can recapitulate, to some extent, early events of embryogenesis. For example, differentiation of the initially naïve cells into cells of the three germ layers (endoderm, mesoderm and ectoderm) and derivation of descendants of these layers can be recapitulated *in vitro* (Liersch et al., 2006, Risau et al., 1988, Smith, 2001). Although the spatial complexity of *in vivo* embryogenesis and organogenesis is not achieved during EB maturation, the dynamics of gene expression *in vitro* mimics the early stages of embryonic development (Bruce et al., 2007, Keller, 2005, Keller et al., 1993) Comparative studies of murine *in vivo* embryonic and *in vitro* EB development have shown that prior to day 3 EB are equivalent to pregastrulation-stage embryos (E4.5-E6.5), between days 3 and 5 EB correspond to gastrulating embryos (E6.5-E7.5) and after day 6 EB are comparable to early organogenesis-stage embryos (E7.5) (Leahy et al., 1999, Vallier et al., 2001, Xiong et al., 1998) (Figure 1.3). Since EB give rise to almost all cell lineages and recapitulate the early events of embryogenesis, their use in studying embryonic development and the signalling events that orchestrate it has been of great importance.

1.6.1.3. Differentiation of ES cells can recapitulate early stages of cardiogenesis

The development of ES cells in culture recapitulates to a large extent the temporal molecular interactions and cellular transitions during specification of naïve cells to progenitors of defined lineages, as discussed above. This system has been particularly useful for studying normal development of cardiac progenitors, for understanding the underlying signalling networks that govern the whole process and for identifying the hierarchy of precursor relationships.

Many studies have shown that the contractile ability and the morphological characteristics of ES cell-derived cardiomyocytes are similar to that of primary cardiomyocytes (Xi et al., 2010). ES cell-derived EB, at any given point during differentiation, contain cardiomyocytes (approximately 30% of the volume of the culture) in different developmental stages with different chamber specificities, electrophysiological properties and myofibrillar organization; ventricular, atrial, His-purkinje and pacemaker (node-like) cells can be found among an ES cell-derived cardiac cell population (Boheler et al., 2002, Fijnvandraat et al., 2003, Hescheler et al., 1997, Hidaka et al., 2003, Sachinidis et al., 2003). Cardiac genes, general or chamber-specific, seem to be expressed in equivalent levels in ES-derived cardiac cells as during early heart development *in vivo; Nkx2.5, Gata-4, Mef2c, Irx4, Anf* and *Connexin40* are only a few of the genes that have been examined (Fijnvandraat et al., 2003).

Also, cardiogenesis *in vitro* can be enhanced or accelerated by a variety of different factors as it happens *in vivo*. Inductive signals, such as BMP2 and TGFβ, have been shown to promote cardiogenic differentiation of ES cells (Menard et al., 2004). In line with these findings, endodermal factors have also been reported to direct differentiation of mouse and human ES cells to the cardiac lineage (Mummery et al., 2003, Rudy-Reil and Lough, 2004). Notch and FGF signalling are implicated in affecting cardiomyocyte fate as well (reviewed by Evans, 2009).

1.6.1.4. Other stem cell categories

Embryonic stem cells have been isolated from other organisms as well, including zebrafish (Collodi et al., 1992) and human (Thomson and Marshall, 1998). Zebrafish ES cells are isolated from blastula-stage embryos and can be maintained in culture in an undifferentiated state on feeder layer cells (Collodi et al., 1992, Fan et al., 2004, Ma et al., 2001, Sun et al., 1995). Despite their isolation almost 20 years ago, a detailed

transcriptome and proteome analysis of different zebrafish ES cell lines remains to be completed (reviewed by Hong et al., 2011). Human ES cells are isolated from blastocyst-stage *in vitro* fertilised embryos or from termination material. They differ substantially in their growth requirements from mouse ES cells, they are more demanding, they do not respond to LIF and they grow poorly on feeder cells when dissociated to single cells (Pera et al., 2000, Thomson and Marshall, 1998). However, their potential for direct therapeutic application and for advancing our understanding of human embryonic development and disease, has made them an attractive tool since their isolation.

Stem cells can be also isolated from adult tissues, including bone marrow, mesenchymal and haematopoietic stem cells (reviewed respectively by Augello et al., 2010, Medvinsky et al., 2011, Walkley, 2011) and from cord blood (reviewed by McKenna and Brunstein, 2011). These cells have the potential to differentiate to a more limited number of cell lineages and will not be examined further here.

1.6.2. Zebrafish

Zebrafish (*Danio rerio* or *Brachydanio rerio*) is a tropical fresh water fish, of Indian origin, that belongs to the *Cyprinidae* family. Adults are typically 4 centimeters (cm) in length, although they can grow up to 6.4 cm. They usually live for approximately 2-3 years but depending on the conditions, their life span can extent to up to 5 years. Mating zebrafish in an aquarium is easy and relatively cheap and can be performed throughout the year. Each female can lay hundreds of eggs in each clutch. These eggs will only grow and develop after external fertilization by the male (spawning). Upon fertilization embryonic development begins. Early cleavage and gastrula stages have been described before and resemble the corresponding stages of other vertebrates. During segmentation (10-24 hpf) somites develop, organ rudiments appear (including the heart, brain, eyes, ears), the embryo elongates, tail morphogenesis is prominent, morphological differentiation of cells takes place and the first bodily movements are observed. The pharyngula period that follows (24-48 hpf) is characterized by the appearance of pectoral fins, pigmentation, blood circulation, pharyngeal arch development and behavioural traits. Development progresses rapidly so that precursors and rudiments of all major organs appear within the first days (up to 48hpf) (Westerfield, 1993). A representative image of a 48 hpf zebrafish embryo is shown in Figure 1.11.

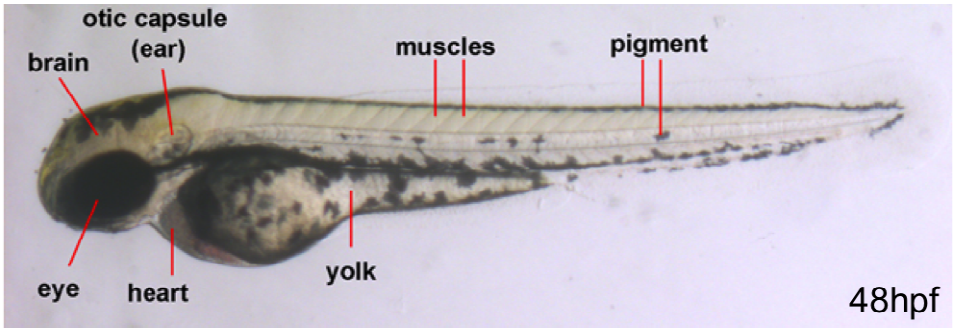

Figure 1. 11: Representative image of a 48 hpf zebrafish embryo in a lateral view. Areas of interest, like the heart, otic vesicle (or capsule), eye, brain, muscle (somites) and others, are shown.

1.6.2.1. Zebrafish as a model for vertebrate embryogenesis and cardiogenesis

Zebrafish is being used extensively as an animal model in developmental biology. As the embryos are transparent and develop *ex utero* they can be directly observed and followed in real time throughout development, a characteristic that has increased its popularity as a developmental research model (Grunwald and Eisen, 2002, Muller and Grossniklaus, 2010). As a vertebrate, it has a high degree of evolutionary conservation with mammalian species and it shares with them fundamental developmental pathways (Ackermann and Paw, 2003, Ingham, 1997). Also, it is amenable to manipulation by exposure to pharmacological agents, by injection with knockdown systems (for example antisense morpholino oligonucleotides) and by generation of transgenic lines, such as GFP and dsRed. *Danio rerio* is particularly well suited for the study of the genetics behind the early steps of heart formation. Although its heart consists of a single atrium and a single ventricle and there is no pulmonary circulation, it is believed that the very early stages of heart cell specification, commitment and differentiation are common in all vertebrate species (Grimes and Kirby, 2009). An additional advantage is the ability of the zebrafish to survive without a fully functional and normal cardiovascular system for up to five days of development (Ackermann and Paw, 2003, Rocke et al., 2009). This allows investigation of mutations or drug treatments that cause early lethality in other species.

1.7. Summary

In this thesis, the canonical Wnt and the JNK signalling pathways are investigated in the context of *in vitro* and *in vivo* cardiac differentiation. In the preceding sections, all areas

of interest were presented in brief. First, an overview of embryonic development introduced the basic concepts and terms of embryonic development. Second, one of the germ layers, mesoderm, and its main derivative, the heart, were thoroughly analysed, focusing on induction, specification, determination and differentiation of cardiac cells, as well as formation and morphogenetic patterning of the heart. Next, the signalling networks of interest were presented, with emphasis on the canonical Wnt, non-canonical Wnt/PCP and JNK. Last, the two experimental models (mouse ES cells and zebrafish embryos) that were selected for the present study were introduced. The hypotheses on which this thesis was based, along with the aims that were set in order for these hypotheses to be tested, are introduced in the next section.

1.8. Aims of the thesis

The regulation of cardiac differentiation is complex and multifactorial and diverse signalling networks and transcriptional cascades have been shown to influence it. In this thesis, two signalling pathways, tightly interconnected between them, were investigated in the context of cardiogenesis; the JNK and the canonical Wnt pathway.

1.8.1. JNK signalling

JNK signalling is the main focus of the current thesis. JNK is a kinase, member of the MAPK family and also, a downstream effector of the non-canonical Wnt/Planar cell polarity (PCP) pathway. The differentiation of the heart and the progression of cardiac disease are two fields in which MAPK members have proven to be very important. Similarly, the Wnt/PCP pathway has been shown to play a defining role in cardiac induction, specification and morphogenesis.

This work was, therefore, based on the hypothesis that JNK, as a mediator of two essential signalling cascades during embryonic development, could represent a central regulator in processes associated with early stages of cardiac induction and specification, with previously unrecognized roles. I, therefore, set out to investigate the involvement of JNK signalling during *in vitro* (mouse ES cell) and *in vivo* (zebrafish embryonic) cardiogenesis. The following aims were set:

1. Characterize all zebrafish *jnk* orthologues that have not been thoroughly investigated previously, with the specific aim of identifying putative new *jnk* genes that arose after the fish genome duplication
2. Elucidate the phylogenetic relations of zebrafish *jnk* genes with their orthologs in other species, including the mouse
3. Establish the expression profiles of *jnk* genes in developing zebrafish embryos and define the role of jnk proteins during zebrafish embryogenesis with a specific focus on cardiogenesis
4. Determine the involvement of Jnk signalling during mouse ES cell differentiation, looking more closely at the generation of ES-derived cardiomyocytes and at the transcriptional networks that govern this process

1.8.2. Canonical Wnt/β-catenin pathway

In addition to JNK, the canonical Wnt pathway is examined in this thesis, in the context of ES cell-derived cardiogenesis, as it has been shown to cross talk extensively with Jnk (Esufali and Bapat, 2004, Liao et al., 2006, Wu et al., 2008). This pathway has long been thought as inhibitory for cardiac induction but recent data suggest that its contribution may be much more complex than initially thought. The intricate relationship and multifaceted cross talk between the canonical and non-canonical Wnt pathways could be one of the factors that add to the suggested complexity of the system. Therefore, the complex and bi-phasic response of cardiogenesis to the canonical Wnt pathway was investigated further with emphasis on the putative cross talk between the canonical and non-canonical branches of the Wnt cascade. It was hypothesized that, as shown before, early activation of the canonical Wnt pathway will have beneficial effects in promoting cardiogenesis, while its late activation will inhibit further cardiac progression. In order to explore this hypothesis the following aims were set:

1. Elucidate the temporally complex role of the canonical Wnt pathway in cardiogenesis *in vitro*
2. Establish potential alterations in the cardiac transcriptional regulatory network after canonical Wnt manipulation
3. Unravel the relationship between canonical and non-canonical Wnt pathway and elucidate how their interaction could affect the process of cardiogenesis

Chapter 2: Materials and methods

All measurements presented in this thesis are shown in SI units and chemicals were obtained from Sigma-Aldrich unless otherwise stated. Some general buffers, reagents and solutions are shown in Table 2.1, while buffers specific for each technique are shown in individual tables.

General buffers, reagents and solutions				
E3	**LB**	**3% methyl-cellulose**	**PBS**	**DEPC H_2O**
5mM NaCl	0.17M NaCl	0.08% Tricaine	10 PBS tablets (Oxoid BR14)	500µl DEPC (Sigma D5758)
0.17mM KCl	1% tryptone	3% methylcellulose	H_2O to 1L	H_2O to 1L
0.33mM $CaCl_2$	0.5% yeast extract	E3 to 1L	autoclaved	autoclaved
0.33mM $MgSO_4$	autoclaved			
0.1% methylene blue				
H_2O to 1L				

Table 2. 1: Table with general buffers, reagents and solutions. The recipes for E3 water, used for zebrafish embryo maintenance, LB (Luria Broth), used for bacteria growth, 3% methylcellulose, used for orientation of zebrafish embryos during microscopic imaging, PBS (phosphate buffered saline), used extensively in many techniques and DEPC (diethylpyrocarbonate) water, free of RNases and used for RNA work, are included in this table.

2.1. Zebrafish techniques

2.1.1. Zebrafish lines

Two transgenic zebrafish lines were used in this study: *Tg(cardiac myosin light chain 2 (cmlc2):GFP)* (Huang et al., 2003) and *Tg(cmlc2:Discosoma (Ds)Red2- nuc)* (Mably et al., 2003). In both lines the *cmlc2* promoter drives the expression of marker proteins. Cardiac-specific GFP expression is observed soon after the onset of *cmlc2* expression (approximately 18 hpf) in cardiomyocytes of *Tg(cmlc2:GFP)* embryos. Cardiac-specific nuclear production of DsRed fluorescent protein in *Tg(cmlc2:DsRed2-nuc)* embryos is

firstly observed after 30 hpf (at least 12 hours after its initial activation by *cmlc2* onset, but usually quite later).

A wild type zebrafish line, *Golden* (Zebrafish International Resource Centre, ZIRC), was also used. These embryos have reduced levels of pigment on their skin, which allows for easier visualisation of organ formation and of the signal from wholemount staining. This zebrafish line was used for whole mount *in situ* hybridization and for RT-PCR analysis.

2.1.2. Zebrafish breeding and mating

Adult *Tg(cmlc2:gfp)*, *Tg(cmlc2:dsNucRed)* or *Golden* fish were put together in special mating tanks that keep them separated overnight and the next morning they were transferred into a single tank to lay eggs. Eggs were collected in 100 mm petri dishes as soon as they were layed. Fertilized eggs (transparent) were separated from unfertilized ones (white) and incubated at 28.5^{o}C at all times, for optimal growth and development. Fish embryos were then used at the appropriate time point depending on the demands of each experiment. If younger than 48 hpf they had to be manually dechorionated before use.

2.1.3. Drug treatment

Fish embryos were incubated in 24-well plates in E3 water (Table 2.1) alone (E3 control) or in E3 water containing the SP600125 drug or dimethylsulfoxide (DMSO) alone (DMSO control), at the appropriate concentration for the required amount of time (5.25-72, 5.25-10, 10-22 and 22-30 hpf). The embryos were then transferred into new wells and washed thoroughly in fresh E3 water until further analysis.

2.1.4. Phenotype scoring, body measurements and embryo collection

Untreated, DMSO-treated and drug-treated fish embryos were phenotypically scored at 24, 48 and 72 hpf under a fluorescence stereoscope (Leica MZ16F stereomicroscope with a Leica DFC 420C digital camera). When necessary, embryos were transferred in 3% methylcellulose (Table 2.1) for better orientation and imaging. Images of the dorsal view of the embryos were taken in order to perform various body measurements (body length, head width, ocular distance, body width). These measurements were done in the

AxioVision image analysis software (AxioVision Rel. 4.8) by drawing lines over the areas of interest and converting pixel differences to metric differences in microns (Figure 2.1).

When necessary, measurements were normalised against values that account for size and length differences for an easier and more accurate comparison of different groups. The ocular distance was normalised against the width of the head so that smaller heads with eyes positioned normally and not further apart or closer together would show the same values as normal sized heads with normally positioned eyes. Under these settings, low values signify eyes located closer together and higher values mark increased eye distances, irrespective of the size of the embryos. Similarly, the width of the body was normalised against the length of the body, as short but normally proportioned fish embryos would be expected to have narrower bodies; so, again in this case high ratios will signify broader bodies, similar to the convergence-extension phenotype, and low ratios will mark narrower bodies.

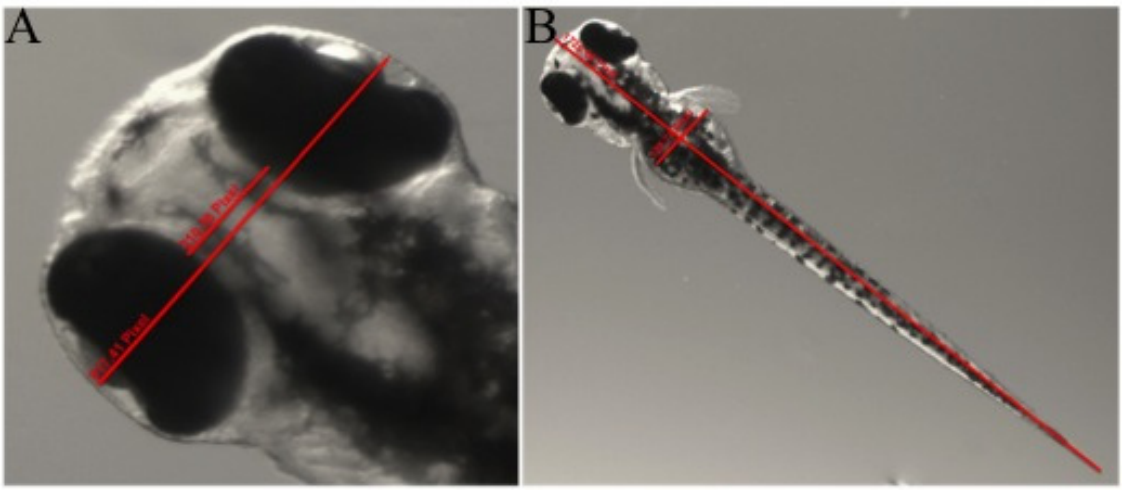

Figure 2. 1: Body measurements on 72 hpf zebrafish embryos. Head measurement, such as width of the head and ocular distance (panel A), and general body measurements, such as body length and body width (panel B) were taken by drawing lines over the areas of interest in the AxioVision (Rel 4.8) software and then converting pixels to microns using a micrometer.

2.1.5. Heart cell counting

Intact immuno-stained (as described in the next section) Tg(*cmlc2:DsRed2-nuc*) embryos were firstly imaged under a fluorescence microscope (Zeiss Axioplan2) and pictures were taken if necessary. For subsequent counting of the cells within their hearts, embryos were placed on a slide (commonly 2-3 embryos at a time) with their

hearts facing upwards. The embryos were then carefully covered with a coverslip and by applying continuous pressure with the thumb on it, squashing of the embryos and their hearts was achieved. The samples were then imaged under the microscope using the appropriate filters. All heart cells in Tg(*cmlc2:DsRed2-nuc*) embryos had red fluorescent nuclei after 48 hpf. The cytoplasm of atrial cells was also counterstained with the S46 antibody; therefore, ventricular cells had red nuclei, while atrial cells had red nuclei and green cytoplasms and could be easily distinguished and counted separately (Figure 2.2). After imaging under the microscope, all pictures were then transferred in an image analysis software (AxioVision Rel 4.8), where nuclei were counted.

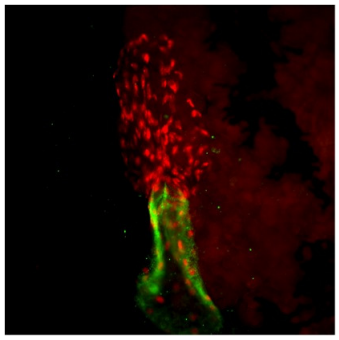

Figure 2. 2: Image of the heart of a *Tg(cmlc2:DsRed2-nuc)* zebrafish embryo after counterstaining with anti-DsRed, shown in red, and S46, shown in green, antibodies. The nuclei of all cardiomyocytes are stained red but only the cytosplasms of atrial cells are stained green.

2.1.6. Wholemount fluorescence immunohistochemistry

Tg(*cmlc2:DsRed2-nuc*) zebrafish embryos were fixed in 4% parafolmadehyde (PFA) (Sigma P6148) at 4^{o}C overnight. The next day embryos were washed twice in PBS, for 5 min each time, at RT and were then transferred into blocking solution consisting of 10% FCS, 2 mg/ml bovine seurm albumin (BSA) (Sigma A2153) and 0.2% saponin (Sigma 84510). Blocking lasted for 1 hour at RT and embryos were then washed 3 times in PBS with 0.2% saponin. Incubation in primary antibody solution followed: anti-dsRed polyclonal antibody was diluted (1:400) in neat mouse monoclonal atrial myosin heavy chain SV46 antibody solution containing 0.2% saponin (Table 2.2). Incubation was performed overnight at 4^{o}C in a humidified chamber in the dark. The following day the primary antibody solution was washed off with two consecutive washes in PBS with 0.2% saponin, at RT, 10 min each. A 2 hours incubation in secondary antibody solution at RT in a dark humidified chamber followed: swine anti-rabbit, TRITC-conjugated and goat anti-mouse IGg1 488 antibodies were used in the appropriate dilutions (1:50 and 1:100, respectively) in PBS (Table 2.2). After two brief

washes in PBS containing 0.2% saponin, samples were stored in the dark at 4°C until further use for fluorescence imaging and heart cell counting (Section 2.1.5, page 55).

Primary antibody				**Secondary antibody**		
Target	**Species**	**Dilution**	**Provider**	**Details**	**Dilution**	**Provider**
dsRed	Rabbit	1:400	Glontech	Swine anti-rabbit, TRITC	1:50	DAKO R0156
S46	Mouse	Neat	Developmental Studies Hybridoma Bank	Goat anti-mouse, IGg1, 488	1:100	Invitrogen, Alexa Fluor, A21121

Table 2. 2: Antibodies used for immunostaining on zebrafish embryos.

2.1.7. Wholemount in situ hybridization

All solutions during the first day were made up with DEPC water (Table 2.1) to prevent the activity of RNases. After day 2 there was no need for DEPC-treated water. After fixation in 4% PFA in DEPC-PBS, embryos were transferred in 100% methanol and stored at -20ºC for at least 2 hours in order to prevent the formation of gas bubbles, until further use. Solutions and buffers used during *in situ* hybridisation are listed in Table 2.4.

The first day embryos were rehydrated passing through a series of methanol / PBT (PBS with 0.1% Tween20) gradient of 75%, 50% and 25% for 5 minutes each, and four washes in 100% PBT, 5 minutes each. Embryos older than 36 hpf were then bleached for 2-3 minutes in a 10% solution of H_20_2 in 0.5xSSC and 5% formamide. After a brief wash in PBT they were subjected to treatment with proteinase K (10 µg/ml) in PBT (Table 2.3 for incubation times). Embryos were then refixed in 4% PFA (in PBS) for 20 minutes and washed in PBT 5 times for 5 minutes each time. After being moved into flat-bottom eppendoft tubes they were incubated in 800µl of pre-heated pre-hybridisation mix for 2-5 hours (typically 3 hours) at 65ºC. After removal of the pre-hybridisation solution, 200 µl of hybridisation mix containing 100-200 ng of digoxygenin (DIG)-labelled antisense RNA probe was added to each tube. Embryos were incubated overnight in a waterbath at 65ºC.

After removal of the hybridisation mix, embryos were briefly washed in hybridisation solution not containing probe at 65ºC. Further washes were carried out in a series of hybridisation mix / 2xSSC gradient of 75%, 50% and 25% for 15 minutes each at 65ºC, followed by a final wash in 2xSSC at 65ºC for another 15 minutes.

Embryos were then further washed in 0.2xSSC at 65ºC twice for 30 minutes and then were passed through a series of 0.2xSSC / PBT gradient of 75%, 50% and 25% for 10 minutes each. After a 10 minute wash in PBT embryos were incubated in 1% blocking solution (Roche, Sigma) in maleic acid buffer (MAB) with 0.1% Tween20 (MABT) for 2 hours to cover non-specific binding sites. Anti-DIG antibody (Roche 11093274910) was added to 1% blocking solution / MABT at a 1:5000 dilution and left to pre-absorb at 4ºC for 1hour, before being added to each tube for an overnight incubation under gentle shake at 4ºC.

Developmental stage	**Proteinase K treatment**
blastula / gastrula	30 seconds
late somitogenesis (14 to 22 somites)	5 minutes
24hpf	15 minutes
36 / 48hpf	30 minutes
72 / 96hpf	40 minutes

Table 2. 3: Incubation times of proteinase K treatment for different zebrafish embryo ages. The older the embryo the longer the treatment has to be.

The third day embryos were subjected to a brief PBT wash, which was followed by seven 15 minute PBT washes. Washes were usually carried out for 2-4 days at RT in 24-well plates before the staining reaction would be initiated. The staining proocedure started with three 5 minute incubations in NTMT staining buffer. The increased pH of the NTMT buffer is optimal for the reaction of the NBT/BCIP (1,4-nitro-blue-tetrazolium-chloride / 5-bromo-4-chloro-3-indoyl-phosphate, Roche 11681451001) developing solution. 50 mg/ml of NBT/BCIP mix were added to the NTMT buffer and 1 ml of this staining solution was added to each well. The plates were left at 4ºC in the dark until staining was detectable. When the desired level of development was reached, the reaction was stopped with extensive PBT washes. Embryos were re-fixed in 4% PFA for 20 minutes and then washed in an increasing gradient of PBT / Methanol (25%, 50%, 75% methanol) finishing in 100% methanol. Embryos were left in 100% methanol at least for 1 hour before being washed down to PBS through a series of decreasing gradient of PBS / Methanol (25%, 50%, 75% PBS) finishing in 100% PBS. Observation of stained embryos was achieved under a dissecting microscope (Leica MZ16F stereomicroscope with a Leica DFC 420C digital camera) with embryos being mounted in 3% methylcellulose for easier orientation.

Negative and positive controls were used for this assay. *Tbx5* (*tbx5a*) was used as a positive control. This provided an excellent comparison measure as it is expressed in most of the areas of interest: the heart, the pectoral fins (or fin buds) and the eyes (or optic primordia) (Begemann and Ingham, 2000, Garrity et al., 2002). In all experiments sense probes were, also, used; these are usually expected to give negative results, as they bind to antisense endogenous mRNA, which is uncommon. However, it has been shown that antisense mRNA is occasionally produced as a control mechanism for gene regulation. It is also known that probes can bind to non-specific targets, due solely to their chemical properties. The sense probe, therefore, gives a measure of non-specific binding, which will be similar to the antisense probe, and accounts for specificity of the signal. In all cases, the sense probe is a valuable internal control; it will either give a negative result or it will show the same or an overlapping expression pattern as the antisense probe, confirming in both cases the specificity of the staining. Sense probe staining patterns are included in the images along with the antisense probe staining for easier comparison. Negative controls, without addition of any probe, were also included.

Solutions and buffers for *in situ* hybridization				
20xSSC	**NTMT**	**MAB**	**Pre-hybridization buffer**	**Hybridization buffer**
1.2M NaCl	100 mM NaCl	0.1M maleic acid	50% formamide	Pre-hybridization buffer
0.3M tri-sodium citrate	100 mM TrisHCl pH 9.5	0.15M NaCl	5xSSC	Probe of interest at 1µg/ml
	50 mM $MgCl_2$	Ph7.5	50 mg/ml yeast tRNA	
	0.1% Tween20		0.1% Tween20	
			50 µg/ml heparin	
			9.2 mM citric acid pH 6.0	

Table 2. 4: Solutions and buffers for *in situ* hybridization. The ingredients of 20xSSC, NTMT, MAB (maleic acid buffer), pre-hybridization and hybridization buffers are shown.

2.1.8. RNA extraction

Total RNA was extracted from zebrafish embryos using the Trizol Reagent RNA extraction protocol (Invitrogen 15596-026) as described in the manufacturer's instructions. Briefly, 1 ml of Trizol was added to each tube containing approximately 20-30 embryos, depending on the age. Trizol maintains RNA integrity during tissue homogenization, while breaking cells and cell components. After thorough mixing for adequate homogenization, tubes were either stored at -80^{o}C until further use or were immediately processed. Tissues were then further homogenized by multiple passing through 21G and 25G syringes, sequentially. After a short incubation at room temperature to ensure complete dissociation of nucleoprotein complexes, 0.2 ml of chloroform were added (per 1ml of Trizol). Rigorous shaking for 15 seconds allowed for proper mixing of the ingredients. Subsequent centrifugation at 12000xg at 4^{o}C for 15 minutes enabled phase separation: the low, organic phase containing mainly chloroform and protein, the intermediate phase (interphase) containing DNA and the upper aqueous phase, containing nearly all of the RNA. The upper phase (approximately 60% of the initial Trizol volume) was then transferred into a new tube and RNA was precipitated from it by adding 0.5 ml of isopropyl alcohol (per 1 ml of Trizol). Precipitation was enhanced by incubation at RT for 10 minutes and subsequent centrifugation at 12000xg at 4^{o}C for another 10 minutes. Removal of the supernatant was followed by ethanol washing of the pellet (1 ml of ethanol for 1 ml of Trizol). Short vortexing that ensures complete ethanol penetration and centrifugation at 7400xg at 4^{o}C for 5 minutes, resulted in a clean RNA product in the pellet that could then be diluted in the appropriate volume of DEPC-treated H_2O (commonly 11 μl). RNA products were then quantified using the NanoDrop ND-1000 Spectrophotometer and by gel electrophoresis in 1% agarose gels, as described in Section 2.1.11 (page 61). Extracted RNA was stored at -80^{o}C until further use.

2.1.9. cDNA synthesis

1 μg of RNA (extracted and quantified as explained in the previous section) was treated with 1 μl DNase I (Invitrogen 18068-015) in a 9 μl solution containing DEPC-treated H_2O and DNase buffer, at RT for 15 minutes, in order to eliminate any DNA contamination. 1 μl of 25 mM EDTA was then added to the mix for the inactivation of the enzyme at 65°C for 10 minutes. The SuperScript II RTase kit (Invitrogen 18080-

044) was used for the reverse transcription of the DNased RNA. 10µl of the DNased mixture were transferred into a tube containing 2µl random primers (200ng) (15-mers, Sigma A1312-002), 10µl dNTPs 10mM, 2µl DEPC-H_2O, 8µl 5x1st strand buffer, 4µl 0.1M DTT, 2µl RNase inhibitor (Promega N2111) and 2µl Reverse Transcriptase. The mix was incubated for at least 1½ hours at 37°C, allowing enough time for reverse transcription to take place. At the end of the incubation, 60µl distilled water were added to the mix. The synthesized cDNA was stored at -20°C until further use.

2.1.10. Polymerase Chain Reaction (PCR)

All amplifications were performed using the PTC-200 (Peltier Thermal cycler) under optimised conditions for each primer set (manually designed and provided by MWG). The PROMEGA Go-taq polymerase kit (Promega M3175) was used for all PCR. All primers were designed to span exon-exon boundaries, where possible, so that genomic DNA contamination is avoided (the sequences and the binding location of jnk primers is shown in Chapter 3). The housekeeping gene *β-actin* was used as an internal reference because of its invariable expression during embryonic development and after drug treatments, as shown recently (McCurley and Callard 2008). The annealing temperature was 58°C and the product sizes along with the primer sequences are shown in Table 3.2 (page 109). Briefly, a 20µl reaction was prepared, containing 2µl dNTP, 4µl 5x buffer, 0.2µl taq enzyme, 1µl of each primer (10µM each), the appropriate amount of cDNA (according to the *β-actin* PCR results) and distilled H_2O to make up the final volume.

2.1.11. Agarose gel electrophoresis

Fresh 2% and 1% agarose (SeaKem LE agarose) gels in 1x Tris-Acetate-EDTA (TAE) were used for electrophoresis of PCR and RNA products, respectively. 100 base pair DNA ladder was used as a size marker (Invitrogen 15628-050). Gel images were captured under ultraviolet light on a SYNGENE transilluminator using the GeneSnap software.

2.1.12. Probe design

All Jnk probes (*jnk3.3, pan-jnk3, pan-jnk1a and jnk2*) were manually designed against the desired gene and isoform (sequences are listed in Table 3.3, page 109). A PCR

reaction (see Section 2.1.10) was then performed on a control cDNA (a sample that is known to express this gene/isoform) in a large volume reaction (50µl). The PCR product was then ran on an agarose gel (see Section 2.1.11), the band was extracted (see next section) and ligated with the appropriate vector (see Section 2.1.12.2) and after bacterial transformation (see Section 2.1.12.3) and selection of the white colonies, plasmid DNA was extracted and linearized (see Section 2.1.12.4). Finally, after confirmation of the orientation of insertion (either by restriction enzyme analysis or by sequencing, see Section 2.1.12.5), the probes were Dig-labelled (see Section 2.1.12.6) and were then ready to use for *in situ* hybridization.

2.1.12.1. Gel extraction

After gel electrophoresis, DNA bands were extracted using the QIAquick Gel Extraction kit (Qiagen), according to the manufacturer's instructions. Briefly, the band was dissected out of the agarose gel using a new, DNA-free scalpel and was incubated at 55^{o}C in QG solution, until its complete dissociation. The solution was then moved in a column and centrifuges at 13000 rpm at RT for 1 minute. The DNA fragments are expected to bind to the column membrane. After two washes in PE buffer and subsequent centrifugations, the DNA product was eluted in a fresh tube with ddH_2O. Extracted products were stored at -20^{o}C until further use.

2.1.12.2. Ligation

The extracted PCR product was flanked on both sides by adenosine (A) and could be readily ligated with a pGEM-T-easy vector (Promega) that contained free thymidine (T) sites within the multi-cloning site (Figure 2.3). 3 µl PCR product were mixed with 1 µl pGEM-T-easy vector, 1 µl T4 DNA ligase and 5 µl ligase buffer (Promega M1801). The mixture was left at RT for 1 hour and was then ready for transformation of competent cells (see below).

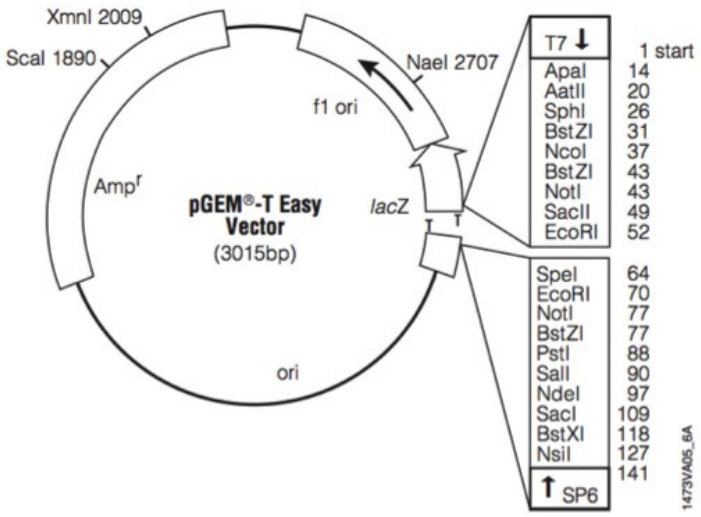

Figure 2. 3: pGEM-T easy vector map and sequence reference points.

2.1.12.3. Bacterial transformation

Competent DH5α bacterial cells (Invitrogen 18265-017) were transformed with pGEM-T-easy plasmids ligated with the gene sequences of interest, as described above. 10-50 ng of ligated plasmid DNA, was added to 25 µl of competent cells and these were left on ice for 30 minutes. The samples were then heat shocked at 37ºC for 90 seconds, then chilled on ice for 3 minutes allowing the plasmids to be inserted into the bacterial cells more efficiently. 950 µl Luria broth (LB, Table 2.1) were added and the samples incubated at 37ºC shaking for 1 hour, allowing for the gene conferring resistance to amplicillin to be expressed. 200 µl of the culture were plated onto X-Gal (5-bromo-4-chloro-3-indolyl-beta-D-galacto-pyranoside, 20mg/ml in 99% dimethylformamide), IPTG (isopropyl-beta-D-thiogalactopyranoside) and ampicillin containing LB plates and left to incubate overnight at 37ºC. The presence of X-Gal allows cells containing plasmids to be identified; they grow white colonies in contrast to the cells not carrying the plasmid that form blue colonies. The production of white colonies is due to the disruption of the gene that encodes for β-galactosidase, the enzyme that catalyzes the reaction that turns the substrate X-Gal into a blue precipitate, caused by the insertion of the gene sequence of interest into the multi cloning site. In contrast, when there is no insert, β-galactosidase is produced and blue precipitate can be observed. The next day, single white colonies were picked from the plates with a P20 tip and grown in 10 ml LB supplemented with 10 µl 500 mg/ml ampicillin overnight shaking at 37ºC.

2.1.12.4. Extraction of plasmid DNA

Plasmid DNA was extracted from bacterial cultures using a miniprep kit (Qiagen 27104) according to the manufacturer's instructions. Briefly, overnight incubation of the transformation mix (see previous section) at 37^{o}C in LB containing ampicillin, has allowed the growth of the bacterial colonies that contain plasmids (which confer ampicillin resistance). Centrifugation of the mixture at 3000 rpm at RT for 5 minutes allows the precipitation of the cells. The supernatant was discarded and the pellet was then resuspended in P1 solution. Alkaline lysis and neutralization of the cells was followed by precipitation of chromosomal DNA and protein debris, while plasmid DNA remained in the supernatant and was collected. After purification in a column, plasmid DNA was eluted with ddH_2O. Tha exracted DNA was stored at -20^{o}C until further use.

2.1.12.5. Restriction enzyme digestion for confirmation and orientation of insertion

With EcoRI digestion of the linearized plasmid it was possible to confirm insertion of the product, since EcoRI restriction sites flank the multi-cloning region and are absent from the rest of the vector. If additional EcoRI sites were located within the insert, more that two different sized products were expected to appear. The NEB (New England Biolabs) cutter V2.0 server was used to predict additional EcoRI cutting sites within the insert. 2-5 μg of circular plasmid were incubated at 37ºC with 2 μl buffer, 2 μl EcoRI and up to 20 μl with H_2O for 2 hours.

After confirmation of the successful insertion of the product, the orientation of the insertion was pursued. Restriction sites uniquely present on the vector and within the insert were chosen, so that after digestion different bands would be generated depending on the orientation of insertion. Failure to identify appropriate cutting sites necessitated sequencing of the ligation products (MWG sequencing service) in order to get information about the orientation of the insert. The NEB (New England Biolabs) cutter V2.0 server was used for identification of restriction cutting sites within the insert sequence.

2.1.12.6. Digoxygenin labelling of RNA probes

After confirmation of the insertion and orientation of the right product into the vector, the probes could then be generated. DNA was transcribed into RNA using the appropriate polymerase, either T7 or SP6 (Table 2.5), in the presence of DIG-UTP that allows for labeling of the riboprobes. Specifically, 1 µg of linearised plasmid DNA was mixed with 2 µl 10x transcription buffer and 2 µl DIG-labelling mix from the Dig-RNA labeling kit (Roche 11277073910), along with 1µl RNase inhibitor (Promega N2111), up to 20 µl DEPC-H20 and 1 µl of the appropriate RNA polymerase (Table 2.5). Samples were incubated for 2½ hours at 37ºC to allow the synthesis of riboprobes containing Dig-UTP. The RNA probes were precipitated by adding 100 µl DEPC TE, 12 µl DEPC sodium acetate, 264 µl 100% ethanol and 1 µl tRNA (Baker's yeast) and leaving the reaction at -20ºC overnight or at -80ºC for 2 hours. Then samples were centrifuged for 20 minutes at 13000 rpm at 4ºC. The supernatant was removed and the RNA pellets washed with 70% DEPC-ethanol. After centrifuging for 5 minutes at 13000 rpm and 4ºC, the ethanol was removed and the pellets were allowed to air dry. Pellets were resuspended in 100 µl DEPC-H_20 and stored at -20ºC. The correct production of a probe was confirmed by 1% agarose gel electrophoresis.

Probe	**Orientation of insertion confirmed by**	**RE and promoter for sense probe**	**RE and promoter for antisense probe**
Pan-jnk1	Sequencing	SalI - T7	ApaI - Sp6
Jnk2	BstxI restriction site cutting	SalI - T7	ApaI - Sp6
Pan jnk3	ApaI restriction site cutting	SalI - T7	ApaI - Sp6
Jnk3.3	Sequencing	NcoI - Sp6	SalI - T7

Table 2. 5: Details about all jnk probes. All probes were inserted into pGem-T easy vectors, which contained an ampicillin-resistance gene. Linearized products were sent for sequencing when restriction enzyme digestion could not reveal the orientation of insertion. RE: restriction enzyme.

2.2. Embryonic stem (ES) cell culture techniques

2.2.1. STO fibroblast culture maintenance

Sim-Thioguanine-Ouabain (STO) fibroblasts, obtained from the American Type Culture Collection (ATCC, CRL-1503), were grown in T75 flasks (Iwaki, 3123-075) in 15 ml STO media (Table 2.6). When cells reached 70-80% confluency, the media was removed and the cells were briefly washed in 10 ml Dublecco's PBS (Gibco 14190). 3 ml of 0.05% trypsin (Gibco 25300) were then added in the flask for 5 minutes at 37^{o}C or until cells get dettached from the bottom. Trypsin was inactivated by the addition of 9 ml of STO media and single cell suspension was achieved by continuous pipetting, avoiding the formation of bubbles. Flask content was then transferred into 15 ml falcon tubes and centrifuged at 1000rpm for 5 minutes at RT. After removal of the supernatant the pellet was resuspended in 5-7 ml of STO media (depending on the dilution required, typically 1:5 or 1:7). 1 ml of the cell suspension was then plated in a new T75 flask containing 14 ml of STO media. Cells were incubated at 37^{o}C under 5% CO_2 in a Heraeus (HERA cell) incubator.

E14	***ES-D3***	***STO***	***Differentiation***	***Freezing***
20% FCS (Gibco 10439-024)	15% FCS (ATCC 30-2020)	10% FCS (ATCC 30-2020)	10% FCS (Gibco 10439-024)	40% FCS
1% L-Glutamine (Gibco 25030-024)	0.1mM 2-mercaptoethanol (Gibco 31350010)	90% DMEM (ATCC 30-2002)	1% L-Glutamine (Gibco 25030-024)	50% DMEM
1% NEAA (Gibco 11140-035)	85% DMEM (ATCC 30-2002)		1% NEAA (Gibco 11140-035)	10% DMSO
0.1mM 2-mercaptoethanol (Gibco 31350010)			0.1mM 2-mercaptoethanol (Gibco 31350010)	
78% DMEM (Gibco 21063-029)			88% DMEM (Gibco 10439-024)	
LIF (Produced in house, 1:500)				

Table 2. 6: Stem cell, differentiation and freezing media. Different stem cell media were used for the culture of E14 and ES-D3 ES cells but during the differentiation assay the same media was employed. Different FCS and DMEM were used for each cell line, depending on the cell provider's instructions for optimal growth and maintenance. In the freezing media the appropriate FCS and DMEM for each cell line were used. Abbreviations: DMEM: Dulbecco's modified eagle medium, NEAA: Non-essential amino acids, DMSO: Dimethylsulfoxide, LIF: Leukemia inhibitory factor, FCS: fetal calf serum.

2.2.2. Preparation of feeder cells by mitotic inactivation of STO fibroblasts

Fibroblast cells (STO) grown as described above, were then used for mitotic inactivation and feeder cell preparation. Mitomycin-C is a light-sensitive compound and had to be handled under minimum light exposure. 2 ml of STO media (Table 2.6) were inserted with a 21G needle (0.45μm) into a fresh mitomycin-C bottle (Sigma M0503). Vigorous shaking mixed the contents of the bottle to a 1 mg/ml solution of mitomycin. The solution was then filtered through a 0.45 μm filter and transferred into a 15 ml falcon tube, covered in foil. 100 μl of the falcon content were added to a T75 flask containing confluent (approximately 75% confluent) STO cells in 10 ml of STO media (final concentration of mitomycin-C was 0.01 mg/ml). A 2 hour incubation at 37^{o}C allowed for mitomycin-C to penetrate the cells and inactivate their mitotic cycle. The flask was then washed thoroughly for at least 3 times in 10 ml of DPBS. Traces of mitomycin-C can severely affect cell culture in downstream procedures. Inactivated STO cells, now called feeder cells, were then counted with a haematocytometer and frozen accordingly, as described below. Typically, $6x10^6$ and $2x10^6$ feeder cells were aliquoted in each cryovial, which would then be used for feeder and stem cell culture in T75 and T25 flasks, respectively. Freezing cells at the correct concentration needed for downstream procedures is essential at this step, since feeder cells cannot proliferate and full coverage of the flask surface is pivotal for optimal ES-D3 cell culture. One day before initiation of ES-D3 cell culture or one day before ES-D3 cell passaging, feeder cells were thawed, as described below, and cultured in STO media. Feeder cells can be kept in culture, with daily media change, for 7-9 days at 37^{o}C under 5% CO_2.

2.2.3. ES-D3 stem cell culture maintenance

ES-D3 cells (ATCC CRL-11632) (Doetschman et al., 1985) require the presence of feeder cells, which secrete leukemia-inhibition factor (LIF) and growth factors, for their optimal maintenance. Cells were typically cultured in T75 or T25 flasks on a confluent layer (approximately $6x10^6$ and $2x10^6$ cells, respectively) of mitotically inactivated STO fibroblasts (feeder cells, as described above) in 12 or 4 ml ES-D3 media (Table 2.6), respectively. Cell passaging was similar to that described for STO cells (Section 2.2.1, page 66) with the following differences: 0.25% trypsin (GIBCO 25200-056) was used for cell dettachment and ES-D3 media was used throughout. Achieving single cell suspension was crucial for the maintenance of stemness, as cells in clumps have been

shown to readily differentiate towards endodermal derivatives (Notarianni and Evans, 2006). Cells were incubated at 37^{o}C under 5% CO_2.

2.2.4. E14 stem cell culture maintenance

Wild type E14Tg2A mouse ES cells, isolated from 129P2/OlaHsd mouse blastocysts (Brennan and Skarnes, 1999, Hooper et al., 1987, Magin et al., 1992) were provided by Dr. Colin Miles (Newcastle University) and were cultured in E14 media (Table 2.6) containing LIF (produced in house, described in section 2.2.11, page 72) on gelatinised T25 flasks: 0.1% gelatin (Sigma G9391) in PBS was applied on the flasks for 5 minutes at 37^{o}C and then removed. Cells were passaged every 2 days, after trypsinisation with 0.05% Trypsin and resuspension in fresh media, as described before. The incubation conditions were 37°C in the presence of 5% CO_2.

2.2.5. Freezing and thawing cells

After trypsinization and centrifugation, as described before, cells were resuspended in freezing media (Table 2.6). The amount of media depends on the cell density and the required freezing concentration. 1 ml of cells in freezing media was quickly transferred in each cryovial. All cryovials were kept in an isopropanol container at -80^{o}C for 24-48 hours for slow freezing and then were moved in a liquid nitrogen tank for long-term storage. DMSO at RT is harmful for the cells so all procedures involving DMSO as a cryo-protective agent were performed rapidly.

Cells were thawed by rapid incubation of the cryovial of interest in a 37^{o}C water bath. The cryovial content was then transferred drop by drop, to avoid cell shocking, in a 15 ml falcon tube containing 9 ml of the appropriate media (STO, ES-D3 or E14). After a 5 minute centrifugation at 1000 rpm at RT and removal of the supernatant, cells were resuspended in 1 ml of media and plated in T25 or T75 flasks already containing 3 or 11 ml of media, respectively. For ES-D3 cells the flask needs to be layered with feeder cells and for E14 cells the flask needs to be coated with 0.1% gelatin.

2.2.6. The differentiation assay

The hanging drop method was used for the differentiation of stem cells (E14 and ES-D3) into embryoid bodies (EB) (Figure 2.3). After trypsinization and centrifugation, as

described before, cells were resuspended in 2 ml of differentiation media (Table 2.6). ES-D3 cells had to be pre-plated in order to get rid of the feeder layer cells, which could deter differentiation by producing LIF and other factors that keep cells in an undifferentiated state. The ES-D3 and feeder layer mixture was thus plated on a T25 flask for 40 minutes (experimentally defined); most of the feeder layer cells were found to be attached to the bottom of the flask by that time, while most of the ES cells were still floating. Therefore, the supernatant contained mainly ES cells and was used for subsequent experiments. E14 cells that were not grown on a feeder layer did not need this pre-plating step. Cells (ES-D3 cells after pre-plating and E14 cells after trypsinization) were then counted with a haematocytometer. A suspension of 15000 cells was achieved by appropriate dilution and 30 µl of this suspension was used for hanging drops. Approximately 80-90 hanging drops, containing 450 cells each, were set on the lid of each 100 mm dish (Iwaki, 3020-100) using a multipipette (Eppendorf Multipipette Plus). 10 ml of DPBS covered the base of the petri dish in order to avoid dessication of the hanging drops. This first day of the experiment was designated as day 0 (d0). After uninterrupted incubation at 37°C, 5% CO_2, the EB that formed within the hanging drops were transferred in suspension in 10 ml differentiation media in bacterial petri dishes and were allowed to grow for another 3 days. At day 5 (d5) EB from ES-D3 and E14 cells were transferred individually in 48 (NELS 3830-048) or 96 (Fischer Scientific TKT-521-110P) well plates in 500 or 200 µl of media, respectively. EB would adhere to the bottom of the wells, spread and grow over the course of the next 6 days. Plated EB were microscopically observed and imaged daily until day 11 (d11). At regular intervals throughout the assay (d0, d5, d11) cells were collected for further analysis.

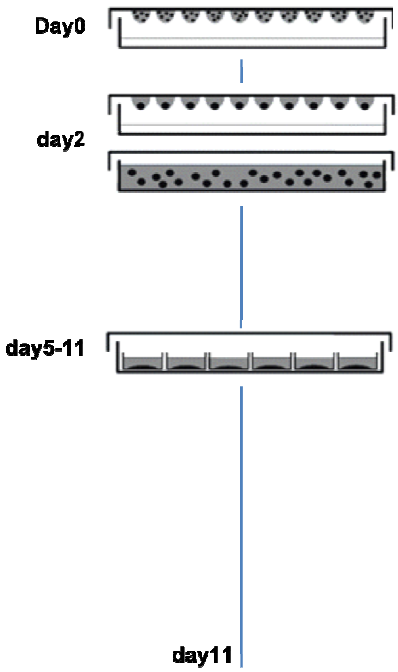

Figure 2. 4: Timeline of the ES cell differentiation assay. ES cells were set into hanging drops at d0 and by d2 EB have formed. EB were then transferred into suspension between days 2 and 5. At d5, EB were plated into the appropriate dishes (for details see text, section 2.2.6) and allowed to attach, spread, grow and differentiate until d11 (or d15 for some experiments, as described in Chapters 5 and 6).

When cells were needed for future immuno-cytochemical applications, EB were plated on round glass coverslips in 24-well plates at d5 and allowed to grow as described above until d11. Coverslips were treated with 0.1% gelatin and autoclaved. For ES-D3 cell experiments, FCS-containing media was used throughout the differentiation assay, while for E14 cell experiments FCS-free media was used after d5.

2.2.7. Use of chemical inhibitors

The appropriate concentration of drug (BIO or SP600125) or DMSO was added at the relevant time points in the culturing media. Thorough washes in DPBS followed removal of the drug or the DMSO to ensure that no traces remained. Drug dilutions were prepared fresh, just before use, from the stocks (Table 2.7).

Compound	**Target protein**	**Stock concentration**	**Working concentration**	**Experimental solvent**	**Experimental control**
BIO (Sigma B1686)	GSK3	1mM	**0.2µM / 1µM** on ES-D3 and E14 ESC	99.5% DMSO	0.1% DMSO
SP600125 (BioMol EI-305)	Jnk	10mM	**3µM** on zebrafish embryos / **5µM** on ES-D3 and E14 ESC	99.5% DMSO	0.03% DMSO 0.05% DMSO

Table 2. 7: Concentrations and details of the inhibitors used. BIO is an inhibitor of GSK3, was kept in a 1 mM stock in DMSO and was used at a concentration of 1 µM on E14 and ES-D3 cells. SP600125 is an inhibitor of Jnk, was kept in a 10 mM stock in DMSO and was used at a concentration of 3 µM and 5 µM on zebrafish embryos and cells (E14 and ES-D3), respectively.

2.2.8. Beating scoring and cell imaging

Scoring of beating was performed daily under a brightfield microscope (Zeiss AxioVert 25) and images were taken under a brightfield microscope (Zeiss AxioVert 200M) connected to a desktop computer.

2.2.9. Cell counting

Counting of cells at days 5, 8 and 11 was performed using the Vi-Cell XR-2.03 Counter (Beckman Coulter, Inc., FACS facility, IHG). This is a video imaging system that automates the widely used trypan blue dye exclusion protocol, which is based on the fact that when cells die their membranes become permeable and allow for the uptake of the trypan blue dye. Therefore, dead cells will appear darker than viable cells; viability can easily be calculated by measuring this contrast. The system can also measure the diameter of the cells (in microns) and their circularity (in units, where 1 represents a perfectly circular cell and 0 the least circular cell). Additionally, a de-clustering tool is available that increases the ability of the software to detect cells that are clumped together and can therefore measure and count them individually. This is of particular importance in this assay as cells within the EB are tightly clumped together and although trypsinization and manual disaggregation is applied before the measurements, this cannot be extended for long as it jeopardizes the quality and integrity of the cells to be analyzed. An extra level of control is provided by the fact that all imported images can be manually analyzed and corrected.

Single cell suspension of the samples of interest was prepared after thorough trypsinization, centrifugation and resuspension of cells in DPBS. Typically, 8-10 EB were used for each sample. Cells were then transferred into special cuvettes, provided at the FACS unit, and introduced in the cell counter.

2.2.10. Collection of cells for RNA extraction

At days 0, 5 and 11 cells were collected for RNA extraction and qPCR analysis. Day 0 and day 5 cells were in suspension and were collected in 15 ml falcon tubes. Day 11 cells were already plated so they had to be trypsinized, centrifuged and then collected in falcon tubes. 1 ml of Trizol reagent (Invitrogen 15596-026) was added to each falcon tube and after thorough mixing the samples were rapidly frozen at -80^{o}C, until further use. The downstream procedures (RNA extraction and cDNA synthesis) are described in Sections 2.1.8 and 2.1.9 (page 60).

2.2.11. Production of LIF

COS-7 cells were transfected with the LIF-producing plasmid pCAGGS-LIF (provided by Dr. Colin Miles, Newcastle University) using the Lipofectamine Transfection Reagent (Invitrogen 11668-027) according to the manufacturer's instructions. In brief, 24µg of the plasmid DNA were diluted to 50 µl and mixed with 1.5 ml of OptiMEM (Invitrogen 51985-026), while 60 µl Lipofectamine Reagent was mixed with 1.5 ml OptiMEM. These solutions were mixed together after a short 5 minute incubation at RT and then added to COS-7 cells, plated at 90-95% confluency in media lacking antibiotics. 6 hours past transfection the transfection mix was removed and replaced with 10% FCS-containing media. Transfected cells were cultured at 37°C, 5% CO_2 uninterrupted for 48 hours. Media containing LIF was generated from four 100 mm dishes (Iwaki 3020-100) and collected after filtration (0.2 µm filters). Testing was carried out for 42 days at various dilutions (1:250, 1:500, 1:1000, 1:2000, 1:4000) on wild type E14 ES cells plated on 6-well plates (Iwaki 3810-006), with each concentration tested in duplicate, in order to identify the optimal concentration for ES cell maintenance. A final concentration of 1:500 was decided as determined by comparison with a known LIF batch, produced and provided by Dr. Colin Miles.

2.2.12. Immunocytochemistry on coverslip-grown EB

EB grown on coverslips in 24-well plates were initially washed thoroughly in PBS in order to get rid of all remains of cell media. Because of the three dimensional structure of the EB prolonged fixation and permeabilization steps were applied and 0.03% Tween-20 (Sigma P1379) was included in all of the washes and incubations. EB were fixed in 4% PFA for 15 minutes at RT and then washed twice in PBS containing Tween for 5 minutes each time. Permeabilization of the cells was achieved by a 15 minute incubation in PBS containing 0.5% Triton-X100 (Sigma T8787), followed by two washes in PBS with Tween, as before. Incubation of the sections in PBS containing 10% fetal bovine serum (FBS, Sigma F7524) efficiently blocked non-specific binding sites. EB were then incubated in primary antibody solution overnight at 4°C in a humidified chamber. The desired dilution of the antibody of interest was performed in PBS containing 2% FCS (Table 2.8). The next day sections were washed twice in PBS, for 5 minutes each time, before being re-blocked in PBS with 10% FCS for another 10 minutes. Incubation in secondary antibody solution in PBS with 2% FCS was

performed for 1-2 hours at RT in a humidified dark chamber. Alexa Fluor (Invitrogen) secondary antibodies were typically used at 1:400 (Table 2.8). Hoerscht solution (Invitrogen) was used for staining the nuclei: 1:1000 dilution of the stock in PBS was applied for 15 minutes at RT in the dark. Two 5 minute PBS washes followed. The round glass coverslips with the EB on them were, then, transferred with forceps on a histobond slide and mounted in Vectashield (Vector Laboratories H-1400) with 25x50mm glass coverslips (VWR 631-0166).

Primary antibody				**Secondary antibody**		
Target	**Species**	**Dilution**	**Provider**	**Details**	**Dilution**	**Provider**
Cardiac TroponinI	Rabbit	1:300	AbCam 58544	Donkey anti-rabbit, 488	1:400	Invitrogen, Alexa Fluor, A21206

Table 2. 8: Details of all antibodies used for immunostaining on EB grown on coverslips (cardiac TroponinI staining).

2.2.13. Quantitative (real-time) PCR

2.2.13.1. An introduction to qPCR

Quantitative PCR (qPCR) is a very useful tool for assessing the levels of expression of genes of interest (Nolan et al., 2006). The SYBR-Green fluorescence technology was used (Ponchel et al., 2003). We used relative qPCR, whereby the relative levels of gene expression of different samples are compared to an internal calibrator. In this case the calibrator was the day 0 sample and its value was set by definition to 1; the levels of all other groups were expressed as fold changes of that. All samples were normalised against two housekeeping genes: *β-actin* (one of the components of the actin cytoskeleton of the cells) and *Rps9* (coding for the 40S ribosomal protein S9, a component of the small ribosomal subunit). Both were found to be expressed constitutively and in fairly stable levels throughout the experimental settings and were evaluated as good candidates. On the contrary, *Gapdh*, which is commonly used as a housekeeping gene in qPCR assays, was found to have a variable expression pattern in our system and was rejected. Therefore, all qPCR data presented in this study have been previously normalized against these two housekeeping genes. A negative control, lacking cDNA template, was included in every reaction and was always performed in triplicate.

2.2.13.2. The reaction

The reactions were prepared to a final volume of 10μl, containing 5μl SYBR Green mix (Sigma, S4438), 3μl distilled water, 0.5μl of each primer (10μM each, provided by MWG) and 1μl of cDNA (diluted 10 times). The reactions were set in 384-well plates (Greiner, 785290) under minimal light exposure. The plates were spun down before the run at 4000 rounds per minute for 5 minutes (Sorvall Evolution). For optimized conditions for each primer set see Table 2.8. After a 15 minute activation step at 95^{o}C, the cDNA template was denatured for 30 seconds at 95^{o}C, followed by primer annealing at 60/65^{o}C (experimentally defined) for 30 seconds and extension for 30 seconds at 72^{o}C. The denaturation-annealing-extension cycle was repeated another 39 times. Data collection for each cycle was performed at a temperature of choice, experimentally defined to match the temperature just before the peak of the melting curve. A dissociation curve was ran at the end of the 40 cycles, starting at a temperature typically 10 degrees lower than the data collection temperature and reaching a maximum of 99^{o}C. This curve was important for assessing the specificity of the fluorescence signal against, mainly, primer dimers.

2.2.13.3. qPCR optimisation

The annealing and melting temperatures of all primers were optimised before use in order to achieve satisfactory efficiencies and optimal amplification plots. Also, the efficiency of all primer sets was evaluated. To achieve this 10 fold dilutions of a control cDNA were used as templates for qPCR reactions with all primers. Efficiency slopes were then constructed and the efficiency of each primer set evaluated. The efficiency of all primer sets was found between 1.75 and 1.95. Specificity of each primer set was confirmed by running the qPCR products in a 2% agarose gel.

2.2.13.4. qPCR data analysis: the ΔΔCt method

qPCR data were analysed by relative quantification. This means that different cDNA were compared to each other and to a calibrator (one of the cDNAs examined that is set, arbitrarily, as 1) and that absolute values were not provided. The ΔΔCt method was used for calculation of the relative quantities (Pfaffl, 2001). Ct is the threshold cycle during a qPCR cycle. It represents the cycle at which the levels of fluorescence for a

given sample reach the threshold. The threshold is manually set, has to be the same for all runs and represents the time when the amount of fluorescence detected surpasses background fluorescence levels.

Gene	T_a	T_m	Melting curve peak
Rps9	60°C	84°C	87°C
β-actin	60°C	84/85°C	88-89°C
Tbx5	60°C	83°C	86°C
Nkx2.5	65°C	85°C	89°C
β-catenin	65°C	81°C	85-86°C
Mlc2v	65°C	81°C	85°C
Mlc2a	65°C	83°C	86°C
Gata-4	65°C	85°C	89-90°C
Brachyury	65°C	85°C	88-89°C
Goosecoid	60°C	83°C	87-88°C
Nanog	65°C	83°C	86-87°C
Oct-04	65°C	83°C	86-87°C
Sox2	65°C	83°C	88°C
Lef-1	65°C	78°C	81-82°C
Cardiac troponinI	60°C	82°C	85-86°C
Flk1	65°C	82°C	85-86°C
Tnnt2	60°C	82°C	85-86°C
Islet1	60°C	81°C	84-85°C
c-Myc	60°C	81°C	84°C
Cyclin-D2	60°C	83°C	86-87°C
Jnk	65°C	78°C	83°C
Connexin43	65°C	79°C	83-84°C
CD31	65°C	82°C	86°C
Hex	65°C	84°C	87-88°C
Dkk1	60°C	82°C	86°C

Table 2. 9: Optimised conditions for all mouse primers used in qPCR analysis. T_a: annealing temperature, T_m: melting temperature. For primer sequences see appendix.

Initially, samples had to be normalized against the housekeeping gene(s). So, the Ct value of the housekeeping gene for each sample (cDNA) was substracted from the Ct value of the gene of interest for the same sample. This value represents the ΔCt value. If more than one housekeeping gene was used, then the average of the Ct values of the housekeeping genes was used for calculation of the ΔCt values. Then, the Ct difference of one sample relative to the calibrator was calculated: the ΔCt value of the calibrator was substracted from the ΔCt value of the sample of interest. This represents the ΔΔCt value. Finally, the relative fold expression was calculated by the following formula: 2^{-}

$^{\Delta\Delta Ct}$. Number 2 represents the amplification efficiency of each gene: this will equal 2 only if after every PCR cycle each amplicon is duplicated. This is, however, not always true and the real primer efficiency of most primer sets is lower than 2. In Section 2.2.13.3 (page 74), it is explained how the efficiency of each gene can be calculated for more accurate results. In fact, in relative quantification the efficiencies of the gene of interest and of the housekeeping gene have to be quite similar; if not the results are not reliable. Below an example of ΔΔCt calculations is given:

> Let's hypothesize that we have *Tbx5*, as the gene of interest, and *Rps9*, as the housekeeping gene, and we want to test the expression levels of *Tbx5* in two cDNA samples: d0 ($cDNA_0$) and d11 ($cDNA_{11}$). We arbitrarily set $cDNA_0$ as the calibrator. The ΔCt values will be $\Delta Ct_0=Ct_{(Tbx5.0)}-Ct_{(Rps9.0)}$ for $cDNA_0$ and $\Delta Ct_{11}=Ct_{(Tbx5.11)}-Ct_{(Rps9.11)}$ for $cDNA_{11}$. The ΔΔCt value of *Tbx5* will be $\Delta\Delta Ct_n= \Delta Ct_n-\Delta Ct_0$, where n is any cDNA. So, the ΔΔCt of *Tbx5* for $cDNA_0$ will be 0 ($\Delta\Delta Ct_0= \Delta Ct_0-\Delta Ct_0$) and the ΔΔCt for $cDNA_{11}$ will be $\Delta\Delta Ct_{11}= \Delta Ct_{11}-\Delta Ct_0$. The relative fold change of *Tbx5* for $cDNA_0$ will be 1 (2^0) and for $cDNA_{11}$ it will be $2^{-\Delta\Delta Ct}{}_{11}$.

2.2.14. Western blotting

Western blotting was performed on ES-D3 cell lysates at d5 for the detection of phospho-Jnk levels. The housekeeping β-tubulin protein levels were used as a loading control. Antibodies used in western blotting are shown in detail in Table 2.9. All buffers used for this technique are described in Table 2.10.

2.2.14.1. Cell lysis

Cells were initially lysed in lysis buffer containing a protease inhibitor cocktail (freshly made solution, ThermoScientific 1862209) in order to maintain proteins intact. Pelleted cells were re-suspended in lysis buffer and incubated shaking on ice for 20 minutes. Any remaining cell clumps were dissociated using a 45μm needle. Samples were then centrifuged at 4°C, 12000 rcf for 20 minutes.

2.2.14.2. Protein measurement

A small aliquot of each sample was then used for protein measurement in the Nanodrop. The BCA assay kit (Thermo Scientific 23225, kindly provided by Dr. Elise Glen, IGM) was used for this purpose, as described by the manufacturer. A protein standard curve was firstly prepared through serial dilutions of an albumin stock of known concentration (2.0 mg/ml, provided with the kit). The albumin concentrations prepared were 0, 5, 25, 50, 125 and 250 μg/ml. Each albumin sample was mixed in a 1:20 ratio with a mixture of A and B reagents (provided with the kit), mixed in a 50:1 ratio. Samples were then incubated for 30 minutes at 37^{o}C. By measuring the absorbance of the purple-coloured product using the NanoDrop ND-1000 Spectrophotometer at 562 nm, a standard curve was prepared. By following the same procedure for the unkown protein samples it was possible to measure the amount of protein in the cell lysates.

2.2.14.3. SDS-PAGE gel running

Equal amounts of all protein samples (10 μg) were incubated with 2x laemli buffer in a 2:1 ratio for 3 minutes at 95^{o}C. This allowed denaturation and charging of the proteins. Samples were then left to cool at RT and were ran in a 10% sodium dodecyl sulfate polyacrylamide gel (SDS-Page, ready precast gels, BioRad 161-1155) along with a pre-stained protein standard size marker (Invitrogen, LC5800). Running buffer was used to fill the tank and the gap between the gel holders. The gel was ran at 100 volts at RT for 1-2 hours, or until the bands separated sufficiently. The proteins were then transferred from the gel to a nitrocellulose membrane, previously incubated for 30 seconds in 100% methanol, 2 minutes in distilled water and 20 minutes in transfer buffer. Blotting papers and sponges were also immersed in transfer buffer. The 'sandwich' structure for the gel transfer was as follows, starting from the cathode (negatively charged electrode): sponge, 2 blotting papers, gel, membrane, 2 blotting papers, sponge. Negatively charged proteins were transferred from the gel to the nitrocellulose membrane forced by the current from the anode to the catode for 1 hour at 4^{o}C at 100 volts.

2.2.14.4. Antibody incubation

After the transfer, the membrane was transferred into a weighing boat, where non-specific binding sites were blocked in Tris-Buffered Saline (TBS) containing Tween20 (TBST) and 5% block reagent (BSA, Sigma A2153, or milk powder) for 1 hour, shaking at RT. The membrane was then incubated in primary antibody solution overnight (Table 2.10), rocking at 4^{o}C, wrapped in sealable bags, cut to size. The appropriate primary antibody was used at 1:1000 dilution in TBST with 5% block reagent (BSA or milk). The next day, after three washes in TBST with 5% block reagent (BSA or milk) in a weighing boat shaking at RT, the membrane was incubated in secondary antibody solution. The appropriate secondary antibody conjugated with horseradish peroxidase (HRP) was used at 1:2000 dilution in TBST with 5% block reagent (BSA or milk), shaking for 1 hour at RT. Three washes in TBST with 5% block reagent (BSA or milk) for 15 minutes each, shaking at RT were followed by another three similar washes in TBST alone.

2.2.14.5. Chemiluminescence and film development

The membrane was then put flat, facing up, on a straightened piece of cling film. 1-3 ml (depending on the size of the membrane, enough to cover the whole surface) of West Dura chemiluminescent substrate (Fischer Scientific, 37071) was added on top of the membrane for 5 minutes at RT. After removing the excess of liquid, the membrane was covered by another piece of cling film, straightened and transferred into a dark box, facing up. In a dark room under red light a piece of photographic film (GE healthcare 28-9068-36) was then placed on top of the membrane. Light emitted by the reaction catalysed by HRP was directly correlated with the location and the amount of the protein of interest and was accurately transferred onto the film. Film development took place in a Medical Film Processor (Model slx-101A).

2.2.14.6. Membrane stripping

After the first chemiluminescence reaction, the membrane can be stripped off the bound antibodies and re-probbed with an antibody against another protein of interest, here β-tubulin. The membrane was incubated in stripping buffer twice for 10 minutes each time, at RT, shaking. It was then sequentially washed in PBS twice, 10 minutes each

time and then in TBS twice, 5 minutes each time, shaking at RT. Then the membrane was ready to be re-blocked and re-probed, as described in Section 2.2.14.4 onwards.

Blocking agent	Primary antibody				Secondary antibody		
	Target	Species	Dilution	Provider	Details	Dilution	Provider
BSA	*Phospho-Jnk*	Rabbit	1:1000	Cell Signalling 9251	Goat anti-rabbit HRP	1:2000	Dako P0448
Milk	*β-tubulin*	Mouse	1:1000	Sigma T-5293	Rabbit anti-mouse, HRP	1:2000	Dako P0260

Table 2. 10: Primary and secondary antibodies used for western blotting. Milk, although cheaper and more commonly used, could not be used as a blocking agent for phospho-Jnk probed membranes, as milk casein is a phospho-protein itself and can cause high background.

Buffers and solutions for western blotting					
10xTBS	**10xRunning buffer**	**10xTransfer buffer**	**Lysis buffer (NP40)**	**2xLaemli buffer**	**Stripping buffer**
24.23g Trizma-HCl	25mM Tris base	48mM Tris base	150mM NaCl	4% SDS	15g Glycine
80.06g NaCl	190mM Glycine	29mM Glycine	1% NP-40 (or TritonX-100)	10% 2-mercaptoethanol	1g SDS
H_2O to 1L	0.1% SDS	0.04% SDS	40mM Tris	0.004% bromophenol blue	10ml Tween20
pH 7.6	pH 8.3		pH 8.0	20% glycerol	H_2O to 1L
				0.125M TrisHCl	pH 2.2
				pH 6.8	

Table 2. 11: Buffers and solutions used for western blotting. Ingredients of lysis buffer, 2x Laemli buffer, stripping buffer and 10x TBS, running buffer and transfer buffer are shown.

2.3. *In silico* techniques

2.3.1. Servers and databases used

Initially, the genes of interest were investigated in online databases, namely Ensembl and NCBI. Through these servers orthologs and homologs of the genes of interest were

investigated. Due to regular updates of online databases it is important to note that the current study was conducted using information mainly from Ensembl release 62. The sequences of different splice variants and protein isoforms were compared between them and with other genes using ClustalW. This server comprises a fully automated program for global multiple alignment of DNA and protein sequences. Global alignments progressively align sequences across their entire length and need to use gaps representing insertions or deletions. Protein analysis and conserved motif investigation were achieved using online servers, such as Prosite, EML, InterProScan, Psipred and others. All databases and servers used in this study are listed in Table 2.12.

Database / Server	Function	URL
National Center for Biotechnology Information (NCBI)	genome database	http://www.ncbi.nlm.nih.gov/
Ensembl	genome database	http://www.ensembl.org/index.html
Eukaryotic Linear Motif (ELM)	protein functional sites search	http://elm.eu.org/
InterProScan (EMBL-EBI)	protein sequence analysis and classification	http://www.ebi.ac.uk/Tools/InterProScan/
PPSearch (EMBL-EBI)	protein motif search	http://www.ebi.ac.uk/Tools/ppsearch/index.html
PSIPRED	protein structure prediction	http://bioinf.cs.ucl.ac.uk/psipred/
ClustalW2 (EMBL-EBI)	sequence alignment	http://www.ebi.ac.uk/Tools/clustalw2/index.html

Table 2. 12: Databases and servers used during the bionformatics approach. Their applications and their URL are shown. Most of the *in silico* results shown in the next chapter (Chapter 3) are a summary of the information collected from all these websites.

2.3.2. Phylogenetic analysis

Phylogenetic and molecular evolutionary analyses were conducted using the Molecular Evolutionary Genetics Analysis (MEGA) software version 5 (Tamura et al., 2011). The method that was used in this study for the construction of phylogenetic trees was the character-based, maximum likelihood method (Felsenstein, 1981, Kishino and Hasegawa, 1990), based on the Jones-Taylor-Thornton (JTT) model for amino acid sequences (Jones et al., 1992) or on the Tamura-Nei model for nucleotide sequences

(Tamura and Nei, 1993), using the nearest-neighbour-interchange (NNI) heuristic method of tree inference, with a 95% site coverage cut-off and 500 repetitions of bootstrap testing.

The JTT model estimates the probabilities of change from one amino acid to another and is able to correct for multiple substitutions (Jones et al., 1992). It is, nowadays, used as a default setting in many maximum likelihood-based phylogenetic analysis tools. The Tamura-Nei model (Tamura and Nei, 1993) corrects for multiple hits, by taking into account the differences in substitution rates between nucleotides and the differences in nucleotide frequencies. It, also, distinguishes substitution rates of transitions (interchange of purines or pyrimidines) and transversions (change of purines to pyrimidines or vice versa).

The NNI method improves the likelihood of a tree by swapping individual subtrees with their neighbours in an attempt to get the tree with the highest probability of occurring. A 95% site coverage cut-off means that all positions that contain fewer than 95% alignment gaps and missing data were eliminated. Bootstrap analysis, explained in Section 3.1.6 (page 89), is essential for ascertaining the reliability of a given tree. 500 bootstrap analysis steps were performed for each inferred tree in the current study.

2.4. Statistical analysis

2.4.1. Experimental design

All experiments were conducted on at least three independent biological replicates (the exact number of repetitions is stated in the respective results sections). For cell experiments one biological replicate represents cells from one frozen batch, while for zebrafish experiments one biological replicate represents one clutch. The number of samples used in each replicate is stated along with the results of each experiment. PCR reactions and immunocytochemistry were performed in triplicate for each biological replicate because of the intrinsic variability of the techniques. In all cases, averages (for numerical data) or representative results (for qualitative data) are shown in the next chapters.

2.4.2. Statistical calculations

All statistical calculations were carried out in the Statistics Package for the Social Sciences (SPSS). For numerical data the normality of the distribution of the values was firstly assessed using the Kolgomorov-Smirnov test. If normality was confirmed, the appropriate parametric test was then carried out. If normality was rejected, the data were transformed to their logarithmic values. The normality of the logarithmic values was, in turn, assessed; if the logarithmic values were found to be normally distributed, the appropriate parametric tests were applied on these data, whereas if the logarithmic values were not found to be normally distributed, the appropriate non-parametric tests were applied in the original (linear) data (Ennos, 2006).

The most commonly used test for parametric data in this study was one-way Anova; if significance was found with one-way Anova testing between any of the groups examined, then a post hoc 2-sided Dunnett test would follow and this would show between which groups there were significant changes (and the exact p values). The most commonly used non-parametric test was the Mann Whitney test. Statistical significance throughout the document will be reported alongside the statistical test used for each specific group of data. For categorical data the chi-squared (χ^2) test or the χ^2 test for associations were used. These tests had to be carried out on raw numbers and not percentages, so, when necessary, statistical testing was conducted before further processing of the data (Ennos, 2006). Throughout this study statistical significance is indicated with asterisks in the corresponding graphs, with *$p<0.05$ and **$p<0.01$. P values lower than 0.000 (for example 10^{-6}) are not provided in SPSS and therefore are stated as 0.000 values here.

Chapter 3. Identification of *jnk* genes in zebrafish

3.1. Introduction

In this chapter, the zebrafish *jnk* genes are presented. Initially, *in silico* investigation led to the identification of all *jnk* genes and isoforms available to date. Further analysis of the structure and conservation of these genes and their corresponding proteins with bioinformatics tools revealed great similarities with known *jnk* genes in other species and confirmed the potential for functional conservation of the kinase activity of zebrafish jnk isoforms. Lastly, exploration of the expression pattern of *jnk* genes throughout zebrafish embryogenesis showed that mRNA of the genes and isoforms examined is produced *in vivo* at early developmental stages.

3.1.1. Fish-specific genome-wide duplication

The first goal of the current study was the identification of *jnk* genes in zebrafish. It was hypothesized that *jnk* genes additional to the three known mammalian *Jnk1, Jnk2* and *Jnk3*, might exist in the zebrafish genome, because of a fish-specific genome-wide duplication event. This took place in the lineage of ray-finned fish after it diverged from the lobe fin lineage (that included avian and mammalian species) approximately 350 million years ago and resulted in many of the genes of land vertebrates being duplicated in the zebrafish genome (Meyer and Van de Peer, 2005, Postlethwait et al., 2000) Examples of such duplications are the discovery of *tbx5a/tbx5b* (Albalat et al., 2010) and *hoxa13a/hoxa13b* (Ahn and Ho, 2008). It is common for one of the members of the duplicated pair (either the original copy or the gene that arose from the duplication) to accumulate mutations over the years, due to reduced evolutionary pressure, and to become inactivated (Postlethwait et al., 2000, Watterson, 1983). So, the number of duplicated genes present in two copies in the zebrafish genome to date is not known (Amores et al., 1998, Ellies et al., 1997, Postlethwait et al., 2000) and it is likely that many such duplicates remain unidentified. Thus, additional, still unidentified, *jnk* duplicates were hypothesized to exist in the zebrafish genome.

3.1.2. Conserved motifs for the regulation and specificity of Jnk signal transduction

The MAPK cascade has the ability to convert a variety of different extracellular stimuli into very specific and targeted cellular responses; therefore its tight regulation, coordination, timing and intensity are of paramount importance for reliable and efficient signal relay. In this section, some of the most important motifs of MAPK in general and JNK in particular are presented, principally associated with activation, inactivation and function of the proteins but also with their interactions with other cellular components.

A key point in the regulation of the MAPK pathway is through the change in the phosphorylation status of the proteins. The conserved T-X-Y motif (where X is glutamic acid, proline or glycine) found in the activation loop of MAPK is essential for their activation. Specifically, JNK proteins exhibit a T-P(proline)-Y motif, where they get phosphorylated, and therefore activated, by MKK4 and MKK7 (Derijard et al., 1994, Lin et al., 1995, Martin et al., 2005, Pearson et al., 2001, Roux and Blenis, 2004). The presence of such a motif (TPY) is essential for the kinases to be activated and further phosphorylate downstream targets.

Most of the kinases in an organism act in a very similar way, targeting in most cases very similar motifs on their substrates. For example, JNK, as proline-directed serine/threonine (S/T) kinases, they can phosphorylate either serine or threonine (S/T) residues within a proline (P)-containing sequence (S/T-P). These motifs are found in approximately 80% of all proteins so additional mechanisms that confer specificity and direct individual kinases towards their correct targets are required (Bardwell and Shah, 2006). One such mechanism is the existence of conserved motifs in molecules that interact with JNK. These motifs are called docking sites or domains (D-sites/domains) and mediate high affinity protein-protein interactions (Bardwell and Shah, 2006, Tanoue et al., 2000, Tanoue and Nishida, 2003). Such sites have been identified in activators, substrates and suppressors of JNK. Similarly, a motif within JNK containing acidic residues has been suggested to establish strong interactions with the basic residues of the D-sites. This domain is called the common docking domain (CD) (Biondi and Nebreda, 2003).

Although a high degree of specificity is conferred at many different levels of MAPK signalling, there is also significant overlap that should not be overlooked. Different subfamilies may share upstream activators and downstream targets, potentially allowing for cross talk and feedback between them (Qi and Elion, 2005, Rose et al., 2010, Turjanski et al., 2007). Additionally, proteins activated by one

pathway may act as negative regulators of another pathway (Juntilla and Koretzky, 2008), further complicating the interactions between the different cascades. In conclusion, MAPK form complex signal transduction networks, induced by a variety of stimuli and propagated through a vast array of mechanisms that confer specificity in order to achieve their multi-functional intracellular goals.

3.1.3. Phylogenetic analysis

In this study, analysis of the phylogenetic relationship of zebrafish *jnk* genes with their homologs from other species was pursued. It is, thus, important to introduce some of the basic concepts of phylogenetic analysis, including phylogenetic tree construction and bootstrapping.

Phylogenetics is the study of the evolutionary relationship between different groups of organisms, commonly using molecular and morphological data (Wiens, 2006). As evolution is a branching process, whereby species diverge, speciate or disappear, phylogenetic estimations are often represented as branching diagrams or trees, called phylograms. The length of the tree branches is proportional to the amount of inferred evolutionary change and, therefore, provides an estimation of the evolutionary relation of different molecules in various organisms. Simplistically put, the divergence between different branches (representing species, genes, taxa etc) is an illustration of how many differences there are between the sequences.

An important concept in phylogenetic analysis is the molecular clock. The molecular clock hypothesis states that DNA and subsequently protein sequences evolve at a relatively constant rate over time and among different organisms (Kimura, 1968, Kumar, 2005). A direct consequence of this hypothesis is that the differences between genetic sequences in any two species will be proportional to the time during which these two species have diverged from their common ancestor. Therefore, this hypothesis provides a useful method for estimating evolutionary relationships. However, this hypothesis does not hold true in all cases and is nowadays thought to be quite simplistic, since the rates of molecular evolution can vary significantly between different species. Most of the models employed today for molecular phylogenetic analysis use the so-called ‘relaxed’ molecular clocks, which allow the molecular evolutionary rates to vary among organisms, but in a limited way or within a specific range (Bromham and Penny, 2003, Weir and Schluter, 2008).

According to the molecular clock hypothesis, the type of mutation that is particularly useful in inferring evolutionary changes is the substitution, the change of one base for another at one specific locus within a DNA sequence. Substitutions are random and therefore, as the model suggests, more time means more chance for them to occur. Based on chemical properties, certain substitutions happen more often than others, and this can be represented by probabilities that are commonly embedded in phylogenetic models. For example transitions, which are interchanges of purines (with two-ring bases, such as Adenine or Guanine) or pyrimidines (with one-ring bases, such as Thymidine or Cytosine), are more frequent than transversions, which are interchanges of purines for pyrimidines and vice versa (Keller et al., 2007). In contrast to substitutions, insertions and deletions, with which large chunks of a gene can be inserted or deleted, respectively, in a short period of time, do not always agree with the molecular clock hypothesis but can be detected and accounted for by sequence alignments (Keller et al., 2007, Schwartz and Mueller, 2010).

3.1.4. Phylogenetic trees

The evolutionary hypothesis of a phylogeny, as instructed by specific models, can be graphically represented in a phylogenetic tree (Figure 3.1). The tree consists of nodes and branches. The tips of the tree (leaves) represent taxa or operational taxonomic units (OTU), which can be any biological unit (an individual, a species or a higher grouping). The branches of the tree connect different leaves and represent the inferred evolutionary divergence between them. Trees can be either rooted or unrooted. A rooted tree has a defined common ancestor, whereas an unrooted tree does not. An outgroup, an OTU that is the least related to the group of taxa of interest, can be used as a tool for rooting trees (Figure 3.1). The nodes are the points where branches separate and represent hypothetical common ancestors. The order of the nodes and the branching pattern of the tree determine its topology and describe how different units have diverged from one another over the course of time. Trees can be rotated at their nodes without changing their topology.

Traditionally, phylogenetic trees were constructed using descriptive morphological observations but nowadays, with the growth of genetic information, it is possible (and common) to use molecular data for inferring evolutionary history. This type of phylogeny is called molecular phylogeny and is typically based on DNA or protein sequences (Felsenstein, 2001).

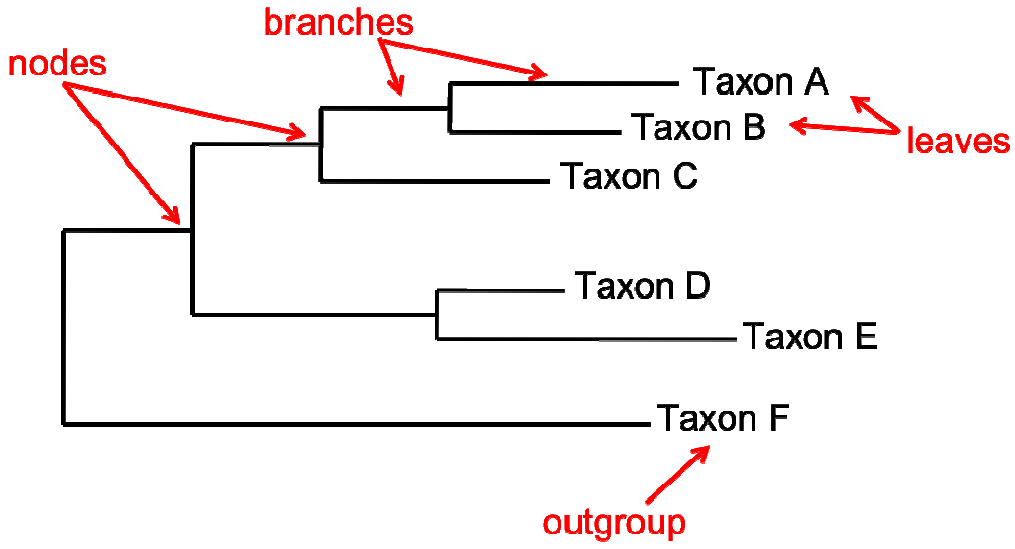

Figure 3. 1: Example of a phylogenetic tree with some points of reference. The tips of the tree, often referred to as leaves, are where the taxa are. A taxon or OTU can be any biological unit: a species, a family or even a whole kingdom. The branches are the lines that connect the leaves and represent the inferred evolutionary relationship between them. The nodes are the points where the branches bifurcate and represent hypothetical ancestral units. The outgroup is used as a basis for the analysis of the phylogenetic relationships.

3.1.5. Constructing molecular phylogenetic trees

There are many different ways for constructing a phylogram, each with its own advantages and disadvantages. The two main categories for constructing molecular phylogenies are distance-based and character-based methods (Felsenstein, 1996, Holmes, 2003, Whelan et al., 2001). The first type is semiparametric and relies on a pairwise measure of genetic 'distance' from multiple sequence alignments. Essentially, these methods convert the observed character differences (differences in amino acids or nucleotides) into distances, comparing two sequences at a time. The main disadvantage of these methods is their inability to use all sequence information at once, as they reduce characters to distances and a lot of information is lost; for example multiple hits and back mutations cannot be detected. Also, because of the pair-wise nature of the comparisons, the distances are never independent. However, they are extremely fast and easy to perform and most of the times they give a good estimate of phylogeny. Two widely used methods of this category are Unweighted Pair Group Method using

Arithmetic averages (UPGMA) and Neighbour Joining (Bruno et al., 2000, Whelan et al., 2001).

The second category for phylogeny construction comprises character-based methods, which use all individual characters (amino acids or nucleotides) in order to infer phylogeny. They estimate the total number of mutations required to explain the observed character sequences and they make use of all known evolutionary information in order to determine the most likely ancestral relationships. The most frequently used character-based methods are the maximum parsimony method, which constructs trees that require the minimal number of changes to explain the current data, and the maximum likelihood method, which creates trees with the highest likelihood of occurring with the given data (Rogers, 1997, Steel and Penny, 2000, Whelan et al., 2001). Although more labour-intensive, computationally demanding and time-consuming than distance-based methods, they give a more reliable phylogenetic tree estimation. A main drawback is the fact that they use the two models of evolution (that of parsimony and maximum likelihood, respectively), which are not necessarily true for all characters (Holmes, 2003).

The approach to adopt is chosen depending on the available data and the required outcome, as exemplified below. UPGMA assumes that all lineages evolve at the same rate (molecular clock hypothesis, explained in detail in Section 3.1.3, page 85), which is sometimes an inaccurate assumption, but is able to provide a rooted tree rapidly. Neighbour Joining is preferable when evolutionary rates are known to vary. Maximum parsimony is ideal for closely related sequences. Maximum likelihood is the most general and statistically robust of all because its assumptions are explicit and can be modified to suit the needs (Holmes, 2003).

The method that is used in this study for the construction of phylogenetic trees is the character-based, maximum likelihood method (Felsenstein, 1981, Kishino and Hasegawa, 1990). This method tests a hypothesis by assessing the probability that the proposed model and the hypothesized evolutionary history would generate the observed data set. The history with a higher probability of generating the current alignment is preferred and the tree with the maximum likelihood is generated. A simplified step-wise description of the procedure would be as follows: an evolutionary model is selected, all possible tree structures are generated for each position of the alignment, the likelihood of all positions in these trees is calculated based on the chosen model, the likelihood for each tree is calculated by multiplying the likelihood for each position within that tree

and the tree with the greatest likelihood is chosen (Guindon and Gascuel, 2003, Holmes, 2003).

A detailed description of how the maximum-likelihood trees were constructed is provided in Chapter 2 (Section 2.3.2, page 80). Briefly, the amino acid or DNA sequences of interest were aligned in ClustalW (Section 2.3.1, page 79) and were then further analyzed in the MEGA5 software (Tamura et al., 2011). The appropriate models (JTT or Tamura-Nei) were selected for estimation of the substitution rates, as described in Section 2.3.2 (page 80).

3.1.6. Bootstrapping

Another important concept in phylogenetic analysis is bootstrapping. Similar to statistics, where the significance of the data is shown with p-values, the evaluation of the reliability of a phylogenetic tree is done by bootstrap analysis (Felsenstein, 2001, Holmes, 2003). The basic idea behind bootstrapping is the re-shuffling of the characters in the alignment data and the construction of a new tree based on the re-shuffled values (Efron et al., 1996). Then, the topology of the new tree is compared to the topology of the original tree. If the new tree is similar to the original tree, then the confidence in the original tree increases. On the other hand, if the new tree is very different to the original tree then the reliability of the original representation is low (Efron et al., 1996, Felsenstein, 2001, Holmes, 2003). This comparison is done by scoring all individual branches of the trees before and after re-shuffling: each interior branch of the original tree that is different from the boostrapped tree is given a score of 0, while interior branches that remain the same after re-shuffling are given a score of 1. By repeating this procedure a number of times (typically hundreds of times), it is possible to score the reliability of each branch of the original tree by calculating the percentage of times each branch was given a value of 1; the higher the bootstrap score the greater the reliability. A score of 95% or higher indicates that the branching is ‘correct’ (Nei and Kumar, 2000).

Boostrap analysis can be performed in the MEGA5 software package (Tamura et al., 2011) used in this study. 500 bootstrap repetitions were performed in this study for each tree in order to quantify certainty and estimate confidence in the constructed trees. The percentage of trees in which the taxa of interest clustered together in 500 boostrap replicates, is shown next to the branches in each tree.

3.2. Aims of the chapter

Jnk genes and proteins have been identified and studied in many organisms. In zebrafish, although a number of studies have explored the putative roles of jnk during embryonic development, the *jnk* genes have not been extensively studied. In this study, I set out to investigate the *jnk* genes and proteins in zebrafish. In order to achieve this the following aims were set:

- Characterize all zebrafish *jnk* orthologues, with a specific focus on identifying new *jnk* genes that arose after the fish genome duplication
- Determine *jnk* splice variants and jnk protein isoforms
- Elucidate the primary and secondary structures of the proteins of interest and identify evolutionarily conserved motifs
- Establish their phylogenetic relations with other species
- Determine their spatial and temporal expression pattern in developing zebrafish embryos

3.3. *In silico* analysis

Initially, I set out to identify and study all *jnk* genes and isoforms in zebrafish. For this purpose, genome databases were examined for the presence of zebrafish *jnk* genes. Among the three available genomic databases (Ensembl, NCBI, UCSC), Ensembl was preferred. Genes in Ensembl are annotated automatically, based on experimental evidence. Manual curation by the HAVANA team supports the automatic annotations. In turn, gene annotation in NCBI (National Centre for Biotechnology Information) is based on published information and is therefore more limited. The UCSC browser accommodates both published and experimentally predicted annotations but does not have a zebrafish entry. Therefore, by using Ensembl (and comparing with NCBI when necessary), it was possible to identify all predicted zebrafish *jnk* genes and study them in detail. Ensembl releases new genebuild findings and updates its browser frequently; since new information is included in every new release, it is important to note that the current data are based on Ensembl Release 62.

Four features of the *jnk* genes were of main interest: the different splice variants of each gene, the structure of the proteins produced by these variants and the similarities

between them, the presence of conserved motifs and the phylogenetic relationship with their orthologues in other species. The findings from the *in silico* investigation are presented below.

3.3.1. Jnk orthologues in zebrafish; characterization of an extra jnk gene

As mentioned earlier, one of the main focus of this study was to identify new *jnk* genes in zebrafish, additional to the three known mammalian genes, that might have arisen from the fish-specific genme-wide duplication event (Meyer and Van de Peer, 2005, Postlethwait et al., 2000). When the current study was being carried out only one jnk gene (*jnk1*) had been identified and studied (Krens et al., 2006). At present, four *jnk* genes have been identified in zebrafish, named *jnk1a-1, jnk1a-2, jnk2* and *jnk3* (Seo et al., 2010), as described in Sections 1.5.2 and 1.5.4 (pages 38 and 41). However, they have not been studied and characterized. In parallel with the aforementioned publication (Seo et al., 2010), the current study was being carried out, focusing on characterizing and further analyzing the identified genes. Following the official nomenclature for duplicated genes proposed by the National Zebrafish Model Organism Database (ZFIN, zebrafish nomenclature guidelines) zebrafish *jnk* genes are named in this study *jnk1a, jnk1b, jnk2* and *jnk3*.

In silico investigation of online databases revealed four orthologues of the three mammalian *Jnk* genes, named (in Ensembl) as follows: *mapk8* (*jnk1,* here called *jnk1a*), *mapk8* (*jnk1,* here called *jnk1b*), *mapk9* (*jnk2*) and *mapk10* (*jnk3*). *Jnk1a* is located on chromosome 12, *jnk1b* on chromosome 13, while *jnk2* and *jnk3* lie on chromosome 21. A table with details about all four genes is presented below (Table 3.1). At the time that this work was being carried out the genes *jnk1b* and *jnk2* had not been identified yet and appeared as unknown, predicted genes (experimentally defined but not published). It was, thus, important to establish whether *jnk1b* arose from a duplication of *jnk1a*, *jnk2* or *jnk3*, as its name at the time did not reveal its origin. In order to elucidate this, three methods were employed: comparison of the divergence of the cDNA sequences of the four genes, analysis of their evolutionary relationship and comparison of the chromosome loci that they occupy. Searching for homology between *jnk1b* on one hand and *jnk1a*, *jnk2* and *jnk3* on the other, it was confirmed that *jnk1b* is likely to have arisen from the duplication of *jnk1a* and not *jnk2* or *jnk3*, as presented below.

Gene Name	Transcript Name	Ensembl Accession Code	Transcript length (bp)	N^{o} of exons	Protein length (aa)	Location
jnk1a	jnk1a.1	ENSDART0000145213	1029	7	256	Chr.12
	jnk1a.2	ENSDART0000086510	943	8	260	
	jnk1a.3	ENSDART0000128677	1287	11	428	
	jnk1a.4	ENSDART0000022471	2059	12	384	
jnk1b	jnk1b.1	ENSDART0000049180	1618	11	427	Chr.13
	jnk1b.2	ENSDART0000139591	1796	12	427	
	jnk1b.3	ENSDART0000132129	2211	12	427	
	jnk1b.4	ENSDART0000146250	421	3	88	
jnk2	jnk2	ENSDART0000112550	1758	12	421	Chr.21
jnk3	jnk3.1	ENSDART0000086521	1293	13	430	Chr.21
	jnk3.2	ENSDART0000042429	1155	11	384	
	jnk3.3	ENSDART0000134892	1756	14	433	
	jnk3.4	ENSDART0000141848	1863	15	430	
	jnk3.5	ENSDART0000086509	1850	16	430	
	jnk3.6	ENSDART0000134195	1887	14	384	
	jnk3.7	ENSDART00000142547	861	6	210	
	jnk3.8	ENSDART0000014434	674	5	102	

Table 3. 1: Zebrafish *jnk* genes and isoforms. Chromosome location, transcript and protein length, as well as the gene identities in Ensembl are shown here. Aa: amino acids, bp: base pairs, chr: chromosome.

Initially, pairwise comparisons of transcripts from all zebrafish *jnk* genes were performed in order to assess the sequence divergence of the genes. For this purpose, cDNA sequences of *jnk* transcripts were aligned using the ClustalW server (Table 2.12, page 80) and then pairwise comparisons were performed using the MEGA5 software (Tamura et al., 2011). Specifically, p-distances between pairs of cDNA sequences were estimated. A p-distance is the proportion of nucleotide sites at which two sequences are different and is obtained by dividing the number of nucleotide differences by the total number of nucleotides. Comparison of the sequence differences between *jnk* transcripts showed that *jnk1a* and *jnk1b* are more similar (in terms of their cDNA sequence) to each other than they are to *jnk2* and to *jnk3* (Figure 3.2). All transcripts of each gene were compared to all transcripts of another gene for an unbiased evaluation and the mean values are presented in Figure 3.2.

An analysis of the evolutionary relations of the four *jnk* genes and their transcripts was also performed and is shown in the tree in Figure 3.3. Coding transcripts (cDNA sequences) of all genes were initially aligned using the ClustalW server and were then further analysed in MEGA5 (Tamura et al., 2011). Evolutionary history was inferred by using the maximum likelihood method based on the Tamura-Nei model (Tamura and Nei, 1993), using the nearest-neighbour-interchange (NNI) heuristic method of tree

inference, with a 95% site coverage cut-off and 500 repetitions of bootstrap testing (see Section 2.3.2 at page 80 for details on these models). From this tree it is evident that *jnk1a* and *jnk1b* transcripts seem to be evolutionarily more closely related between them than either of them is with *jnk2* and *jnk3* transcripts (Figure 3.3). Specifically, all transcripts of *jnk1a* and *jnk1b* cluster close to each other, with excellent bootstrap scores (100%), which ascertain the reliability of the tree topology. A bootstrap value of 100% means that all the trees that were constructed after re-shufflling the data (500 times) agreed on the current topology of the branches. Therefore, it seems likely that *jnk1a* and *jnk1b* are members of a duplicated gene pair.

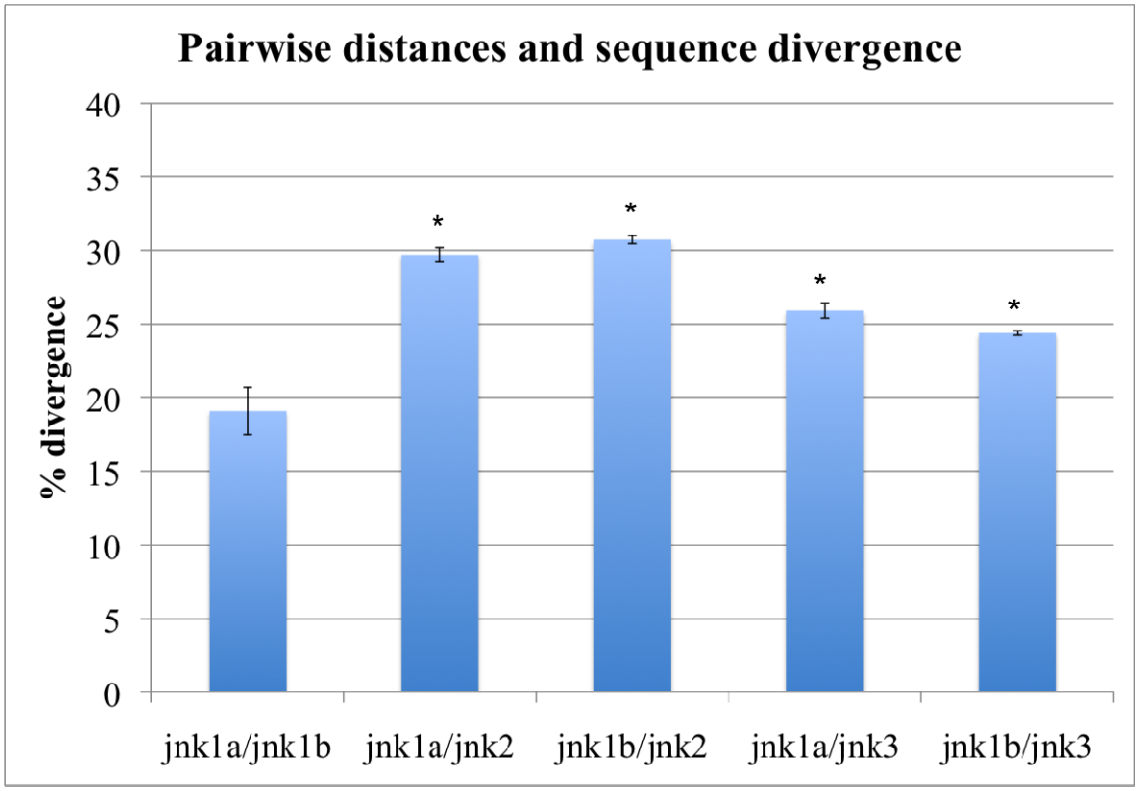

Figure 3. 2: Graphic representation of the percentage of sequence divergence between zebrafish *jnk* cDNA. Pairwise distances were calculated using the MEGA5 software and were converted to sequence divergence percentages. Information from all transcripts of each gene was included in the calculations. Shown are the mean values of all transcripts for one gene against the mean values of all transcripts for another gene: for example the differences between *jnk1a* transcripts and *jnk1b* transcripts are shown in the first column. More differences mean more distantly related genes. Non-parametric statistical testing was used (Mann Whitney test). Asterisks indicate statistical significance compared to the jnk1a/jnk1b values. *p<0.05.

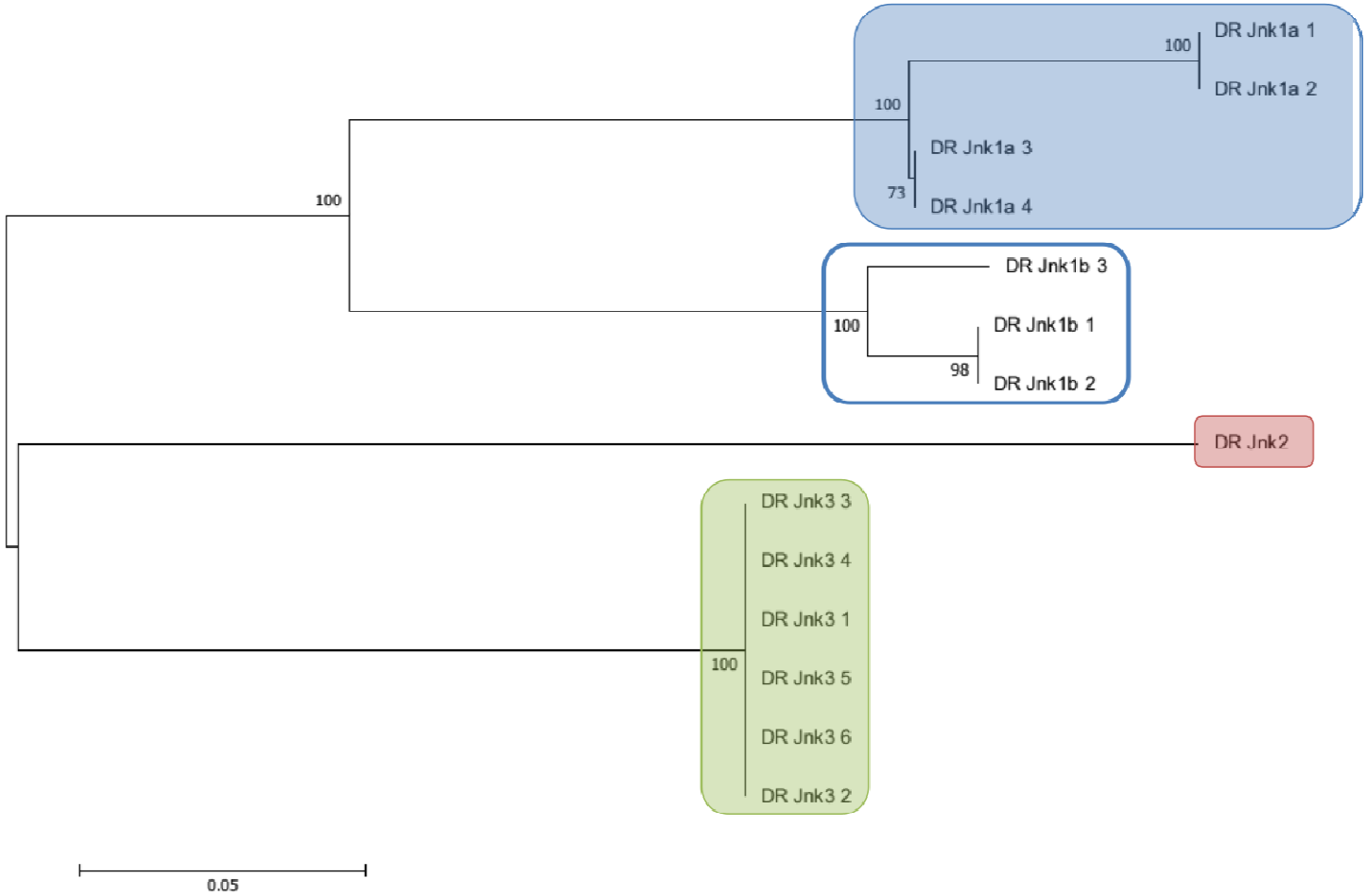

Figure 3. 3: Molecular analysis showing the evolutionary relation of *jnk* nucleotide sequences in zebrafish (*Danio rerio*, DR). Evolutionary history was inferred by using the maximum likelihood method based on the Tamura-Nei model. The tree with the highest likelihood is shown. The percentage of replicate trees in which the associated groups clustered together in the bootstrap test (500 replicates) is shown next to the branches. The tree is drawn to scale with branch lengths measured as the number of substitutions per site (the scale bar indicates 0.05 substitutions per site). The analysis involved 14 nucleotide sequences and was conducted in MEGA5.

Additionally, the chromosome locations of the zebrafish *jnk* genes were compared, because any genome duplication event would have included duplication of large areas of the chromosome, spanning probably more than one gene. The genes surrounding the *jnk1a* and *jnk1b* loci in chromosomes 12 and 13, respectively, were found to share high levels of paralogy: four genes, namely FRMPD2, ARHGAP22, LRRC18 and C10orf72 lie on either side of *jnk1a*, while putative paralogues of these genes lie on either side of *jnk1b* (ntpn20, ARHGAP22, LRRC18, C10orf72) (Figure 3.4). Similar comparisons of the *jnk1b* loci with the *jnk2* and *jnk3* loci did not yield similar associations. This observation reinforces the notion that *jnk1a* and *jnk1b* form a pair of duplicated genes, with one having arisen from the other.

Although *jnk1a* was identified first (*jnk1* in Krens et al. 2006), it is not clear if it was the chromosomal locus around *jnk1a* or *jnk1b* that became duplicated and gave rise to the other gene. Duplication of the regions around *jnk2* and *jnk3* were not detected (Ensembl release 62) but future Ensembl releases may reveal additional genes.

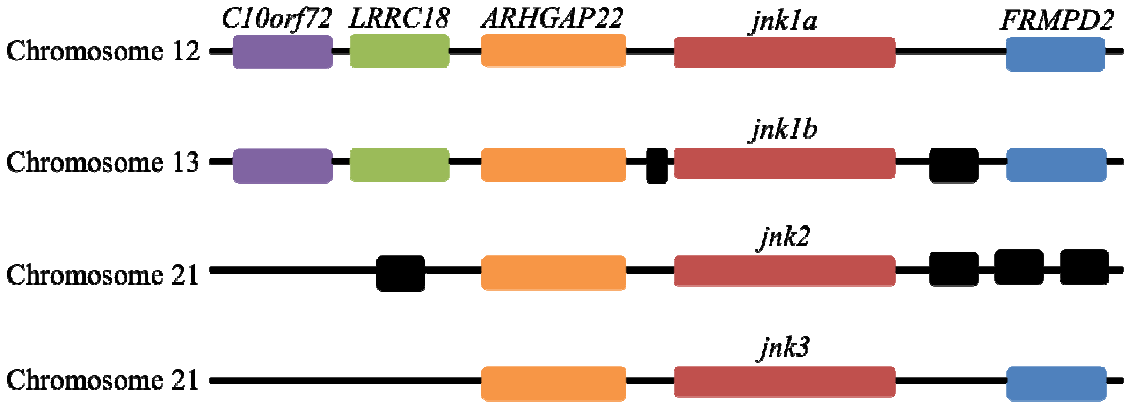

Figure 3. 4: Comparison of the jnk loci in chromosomes 12, 13 and 21. *Jnk1a* is flanked by 4 genes, copies (paralogues) of which are also found around *jnk1b*. A copy of one of the genes that is adjacent to *jnk1a* is also found in the area where *jnk2* lies, while copies of two genes flanking *jnk1a* are also found in the chromosome 21 locus where *jnk3* lies. Genes are represented in boxes. Same coloured boxes indicate paralogy. Black boxes indicate genes that were found not to have any associations between the different chromosomes. The length of the boxes is not necessarily proportional to the length of the genes.

3.3.1.1. Alternative splice variants of jnk1a, jnk1b, jnk2 and jnk3

After identification of the zebrafish *jnk* genes in online databases, analysis of their transcript variants was of interest. *Jnk2* contains one transcript of 1758 base pairs in

length, which contains 12 exons and encodes a 421 amino acids protein (Table 3.1). In contrast, *jnk1a, jnk1b* and *jnk3* were found to contain more than one transcript, which through alternative splicing lead to the production of different protein isoforms. Specifically, *jnk1a* was found to contain four splice variants, 1287, 2059, 943 and 1029 base pairs in length, containing 11, 12, 8 and 7 exons and coding for 428, 384, 260 and 256 amino acids proteins, respectively. Similarly, *jnk1b* was found to contain four protein-coding splice variants (and one non-protein coding transcript), 2211, 421, 1618 and 1796 base pairs in length, containing 12, 3, 11 and 12 exons and coding for 427, 88, 427 and 427 amino acids proteins, respectively. *Jnk3* has eight protein-coding splice variants (and one non-protein coding), 1155, 1850, 1293, 861, 674, 1756, 1863 and 1887 base pairs in length, containing 11, 16, 13, 6, 5, 14, 15 and 14 exons and encoding 384, 430, 430, 210, 102, 433, 430 and 384 amino acids proteins, respectively (Table 3.1). Most of the differences between the transcripts of each gene lie in the 5' and 3' untranslated regions and in the first few or last few exons. The central exons are shared between all transcripts, indicating, as will be shown in the next few sections, that the core domain of the proteins that are produced by these transcripts is present in all of them. In fact, most of the exons are shared between isoforms of all four genes (Figure 3.4). One extra exon appears to be present in *jnk3* splice variants, missing altogether from *jnk1a, jnk1b* and *jnk2*.

Taken together, the four *jnk* genes that were identified in the zebrafish genome in online databases have 19 transcripts (splice variants), 17 of which code for proteins of different sizes. Next, the jnk proteins were studied in more detail, by looking at their primary and secondary structure.

3.3.1.2. Primary structure of jnk proteins in zebrafish

Next, the primary structure of all variants of the jnk proteins was investigated in order to evaluate where the differences and similarities between them lie. This was performed by pairwise alignment of their amino acid sequences in ClustalW. Only small differences could be observed (Figures 3.4 and 3.5) between the amino acid sequences of the examined proteins. Jnk1a.1 and jnk1a.2 only have minor differences in the carboxyl (C)-terminal region. Similarly, jnk1a.3 and jnk1a.4 differ only in their last amino acids. The differences between jnk1a.1 and jnk1a.2 on one side and jnk1a.3 and jnk1a.4 on the other are again restricted in their C-terminal region, making the two latter variants (jnk1a.3 and jnk1a.4) longer than the former ones (jnk1a.1 and jnk1a.2).

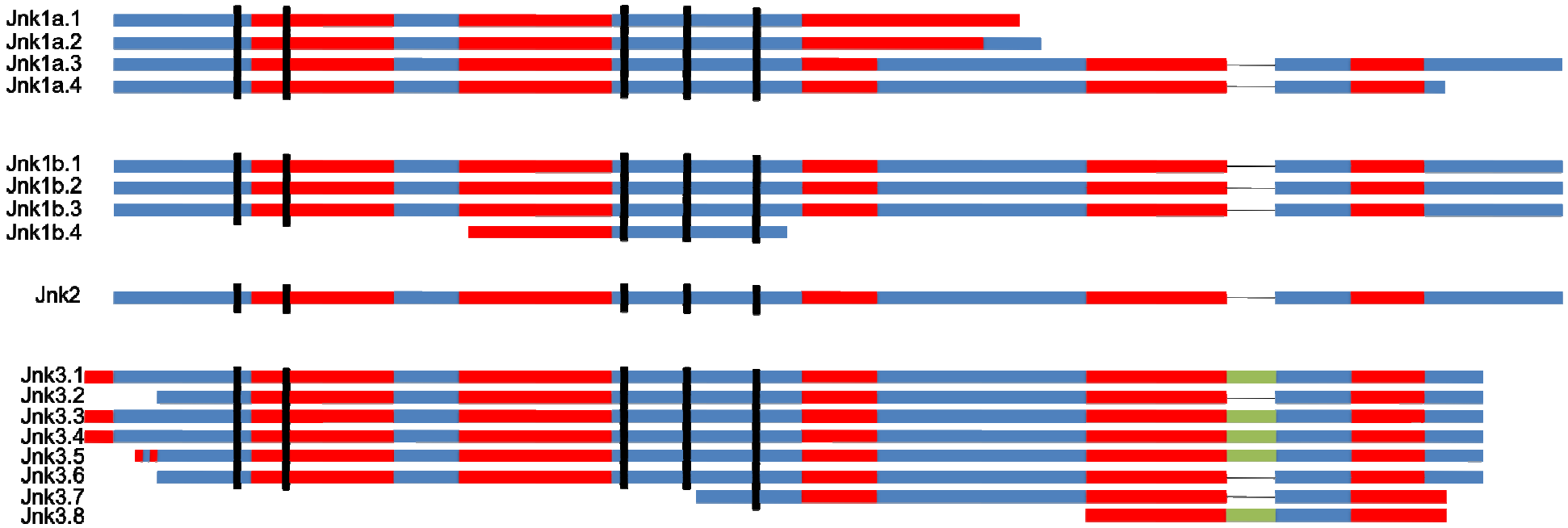

Figure 3. 5: Schematic representation of *jnk* genes in zebrafish. Splice variants of all genes are shown here: four transcripts of *jnk1a*, four transcripts of *jnk1b*, one transcript of *jnk2* and eight transcripts of *jnk3*. Alternate exons are shown in alternate colours. The length of each exon is proportional to its nucleotide and amino acid length. Introns are not shown in this diagram. The horizontal thin grey lines in *jnk1a*, *jnk1b*, *jnk2* and some *jnk3* isoforms highlight the area where the 'green' exon of *jnk3* is. This exon is absent in *jnk1a*, *jnk1b*, *jnk2* and some *jnk3* isoforms. Vertical black lines represent areas, where important motifs of the proteins lie, as discussed in Section 3.3.1.3 (page 99). This schematic representation was manually drawn using information from nucleotide and amino acid sequences of all transcripts.

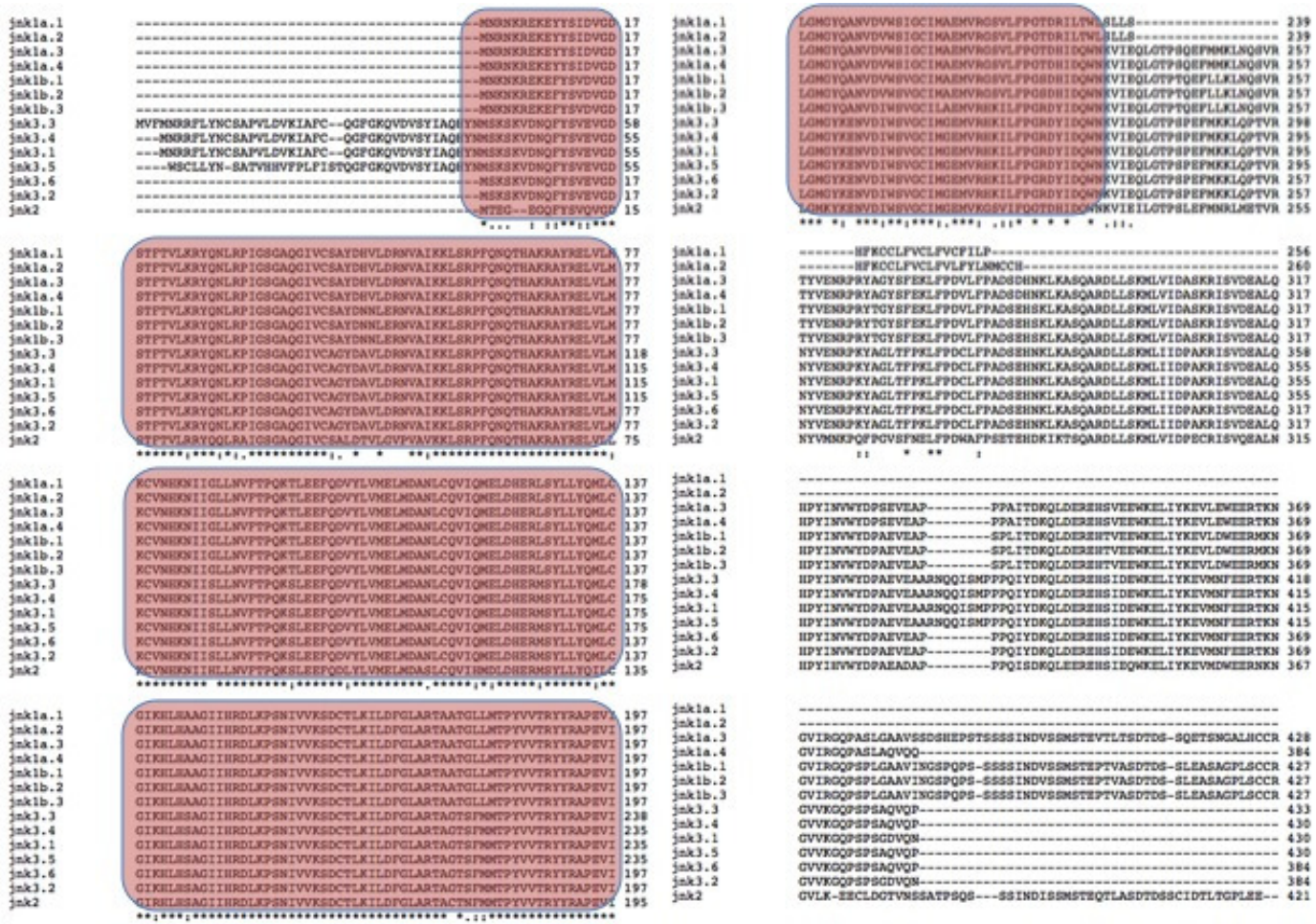

Figure 3. 6: Alignment and comparison of the zebrafish jnk amino acid sequences. Only non-redundant sequences were used. The alignment is shown in two columns. Highlighted in red is the core area of high conservation. (*) shows identical residues in all sequences of one column, (:) shows conserved substitutions (substitution of one amino acid with another one of similar properties) and (.) shows semi-conserved substitutions (substitution of one amino acid with another of similar steric conformation but different chemical properties). The sequences are presented in single letter code. The alignment was performed using the ClustalW online server.

Jnk3.1, jnk3.3, jnk3.4 and jnk3.5 exhibit only a few amino acid differences in their amino (N)-terminal domain but are identical in the rest of the sequence. Jnk3.2 and jnk3.6 are identical in length and present negligible amino acid substitutions. Interestingly, all jnk protein isoforms of all four genes seem to share approximately 69-82% of their amino acid sequence, with changes mainly observed outside the core (middle) region of the protein and located at its termini (Figures 3.5 and 3.6). Whether these seemingly insignificant amino acid differences bear structural or functional importance is examined below.

3.3.1.3. Secondary structure and conserved motifs of jnk proteins in zebrafish

The next aim of the current study was to detect conserved motifs in the newly identified protein isoforms that would relate to the functionality of the proteins. Therefore, the amino acid sequences of jnk were further analysed using online databases and servers that can predict the secondary and tertiary structure of the proteins, as well as indicate conserved domains and short motifs related to their functionality and activity. The bioinformatics tools used in this study are listed in Table 2.12 (page 80) and the information provided below represents a summary of all the findings collected from these tools.

First, the secondary structure of the proteins of interest was examined. It was shown that the secondary structure of all proteins was similar, containing mainly β-strands on the N-terminus and α-helices in the C-terminus. This conformation matches perfectly the typical eukaryotic protein kinase fold, which comprises two lobes, the N-terminal one that is rich in β-structures and the C-terminal one, rich in α-helices (Bogoyevitch, 2006). β-structures or β-strands are stretches of polypeptide chains typically 3-10 amino acids, in an almost fully extended conformation. In fact, the proteins examined seem to differ only in their length and therefore in the number of helices they contain in the C-terminus, while the N-terminus and the core of the molecule appear indistinguishable (Figure 3.7).

Figure 3. 7: Secondary structure of zebrafish jnk proteins. Only one sequence is shown here for a clearer representation but all of them were identical. β-strands are shown with brown boxes. Strands are connected laterally by 2-3 hydrogen bonds, forming β-sheets. Helices, shown in yellow, represent α-helices.

Additionally, using the EML and InterProScan databases all of the jnk isoforms were found to comprise the same conserved domains: among others, a serine/threonine-protein kinase domain, a MAPK conserved site and an ATP-binding site, all of which are important for the activity of the MAPK and therefore the JNK proteins (Figure 3.8). Characteristic of JNK proteins is the presence of a glycine (G)-rich motif in the vicinity of a lysine (K), involved in ATP binding, and an aspartic acid residue (D), important for the catalytic activity of the kinase (Knighton et al., 1991). As shown in Figure 3.8 these conserved residues were found in all predicted jnk proteins examined. Additionally, T-P-Y motifs, which are essential for activation by upstream kinases, were found in all protein structures (shown with black lines in Figure 3.5). The MAPK signature motif, which is located adjacent to the TPY motif, was, also, identified in all isoforms. This region contains a phenylalanine (F) and a cysteine (C) at the two extremities of the region of interest that are MAPK-specific. The arginine (R) and glutamic acid (E) in the first part of the pattern, and the arginine (R), aspartic acid (D) and lysine (K) in the second part, are shared by many additional protein kinases (Dorin et al., 1999).

Detection of the aforementioned conserved motifs in the newly studied jnk proteins is a good indication of the potential functionality of the isoforms. Although the presence of the domains, which are essential for kinase activation and activity, is essential for the proteins to work, it does not ascertain that the proteins are actually produced and are active *in vivo*. Their *in vivo* production can only be confirmed by western blot analysis and *in situ* staining and cannot be predicted by *in silico* studies. The next goal was to determine the phylogenetic relationships of the zebrafish jnk genes and proteins with their known homologues in other species.

3.3.2. Evolutionary conservation of jnk amino acid sequences

The evolutionary conservation of the proteins of interest was evaluated and their structures were compared to their *Caenorhabditis elegans* (roundworm), *Drosophila melanogaster* (fruit fly), *Gallus gallus* (chicken) and *Mus musculus* (mouse) orthologues (Figure 3.9). *C.elegans* was selected as a simple, multicellular, low eukaryote, *D.melanogaster* as an invertebrate arthropod, *G.gallus* as an amniotic vertebrate and *M.musculus* as a mammal. Non-redundant amino acid sequences from all species were used for the construction of a phylogenetic tree. We were interested in looking at the conservation of the protein structure between different organisms, as this would, to some extent, entail conservation of protein function.

Figure 3. 8: Conserved residues in catalytic motifs of zebrafish jnk proteins. A) A G-rich stretch of residues (highlighted in yellow) in the N-terminal extremity of the catalytic region (G-X-G-X-X-G-X-X motif, where X is any amino acid) usually precedes a K (highlighted in green), shown to be involved in ATP binding. A conserved D (highlighted in red), commonly found in the central part of the catalytic domain, has been shown to be important for the catalytic activity of the enzyme. B) The MAPK signature motif is shown. The area shown here is located just after the conserved TPY motif (shown with vertical black lines in Figure 3.5) and is characteristic of all MAPK. The F and C residues at the extremity of the region shown are MAPK-specific, whereas the rest of the highlighted amino acids (R, E, R, D, K) are shared by additional kinases. The sequences are presented in single letter code. G: glycine, D: aspartic acid, K: lysine, F: phenylalanine, C: cysteine, R: arginine, E: glutamic acid.

Amino acid sequences were initially aligned in the ClustalW server. The alignment files were then further analysed in the MEGA5 software. The maximum likelihood method was used for phylogenetic reconstruction and statistical analysis, under the Jones-Taylor-Thornton (JTT) model of evolution, using the nearest-neighbour-interchange (NNI) heuristic method of tree inference, with a 95% site coverage cut-off and 500 repetitions of bootstrap testing. Details about these models are given in Section 2.3.2 (page 80).

The tree that was constructed is shown in Figure 3.9. Jnk1 is highlighted in blue, Jnk2 in red and Jnk3 in green. Zebrafish isoforms are illustrated in shaded boxes of the same colours, respectively. Jnk orthologs from other species, such as Drosophila, *C.elegans*, mouse and chicken were retrieved from Ensembl. *D.melanogaster* has only one *jnk* orthologue, called basket (Gettings et al., 2010, Riesgo-Escovar et al., 1996). *C.elegans* has two confirmed jnk orthologues, called jnk1 and kgb1 (Orsborn et al., 2007). The phylogenetic relationships of all confirmed *Jnk* proteins in the species of interest are shown in Figure 3.9.

C.elegans kgb1 seems to represent a more ancestral protein and appears to have been present even before the emergence of distinct jnk proteins. Similarly, basket in *D.melanogaster* diverged from the original common ancestor before the separation of the jnk lineage to jnk1, jnk2 and jnk3. The presence of a second jnk orthologue in *C.elegans* suggests that a duplication event might have taken place in its genome, giving rise to a new jnk isoform, which diverged to jnk1. *C.elegans* jnk1 might represent an ancestral form from which further duplication events and divergence led to the emergence of initially separate jnk1 and jnk2/jnk3 lineages and finally even further to separate jnk2 and jnk3 branches.

The separation of the jnk proteins in these three lineages (jnk1, jnk2 and jnk3) is quite distinct in all vertebrates examined: jnk1 proteins in one species only cluster with jnk1 in other species, jnk2 with jnk2 and jnk3 with jnk3. Also, not surprisingly, isoforms from one species tend to be closer to other isoforms of the same protein in the same species than to isoforms of the same protein in other species: for example, all zebrafish jnk3 isoforms are closer to each other than to the mouse jnk3 isoforms (Figure 3.8). The fact that the zebrafish jnk1a and jnk1b clusters are so close and only one node away from each other, reinforces the notion that they may have arisen from a duplication of the original single *jnk1* gene.

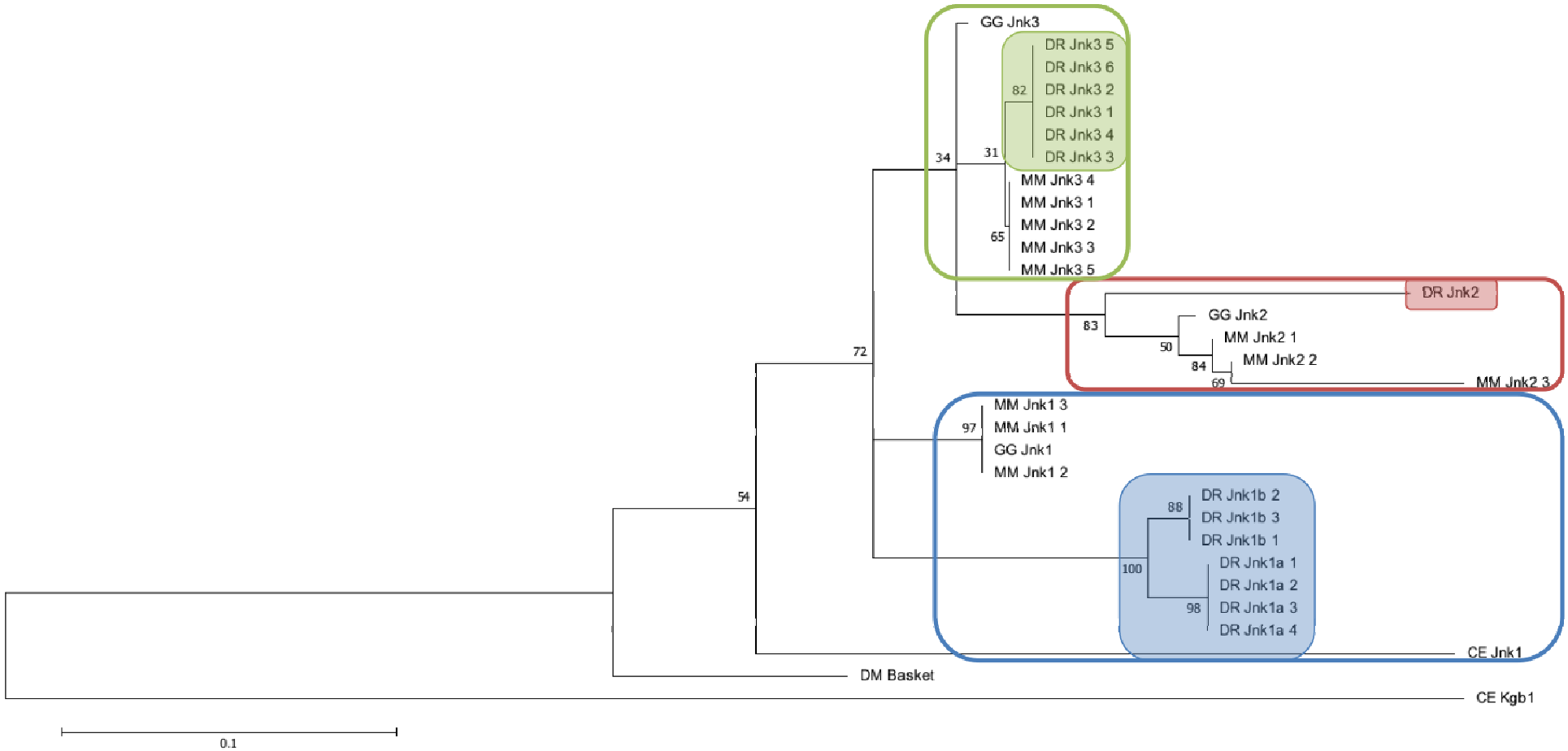

Figure 3. 9: Molecular phylogenetic analysis showing the evolutionary relation of Jnk proteins in different species: *Caenorhabditis elegans* (CE, roundworm), *Drosophila melanogaster* (DM, fruitfly), *Mus musculus* (MM, mouse), *Gallus gallus* (GG, chicken), *Danio rerio* (DR, zebrafish). Evolutionary history was inferred by using the maximum likelihood method based on the JTT matrix based model. The tree with the highest likelihood is shown. The percentage of replicate trees in which the associated taxa clustered together in the bootstrap test (500 replicates) is shown next to the branches. The tree is drawn to scale with branch lengths measured as the number of substitutions per site (the scalebar indicates 0.1 substitutions per site). The analysis involved 31 amino acid sequences and was conducted in MEGA5.

Nevertheless, the bootstrap values for some of the nodes are relatively low, which suggests that the topology of these nodes is not very reliable. For example, the node that represents the hypothetical common ancestor of the mouse Jnk3 and the zebrafish jnk3 is given a bootstrap value of 31. This means that the current conformation of this node was reproduced in 31% of the trees that were constructed by data re-shuffling, while in 69% of the reconstructed trees the topology was different. Similarly, the node that separates Jnk2 (in all species) from chicken Jnk3 and the group of zebrafish jnk3/mouse Jnk3 was given a boostrap value of 34%. Higher, but still not sufficiently reliable, bootstrap values were given to the node separating the chicken and mouse Jnk2 (50%) and to the node that separates the *C.elegans* jnk1 with the common ancestor of all Jnk genes in mouse, chicken and zebrafish (54%). The low reliability of the current protein tree is one of the reasons why a tree based on nucleotide sequences was also constructed (see below).

3.3.3. Evolutionary conservation of Jnk nucleotide sequences

After evaluation of the evolutionary relationship of the Jnk proteins between the species of interest, it became evident that the same should be carried out for the nucleotide sequences. The reasons for this were three. The first, as mentioned before, is that the tree, constructed based on the amino acid sequences, was not very reliable, as shown by low boostrap values (Figure 3.9). The second reason is related to the evolutionary pressure that proteins receive. As explained before, the amino acid conservation varies significantly in different regions of the protein: high conservation in the core part of the sequences, where the important function-related domains are, and low conservation in the rest of the sequence. Comparison of nucleotide instead of amino acid sequences can account for this uneven conservation since mutations at the DNA level are not related to the functionality of the protein and do not receive the same evolutionary pressure. Thirdly, not all mutations that happen at the DNA level are directly translated to amino acid changes because of the degeneration of the genetic code. For example the amino acid glycine can be encoded by four different codons (GGA, GGC, GGG and GGT) and, thus, any change in the last nucleotide of the codon will not be translated to an amino acid change. Therefore, phylogenetic trees based on nucleotide comparisons are likely to give better estimations of evolutionary time. For the reasons presented above, a tree based on the nucleotide sequences of *jnk* transcripts was also constructed (Figure 3.10).

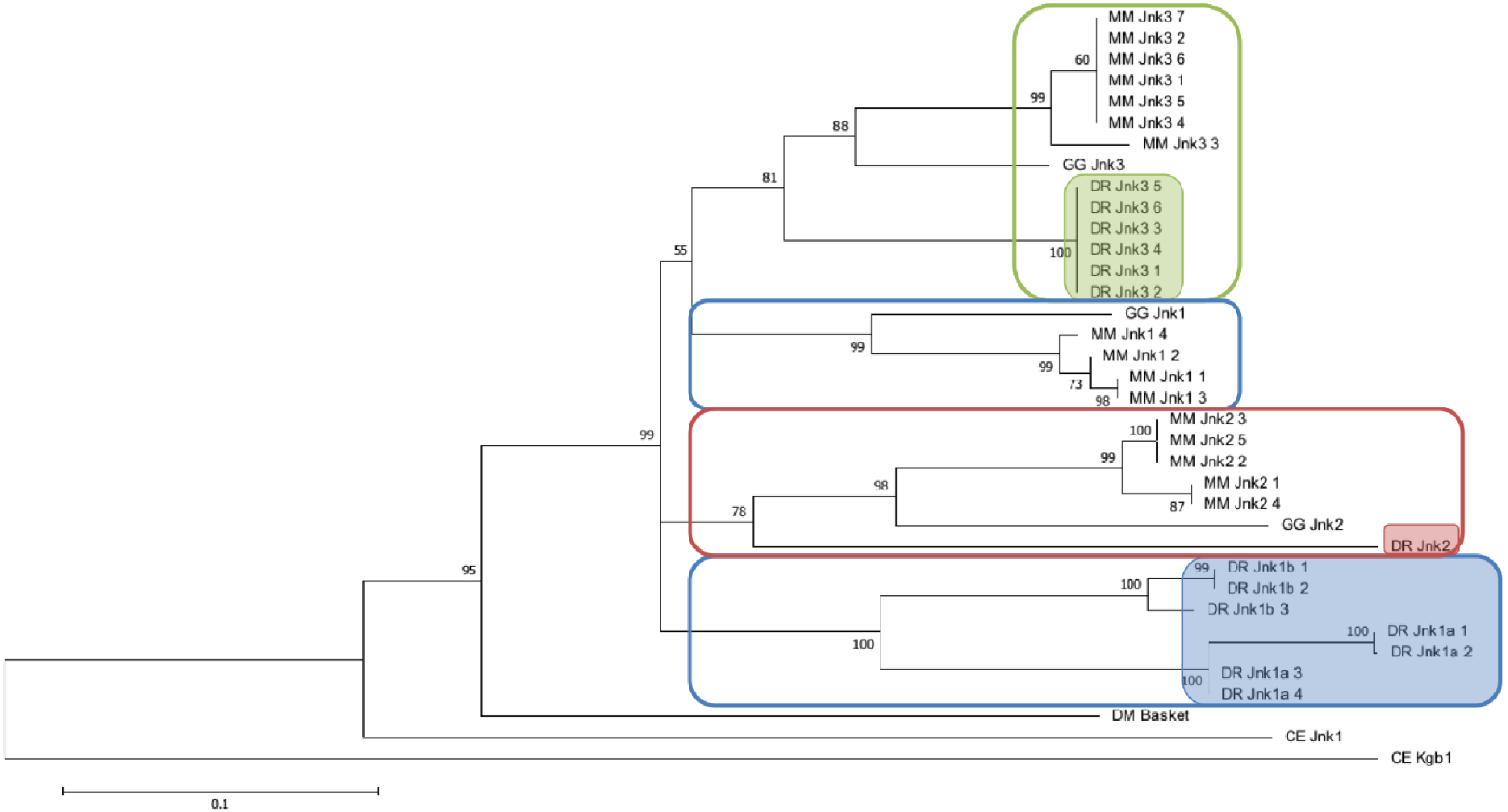

Figure 3. 10: Molecular phylogenetic analysis showing the evolutionary relation of Jnk nucleotide sequences in different species: *Caenorhabditis elegans* (CE, roundworm), *Drosophila melanogaster* (DM, fruitfly), *Mus musculus* (MM, mouse), *Gallus gallus* (GG, chicken), *Danio rerio* (DR, zebrafish). Evolutionary history was inferred by using the maximum likelihood method based on the Tamura-Nei model. The tree with the highest likelihood is shown. The percentage of replicate trees in which the associated taxa clustered together in the bootstrap test (500 replicates) is shown next to the branches. The tree is drawn to scale with branch lengths measured as the number of substitutions per site (the scalebar indicates 0.1 substitutions per site). The analysis involved 36 nucleotide sequences and was conducted in MEGA5.

No major differences were observed between the two trees (based on amino acid and nucleotide sequences). Clustering of *Jnk2* and *Jnk3* transcripts was as expected and as shown before in the protein phylogenetic tree (Figure 3.9). The *Jnk1* family was, however, more scattered. Mouse and chicken sequences clustered together, while zebrafish orthologues appeared in a separate subtree. Zebrafish *jnk1a* and *jnk1b* transcripts remained very closely related. The *C.elegans Kgb1* transcript seems to correspond to an ancestral form, as was shown with the protein tree too. However, in this tree, contrarily to what was shown by the protein tree, the *C.elegans Jnk1* isoform seems to have diverged before the emergence of a separate *Jnk1* gene in other species. Although this finding is unexpected and difficult to interpret, its bootstrap value is 95%, which reinforces the reliability of the current tree conformation. The respective bootstrap value of that branch in the protein tree is a mere 54%, as explained before. In fact, the boostrap values in all nodes of the tree are high, with the lowest ones being 55% and 60% (Figure 3.10). This highlights the reliability and robustness of the nucleotide-based tree, compared to the protein-based tree. Of note, any phylogenetic tree is as good as the data that were used to construct it. Additional information (using genes from more species for example) could generate some changes in the topology of the tree. For the purposes of this study, however, the analysis performed is adequate and reliable.

Overall, the *in silico* investigation and subsequent bioinformatics analysis confirmed the presence of an additional *jnk*-like gene (*jnk1b*), ortholog to vertebrate *Jnk1* and paralog to zebrafish *jnk1a*. *Jnk1b* showed high evolutionary conservation with other zebrafish *jnk* genes (*jnk1*, *jnk2* and *jnk3*) and with *Jnk* genes from other species (mouse, chicken, fruit-fly and roundworm). Sites of high evolutionary similarity were located in the core part of the genes, which correspond to the essential activation and activity domains of the kinases, while lower conservation was observed in the two termini of the genes and subsequently of the proteins. It was, also, shown that phylogenetic trees based on nucleotide sequences are more reliable than trees based on amino acid sequences, as suggested by bootstrap analysis of both types of trees. The *jnk* gene-based phylogenetic tree revealed that *kgb1* (one of the *Jnk* genes in *C.elegans*) might represent an ancestral form of the protein that gave rise to all different *jnk* genes.

3.4. *In vivo* analysis

After *in silico* identification and characterization of the zebrafish *jnk* genes, the onset of their expression and their expression pattern were examined in detail. Two main tools were used in order to achieve this: reverse transcriptase (RT)-PCR to look at the temporal gene expression pattern in development and in adulthood and whole mount *in situ* hybridization to study the pattern of expression of these genes.

RNA was extracted from three different batches of *golden* zebrafish embryos (biological replicates: 10-20 embryos, depending on the age, from three different clutches) at various developmental stages and was transcribed to cDNA. PCR reactions were repeated three times on each cDNA set (experimental replicates). Results from one representative set are shown here. Primers were designed to either bind specific isoforms only or to bind all isoforms of one gene, as shown in Figure 3.11 (primer sequences are shown in Table 3.2). Primer design was based on the gene information available at the time and therefore does not include all splice variants. Specifically, jnk1a.1, jnk1a.2, jnk3.1, jnk3.2 and jnk3.3 were the only variants that were individually detected. All other variants were detected by the common primer sets.

The housekeeping gene *β-actin* was used as an internal control for RT-PCR, providing a reference of the cDNA input and the baseline gene expression. Primer sets (*jnk* and *β-actin*) were optimised individually but were found to work optimally under similar conditions, as they were designed to have similar properties (nucleotide length, GC content etc). The same number of PCR cycles was used for all reactions in order for the PCR products to be comparable between them. Also, the UV light exposure during agarose gel imaging was the same for all gels.

Although semi-quantitation was possible with the technique used, the main aim of the current approach was to establish that the genes of interest were expressed during development and not to accurately characterize the levels of their expression. Quantitative RT-PCR (qPCR) could have been employed instead, if a precise expression analysis was required. A no-template control was included in all reactions to ascertain that the products were specific and not due to contamination. More details on practical aspects of these methods are given in Sections 2.1.7 (page 57, for wholemount *in situ* hybridization) and 2.1.10 (page 61, for RT-PCR).

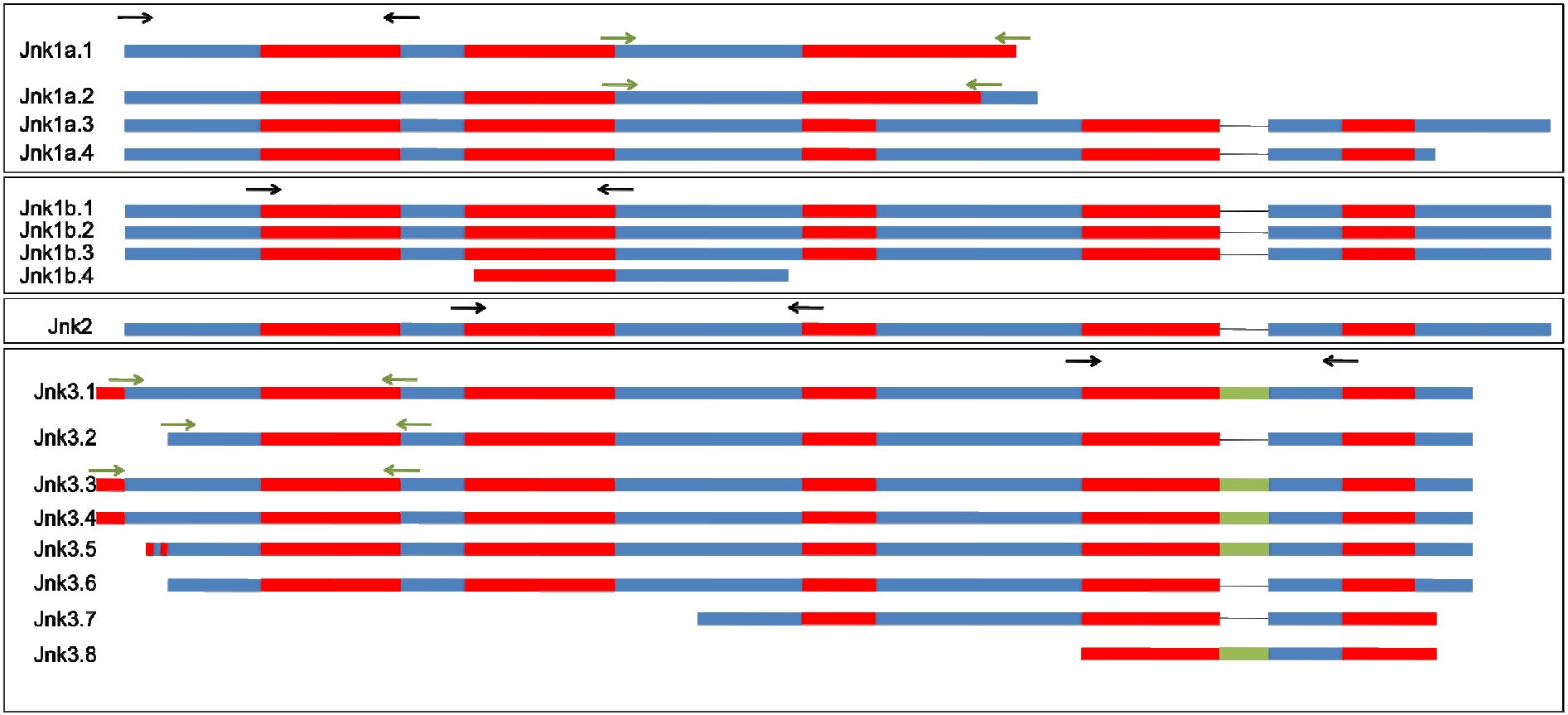

Figure 3. 11: Location of manually designed jnk primers. Black arrows represent primers that bind to all transcripts of one gene, while green arrows show primers that are specific for one gene isoform. Although, the sequences between different genes appear indistinguishable in this representation, in fact, there are enough point mutations that allow for the design of gene-specific primers that do not bind to any other *jnk* genes. Each gene (*jnk1a, jnk1b, jnk2* and *jnk3*) is shown in a separate box.

Whole mount *in situ* hybridization was performed three independent times on *Golden* zebrafish embryos of different clutches at different developmental stages. 20 embryos were commonly used for each reaction. The most representative staining patterns are shown here. Probes were designed to either bind specific isoforms only or to bind all isoforms of one gene (sequences shown in Table 3.3), as explained in Section 2.1.12 (page 61). Sense-probe and no-probe controls were used for confirmation of the specificity of the staining. Staining with a *tbx5* (*tbx5a*) probe was used as a positive control. More details about this method are given in Section 2.1.7 (page 57).

Genes	**Size (bp)**	**Forward sequence**	**Reverse Sequence**
β-actin	105	GAGCAGGAGATGGGAACC	CAACGGAAACGCTCATTGC
Pan-jnk1a	253	CGCTGAGAAGACCCCAGTGTT	TACGCTGAGCAGACGATGCC
Jnk1a.1	240	TCGGACCACAACAAACTCAA	CCATTCCAGCACTTCCTTGT
Jnk1a.2	190	GGGCATGGGTTATCAAGCTA	TCAATGGCAACACATATTAAGG
Pan-jnk1b	179	CAGGGACCTGAAACCCAGTA	ACACATCCACATTGGCTTGA
Jnk2	407	TCACAGGGATCTGAAGCCCA	TCTCTGATGGGAAGGCCCAG
Pan-jnk3	290	GGGCATGGGCTACAAGGAGA	GTGCCTGACTCGCTTTGAGT
Jnk3.1	270	TCAGTCCTTTGGAGCTGCTT	GTCCAGGACGGCATCATATC
Jnk3.2	150	TGAGAAACCCTCCCATTGTG	AACACTACAGCAAACAACACCA
Jnk3.3	237	TGCCTTTTGTCAGGTGTGTG	GTCCAGGACGGCATCATATC

Table 3. 2: Zebrafish RT-PCR primer sequences. All jnk primer sets were manually designed to span exon-exon boundaries (when possible) in order to avoid genomic DNA contamination. The sequences of *β-actin* were retrieved from previously published work (McCurley and Callard, 2008).

Target gene	**Forward sequence**	**Reverse Sequence**
Pan-jnk1a	CTGAGAAGACCCCAGTGTTT	GCAGAGCATCTGATAGAGCA
Jnk2	CAACGGTCAGTCATGCCACA	CAGAGCGGAGCAGACGATAC
Pan-jnk3	TCTTACATTGCCCAGCATTA	ATCCACGTTCTCCTTGTAGC
Jnk3.3	CCATAATGGTACAGGCATCA	CAGCACACACTATTCCCTGA

Table 3. 3: Sequences of zebrafish primers that were used for making the probes for wholemount *in situ* hybridization. Primer sets were designed to span different exons, when possible, to give large PCR products and not to recognize other *jnk* genes.

3.4.1. Temporal expression analysis of jnk in zebrafish

As mentioned before, *β-actin* was used as a housekeeping gene for the RT-PCR analysis presented here. The expression of this gene, shown previously to be expressed at stable levels throughout development and following chemical treatment in zebrafish (McCurley and Callard, 2008), was used as a measure of the cDNA input for each PCR reaction. The same amount of cDNA was used for the *β-actin* reaction and for all *jnk* reactions at one specific developmental stage.

As shown in Figure 3.12, the temporal expression profile of the various isoforms is distinct. *Jnk1a.1* is expressed throughout development, from 20 minutes after fertilization onwards with small fluctuations in the levels of expression. Highest levels are observed at 3 hpf and after 48 hpf, as well as in day 5 (d5) embryos and in the adult heart. 3 hpf represents the mid-blastula transition, when the embryonic genome becomes activated (see Section 1.2.1 at page 2 for more details on this). Therefore, increased mRNA levels at that time point reflect the onset of expression of the embryonic *jnk1a.1* gene. Before 3 hpf only maternal *jnk1a.1* mRNA was probably present. Similarly, *jnk1a.2* was maternally expressed at 20 minutes, reached maximal levels at 3 hpf, when embryonic expression started, and faded away after 48 hpf. Its expression in older embryos (5 days old) and in adult tissues (brain and heart) was abundant. RT-PCR with the pan-*jnk1a* primers recapitulates to some extent the expression patterns of *jnk1a.1* and *jnk1a.2*. This suggests that the other *jnk1a* splice isoforms are either not expressed at the developmental stages examined or are expressed in a very similar pattern as *jnk1a.1* and *jnk1a.2*.

Jnk1b remained modestly expressed until 10 hpf, picked up between 20 hpf and 48 hpf and disappeared at 72 hpf, while it became again abundantly present after 5 days of development. The fact that there was no peak at 3 hpf possibly indicates that the activation of embryonic *jnk1b* did not take place until later in development. Thus, it is possible that most of the *jnk1b* mRNA that was detected until 10 hpf was of maternal origin (Figure 3.12). *Jnk2*, although present since 20 minutes after fertilization, was expressed at very low levels throughout development with highest expression levels observed in d5 old fish and in adult tissues. As with *jnk1b*, no peak was observed at 3 hpf and therefore, it is possible that most of the detected mRNA was of maternal and not embryonic origin until later in development.

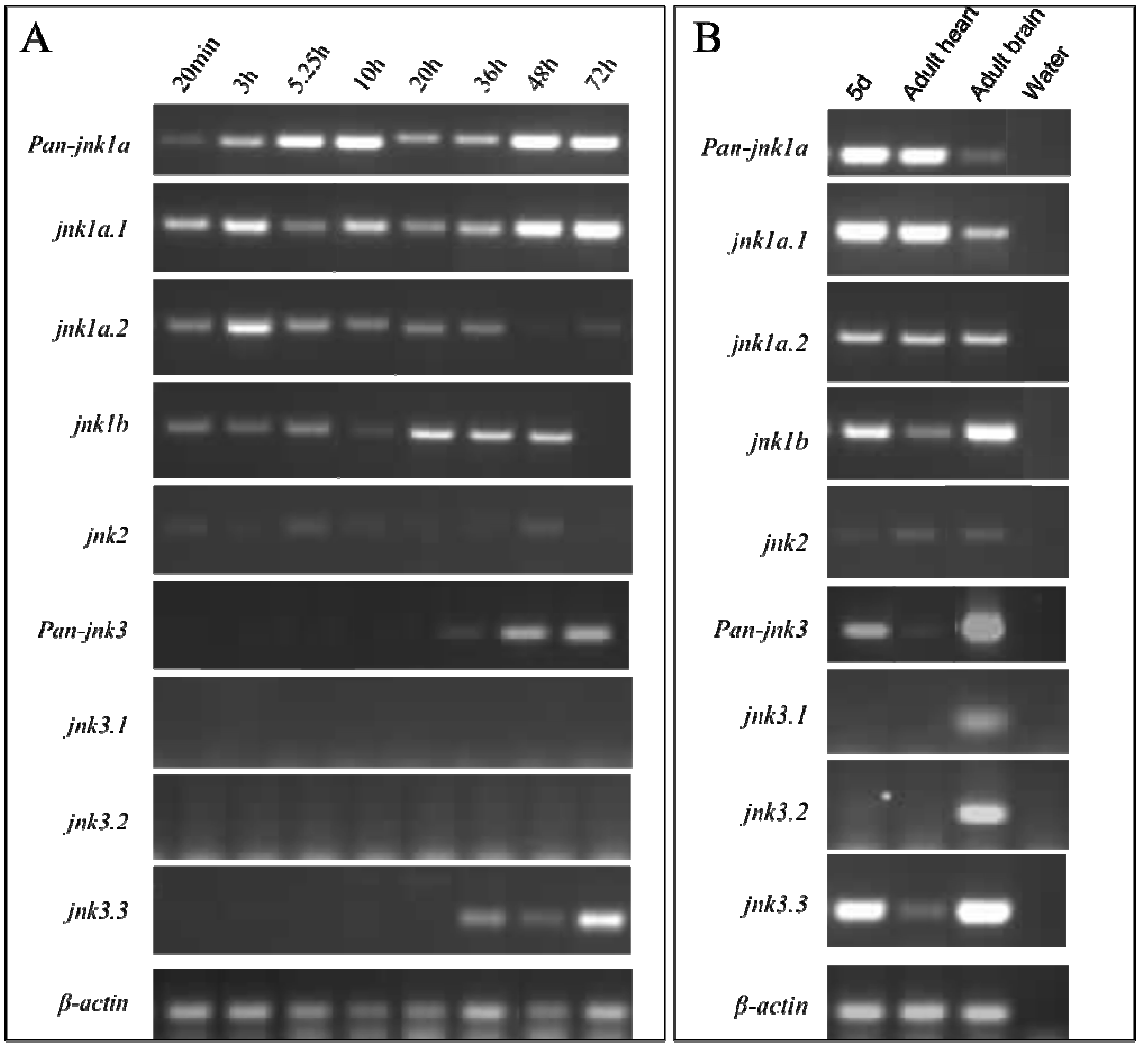

Figure 3. 12: RT-PCR analysis of *jnk* isoforms (*jnk1a.1, jnk1a.2, jnk1b, jnk2, jnk3.1, jnk3.2, jnk3.3*). The housekeeping gene *β-actin* was used as an internal control. cDNA from many stages of embryonic development was used. A) Expression levels of *jnk* genes during the first few days of development are shown, starting at 20 minutes after fertilization and reaching 72 hpf. B) The expression pattern of *jnk* genes in 5 days old fish and adult tissues (heart and brain) is shown. *Jnk1a* and *jnk1b* were abundantly expressed throughout embryonic development, while *jnk2*, was only present at very low levels. *Jnk3.3* came on only after 36 hpf, while the other two *jnk3* transcripts (*jnk3.1* and *jnk3.2*) were only expressed in the adult brain.

The fact that *jnk2* was found to be expressed at very low levels throughout zebrafish embryonic development contradicts previous findings, which suggested that *jnk2* was the most important *jnk* gene during gastrulation (Seo et al., 2010). However, a peak in the expression levels of *jnk2* can be seen at 5.25 hpf, which marks the onset of gastrulation (Figure 3.12). The robustness and reliability of the method used in this study for RT-PCR analysis are further discussed in Section 3.5.4 (page 128).

Three *jnk3* transcripts were examined: *jnk3.1, jnk3.2* and *jnk3.3*. They showed a different pattern and a later onset of expression (Figure 3.12). *Jnk3.1* and *jnk3.2* were not expressed at all during development and were only found in the adult brain, while *jnk3.3* was present after 36 hpf and was, also, expressed in d5 fish and in adult tissues, both the heart (at low levels) and the brain (at high levels). Its presence in the adult heart made it the only *jnk3* isoform expressed in the fully formed and functional heart. Recapitulation of the *jnk3.3* expression pattern with the pan-*jnk3* primers suggests that the rest of the *jnk3* variants are not expressed during development (like *jnk3.1* and *jnk3.2*) or that they are expressed in a similar manner to *jnk3.3*. In either case, *jnk3* was not expressed at all in the early stages of development. Therefore, only *jnk1a*, *jnk1b* and *jnk2* are expected to be involved in most of the early events of gastrulation, cell specification, organogenesis and morphogenesis that happen before 36 hpf, when one of the *jnk3* isoforms is firstly expressed.

Taken together, the RT-PCR data revealed that mRNA of the isoforms of interest is produced *in vivo*. Also, it showed that *jnk1a, jnk1b, jnk2* and *jnk3* have distinct expression patterns, with *jnk1a* and *jnk1b* being the most highly expressed genes during the early embryogenesis stages. Next, the *in vivo* spatial expression profile of *jnk* during the first days of zebrafish development was investigated.

3.4.2. Spatial expression analysis of jnk in zebrafish

After *jnk* mRNA detection with RT-PCR that revealed the timely expression pattern of the genes, their spatial expression pattern was also examined at different time points. Four antisense probes were used in this assay: against *jnk2*, all *jnk1a* isoforms (pan-*jnk1a*), all *jnk3* isoforms (pan-*jnk3*) and *jnk3.3*. Since no other *jnk3* transcript, besides *jnk3.3*, was expressed until adulthood, the pan-*jnk3* probe was used as a control to confirm the specificity of *jnk3.3* probe staining. *Tbx5a* was used as a positive control, while sense probes or no probes were used as negative controls at all ages examined. The sense *jnk* and the *tbx5* staining are shown along with the antisense *jnk* staining (Figures 3.14, 3.15, 3.16 and 3.17) allowing for direct comparison of the expression patterns, while the negative controls are presented in a separate figure because of space limitation (Figure 3.13). *Golden* embryos were used for this analysis because, due to their low pigmentation, they allow for easier visualization.

Whole mount *in situ* hybridization (WISH) without any probe (negative control) confirmed the absence of unspecific background staining (Figure 3.1.3). *Tbx5* staining

followed the expected pattern of expression, as suggested by previously published work (Begemann and Ingham, 2000). It was shown to be expressed in the forming pectoral fin buds and subsequently in the developing fins, in the embryonic heart and in the eyes (Figures 3.14, 3.15, 3.16 and 3.17). The fact that *tbx5* staining appeared as expected increased the reliability of the method and of the findings thereafter.

WISH at 24 hpf with a pan-*jnk3* and a *jnk3.3* probe showed formation of blue precipitate in the area lining the yolk sac, covering the presumptive pharyngeal region and the area where the heart tube lies (Figures 3.14 and 3.15). The RT-PCR results presented in Figure 3.12 show that at 20 hpf none of the *jnk3* transcripts was present, while at 36 hpf *jnk3.3* was already quite highly expressed. Therefore, although 24 hpf is not included in the RT-PCR analysis in Figure 3.12, it seems likely from the WISH analysis that the onset of *jnk3.3* (detected by both pan-*jnk3* and *jnk3.3* probes) expression was between 20 and 24 hpf. At 36 hpf staining with *jnk3.3* and pan-*jnk3* was more specific in the hypothalamus of the brain and the developing otic vesicles (Figures 3.14 and 3.15). At 96 hpf expression of *jnk3.3* was apparent in the area around the heart. Staining with the anti-*jnk3.3* probe showed clearer staining in the heart area, where it was shown that possibly not the whole heart was stained (Figure 3.15). The gut was also stained at 96 hpf with both probes. The sense probes of both *jnk3.3* and pan-*jnk3* probes showed no staining at all, confirming that the expression pattern seen with the antisense probes was real and specific.

Three ages were examined for *jnk1a* and *jnk2* expression: 13, 24 and 36 hpf. At 13 hpf both *jnk1a* and *jnk2* appeared ubiquitously expressed, with possibly higher expression levels in the head (Figures 3.16 and 3.17). At 24 hpf *jnk1a* was highly expressed in anterior structures, covering the whole head, the heart area and most of the trunk. At 36 hpf staining with the pan-*jnk1a* probe was fairly faint but appeared in the presumptive gut area and possibly the eyes (Figure 3.16). *Jnk2* followed a similar expression pattern. At 24 hpf it was present in the pharyngeal area and the presumptive gut and heart, while at 36 hpf it was found in the brain, the pharyngeal region and the heart (Figure 3.17). The sense probes for *jnk1a* and *jnk2* showed some staining as well, but the areas in which it appeared generally overlapped with the areas stained by the antisense probes.

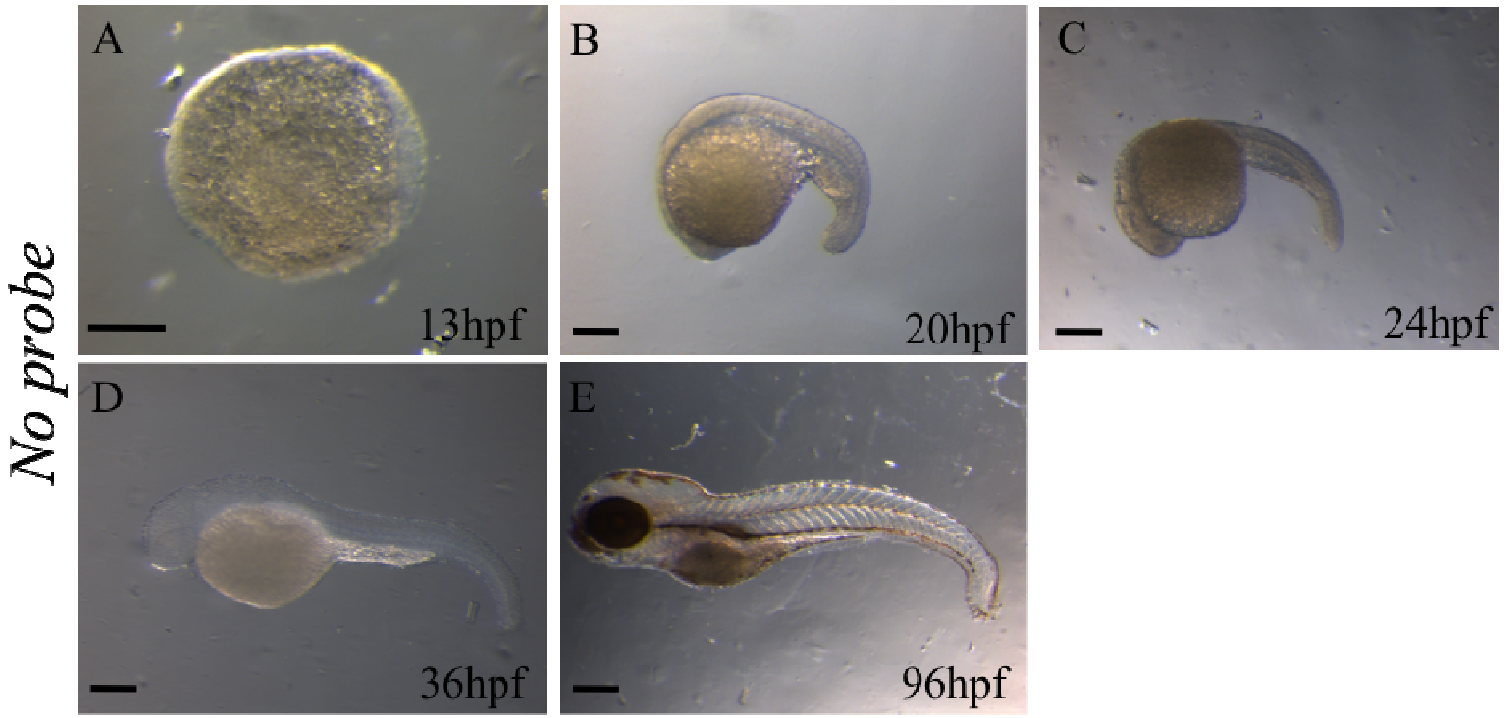

Figure 3. 13: Negative control for the *in situ* hybridization analysis. No probe was added to the hybridization mix during wholemount *in situ* hybridization of these embryos. No staining was observed in any of the ages examined, suggesting that any staining that would appear in the probed embryos is real.

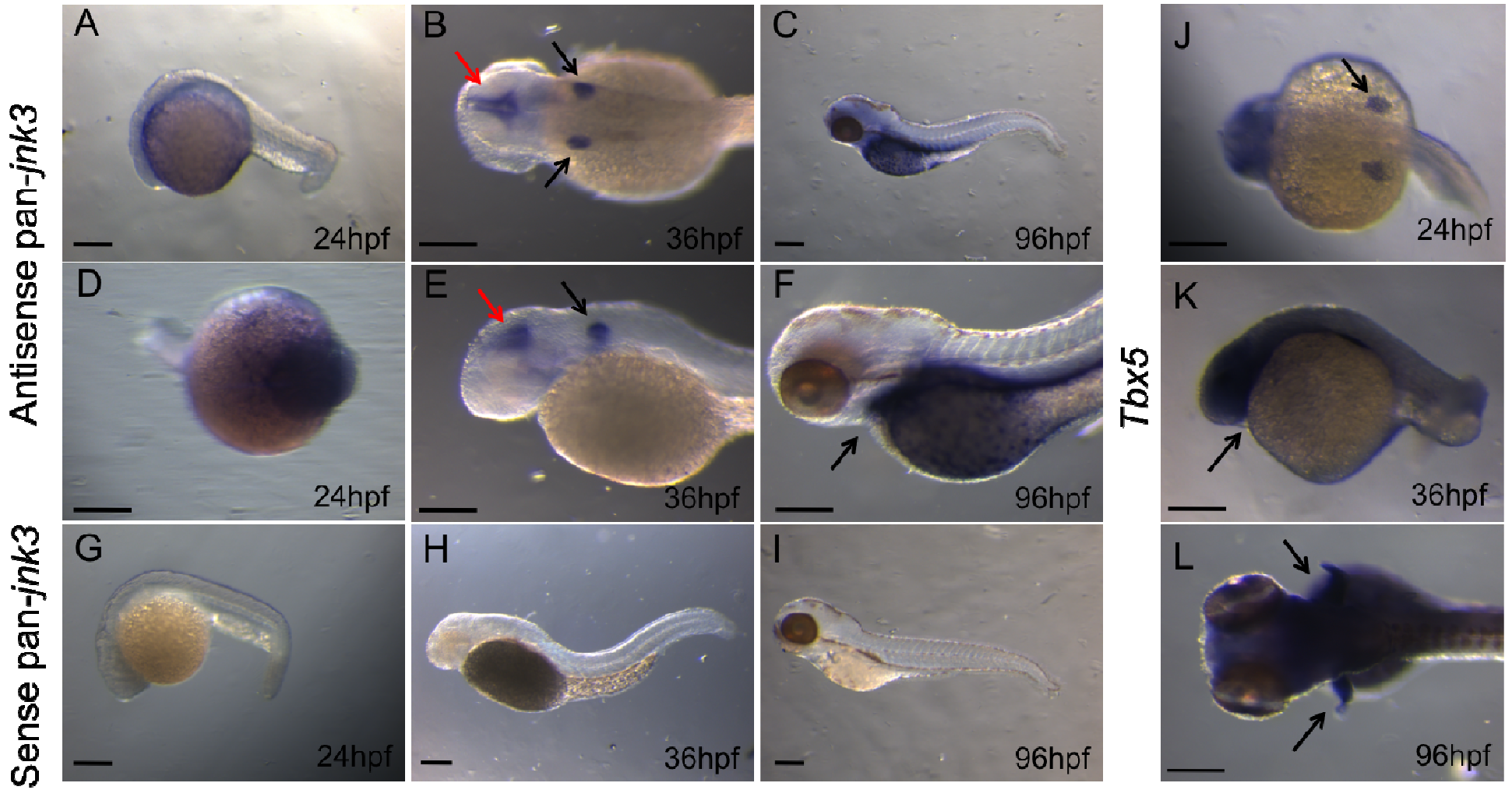
Antisense pan-jnk3
Sense pan-jnk3
Tbx5
A
B
C
D
E
F
G
H
I
J
K
L
24hpf
36hpf
96hpf
24hpf
36hpf
96hpf
24hpf
36hpf
96hpf
24hpf
36hpf
96hpf

Figure 3. 14: In situ hybridization of 24, 36 and 96 hpf *golden* zebrafish embryos with a pan-*jnk3* probe. A) and D) show 24 hpf fish stained in the area lining the yolk sac, in the presumptive gut and heart regions. B) and E) show 36 hpf embryos stained in the hypothalamus (red arrow) and otic vesicles (black arrows). C) and F) show 96 hpf fish with staining in the heart (arrow) and gut regions. G-I) represent negative controls for each age, respectively. These were stained with sense probes that are not expected to bind to the target mRNA. (J-L) show 24, 36 and 96 hpf embryos stained with a *tbx5* probe, used as a positive control. The arrow in (J) shows one of the fin buds, in (K) the heart region and in (L) the fins. Scale bars show 200µm.

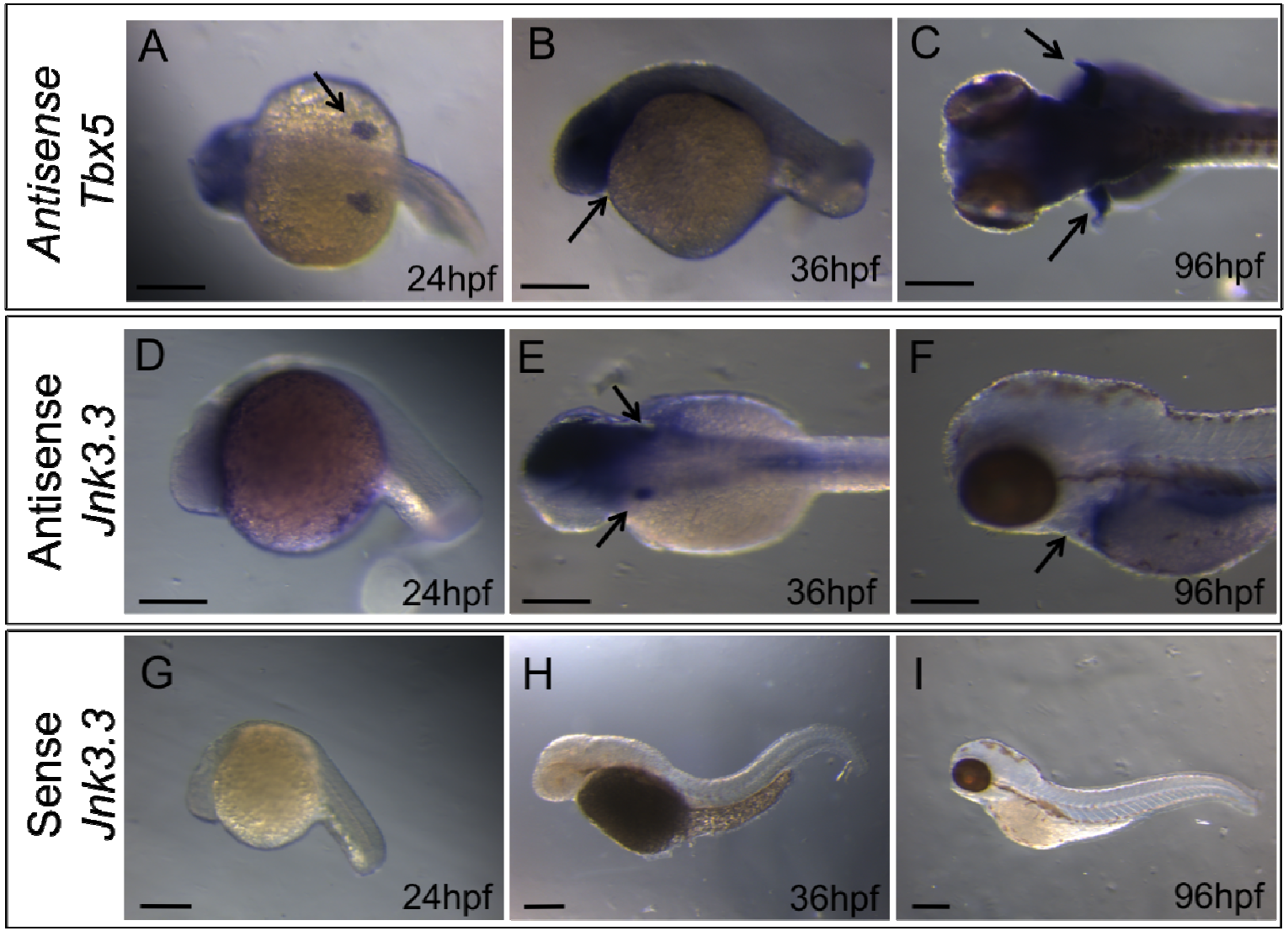
Antisense Tbx5
A
24hpf
B
36hpf
C
96hpf
Antisense Jnk3.3
D
24hpf
E
36hpf
F
96hpf
Sense Jnk3.3
G
24hpf
H
36hpf
I
96hpf

Figure 3. 15: In situ hybridization of 24, 36 and 96 hpf *golden* zebrafish embryos with a *tbx5* and a *jnk3.3* probe. (A-C) *Tbx5* staining of 24, 36 and 96 hpf embryos, respectively. The arrow in (A) shows one of the fin buds, in (B) the heart region and in (C) the fins. (D-F) Antisense *jnk3.3* staining. D) shows 24 hpf fish stained in the area lining the yolk sac, in the presumptive gut and heart regions. E) shows 36 hpf embryos stained in the hypothalamus and otic vesicles (arrows). F) shows 96 hpf fish stained in the heart (arrow) and gut regions. G-I) Sense jnk3.3 staining, used as negative controls for each age (24, 36 and 96 hpf, respectively). These were stained with sense *jnk3.3* probe that is not expected to bind to the target mRNA. Scale bars show 200µm.

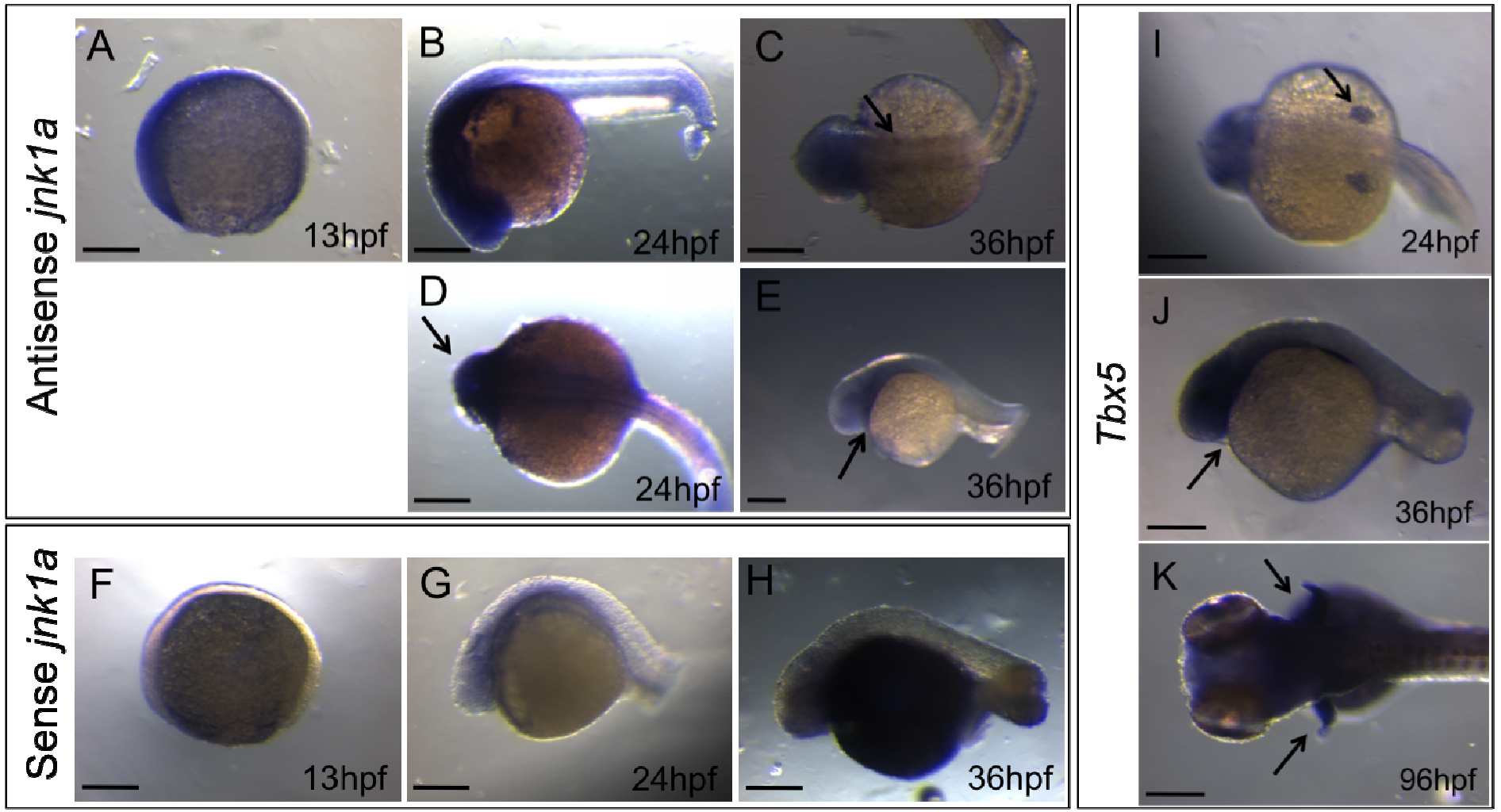
Antisense jnk1a
A
13hpf
B
24hpf
C
36hpf
D
24hpf
E
36hpf
Sense jnk1a
F
13hpf
G
24hpf
H
36hpf
Tbx5
I
24hpf
J
36hpf
K
96hpf

Figure 3. 16: In situ hybridization of 13, 24 and 36 hpf *golden* zebrafish embryos with a pan-*jnk1a* probe. A) shows 13 hpf fish stained predominantly in the anterior area (anterior to the left). B) and D) show 24 hpf embryos stained heavily in the head (aarow). C) and E) show 36 hpf fish with faint staining in the head, presumptive gut regions and potentially the fin buds (arrow in C) and the heart (arrow in E). F-H) represent negative controls for each age, respectively. These were stained with sense probes that are not expected to bind to the target mRNA. Residual staining in the negative control is similar to the real staining. (I-K) show 24, 36 and 96 hpf embryos stained with a *tbx5a* probe, used as a positive control. The arrow in (I) shows one of the fin buds, in (J) the heart region and in (K) the fins. Scale bars show 200µm.

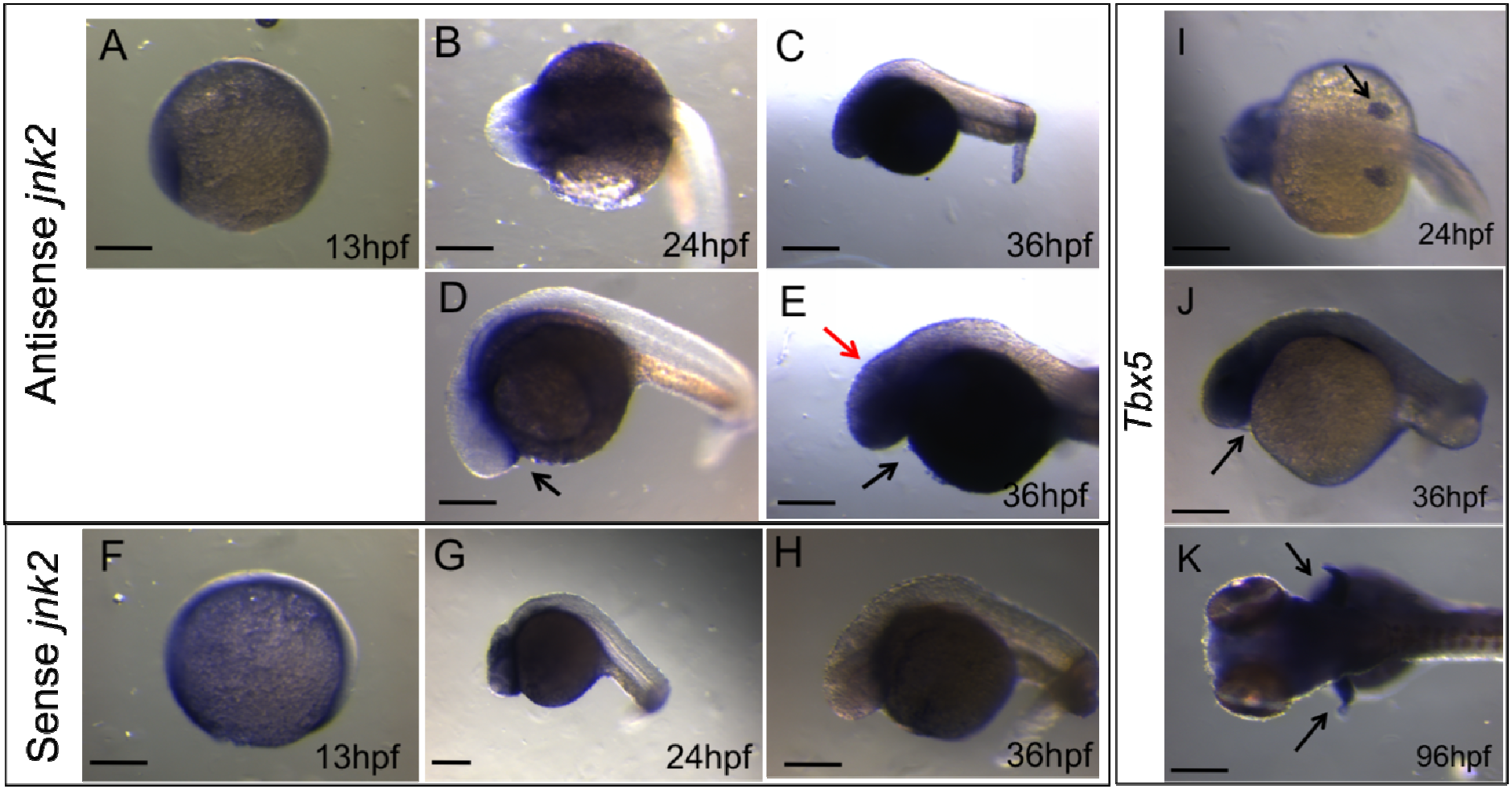
Antisense jnk2
A
13hpf
B
24hpf
C
36hpf
D
E
36hpf
Sense jnk2
F
13hpf
G
24hpf
H
36hpf
Tbx5
I
24hpf
J
36hpf
K
96hpf

Figure 3. 17: In situ hybridization of 13, 24 and 36 hpf *golden* zebrafish embryos with a *jnk2* probe. A) shows 13 hpf embryos stained predominantly in the anterior area (anterior to the left). B) and D) show 24 hpf embryos stained in the area lining the yolk sac and in the presumptive heart (arrow) and gut regions. C) and E) show 36 hpf fish with strong staining in the head and anterior structures (red arrow) and potentially in the heart (black arrow). F-H) represent negative controls for each age, 13, 24 and 36 hpf, respectively. These were stained with sense probes that are not expected to bind to the target mRNA. Residual staining in the negative control is similar to the real staining. (I-K) show 24, 36 and 96 hpf embryos stained with a *tbx5* probe, used as a positive control. The arrow in (I) shows one of the fin buds, in (J) the heart region and in (K) the fins. Scale bars show 200µm.

Further analysis and undoubtful confirmation of the expression profiles of *jnk* during zebrafish embryonic development could have been achieved by embedding (in wax or resin for example) and sectioning stained embryos and closely looking at the staining pattern in structures of interest. Also, antibody analysis would have been useful for evaluating the presence, not only of the transcripts, but also of the protein products. However, time limitations did not allow for such analyses. Taken together, the temporal and spatial expression patterns of *jnk* genes were determined. RT-PCR analysis showed that *jnk1a* and *jnk1b* were the most predominantly expressed genes during early stages of embryogenesis, with *jnk2* being expressed at very low levels and *jnk3* only coming on later in development. WISH experiments revealed abundant expression of *jnk1a* and *jnk2*. *In situ* expression analysis provided insight into the spatial distribution of the genes but not in an absolutely conclusive manner because of the inability to visualize specific organs. Therefore, the exact domains of expression of the genes have not been determined due to, as explained above, time limitations.

3.5. Discussion

In this chapter zebrafish jnk genes and proteins were examined. Initially, a bioinformatics approach enabled thorough investigation of jnk splice variants and protein isoforms and confirmed the presence of an additional gene compared to mammals. *In vivo* and *in situ* studies of the identified genes confirmed their expression and showed differential temporal and spatial patterns.

3.5.1. In silico identification of four jnk genes in zebrafish

Rather than the expected three *Jnk* genes observed in other mammals, four *jnk* genes were found in zebrafish in online databases after thorough *in silico* investigation: *jnk1*, *jnk2* and *jnk3*, orthologues of mammalian *Jnk1*, *Jnk2* and *Jnk3*, and an additional *jnk1*-like gene. The two *jnk1* genes were called *jnk1a* and *jnk1b* following the official nomenclature for duplicated gene pairs. The locus in chromosome 13, where *jnk1b* lies, appears to be member of a duplicated pair that includes a region of chromosome 12, where *jnk1a* is located. Measurement of the evolutionary divergence of all *jnk* genes in zebrafish showed that *jnk1a* and *jnk1b* share significantly more similarities than *jnk1b* does with either *jnk2* or *jnk3*. Subsequent phylogenetic analysis revealed the expected

clustering of zebrafish *jnk* genes and proteins with their corresponding orthologues in other species (chicken, mouse, roundworm and fruitfly). *Jnk1b* clustered with zebrafish *jnk1a* and with other *Jnk1* orthologues. Interestingly, *Jnk1* appears to have diverged from the common ancestor before the divergence of *Jnk2* and *Jnk3*.

Emergence of additional genes in zebrafish was not unexpected. A genome-wide duplication event took place approximately 350 million years ago in the lineage of ray-finned fish, after its divergence from the lobe-fin lineage that includes avians and mammals. Therefore, many of the genes of land vertebrates are duplicated in zebrafish (Meyer and Van de Peer, 2005, Postlethwait et al., 2000). A usual but not certain fate of duplicated gene pairs is loss of one of the members by mutations; genes can either turn into pseudogenes (explained in detail below) and become inactive or they can be lost by further chromosomal rearrangements (Postlethwait et al., 2000, Watterson, 1983). Therefore, the number of duplicated genes that are present in two copies in the zebrafish genome is not known and possibly many duplicates remain unidentified to date (Amores et al., 1998, Ellies et al., 1997, Postlethwait et al., 2000).

The process of identification of duplicated pairs may be further complicated by the excess of chromosome fusions that likely occurred in the fish lineage after duplication of its genome. This is suggested by the fish fusion model. According to this model, the fact that fish (25 chromosomal pairs) do not have twice as many chromosomes as humans (23 chromosomal pairs), although their whole genome was duplicated, is due to excessive fusion of chromosome segments that re-established the original number of chromosomes (Postlethwait et al., 2000). An alternative theory, supported by the tetrapod fission model, suggests that the ancestral state was of approximately 12 chromosomes, which doubled in the fish lineage and fragmented in tetrapod lineages (Postlethwait et al., 2000). Both these theories explain the current karyotypic status of fish and tetrapods but it still remains unclear which one more accurately describes the real evolutionary history (Goode et al., 2011).

3.5.2. Pseudogenes and the fate of duplicated gene pairs

As mentioned before, it is not uncommon for duplicated genes to become inactivated and turn into pseudogenes (Postlethwait et al., 2000, Watterson, 1983). Pseudogenes are DNA sequences that resemble functional genes but in fact do not have, or are thought not to have, any known function (Jacq et al., 1977). The loss of function of pseudogenes is usually due to either failure of transcription and/or translation or due to production of

a defective protein (Mighell et al., 2000, Vanin, 1985, Yao et al., 2006). They are commonly derived from duplications of existing genes and are located either at different chromosomes to their functional counterparts or in clusters with them (Lee et al., 2003, Long and Langley, 1993). They may be complete or incomplete copies of the original genes or they may comprise mixtures of different genes (Lee et al., 2003). Some form of short mRNA is likely to be produced from pseudogenes, depending on the mutations they have accumulated over time and the damage that has been caused to the original gene sequence, as shown for a few pseudogenes in the past (selected publications: Balakirev and Ayala, 2003, Berger et al., 2005, Edgar, 2002, Guo et al., 1998). Their full expression is, however, usually disrupted by misplaced stop codons, deletions, insertions or other kinds of mutations. It is thought that pseudogenes are good examples of common ancestry, when shared by different species, and are commonly used by evolutionary biologists for phylogenetic analysis (Balakirev and Ayala, 2003). It has, also, been shown that some pseudogenes serve as regulators of the expression levels of their paralogous coding genes (Hirotsune et al., 2003).

Online databases are able to identify and highlight pseudogenes. *Jnk1b* was not identified as a pseudogene in online databases. Also, the confirmation of its presence in our *in vitro* approach and its alignment with *jnk1a* revealed that this gene was neither lost nor severely altered during fragmentation or rearrangement of chromosomes. Of note, the Ensembl genome database is an automated system and as such, it has both the benefits (objectivity, reproducibility and speed) and drawbacks (absence of the human expertise and curation) associated with automation. Automatic pseudogene annotation in the database relies on some basic criteria for pseudogene identification (presence of single exons, absence of methionine at the beginning of the translation start point, presence of in-frame stop codons etc). These are, however, only guidelines and are likely not to identify all pseudogenes in all occasions. Therefore, manual pseudogene flagging, on top of automatic predictions, is preferable. The HAVANA group at the Welcome Trust Sanger Institute provides manual curation of Ensembl predictions (confirmation of automatically collected data with human expertise) and displays its results in a separate track in the Ensembl browser. The conclusions drawn and presented here are based on information gathered by both automatic annotation and manual curation.

Overall, it is most likely that the newly identified *jnk1b* gene has not been inactivated in the course of time since the duplication event. Also, the fact that in the meantime (as this work was being carried out) *in vivo* information about *jnk1b* was

published (Seo et al., 2010), does not allow for much doubt. However, the only definite confirmation for this would be the undoubtful detection of phospho-jnk1b levels (the activated form of jnk proteins) *in vivo*, which was not pursued here.

3.5.3. Zebrafish jnk genes in the literature

The two zebrafish *jnk1* genes were described in the literature for the first time when the current study was being carried out (Seo et al., 2010). They presented four genes, *jnk1a-1*, *jnk1a-2*, *jnk2* and *jnk3*, among which the first three were found to be expressed during gastrulation. Knockdown of *jnk1a-1* and *jnk1a-2* with morpholino injections showed no gross morphological abnormalities, while *jnk2* downregulation caused severe defects in anterior-posterior extension and mediolateral convergence of the body, producing a convergence-extension-like (CE-like) phenotype (Seo et al., 2010). It was, also, shown that Wnt11, a ligand of the non-canonical Wnt pathway, is a target of Mkk4-Jnk signalling and possibly mediates regulation of CE movements (Seo et al., 2010). However, in this publication no gene expression or bioinformatics analyses of the newly identified genes were conducted. Given the lack of *in silico* investigation in the work by Seo et al. (2010), it is possible that their splice morpholinos, instead of knocking down jnk, may in fact have inadvertedly produced alternative jnk isoforms. This idea is supported by the bioinformatics approach presented in this thesis, which showed that most of the jnk splice variants differ very little between them.

Therefore, there are three reasons why the current study is not severely compromised from the publication of the work just described. The first is that this publication did not address other features of zebrafish development, besides gastrulation. For example, formation of the heart, as well as formation of other organs, were not assessed but are of interest in this study (presented in the next chapter). The second reason is that Seo et al. (2010) did not take into account the different splice variants of the zebrafish *jnk* genes. From my work, it is evident that *jnk* genes have many splice variants, most of which produce potentially functional protein isoforms. These variants are shown to be expressed in a spatially and temporally specific manner. The fact that Seo et al. (2010) did not look at splice isoforms of the genes they examined, means that functional redundancy may have been overlooked. The splice morpholinos that were used in their study were designed against each gene (*jnk1a-1, jnk1a-2, jnk2* and *jnk3*) but whether they blocked correct splicing of all variants was not specified (Seo et al., 2010). After a scrutinous investigation and comparison of the

available sequences in genome databases, it was revealed that the morpholinos designed against *jnk1a-1, jnk1a-2, jnk2* and *jnk3* in the work of Seo et al. (2010) bind to most but not all of the transcripts. Specifically, the short transcripts, shown in Figure 3.5 (*jnk1b.4, jnk3.7* and *jnk3.8*) were not targeted by these splice morpholinos. Although it is not clear whether these short isoforms are in fact functional, it is important to take into account that production of even small levels of properly spliced *jnk* mRNA could compensate to some extent for the loss of the other isoforms. This observation highlights the third reason why the work presented in this chapter is of importance: it provides a comprehensive and detailed analysis of the four *jnk* genes, their splice variants, their putative protein isoforms and their evolutionary and phylogenetic relations, which has not been conducted in the past. The presence of additional putative paralogs or variants (for example an additional *jnk2* or *jnk3* gene) was investigated thoroughly and was disproved. This observation is based on the information currently available in online databases (Ensembl release 62). Such an approach facilitates further investigation of the timely and spatial roles of individual genes or variants, avoiding unknown confounding redundancy effects.

Previously published work carried out mainly on frog and mouse embryos has shown that the JNK signal transduction pathway is important in regulating CE movements (Asaoka and Nishina, 2010, Yamanaka et al., 2002). However, no distinction between different *jnk* genes was made in any of them. In the study by Seo et al. (2010) *jnk2* was shown to have more important roles in the regulation of CE movements during gastrulation than *jnk1* (*jnk1a-1* and *jnk1a-2*) and *jnk3* (Seo et al., 2010). It has been suggested in the past that *Jnk1* and *Jnk2*, although concurrently and ubiquitously expressed in mammalian embryos, may in fact have substantially different contributions in cellular processes depending on the physiological content, the presence or absence of interacting partners, the activating stimulus and the timing (reviewed by Bode and Dong, 2007). Intriguingly, most of the known Jnk substrates to date can be bound and become phosphorylated by all Jnk kinases (some exceptions are mentioned in Section 1.5.2, page 38) but to different degrees, with different affinities and with different, even contradictory, outcomes (Bode and Dong, 2007, Gupta et al., 1996, Hochedlinger et al., 2002, Sabapathy et al., 2004, Sabapathy et al., 2001, Sabapathy and Wagner, 2004); for example, Jnk2 has been shown to have a greater affinity for binding to c-Jun and targeting it for ubiquitination and degradation, while Jnk1 is more efficient in phosphorylating and thus activating it (Bode and Dong, 2007, Gupta et al., 1996). The function of each *Jnk* gene can be also greatly modified depending upon the

expression and activation status of the other Jnk genes; for example, *Jnk1* was shown to be greatly upregulated in *Jnk2*$^{-/-}$ mouse embryonic fibroblasts and to compensate for the loss of Jnk2 activity (Jaeschke et al., 2006, Jaeschke et al., 2005). New specific targets for the three *Jnk* genes are yet to be identified but are likely to exist. Taken together, the data presented above highlight the necessity for investigation of the individual contributions of *jnk* genes and isoforms, which have been shown in the past to be differentially regulated.

3.5.4. In vivo expression analysis of zebrafish jnk genes and proteins

The expression pattern of the identified zebrafish *jnk* genes was examined with two *in vivo* complimentary methods: RT-PCR and *in situ* whole mount hybridization (WISH). The former was mainly used for establishment of the timing of *jnk* expression and the latter for establishment of the localization of *jnk* expression. *Jnk1a* was shown to be abundantly expressed from fertilization until late developmental stages, with zygotic (embryonic) gene expression possibly activated at approximately 3 hpf during the mid-blastula transition, as shown by RT-PCR analysis. *In situ* spatial expression analysis confirmed abundant production of *jnk1a* mRNA, mainly in anterior structures, such as the brain and possibly the heart, but also in the presumptive gut. This pattern of expression fits in with previously published work that showed expression of zebrafish *jnk1* throughout development, mainly localized in the telencephalon and hypothalamus of the brain and in the presumptive gut (Krens et al., 2006).

Jnk2 was shown by RT-PCR analysis to be expressed at low levels during embryonic development, with a putative peak at the onset of gastrulation (5.25 hpf). In contrast, *in situ* hybridization with an anti-*jnk2* probe showed abundant expression of this gene at 13, 24 and 36 hpf, very similar to the expression pattern of *jnk1a*. This discrepancy can be partly explained by the differential sensitivity and specificity of the two methods. PCR is a highly sensitive technique. However, its efficiency and reliability depend greatly on the quality of the primers and on the optimisation of the protocol; suboptimal conditions may have significantly reduced yield and provide underestimated levels of gene expression. Although primers were carefully designed and the reaction was thoroughly optimised, the possibility that further optimisation could have been achieved cannot be excluded. In turn, *in situ* hybridization is a highly sensitive technique that can detect even as little as 10-20 copies of mRNA per cell (Thisse et al., 2004, Thisse and Thisse, 2008). The design of long probes (of around

400-500 base pairs) that recognize and bind to a large area of the mRNA that is produced in the cell, enhances the specificity and intensity of the signal and provides a reliable read-out of the levels of gene expression. Optimisation is required for this technique as well, in order to achieve the best levels of resolution with the highest levels of stringency. Of note, neither of these techniques is suited for strict quantitative analysis and they are both used in this study for the qualitative detection (spatial and temporal) of *jnk* genes and not for accurate measurement of their expression levels. It is, therefore possible that the differences in the expression levels of *jnk2* detected by RT-PCR and by WISH are mainly due to the limitations of the two techniques in providing reliable quantitative information. If accurate quantitation of *jnk* expression levels was of interest here, quantitative real-time PCR could and would have been employed (described in Chapter 2, page 73 and used for the data presented in Chapters 5 and 6). Also, the use of different primers/probes suited to the optimal requirements of each technique individually (short in RT-PCR analysis for increased specificity and efficiency, long in WISH for enhanced signal detection and specificity), are likely to be another reason for the discrepancy. Given the data presented by Seo et al. (2010) that suggested *jnk2* as being the most important *jnk* gene expressed during gastrulation (Seo et al., 2010), it is likely that the WISH results obtained here more accurately represent the real expression levels of *jnk2* during zebrafish development than the RT-PCR results.

Jnk3 expression was absent at 20 hpf and firstly detected by RT-PCR at 36 hpf. However, WISH analysis showed low levels of *jnk3* expression already at 24 hpf, a time point not included in the PCR analysis. Thus, onset of expression of *jnk3* is likely to be between 20 hpf and 24 hpf. At this stage (20-24 hpf) and up to at least 5 days of embryonic development only *jnk3.3*, among the *jnk3* variants examined here, was found to be expressed, so any mRNA signal detected by WISH analysis with the pan-*jnk3* probe at 24, 36 and 96 hpf is likely to represent *jnk3.3* mRNA. Hybridization with a specific anti-*jnk3.3* probe reproduced the expression pattern detected by the pan-*jnk3* probe and reiterated the notion that throughout development only *jnk3.3* mRNA, among the *jnk3* splice variants, is produced.

Sense probes were used as controls for each antisense probe. Antisense probes are designed so that they can bind to endogenously produced mRNA. Sense probes, in contrast, are designed to bind to antisense mRNA that is not commonly produced endogenously. So, it is commonly expected that staining with sense probes does not give any blue-purple precipitate, emphasizing the specificity of the antisense probe.

This was the case for sense *jnk3* and *jnk3.3* staining, but not for sense *jnk1* and *jnk2*. A possible reason for detection of product after staining with sense *jnk1* and *jnk2* probes at 13 and 24 hpf (no staining was observed at 36 hpf) is internal regulation of the levels of mRNA production: antisense mRNA may be produced endogenously as a regulatory mechanism for controlling the levels of expression of sense mRNA (that will be translated and will produce the corresponding protein). If this scenario is true, the expression domains of sense and antisense mRNA and thus the staining pattern of antisense and sense probes, respectively, are expected to be quite similar but possibly not identical (due to the effect of regulation). This is, in fact, what is observed here, with *jnk1* and *jnk2* sense probes giving a similar (anterior-dense) staining pattern as their antisense counterparts. Overall, the main areas of *jnk* expression, as revealed with the current approaches, are anterior structures, such as the brain, the heart, the otic vesicles, the presumptive gut and possibly the fin buds.

3.5.5. Advantages and disadvantages of the current study

In the current study three complementary methods were used for the identification of zebrafish jnk orthologs. *In silico* investigation and bioinformatics analysis were complemented by *in vitro* and *in vivo* gene expression examination, providing a thorough overview of zebrafish *jnk* genes. The most up to date information was used for all the analyses and, with the use of appropriate controls, comprehensive and reliable results were obtained. An obvious observation from the data presented in previous sections is the fact that not all *jnk* transcripts identified *in silico* were further examined *in vivo* and *in situ*. The main reason for that was the constant update of online databases. Ensembl provides very regular updates of its online information and different or newly predicted transcripts appear frequently. This made the follow up studies cumbersome and sometimes even impossible. For example, the identification of *jnk1b* (the 'extra' zebrafish *jnk1* gene) took place after the completion of the *in vivo* zebrafish work (shortly before its publication by Seo et al., 2010) and therefore, could only be included in the *in silico* studies and the phylogenetic analyses (and not in the *in situ* expression analysis). Primers (against all transcripts of the gene at the time, Ensembl release 62) for RT-PCR analysis were however designed against *jnk1b*, as it was important to assess its presence, at least *in vitro*. Fortunately, the general *jnk1*a RT-PCR primers that were initially designed against common areas of *jnk1a* transcripts (two at the time), were found to also pick up the newly identified (after the initial primer design) *jnk1a*

transcripts (four currently, Ensembl release 62). So, the RT-PCR panel shows a representative illustration of the temporal expression pattern of *jnk1a*. Also, it is important to note that most of the information provided by the online databases corresponds to predictions, which do not necessarily respond to reality. The *in silico* and bioinformatics analyses were, thus, based on predicted sequences. *In vivo* analyses confirmed, at least some, of the predictions, by showing that mRNA of some of the newly identified *jnk* transcripts is produced in developing zebrafish embryos. A downside of the current study was the detection of mRNA only and not protein, during the *in vivo* approaches. As there are many steps after transcription that regulate gene expression and many steps of protein synthesis, maturation and modification before the production of a functional protein, production of mRNA is not linearly correlated with protein production. However, mRNA detection is commonly used as a method for assessing gene expression and functionality.

3.5.6. Summary and conclusions

In this chapter the zebrafish *jnk* genes were examined in detail. Initially, *in silico* investigation of online genomic databases revealed (or in fact confirmed) the presence of a fourth *jnk* gene, additional to the three known mammalian *jnk* orthologs. This gene, named *jnk1b*, following the ZFIN guidelines for naming genes of duplicated pairs, showed high evolutionary conservation with *jnk1a* and was, thus, classified as a duplicated *jnk1a* paralog. However, it is still not clear which one of the two is the original gene and which one arose after the duplication. Bioinformatics and phylogenetic analysis of the structure of zebrafish jnk genes and proteins revealed conservation of essential motifs and of the overall morphology of the kinases, which reinforces the possibility that the identified isoforms can, in fact, be functional if produced *in vivo*. This observation led us to the next milestone of the current study, which was the investigation of the *in vivo* production of *jnk* mRNA, which is a good indication of putative *in vivo* protein production. All of the isoforms examined were shown to be produced, at least at the mRNA level, in developing zebrafish embryos. Their expression patterns were distinct but were mainly localised in anterior structures (such as brain, heart, otic vesicles). In the next chapter, global inhibition of all jnk protein isoforms by a pharmacological agent (SP600125) is conducted, in order to elucidate their role during zebrafish development and in particular during zebrafish cardiogenesis.

Chapter 4. Investigation of the role of jnk during zebrafish embryogenesis

4.1. Introduction

In the previous chapter (Chapter 3), *in silico* investigation and bioinformatics analysis revealed the presence of four *jnk* genes in the zebrafish genome (*jnk1a, jnk1b, jnk2* and *jnk3*), which are expressed and are potentially active during the first days of embryogenesis. In this chapter, the putative roles of jnk during zebrafish embryonic development are investigated. In order to achieve this, chemical inhibition of the activity of jnk proteins was performed at distinct time intervals during gastrulation, segmentation and later stages of zebrafish embryonic development. General body defects and, in particular, cardiac abnormalities arising after jnk inhibition were of interest. Below, an overview of the chemical inhibitor that was used in this study is presented.

4.1.1. SP600125, a potent pharmacological inhibitor of Jnk

SP600125 [anthra(1,9-cd)pyrazol-6(2H)-one] is a potent, cell-permeable, reversible ATP-competitive inhibitor that binds and inactivates Jnk (Bennett et al., 2001). It is a small hydrophobic molecule, with a nitrogen-containing ring system, which was shown to make optimal binding in the ATP pocket of Jnk. By binding to this area, SP600125 prevents ATP from binding and therefore Jnk can no longer phosphorylate its downstream targets. The chemical structure of SP600125 (three fused rings containing nitrogen residues), which makes its affinity with the ATP pocket of Jnk strong, also makes the molecule poorly soluble in water, a difficulty easily overcome by the addition of dimethylsulfoxide (DMSO).

SP600125 binds and inactivates all Jnk isoforms with half maximal inhibitory concentration (IC_{50}) values for mammalian Jnk1, Jnk2 and Jnk3 being 40, 40 and 90 nM, respectively (Bennett et al., 2001). It exhibits 300 fold greater selectivity for Jnk over related MAPK (Erk1 and p38) and between 10 fold and 100 fold selectivity over another 14 protein kinases tested. Interactions between SP600125 and Jnk have been explored by co-crystallization of SP600125 with Jnk3 (Scapin et al., 2003). It was

shown that residues specific for Jnk, but absent in related MAPK, such as p38, are important in producing a narrow ATP-binding pocket that can accommodate SP600125, contributing to the specificity of the drug (Scapin et al., 2003). These observations suggest high affinity and specific interactions of SP600125 with Jnk.

Over 200 publications have reported the use of SP600125 as a chemical inhibitor for the assessment of Jnk-dependent events in cells and *in vivo*. Among others, SP600125 has been shown to inhibit a number of apoptotic events (activation of pro-apoptotic Bcl2, release of mitochondrial cytochrome-c etc), to modulate immune responses and to prevent cells from entering mitosis (Bogoyevitch and Arthur, 2008).

Despite its extensive use in both *in vitro* and *in vivo* studies, some scepticism surrounds its repeated use, mainly associated with the claimed specificity for Jnk. After its initial characterization (Bennett et al., 2001), subsequent testing has shown that SP600125 can also inhibit a number of other protein kinases, like serum and glucocorticoid-regulated kinase, AMP-dependent protein kinase and others (Bain et al., 2003). Nevertheless, the concentration of the drug has to be quite high for these effects to take place (much higher than the IC_{50} of the drug) and for many years SP600125 continued to be the preferred chemical Jnk inhibitor (Bogoyevitch and Arthur, 2008). In the present study, SP600125 was used as an inhibitor of Jnk at low, compared to previously published work, concentration (3μM and 5μM).

Recently, new inhibitors of Jnk have started to be developed. The most specific and potent among the new drugs are peptide inhibitors that can interfere with protein-protein interactions. Their main advantages are high specificity and reduced side effects compared to small molecule inhibitors. However, a great problem associated with their use is their rapid breakdown and their difficult delivery into the cell (Waetzig and Herdegen, 2005). Additionally, Jnk-interacting peptide (JIP)-targeting inhibitors have recently started to be developed. JIP are scaffolding proteins that contain a docking domain (D-domain, essential for binding to Jnk, further described in Section 3.1.2, page 84) and interact with Jnk. This interaction has been shown to be essential for further activation of Jnk (Kallunki et al., 1996, Yang et al., 1998). Peptides that correspond to the D-domain of JIP or chemical inhibitors that target the JIP-Jnk interaction site have been shown to inhibit Jnk activity in a remarkably selective way (Barr et al., 2002, De et al., 2009a, De et al., 2009b, Heo et al., 2004). These inhibitors have, however, not been tested and used extensively yet.

In summary, SP600125 is a selective Jnk inhibitor that competes with ATP for binding at a Jnk-specific site of the ATP-binding pocket. Although, new drugs are being

rapidly developed and the specificity of the existing inhibitors is coming into question, SP600125 remains a widely accepted and extensively used inhibitor of Jnk.

4.2. Aims of the chapter

JNK, as a member of the MAPK family and the Wnt/PCP pathway, has been shown to be involved in a vast array of cellular and morphogenetic processes. Members of both cascades (MAPK and PCP) have been shown to be involved in different aspects of heart development and disease, in animal models (mouse, chicken, frog, zebrafish) and in cultured cells (primary, carcinoma, embryonic stem cells). It was, thus, hypothesized that JNK may represent the culmination of the activity of the two highly conserved and important pathways during heart specification and development. Therefore, the main focus of the current study was to investigate the requirement of jnk signalling during zebrafish development. In order to achieve this the following aims were set:

- Define the role of zebrafish jnk proteins (identified in the previous chapter) at distinct time intervals during embryonic development by inactivating them with SP600125
- Determine their roles during zebrafish cardiogenesis with SP600125 treatment

4.3. Chemical inhibition of jnk in zebrafish

The contribution of jnk during zebrafish embryogenesis was investigated by chemically inhibiting all jnk protein isoforms with SP600125 at distinct time intervals. Initially, the dosage of the inhibitor was assessed and then its effects were analysed. Understanding how inactivation of jnk affects normal embryonic development generally was of interest, but also more specifically how it influences heart specification and morphogenesis. In all sections that follow the transgenic Tg*(cmlc2;gfp)* zebrafish line was used, unless otherwise stated. For more details about the transgenic lines refer to Chapter 2 (Section 2.1.1, page 53).

4.3.1. SP600125 dosage assessment

Initially, a wide range of SP600125 dosages was examined in order to find the appropriate concentration for treatment of zebrafish embryos. SP600125 was diluted in dimethylsulfoxide (DMSO) because its ring structure makes it insoluble in water. Therefore, a control containing DMSO alone was, also, used alongside the E3 water control. Both controls are presented here. 50 zebrafish embryos were used for each treatment and for each control in every experiment. The overall number of embryos used for each condition is shown within the graphs. Each experiment was performed on the same clutch of eggs. Three repetitions of the experiment were performed at different days and with eggs from different clutches. The embryos were washed thoroughly after each treatment and were transferred into new dishes. The results presented here were collected at 72 hpf and represent the mean values of three experiments.

In the preliminary dosage assessment experiments, the inhibitor was introduced into the water at distinct time intervals: 0-5.25 hpf, 5.25-10 hpf, 10-22 hpf and 22-30 hpf. These intervals trail some of the important events during normal embryonic and heart development. 0-5.25 hpf is the time when cleavages take place and blastula embryos form; between 5.25 and 10 hpf gastrulation is under way, atrial and ventricular cells are being specified and myocardial precursors involute; at 10-22 hpf body segmentation occurs, most of the organ rudiments appear (otic vesicle, optic primordia, fin buds) and heart cells form the cone and later the heart tube; 22-30 hpf, is the time when pharyngeal arches develop, organs (including the heart) attain their final positions and conformation while the body straightens and lengthens (see Section 1.2 at page 2 for more details on zebrafish embryonic development). Dosages ranging from 1 μM to 25 μM were tested (1μM, 3μM, 6μM, 12μM and 25μM). These dosages were adjusted and expanded from previously published work on animal models and cells (Moon et al., 2008, Nakaya et al., 2009, Naruishi et al., 2003, Tanemura et al., 2009, Zhu et al., 2008).

In Figure 4.1 an overview of the results obtained from the dosage assessment experiments is presented. Representative images of the SP600125-treated embryos are shown, when possible. When viability was very low after jnk inhibition and a representative image could not be obtained (very few embryos surviving with a variable phenotype), a graph showing the viability is shown instead. Results obtained from the 3μM SP600125 experiments are not included in this figure but are presented in detail in the next sections.

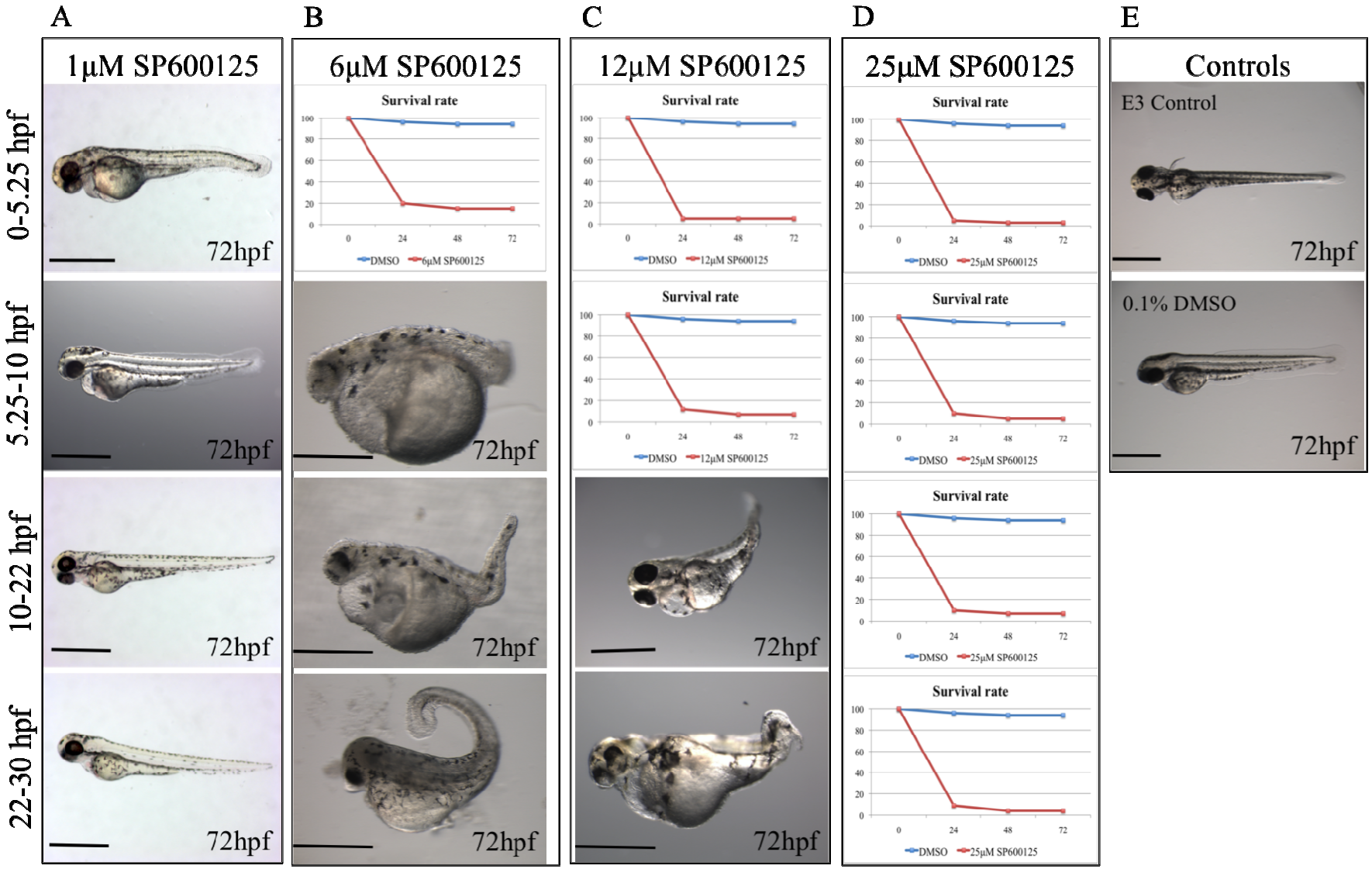
A
B
C
D
E
1µM SP600125
6µM SP600125
12µM SP600125
25µM SP600125
Controls
0-5.25 hpf
5.25-10 hpf
10-22 hpf
22-30 hpf
72hpf
Survival rate
DMSO
6µM SP600125
12µM SP600125
25µM SP600125
E3 Control
0.1% DMSO

Figure 4. 1: SP600125 dosage assessment. SP600125 was initially used at 5 different concentrations (1μM, 3μM, 6μM, 12μM and 25μM), four of which are shown here: (A) 1μM, (B) 6μM, (C) 12μM and (D) 25μM (the 3μM concentration is not shown here as it is the one used for the rest of the experiments, presented in the next sections). (E) Untreated and DMSO-treated (0-30 hpf) zebrafish embryos were used as controls. Treatment with the drug was conducted in four different time intervals: 0-5.25 hpf, 5.25-10 hpf, 10-22 hpf and 22-30 hpf. All figures represent representative images of the majority (but not all) of the embryos for each condition. High lethality was observed after 0-5.25 hpf treatment with 6, 12 and 25 μM SP600125, after 5.25-10 hpf treatment with 12 and 25 μM SP600125 and after the two late treatments (10-22 and 22-30 hpf) with 25μM SP600125. In the cases where high lethality was observed and therefore not enough embryos were available for phenotype assessment, a graph representing the survival curve of SP600125-treated embryos compared to DMSO-treated embryos is shown. In these graphs the survival rates of untreated embryos are not included for clarity of illustration, but were very similar to that of DMSO-treated embryos. Scale bars represent 200 μm.

The 25 μM SP600125 concentration was found to be lethal from fertilization until 30 hpf (Figure 4.1). The period between fertilization and initiation of gastrulation (0-5.25 hpf) is a tightly regulated, finely tuned and very important phase, commonly disturbed by chemical manipulation. Treatment with 12 μM of the inhibitor in the first two time intervals (0-5.25 hpf and 5.25-10 hpf) caused lethality to more than 90% of embryos, while its later administration proved viable but highly toxic (misshapen embryos). Similarly, 6 μM SP600125 treatment between fertilization and gastrulation (0-5.25 hpf) caused high levels of lethality, while between 5.25 and 30 hpf (5.25-10, 10-22, 22-30 hpf) it was viable but toxic for the embryos (Figure 4.1). The most prevalent abnormalities caused by high dosages of SP600125 were severe cardiac oedema, yolk sac anomalies, tail shortening and curving and general body plan disturbance. In contrast, 1 μM of SP600125 had no superficial effect on the morphology and viability of the embryos (Figure 4.1). Comparisons were made to the two controls: E3 water and DMSO. It was therefore concluded that the most potent, but not toxic concentration to be used and assessed further was 3 μM. This concentration, however, caused high lethality at the time interval between fertilization and initiation of gastrulation (0-5.25 hpf), which, as discussed before, is a highly sensitive period. The experiments presented and analysed in this section were performed using this concentration of SP600125. 3μM of SP600125 is considered a fairly low concentration, not likely to cause unspecific effects, as discussed in Section 4.1.1 (page 132).

4.3.2. Analysis of the general phenotype of zebrafish embryos after SP600125 treatment; convergence-extension-like phenotype observed

Once the concentration of the inhibitor was decided (3μM), the temporal-specific role of jnk was further investigated. The following time intervals were investigated: 5.25-10 hpf, 10-22 hpf and 22-30 hpf, excluding the 0-5.25 hpf phase, which, as shown before, was sensitive to treatment even with small concentrations of SP600125. Two methods were used to assess the phenotype in the domains of interest: microscopic observation and phenotypic scoring for qualitative assessment, and various body measurements for quantitative assessment. The following measurements were taken: the distance between the eyes (ocular distance), the width of the head, the length and width of the body. These body features are commonly disturbed in known mutant zebrafish lines (Heisenberg et al., 2000, Jessen et al., 2002, Kilian et al., 2003, Topczewski et al.,

2001). When necessary, measurements were normalised against the body size (either body length or head width), as explained in more detail in Section 2.1.4 (page 54).

4.3.2.1. Convergence extension-like phenotype

Initially, we assessed the overall body size and shape of SP600125-treated embryos compared to controls, as explained in Section 2.1.4 (page 54). These features were of interest because they are commonly disturbed in PCP mutants that exhibit convergence-extension abnormalities (see Section 1.4.2.1 at page 32). At 72 hpf, embryos of all treatment groups appeared significantly shorter than untreated and DMSO-treated ($p=0.000$) embryos, while the two latter groups did not show any differences between them ($p=0.42$) (Figure 4.2A). Specifically, 5.25-10 hpf SP600125-treated embryos were on average 4816μm long (standard error, se=322), 10-22 hpf SP600125-treated embryos were 5041μm long (se=36) and 22-30 hpf SP600125-treated embryos were 4669μm long (se=253) at 72 hpf. At the same stage of development, untreated fish were on average 5285μm long (se=50) and DMSO-treated embryos were 5337μm long (se=68). Overall, treatment of zebrafish embryos with 3μM SP600125 caused a severe decrease in body length, regardless of the time of drug administration.

Next, the ratio of body width to body length (width:length) was investigated as it is a good indication of CE progression: if CE is defective, shorter and wider embryos (higher width:length ratio) are expected to develop. The width:length was only significantly increased in the first SP600125 treatment group (5.25-10 hpf, $p=0.027$), but was not altered in all later SP600125 treatment groups ($p>0.06$ for the 10-22 hpf and 22-30 hpf) compared to both untreated and DMSO-treated embryos (Figure 4.2C). At 72 hpf, 5.25-10 hpf SP600125-treated embryos had a width:length ratio of approximately 0.082, 10-22 hpf SP600125-treated fish 0.077, 22-30 hpf SP600125-treated embryos 0.078, while untreated fish embryos had width:length ratios of 0.074 and DMSO-treated embryos 0.076. No significant differences were observed between the two control groups. Overall, 5.25-10 hpf SP600125-treated zebrafish embryos had increased body width:length ratios, representing both wider and shorter body axes, a feature commonly seen in mutants with defective CE movements.

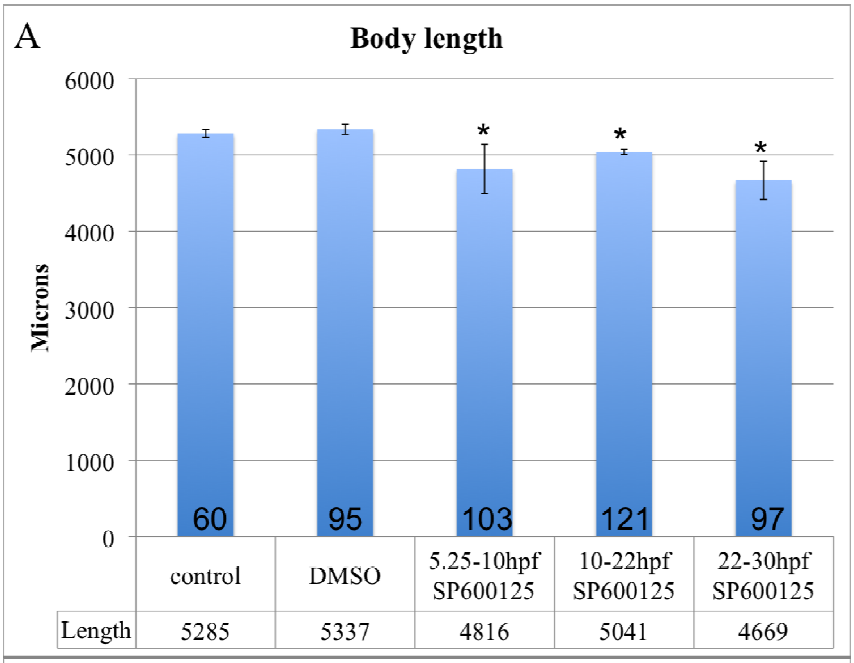
A
Body length
Microns
6000
5000
4000
3000
2000
1000
0
60
95
103
121
97
*
*
*
control
DMSO
5.25-10hpf SP600125
10-22hpf SP600125
22-30hpf SP600125
Length
5285
5337
4816
5041
4669

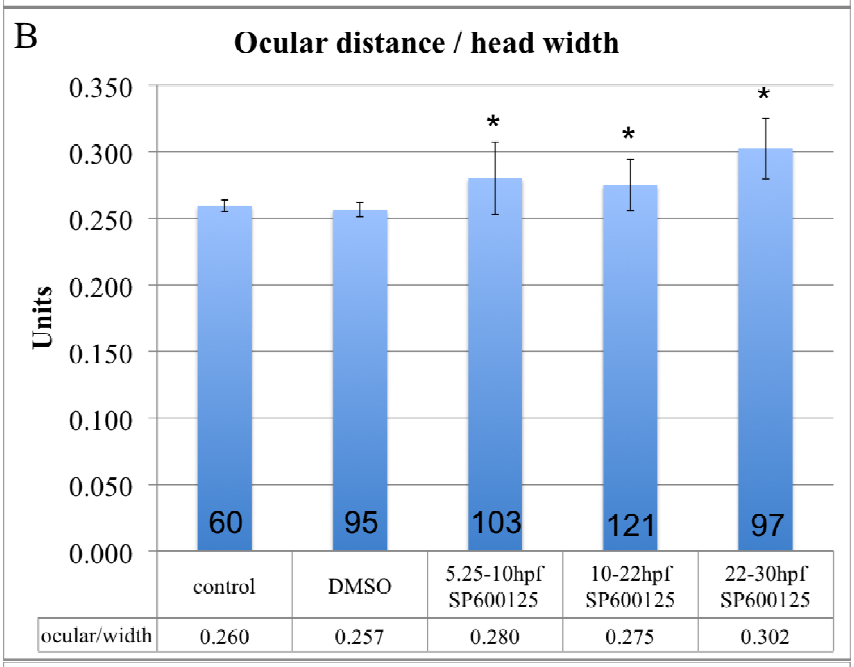
B
Ocular distance / head width
Units
0.350
0.300
0.250
0.200
0.150
0.100
0.050
0.000
60
95
103
121
97
*
*
*
control
DMSO
5.25-10hpf SP600125
10-22hpf SP600125
22-30hpf SP600125
ocular/width
0.260
0.257
0.280
0.275
0.302

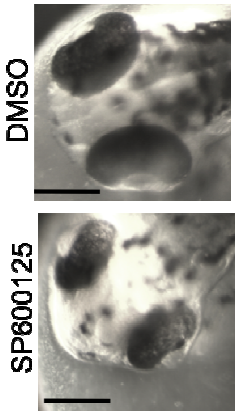
DMSO
SP600125

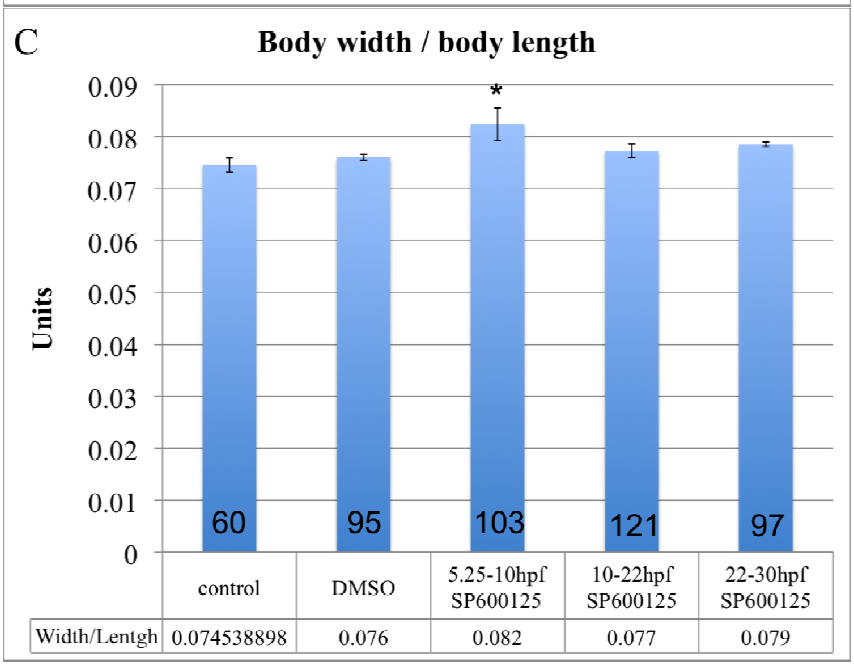
C
Body width / body length
Units
0.09
0.08
0.07
0.06
0.05
0.04
0.03
0.02
0.01
0
60
95
103
121
97
*
control
DMSO
5.25-10hpf SP600125
10-22hpf SP600125
22-30hpf SP600125
Width/Lentgh
0.074538898
0.076
0.082
0.077
0.079

Figure 4. 2: Body measurements after jnk inhibition. A) The length of the body of treated embryos was significantly decreased at 72 hpf after 5.25-10, 10-22 and 22-30 hpf SP600125 treatment compared to untreated and DMSO-treated embryos. B) The distance between the eyes, normalized against the width of the head was, also, shown to be statistically significant in all SP600125 treatment groups, compared to controls. A representative image of a control and a SP600125-treated embryo at 72 hpf is shown on the right. C) After 5.25-10 hpf SP600125 treatment a convergence-extension like phenotype was observed, with the body width to body length ratio severely affected. Later treatments (10-22 and 22-30 hpf) did not affect the body shape. Statistical analysis was performed with one-way Anova testing, followed by a 2-sided Dunnet test. Asterisk (*) shows statistical significance compared to both control groups, with $p<0.05$.

4.3.2.2. Ocular distance abnormalities

It was also of interest to score the distance between the eyes in SP600125-treated, DMSO-treated and untreated embryos, as disturbed ocular distance is one of the features commonly associated with, among others, PCP mutants (Heisenberg and Nusslein-Volhard, 1997, Heisenberg et al., 2000). Indeed, embryos of all SP600125 treatment groups exhibited disturbances in the positioning of their eyes: eyes were located further apart from each other than in control embryos (Figure 4.2B). Specifically, at 72 hpf the ratio of the distance between the eyes normalised against the width of the head (eyes/width), to account for head size differences (associated with body size differences), was on average 0.260 for untreated, 0.257 for DMSO-treated, 0.280 for 5.25-10 hpf SP600125-treated, 0.275 for 10-22 hpf SP600125-treated and 0.302 for 22-30 hpf SP600125-treated embryos (Figure 4.2B). Differences between treatment groups and controls were found to be significant ($p<0.05$ for all groups compared to both DMSO and E3 controls). Overall, 3μM SP600125 treatment caused an increase in the ocular distance of developing zebrafish embryos, regardless of the time of drug administration.

4.3.2.3. Jnk inhibition did not affect the formation of fins and somites but caused low prevalence abnormalities in the eyes, otic vesicles and tails

I was then interested to look at how the general morphology of some important organs and structures of zebrafish embryos changed after inhibition of jnk, focusing mainly on the fins, the eyes, the otic vesicles, the somites and the tail (Figures 4.3 and 4.4). An unusual eye phenotype was observed in a small percentage (4%) of 10-22 hpf SP600125-treated embryos, whereby only half of the eye was pigmented, showing a coloboma-like phenotype. However, it was unclear whether the pigmentation only or the underlying structure as well was missing. DMSO-treated, untreated and 5.25-10 hpf and 22-30 hpf SP600125-treated embryos did not exhibit this phenotype (Figure 4.3A).

Additionally, otic vesicle defects were observed in all groups, with the highest occurrence (but still fairly low) in the early treatment group (9% in 5.25-10 hpf SP600125-treated embryos) and decreasing incidence as development proceeded (5% in 10-22 hpf and 1% in 22-30 hpf SP600125-treated embryos). These defects included small otic vesicles and otolith abnormalities, such as absence of one otolith, and smaller or malpositioned otoliths (Figure 4.3B).

A

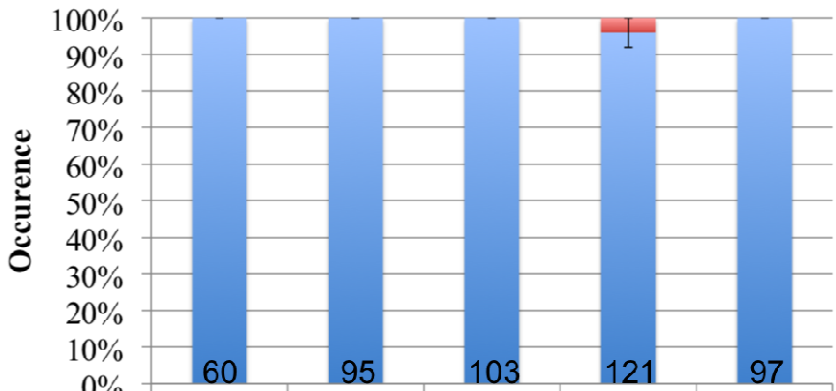

	control	DMSO	5.25-10 SP600125	10-22 SP600125	22-30 SP600125
abnormal	0	0	0	4	0
normal	100	100	100	96	100

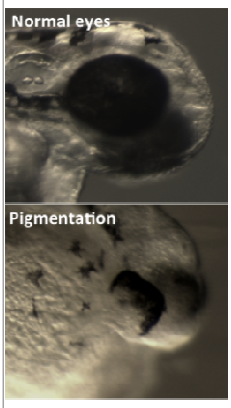

B

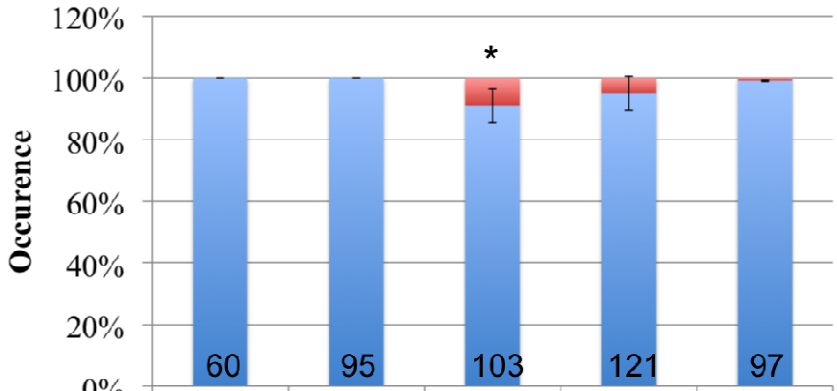

	control	DMSO	5.25-10 SP600125	10-22 SP600125	22-30 SP600125
abnormal	0	0	9	5	1
normal	100	100	91	95	99

C

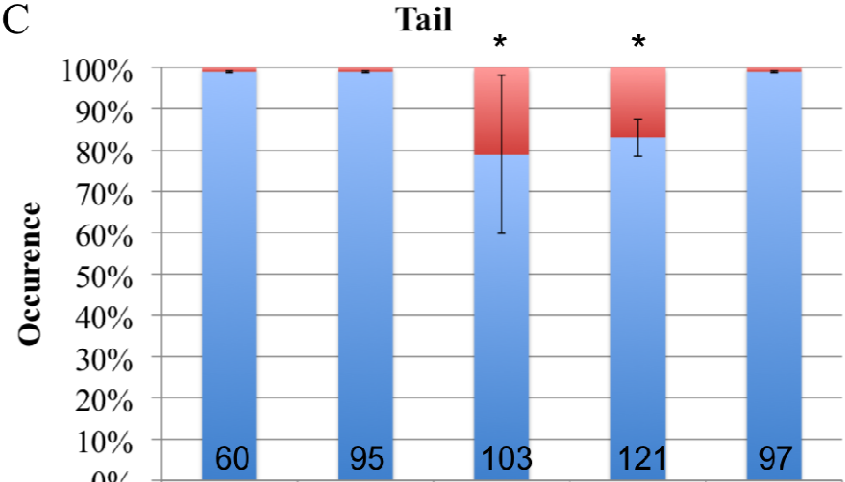

	control	DMSO	5.25-10 SP600125	10-22 SP600125	22-30 SP600125
abnormal	1	1	21	17	1
normal	99	99	79	83	99

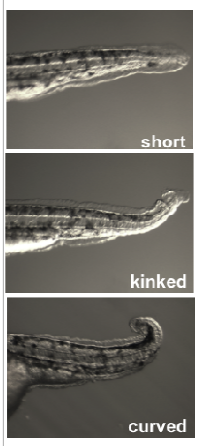

Figure 4. 3: Eyes, otic vesicle and tail development after treatment with SP600125. A) Development of the eyes was not severely affected after 10-22 hpf SP600125 treatment. Only a small and not significant percentage of embryos exhibited a coloboma-like phenotype, shown in the figure on the right. B) The formation of the otic vesicles was defective after 5.25-10 hpf SP600125 treatment in 9% of the embryos. Later treatment groups (10-22 and 22-30 hpf) remained unaffected. The most common otic vesicle phenotypes are shown in the figure on the right. Otoliths were either missing, misplaced or smaller in size, compared to controls. C) Tail abnormalities were observed after the two early SP600125 treatments (5.25-10 and 10-22 hpf), but not after the 22-30 hpf SP600125 treatment. Curved and kinked tails were most commonly seen in abnormal embryos. Data are tabulated underneath the graph. Statistical significance was assessed with the χ^2 test for association of categorical data and is shown with an asterisk (*$p<0.05$).

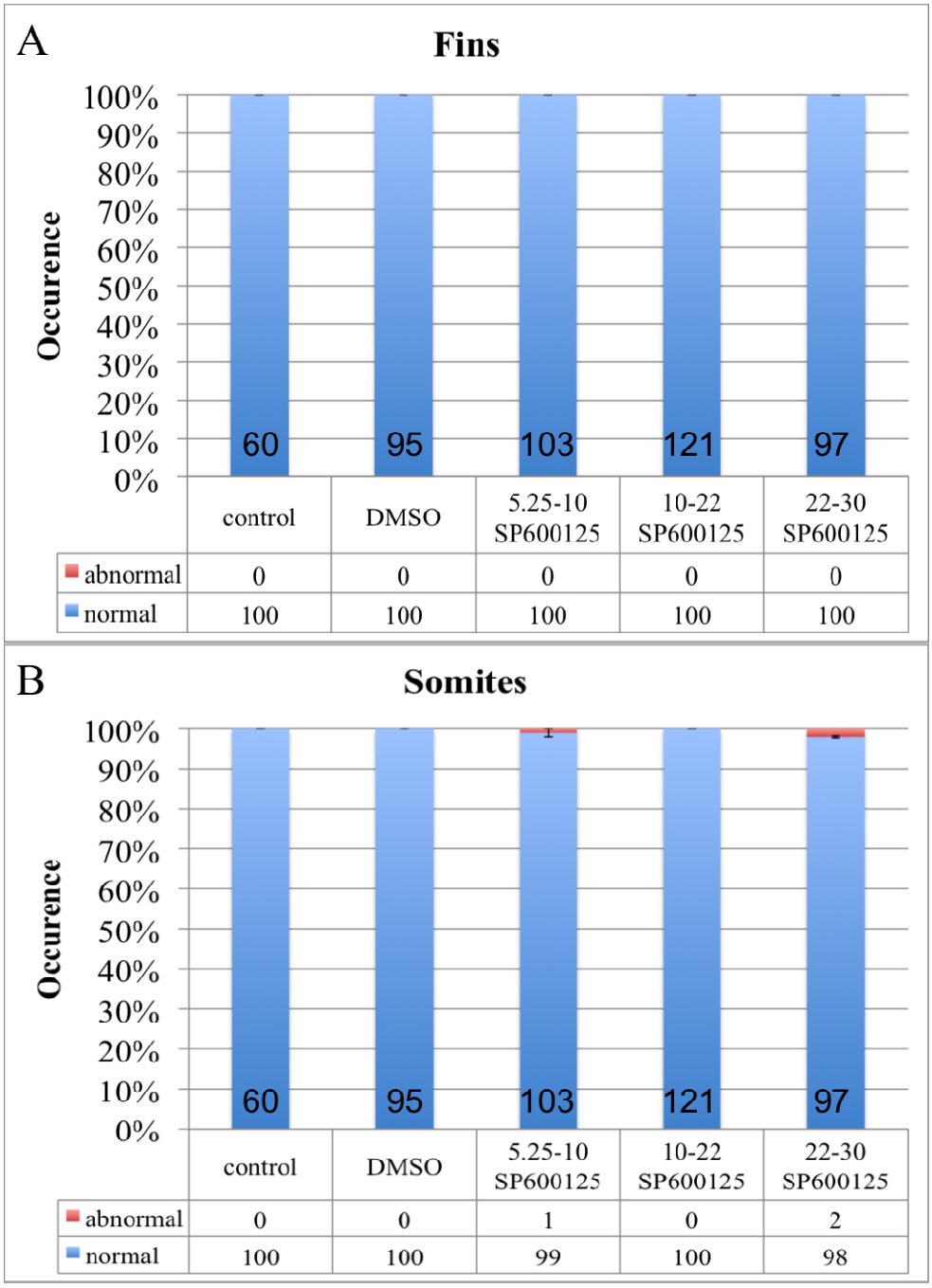

Figure 4. 4: Development of the fins and somites after SP600125 treatment. A) Formation of the fins was not shown to be affected by any of the SP600125 treatments (5.25-10, 10-22 and 22-30 hpf). B) Development of the somites was not significantly affected after jnk inhibition at any time interval examined here. Statistical significance was assessed with the χ^2 test for association of categorical data.

Abnormalities associated with the tail were seen in all SP600125 treatment groups examined here. Their occurrence in the control groups (DMSO and E3) and in the late SP600125 treatment group (22-30 hpf) was only 1%, while this percentage was higher in the earlier SP600125 treatment groups: 17% in the 10-22 hpf and 21% in the 22-30 hpf SP600125 treatment groups. Tail anomalies were mainly associated with a curly or kinky phenotype of the tip of the tail.

In contrast, the development of the fins did not seem to be affected under any of the conditions, signifying that jnk is probably not important during this process (Figure 4.4A). Similarly, formation of the somites was not severely affected, as only a few abnormal embryos were seen after the 5.25-10 hpf (1%) and the 22-30 hpf (2%) SP600125 treatments (Figure 4.4B). So, the development of the fins and the somites was not affected by jnk inhibition throughout embryonic development.

Although differences in the fin, eye and somite development were observed between SP600125-treated and untreated or DMSO-treated embryos, in none of the treatment groups were the observed differences statistically significant compared to the two control groups. Statistical significance was assessed with the χ^2 test for associations of categorical data and p was found to be higher than 0.05 for all SP600125 treatment groups for the fins, eyes and somites phenotypes. In contrast, formation of the otic vesicles and the tail was significantly abnormal ($p<0.05$ compared to both control groups) after 5.25-10 hpf SP600125 treatment (for the otic vesicle) and after the 5.25-10 and 10-22 hpf SP600125 treatments (for the tail).

Taken together, jnk inhibition at 5.25-10 hpf caused a significant occurrence of abnormalities in the development of the otic vesicles and the tail, while jnk inhibition at 10-22 hpf caused a significant occurrence of tail abnormalities. The eye defects that were observed in the 10-22 hpf SP600125 treatment group, although interesting, were at low prevalence.

4.3.3. Analysis of the heart phenotype after SP600126 treatment

One of the main interests of the current study was to characterize putative roles of jnk during zebrafish cardiogenesis. In order to achieve this, the development of the embryonic zebrafish heart was examined after timely SP600125 treatment. More specifically, the segmentation of the heart into two chambers (atrium and ventricle), the relative sizes of the two chambers, the looping of the linear heart tube and formation of pericardial oedema were examined in detail. These features provide a good

morphological evaluation of progression of cardiogenesis the first 3 days of zebrafish embryonic development.

Normal 72 hpf zebrafish hearts are expected to be segmented into equally sized chambers (an atrium and a ventricle), looped towards the right with the ventricle lying on the anterior and right side of the atrium (looking at the embryos dorsally) and without any noticeable cardiac oedema. As expected, under control conditions and after DMSO treatment, almost all of the embryos exhibited the features described above, with only an insignificant ($p<0.05$) 1% of them showing leftwards instead of rightwards looping.

4.3.3.1. Small occurrence of mild pericardial oedema

Pericardial oedema, commonly a marker of cardiac dysfunction or fluid homeostasis disruption, was absent after late SP600125 treatment (22-30 hpf) but present in embryos treated with SP600125 between 5.25-10 hpf and 10-22 hpf. 5.2% of early SP600125-treated embryos (5.25-10 hpf) exhibited minimal enlargement of the pericardial cavity, 2.8% of them had mild cardiac oedema and 92% were normal (Figure 4.5A). Illustration of the categorization of mild and minimal pericardial oedema is shown in Figure 4.5A (embryo images on the right). The respective percentages for 10-22 hpf SP600125-treated fish were 4.5% (minimal), 7.5% (mild) and 88% (normal), showing increased severity of the phenotype.

The overall number of embryos with abnormally swollen pericardial cavities was shown to be statistically significant compared to control embryos ($p=0.009$, shown with the χ^2 test for associations). However, individual subcategories of abnormal embryos (with minimally and mildly swollen cardiac cavities separately) did not exhibit statistical significance compared to controls ($p>0.1$). Despite the significance shown by the statistical tests, in all treatment groups the pericardial cavity was only slightly enlarged (either minimally or mildly, as shown in Figure 4.5A), which is unlikely to be disruptive for proper heart morphology and function, as it does not seem to stretch and distort the heart.

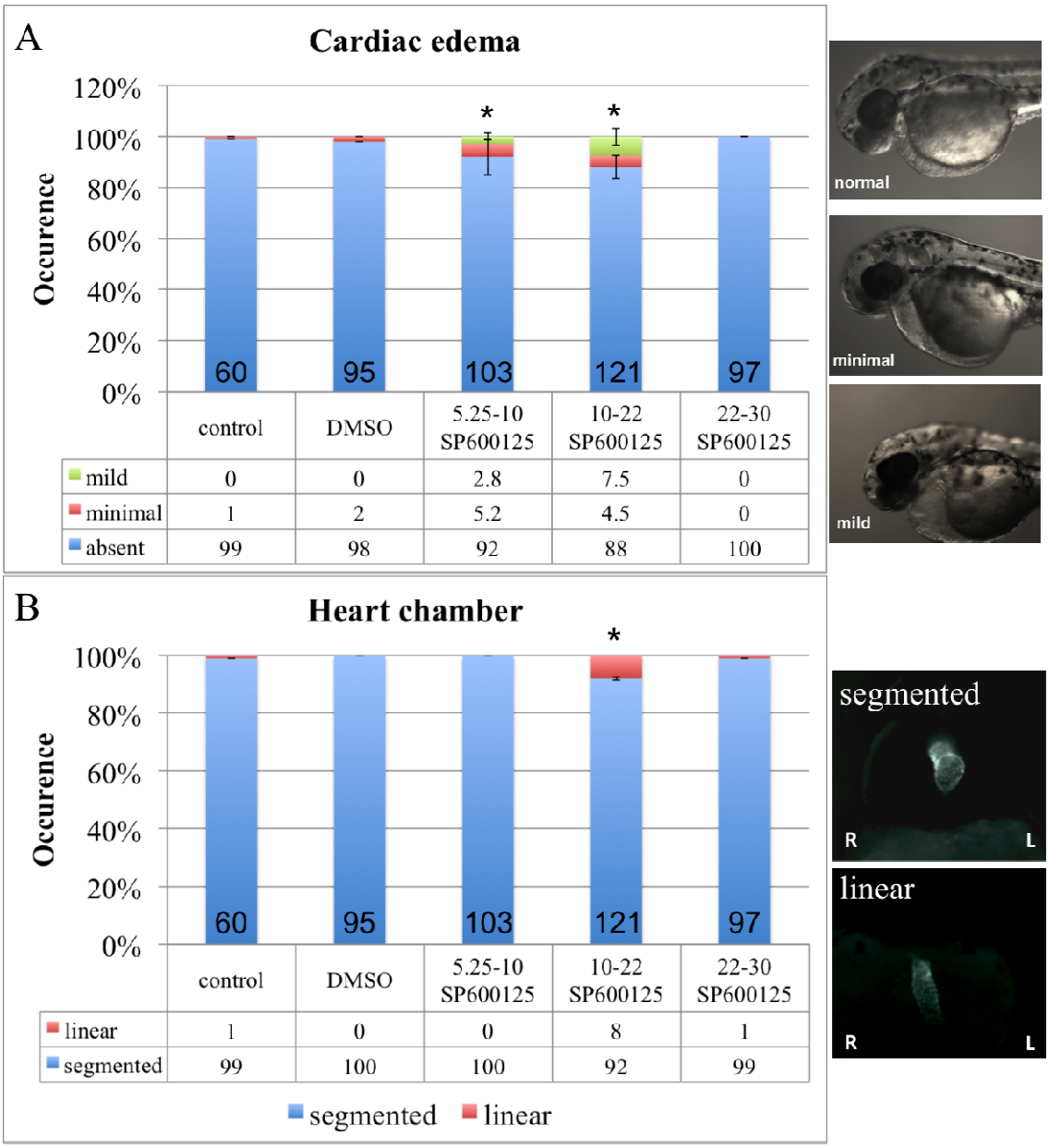

Figure 4. 5: Cardiac oedema and heart chamber segmentation after SP600125 treatment. A) Swelling of the pericardial cavity was observed in 8% and 12% of 5.25-10 and 10-22 hpf SP600125-treated embryos. The occurrence of abnormal pericardial oedema was significantly higher in treated compared to untreated and DMSO-treated embryos (p=0.009). 65% of the embryos with abnormally enlarged cardiac cavities had minimal oedema (5.2% of the overall embryos), while 35% of them (2.8% of the overall embryos) showed mild oedema, as shown in the image on the right. B) Only 10-22 hpf SP600125-treated embryos showed abnormalities in the segmentation of their heart chambers, with 8% of them having non-segmented linear hearts at 72 hpf. Representative images of the phenotype are shown on the right side (ventral views of embryos, anterior to the top). The other treatment groups (5.25-10 and 22-30 hpf) were not affected. Statistical significance was assessed with the χ^2 test for association of categorical data and is shown with asterisks in the graphs (*p<0.05).

4.3.3.2. Segmentation of the heart and relative chamber sizes were affected

Next, heart chamber segmentation and proportions were of interest, in order to assess progression of cardiogenesis. There was only a minor percentage (8%) of zebrafish embryos treated with SP600125 between 10-22 hpf that showed non-segmented hearts ($p=0.046$), resembling primitive linear heart tubes, with no obvious distinction between an atrium and a ventricle (Figure 4.5B). No such phenotype was observed after 5.25-10 hpf and 22-30 hpf SP600125 treatment ($p>0.05$) compared to both controls (DMSO and E3).

The relative sizes of the two heart chambers were subsequently examined in untreated, DMSO-treated and SP600125-treated embryos. The ventricle and the atrium would normally be expected to be approximately equal to each other, as shown in the untreated and DMSO-treated embryos (Figure 4.6A). After SP600125 treatment, the heart chamber proportion was found to be altered. In 8% and 21% of zebrafish embryos treated with SP600125 at 5.25 hpf (until 10 hpf) and at 10 hpf (until 22 hpf), respectively, the atrium appeared bigger than the ventricle (A>V), due to either enlargement of the atrium or shrinkage of the ventricle (Figure 4.6A). This issue will be discussed in more detail later on, as, by counting the cells within the heart, it is possible to assess if the ventricle is smaller or if the atrium is bigger than normal.

Statistical analysis showed significant differences in both groups compared to the two controls: $p=0.016$ and $p=0.006$ after 5.25-10 and 10-22 hpf SP600125 treatment, respectively. 22-30 hpf SP600125 treatment did not affect the relative sizes of the heart chambers ($p=0.837$ compared to controls). Overall, 5.25-10 hpf SP600125 treatment caused a significant occurrence of altered heart chamber proportions (A>V), 10-22 hpf SP600125 treatment caused significant occurrence of disturbed chamber morphogenesis (no obvious chamber segregation) and chamber proportions (A>V), while 22-30 hpf SP600125 treatment did not significantly alter the heart chambers.

4.4.3.3. Looping of the heart was severely affected

The most intriguing heart-related phenotype was the looping of the heart. Rightward looping was observed in 99% of control embryos (untreated and DMSO-treated) and leftward looping was seen in the remaining 1% of the embryos. The percentages were very similar (98% and 2%, respectively) for the late SP600125 treatment group (22-30 hpf). However, in the other treatment groups the situation was different (Figure 4.6B).

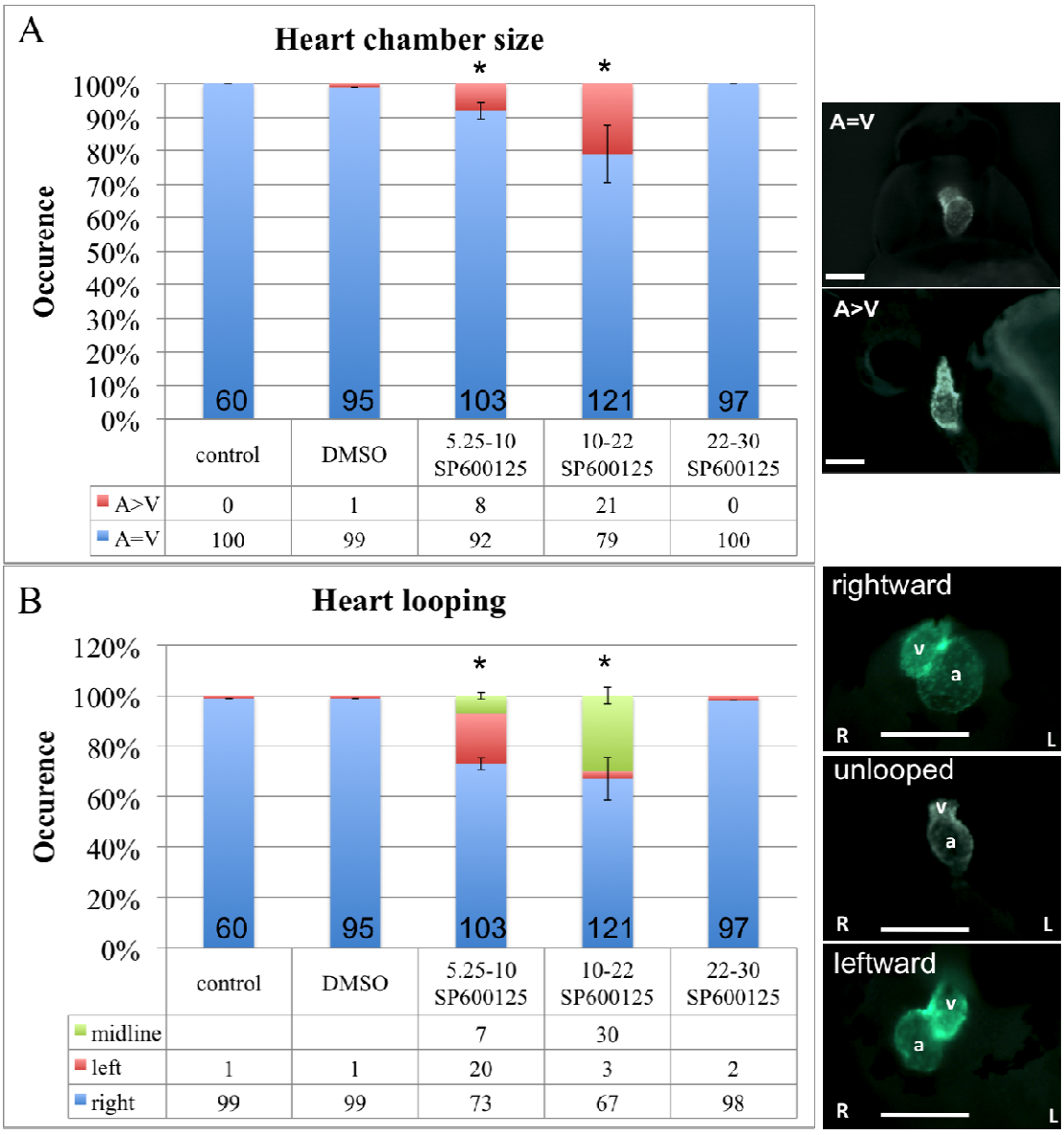

Figure 4. 6: Heart chamber size and cardiac looping after SP600125 treatment. A) The relative sizes of the heart chambers were altered after jnk inhibition. 8% and 21% of 5.25-10 and 10-22 hpf SP600125-treated embryos, respectively, had an atrium bigger than the ventricle (A>V), showing either enlargement of the atrium or shrinkage of the ventricle. Both values were found to be significantly different compared to controls (E3 and DMSO), with p values 0.016 and 0.006, respectively. The late SP600125 treatment group (22-30 hpf) was not affected. B) The looping of the heart was, also, affected after SP600125 treatment. 73% of 5.25-10 hpf SP600125-treated embryos had a normal rightward-looped heart, 20% had a leftward-looped heart (p=0.000) and 7% had unlooped hearts (p=0.046). After the 10-22 hpf SP600125 treatment 68% of embryos exhibited normal looping, 2% showed reverse looping (p=0.387 compared to controls) and 30% had unlooped hearts (p=0.000 compared to controls). Representative images of the phenotype are shown on the right (ventral views, anterior to the top). Statistical significance, in comparison to both control groups, was assessed with the χ^2 test for association of categorical data and is shown with asterisks in the graphs (*p<0.05). R: right, L: left, A: atrium, V: ventricle.

After the early (5.25-10 hpf) SP600125 treatment, only 73% of the embryos had a normal rightward-looped heart, while 20% had a leftward-looped heart (p=0.000 compared to E3 and DMSO controls) and 7% had their segmented hearts positioned in the midline without any apparent looping (p=0.046 compared to controls). So, the occurrence of reverse looping increased approximately ten fold compared to controls, while the incidence of unlooped hearts was fairly small but still significantly different from controls (Figure 4.6B). The looping of the heart was also affected after the 10-22 hpf SP600125 treatment: 68% exhibited normal looping (rightward), 2% showed reverse looping (leftward, p=0.387 compared to controls) and 30% had unlooped hearts positioned in the midline (p=0.000 compared to controls).

Overall, the looping of the heart was a significantly affected feature in 5.25-10 and 10-22 hpf SP600125-treated embryos, with the former exhibiting mainly leftward (reverse) looping and the latter showing predominantly absence of looping. Statistical significance was assessed with the χ^2 test for association of categorical data.

4.3.3.4. Heart cell counting revealed cell fate changes

In order to elucidate whether atrial and ventricular cells were differentially affected by SP600125 treatment, as suggested by the morphological differences in the two chambers of SP600125-treated embryos compared to controls, the number of cells within the hearts of SP600125-treated, DMSO-treated and untreated embryos was measured. A method adapted from previously published work (Schoenebeck et al., 2007) was employed. Tg*(cmlc2;DsRed2-nuc)* zebrafish embryos, counterstained with anti-DsRed and SV46 antibodies were used, as described in more detail in Chapter 2 (Sections 2.1.5 and 2.1.6, pages 55 and 56). 10 embryos for each condition were counted in each of the three experiments and the averages are presented in the graph in Figure 4.7.

It was shown that after 5.25-10 hpf SP600125 treatment, the overall number of heart cells was significantly decreased (p=0.0104 and p=0.0148 compared to untreated and DMSO-treated embryos, respectively): 89 cells (se=1) in the SP600125-treated, 101 cells (se=6) in the untreated and 102 cells (se=11) in the DMSO-treated group. However, the relative proportion of atrial and ventricular cells was not altered (p=0.097 and p=0.332 for atrial and ventricular cells, respectively, compared with the two controls); it remained at approximately 1.4 ventricular cell(s) for every atrial cell (ventricular:atrial=1.4, shown by the blue dashed line in Figure 4.7).

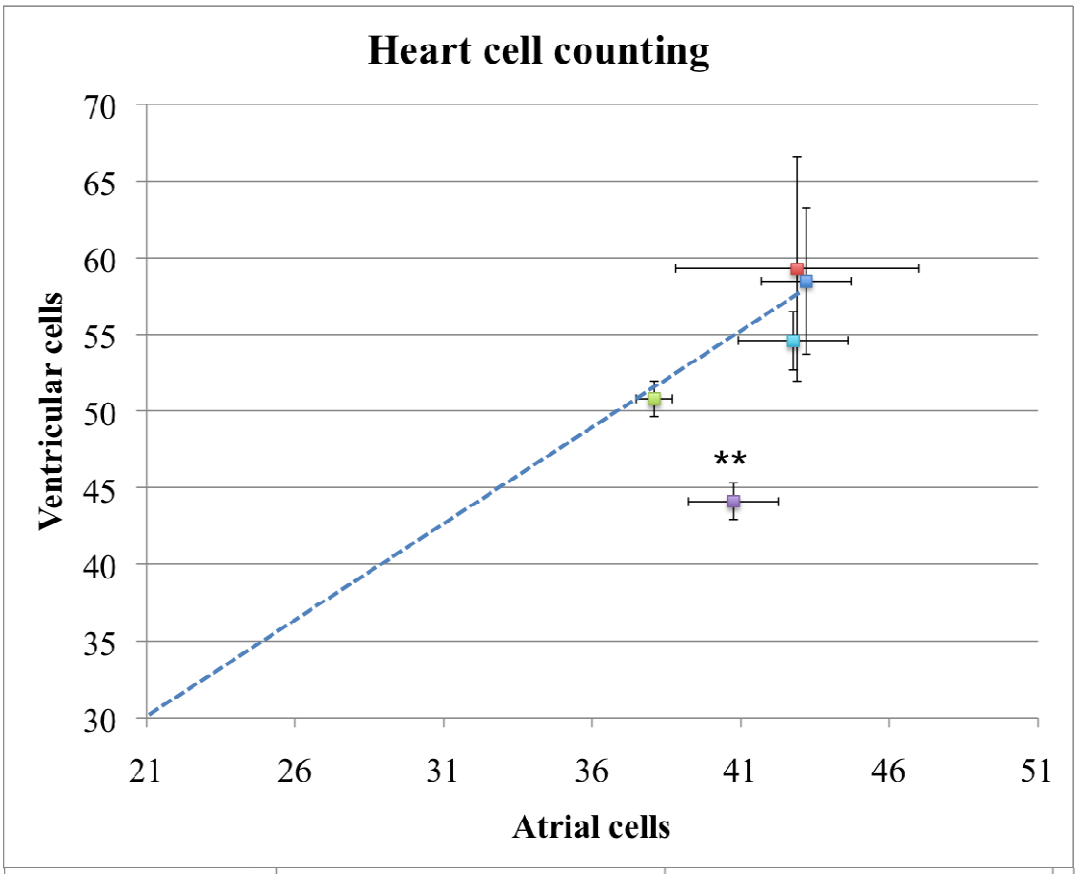

	Atrial	Ventricular
control, 101	43	58
DMSO, 102	43	59
5.25-10 SP, 89	38	51
10-22 SP, 85	41	44
22-30 SP, 98	43	55

Figure 4. 7: Counting of heart cells (atrial and ventricular) after treatment with SP600125, between 5.25-10, 10-22 and 22-30 hpf. Values show the means of three independent experiments and error bars represent standard errors of the mean. The overall number of heart cells is indicated in the legend of the graph (101 cells for untreated, 102 cells for DMSO-treated, 89 cells for 5.25-10 hpf SP600125-treated, 85 cells for 10-22 hof SP600125-treated and 98 cells for 22-30 hpf SP600125-treated embryos). Numerical data are tabulated underneath the graph. The blue dashed line represents the expected ratio between ventricular and atrial cells (1.4:1). Statistical significance was assessed with one-way Anova, followed by a 2-sided Dunnett test (p<0.01). Data had to be transformed to their logarithmic values to attain normality and although statistical analysis was performed on the logarithms, the linear values are shown in the graph. Mean values cannot accurately represent a not normally distributed population but are used in this graph for easier visualization. Statistical analysis and significance remain the same in both representations.**

The 10-22 hpf SP600125 treatment group also showed a significant reduction (p=0.011 and p=0.046 against E3 and DMSO controls, respectively) in the overall number of heart cells (85 cells, se=2) (Figure 4.7). Interestingly, the ventricular cells were more severely affected than the atrial cells; the ventricular:atrial ratio was close to 1:1 compared to 1.4:1 in control conditions. Specifically, in the 10-22 hpf SP600125-treated embryos there were 44 (se=1.2) ventricular and 41 (se=1.5) atrial cells, in the DMSO-treated embryos there were 59 (se=1.7) ventricular and 43 (se=1.3) atrial cells and in the untreated zebrafish embryos there were 58 (se=1.7) ventricular and 43 (se=1.1) atrial cells. This showed a significant loss of ventricular cells after inhibition of jnk at 10-22 hpf (p=0.000 and p=0.004 compared with the E3 and DMSO controls, respectively), while atrial cell numbers were not significantly affected (p=0.097 for all groups compared with the two controls).

As expected, after the late SP600125 treatment (22-30 hpf) no significant effect (p>0.1 for all groups compared with controls) on the number of heart cells (98 cells, se=3) or on the ventricular-to-atrial ratio (1.3 instead of 1.4) was observed (Figure 4.7). Overall, at 72 hpf, 5.25-10 hpf SP600125-treated embryos had smaller but correctly proportioned hearts, 10-22 hpf SP600125-treated embryos had smaller and disproportionate hearts (the loss in heart cell number was due to a specific loss of ventricular cells), while the hearts of 22-30 hpf SP600125-treated embryos remained unaffected.

4.3.3.5. Heart cell loss compared to body length decrease

It was previously shown (Section 4.3.2.1, page 139) that the body length of 5.25-10 hpf, 10-22 hpf and 22-30 hpf SP600125-treated embryos was significantly decreased compared to controls. Concomitantly, the total number of cardiomyocytes was significantly decreased after 5.25-10 hpf and 10-22 hpf SP600125 treatment, as explained in detail in the previous section. What remained to be elucidated was whether the loss of heart cells in 5.25-10 hpf and 10-22 hpf SP600125-treated embryos was associated with an overall decrease in the size of the embryos, or whether there was a specific loss of heart cells after jnk inhibition. In order to address this, a graph illustrating changes in the length of the body against changes in the number of total heart cells was made (Figure 4.8). A line (blue dashed line in Figure 4.8) shows the known (experimentally defined) count of heart cells at two different body lengths (corresponding to 48 and 72 hpf untreated embryos). This line represents the expected

relationship between body length and number of cardiomyocytes at these two time points, based on experimental data. Significant differences in body length are shown with blue asterisks and significant differences in the number of cardiomyocytes are shown with black asterisks in Figure 4.8. Values above or below the dashed line deviate from the expected relationship between the number of heart cells and the length of the body. Embryos with values that fall above the dashed line are likely to show more severe disturbances in the number of cardiomyocytes than in their body size. This means that the reduction in the body length of these embryos cannot fully account for the reduction in the number of cardiomyocytes. In contrast, embryos with values below the line are expected to have more severely affected body size and less severely affected cardiomyocyte numbers. This suggests that the loss of cardiomyocytes observed in these embryos is mainly due to a general decrease in the size of the embryo and is not necessarily cardiac-specific.

Figure 4.8 shows that the hearts of 5.25-10 hpf SP600125-treated embryos were not preferentially affected by jnk inhibition, as the decrease in the number of cardiomyocytes was accompanied by a concomitant decrease in the length of the body. In contrast, in 10-22 hpf SP600125-treated embryos, the significant decrease in the size of the embryo is not likely to fully account for the loss of cardiomyocytes, as explained before. This observation suggests that the loss of cardiomyocytes due to 10-22 hpf SP600125 treatment is not uniquely due to a decrease in the size of the embryos, but may in fact be caused by jnk-specific effects in the heart. Since loss of ventricular cells but not atrial cells was shown to cause the observed decrease in heart cell numbers in 10-22 hpf SP600125-treated embryos, inhibition of jnk may have specific effects on the ventricle, rather than the whole heart. What these effects may be is discussed further in the next sections. In contrast, 22-30 hpf SP600125-treated zebrafish embryos, showed a significant decrease in body length but not in the number of cells within their hearts.

4.3.4. Summary

Overall, treatment with 3μM SP600125 was shown to affect many aspects of zebrafish embryogenesis. It was shown to cause low penetrance alterations in the body ratios of developing embryos producing a CE-like phenotype, in the localization of the eyes and in the formation of otic vesicles and of the tail. Higher prevalence phenotypes caused by SP600125 treatment were observed in the hearts of developing zebrafish embryos: swelling of the pericardial cavity, lack of segmentation of the linear heart tube,

alterations in the relative sizes of the heart chambers, lack or reversal of the looping process and loss of ventricular cells. The way these abnormalities may have arisen, related to the timing of SP600125 treatment, is discussed in the next section.

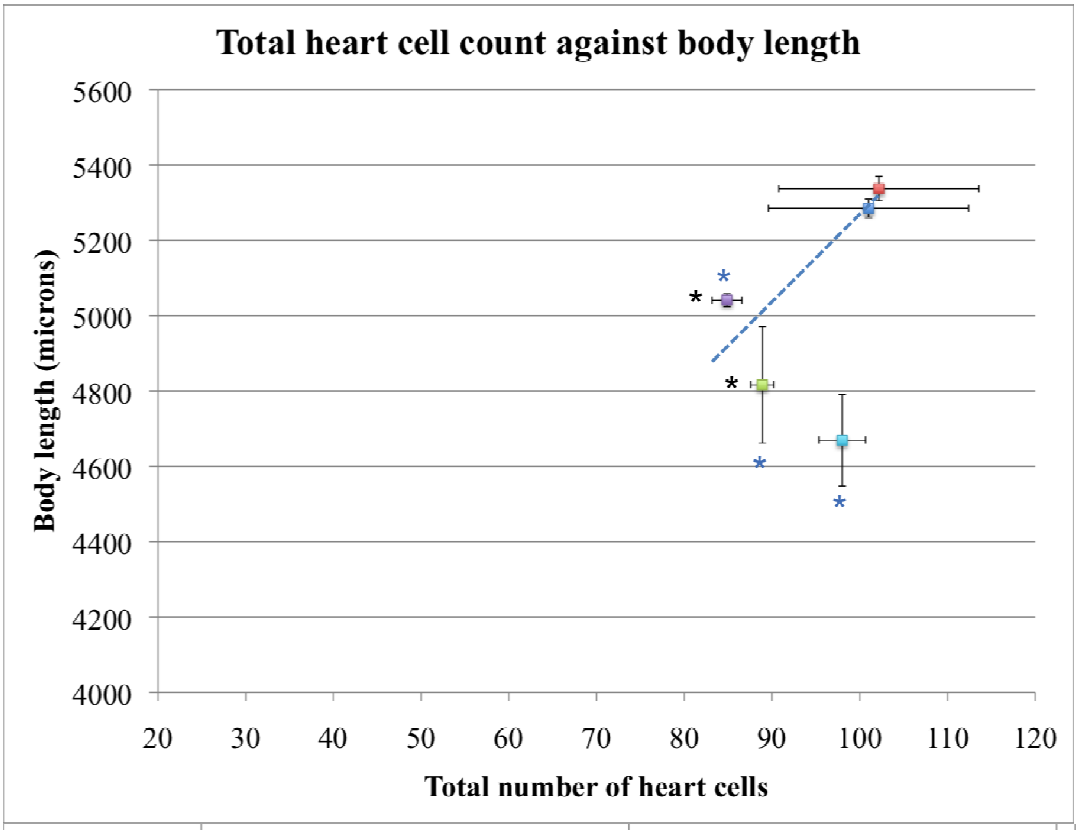

	Total number of heart cells	Body length
control	101	5285
DMSO	102	5337
5.25-10 SP	89	4816
10-22 SP	85	5041
22-30 SP	98	4669

Figure 4. 8: Total cardiomyocyte count against embryo body length after jnk inhibition. The dashed line shows the expected relation between the two values. 5.25-10 hpf SP600125-treated embryos showed equal decreases in their body length and heart cell count, 10-22 hpf SP600125-treated embryos had more severely affected hearts, while 22-30 hpf SP600125-treated embryos had unaffected hearts but severely reduced body size. Mean values and standard errors of the mean are shown. Statistical significance was assessed for body length and heart cell count individually, as described before, and is shown with asterisks (blue asterisks for body length and black asterisks for heart cell count, *p<0.05).

4.4. Discussion

In this chapter, inhibition of the activity of all zebrafish protein isoforms, identified in the previous chapter, by SP600125, a global jnk inhibitor, resulted in severe cardiac malformations in developing zebrafish embryos, associated with mild general body disturbances. In the following sections all these aspects are individually discussed.

4.4.1. Jnk inhibition affects body measurements and general aspects of zebrafish embryonic development

After initial identification and characterization of zebrafish jnk genes and proteins in Chapter 3, the next step was to globally inhibit all jnk isoforms at different time points during zebrafish development and to assess the resulting abnormalities. Interesting eye, ear and tail defects arose after jnk inhibition, concomitantly with a CE-like body phenotype. Although the prevalence of these defects was low, it is interesting to briefly mention them here, as they recapitulate the phenotype of known PCP mutants and, to a lesser degree, of MAPK mutants. Specifically, eyes were located further apart from each other, otic vesicles were malformed, containing no or small otoliths, the tail was curved or kinked and the body appeared shorter and fatter. Seo et al. (2010) reported severe abnormalities during gastrulation and CE-like defects after morpholino disruption of *jnk* genes in developing zebrafish embryos, but did not mention any defects associated with specific organs (Seo et al., 2010). In fact, the disruption of gastrulation movements, which in turn causes a CE phenotype, is characteristic of PCP mutations. Specifically, CE defects have been observed in many PCP zebrafish mutants, including pipe-tail (*wnt5b*) (Hammerschmidt et al., 1996, Rauch et al., 1997), silberblick *(wnt11*) (Heisenberg and Nusslein-Volhard, 1997, Heisenberg et al., 2000), knypek (*glypican 4*) (Solnica-Krezel et al., 1996, Topczewski et al., 2001) and trilobite (*vang-like 2*) (Hammerschmidt et al., 1996, Jessen et al., 2002, Solnica-Krezel et al., 1996). Gastrulation defects have been observed in MAPK mutants (JNK, Erk1, Erk2, MAPKAPK2, p38) as well (Krens et al., 2008, Krens et al., 2006, Matsui et al., 2005, Schwarz-Romond et al., 2002). Abnormalities in the eyes and the otic vesicles, similar to the ones described in this study, have been observed in many of the PCP mutants presented above (Hammerschmidt et al., 1996, Heisenberg and Nusslein-Volhard, 1997, Heisenberg et al., 2000, Jessen et al., 2002, Rauch et al., 1997, Solnica-Krezel et al., 1996, Topczewski et al., 2001). In fact, direct involvement of the Wnt pathway in some

of the processes disrupted in the jnk-inhibited embryos, has been previously reported. For example, induction of the eye field within the anterior neural plate (Wilson and Houart, 2004) and specification of the telencephalic and eye identity (Cavodeassi et al., 2005, Heisenberg and Nusslein-Volhard, 1997, Houart et al., 2002, Kim et al., 2002) have been shown to be influenced by both canonical and non-canonical Wnt signals. Specifically, Wnt11 has been shown to promote coherence of eye field cells and to coordinate morphogenetic movements in the nascent eye in zebrafish embryos (Cavodeassi et al., 2005); its absence caused partial fusion of the eyes, possibly due to defective signalling from the underlying mesendoderm (Cavodeassi et al., 2005, Heisenberg and Nusslein-Volhard, 1997, Marlow et al., 1998). Of note, mkk4b (an activator of jnk) and jnk were shown to inhibit transcription of Wnt11 in developing zebrafish embryos (Seo et al., 2010).

Members of the MAPK have not been extensively studied in zebrafish. However, mutations within the Ras/MAPK pathway are known to be involved in progression of the cardio-facio-cutaneous (CFC) syndrome in humans, characterized by a typical facial appearance, heart, skin and hair defects and mental retardation (Rodriguez-Viciana et al., 2006, Tidyman and Rauen, 2008). Similar defects were observed in CFC zebrafish mutants (Anastasaki et al., 2009). The phenotype was rescued by injection of *erk* (one of the Ras/Map kinases) mRNA (Anastasaki et al., 2009). Additionally, MAPK signalling, in association with fgf19, has been shown to regulate the development of the cornea in developing zebrafish embryos (Acharya et al., 2011, Tamimi et al., 2006). Also, activation of the Erk (member of the MAPK family) pathway in developing zebrafish embryos caused a dorsalized phenotype, rescued after activation of a phosphatase, inhibiting Erk (Furthauer et al., 2002, Snaar-Jagalska et al., 2003, Tsang et al., 2004). Similarly, inhibition of jnk (with morpholino injections) was shown to cause ventralization of the body of zebrafish embryos (Rui et al., 2007). Asymmetric activation of p38a (MAPK14a) was observed in zebrafish blastodiscs during the early cleavage period (0.75-2.25 hpf) and it was suggested to be related to the machinery that controls dorsalization signals (Fujii et al., 2000).

The typical PCP eye phenotype, as described before, is decreased ocular distance or even partial fusion of the eyes (cyclopia) (Cavodeassi et al., 2005, Heisenberg and Nusslein-Volhard, 1997, Marlow et al., 1998). In this study, however, the opposite phenotype was observed: the eyes of SP600125-treated embryos were located further apart from each other. This observation is probably an indication that other pathways, along with the Wnt/PCP pathway, may in fact be altered by SP600125 treatment due to

jnk inhibition and thus, they may affect the formation, morphogenesis and localization of organs during zebrafish development.

RhoA morphants (embryos that have been injected with RhoA morpholinos) show abnormalities very similar to the defects seen in jnk-inhibited embryos: short anterior-posterior axis, reduced head structures, CE defects, impaired tail formation, loss of one otolith and increased apoptosis (Zhu et al., 2008, Zhu et al., 2006). RhoA is a small GTPase of the Ras family and is known to participate in the non-canonical Wnt/PCP pathway, whereby it acts by phosphorylating and thus activating ROCK. Nevertheless, RhoA has PCP-independent effects as well, activating a multitude of downstream targets (such as p21-activated kinase, myosin phosphatase, protein kinase-N) and participating in diverse biological processes (including actin cytoskeleton organization, microtubule dynamics, gene transcription, cell cycle progression) (reviewed by Boureux et al., 2007). Also, Shh mutants and morphants exhibit head deformities, underdevelopment and malpositioning of the eyes, tail bending and poor trunk formation (Ekker et al., 1995, Feijoo et al., 2011, Jackman et al., 2010, Ribes et al., 2010, Strahle et al., 1996), similar to the defects seen in the jnk-inhibited embryos in this study. Taken together, although the overall resemblance between jnk-inhibited zebrafish embryos and PCP mutants is striking, contribution from other pathways in the establishment of this phenotype cannot be overlooked, as suggested by similar defects observed in mutants of other pathways.

The general body and organ defects were only observed in a small percentage of SP600125-treated zebrafish embryos and only after 5.25-10 hpf (gastrulation period) and 10-22 hpf (segmentation period) treatments. This observation is not surprising, as the time interval between 5.25 hpf and 22 hpf is critical for proper cell migration, body patterning, tissue specification and organ morphogenesis. The RT-PCR data in Chapter 3 showed that until 20-24 hpf only *jnk1* (*jnk1a* and *jnk1b*) and *jnk2* are expressed in detectable levels in developing zebrafish embryos. The absence of *jnk3* expression at the time of the 5.25-10 hpf and 10-22 hpf SP600125 treatments suggests that any defects seen in the 5.25-10 hpf and 10-22 hpf treated embryos will be due to inhibition of jnk1 and jnk2 alone (assuming that protein levels correspond roughly to mRNA levels). The first day of development, *jnk1* and *jnk2* were expressed mainly in the anterior part of the embryos (Chapter 3); therefore, deformities associated with anterior structures, such as the brain (including the eyes), the ears (otic vesicles) and the heart would be expected to arise after jnk1 and jnk2 inhibition. They were, also, found to be expressed in the presumptive gut but abnormalities in this organ would likely not be

directly visible under a microscope because of its position within the embryonic body. Later treatment (22-30 hpf) did not cause abnormalities in the eyes, fins, somites, otic vesicles and tail. During this late treatment (22-30 hpf) inhibition of all three proteins (jnk1, jnk2, jnk3) by SP600125 is expected, since all three genes were shown to be expressed at that time (Chapter 3). Strong expression of *jnk3* (specifically *jnk3.3*) in the otic vesicles and the hypothalamus of the embryos suggests that these structures are expected to be severely affected by SP600125 treatment. In contrast, only abnormalities in the length of the embryos (shorter than controls) and the ocular distance (larger than in controls) were observed. This discrepancy between expression pattern and abnormalities is probably due to the fact that many of the processes that establish body patterns and organ morphogenesis have either already been completed or are well underway and cannot be affected at that time (22-30 hpf) by SP600126 treatment. Of note, the examination of the general body morphology and the development of some organs was only conducted superficially with microscopic observation and thus, the presence of abnormalities that could not be detected with the current approach, cannot be excluded.

4.4.2. Jnk inhibition causes abnormalities in the formation and morphogenesis of the hearts in developing zebrafish embryos

Of pivotal importance for our research group, was the heart-related phenotype of SP600125-treated zebrafish embryos. A small but significant percentage of 5.25-10 hpf SP600125-treated embryos had abnormal hearts that were reversely (leftwards) looped and surrounded by mild pericardial oedema. A considerable percentage of 10-22 hpf SP600125-treated fish showed more severe and prevalent cardiac defects, including pericardial oedema, lack of chamber morphogenesis, disturbed chamber specification and absence of looping. In contrast, 22-30 hpf SP600125-treated embryos did not exhibit obvious cardiac-specific abnormalities, as assessed by the current approach.

Swollen pericardial cavities in zebrafish embryos usually indicate problems with the function of the heart or with the circulation of fluid around the body and commonly disturb proper morphogenesis of the heart. Therefore, it seems possible that SP600125 treatment affects the function of the heart or fluid homeostasis, as suggested by the formation of oedema around the heart, but the small size of the swelling is probably not sufficient for distortion of the heart itself.

4.4.2.1. Left-right patterning and looping morphogenesis

Left-right patterning is a major determinant of correct heart morphogenesis and abnormal looping has been commonly associated with defects in this process (Bisgrove et al., 2000, Chen and Fishman, 2000a, Chen and Fishman, 2000b, Chen et al., 1997, Chin et al., 2000, Glickman and Yelon, 2002, Kathiriya and Srivastava, 2000, Yan et al., 1999). The initial symmetry breaking at the mouse node (or Kupffer's vesicle in zebrafish) and the subsequent asymmetric gene expression at the lateral plate mesoderm (LPM) have been discussed thoroughly before (Section 1.2.4, page 6). The PCP pathway has been recently shown to be essential for correct (posterior) positioning of the cilia in the cells of the node (Borovina et al., 2010, Guirao et al., 2010, Okada et al., 2005, Song et al., 2010). Posterior localization of the cilia dictates the direction of their rotation and enables proper establishment of left-right identities in the mouse embryo (Nonaka et al., 2005, Song et al., 2010). Translation of the initial asymmetric signals from the node to the LPM dictates the directionality of subsequent organ morphogenesis, such as the looping of the heart (Aw and Levin, 2008, Capdevila et al., 2000, Collignon et al., 1996, Ibanes and Izpisua Belmonte, 2009, Kawasumi et al., 2011). Nodal signalling, the main asymmetrically expressed cascade at the LPM, has been shown to determine, to a large extent, left-right patterning (Ahmad et al., 2004, Brennan et al., 2002, Duboc et al., 2005, Kawasumi et al., 2011, Saijoh et al., 2003). In zebrafish, three nodal genes have been described (*cyclops, squint* and *southpaw*), with different ranges of action but same targets (Erter et al., 1998, Feldman et al., 1998, Long et al., 2003, Schier, 2009).

Interestingly, a connection between Nodal signalling (member of the TGFβ superfamily) and the MAPK pathway has been established (Dennler et al., 2000, Hagemann and Blank, 2001). Specifically, Smad proteins (Smad2/3), which are known downstream targets of Nodal signalling and participate in the establishment of asymmetric gene expression (Kawasumi et al., 2011, see section 1.2.4, page 6 for more details on this), have been shown to be activated by MEKK1 (MAPK/Erk kinase kinase1 or MAPKKK1, an upstream activator of MKK4 and MKK7, which in turn activate JNK). In fact, dominant-negative MEKK1 expression in cultured cells has been shown to inhibit TGFβ-mediated induction of Smad-regulated transcription. In contrast, JNK and c-Jun have been shown to mediate inhibition of Smad3, without affecting its cellular localization (Dennler et al., 2000). Overall, the TGFβ/MEKK1/JNK-mediated

regulation of Smad2 and Smad3 proteins is likely to be complex and still not fully elucidated.

Symmetry breaking and left-right patterning are important for heart morphogenesis, as briefly mentioned before. In fact, the heart is the first organ, in most animals, to break the embryonic symmetry, in response to left-right asymmetry signals already established. Heart jogging at approximately 19 hpf is the first sign of cardiac left-right asymmetry in zebrafish (Baker et al., 2008, Kathiriya and Srivastava, 2000). Asymmetric Nodal signalling and subsequent asymmetric gene expression (such as *Pitx2, Lefty-1, Lefty-2*) have been shown to be highly involved in establishing the directionality of this process (Baker et al., 2008). In turn, the direction of heart jogging is highly correlated with the direction of looping in subsequent stages of heart development (starting at approximately 30 hpf). So, although heart looping itself is not directly dependent upon establishment of Nodal-induced asymmetric gene expression at the node and at the LPM, it relies on proper heart jogging (Baker et al., 2008). Incorrect jogging and/or looping (reverse, incomplete or absent) have been correlated with left-right patterning defects or with inability to interpret left-right cues (Ahmad et al., 2004, Chin et al., 2000). Also, modifications in the proliferation, migration, differentiation and death levels of cells are suggested to be involved in the heart jogging and looping processes (Kathiriya and Srivastava, 2000).

Inhibition of jnk during gastrulation (5.25-10 hpf), which caused a high incidence of reverse looping, is unlikely to directly affect jogging-related processes as these take place later (starting at approximately 19 hpf). Also, jnk proteins are not known to be directly involved in left-right patterning, although there is evidence to suggest that, directly or indirectly, the non-canonical Wnt/PCP pathway (Antic et al., 2010, Song et al., 2010) and members of the MAPK cascade (Dennler et al., 2000, Hagemann and Blank, 2001) are, as discussed before. Early inhibition of jnk may, therefore, indirectly affect establishment of the left-right axis, not specifically in the heart but globally in the whole embryo. It could affect the formation of the Kupffer's vesicle, the initial localization of cilia within Kupffer's vesicle cells (along with other PCP members), the establishment of the appropriate left-right gene expression pattern and/or the interpretation of left-right cues (possibly through Smad-related interactions), the transmission of the left-right asymmetry from the node to the LPM and the migration and polarization of cells during convergence and extension movements (through both PCP and MAPK interactions). Abnormalities in any of these procedures could cause defects or even randomization of left-right patterning, which would affect downstream

organ localization, directionality and morphogenesis. A number of zebrafish mutants show abnormalities in cardiac looping. In these mutants, reverse looping has been commonly associated with defective left-right patterning of the embryonic axis (Bisgrove et al., 2000, Chen et al., 1997, Chin et al., 2000, Glickman and Yelon, 2002, Yan et al., 1999). These are only hypotheses, based on current information about the activity of Jnk, that need further work in order to be elucidated.

SP600125 treatment during the segmentation period (10-22 hpf), which caused high occurrence of absence of looping, could have broader effects than the gastrulation treatment, as it encompasses many processes. During the first hours of the treatment (10-19 hpf), inhibition of jnk may affect processes preceding cardiac jogging, such as the ones described above (Kupffer's vesicle formation, ciliogenesis, left-right gene expression patterning and cell migration and/or polarization). However, defects in these processes would be expected, as described above, to cause reversal or randomisation of looping (as observed after the 5.25-10 hpf SP600125 treatment) and not to inhibit it altogether, since they are not directly related with looping morphogenesis but mainly affect left-right patterning. After 19 hpf, jogging-related modifications in cell proliferation, apoptosis, migration, differentiation and gene expression take place (Kathiriya and Srivastava, 2000). Treatment with SP600125 at that time interval is likely to affect the directionality of jogging through deregulation of one or more of these processes, as jnk has been shown to be highly involved in these procedures in other contexts (reviewed by Bogoyevitch and Kobe, 2006). Specifically, jnk could be affecting the tilting and migration of the cardiac cells during jogging of the cardiac cone, which starts at approximately 19 hpf and is complete by 22-24 hpf (Chen et al., 1997, Rohr et al., 2008, Stainier and Fishman, 1992, Yelon and Stainier, 1999). Defective migration could lead to improper jogging, abnormal positioning and possibly formation of the heart tube and could cause complications in downstream cardiac morphogenesis events. Alternatively, jnk could be affecting the expression of genes within the heart population, possibly through differential effects on atrial and ventricular cells. The dynamics of cell proliferation, death and differentiation could also be affected by inhibition of jnk, influencing majorly the process of cardiac jogging and subsequently of cardiac looping. Absence of looping has been previously linked with defects in the interpretation of left-right cues or in the molecular mechanisms that guide and orchestrate looping in zebrafish mutants (Ahmad et al., 2004).

4.4.2.2. Chamber specification

Another aspect of heart formation that was investigated was chamber specification. 5.25-10 hpf SP600125 treatment caused increased atrial compared to ventricular size in significantly more embryos than no treatment or DMSO treatment did, but this change was not accompanied by a difference in the numbers of atrial and ventricular cells in the two chambers. This probably indicates that the observed size difference was due either to a swelling of the atrium or an increase in the size of the cells, which were not accompanied by an increase in cell numbers. Further work counting proliferating cells (BrdU staining) and cells undergoing programmed cell death (TUNEL staining) would be required in order to fully elucidate how inhibition of jnk between 5.25 and 10 hpf causes the observed phenotype.

Chamber specification was dramatically affected after the 10-22 hpf SP600125 treatment. The atrium appeared markedly larger than the ventricle after microscopical observation and this was found to be due to a specific loss of ventricular cells and, thus, shrinkage of the ventricle, rather than to an enlargement of the atrium. Ventricular and atrial cell specification takes place very early during zebrafish development. Already in late blastula-stage embryos (at 40% epiboly, approximately 5 hpf) ventricular and atrial myocardial progenitors are thought to be differentially positioned, with ventricular cells located closer to the embryonic margin and towards the dorsal midline than atrial cells (Keegan et al., 2004). Subsequent migration during gastrulation (5.25-10 hpf) maintains the physical separation of these cell populations so that in the LPM ventricular progenitors become positioned medially and rostrally in relation to atrial progenitors (Keegan et al., 2004, Yelon and Stainier, 1999). It is, thus, evident that jnk inhibition between 10 and 22 hpf could not explain a difference in atrial versus ventricular specification, as this has taken place before administration of the drug. The proliferation and apoptosis rates of cardiomyocytes could be, however, affected by jnk inhibition. Previous studies have shown that smaller hearts or hearts with one smaller chamber can be caused by defective proliferation of cardiomyocytes during the heart tube stage, while programmed cell death is not a major contributor to the first days of cardiac morphogenesis (Ribeiro et al., 2007, Sedletcaia and Evans, 2011). The fact that JNK is thought to be important in regulation of both apoptosis and proliferation rates in many different contexts (reviewed by Bogoyevitch and Kobe, 2006) suggests that SP600125 treatment between 10 and 22 hpf may have detrimental effects on the proliferation of both or one of the heart chambers. The reason why one of the heart lineages (atrial or

ventricular cells) might be more severely affected than the other by the absence of jnk remains to be determined; differential expression of jnk proteins and/or protein isoforms in the two presumptive chambers (which was not examined here) is a possible explanation.

4.4.2.3. Overview of the known contribution of MAPK and Wnt/PCP in the heart

The MAPK and the Wnt/PCP signalling pathways have been studied extensively in heart development and disease in the past (reviewed by Muslin, 2008, Rose et al., 2010). The three main MAPK cascades involve ERK, p38 and JNK and are shown to be involved in many aspects of cell physiology (Raman et al., 2007). Most of the contribution of ERK1/2 signalling to heart development is due to its role in FGF and other growth factor signalling. However, its role is not fully established. ERK1/2 has been shown to be vital for cardiogenesis and for differentiation of beating clusters in ES-derived EB (Dell'Era et al., 2003, Schonwasser et al., 1998). Also, ERK1/2 mediating FGF signalling has been suggested to play critical roles in morphogenesis and growth throughout cardiac development (Lincoln et al., 2006, Zhao et al., 2007). Deletion of ERK5 in mouse embryos caused underdevelopment of the myocardium, disorganization of trabeculae, vascular defects and early leathality (Hayashi and Lee, 2004, Regan et al., 2002). However, in other studies, inhibition of ERK1/2 has been shown not to affect cardiomyocyte differentiation (Davidson and Morange, 2000, Eriksson and Leppa, 2002). Importantly, members of the ERK branch of the MAPK cascade were found to be causative for Noonan Syndrome (Carta et al., 2006, Roberts et al., 2007, Schubbert et al., 2006) and involved in Costello and Cardio-Facio-Cutaneous syndromes (Aoki et al., 2005, Niihori et al., 2006, Schubbert et al., 2007). All of these syndromes in humans are associated with congenital heart defects, including hypertrophic cardiomyopathy, electrophysiological abnormalities and septal defects (briefly discussed in Section 1.1 page 1).

Similarly, p38 is thought to be an important regulator of cardiomyocyte differentiation. Among others, it has been shown to be required for cardiac differentiation of P19 carcinoma cells (Eriksson and Leppa, 2002), to promote cardiogenesis over neurogenesis in ES cells (Aouadi et al., 2006) and to be implicated in reactive oxygen species (ROS)-mediated cardiac differentiation of mouse ES cells (Ding et al., 2008, Wo et al., 2008). In contrast, inhibition of p38 has been shown to promote differentiation of human ES cells into cardiomyocytes (Graichen et al., 2008).

Interestingly, this effect was only seen in low concentrations of the p38 inhibitor, while in high concentrations cardiogenesis was strongly inhibited (Graichen et al., 2008). A similar controversy about the role of p38 exists in the field of cardiac disease. It is generally believed that activation of p38 is detrimental for cardiac pathology and recovery after ischemia and therefore its inhibition has beneficial outcomes (Ma et al., 1999, Mackay and Mochly-Rosen, 1999). However, some reports suggest protective effects of p38 MAPK activation in cardioprotection (Maulik et al., 1998, Mocanu et al., 2000, Muslin, 2008, Rose et al., 2010, Weinbrenner et al., 1997). Overall, p38 is thought to have both protective and pathological roles in the differentiation, proliferation and function of the heart (Kerkela and Force, 2006, Liao et al., 2002, Muslin, 2008, Rose et al., 2010).

The JNK pathway has also been studied during heart development and disease. Its role is best characterized through its function in the non-canonical Wnt/PCP signalling, which is a known important player in cardiogenesis. Activation of the PCP pathway has been shown to promote cardiogenic differentiation and cardiac gene expression in cultured cells and in animal models (Belema Bedada et al., 2005, Eisenberg and Eisenberg, 1999, Eisenberg et al., 1997, Garriock et al., 2005, Pandur et al., 2002, Schulze et al., 2005, Terami et al., 2004), while deletion of upstream or downstream effectors of the pathway has been shown to cause severe cardiac defects in mouse and zebrafish embryos (Hamblet et al., 2002, Henderson et al., 2001, Matsui et al., 2005, Phillips et al., 2007, Wei et al., 2001). Additionally, JNK, activated by the Wnt/PCP pathway (Wnt11) and acting through TGFβ-2, has also been shown to be required for proper outflow tract formation in the mouse (Zhou et al., 2007). What is not clear from the studies that are available to date is the extent to which Jnk is involved in these Wnt/PCP-mediated functions, as Jnk-deficient mice have not been shown to display significant defects in cardiogenesis (Gerits et al., 2007). This might, however, reflect the early lethality of double *Jnk1* and *Jnk2* mouse mutatnts ($Jnk1^{-/-}$;$Jnk2^{-/-}$) due to brain abnormalities (Aouadi et al., 2006, Kuan et al., 1999), which does not allow for further investigation of the heart phenotype, and putative redundancy in other combinatorial deletions ($Jnk1^{-/-}$;$Jnk2^{+/-}$, $Jnk1^{+/-}$;$Jnk2^{-/-}$, $Jnk2^{-/-}$;$Jnk3^{-/-}$ or $Jnk1^{-/-}$;$Jnk3^{-/-}$), which do not allow for the whole spectrum of actions to be revealed. Interestingly, $c\text{-}Jun^{-/-}$ (direct target of Jnk) mouse embryos show malformations of the cardiac outflow tract that resemble truncus arteriosus persistens (Eferl et al., 1999). The role of Jnk in cardiac disease has also been the focus of many studies in the past; however, a lot of controversy surrounds the data available to date. Overall, it has been shown to have

both protective and pathological roles in cardiac physiology (including regulation of hypertrophy, cardiomyocyte death and survival, remodelling after ischemia) depending on the context, the cell type and the timing (reviewed in (Rose et al., 2010) and described in detail in Section 1.5.6, page 43).

Taken together, JNK, as a member of the MAPK family and a downstream effector of the non-canonical Wnt/PCP pathway, is involved in a variety of cellular and morphogenetic processes throughout development and in adulthood. In the context of this study, the roles of JNK within the two cascades (MAPK and Wnt) cannot be distinguished and are likely to be tightly interconnected, with complex interactions and extensive cross talk between them. Analysis of the known roles of other MAPK and PCP members in development and cardiogenesis highlights the complex and often contradictory contributions of the two pathways and partially explains the discrepancy between some of the observations made in this study and published work. The strong and weak features of this study are analysed below.

4.5. Advantages and disadvantages of this study

In the current study the role of jnk during zebrafish development was investigated by using a chemical inhibitor, SP600125. The use of SP600125 was an advantage of the current study. This chemical is a specific inhibitor of Jnk with an IC_{50} (half maximal inhibitory concentration) for Jnk much lower (40, 40 and 90 nM for Jnk1, Jnk2 and Jnk3, respectively) than the IC_{50} for other kinases of the same family. The second lowest IC_{50} after Jnk is 400 nM against Mkk4 (Bennett et al., 2001), which is primarily an upstream activator of Jnk and to a lesser degree of p38 (Gerits et al., 2007). Although recent studies have questioned its claimed specificity (Bain et al., 2003), it continues to be used extensively as an inhibitor against Jnk (Bogoyevitch and Arthur, 2008).

In this study, SP600125 was preferred over morpholino injections (these are discussed in detail in Section 4.6, page 169) for two essential reasons. The first was the fact that it inactivates all Jnk proteins, even unidentified isoforms, as it targets the ATP binding pocket of the enzyme, which is highly conserved and omnipresent in all active forms of Jnk proteins. This is very important because it avoids modification of the observed phenotype due to redundancy. Morpholinos, on the contrary, are designed against specific transcripts or isoforms and simultaneous injection of multiple constructs would be required in order to get global inhibition of Jnk proteins. This is practically impossible, since injection of more than 2-3 morpholinos is unreliable and can cause

severe unspecific morphological defects. It is also problematic if not all isoforms have been identified, as the design of the constructs has to be tailor-made against specific sequences.

The second reason for choosing SP600125 in this study was the need for timely inhibition of the proteins of interest. The drug can be administered at any experimentally defined time during development and for as long as it is required. In this way, specific developmental processes can be targeted, which could not be achieved with morpholino injections that have to be carried out at the 1-2 cell stage. Thus, the use of a chemical inhibitor allowed for a more comprehensive and global investigation of the effects of jnk inactivation during zebrafish development. Although chemical inhibition was the preferred approach for this study for the reasons described above, morpholino injections have significant advantages that cannot be overlooked and are, thus, analysed in Section 4.6 (page 169). The main one of these advantages is the specificity. Although SP600125 is a specific inhibitor, its specificity (in fact the specificity of any chemical inhibitor) cannot reach the tailor-made specificity of morpholinos, which are designed to target only one specific gene and not a whole family.

Another positive feature of the current study was the fact that the analysis of cardiac-specific phenotypes, which were the main interest here, was carried out concomitantly with analysis of the general phenotype. This is essential when analysing organ-specific abnormalities because it puts them into context and does not isolate them from the events that take place in the rest of the body due to the drug. In this study we observed severe cardiac defects in a large proportion of SP600125-treated embryos and it was important to assess whether these abnormalities arose from a general disorganization of the body plan and of surrounding tissues, or whether they were intrinsic to the heart. Put simply, it was important to examine whether what we observed was an abnormal heart within a severely abnormal body or a defective heart within a normal body. Only a small percentage of embryos exhibited cardiac-unrelated abnormalities, much smaller than the percentage with cardiac defects, and these anomalies were not severe. However, the length of the body of SP600125-treated embryos (5.25-10, 10-22 and 22-30 hpf) was significantly decreased compared to controls. This was shown to probably be the main reason (or one of them) for the reduced heart cell count observed in 5.25-10 hpf SP600125-treated embryos; the reduction in heart cells (both atrial and ventricular) was accompanied by a concurrent decrease in the length of the body. This did not hold true for 10-22 hpf SP600125-

treated embryos, which had more severely reduced heart cell numbers (ventricular cells more affected than atrial cells) compared to the reduction of their body size. Thus, both extra- and intra- cardiac effects caused by absence of jnk are likely to account for the observed phenotype, possibly depending on the timing of the drug administration. One of the extra-cardiac effects is the putative reversal of left-right patterning of the body that in turn affects the directionality and positioning of the heart, as described in previous sections. Closer examination of the positioning and morphogenesis of other organs, such as the gut, would elucidate whether left-right patterning was indeed reversed or randomized, or whether the heart was specifically affected.

Additionally, the use of transgenic zebrafish lines greatly improved the resolution of our observations and allowed for accurate scoring and measurement of the features of interest. Both lines used, *Tg(cmlc2:GFP)* (Huang et al., 2003b) and *Tg(cmlc2:DsRed2-nuc)* (Mably et al., 2003), had cardiac-specific constructs that facilitated visualization of the heart from early developmental stages onwards and made even early observations possible.

Finally, in depth and accurate statistical analysis was another positive attribute of the current study. Assumptions that couldn't be tested were not made and for all data, the appropriate parametric or non-parametric tests were used, after thorough investigation of the fitness of each test and its suitability for the current data sets. Also, categorical data, which are usually troublesome in their statistical analysis, were examined under the correct null hypotheses and using suitable tests (Ennos, 2006).

However, some aspects of the current work could be improved. An important downside of the present study was the lack of investigation of the effectiveness of the drug. This was due to the fact that commercial antibodies (against phospho-Jnk, as the one used in Chapter 5) did not specify their cross-reactivity with zebrafish and it was uncertain whether they would specifically bind the activated form of the protein. This was exacerbated by analysis of the predicted protein weights of different jnk isoforms that were between 46 and 50 kDa for most proteins, differing from mammalian jnk proteins that give 46 and 54 kDa bands in SDS-Page electrophoresis (Chan et al., 1997, Masamune et al., 2004). These are the reasons why western blot analysis was not conducted on SP600125-treated embryos to affirm effective downregulation of jnk. This issue could be overcome by using splice-blocking morpholino injections to confirm the phenotype, since the end point of such an inactivation is readily testable with RT-PCR analysis. Splice morpholinos have already been designed against *jnk1a, jnk1b* and *jnk2* (*jnk3* is only expressed after 20-24 hpf) and the work is due to be carried out in the near

future by new members of our research group. The advantages and disadvantages that morpholino work entails are described below.

Also, rescue experiments should have ideally been conducted in order to assess the specificity of the drug. This is usually performed with injection of mRNA of the gene of interest at the 1-2 cell stage. This would not be useful for reversing (rescuing) the effect of SP600125 treatment, since the drug acts on the protein and inhibits its association with ATP, but is not expected to affect the transcription levels of the gene. Expression of a dominant active form of the protein, not affected by the drug, would be a better candidate for rescue experiments.

4.6. Further work

The next step to take in order to advance this study would be, as described before, to perform morpholino injections. Morpholinos are synthetic sequences of nucleotides that can silence transcription or translation of the genes of interest. Their backbone is made of 6-membered morpholine rings that carry one of the four known bases of DNA/RNA molecules and can be microinjected into the cytosol of zygotes for targeted gene inactivation. There, they block mRNA splicing or initiation of translation by preventing the respective complexes (the splicing or ribosomal machinery, respectively) to bind to the substrate (Sumanas and Larson, 2002). The main asset of using morpholinos for gene inactivation is their specificity. Careful design of morpholinos according to published guidelines (Eisen and Smith, 2008, Kamachi et al., 2008, Morcos, 2007) can lead to the production of highly specific products that reliably and efficiently inactivate the gene(s) of interest. Moreover, targeting of specific transcripts or individual genes that are very similar to other genes of the same family, can be achieved. Another important benefit of using splice-blocking (but not translation-blocking) morhpolinos is the fact that their effectiveness can be readily detected by PCR analysis: misplicing of an mRNA product will change (usually shorten) its size, which can be easily visualized after PCR analysis on an agarose gel (Eisen and Smith, 2008). Detection of the end point of translation-blocking morpholinos can be achieved, similarly to chemically inhibited products, with western blot analysis for detection of the absence of the protein of interest. In this case, though, antibodies that recognize the protein and not necessarily the active form of the protein (as would be required for chemical inhibition) can be used.

Disadvantages of the morpholino approach, as briefly mentioned before (Section 4.5, page 166), include off-target effects due mainly to activation of p53 (Sumanas and Larson, 2002), inability to cross the plasma membrane (which dictates their injection only during the first few cell divisions), delivery inconsistencies due to subjective evaluation of the size of the morpholino droplet and dependence of the efficiency of gene inactivation (and absence of redundancy) upon knowledge of all protein-coding transcripts. The reasons, why chemical inhibition by SP600125 was preferred over moprholinos in this study, are clear and are explained before (Section 4.5, page 166). However, confirmation of the observed phenotype, extension of the findings and analysis of putative redundancy between jnk isoforms using morpholino injections would be important.

In addition to morpholino injections, it would also be interesting to find the mechanism of how jnk exerts its effects on the heart during development. Five main ideas, some of which are already being implemented by new members of our research group, could significantly move this project further. They are explained in detail below.

The first one is the examination of cell death and proliferation rates in the hearts of developing SP600125-treated and untreated embryos. Jnk is a major regulator of both these processes (reviewed by Bogoyevitch and Kobe, 2006) and, as suggested by the reduction of ventricular cells in hearts of SP600125-treated embryos, its inactivation could cause destabilization of their intricate balance. Assessment of cell death and proliferation rates is readily achievable by TUNEL and BrdU staining in zebrafish hearts, respectively (Ribeiro et al., 2007, Sedletcaia and Evans, 2011).

The second future plan is the investigation of the specification and migration of cardiac cells. Myocardial cells can be followed through their migratory journey by *in situ* hybridization with a *cmlc2* probe at different time intervals during zebrafish development. Comparing the correlation of somite numbers (indication of overall developmental progression) with *cmlc2* expression pattern (bilaterally, V-shaped, cone, linear heart tube etc) between treated and untreated embryos, would give us an indication of how migration progresses. For an earlier visualization of cardiac progenitors a different approach can be employed. *Goosecoid*-mCherry transgenes constructed using the Tol2-Gateway system (currently being established in the lab by David Burns) can be injected into zebrafish eggs with KikGR mRNA (coding for a photo-convertible green-to-red fluorescent protein). After identification of the first two tiers in the margin of the embryo (see Section 1.3.2 and 1.3.3 at pages 11-13 for details) photo-activation of the desired cells or layers of cells will be achieved with UV light

exposure. Photo-activated precursors, turned red after UV exposure, can be followed using time-lapse fluorescence microscopy and the directionality and rate of their migration can be measured. Changes in these procedures after jnk inactivation (by chemical inhibition or by morpholino injections) would reveal how (and if) jnk is involved in them.

Thirdly, examination of the function of the hearts of SP600125-treated (or morpholino-injected) and untreated fish embryos would add invaluable understanding to the role that jnk plays during zebrafish heart development. The function of the heart and the flow of blood have been shown to be important in shaping the heart itself (Bartman and Hove, 2005, Hove et al., 2004, Ingber, 2006); so analysis of potential defects in heart function and blood circulation could shed more light in our current knowledge of why jnk inhibition causes heart defects. These analyses can be achieved by counting heart rates and by high-speed video recording of circulating red blood cells in the dorsal aorta. This work is currently being conducted in the lab by a new PhD student, Paul Chrystal.

Moreover, investigation of putative alterations in the expression of essential genes after inactivation of jnk enzymatic activity would, also, be interesting and beneficial. For example, changes in the expression levels or patterns of important early cardiac regulators, such as *gata-4* and *nkx2.5*, could have detrimental effects on the specification and differentiation of myocardial progenitors. Analysis of their spatial expression pattern before and after SP600125 treatment could be achieved by *in situ* hybridization, while potential alterations in their expression levels could be revealed by quantitative RT-PCR.

Lastly, examination of left-right patterning defects in SP600125-treated embryos would be of relevance and of interest. Establishment of the left-right axis could be assessed by looking at organs or structures that commonly exhibit left-right directionality (such as the heart and the gut) and by defining asymmetric gene expression in the LPM and thereafter. *Nodal* (*cyclops*, *squint*, *southpaw*) and downstream genes (*lefty-1, lefty-2, pitx2*) are expected to be predominantly expressed on the left side of the midline in the LPM of forming zebrafish embryos. Also, *cyclops*, *lefty-1* and *pitx2* have been shown to be preferentially expressed in the left diencephalon, *cyclops*, *lefty-2* and *pitx2* in the left heart field and *cyclops* and *pitx2* in the left gut primordium (Bisgrove et al., 2000). These asymmetries are useful predictors of organ situs. If reversed or randomized left-right body patterning is observed, then investigation of the underlying mechanism would follow: formation of the Kuppfer's

vesicle, ciliogenesis, polarized positioning of cilia within the cells, transmission of left-right signal(s) from the Kuppfer's vesicle to the LPM and correct interpretation of the left-right cues for subsequent organ morphogenesis would be examined.

Finally, a correlation between the age of the embryos and their developmental progression should also be carried out and has, to some extent, been carried out (not presented here because, due to technical reasons, it was not repeated sufficient times in order to give a reliable pattern). This can be achieved by correlating the number of somites with the age of developing embryos, which is a good indication of developmental progression and can be readily performed under a dissecting microscope. Developmental delay of SP600125-treated embryos, if any, would be revealed with this method. Embryos that are developmentally delayed are expected, despite their age, to exhibit premature features of younger embryos, such as a linear instead of a looped heart tube at 48 or 72 hpf.

4.7. Conclusion

In the work presented in this chapter, inhibition of all proteins produced by the *jnk* genes, identified in Chapter 3, was achieved with the chemical SP600125. Inactivation of jnk during gastrulation (5.25-10 hpf) caused low occurrence of ocular distance, CE and otic vesicle abnormalities and higher incidence of abnormally formed tails, cardiac oedema, atrium enlargement and reverse cardiac looping. Similarly, inhibition of jnk during the segmentation period (10-22 hpf) generated embryos with ocular distance, CE, otic vesicle and tail defects in small percentages and abnormalities associated with the pericardial cavity, heart chamber segmentation, heart chamber specification and/or expansion and cardiac looping in higher occurrence. In contrast, treatment with SP600125 later in zebrafish development (22-30 hpf) affected only the ocular distance (it increased it) and the body length (it decreased it) of treated embryos. Overall, jnk was found to play significant roles during heart formation in zebrafish. So, the next aim of this study was to investigate the role of Jnk in mouse embryonic stem (ES) cells (Chapter 5). This was pursued for two reasons. Firstly, *in vitro* experiments, due to the simpler organization and easier manipulation of the system, can reveal additional information, especially about the early stages of commitment and specification of the cells that are more difficult to approach in a whole organism. Secondly, the origin of ES cells from a different species (mouse instead of zebrafish) is expected to provide a more comprehensive insight to evolutionarily conserved roles of jnk.

Chapter 5. Investigating the role of Jnk during mouse embryonic stem cell differentiation

5.1. Introduction

In this chapter, evaluation of the role of Jnk signalling during differentiation of mouse embryonic stem (ES) cells is conducted. Inhibition of Jnk at distinct time intervals throughout *in vitro* differentiation was performed with SP600125 (a specific pharmacological agent against Jnk, discussed in Section 4.1.1, page 132 and Section 4.5, page 166) and the results obtained are presented below. A short introduction on the ES cell line used in this study (ES-D3) and its special maintenance requirements are discussed in the following section, followed by a brief overview of the genes that have been used as markers of various lineages and differentiation-associated procedures in the PCR analysis.

5.1.2. ES-D3 stem cell line and STO fibroblasts

ES-D3 was one of the first murine ES cell lines to be established, isolated from day 4 129S2/SvPas blastocysts (Doetschman et al., 1985). Its *in vitro* optimal maintenance has been shown to be dependent on the presence of a fibroblast feeder monolayer, LIF and stem cell qualified serum (see Section 1.6.1.1, page 45 for details) (Doetschman et al., 1985, Pease et al., 1990, Toumadje et al., 2003), as explained in more detail below.

The fibroblast feeder layer consists of mitotically inactivated fibroblasts that provide the necessary attachment surface and soluble factors (LIF, nutrients and growth factors) important for the long-term survival and growth of stem cells in an undifferentiated state (Smith et al., 1988). There are two main types of feeder cells that can be used: mouse embryonic fibroblasts (MEF) or Sim-Thioguanine-Ouabain (STO) fibroblasts. MEF are primary cells that provide a reliable, potent and reproducible source of feeder cells after their mitotic inactivation (Evans and Kaufman, 1981). However, as primary cells, they have a limited life span and cannot be maintained indefinitely in culture. In fact, they can only be used efficiently as feeders and support stem cell culture during their first 3-6 passages *in vitro*. Their tedious isolation from

E12.5-E14.5 mouse embryos and their continuous need for stock replenishing make their use difficult and time-consuming (Notarianni and Evans, 2006). Despite these disadvantages, they are extensively used in stem cell research, as they can be obtained relatively cheaply from wild type mice and they have proven to be efficient and reliable. STO on the other hand is an established cell line derived from Sandos Inbred Mouse (SIM) fibroblasts (Notarianni and Evans, 2006). These cells are thioguanine and ouabain resistant, grow well and effortlessly in culture and are easy to obtain, with no need for tedious and lengthy methods of stock replenishing. However, they are expensive and, as they can be kept for long periods in culture, their quality and health can be significantly diminished if optimal conditions are not maintained throughout (Notarianni and Evans, 2006). The ES-D3 cell line, used for all experiments described in this chapter, was obtained from the American Type Culture Collection (ATCC). The stem cell maintenance protocol was performed exactly as recommended by the provider in order to achieve optimal culture conditions, as described in detail in Chapter 2.

5.1.3. Genes used as markers

JNK is a major regulator of transcription and has been shown to affect several cellular processes (reviewed by (Bogoyevitch and Kobe, 2006). The expression of several genes that mark some of these processes was assessed after inhibition of Jnk. Cardiac-related genes, associated with important cardiac differentiation procedures, are examined in this chapter and have been presented before (Section 1.3.5, page 14). Cardiac-unrelated genes are examined as well and are presented below.

5.1.3.1. Markers of cell lineages

Markers of four cell populations outside the cardiac lineage were examined. *Brachyury*, marker of mesoderm, *Hex*, marker of endoderm and early hematopoietic precursors, *Flk1*, marker of early hemangioblasts and endothelial cells, and *CD31*, marker of endothelial cells.

Brachyury (*Bry*), also known as *T*, is a transcription factor essential for the activation of genes required for mesoderm formation and differentiation. It is transiently expressed throughout the primitive streak and nascent mesoderm (Herrmann and Kispert, 1994) and is required for axis development and notochord formation (Technau, 2001). Its connection with β-catenin signalling has been known for years: it was initially

shown to be a direct target of the canonical Wnt pathway (Arnold et al., 2000, Vonica and Gumbiner, 2002, Yamaguchi et al., 1999) and more recently it was suggested to participate in a positive autoregulatory loop with β-catenin that maintains mesodermal progenitors and facilitates posterior somite development (Martin and Kimelman, 2008).

Haematopoietically-expressed homeobox (*Hex*) is a homeobox gene expressed in many tissues during early embryonic development, including primitive endoderm, some endoderm-derived tissues and endothelial and haematopoietic precursors. However, its expression is turned off during terminal differentiation of endothelial and haematopoietic cells (Bedford et al., 1993, Pellizzari et al., 2000, Thomas et al., 1998). *Hex* has also been shown to have a cardiogenic function, as suggested by experiments in frogs and chicks (Schneider and Mercola, 2001, Yatskievych et al., 1999), in human and murine ES cells (Mummery et al., 2003) and in mouse (Hallaq et al., 2004). Recently, a connection between the Wnt network and *Hex* was unravelled. Specifically, experiments on Xenopus showed that during early embryonic development *Hex* has an amplifying effect on canonical Wnt signalling by repressing Wnt antagonists (Zamparini et al., 2006), while later it seems to be induced by canonical Wnt antagonists (such as Dickkopf-1) in the endoderm. This, in turn, activates a yet unknown diffusible factor that acts on mesoderm, where it promotes early heart induction (Foley et al., 2006, Foley and Mercola, 2005). However, it is known that *Hex* can activate early cardiac genes, such as *Nkx2.5* and *Tbx5*, but not later myocardial markers, like cardiac myosins and troponins (Foley et al., 2006, Foley and Mercola, 2005).

The mouse gene *Flk1*, also known as *VEGFR-2* (Vascular endothelial growth factor receptor-2), codes for the main receptor of vascular endothelial growth factor-A (Vegf-A). It plays an essential role during the development of the vascular and haematopoietic system in the early embryo (Ema et al., 2006, Shalaby et al., 1997). This gene is traditionally used as a marker of haemangioblasts, the common mesodermal progenitors of the haematopoietic and vascular lineages, in mouse, differentiating ES cells and zebrafish (Huber et al., 2004, Vogeli et al., 2006). However, there is evidence to suggest that *Flk1* expression marks mesodermal cells with broader differentiation potential (Yamashita et al., 2000). Specifically, it was shown that $Flk1^{-}/Bry^{+}$ mesodermal cells can sequentially give rise to two distinct $Flk1^{+}/Bry^{+}$ cell populations in culture; the first one is the haemangioblast mentioned earlier and the second one is a common progenitor for cardiac myocytes (of both the PHF and SHF), vascular smooth muscle and endothelial cells. The latter population is commonly referred to as the

cardiovascular colony-forming cell (further discussed in Section 1.3.2, page 11) and expresses *Flk1* and *Bry* prior to early cardiac markers, such as *Nkx2.5*, *Gata-4* and *Mef2c* (Garry and Olson, 2006, Kattman et al., 2006). Concomitantly, it was shown that *Nkx2.5*$^{+}$ cells do not express endothelial cell markers, suggesting that the endothelial and myogenic cell lineages have already diverged before the onset of *Nkx2.5* expression (Garry and Olson, 2006, Wu et al., 2006).

Platelet endothelial cell adhesion molecule-1 (PECAM-1 or CD31) is a signalling and cell adhesion molecule, expressed on the membrane of haematopoietic and endothelial cells (Albelda, 1991, Albelda et al., 1991, Tang et al., 1993, Zehnder et al., 1992). This protein is vital for the regulation of angiogenesis and inflammatory responses, facilitating leukocyte migration, transducing mechanical signals in endothelial cells, suppressing pro-inflammatory cytokine production, maintaining vascular integrity and more (reviewed by Privratsky et al., 2010). It is normally found in endothelial cells, platelets and macrophages. It is commonly used as an endothelial cell marker (Luu et al., 2003).

5.1.3.2. Wnt targets

Great overlap between the canonical and non-canonical Wnt pathways has been revealed over the past few years (selected publications: Caneparo et al., 2007, Maye et al., 2004, Tahinci et al., 2007, for more details refer to Section 1.4.4, page 35). Therefore, it was important to assess the cross talk between them, when manipulating either of them individually. *Dickkopf-1* and *Lef-1* were used in this study to assess the effects of Jnk inhibition on the canonical Wnt pathway.

Dickkopf-1 (Dkk-1) is a secreted antagonist of the canonical Wnt/β-catenin pathway (shown in Figure 1.8, page 26). It has been shown to bind to the LRP5/6 co-receptor and prevent the formation of an active Wnt-Frizzled-LRP5/6 complex, thus blocking transmission of canonical Wnt signal (Bafico et al., 2001, Kawano and Kypta, 2003, Mao et al., 2001). Surprisingly, the activation of β-catenin has positive effects on the transcription of Dkk-1, creating a negative feedback loop (Gonzalez-Sancho et al., 2005). A characteristic developmental function of Dkk-1 is its head-inducing capacity by antagonizing the posterior-inducing activity of canonical Wnt signals (Glinka et al., 1998, Mukhopadhyay et al., 2001). Dkk-1 has also been shown to be an important regulator of programmed cell death, an effect exerted mainly through activation of *c-Jun* (Grotewold and Ruther, 2002b), but also through signals from BMP, FGF and Wnt

(Grotewold and Ruther, 2002). c-Jun was shown to be able to induce *Dkk-1* expression *in vivo*, while the expression of both *c-Jun* and *Dkk-1* was shown to be rapidly downregulated after serum withdrawal (Grotewold and Ruther, 2002b).

Lymphoid enhancer-binding factor-1 (*Lef-1*) encodes a transcription factor that can bind to T-cell factor (TCF) proteins, forming potent transcriptional complexes. These complexes participate in the canonical Wnt signalling pathway by recruiting β-catenin, which lacks the ability to directly bind DNA, to Wnt-target genes (Barolo, 2006, Behrens et al., 1996, Huber et al., 1996, Roel et al., 2002, Seidensticker and Behrens, 2000). In many developmental systems, Lef-1 has been shown to be sufficient for inducing a Wnt-like developmental process (Hammerlein et al., 2005, Kengaku et al., 1998, Merrill et al., 2004) and null mutations in *Lef-1/TCF-1* generated a mouse phenotype identical to that seen in Wnt3a-deficient mice (Galceran et al., 1999). It was recently suggested that *Lef-1* itself may in fact be a transcriptional target of β-catenin, either through activation by a β-catenin/TCF-1/Lef-1 complex (Hovanes et al., 2001, Hovanes et al., 2000, Vadlamudi et al., 2005) or through Wnt-induced non Lef/TCF-mediated activation (Filali et al., 2002). Although, it is evident that *Lef-1* is an important regulator of the canonical Wnt pathway and participates in a positive feedback loop enhancing its activity, it has also been shown to be activated by TGF-β signalling in SMAD-dependent (Cordray and Satterwhite, 2005) and SMAD-independent ways (Labbe et al., 2000).

5.1.3.3. Proliferation markers

JNK has been shown to be a critical regulator of proliferation levels in cells (reviewed by Bogoyevitch and Kobe, 2006). Therefore, progression of the cell cycle was assessed by examining the expression levels of *Cyclin-D2* and *c-Myc*.

Cyclin-D2, encoded by the gene *Ccnd2*, belongs to the D-type cyclins, which are regulatory subunits of cyclin-dependent kinases (CDK). Their main role is to regulate G1 phase progression during the cell cycle; their degradation during the G1 phase correlates with the cell failing to enter the S-phase, while its overexpression at that time considerably shortens the G1 interval (reviewed in (Satyanarayana and Kaldis, 2009). Cyclin-D2 is a very labile protein and degrades rapidly after removal of mitogens or other factors that promote cell cycle progression (Schang, 2003, Sherr, 1995). Transgenic mice expressing Cyclin-D2 in the myocardium (αMHC-CycD2) showed 20-30% increase in the size of their hearts, increased DNA synthesis and increased

cardiomyocyte numbers (Lafontant and Field, 2006, Pasumarthi et al., 2005, Soonpaa et al., 1997). Deregulation of D-type cyclins has been associated with cancer progression (Bai et al., 2005, Denicourt et al., 2008).

The gene *c-Myc* encodes an evolutionarily conserved basic Helix-Loop-Helix/Leucine Zipper transcription factor that is known to regulate the expression of a vast array of genes upon stimulation by mitogenic signals (Brenner et al., 2005, Grandori et al., 2000). It has been shown to be activated by Wnt (He et al., 1998, Myant and Sansom, 2011, Sansom et al., 2007, You et al., 2002), Shh (Rao et al., 2003), MAPK/Erk (Armstrong et al., 2006) and other signals and to be involved in a range of downstream cellular processes, such as proliferation and cell growth regulation (Amati et al., 2001, de Alboran et al., 2001, Eilers, 1999, Heikkila et al., 1987), apoptosis and stem cell self-renewal (Smith and Dalton, 2010). Aberrant regulation of the gene that leads to upregulation of its activity has been associated with cancer (reviewed by Pelengaris et al., 2002). JNK (Gupta and Davis, 1994, Noguchi et al., 1999, Alarcon-Vargas and Ronai, 2004) and cyclins (Kanazawa et al., 2003) are known interacting partners of c-Myc. In fact, it has been shown that c-Myc promotes cell cycle progression at least in part through the transcriptional upregulation of Cyclin-D2, with which it can bind directly (Bouchard et al., 2001, Bouchard et al., 1999, Coller et al., 2000). c-Myc is not only activated by Wnt signals but it can also activate the canonical Wnt pathway by suppressing Wnt inhibitors, such as Dkk-1 (Cowling and Cole, 2007, Cowling et al., 2007).

5.1.3.4. Connexin-43, a marker of gap junctions

Connexin-43 (Cx-43) is encoded by the gene *Gja1* (Gap Junction α1) and belongs to a family of oligomerizing transmembrane proteins that form hexameric structures, called connexons. These structures form channels, called gap junctions, which connect neighbouring cells and allow for the transfer of ions and small metabolites (Prochnow and Dermietzel, 2008, Sohl et al., 2003). Cx-43 is expressed in many tissues, including epithelium, myocardium and smooth muscle and its expression is regulated through complex mechanisms, often cell- or tissue-specific (Granot et al., 2002, Pfeifer et al., 2004). Their export to the plasma membrane, their assembly into junctions and their degradation are all regulated via post-translational modifications and, since many of the connexins are phosphoproteins, phosphorylation and dephosphorylation are likely to be essential regulators of their activity (Lampe and Lau, 2004, Solan and Lampe, 2005,

Solan and Lampe, 2009). In fact, MAPK, among others, have been shown to phosphorylate Cx-43 and downregulate gap junction communication (Cameron et al., 2003, Solan and Lampe, 2008). More specifically, activation of JNK in cardiomyocytes resulted in significant reduction in Cx-43 expression at both mRNA and protein levels and caused impaired cell-cell communication (Petrich et al., 2002).

5.2. Aims of the chapter

Jnk is involved in a variety of cellular processes, ranging from cell proliferation and apoptosis to cell migration and differentiation. As a member of the MAPK family and a downstream effector of the non-canonical Wnt/PCP pathway, it is expected to participate, among others, in the transduction of essential signals during cardiac development, possibly affecting the proliferation or apoptosis levels and the differentiation potential of cells. Therefore, the main focus of the current chapter was to investigate whether Jnk is required during mouse ES cell-derived cardiogenesis. In order to achieve this the following aims were set:

- Establish the effect of DMSO (in which SP600125 is diluted) on the differentiation of ES-D3 cells by looking at their morphology, general properties, beating behaviour and gene expression profiles
- Determine the involvement of Jnk signalling on the morphology and growth of differentiating ES-D3 cells during EB formation by inhibiting it with the pharmacological agent SP600125
- Elucidate the effect of suppression of the Jnk pathway by SP600125 on the beating behaviour of differentiating ES-D3 cells, before and after initiation of beating
- Confirm the findings related to the beating behaviour of ES-D3 cells with differentiating E14 ES cells
- Analyse the gene expression profiles of differentiating ES-D3 cells under timely inhibition of the Jnk pathway by SP600125 and determine its involvement in the process

5.3. Assessment of the effect of DMSO on differentiating ES-D3 cells

DMSO was used as the experimental solvent of SP600125, the chemical inhibitor of Jnk. Thus, experiments conducted in the presence of DMSO alone (0.1% DMSO, corresponding to the amount used for SP600125 dilution) should always be included in the analysis in order to ascertain that any observations made after SP600125 treatment were not caused by DMSO but by the drug itself. Therefore, before analysing the effect of the drug on differentiating ES cells, it was important to examine whether DMSO on its own had any effects. The shape, size and morphology of the cells, as well as their beating behaviour and their gene expression profiles were assessed, after administration of DMSO during the ES cell differentiation assay. Briefly, EB were formed in hanging drops from ES-D3 cells between days 0 and 2 of differentiation, were grown in suspension for another three days (d2-d5) and were then plated in 48-well plates (d5-d11). The properties, the morphology and the beating behaviour of the forming EB were assessed at d5 onwards. An untreated group, grown in differentiation media with no additions, was used as the basic comparator.

5.3.1. 0.1% DMSO did not alter the properties and morphology of the cells

Untreated and DMSO-treated EB did not look considerably different at days 5-11, as examined by microscopical observation. At d5, EB, still in suspension, appeared like large spherical, well-formed and well-defined aggregates under both conditions. Between days 5 and 6, cells started migrating away from the adhesion point and EB started to spread along the surface of the well (Figure 5.1). At d8, many cells had migrated away from the initial attachment point but this was still identifiable. At d10, cells had covered a large part of the well surface and EB had spread excessively. All these processes took place in a very similar manner between untreated and DMSO-treated EB.

In parallel, some important cell measurements were taken: the diameter, circularity and viability of the cells were measured and the total number of cells within each EB was assessed. In order to achieve this a Vi-Cell XR-2.03 Counter was employed, details about which are given in Section 2.2.9 (page 71). Cells from 10-12 EB from each condition were pooled together and measured. Three biological replicates (different cells, different days) were assessed for each condition. No significant differences were observed in any of these measurements between the no-treatment and

DMSO-treatment groups. All numerical data are analytically presented in tables and illustrated in graphs.

The average diameter of each cell for the media control group was 10.4μm (se=0.2), 10.3μm (se=0.2) and 9.8μm (se=0.9) at d5, d8 and d11, respectively. The values for the DMSO treatment were found to be similar to that of the no-treatment control: 10.5μm (se=0.2), 9.7μm (se=0.2) and 8.6μm (se=0.2) at d5, d8 and d11, respectively (Figure 5.2). Similarly, the average circularity (counted in units, with 1 being a perfectly circular cell, see Section 2.2.9, page 71) of the cells within untreated and DMSO-treated EB was not affected. For the untreated group it was 0.8 (se=0.02), 0.7 (se=0.01) and 0.7 (se=0.01) at days 5, 8 and 11, respectively. The circularity values for the DMSO treatment group were 0.7 (se=0.01), 0.7 (se=0.01) and 0.7 (se=0.01) at days 5, 8 and 11, respectively.

At d5, the viability of the cells within each EB was 77% (se=1) for the no-treatment and 76% (se=2) for the DMSO-treatment group, which means that at the time of the measurement approximately 77% of the cells within each EB under control conditions were alive. The viability was also measured at days 8 and 11 and was found to be very similar between the two groups examined here: it was 80% (se=4) and 77% (se=3) for the untreated and the DMSO-treated EB at d8, and 74% (se=8) and 67% (se=3) for the respective groups at d11. The total number of cells (dead and alive at the time of the measurement) within each EB was also counted at d5, d8 and d11. The average number of cells per EB was 60174 cells (se=8623), 170247 (se=42049) and 355443 (se=9042) at days 5, 8 and 11 for the media control and 67449 cells (se=10158), 210208 (se=110409) and 478050 (se=101843) at days 5, 8 and 11 for the DMSO control. All experiments started with the same amount of cells (450 cells per hanging drop) so any difference in the number of cells that make up each EB would be expected to be due mainly to different levels of proliferation and cell death. The survival levels (% viability) could be correlated with the levels of cell death within the developing EB at the time of the measurement.

From the data presented above it is clear that no major differences were observed in the morphology and properties of the cells within untreated and DMSO-treated conditions, which suggests that DMSO did not have any adverse effect on the cells. These differences were statistically examined and were found not significant, with p values consistently above 0.1.

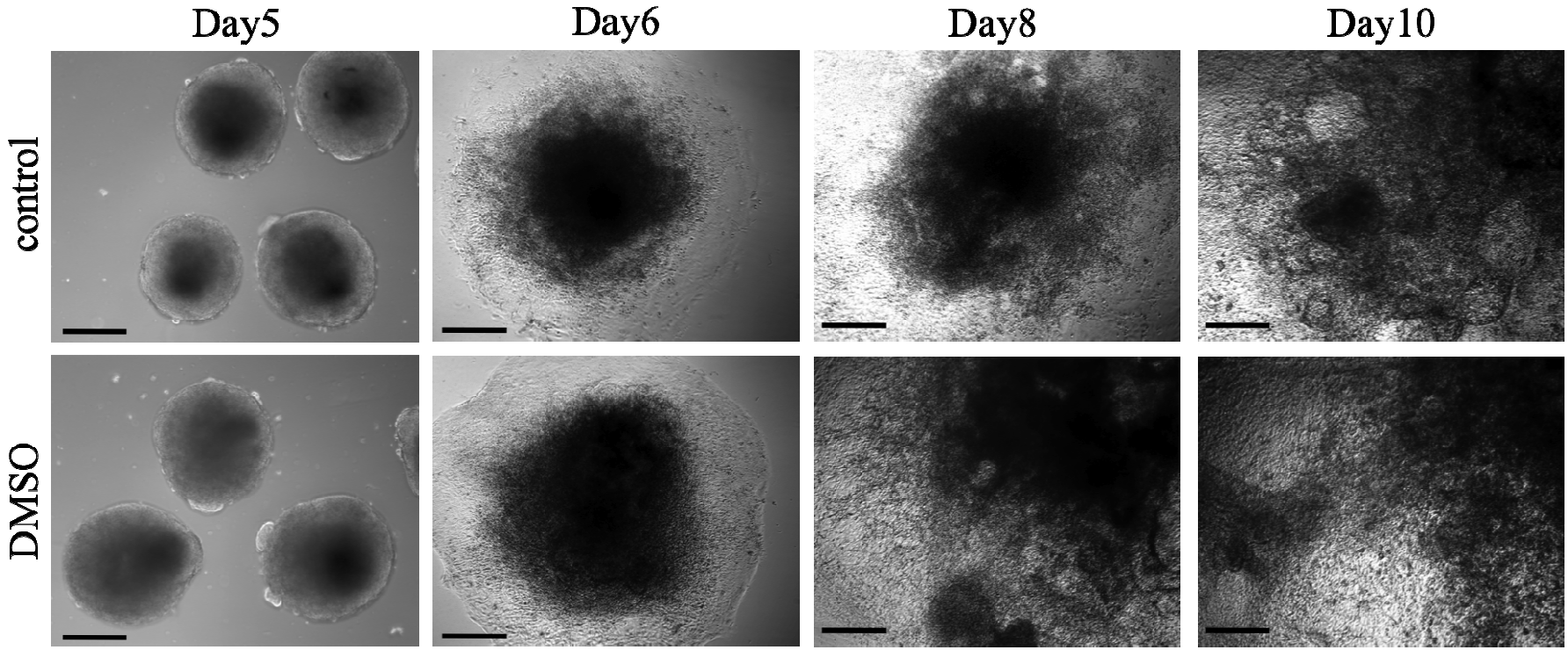

Figure 5. 1: DMSO did not affect the morphology of differentiating EB. Control and 0.1% DMSO-treated EB, one day after plating (d6), still resembled EB in suspension with only a few cells migrating away from the main mass of cells. Three days after plating (d8) many cells have migrated away from the attachment point and have differentiated towards other cell lineages. At d10, a large proportion of the surface of the well was covered by cells and the initial attachment point of the EB was no longer visible. No major differences were observed between untreated and DMSO-treated EB during this process. Scale bars show 200 µm.

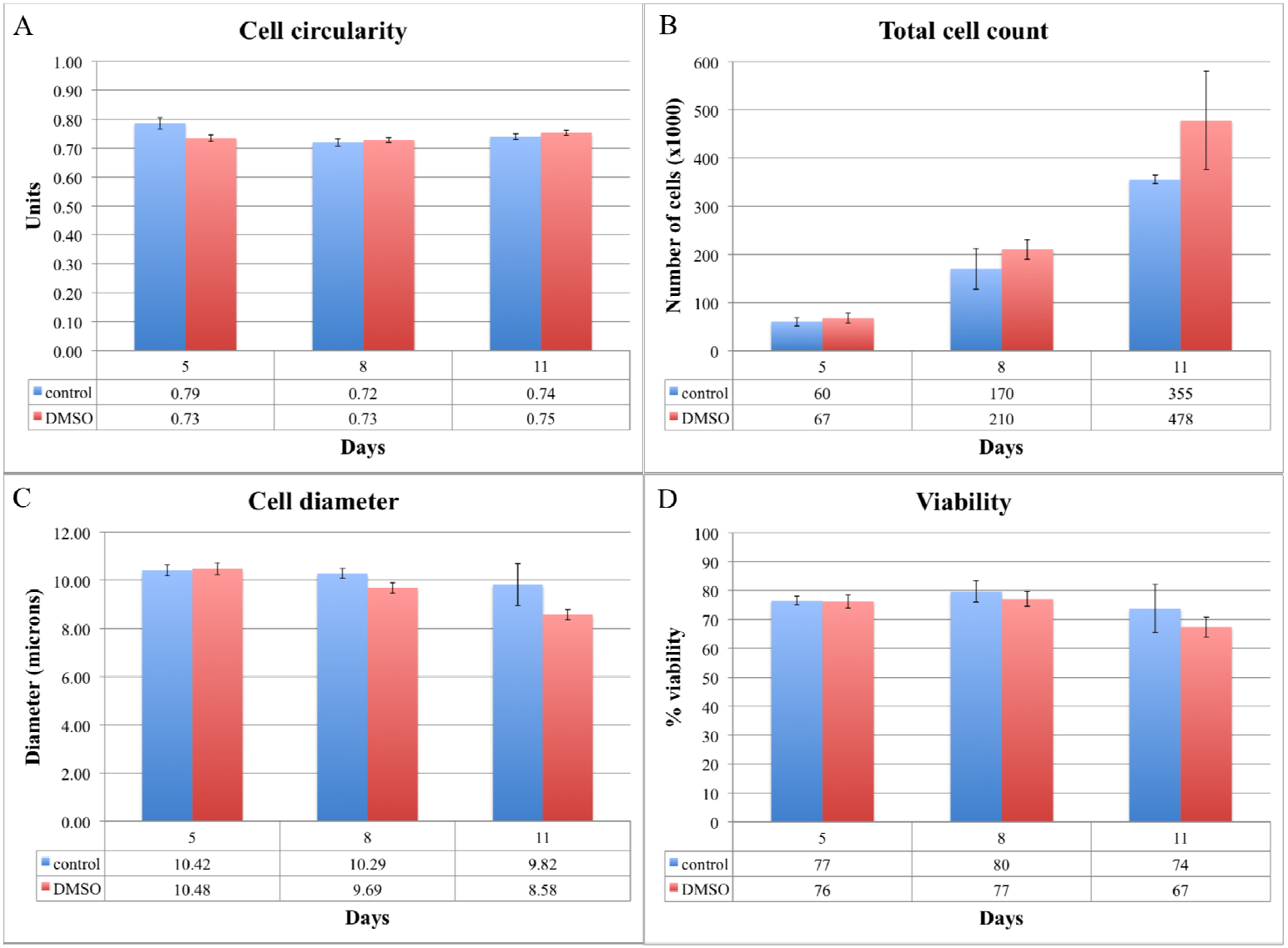

Figure 5. 2: DMSO did not affect the basic cell properties of differentiating EB. Control and 0.1% DMSO-treated EB at days 5, 8 and 11 did not show statistically significant differences in the circularity (A), total count (B), diameter (C) and viability (D) of their cells. The circularity, diameter and viability did not considerably change in either group (no treatment and DMSO-treatment) between days 5 and 11, while there was a gradual increase in the total number of cells per EB from d5 to d11. All numerical data are shown in the tables underneath the graphs. Statistical analysis was performed using one-way Anova testing.

5.3.2. 0.1% DMSO did not alter the beating behaviour of the EB

The beating behaviour of EB after DMSO treatment was examined in comparison to the beating behaviour of untreated EB. It was shown that DMSO did not affect the beating behaviour of the cells within EB in three independent experiments, compared to untreated cells (Figure 5.3). The onset of contraction was at d7 for both media alone and DMSO, when approximately 5% (se=3) and 11% (se=2) of the EB had already initiated spontaneous contraction. Subsequently, with a gradual increase from d7 to d11, the maximal number of EB with beating foci was 51% (se=4) and 46% (se=6) for the media only and the DMSO, respectively. The percentages of EB that contained beating foci at days 5-11 without any treatment and after DMSO treatment are presented in a table and graph format in Figure 5.3.

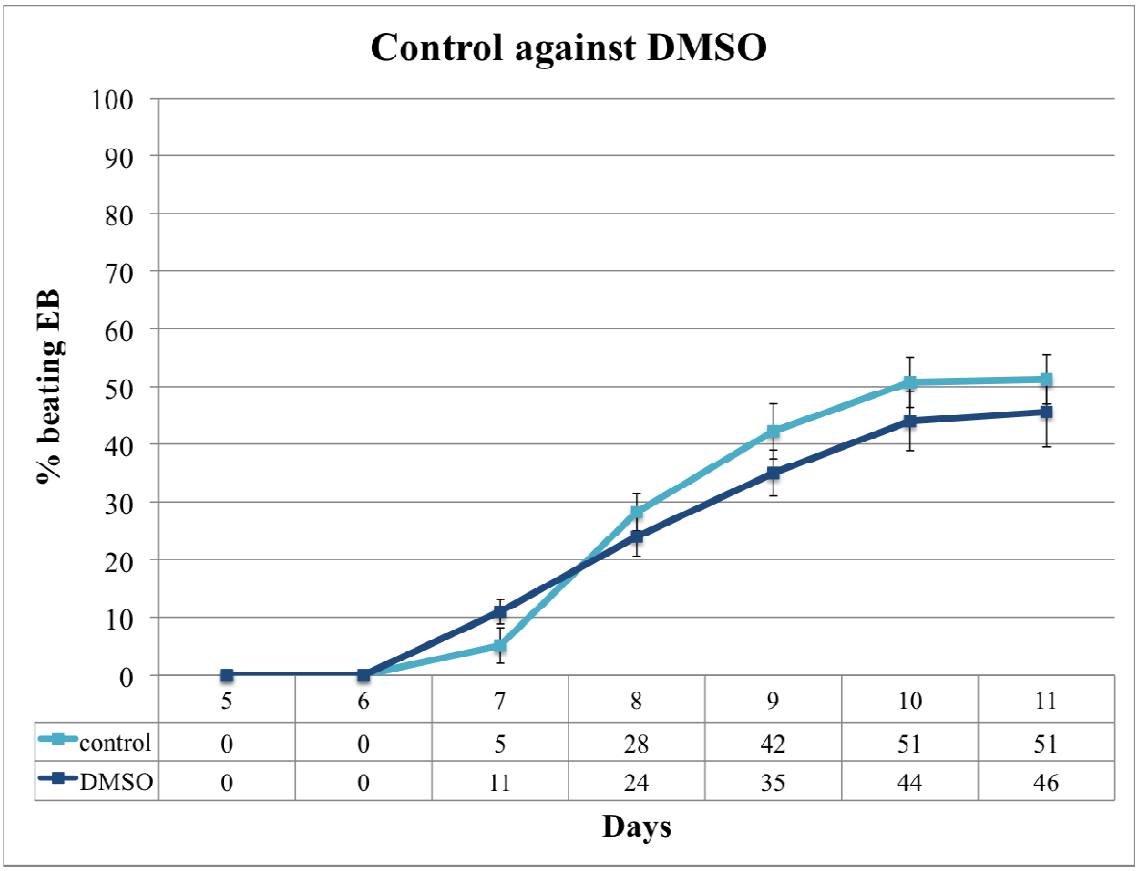

	5	6	7	8	9	10	11
control	0	0	5	28	42	51	51
DMSO	0	0	11	24	35	44	46

Figure 5. 3: DMSO did not affect the beating behaviour of differentiating EB. No major differences were observed in the beating capacity of untreated (control) and 0.1% DMSO-treated (DMSO) EB. Initiation of contraction occured at d7, with 5% and 11% of EB containing beating foci in the no-treatment and DMSO-treatment group, respectively. A gradual increase from d7 onwards led to 51% and 46% beating EB at d11 for the two groups, respectively. All numerical data are tabulated underneath the graph. Statistical significance was assessed with the non-parametric Mann Whitney test.

From the data presented above it is evident that DMSO did not positively or negatively influence any of the aspects of cell differentiation examined here and could, therefore, reliably be used as an experimental control instead of the no-treatment control. However, it was, also, important to assess the gene expression profile of DMSO-treated EB compared to untreated EB.

5.3.3. DMSO treatment did not alter the gene profile of differentiating EB

The expression of several genes of interest was examined in untreated (media) and 0.1% DMSO-treated (DMSO) EB, in order to assess the effect of DMSO in their differentiation potential. Most of the genes examined (shown in detail below) were not altered after 0.1% DMSO treatment at days 0, 5 and 11, compared to the gene expression profile of untreated EB. Lineage markers (cardiac, endothelial, haematopoietic, mesodermal), Wnt targets (Lef-1, Dkk-1), proliferation markers (c-myc, cyclin-D2) and others (Connexin-43) were examined, before and after 0.1% DMSO treatment.

Initially, lineage markers were examined. *Brachyury* met a 35 and 40 fold increase from d0 to d5 and a 9 and 2 fold decreased from d5 to d11 in its expression in the media and DMSO groups, respectively (Figure 5.4). *CD31* transiently decreased at d5 (10 fold from d0 to d5 for both groups) and then increase at d11 (14 fold from d5 to d11 for both groups). *Hex* expression gradually increased from d0 to d11: it increased 2.5 and 5 fold at d5 and then, 8 and 3 fold at d11 in the media and DMSO groups, respectively. The expression of *Flk1* was transiently increased at d5 (3 and 2 fold compared to d0 for media and DMSO, respectively) and then was decreased to levels similar to d0 (Figure 5.4). No statistically significant differences were observed in these genes between untreated and 0.1% DMSO-treated EB at days 5, 8 and 11: $p>0.1$ at all cases as assessed with the one-way Anova test.

Cardiac lineage markers were also assessed. *Mlc2a* decreased approximately 2 fold from d0 to d5 and then increased 3 fold from d5 to d11 in the media control, while it remained unchanged between days 0 and 5 and increased approximately 3 fold from d5 to d11 in the DMSO control (Figure 5.5). *Mlc2v* and *Gata-4* expressions were gradually increased from d0 to 11 in the two groups. Expression of *Mlc2v* was increased 2.5 fold from d0 to d5 and then, 3 and 4 fold from d5 to d11 for the two controls, respectively. *Gata-4* met a 10 and 8 fold increase at d5, followed by a 6 and 9 fold

increase at d11, for media and DMSO, respectively (Figure 5.5). Although some small fluctuations in the expression levels of these genes were observed between untreated and 0.1% DMSO-treated EB, no statistical significance was found in any of them at days 0, 5 and 11 ($p>0.06$).

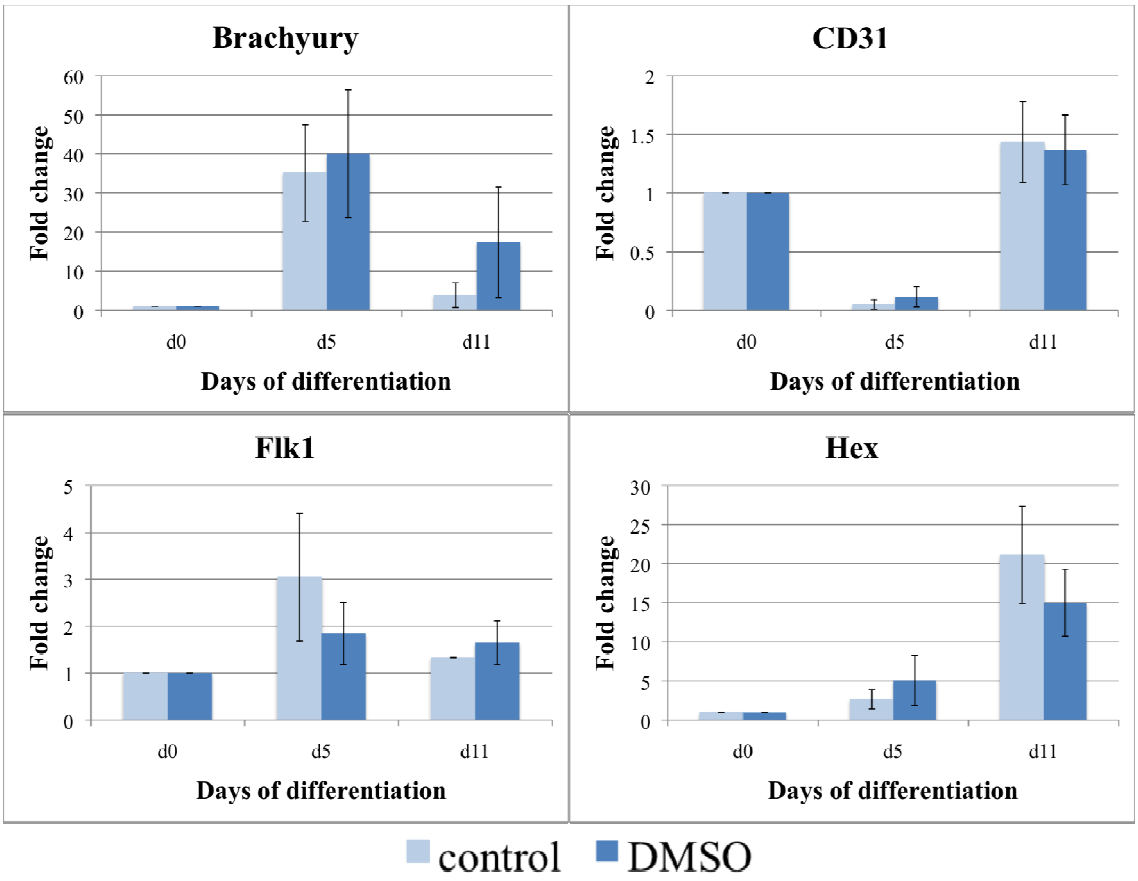

Figure 5. 4: qPCR analysis of lineage markers after 0.1% DMSO treatment. Addition of DMSO in the culturing media between days 0 and 11 did not severely affect the expression of the lineage markers examined here. The expression levels of *Brachyury, CD31, Flk1* and *Hex* were examined at days 0, 5 and 11. All genes were normalized against two housekeeping genes (*β-actin* and *Rps9*) and compared to d0 values (set as the calibrator, equal to 1). Relative quantities expressed as fold changes are shown in the graphs. Mean values of three independent experiments are represented in the graphs, with error bars showing standard errors of the mean. Statistical significance was assessed using one-way Anova testing, followed, when necessary by a 2-sided Dunnett test.

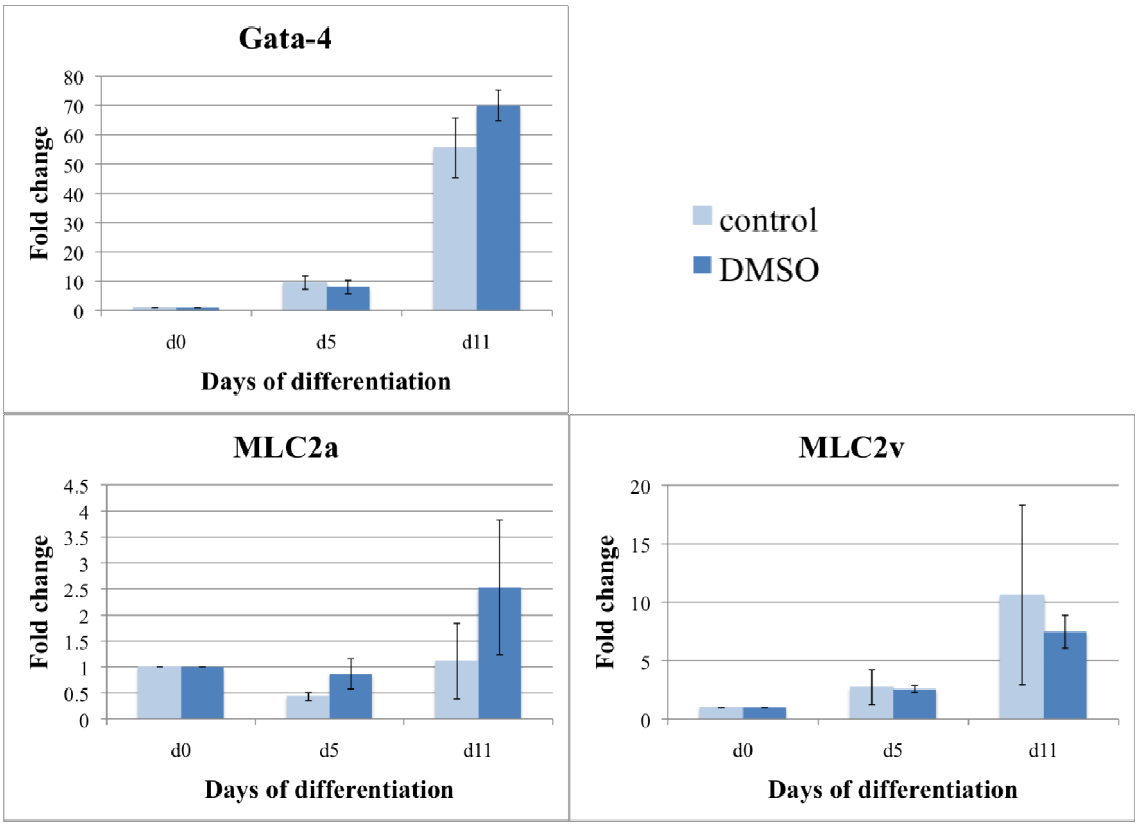

Figure 5. 5: qPCR analysis of cardiac markers after 0.1% DMSO treatment. Addition of DMSO in the culturing media between days 0 and 11 did not severely affect the expression of the lineage markers examined here. The expression levels of *Mlc2a, Mlc2v* and *Gata-4* were examined at days 0, 5 and 11. All genes were normalized against two housekeeping genes (*ß-actin* and *Rps9*) and compared to d0 values (set as the calibrator, equal to 1). Relative quantities expressed as fold changes are shown in the graphs. Mean values of three independent experiments are represented in the graphs, with error bars showing standard error of the mean. Statistical significance was assessed using one-way Anova testing.

Other genes, like proliferation and gap junction markers, inhibitors and downstream components of the Wnt pathway and *Jnk* itself were also examined (Figure 5.6). Expression of *c-Myc* showed a high increase at d5 for both groups (11 and 12 fold for media and DMSO, respectively) and remained fairly unchanged at d11. *Cyclin-D2* expression gradually increased from d0 to d5 (4 and 5 fold for media and DMSO, respectively) and then to d11 (8 and 6 fold for media and DMSO, respectively). *Connexin-43* and *Jnk* met a transient increase from d0 to d5 (51 and 39 fold for *Cx-43*, 3 and 4 fold for *Jnk*, for media and DMSO) and a fall from d5 to d11 (4 and 2 fold for *Cx-43* and 2 and 3 fold for *Jnk*, for media and DMSO). Similarly, Dkk-1 expression was upregulated 80 and 59 fold from d0 to d5 and downregulated 4 and 3 fold from d5 to d11, in the media and DMSO groups, respectively. No statistically significant difference was observed between the two groups (untreated and 0.1% DMSO-treated EB) for the genes examined here at days 0, 5 and 11 as assessed with the one-way Anova test.

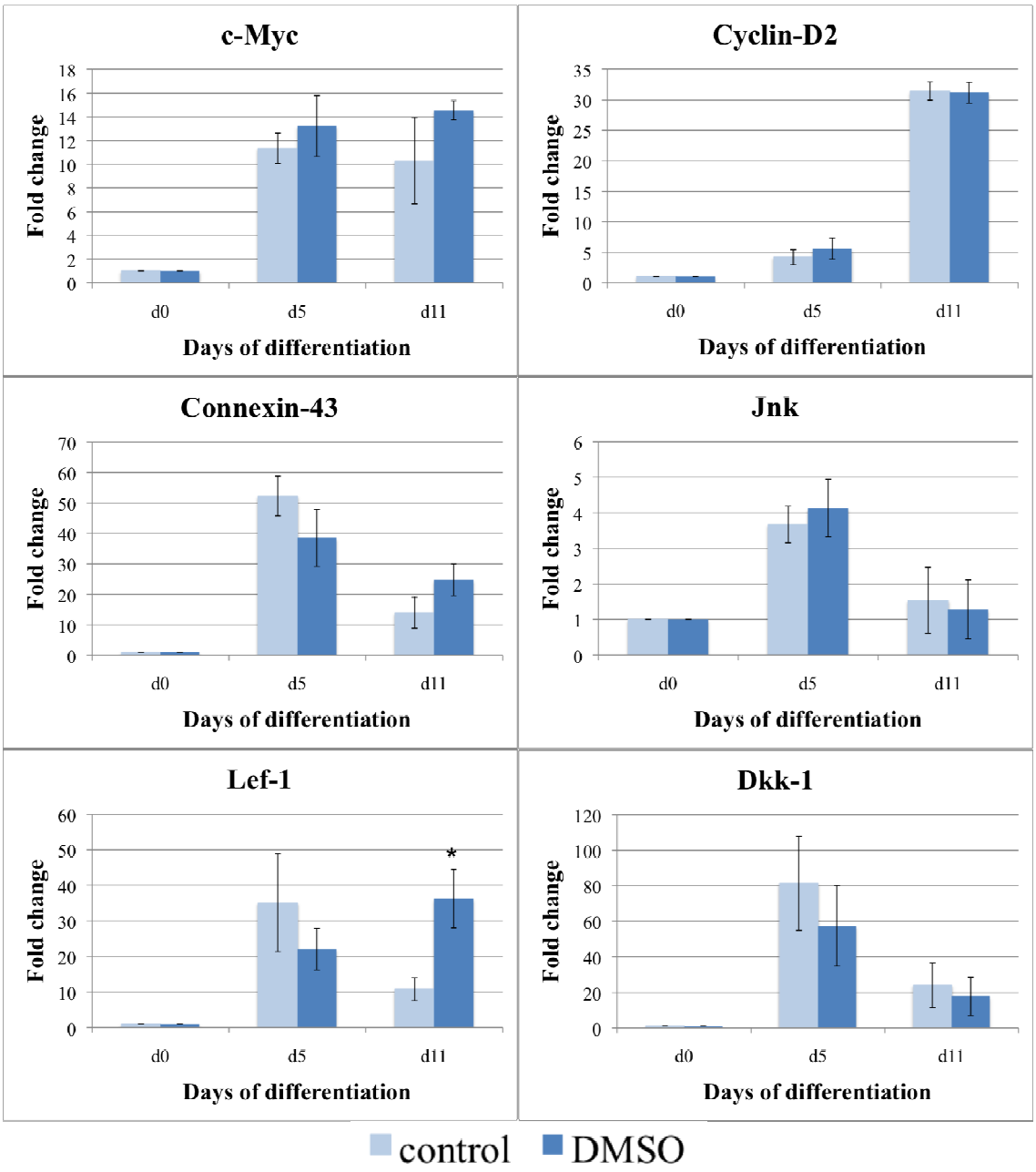

Figure 5. 6: qPCR analysis of downstream Wnt targets, proliferation markers and other genes after 0.1% DMSO treatment. Addition of DMSO in the culturing media between days 0 and 11 did not severely affect the expression of the genes examined here, at days 0, 5 and 11: *c-Myc, Cyclin-D2, Cx-43, Jnk, Lef-1* and *Dkk-1*. All genes were normalized against two housekeeping genes (*β-actin* and *Rps9*) and compared to d0 values (set as the calibrator, equal to 1). Relative quantities expressed as fold changes are shown in the graphs. Mean values of three independent experiments are represented in the graphs, with error bars showing standard errors of the mean. Statistical significance was assessed using one-way Anova testing.

Lef-1 was the only gene that showed differential levels of expression between the media and DMSO groups. At d5 its expression was 35 and 22 fold higher than d0 for the two controls respectively, but at d11 its levels dropped in the media control (3 fold), while they increased in the DMSO control, almost 2 fold (Figure 5.6). This difference

was shown to be statistically significant by one-way Anova testing (p=0.029). This observation will be important when assessing the levels of expression of SP600125-treated EB in the next section.

From the data presented in this section, it becomes evident that administration of 0.1% DMSO during embryonic stem differentiation did not severely affect the gene expression profile (except Lef-1) and, thus, the differentiation potential and progression of cells. Taken together, the use of DMSO as the solvent of SP600125 dictates its use as an experimental control throughout all data analysis and since 0.1% DMSO was not shown to considerably change the properties, morphology and behaviour of differentiating cells, it can be used as the only control from this point forward.

Importantly, the expected expression profiles of the genes of interest during ES cell differentiation were revealed in the last section under both control conditions. This pattern will be used as a comparator for subsequent analysis of the effect of SP600125 administration, and therefore Jnk inhibition, on the differentiation potential of cells.

5.4. Assessment of SP600125 dosage

Initially, the dosage of SP600125 was assessed. After a wide literature search, four concentrations were selected: 1μM, 5μM, 10μM and 20μM (selected publications: (Lu et al., 2008, Moon et al., 2008, Renlund et al., 2008, Tanemura et al., 2009). All four concentrations were tested throughout the experimental time frame, from day 0 until day 11, in order to assess their effectiveness and their potential toxicity at all stages. Once this was completed, the most appropriate concentration, as assessed by the morphology and the beating behaviour of the treated cells compared to controls, was further used for targeted temporal experiments.

5.4.1. High dosages of SP600125 affected the morphology and size of growing EB

After treatment with SP600125 between days 0 and 11 we observed a dose-dependent decrease in the size of the EB at d5: the 20 μM treatment had a detrimental effect on the size and morphology of the EB, the 10 μM had a severe effect, the 5 μM had a mild effect, while the 1 μM treatment did not considerably change their overall morphology (Figure 5.7). The 20 μM SP600125-treated EB, the most severely affected treatment, looked like irregular-shaped, small clumps of cells rather than well-formed multi-

cellular, round and well-defined aggregates. Cell counting was performed using specialised equipment, as described in Sections 2.2.9 (page 71).

5.4.2. The beating pattern of EB was affected in a dose-dependent manner

Next, the beating behaviour of 0.1% DMSO-treated and SP600125-treated EB (at different concentrations) was examined, in order to elucidate which dosage of SP600125 was the most potent and less toxic to be used in further experiments. The beating pattern of SP600125-treated EB was altered compared to the DMSO control in a dose-dependent manner. As described before, DMSO-treated EB initiated spontaneous contraction at d7 (11% beating EB, se=2) and reached a maximum plateau phase at d11, whereby 46% (se=6) of DMSO-treated EB were beating. In contrast, 10 μM and 20 μM SP600125-treated EB showed considerable decreases in their beating ability (not statistically significant, p=0.069, for the 10 μM treatment, but statistically significant, p=0.028, for the 20 μM treatment at d11, compared to DMSO), with the first reaching a maximum of 32% (se=7) beating at d11 and the latter not showing any beating at all, probably reflecting the abnormal differentiation of these EB (Figure 5.8). Interestingly, 1 μM and 5 μM SP600125-treated EB showed increased beating (not statistically significant, p=0.067, and statistically significant, p=0.046, respectively, at d11 compared to DMSO), reaching a maximum of 57% (se=13) and 72% (se=13) beating EB, respectively. Although the 1 μM and 10 μM data were not significantly distinct from controls for most time points between d5 and d11, the 5 μM and 20 μM data were significantly different. The statistically assessed significance values (p) for the 1μM treatment group were higher than 0.05 at d6-d11 compared to DMSO, indicating that no significant differences were observed between the two groups throughout ES cell-derived differentiation. For the 10μM SP600125 treatment statistical significance was observed only at d7 (p=0.046 compared to DMSO), but no significant changes were found at d8 onwards (p>0.05 for d8-d11 compared to DMSO). For the 20μM SP600125 treatment p<0.05 at all time points, indicating significant reductions in the beating capacity of the cells. In contrast, after the 5μM treatment p>0.06 at days 7 and 8 (no statistically significant difference compared to DMSO) and p<0.05 at d9-d11, showing significant increase in the beating behaviour of the cells compared to DMSO. These results were highly reproducible; the pattern was the same in all three independent experiments examined. Under all treatments analysed here, the timing of onset of

beating was not altered; it remained at d7, except after the 20μM treatment, whereby no beating was observed at all.

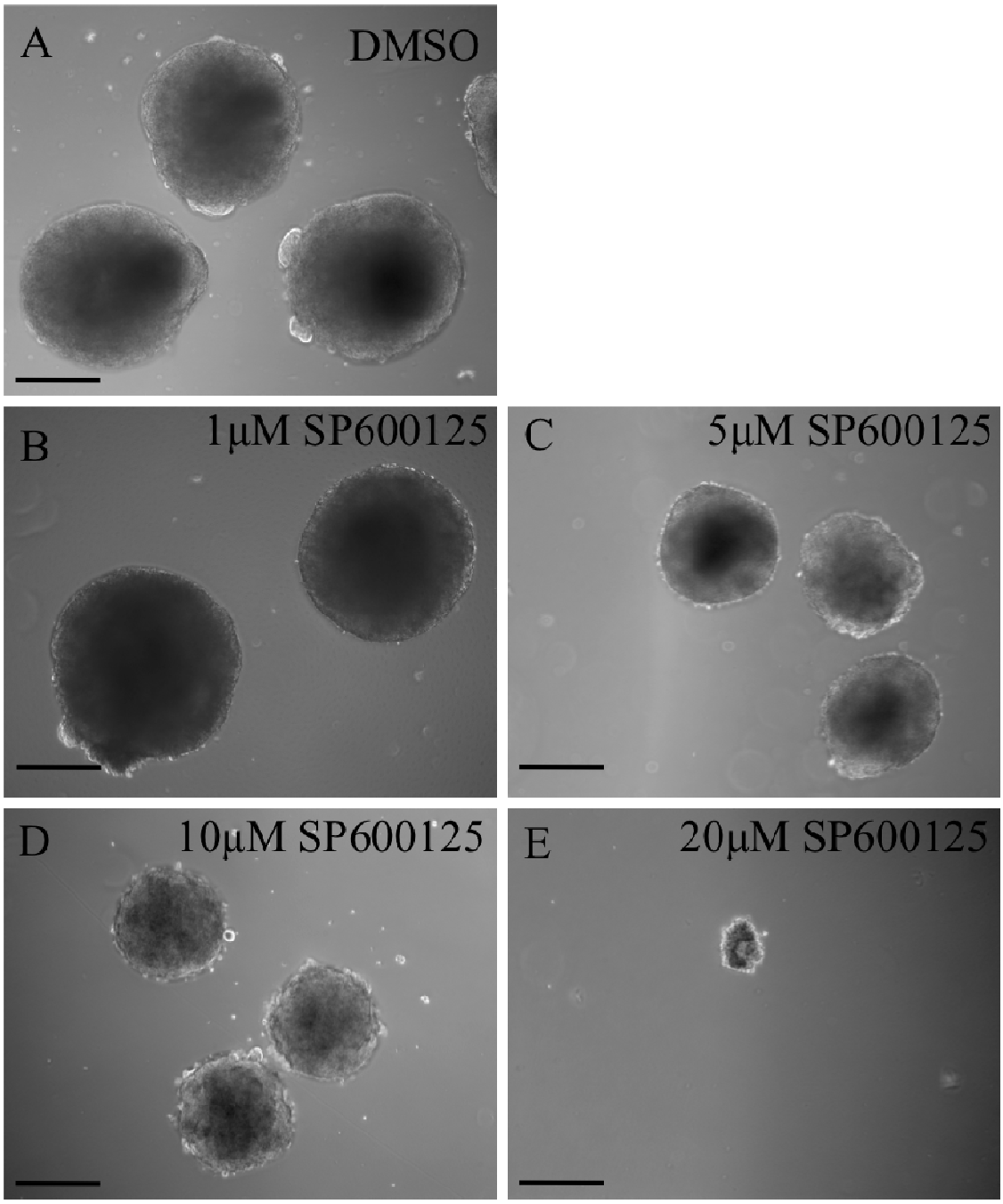

Figure 5. 7: Morphology of EB after SP600125 treatment at various dosages. 1 μM SP600125-treated EB were similar in size with DMSO-treated EB, while 5 μM, 10 μM and 20 μM SP600125-treated EB showed a dose-dependent decrease in their size at d5. 5 μM and 10 μM treated EB appeared like normal, albeit smaller, EB, while 20 μM treated EB appeared like small, irregularly shaped and unhealthy clumps of cells. Scale bars show 200 μm.

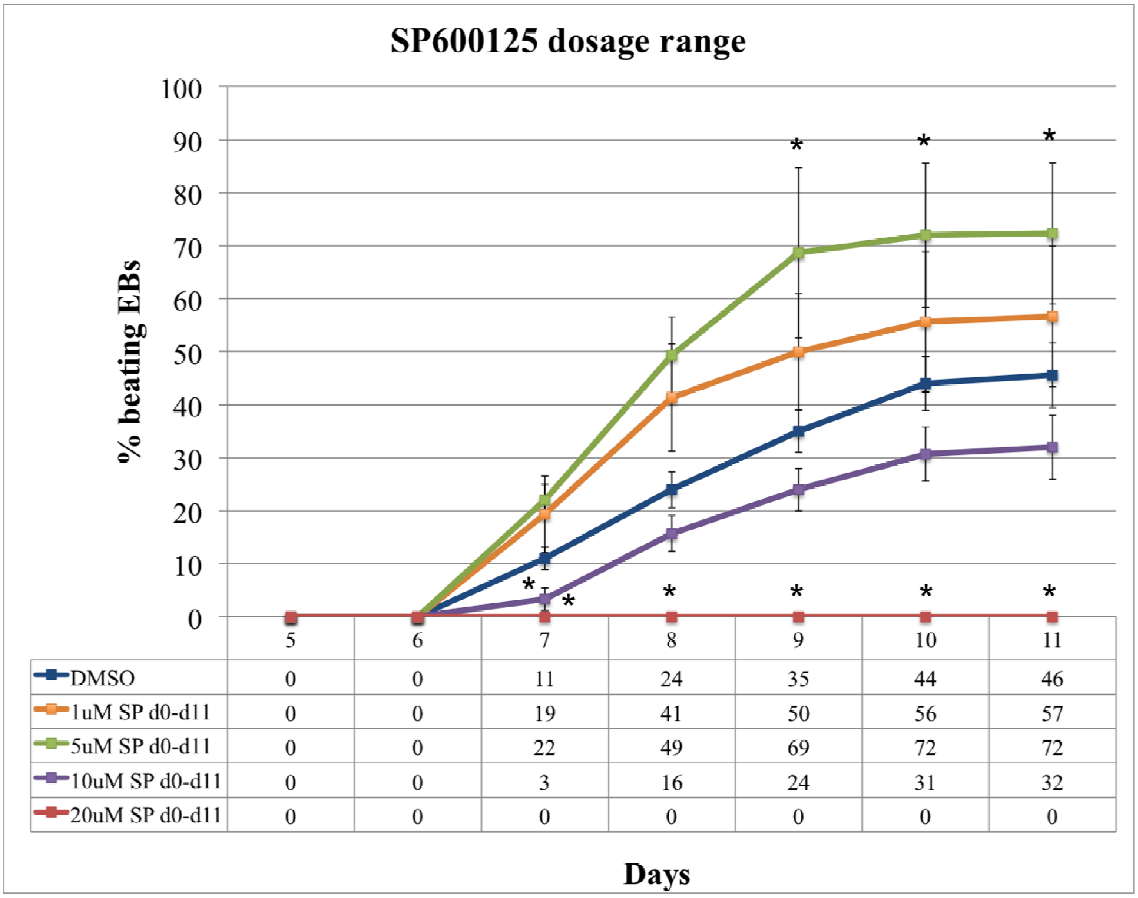

Figure 5. 8: Dose-dependent effect of SP600125 on the beating behaviour of EB. All treatments were performed between days 0 and 11. Mean values from three independent experiments are shown here, with error bars representing the standard errors of the mean. 0.1% DMSO-treated EB showed a gradual increase in their beating ability from d7 (11%, se=2) to d11 (46%, se=6). 1 µM SP600125-treated EB behaved similarly to DMSO controls with an increase from 19% (se=7) beating at d7 to 57% (se=13) beating at d11. 5 µM SP600125-treated cells showed a marked upregulation in their beating behaviour: already at d7 22% (se=3) of EB contained beating foci and at d11 this percentage reached 72% (se=13). Treatment with 10 µM SP600125 slightly affected the number of EB that initiated spontaneous contraction: 3% (se=1) and 32% (se=7) beating EB were seen at d5 and d11, respectively. Addition of 20 µM SP600125 in the culture media had a detrimental effect on the beating behaviour and the overall differentiation of the cells, as none of them achieved contraction within the 11 days of the experiment. Statistical significance, shown with asterisks (*p<0.05) in the graph, was assessed using the non-parametric Mann Whitney test.

We can therefore conclude that, of the doses tested, 5 µM is the concentration at which the inhibitor exerts its maximal positive effect on the differentiation of the cells. 20 µM is highly toxic for the cells, while 1 µM and 10µM are probably not adequate for the drug to exert its full effect: 1µM is possibly very low and 10µM may show low levels of toxicity that do not allow for the drug to exert its effects. In the following sections, experiments performed with 1, 5 and 10 µM of SP600125 are presented, but only the intermediate concentration (5 µM) was used for the more refined experiments.

5.4.3. Effective down-regulation of the levels of activated Jnk after 5μM SP600125 treatment

Before further usage of the drug at 5 μM, it was essential to assess its inhibitory efficiency. 10 μg of d5 total protein lysate from cells grown under different conditions were probed with a specific anti-phospho-Jnk antibody on a western blot. This antibody specifically recognizes endogenous levels of the 46 kDa (Jnk1) and 54 kDa (Jnk2 and Jnk3) Jnk proteins, dually phosphorylated at threonine 183 and tyrosine 185. Adult mouse brain, where Jnk is known to be highly active (Bogoyevitch and Kobe, 2006, Martin et al., 1996, Mohit et al., 1995) was used as a positive control. Treatment with 5 μM SP600125 between days 0 and 5 significantly decreased the levels of active Jnk proteins at d5, although the knock-down was not complete. Recovery of the activity of the proteins was achieved rapidly after removal of the drug, as shown by the d0-d2 treated protein lysate at d5 (Figure 5.9), as assessed by densitometry analysis.

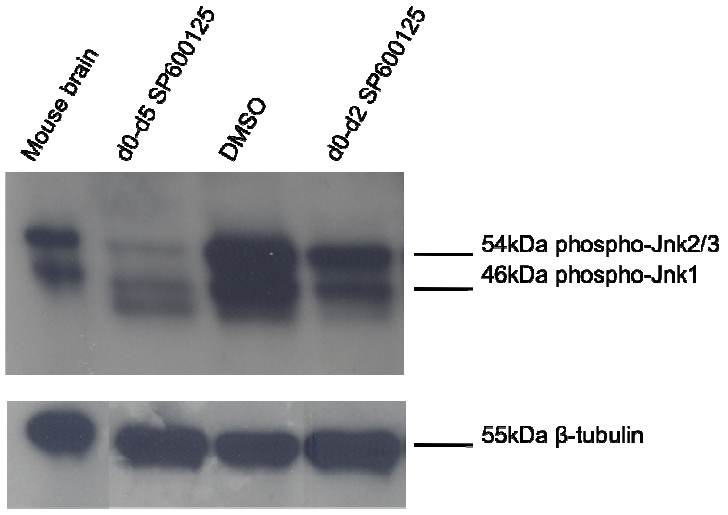

Figure 5. 9: Western blot analysis of d5 DMSO-treated and SP600125-treated EB. The levels of phospho-Jnk were examined and measured with densitometry in adult mouse brain, d0-d5 SP600125, d0-d2 SP600125 and DMSO-treated EB at d5. The levels of phospho-Jnk in d0-d5 SP600125-treated EB were 6 fold lower than that of DMSO-treated EB at d5, showing a significant decrease in the levels of active protein. In contrast, the levels of phospho-Jnk in d0-d2 SP600125-treated EB was only 2 fold lower compared to DMSO-treated EB, indicating that the effect of the drug is reversible. 10μg of each protein lysate were loaded on the SDS-Page. β-tubulin, which was used as a loading control, showed stable expression levels in all samples. The image shown here is representative of images taken from three independent experiments.

5.5. Examination of the effect of serum during the differentiation assay

Next, the effect of foetal calf serum (FCS) on the differentiation of ES cells into cardiomyocytes, in the presence and absence of SP600125, was examined (see Section 1.6.1.1 for a thorough discussion of serum in stem cell culture). Initially, the morphology and beating ability of EB were examined under serum-free conditions and then in serum-free and JNK-free (in the presence of SP600125) conditions. Serum removal was only performed after d5 as up until that time point it was essential for proper growth of the cells within the EB; its earlier removal did not allow the formation of EB at all (refer to Section 2.2.6, page 68 for more details on this).

5.5.1. Serum starvation reduced the adhesion properties and spreading ability of EB in the presence and absence of SP600125

Removal of FCS after d5 caused considerable changes in the morphology, but not the size, of growing EB. EB grown under serum-containing conditions became attached to the bottom of the well soon after their plating at d5. Rapidly, cells started migrating away from the initial adhesion centre and spread out, covering, by the end of the experimental period (d11), a large part of the well. In contrast, EB grown under serum-free conditions did not attach well to the bottom of the wells after plating at d5 and did not spread. Instead they retained, in most cases, their spherical appearance and their contacts with the bottom of the well were minimal (Figure 5.10).

5.5.2. Serum starvation reduced the beating capacity of EB in the presence and absence of SP600125

Removal of FCS caused a severe reduction in the beating ability of EB. Cells grown under serum-free conditions attained a mere 13% (se=4) beating by d11, compared to the DMSO control (EB grown in DMSO- and serum-containing conditions) that exhibited a percentage of 46% (se=6) beating EB at d11 (Figure 5.11). This suggests that one factor, or more likely a combination of factors, within the FCS was important for cells to differentiate properly and to initiate spontaneous contraction.

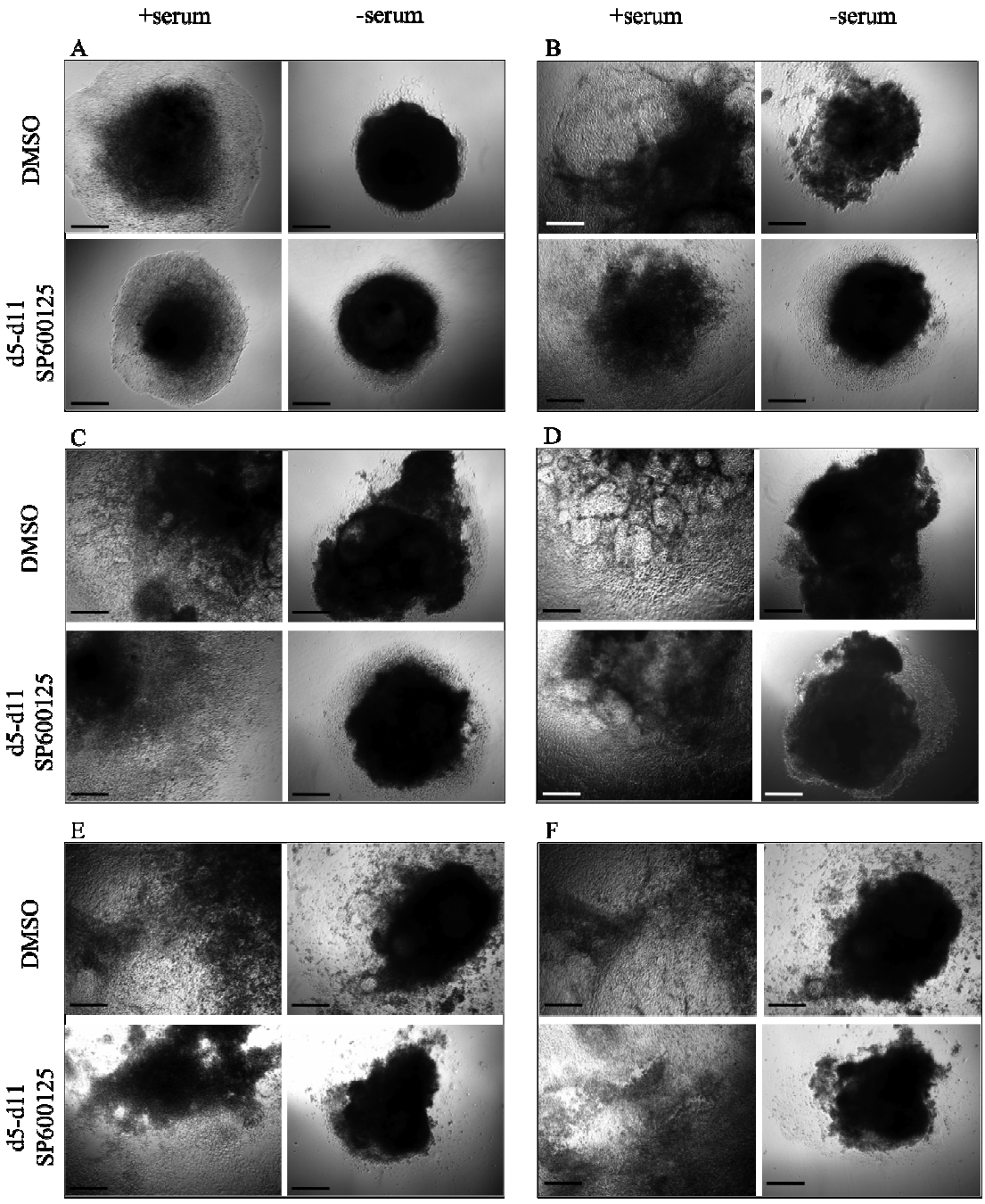

Figure 5. 10: Morphology of EB in the presence of DMSO or SP600125 after serum starvation. A) d6, B) d7, C) d8, D) d9, E) d10 and F) d11 EB are shown. Serum-deprived EB failed to properly adhere to the bottom of the culture dish and to spread allowing for differentiation of the cells. The presence of SP600125 did not alter this effect and did not manage to further promote differentiation. Scale bars show 200 µm.

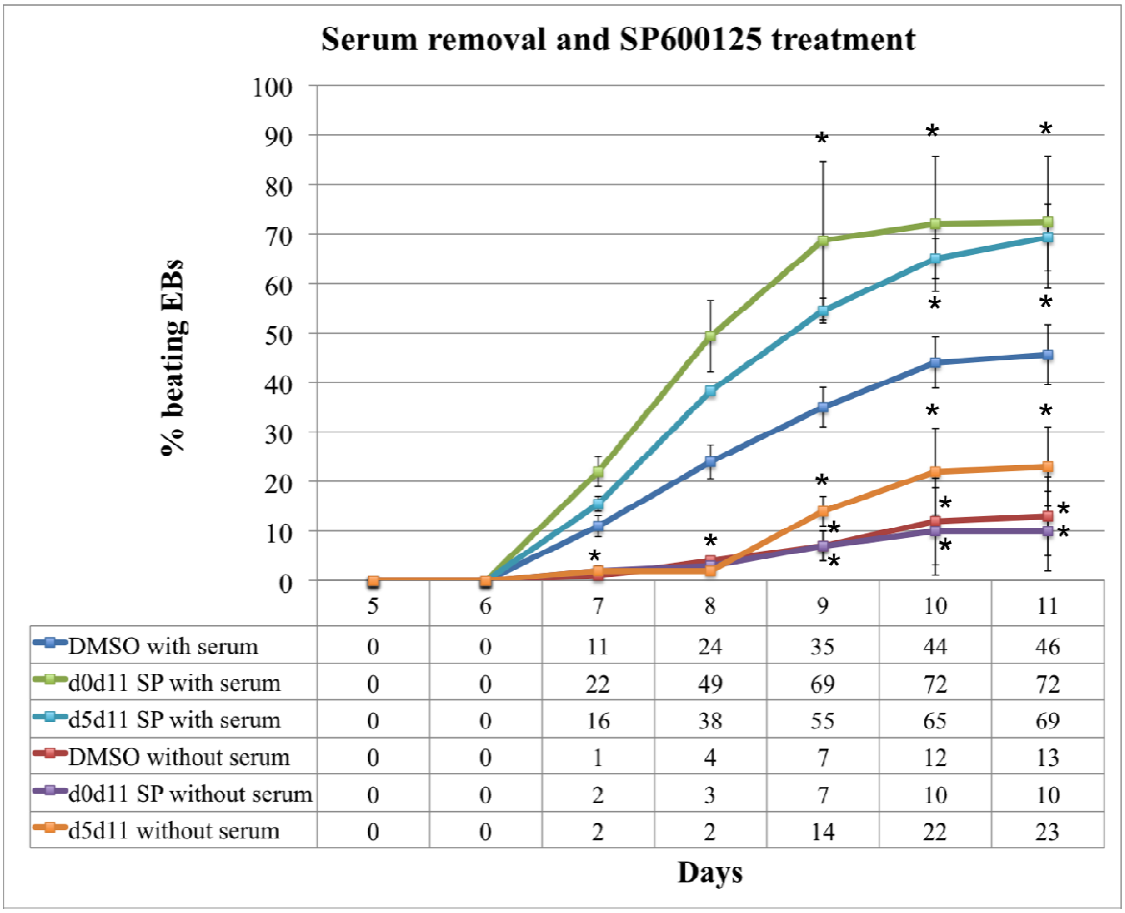

	5	6	7	8	9	10	11
DMSO with serum	0	0	11	24	35	44	46
d0d11 SP with serum	0	0	22	49	69	72	72
d5d11 SP with serum	0	0	16	38	55	65	69
DMSO without serum	0	0	1	4	7	12	13
d0d11 SP without serum	0	0	2	3	7	10	10
d5d11 without serum	0	0	2	2	14	22	23

Figure 5. 11: Beating assessment after serum removal in the presence of SP600125. Absence of serum in the presence of SP600125 had similar effects as in the DMSO-treated EB: it did not allow beating to occur at the expected levels. In the presence of serum 46%, 72% and 69% of DMSO-treated, d0-d11 SP600125-treated and d5-d11 SP600125-treated EB exhibited spontaneous contraction, respectively, while after serum starvation the respective percentages were 13%, 10% and 23%. In the absence of serum, the upregulation of the beating activity of EB observed after SP600125 treatment was lost. Statistical significance, shown with asterisks (*p<0.05), was assessed using the non-parametric Mann Whitney test.

As already mentioned, inhibition of Jnk with 5μM SP600125 increased the occurrence of beating during ES cell differentiation (Section 5.4.2, page 190, Figure 5.8) while removal of serum did not allow proper differentiation and cardiogenesis to take place (Figure 5.11). The next question that arose was how would inhibition of Jnk in serum-free conditions affect the beating behaviour of the cells. In order to answer this question 5μM SP600125 was added to both serum-free and serum-containing medium at different time intervals during ES cell differentiation: d0-d11 and d5-d11. Serum-free medium was only used after d5, as explained in Chapter 2.

Addition of SP600125 in this context did not cause an increase in the occurrence of beating (Figure 5.11) as it did when serum was present. In fact, addition of SP600125 in serum-free media did not seem to have any effect on the beating ability of EB compared to serum-free media alone. 2% and 10% beating EB were seen at d7 and d11

after d0-d11 SP600125 treatment under serum-free conditions, compared to 22% and 72% under serum-containing conditions, respectively. Similarly, after d5-d11 SP600125 treatment in the absence of serum, only 2% and 23% of EB contained beating foci at d7 and d11, respectively, while the respective percentages in the presence of serum were 16% and 69%. So, it is the combination of serum and SP600125 after d5 that increased the beating ability of the cells, since either one on its own did not have this effect. Also, the presence of SP600125 and serum in the period between d0 and d5 did not seem to be sufficient for upregulation of contraction, if serum was removed after d5. Therefore, the results presented in this chapter hereafter were obtained from experiments performed in the presence of FCS throughout the differentiation period.

5.6. Examination of the beating behaviour of EB after timely inhibition of Jnk

The 5 μM SP600125 concentration was used throughout the experiments, as it was found to promote beating with no evidence of toxicity. However, as mentioned before, the 1 μM and 10 μM SP600125 dosages were also included in some of the assessments because it was thought that these dosages given for shorter amounts of time might have different effects and could provide useful comparisons. The time intervals for SP600125 treatment had to be refined, as we were interested in understanding the precise temporal role of Jnk during ES cell differentiation into cardiomyocytes. Our interest was mainly focused on pre-beating stages of differentiation that are related to zebrafish heart tube stages before the initiation of spontaneous contraction, as discussed in Chapter 4. However, we also wanted to gain insight into the later stages of differentiation. Therefore, we selected the following time treatments: d0-d5 for three dosages (1μM, 5μM and 10μM) and d0-d2, d2-d5 and d5-d11 for the optimal dosage only (5μM).

5.6.1. 1μM and 10μM SP600125 did not exhibit a stage-specific effect on beating

When SP600125 was added at a concentration of 1 μM between days 0 and 5 only, the beating behaviour of the cells was not altered compared to DMSO-treated cells. 10% (se=5) and 50% (se=12) of EB were beating at d7 and d11, respectively, after d0-d5 treatment with 1μM SP600125. The respective percentages for DMSO-treated EB were 11% (se=2) and 45% (se=6) and for d0-d11 treated EB they were 19% (se=7) and 57% (se=13) at days7 and 11, respectively (Figure 5.12).

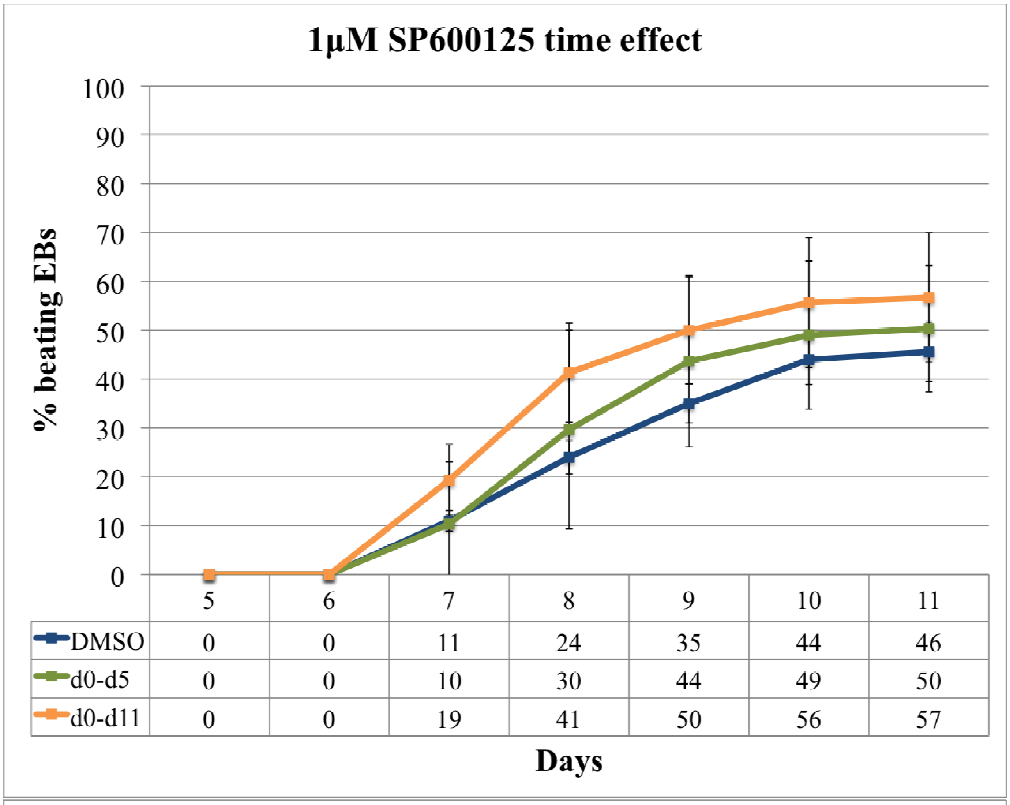

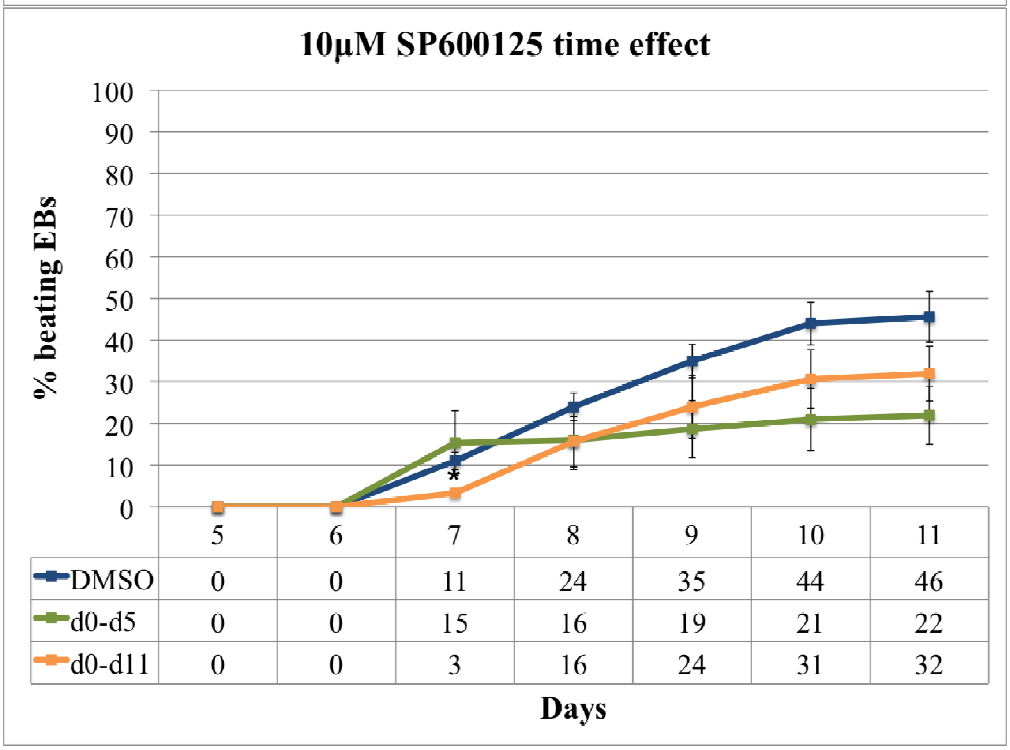

Figure 5. 12: Timely assessment of the beating behaviour of 1µM and 10µM SP600125-treated EB. No major differences were observed in their beating capacity regardless of when and for how long the drug was applied. 10% (se=5) and 50% (se=12) of EB were beating at d7 and d11, respectively after treatment with 1 µM SP600125 between days 0 and 5, while the respective percentages for the d0-d11 1 µM treatment were 19% (se=7) and 57% (se=13). Similarly, at d7 15% (se=8) and 3% (se=1) of d0-d5 and d0-d11 treated EB were beating and at d11 the respective percentages were 22% (se=7) and 32% (se=7). These percentages did not show considerable differences compared to DMSO controls: at d7 11% (se=2) and at d11 45% (se=6) of DMSO-treated EB exhibited contractile activity. Statistical significance, shown with asterisks (*p<0.05) in the graph, was assessed using the non-parametric Mann Whitney test.

Similarly, addition of 10μM SP600125 to the culture media at d0-d5 did not considerably alter the beating ability of EB, compared to DMSO-treated EB. 22% (se=7) of EB were beating at d11 after d0-d5 Jnk inhibition with 10μM SP600125 compared to 45% (se=6) of DMSO-treated beating EB. The respective percentage of d0-d11 SP600125 (10μM)-treated EB was 32% (se=7) at d11 (Figure 5.12). Interestingly, at d7, only the d0-d11 but not the d0-d5 SP600125 treatment caused a transient but significant decrease in the beating ability of EB (asterisk in Figure 5.12).

These observation support the suggestion that 1μM is possibly a very low dosage for Jnk inhibition, regardless of the timing of the treatment and that 10 μM is not an appropriate concentration to be used, since it probably shows some levels of toxicity.

5.6.2. 5μM SP600125 exhibited a stage-specific effect on beating

Focusing more on the concentration of interest, as explained before, 5 μM, both pre-beating (d0-d2 and d2-d5) and post-beating (d5-d11) treatment stages were examined and compared to the DMSO control. Treatment between days 0 and 2 did not affect the beating activity of the cells (Figure 5.13). The percentages of EB with beating foci at days 7 and 11 were 20% (se=2) and 52% (se=6) for this group, compared to 11% (se=2) and 46% (se=6) for the DMSO group, respectively, with p values higher than 0.05 at all time points. The d2-d5 and d5-d11 treatment groups exhibited similar patterns between them, but were markedly different to that of the DMSO group, especially at later stages of differentiation (after d8).

Similarly to the d0-d11 treatment discussed earlier (Section 5.4.2, Figure 5.8), d2-d5 and d5-d11 Jnk inhibition (5 μM SP600125) caused an increase in the beating capacity of EB. At d7 30% (se=1) and 16% (se=2) of d2-d5 and d5-d11 SP600125-treated EB were beating, showing no major differences compared to DMSO (p=0.064 and p=0.384, respectively), but at d11 the respective percentages were 62% (se=7) and 69% (se=7), which were both significantly different compared to DMSO (p=0.046 and p=0.023, respectively). Of note, d5-d11 SP600125-treated EB exhibited a significant increase in their beating behaviour only at d10 and d11, while d2-d5 SP600125-treated EB showed significantly increased beating already at d8. This delay may be attributed to a delay in the action of the drug and to the different phase that cells are going through, depending on their differentiation status at the time that the drug is administered.

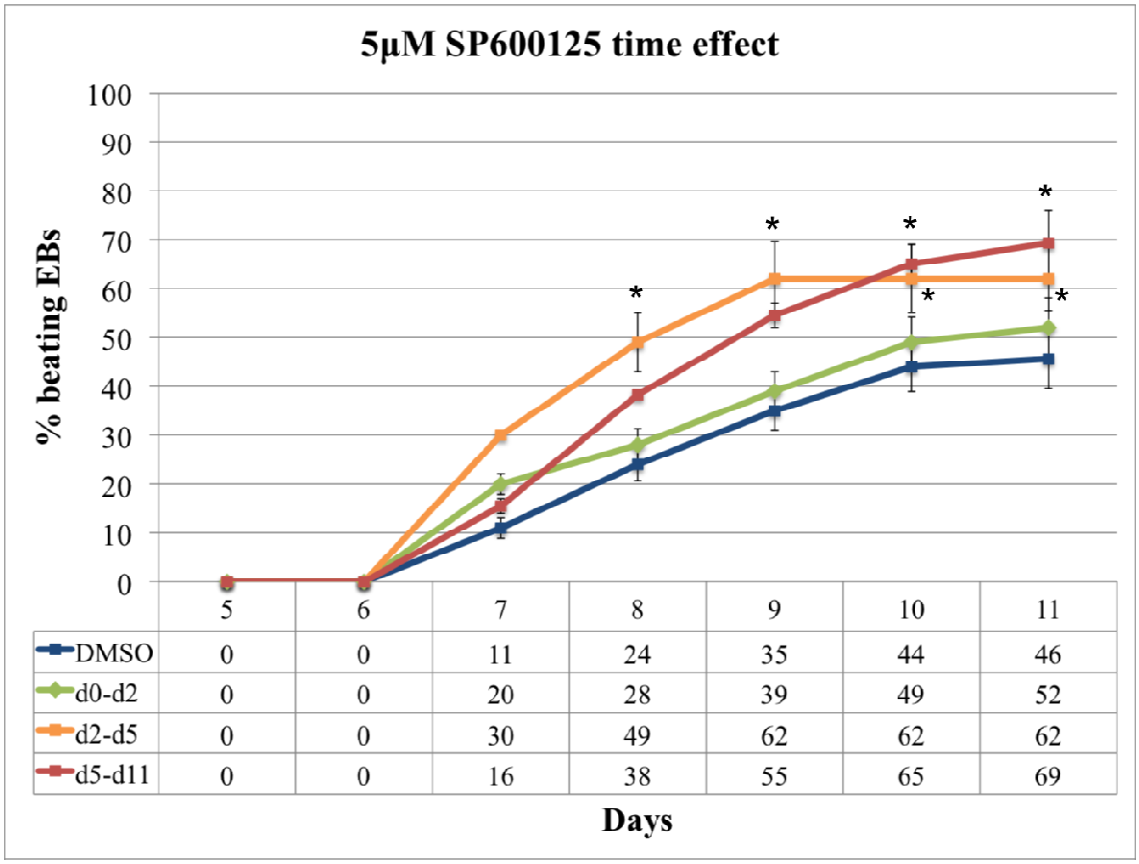

	5	6	7	8	9	10	11
DMSO	0	0	11	24	35	44	46
d0-d2	0	0	20	28	39	49	52
d2-d5	0	0	30	49	62	62	62
d5-d11	0	0	16	38	55	65	69

Figure 5. 13: Time effect of 5 µM SP600125 treatment on the beating behaviour of the cells. No major differences were observed in the beating capacity of d0-d2 SP600125-treated EB compared to the DMSO control (p>0.05 at d6-d11). 20% (se=2) and 52% (se=6) of beating EB were observed after d0-d2 SP600125 treatment, percentages very similar to DMSO (11% and 46% at days 7 and 11, respectively). After the d2-d5 and d5-d11 treatment, though, a clear upregulation of the beating capacity of the EB was observed after (including) d8 and d10, respectively. At d7 30% (se=1) and 16% (se=2) and at d11 62% (se=7) and 69% (se=7) of beating EB were observed in the d2-d5 and d5-d11 SP600125 treatment groups, respectively. At d11 the respective percentages were 62% (se=7) and 69% (se=7). Statistical significance, shown with asterisks (*p<0.05) in the graph, was assessed using the non-parametric Mann Whitney test.

Therefore, it is concluded that between days 0 and 2, Jnk either does not play an important role in regulating the events that lead to the emergence of beating, or is not highly expressed (or highly activated) and, thus, its inhibition does not severely affect the behaviour of the cells. After d2, however, the timing of Jnk inhibition does not seem to play an important role in cardiogenesis; its effect is always the same (increased beating) regardless of the time of the drug administration. It is only the timing and the duration of the effect that differs between the two later SP600125 treatments (d2-d5 and d5-d11).

5.6.3. 5 μM SP600125 had similar effects on the beating ability of E14 ES cells

The effect of Jnk inhibition was also assessed on differentiating E14 ES cells, exactly as described for ES-D3 cells. This comparison was performed in order to assess whether the observed effect of the SP600125 drug on differentiating ES-D3 cells was only specific to this cell line, or whether it was a more general effect. It also allowed for a comparison with the data obtained from the E14 cell line, presented in Chapter 6. The beating graph obtained from this experiment is shown in Figure 5.14.

	5	6	7	8	9	10	11
media	0	15	50	53	55	55	56
DMSO	0	28	53	55	57	60	60
d0d5 SP	0	17	54	69	79	79	79
d5d11 SP	0	20	65	78	85	85	85

Figure 5. 14: Time effect of 5 μM SP600125 treatment on the beating behaviour of differentiating E14 ES cells. A slight but not significant upregulation of beating was observed after d0-d5 and d5-d11 treatment. At d11 56% (se=15), 60% (se=4), 79% (se=8) and 85% (se=11) of EB contained beating foci under control, DMSO, d0-d5 treatment and d5-d11 treatment conditions, respectively. In this graph, the mean values of 3 independent experiments are shown, with error bars representing standard error of the mean. Statistical significance was assessed using the non-parametric Mann Whitney test.

SP600125 introduced in the media between days 0 and 5 and days 5 and 11 was shown to increase the beating ability of differentiating E14 ES cells (Figure 5.14), in a similar way to what is shown in Figures 5.8 and 5.13 for ES-D3 cells. However, its effect was not statistically significant ($p>0.05$ at all time points, compared to DMSO), likely due to increased biological variability, indicated in the graph (Figure 5.14) with large error bars that represent the standard errors of the mean. More repetitions would probably be required for statistical significance to be observed.

5.7. Examination of the effect of Jnk inhibition on the size, shape, viability and numbers of cells within EB

In parallel, we also looked at the size, shape and viability of the cells within EB grown under different conditions at d5, d8 and d11. This would give us an insight into how cells are behaving within the EB and it would allow us to understand how inhibition of Jnk can interfere with it. For the d5 measurements, EB treated with 5 μM SP600125 between d0-d2 and d2-d5 were used, while for the d8 and d11 measurements EB treated with 5 μM SP600125 between d0-d2, d2-d5 and d5-d11 were used. 10 EB, thoroughly disaggregated with trypsin (refer to Section 2.2.9 for more details), were used for the measurements for each condition and the experiment was repeated three times. Average values from three independent experiments are shown in the graphs, with error bars representing standard errors of the mean and asterisks indicating statistical significance, as assessed with the parametric one-way Anova test, followed when necessary (as explained in Section 2.6, page 81) with a 2-sided Dunnett test.

5.7.1. Jnk inhibition did not affect the shape and size of cells

Initially, the size and shape of the cells within the EB were of interest so we counted the diameter and circularity of the cells in all groups using a Vi-Cell XR-2.03 Counter, as described in more detail in Section 2.2.9 (page 71). The diameter of the cells is an indication of their size, while the circularity is an indication of how regular their shape is. All numerical data are tabulated underneath the graphs for easier observation (Figure 5.15). The average diameter of each cell for the DMSO control group was 10.5μm (se=0.2), 9.7μm (se=0.2) and 8.6μm (se=0.2) at d5, d8 and d11, respectively. No statistically significant differences were observed between the DMSO and the SP600125 treatment groups ($p>0.06$ in all cases). D0-d2 SP600125-treated cell diameter

was 10.9μm (se=1.3), 9.9μm (se=0.4) and 8.6μm (se=0.3) at d5, d8 and d11, respectively. The average values for d2-d5 SP600125-treated cells were 11.7μm (se=0.3), 9.7μm (se=0.3) and 8.9μm (se=0.3) at d5, d8 and d11, respectively, and for d5-d11 SP600125-treated cells 9.3μm (se=0.6) and 8.1μm (se=0.1) at d8 and d11, respectively (at d5 the drug was not yet applied). These findings indicate that the size of the cells was not altered after inhibition of Jnk (Figure 5.15).

Similarly, the circularity of the cells was shown not to be affected after SP600125 treatment. At d5 this value was 0.7 (se=0.01), 0.8 (se=0.02), 0.8 (se=0.01) and 0.8 (se=0.02) for the DMSO, d0-d2, d2-d5 and d5-d11 SP600125 treatment, respectively, with values closer to 1 showing perfect circularity and values closer to 0 showing irregular cell shape (Figure 5.15). The respective values for d8 were 0.7 (se=0.01), 0.7 (se=0.01), 0.7 (se=0.02) and 0.7 (se=0.02) and for d11 they were 0.7 (se=0.01), 0.8 (se=0.02), 0.7 (se=0.02) and 0.8 (se=0.01). Statistical significance was low for the observed minor differences between the different groups with $p>0.35$ in all cases. Therefore, no difference was observed in the shape of the cells after inhibition of Jnk.

5.7.2. Jnk inhibition did not affect the viability of cells but reduced the number of cells per EB at d8

At d5, the average viability was 76% (se=2) for the DMSO control, which means that at the time of the measurement approximately 76% of the cells within one EB, under control conditions, were alive. Viability was not severely altered after d0-d2 and d2-d5 5μM SP600125 treatment. The respective percentages were 81% (se=3) and 83% (se=5). The viability was also measured at days 8 and 11 but no significant differences were observed at either time point for any of the conditions (Figure 5.16). At d8, the percentage of viable cells was 77% (se=3), 74% (se=9), 80% (se=6) and 78% (se=3) for the DMSO control, d0-d2, d2-d5 and d5-d11 SP600125 treatment groups, respectively. Similarly, at d11 the respective percentages were 67% (se=3), 64% (se=7), 65% (se=4) and 59% (se=0.04). Although there was some variation in the survival rates of cells within treated and untreated EB at days 5, 8 and 11, the differences were not statistically significant ($p>0.09$ for all groups compared to DMSO). Survival could be used as a measure of the levels of cell death.

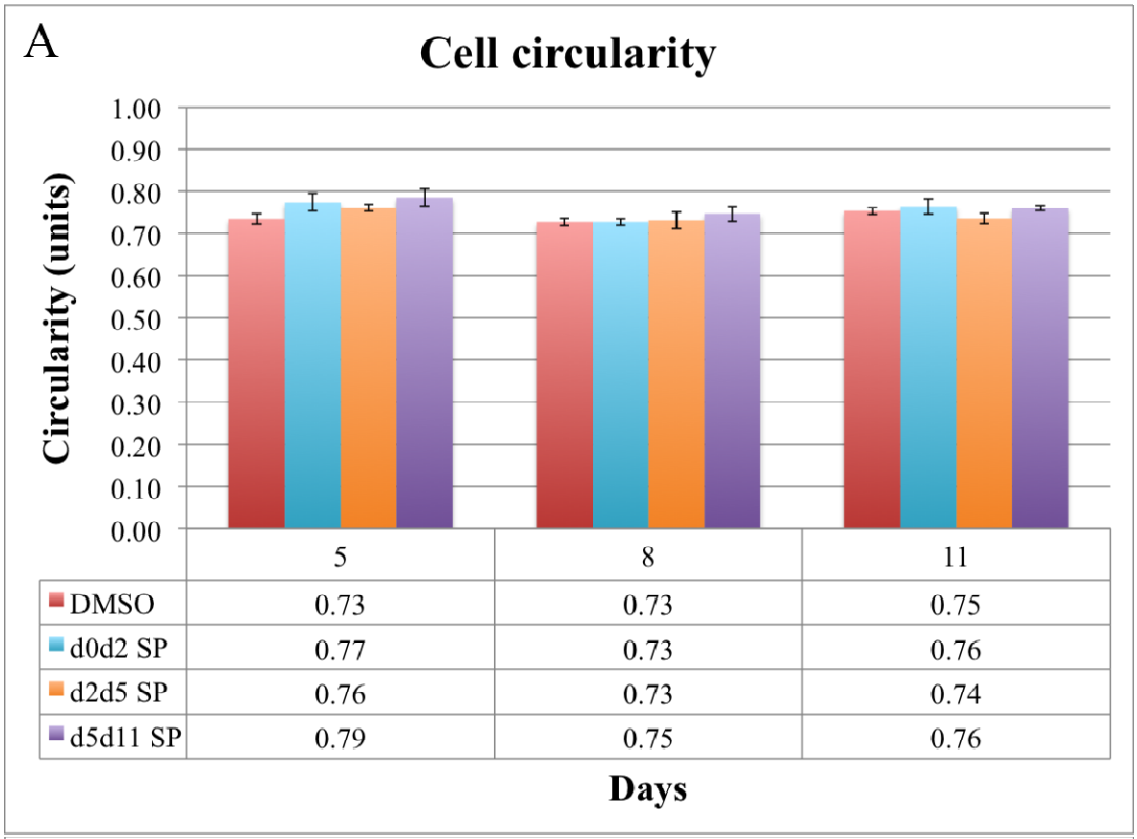

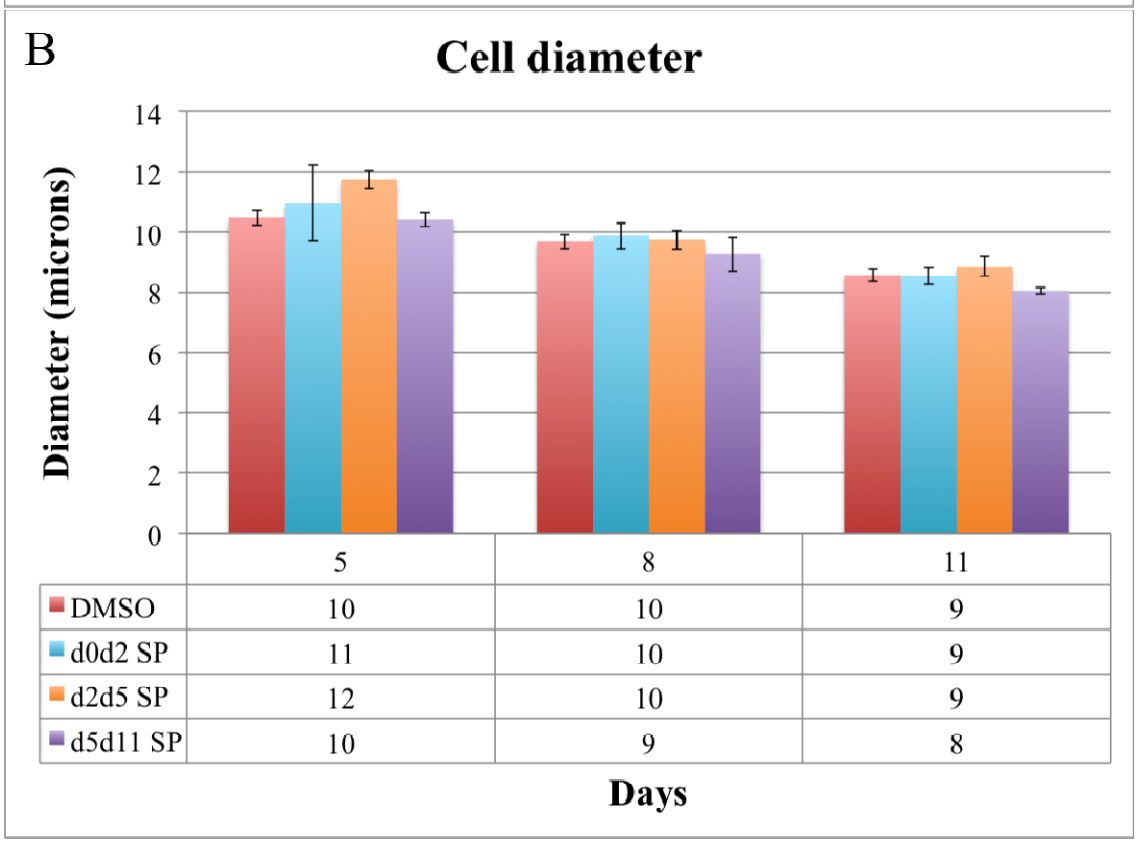

Figure 5. 15: Cell diameter and circularity at days 5, 8 and 11 after Jnk inhibition. Neither the size nor the shape of the cells was affected (p>0.06) at the time points examined by any of the SP600125 treatments (d0-d2, d2-d5 and d5-d11). The average diameter decreased over time in all groups from on average 11 μm at d5 to 9 μm at d11, while the average circularity transiently decreased from d5 (0.76 units) to d8 (0.74 units) and then increased again at d11 (0.75 units). These changes were observed in all groups. Statistical significance was assessed with one-way Anova testing.

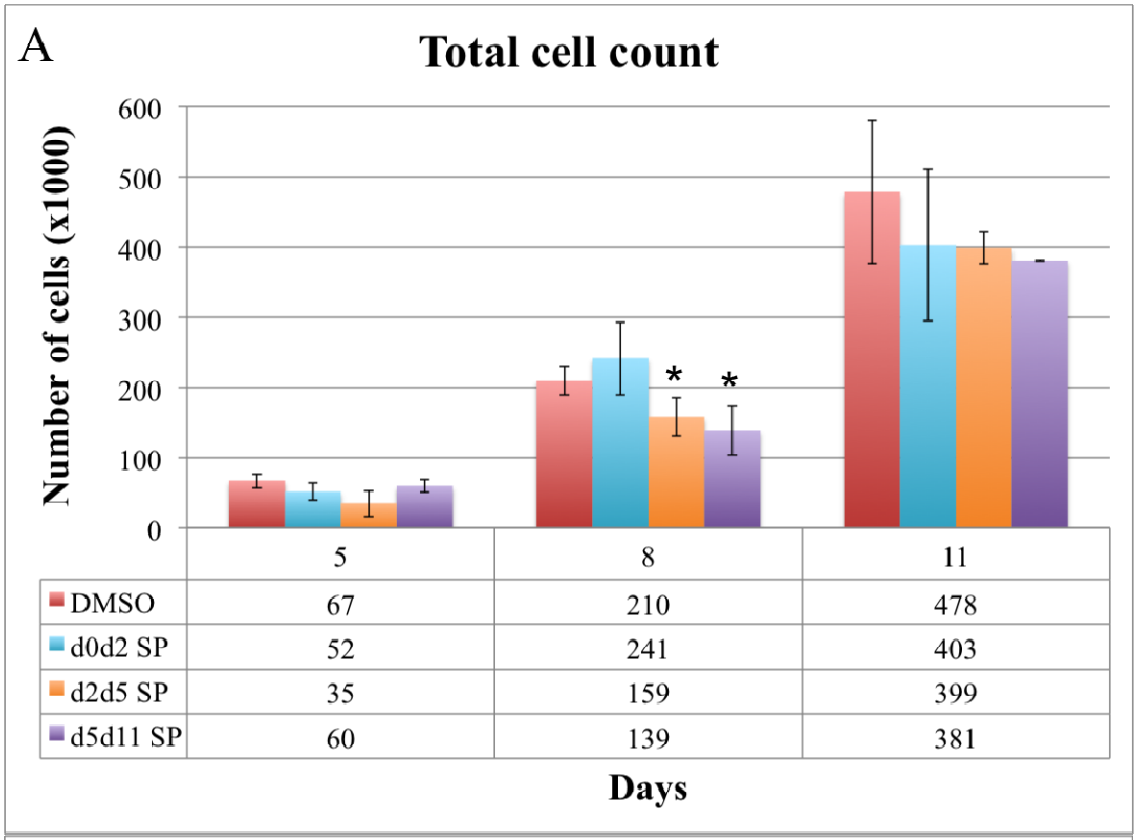

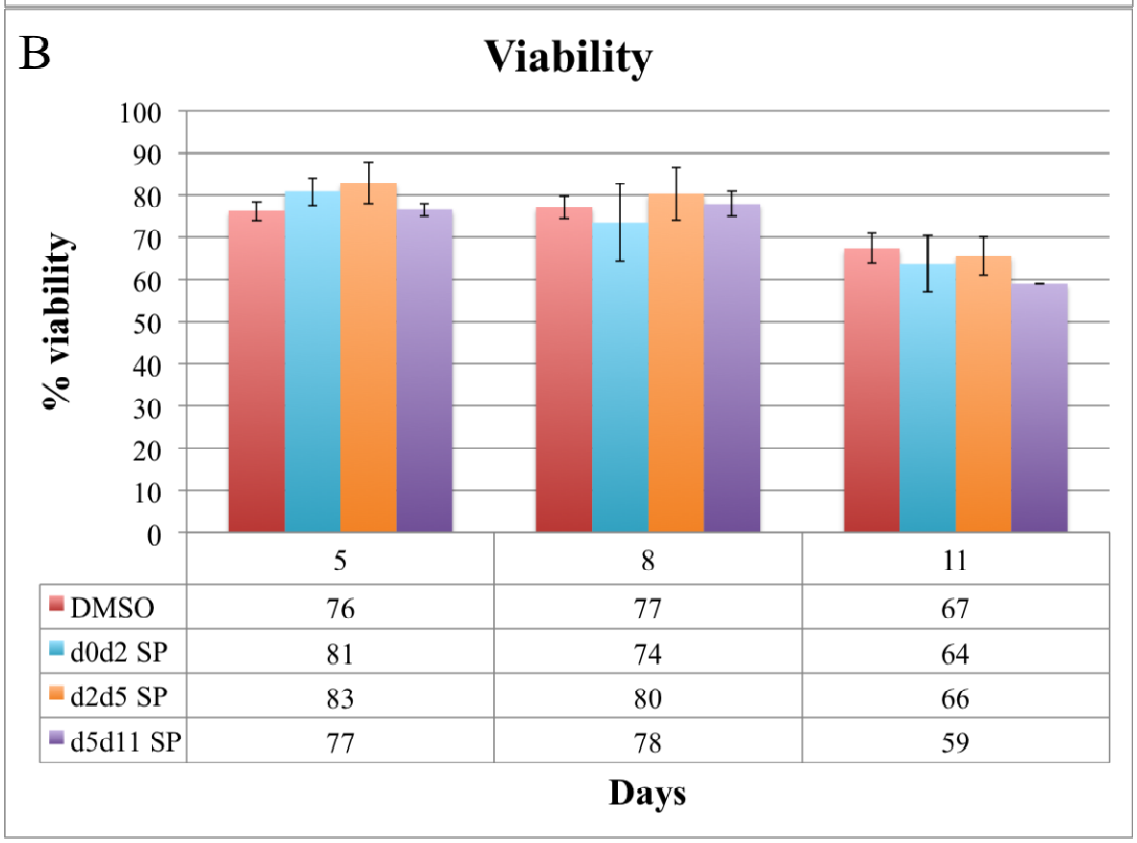

Figure 5. 16: Cell viability and total cell count at d5, d8 and d11 after Jnk inhibition. The viability of the cells was not significantly affected after any of the SP600125 treatments at any of the time points examined here, compared to DMSO (p>0.09). The total cell count, though, was significantly reduced at d8 after the d2-d5 and d5-d11 treatments compared to DMSO: p=0.02 and p=0.04, respectively, shown with the asterisks in (A). At d5 and d11 the differences were not significant. Statistical significance was assessed using one-way Anova, followed by a 2-sided Dunnet test, in SPSS.

The total number of cells in each EB was also counted at d5, d8 and d11. All experiments started with the same amount of cells (450 cells per hanging drop) so any difference in the number of cells that make up each EB will be due to different levels of proliferation and cell death. In the DMSO group the average number of cells per EB was 67449 cells (se=10158), 210208 (se=110409) and 478050 (se=101843) at days 5, 8 and 11, respectively. After 5 μM d0-d2 SP600125 treatment the amount of cells per EB was not significantly affected ($p>0.40$) compared to controls: 52402 cells (se=11745), 241421 (se=51608) and 402798 (se=107417) at days 5, 8 and 11, respectively (Figure 5.16).

Similarly, after 5 μM d2-d5 SP600125 treatment the number of cells was not significantly altered ($p>0.28$) at days 5 and 11, but it was significantly affected at d8 ($p=0.02$ compared to DMSO). The counts were 35210 (se=18287), 158556 (se=47253) and 398896 (se=23003) cells at days 5, 8 and 11, respectively. D5-d11 SP600125 treatment had a similar effect: at d8 there was a significant reduction in the overall number of cells between SP600125-treated and DMSO-treated EB ($p=0.04$), whereas the differences at d11 were insignificant. The actual numbers were: 139139 (se=35065) and 381083 (se=1382) cells at days 5, 8 and 11, respectively (Figure 5.16). The observed reduction in the total amount of cells at d8 is in keeping with the morphological observations, presented before, that showed smaller EB, probably consisting of fewer cells, after 5 μM SP600125 treatment compared to controls.

5.8. Quantitative PCR analysis: treatment with SP600125 caused considerable changes in the expression profiles of differentiating stem cells

The expression profile of SP600125-treated and DMSO-treated EB was also examined by quantitative PCR analysis at days 0, 5 and 11. Changes in gene expression reflect potential changes in the differentiation potential and status of the cells and were, therefore, considered essential in our assessment of the effect of Jnk during ES cell differentiation. The genes used here were described earlier (Sections 1.3.5, page 14 and 5.1.3, page 174): *Brachyury, CD31, Flk1, Hex, Mlc2v, Mlc2a, Gata-4, c-Myc, Cyclin-D2, Connexin-43, Jnk, Lef-1, Dkk-1*. Comparison of the expression profile of untreated and DMSO-treated EB was presented in Section 5.3.3 (page 185) and revealed the baseline expression of the genes of interest. Here the expression profiles of the genes of interest after SP600125 treatment (d0-d2, d2-d5 and d5-d11) are shown in comparison to DMSO alone. The mean values of three independent experiments are shown in the

graphs that follow. All reactions were performed in triplicates (for each biological repetition) and data were analysed manually using the ΔΔCt method (refer to Section 2.2.13.4, page 74, for details). Significance was assessed with one-way Anova test, followed when necessary by a 2-sided Dunnett test, as explained in detail in Section 2.6 (page 81).

Some of the lineage markers examined showed considerable changes in their expression levels after Jnk inhibition (Figure 5.17). At d5 expression of *Brachyury* was unaltered after d0-d2 SP600125 treatment and was 5 fold decreased (not statistically significant, p=0.06) after d2-d5 SP600125 treatment, while at d11, although some changes were observed, the expression levels were practically the same in all groups. The expression of *Flk1* at d5 was affected in a similar way to *Brachyury* (no statistical significance, p>0.06 for all groups compared to DMSO) but at d11 there was a 3 fold significant increase after d0-d2 treatment (p=0.046), while d2-d5 and d5-d11 SP600125 treatments caused a slight but not significant decrease in its expression. *Hex* and *CD31* expressions were not severely affected by SP600125 treatment: their levels after Jnk inhibition were similar to the DMSO levels, with only a slight, but not significant, decrease (2 fold) in *CD31* expression at d11 after d5-d11 SP600125 addition (Figure 5.17). These observations indicate that no major changes in the expression profiles of lineage markers were observed after SP600125 treatment. This means that inhibition of Jnk did not have adverse effects on the differentiation potential of ES cell towards mesodermal, endothelial and hematopoietic cell fates. However, significantly increased expression of *Flk1* at d11 after d0-d2 SP600125 treatment indicates an increase in endothelial and/or hematopoietic cells.

Interestingly, the levels of *Mlc2a* were unaltered at d5 after all SP600125 treatments compared to DMSO, but were downregulated at d11 (3, 8 and 8 fold decrease after d0-d2, d2-d5 and d5-d11 treatments, respectively), as shown in Figure 5.18. The respective significance values (p) at d11 compared to DMSO were: 0.386, 0.046 and 0.029, showing that only the two latter groups were significantly altered. *MLc2v* was affected in the opposite way but not to a significant extent (p>0.05 at all time points and for all treatments): at d5 its levels were unaffected but at d11 they were increased (2 and 2.5 fold after d0-d2 and d5-d11 treatments, respectively) or remained unchanged (no change after d2-d5 treatment). *Gata-4* remained unchanged at d5 but was upregulated at d11 after d0-d2 and d2-d5 treatments (4 and 3 fold with p=0.029 and p=0.038, respectively) and remained unaltered after d5-d11 treatment (Figure 5.18).

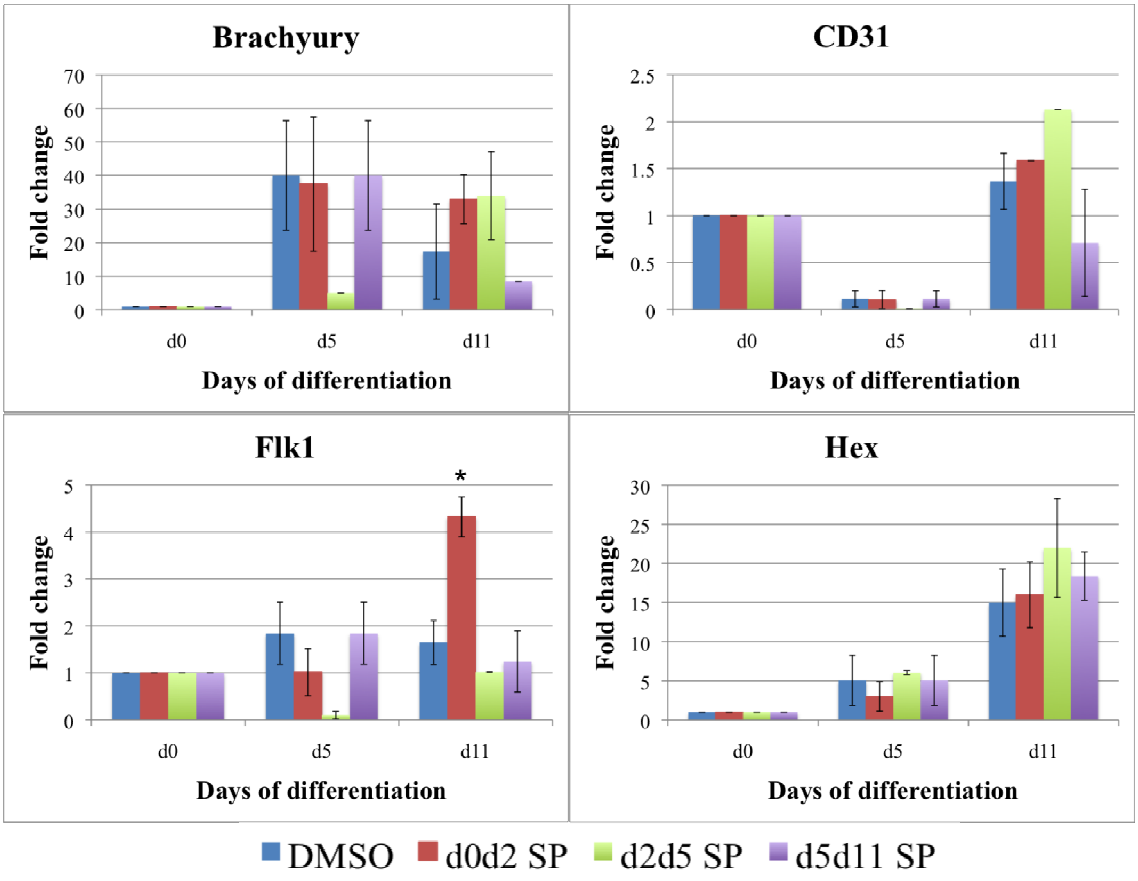

Figure 5. 17: qPCR analysis of lineage markers after SP600125 treatment. Expression of *Brachyury, CD31, Flk1* and *Hex* was examined at days 0, 5 and 11 after d0-d2, d2-d5 and d5-d11 SP600125 treatments. Changes in the expression levels were observed in mesodermal and endothelial genes. All genes were normalized against two housekeeping genes (*ß-actin* and *Rps9*) and compared to d0 values (set as the calibrator, equal to 1). Relative quantities expressed as fold changes are shown in the graphs. Mean values of three independent experiments are represented in the graphs, with error bars showing standard error of the mean. Statistical significance was assessed using one-way Anova testing, followed, when necessary by a 2-sided Dunnett test.

The fact that the cardiac genes examined here (Figure 5.18) were not altered at d5 indicates that no major differences in the specification of ES cell-derived cardiomyocytes were observed. Increased expression of *Gata-4* at d11 is likely to represent not only cardiac-specific, but possibly cardiac-unrelated events as well, as *Gata-4* is not uniquely expressed in cardiac cells, especially later in differentiation (Burch, 2005, Molkentin et al., 2000, Patient and McGhee, 2002, refer to Section 1.3.5.2, page 16, for more details). Decreased *Mlc2a* expression at d11 after d0-d2 and d2-d5 SP600125 treatment suggests a specific loss of atrial cells.

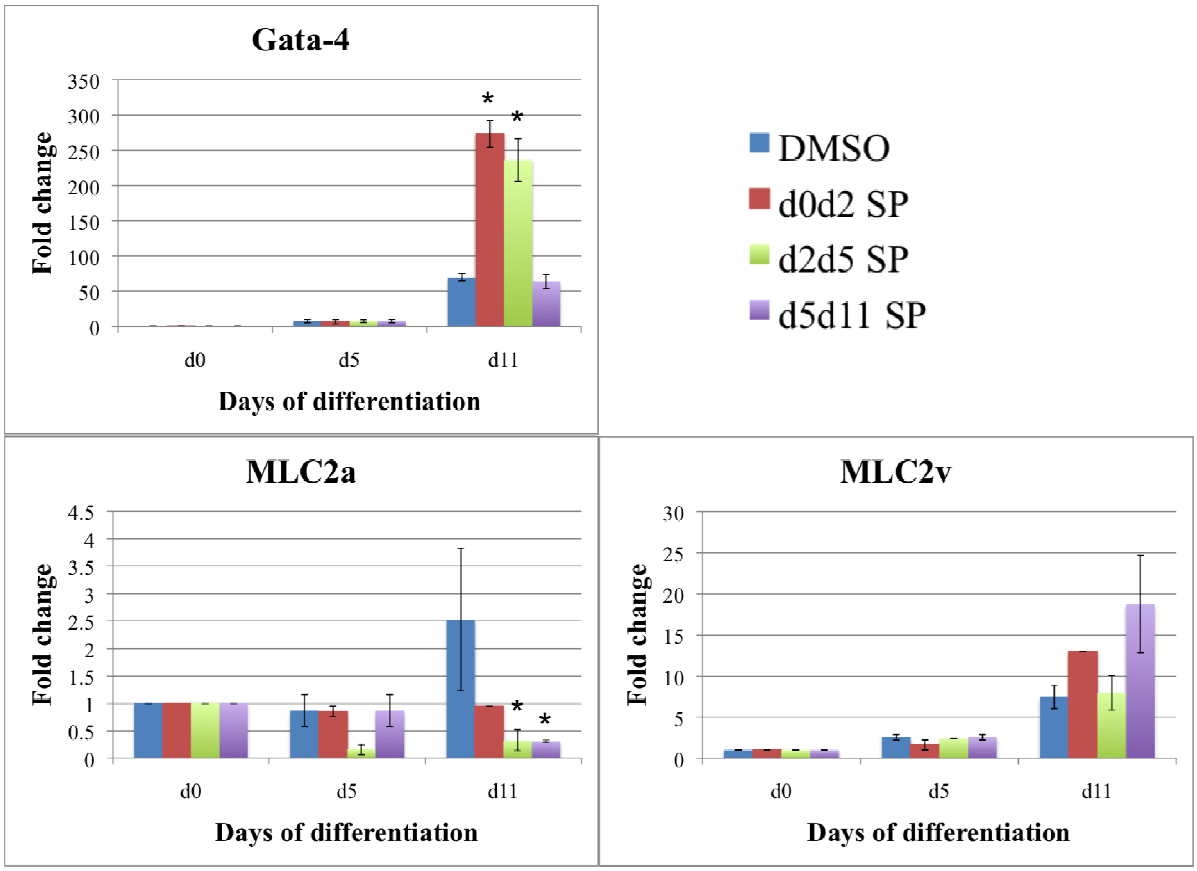

Figure 5. 18: qPCR analysis of cardiac markers after SP600125 treatment. Expression of *Mlc2a, Mlc2v* and *Gata-4* was examined at days 0, 5 and 11 after d0-d2, d2-d5 and d5-d11 treatments. Changes in the expression levels were observed in *Gata-4* and *Mlc2a*. All genes were normalized against two housekeeping genes (*β-actin* and *Rps9*) and compared to d0 values (set as the calibrator, equal to 1). Relative quantities expressed as fold changes are shown in the graphs. Mean values of three independent experiments are represented in the graphs, with error bars showing standard error of the mean. Statistical significance was assessed using one-way Anova testing, followed, when necessary by a 2-sided Dunnett test.

Some but not all of the other markers examined (proliferation, Wnt targets, Connexin-43), also showed considerable changes after Jnk inhibition (Figure 5.19). Expression of *c-Myc* was significantly 2.5 fold decreased at d5 after d0-d2 (p=0.046 compared to DMSO) and d2-d5 (p=0.046 compared to DMSO) SP600125 treatments but was not significantly altered, although slightly different, at d11 after all treatments (p>0.05). In contrast, *Cyclin-D2* was unchanged at d5 after d0-d2 treatment but significantly decreased after d2-d5 treatment (p=0.046). At d11 it was 4 fold decreased after d2-d5 SP600125 treatment (statistically significant, with p=0.027). D0-d2 and d5-d11 SP600125 treatments did not alter its expression at d11. A decrease in the expression levels of c-Myc and Cyclin-D2 indicate a decrease in the proliferation rate of the cells, as they are both involved in progression of the cell cycle (Brenner et al., 2005, Grandori et al., 2000, Satyanarayana and Kaldis, 2009) (see Section 5.1.3, page 174).

Cx-43 expression was significantly downregulated at d5 after d0-d2 and d2-d5 SP600125 reatments (20 fold, p=0.029) but was not significantly different at d11 after d2-d5 (2 fold decrease compared to DMSO) and d5-d11 (2 fold reduction compared to DMSO) SP600125 treatments (Figure 5.19). It was, however, significantly reduced at d11 after d0-d2 SP600125 treatment (3 fold decrease compared to DMSO, p=0.046). Cx-43 is a marker of cellular gap junctions. The decrease in its expression levels after SP600125 treatment, if translated into decreased protein production and activity of the protein, could adversely affect the formation and effectiveness of gap junctions and thus, decrease the communication between the cells.

Surprisingly, expression of *Jnk* was reduced at d5 (20 fold decrease after d0-d2 and d2-d5 SP600125 treatments, p=0.039) (Figure 5.19). At d11 its expression was significantly 4 fold increased after d0-d2 SP600125 treatment (p=0.046), unaltered after d2-d5 SP600125 treatment and slightly decreased (2 fold) after d5-d11 treatment (p=0.137). These are surprising findings as SP600125 has not been shown to have direct effects on the transcription of *Jnk*, but rather only affects the activation and activity status of the protein (Bennett et al., 2001).

Lef-1 showed decreased, but not to a significant extent, expression levels at d5 after d0-d2 and d2-d5 SP600125 treatments (3 and 2 fold decrease, p>0.05). At d11 its expression was significantly 2 fold higher (p=0.029), unaltered (p=0.230) and significantly 4 fold lower (p=0.046) than DMSO after d0-d2, d2-d5 and d5-d11 SP600125 treatments, respectively (Figure 5.19). *Lef-1* was shown to be upregulated after DMSO treatment alone (refer to Section 5.3.3, page 185 and Figure 5.6, page 188) at d11, so its increased expression levels after d0-d2 SP600125 at d11 could be mainly due to the effect of DMSO. In contrast, decreased expression levels at d11 after d5-d11 SP600125 treatment indicate a severe reduction in canonical Wnt signalling.

Dkk-1 expression, although not affected by Jnk inhibition at d5 and d11 after d0-d2 and d2-5 treatments, was significantly 5 fold higher (p=0.037) at d11 compared to DMSO after d5-d11 SP600125 treatment (Figure 5.19). Dkk-1 is an inhibitor of the canonical Wnt pathway (Bafico et al., 2001, Kawano and Kypta, 2003, Mao et al., 2001) and therefore, it is likely that its increased expression at d11 after d5-d11 treatment will adversely affect signalling through the canonical Wnt cascade.

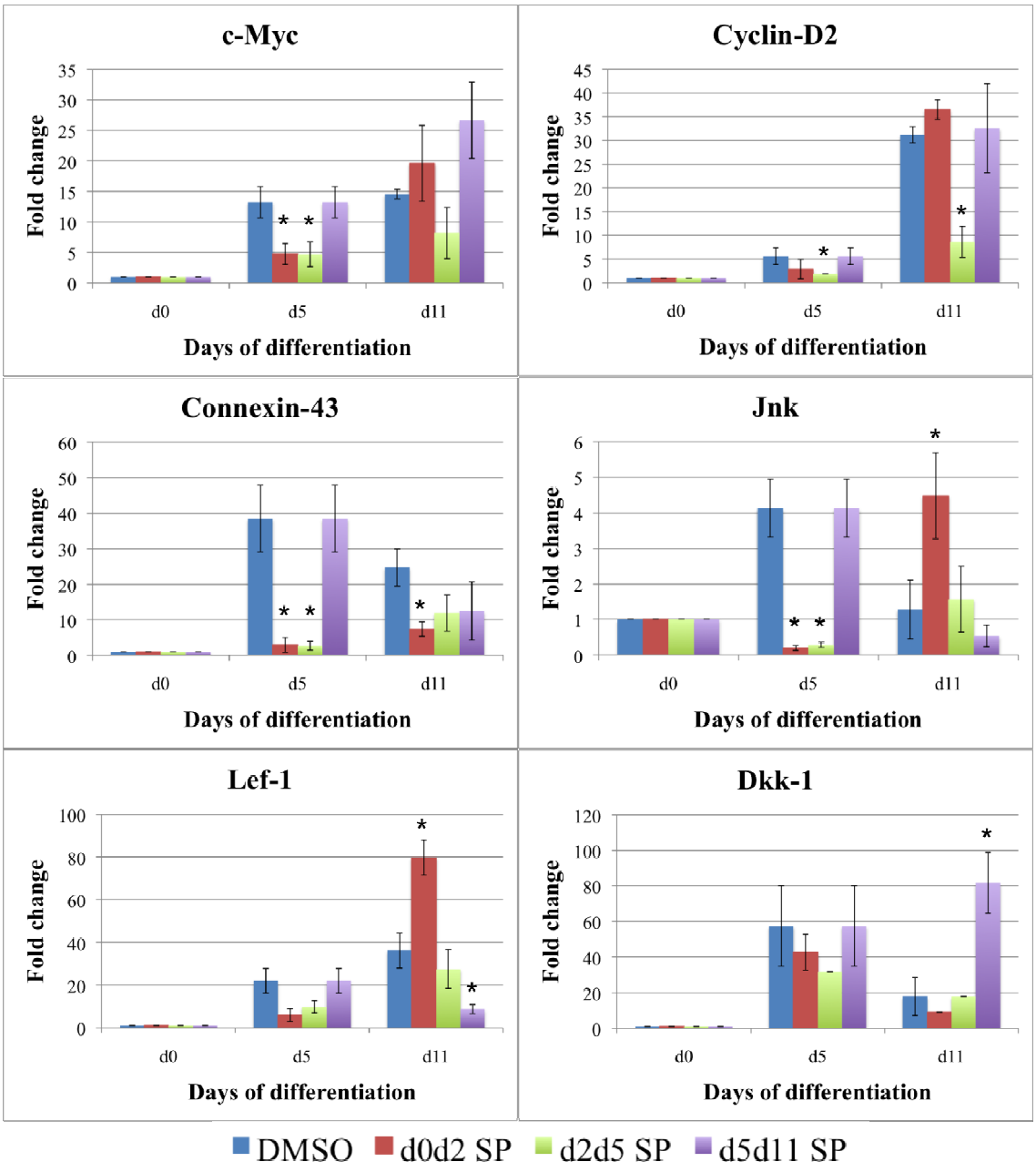

Figure 5. 19: qPCR analysis of downstream Wnt targets, proliferation markers and other genes after SP600125 treatment. Expression of *c-Myc, Cyclin-D2, Cx-43, Jnk, Lef-1* and *Dkk-1* was examined at days 0, 5 and 11 after d0-d2, d2-d5 and d5-d11 treatments. Changes in the expression levels were observed in genes examined here. All genes were normalized against two housekeeping genes (*ß-actin* and *Rps9*) and compared to d0 values (set as the calibrator, equal to 1). Relative quantities expressed as fold changes are shown in the graphs. Mean values of three independent experiments are represented in the graphs, with error bars showing standard error of the mean. Statistical significance was assessed using one-way Anova testing, followed, when necessary by a 2-sided Dunnett test.

5.9. Organization of beating clusters within treated and untreated EB

The examination of the gene expression profile of differentiating EB before and after SP600125 administration was revealing about how Jnk could be involved in the process. However, the morphology of the beating clusters within the EB was also of interest, in order to elucidate how the beating cells are organized and arranged within the EB. Cardiac TroponinI (cTnI) is present in beating cells and is commonly used as a marker of differentiated cardiomyocytes, as described before (Kattman et al., 2011). So, by staining d11 EB grown under different conditions with an anti-cTnI antibody it was possible to visualize beating foci. EB were grown on gelatin-coated glass coverslips and only the beating ones were selected for antibody staining. The images shown in Figure 5.20 are representative images of EB from three independent experiments. Untreated EB, along with DMSO-treated EB, are also shown here (Figure 5.20) in order to emphasize the reproducibility of the phenotype before SP600125 treatment.

As expected, the negative control (probed only with secondary antibody) showed no staining under identical experimental conditions and light exposure. cTnI-positive cells were scattered throughout the EB in untreated and DMSO-treated EB, as shown by the green staining in Figure 5.20. A noticeable difference was observed in the SP600125-treated EB. Although the overall area covered by the staining did not seem to be significantly altered, the pattern of organization of the positive cells was intriguingly different: there were patches of tightly packed cTnI-positive cells in the d2-d5 and d5-d11 SP600125-treated EB, a conformation not seen in the control EB. The pattern of organization of d0-d2 SP600125-treated cells, although not identical to controls, was however not as distinct as in the other SP600125 treatment groups.

Although counting the overall number of cTnI-positive cells would give us useful insight into whether Jnk inhbition also affects the number of beating cells (technique currently being optimised in the lab), the way these cells are organized in beating clusters is also important, as shown here. The fact that enhanced beating, observed after Jnk inhibition (d2-d5 and d5-d11 SP600125 treatments), could be related to the organization of beating cells and not to their cardiogenic potential is intriguing, as will be discussed in the next section.

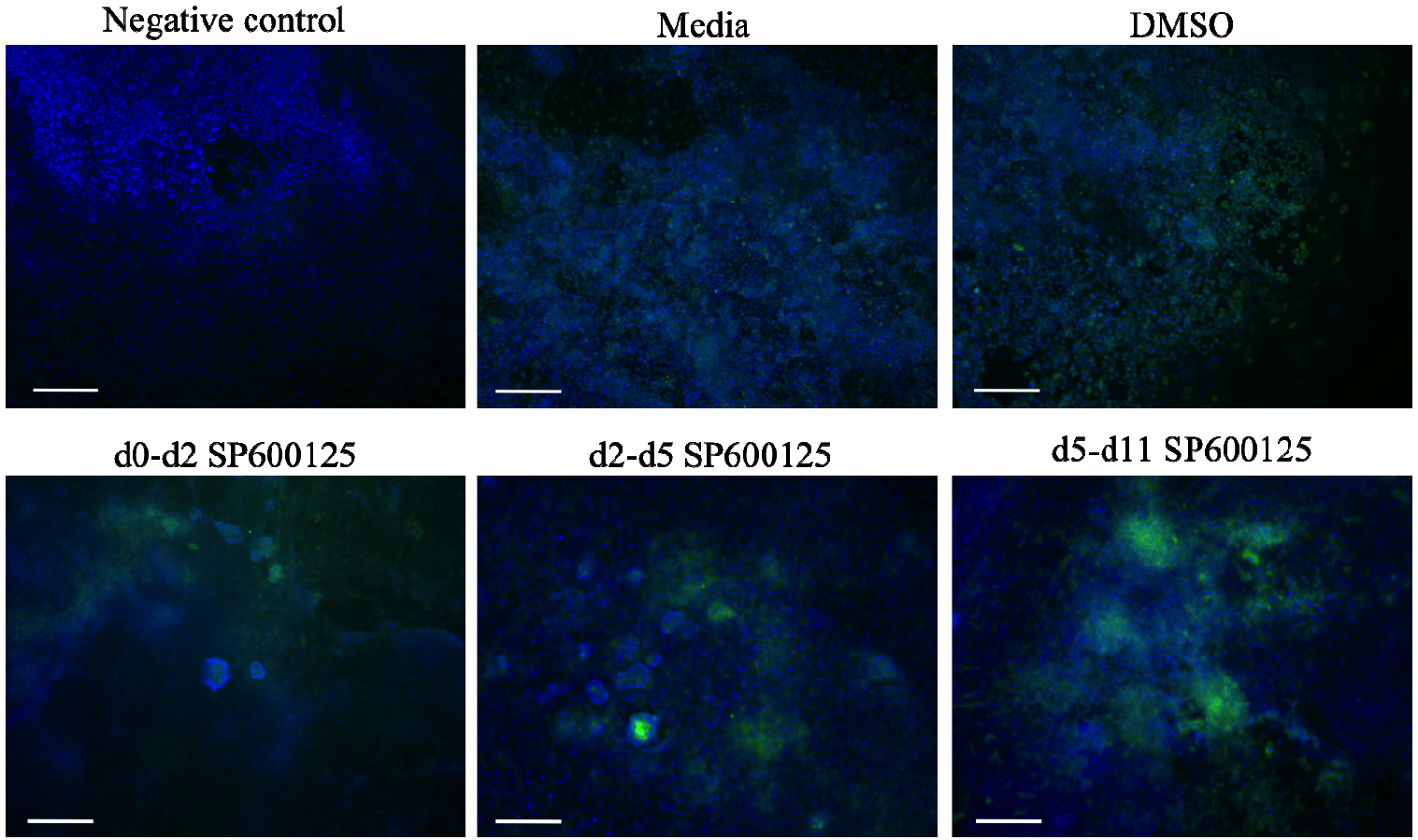

Figure 5. 20: Cardiac TroponinI (cTnI) antibody staining on whole EB grown on glass coverslips. Blue shows nuclear DAPI staining, while green shows cytoplasmic cTnI staining. The negative control showed no staining in the absence of primary antibody. Untreated and DMSO-treated EB showered scattered cTnI staining, intermingled with cells without staining. SP600125-treated EB revealed a more organized pattern of cTnI positive cells: they were shown to be grouped in clusters, possibly corresponding to beating foci. This organization was more apparent in the d2-d5 and d5-d11 SP600125 treatment groups. Scale bars represent 200 µm.

5.10. Discussion

JNK, as a downstream effector of the non-canonical Wnt pathway and a member of the MAPK family, has been recognised as an important player in many cellular and physiological processes. In this chapter, the role of Jnk during *in vitro* ES cell-derived cardiogenesis was investigated.

In summary, treatment with SP600125, a specific inhibitor of Jnk1, Jnk2 and Jnk3, caused a considerable increase in the beating ability of EB in a time-specific manner. Jnk inhibition between days 0 and 2 did not affect cardiogenesis, but all later SP600125 treatments (d2-d5 and d5-d11) increased the occurrence of spontaneous contraction. However, the cardiac genes that were examined did not show significant changes after SP600125 treatment, suggesting that specification of cardiac progenitors took place normally. It was initially thought that alterations in the levels of Connexin-43, a downstream target of Jnk (Petrich et al., 2002), could be a defining factor. Inhibition of Cx-43 (at both transcriptional and translational/post-translational level) caused by activation of Jnk has been shown before to impair cell-cell communication via gap junctions (Petrich et al., 2002). Therefore, it would be possible that inhibition of Jnk in this study may cause an upregulation in Cx-43 levels, which would then allow for the formation of more gap junctions. This, in turn, could have positive effects on the communication and propagation of signals between cells, which in cardiac cells could be manifested with more and better coordinated beating. Nevertheless, a decrease, instead of an increase, in the expression levels of Cx-43 was observed after inactivation of Jnk, a finding that does not support the proposed hypothesis. The question, however, about how inhibition of Jnk may have affected post-translational modifications of this protein, as shown in previous studies (Cameron et al., 2003, Petrich et al., 2002, Solan and Lampe, 2008), remains unanswered.

On a similar note, cardiac Troponin I (cTnI) antibody staining on treated EB revealed a clear change in the organization of beating areas, rather than an obvious alteration in the overall number of beating cells (cTnI-positive, which were not, however, counted), compared to control EB. Beating cells were organized in clusters in a much more packed conformation after SP600125 treatment compared to untreated and DMSO-treated EB. This was highly reproducible in the three experiments performed in the current study. An additional important observation was also made: d0-d2 SP600125-treated EB did not show such a marked change in the organization of beating clusters as the d2-d5 and d5-d11 SP600125-treated EB. This is intriguing since d0-d2 treated EB

did not exhibit as profound differences in their beating behaviour as did d2-d5 and d5-d11 SP00125-treated EB. Although more work is required in order to definitely conclude that a conformational change in the arrangement of beating cells rather than a change in the specification of cardiac cells explains the differences in the beating behaviour of the cells, it remains a fascinating hypothesis.

Interestingly, a significant loss of atrial-marker gene expression was observed in EB after d2-d5 and d5-d11 SP600125 treatment. This decrease was not accompanied by a concomitant increase in ventricular-marker gene expression. It would be interesting to count atrial and ventricular cells accurately in order to investigate whether the observed differences in the gene expression profiles of *Mlc2a* and *Mlc2v* recapitulate changes in the specification status of the treated cells. Also, given that *Mlc2a* and *Mlc2v* are not chamber-specific at all times (see Section 1.3.4, page 13) (Bruneau et al., 2000, Christoffels et al., 2000, Kubalak et al., 1994, O'Brien et al., 1993, Small and Krieg, 2004), the expression levels of these genes in differentiating ES cells are not directly correlated with specification towards one of the two lineages.

An additional interesting finding was the observation that SP600125-treated EB (5μM) were smaller than their control counterparts at d5 of differentiation. This observation was, however, not associated with decreased cell diameter (an indication of decreased cell size) or decreased cell count within the treated EB. In fact, only a transient decrease in the number of cells within treated EB was observed at d8. Therefore, the fact that EB appeared smaller but did not contain smaller or less cells after Jnk inhibition suggests either that cells are more tightly packed within treated EB or that the cavity, which occupies the centre of the EB at d5 (Hernandez-Garcia et al., 2008), is not properly formed when Jnk is inhibited. Defects in the formation of the central cavity in EB have been associated in the past with anomalous differentiation (Hernandez-Garcia et al., 2008), but not with increased beating or upregulation of cardiogenesis. Also, there is no evidence in the literature to suggest that abnormal cavitation preferentially affects the differentiation of one lineage over others; for example, it could affect endoderm that is essential for cardiac differentiation or neuronal development that is inhibitory for cardiogenesis *in vitro*. Therefore, whether increased beating is associated with the different size of treated EB remains to be elucidated. Of note, Jnk deficiency ($Jnk1^{-/-}$;$Jnk2^{-/-}$ cells) has been associated with defective EB cavitation and growth (Xu and Davis, 2010).

The complex interplay between canonical and non-canonical Wnt pathways and the importance of integrative approaches that include the whole network and not

individual pathways have been discussed before (Section 1.4.4, page 35). Thus, possible alterations in the canonical Wnt pathway caused by Jnk inhibition were also examined. Specifically, the expression levels of *Dkk-1* and *Lef-1* were analysed. *Dkk-1* is an inhibitor of the canonical Wnt pathway (Bafico et al., 2001, Kawano and Kypta, 2003, Mao et al., 2001) but also a downstream target of β-catenin (Gonzalez-Sancho et al., 2005) and c-Jun (Grotewold and Ruther, 2002). The latter protein is a transcription factor, firstly identified as an important and direct target of Jnk (Derijard et al., 1994). *Dkk-1* was found to be significantly upregulated at d11 after d5-d11 SP600125 treatment in this study. *Lef-1* is a downstream target of β-catenin and an effector of the canonical Wnt pathway (Barolo, 2006) and was found to be significantly upregulated after d0-d2 SP600125 treatment and significantly downregulated after d5-d11 treatment. The observed increase after the d0-d2 SP600125 treatment could be due to the presence of DMSO and not to the drug, as it was shown that DMSO alone also caused a significant upregulation in the expression levels of *Lef-1* at d11, compared to its levels without any treatment. Activation of the canonical Wnt pathway by either DMSO or SP600125, shown by increased *Lef-1* transcription after d0-d2 SP600125 treatment, could have severe effects on the beating ability of differentiating cells, as will be discussed in Chapter 6 in detail (activation of the canonical Wnt pathway was shown to severely suppress the beating ability of EB). The observed downregulation of *Lef-1* (downstream effector of the canonical Wnt pathway) at d11 after d5-d11 SP600125 treatment did not come as a surprise since levels of *Dkk-1* (inhibitor of canonical Wnt signalling) were increased after d5-d11 SP600125 treatment and thus, canonical Wnt signalling was expected to be inhibited. The cross talk between the different Wnt pathways is crucial and needs to be taken into account, since, as described in Section 1.4.4 (page 35), they work as a network and not independently.

Downstream targets of Jnk, which are also associated with the canonical Wnt pathway and with regulation of proliferation, were concomitantly assessed. The expression of *c-Myc* was decreased at d5 after d0-d2 and d2-d5 SP600125 treatment but remained unaffected at d11 after all treatments. In contrast, *Cyclin-D2* expression levels were significantly downregulated at d5 and d11 after d2-d5 SP600125 treatment. These proteins are common markers of proliferation; they participate in cell cycle progression in response to mitogenic signals and their inhibition has been associated with decreased cell turnover (Brenner et al., 2005, Grandori et al., 2000, Satyanarayana and Kaldis, 2009). Mitogenic signals, such as MAPK (Armstrong et al., 2006) and Wnt (He et al., 1998, Myant and Sansom, 2011, Sansom et al., 2007, You et al., 2002), are able to

activate c-Myc. In turn, c-Myc has been shown to activate the highly labile protein Cyclin-D2 and to suppress inhibitors of the canonical Wnt pathway, like Dkk-1 (Cowling and Cole, 2007, Cowling et al., 2007). Decreased levels of *c-Myc* at d5 were associated with significantly increased expression of *Lef-1* at d11 (after d0-d2 SP600125 treatment), showing a potential effect on the canonical Wnt pathway (Arce et al., 2006, Barolo, 2006). Inhibition of c-Myc and Cyclin-D2, especially after the d2-d5 SP600125 treatment, possibly reflects decreased levels of proliferation at d5. Although the total number of cells in each SP600125-treated EB was not altered at d5, it was significantly, albeit transiently, decreased at d8. It is, therefore, possible that decreased activity of c-Myc and Cyclin-D2 at d5 caused a transient halt of cell proliferation in treated EB between days 5 and 8, which in turn reduced the total number of cells that each SP600125-treated EB contained at d8. Removal of the drug allowed for the expression levels of c-Myc and Cyclin-D2 to recover and for cell cycle progression to be restored; hence the normal cell count in treated EB at d11.

Jnk is part of the non-canonical Wnt pathway and as such it might be expected to enhance cardiogenesis, as discussed in Section 1.4.2.2 at page 33 (Garriock et al., 2005, Pandur et al., 2002, Terami et al., 2004). Therefore, its reduction after inhibition by SP600125 would be expected to deplete cardiogenesis or to downregulate it to some extent. However, data obtained from the present study showed the exact opposite: inhibition of Jnk after d2 of differentiation enhances the beating capacity of cells. It is not clear whether this observation is necessarily associated with increased cardiac differentiation, as discussed earlier in this section, but it is still contradictory to the expected effect after depletion of the non-canonical Wnt pathway. Previous work (MSc dissertation) on differentiating E14 stem cells (shown in the appendix) showed that inhibition of the non-canonical components Rac (NSC23766 drug, n=5) and ROCK (Y17632 drug, n=4) had similar effects on the beating behaviour of cells: early inhibition (between days 0 and 5) had no effect on beating, whereas late inhibition (between days 5 and 11) significantly increased the occurrence of beating. These findings, although performed on a different cell line (E14 instead of ES-D3), are indicative of a common mechanism or pathway for the observed changes in beating. It is, however, noteworthy that the data are not identical between Jnk and Rac/ROCK inhibition. SP600125 (Jnk) treatment between days 2 and 5 caused an upregulation in the occurrence of beating, while NSC23766 (Rac) and Y27632 (ROCK) treatments did not. This discrepancy suggests that Jnk may have additional roles during the differentiation process, independent of the Wnt pathway. The fact that Jnk is also

activated by the MAPK cascade and is highly involved in regulating and responding to stress (Xie et al., 2006, Zhong et al., 2007, Zhong and Kyriakis, 2007), may partly explain the additional effects that Jnk inhibition is causing during ES cell differentiation. In effect, the stress levels of different systems, which determine to some extent the phosphorylation and, therefore, activation status of Jnk and other stress-activated protein kinases, have been shown to markedly affect the differentiation process (Zhong et al., 2007). Although it is not possible to measure the stress levels of the system used here, it is important to take into account that differentiation is a stressful condition for the cells and activation of Jnk may be an important protection mechanism.

An evident observation from the data presented in the current chapter is that the canonical and non-canonical Wnt pathways may overlap, interact and antagonize each other more than previously thought. This study highlights the importance of investigating the Wnt network as a whole and not individually. The following chapter deals with the effect of the activation of the canonical Wnt pathway in ES cell differentiation and cardiogenesis and underpins the aforementioned concept. Also, additional roles for Jnk, potentially independent of Wnt, were unravelled. Although with the current tools it is not possible to definitely distinguish between Wnt-related and Wnt-independent effects of Jnk, it appears likely that both paths are involved.

5.11. Advantages and disadvantages of the study

Some features of this study make it reliable, powerful and comprehensive and it is important to emphasize them. Firstly, the confirmation of successful downregulation of the target protein was essential. The levels of phospho-Jnk (Jnk1, Jnk2 and Jnk3) were markedly reduced after SP600125 treatment, indicating that the activity of the kinase was severely compromised. The broad range of downstream targets of phospho-Jnk and the multitude of other signalling pathways that activate the same targets, did not allow for further confirmation of inhibition of the activity of Jnk. The efficacy and specificity of the drug have been discussed before (Sections 4.1.1, page 132 and 4.5, page 166). Of note, the specificity of the drug has not been tested in this study (by looking at how SP600125 affects the activation status of other related kinases) and is essential to take it into account.

Secondly, the assay itself provided a reliable framework for the studies performed here. Differentiation of ES cells into EB using the hanging drop method has been shown

to be highly reliable, reproducible and uniform (Dang et al., 2002, Kurosawa, 2007), compared to other methods, such as spontaneous aggregation of cells in low-adherens plates (Ng et al., 2005) or in suspension culture in semi-solid methylcellulose media (Kurosawa, 2007, Kurosawa et al., 2003) The controlled aggregation of an experimentally predetermined number of ES cells (450 cells here) in hanging drops allows for the formation of homogeneous and comparable EB and reduces variability within individual EB and between different batches (experiments) of EB. Formation of EB with the hanging drop method has been used to generate a broad spectrum of cell lineages, including cardiomyocytes (Metzger et al., 1994, Takahashi et al., 2003, Wobus et al., 1991), neurons (He et al., 2006), haematopoietic cells (Dang et al., 2002) and smooth muscle cells (Drab et al., 1997, Yamada et al., 2002). The disadvantages of this method are mainly practical: setting cells in hanging drops is time-consuming, while media exchange and direct microscopic observation, when cells are in hanging drops, are difficult or even impossible (Kurosawa, 2007).

The detailed and thorough deconstruction of the differentiation assay into shorter intervals, during which inhibition of Jnk was examined, boosted the efficiency and comprehensibility of the data obtained. The reproducibility of the findings was also an important positive aspect of the assay; even if the actual numbers were different, the pattern was similar in all experiments performed. An additional confirmation of the validity of the obtained data came from the verification that inhibition of Jnk had similar effects on a different cell line. The variability in the new cell line (E14) was greater than in the old one (ES-D3) but the trend was the same.

Additionally, thorough statistical analysis was performed, using the appropriate parametric or non-parametric tests in each occasion, without making assumptions that could not be supported by the available data. This is an essential aspect of biological data analysis, as variation, both experimental and biological, can significantly mislead interpretation of the results.

Nevertheless, some assets of the assay could be altered and improved. One of them is the inclusion of FCS in the culturing media. I showed that serum starvation after d5 was not beneficial for the growth and differentiation of ES-D3 cells. Specifically, a severe reduction in the beating ability and the adhesive and spreading properties of EB was observed after serum removal. Although enhancement of cardiogenesis has been observed after serum withdrawal in some studies in the past (Gissel et al., 2006, Goldman and Wurzel, 1992, Sachinidis et al., 2003), serum is generally considered an essential additive to ES cell culture and its removal is usually accompanied by

substitution with chemically defined serum replacement factors (Sachinidis et al., 2003). Even in the presence of SP600125, the absence of serum was sufficient to deter differentiation. BMP4 is commonly thought to be an essential component of serum (ten Berge et al., 2008), in the absence of which differentiation in general and cardiogenesis particularly cannot proceed. In the current study the absence of serum and the lack of use of serum replacement factors did not allow for proper stem cell differentiation. This forced us to include serum in all subsequent studies on this cell line, which may hinder some aspects of the differentiation process.

The second aspect of the assay that could be improved is associated with accurate counting of cardiomyocytes. Although measurements about the expression levels of cardiac genes are useful in understanding how the process of cardiogenesis is affected by treatment with SP600125, the exact number of cardiomyocytes that are produced in the absence and presence of the drug would be a valuable addition to our understanding of the system. A reliable way to achieve this would be via the establishment of a reporter system that marks cardiomyocytes *in vitro*. For example a reporter, such as GFP, driven by the promoter of a cardiac gene, like *cardiac Toponin I* (*cTnI*), could be used as a marker of cardiomyocytes, which could then be analysed and measured using fluorescence-activated cell sorting (FACS). An alternative approach that involves fluorescence staining of unlabelled differentiated cells with an anti-cTnI antibody, followed by FACS, is under optimisation in the laboratory and has been used in the past for similar analyses (Kattman et al., 2011b, Kattman et al., 2011a). The latter technique avoids time consuming transfections and laborious establishment of transfected cell lines.

Additionally, an altogether different approach could have been employed in order to establish the role of Jnk signalling in differentiating ES cells. $Jnk^{-/-}$ ES cells, isolated from genetically modified mouse blastocysts could have been used. With this approach the use of a chemical inhibitor would have been avoided and the specificity problems associated with it would have been overcome. However, three main drawbacks are correlated with this method. The first one is the need for establishment of a genetically modified mouse strain ($Jnk^{-/-}$), which is both time-consuming and expensive. The second is associated with the existence of more than one *Jnk* genes. In fact, there are three *Jnk* genes in mouse, all of which would have to be genetically inactivated in order to avoid redundancy between them. This would require more time-consuming mouse crosses and expensive maintenance of additional mouse colonies. Thirdly, investigation

of time-specific roles of Jnk could not be conducted since Jnk would be genetically and irreversibly inactivated.

Finally, although analysis of mRNA levels of the genes of interest is an essential component of unravelling the effect of the drug, especially since most of the targets of the protein that is being inhibited are transcription factors, mRNA levels are not always directly associated with protein levels and even more so with the levels of active protein. Therefore, more protein analysis could be employed in similar studies in the future. This, however, entails disadvantages itself, with the most important one being the high cost of antibodies, whereas qPCR analysis is a fairly inexpensive technique. Also, as mentioned before, it is not just the presence of the protein that is important to be detected, but the presence of the active form of the protein. This, in some cases, may depend on complex post-translational modifications that are not always detectable by commercial antibodies.

5.12. Further work

This work could be extended in a number of ways in order to further advance our understanding and our knowledge on Jnk signalling. Firstly, it would be interesting to rescue the phenotype. Activation of the non-canonical Wnt pathway is not expected to fully counteract the observed changes caused by Jnk inhibition, because, as mentioned before, Jnk has pleiotropic inputs and outputs that are not all related to the Wnt cascade.

Secondly, as described before, counting of cardiomyocytes using FACS would enrich our understanding on how SP600125 and inhibition of Jnk signalling affects cardiogenesis and beating. It would also be interesting to look into the morphology of individual cells within the EB in order to evaluate possible changes in their conformation, their communication and their adhesion properties.

Lastly, a thorough analysis of the effects of inhibitors of other components of the Wnt and MAPK cascades would provide valuable insight about the cross talk between the two pathways and the divergence of their activities. In fact, analysis of the effect of a canonical Wnt pathway activator has already been carried out and is discussed in the next chapter, while inhibition of p38, a downstream effector of the MAPK pathway, is being currently carried out in the laboratory by other members of the research group. Preliminary results from that study show very similar responses.

5.13. Summary and conclusion

In this chapter, I showed that treatment of differentiating ES cells with a specific Jnk inhibitor upregulated the beating ability of cells in a time-specific manner; undifferentiated cells treated with the drug did not show altered beating behaviour, while cells that were undergoing differentiation, either at early (d2-d5) or late stages (d5-d11), exhibited increased occurrence of beating after inhibition of Jnk. This increase did not seem to be associated with amplified cardiogenic specification and differentiation, but rather appeared to be a result of changes in the organization and conformation of cells within the EB. Transient alterations in the cell cycle regulation of EB caused a temporary decrease in their proliferation rates and their size, which, however, did not negatively affect their differentiation potential. Considerable alterations in the expression levels of downstream targets of the canonical Wnt pathway were observed after SP600125 treatment (Jnk inhibition), which highlight the importance of examining the Wnt pathways as a network and not individually. Based on this observation and on previously published work linking Jnk with the canonical Wnt pathway (Esufali and Bapat, 2004, Liao et al., 2006, Wu et al., 2008), it was decided that manipulating the canonical Wnt pathway and examining the resulting effects would be important in further elucidating the role of both pathways during *in vitro* cardiogenesis and understanding their cross talk. The next chapter addresses this issue.

Chapter 6. The Wnt/β-catenin pathway during *in vitro* cardiogenesis

6.1. Introduction

The Wnt pathway has been the focus of research over the last decades in many different contexts and has been shown to play essential roles during embryonic development and stem cell biology. The canonical branch of this pathway, which signals through β-catenin, was shown to participate in heart development in vertebrates and in *in vitro* differentiation of stem cells into cardiomyocytes. However, its suggested role in these processes has often met controversy. In the introduction of this chapter, some general aspects that are associated with the data presented here will be discussed. Genes that have been used as markers of lineages or of specific processes in the PCR analysis are presented below, along with some details about the cell line used in this study (E14 ES cell line) and its special requirements. BIO, the pharmacological agent that was used throughout this study for canonical Wnt activation is also presented.

6.1.1. The genes used as markers

In this study, I was interested in studying the progression of stem cell differentiation into cardiomyocytes and in understanding how this process is affected by activation of the canonical Wnt pathway. In order to do this, a range of pluripotency and differentiation markers was used to look at different aspects of this process. Most of the genes used as markers here have been discussed in detail in previous chapters (Sections 1.3.5, page 14 and 5.1.3, page 174). These are cardiac genes, such as *Nkx2.5, Gata-4, Tbx5, Isl1, Mlc2a, Mlc2v, cTroponinI* and *Tnnt2*, and other lineage markers, such as *Hex, Flk1* and *Brachyury*.

Additional genes were also employed for the expression profile analysis of differentiating ES cells in this study. As pluripotency markers we used the commonly used trinity of *Nanog*, *Oct4* and *Sox2* (briefly mentioned in Section 1.6.1.1, page 45). It has been shown that it is not their individual presence or absence within a cell, but the integrated activity of all three of them as a network that is essential for maintenance of

pluripotency (Kalmar et al., 2009). For example, it has been suggested that loss of *Nanog* expression may increase the probability of differentiation but does not abolish pluripotency altogether (Silva et al., 2008). The SON (*Sox2, Oct4, Nanog*) network within the cell prevents differentiation by suppressing the activity and expression of lineage-specific factors (Niwa, 2007, Smith, 2005).

Mesodermal differentiation was of particular interest here, as the canonical Wnt pathway has been shown to be involved in mesoderm induction (Arnold et al., 2000, Martin and Kimelman, 2008, Vonica and Gumbiner, 2002, Yamaguchi et al., 1999). Therefore, an additional and earlier mesodermal marker was employed, alongside *Brachyury*. *Goosecoid* (*Gsc*) is a homeobox gene that has been implicated in a variety of key developmental processes. It was initially found in the vertebrate organizer, where it was shown to be involved in dorsoventral patterning of mesoderm and in organizing the embryo (Boncinelli and Mallamaci, 1995, Nakaya et al., 2008). *Gsc* has also been found during organogenesis in tissues undergoing morphogenesis, most notably the brain, limbs and ventrolateral body wall (Gaunt et al., 1993, Yamada et al., 1995). It is widely used as an early mesodermal marker, most commonly in association with *Bry*.

6.1.2. E14 stem cell line

In these experiments the E14Tg2A stem cell line was used. This line is a spontaneous hypoxanthine phosphoribosyltransferase (HPRT) deficient derivative of the wild type E14 line, which was isolated from 129P2/OlaHsd mouse blastocysts (Brennan and Skarnes, 1999, Hooper et al., 1987, Magin et al., 1992). These cells are resistant to 0.06 mM 6-thioguanine, are easy to maintain and significantly reduce the amount of tissue culture required. It is a feeder-free cell line and therefore requires exogenous addition of LIF for self-renewal. E14Tg2A cells have been extensively used in a variety of *in vitro* differentiation studies. Specifically, they have been differentiated, among others, into cardiomyocytes (Yamashita et al., 2005, Deacon et al., 1998), neurons (Gaspard et al., 2009) and adipocytes (Dani et al., 1997).

6.1.3. BIO, as a potent pharmacological activator of ß-catenin signalling

Until recently only a limited number of pharmacological inhibitors of glycogen synthase kinase-3 (GSK3) were available (Martinez et al., 2002) with lithium chloride (LiCl)

being one of the most frequently used. However, its half maximal inhibitory concentration (IC_{50}) is relatively high (10–20 mM) and its additional effects on inositol phosphatases are widely known (Patel et al., 2002, Sinha et al., 2005).

BIO, (2'Z,3'E)-6-Bromoindirubin-3'-oxime, is an ATP-competitive, cell-permeable and reversible GSK3 inhibitor (IC_{50} value is 5nM). Its bromine group makes strong bonds with hydrophobic residues (commonly Leucine) in the ATP pocket of GSK3 (Meijer et al., 2003), making it unavailable for binding of ATP molecules and therefore rendering the kinase unable to phosphorylate its downstream targets. Due to its preference for hydrophobic environments, BIO is poorly soluble in water and requires the presence of dimethylsulfoxide (DMSO) for increased solubility (Meijer et al., 2003).

BIO has also been tested for its specificity against other common kinases, including MAPK (mitogen-activated protein kinases), PKA (protein kinase A), PKC (protein kinase C) and others, but its IC_{50} for these proteins is more than 10μM (Meijer et al., 2003, Polychronopoulos et al., 2004). Therefore, its effect at small concentrations is expected to be highly specific for GSK3.

GSK3 inhibits the canonical Wnt pathway by phosphorylating and inactivating β-catenin. So, BIO, by inhibiting GSK3, in fact activates the pathway and stabilizes the levels of β-catenin (Meijer et al., 2003). In previous studies, BIO was shown to sustain pluripotency (Sato et al., 2004), to induce self-renewal in human and murine ES cells, and to induce differentiation of neonatal cardiomyocytes (Tseng et al., 2006). Although BIO has been shown to be specific for GSK3 (Meijer et al., 2003), it is important to note that GSK3 is not only part of the canonical Wnt pathway. It, also, participates in the Hedgehog signalling pathway, where it facilitates proteolysis of the protein Cubitus interruptus (Ci) (Kalderon, 2002, Nusse, 2003). Therefore, when using BIO it is essential to take into account this additional activity area of GSK3. However, BIO has been extensively used as an activator of the canonical Wnt pathway and has been shown to recapitulate the axis-duplication phenotype caused by other Wnt activators (Manisastry et al., 2006, Martin et al., 2010, Meijer et al., 2003, Ueno et al., 2007).

6.2. Aims of the current study

The canonical Wnt/β-catenin pathway and its involvement in various developmental processes, including cardiogenesis, have been extensively studied in the past. However,

controversy still prevails in the field as to the exact role that β-catenin signalling plays during the commitment, specification and differentiation of cardiac progenitors and during subsequent heart morphogenesis. The main focus of the current study was to shed more light to the cardiogenic role of β-catenin. Specifically, the aim of this study was to investigate the requirement of canonical Wnt signalling during ES cell-derived cardiogenesis. In order to achieve this, the following aims were set:

- Establish the effect of DMSO (in which the drug BIO is diluted) during differentiation of E14 ES cells by looking at their morphology, beating behaviour and expression profiles
- Elucidate the effect of canonical Wnt activation by treatment with BIO on the morphology and growth of differentiating E14 ES cells
- Define the effect of canonical Wnt activation by treatment with BIO on the beating behaviour of differentiating E14 ES cells, focusing on individual time intervals during differentiation
- Confirm the findings related to the beating behaviour of E14 cells with differentiating ES-D3 cells
- Establish the gene expression profiles of differentiating ES-D3 cells under timely activation of the canonical Wnt pathway by BIO

6.3. Investigation of the effect of DMSO on the morphology, growth and beating potential of EB

DMSO was used as the experimental solvent for BIO, the chemical used in this study for canonical Wnt signalling activation. Thus, experiments conducted in the presence of DMSO alone (0.1% DMSO, corresponding to the amount used for BIO dilution) should always be included in the analysis in order to ascertain that any observations made after BIO treatment were not caused by DMSO but by the drug itself. Therefore, it was important to examine whether DMSO on its own had any effects. The shape, size and morphology of the cells, as well as their beating behaviour and their gene expression profiles were assessed, after administration of DMSO during ES cell differentiation. Briefly, EB were formed in hanging drops from E14 ES cells between days 0 and 2 of differentiation, were grown in suspension for another three days (d2-d5) and were then plated in 96-well plates (d5-d11). The properties, the morphology and the beating

behaviour of the forming EB were assessed at d5 onwards. An untreated group, grown in differentiation media with no additions, was used as the basic comparator.

A similar assessment of the effect of DMSO on differentiating ES cells is presented in Chapter 5. However, it has to be reminded that two different cell lines were used in the two studies: ES-D3 cells in Chapter 5 and E14 ES cells here (Chapter 6). So, it was important to examine the effect of DMSO on this new cell line before use of the inhibitor and to define the expected morphology, properties and expression profiles of differentiating E14 cells. Data from the DMSO treatment of E14 cells that were similar to that with ES-D3 cells are presented in the appendix, while here only deviations from the previously described expected patterns (Chapter 5, DMSO on ES-D3 cells) are shown.

6.3.1. 0.1% DMSO did not alter the properties and morphology of the cells

The morphological and cell measurement data after DMSO treatment are all presented here, as they are intrinsic to each cell line and are expected to be even slightly different between ES-D3 cells (Chapter 5) and E14 ES cells (here). The EB that formed within the hanging drops were initially small (hardly detectable with naked eye) and uniform in size. The uniformity is, in fact, one of the main advantages of using the hanging-drop method for generating EB (Dang et al., 2002, Kurosawa et al., 2003). EB were then left in suspension, where they grew in size as cells proliferated and differentiated. After d5, when EB were plated, cells attached to the bottom of 96-well plates and spread in all directions, covering, after a few days, a large proportion of the well. No noticeable differences were observed in the morphology of untreated and DMSO-treated EB, as shown in Figure 6.1. They both appeared like large spherical, well-formed and well-defined aggregates under both conditions. Therefore, DMSO did not adversely affect the morphology of forming and developing EB.

In parallel, some important cell measurements were taken at d5: the diameter, circularity, total cell count and viability of the cells. A Vi-Cell XR-2.03 Counter was employed for these measurements (Section 2.2.9, page 71). No significant differences were observed in any of these measurements between the two groups. Small differences in the various cell measurements were observed between the E14 cell line, used in this study, and ES-D3 cells, used in Chapter 5 (highlighted in the next sections). All numerical data are presented in tables and illustrated in graphs (Figure 6.2). Twelve EB

were pooled together for each measurement and each condition. All measurements were repeated on samples from three independent experiments.

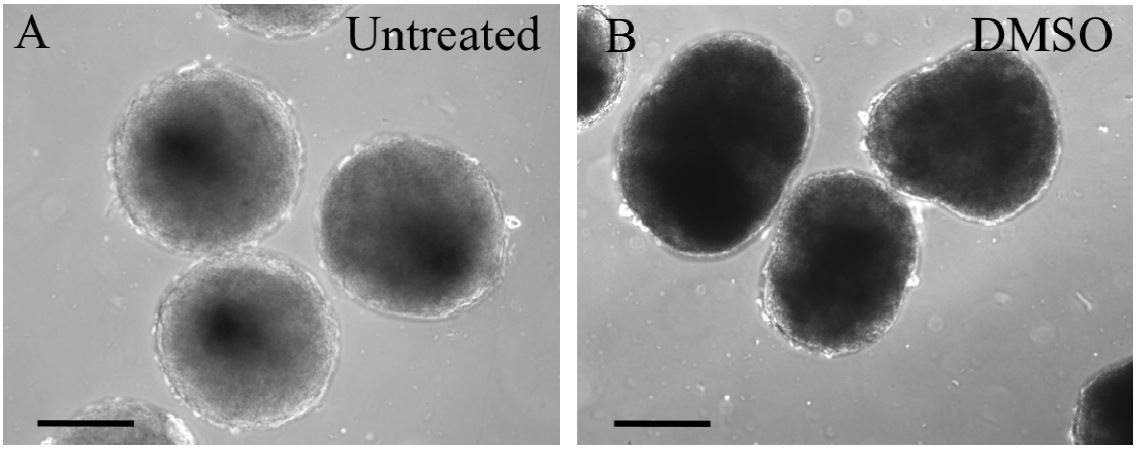

Figure 6. 1: Morphology of EB after DMSO treatment. Shown are bright-field microscopy images of d5 untreated and 0.1% DMSO-treated EB. Addition of DMSO did not noticeably affect the size and morphology of EB at d5. Untreated and DMSO-treated EB do not differ in size. Scale bars represent 200 μm.

The average diameter of E14-derived cells for the media control group at d5 was 9.8 μm (se=0.5) and for the DMSO 8.7 μm (se=0.5) (Figure 6.2). No significant difference was observed between these values (p=0.447). Similarly, the average circularity of E14-derived cells within untreated and DMSO-treated EB at d5 was found not to be affected. For the untreated group it was 0.81 (se=0.01) and for the DMSO group it was 0.79 (se=0.01). A high p value (p=0.163) showed that these measurements were not significantly different from each other and therefore DMSO did not affect the circularity and hence the shape of differentiating cells (Figure 6.2). Untreated and DMSO-treated ES-D3-derived cells at d5 were equally circular (0.76 units on average) but slightly larger (10.45 μm on average) than E14-derived cells.

The viability of E14-derived cells within each EB was 83% (se=3) for the no-treatment and 71% (se=3) for the DMSO-treatment group at d5, which means that at the time of the measurement on average 77% of the cells within each EB under control conditions were alive (Figure 6.2). Although a small decline in the viability of the cells was observed after DMSO treatment, this decrease was not found to be statistically significant (p=0.171). The total number of cells within each EB was also counted at d5 and revealed no changes between untreated and DMSO-treated E14-derived EB (p=0.748). The average number of cells per EB (E14-derived) was 52300 cells (se=4485) for the media control and 51500 cells (se=4991) for the DMSO control.

Control ES-D3-derived EB were more cell-dense (63500 cells per EB on average) than E14-derived EB, but had the same viability rates (77% on average).

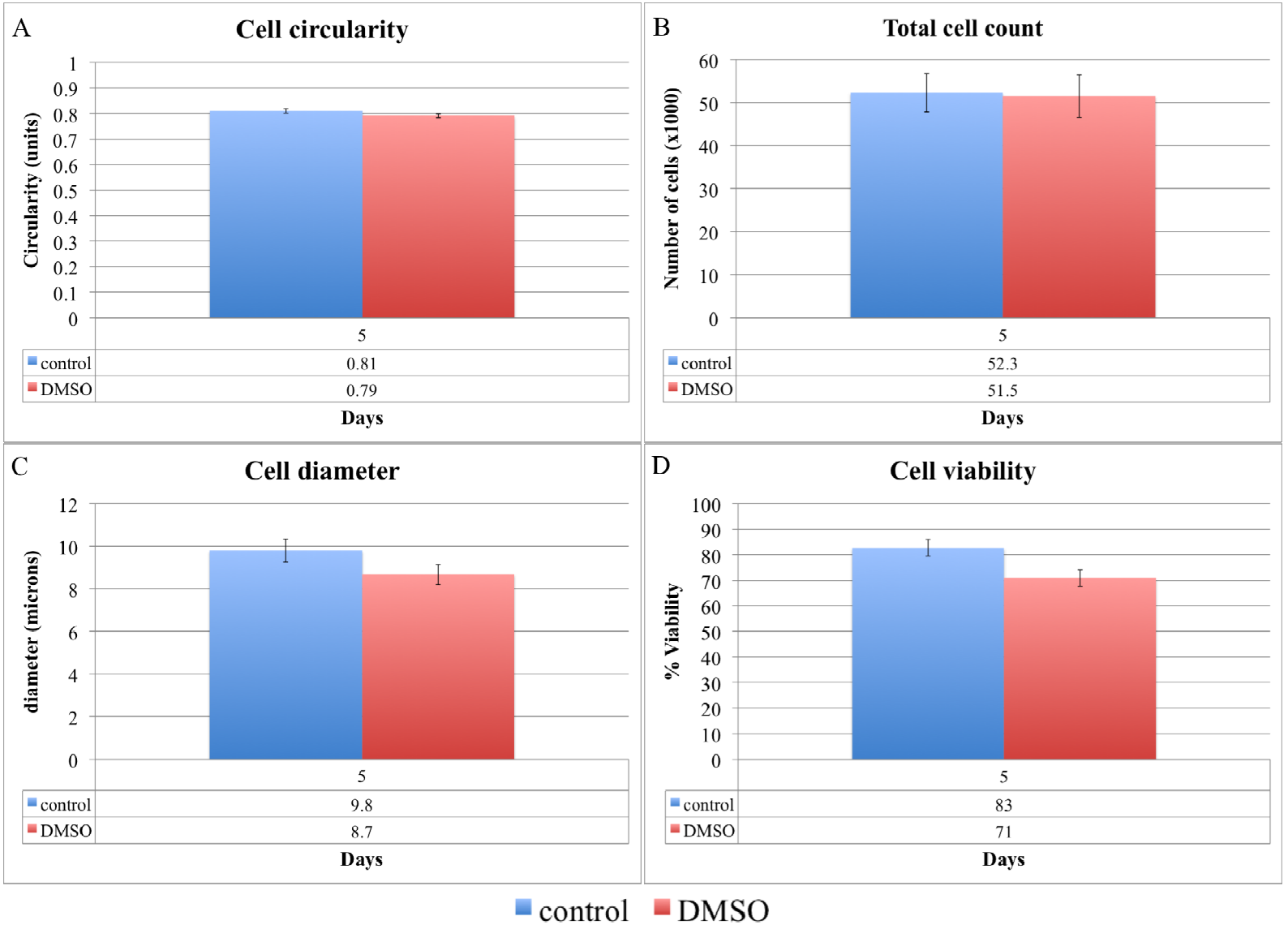

Figure 6. 2: DMSO did not affect the basic cell properties of differentiating EB. Untreated and 0.1% DMSO-treated EB at d5 did not show statistically significant differences in the circularity (A), total count (B), diameter (C) and viability (D) of their cells. All numerical data are shown in the tables underneath the graphs. Statistical analysis was performed using one-way Anova testing.

From the data presented above, it is evident that no statistically significant differences were observed in the morphology and properties of cells within untreated and DMSO-treated E14-derived EB, which suggests that DMSO did not have any adverse effects on the cells. Additionally, no major differences in the cell measurement data between the two cell lines (ES-D3 and E14) were observed. The next step was to assess how DMSO could be affecting the beating behaviour of differentiating E14 ES cells, as the main focus of the current study was the process of cardiogenesis.

6.3.2. 0.1% DMSO did not alter the beating behaviour of the EB

The beating behaviour of E14-derived EB after DMSO treatment was examined in comparison to the beating behaviour of untreated E14-derived EB. DMSO did not affect the beating behaviour of the cells within EB in three independent experiments, compared to untreated cells (Figure 6.3). DMSO was introduced into the media at 5 different intervals, reflecting the time intervals during which BIO would be administered. These were d0-d2, d2-d5, d5-d7, d7-d9 and d9-d11. No significant differences were observed between the different DMSO treatment groups or between the DMSO treatment and the no treatment groups (Figure 6.3).

Untreated E14-derived EB first exhibited contractile activity at day 6, when on average 28% (se=5) of the EB were beating. By d11, approximately 69% (se=2) of the EB showed signs of contraction and were grouped as beating EB. By comparing untreated EB and DMSO-treated EB at all time intervals examined (d0-d2, d2-d5, d5-d7, d7-d9 and d9-d11), no difference was observed (Figure 6.3). This confirmed the common notion that DMSO at very low concentrations (0.1% in this study) does not severely alter the *in vitro* behaviour of ES cell-derived cardiac cells, although in higher concentrations it has been used as a cardiac-enhancing factor (McBurney et al. 1982, Ventura and Maioli 2000, Sachinidis et al. 2003). The percentages of EB that contained beating foci at days 5-11 without any treatment and after all DMSO treatments are presented in a table and graph format in Figure 6.3.

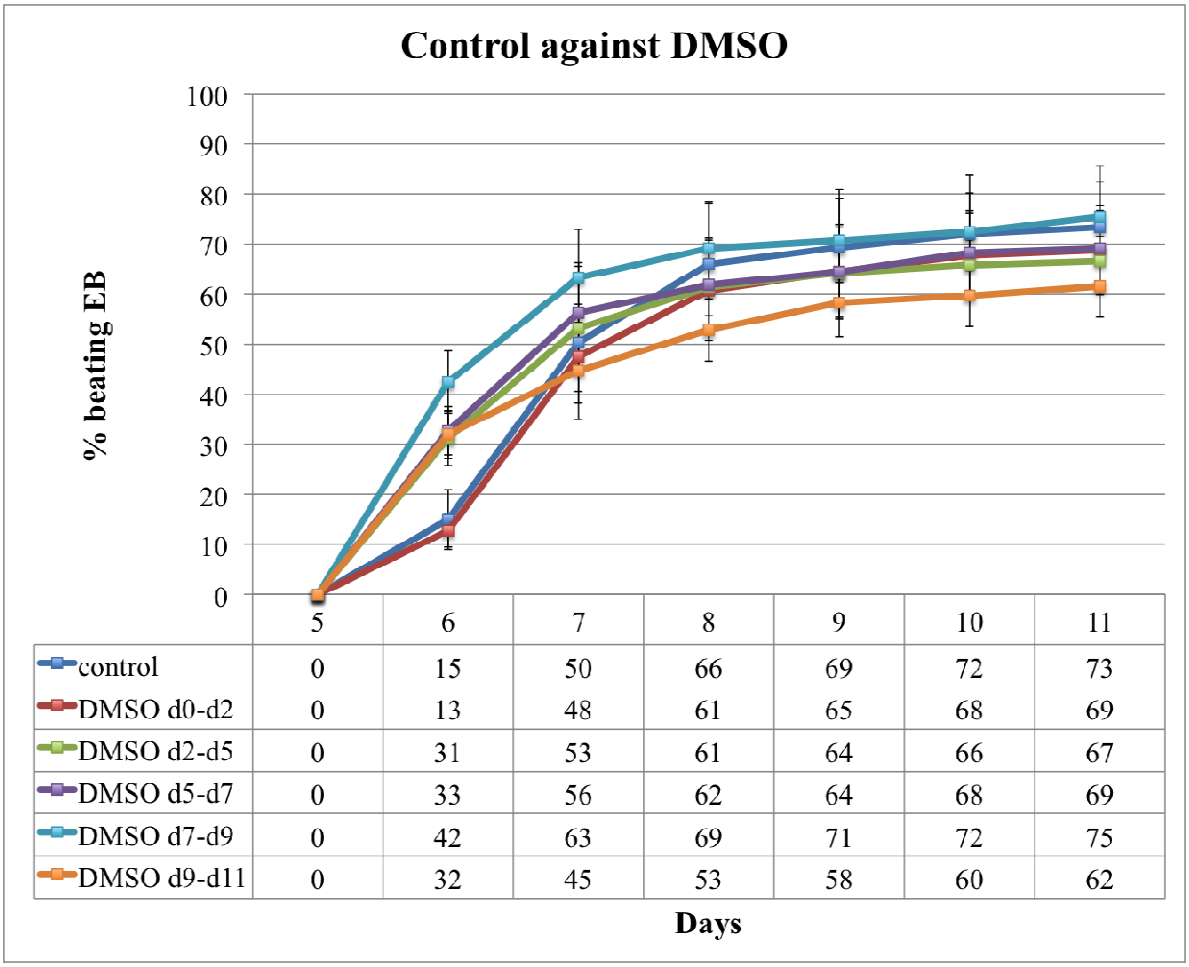

	5	6	7	8	9	10	11
control	0	15	50	66	69	72	73
DMSO d0-d2	0	13	48	61	65	68	69
DMSO d2-d5	0	31	53	61	64	66	67
DMSO d5-d7	0	33	56	62	64	68	69
DMSO d7-d9	0	42	63	69	71	72	75
DMSO d9-d11	0	32	45	53	58	60	62

Figure 6. 3: DMSO did not affect the beating behaviour of differentiating EB. No major differences were observed in the beating capacity of untreated (control) and 0.1% DMSO-treated EB. Initiation of contraction occured at d6, with 15% and 30% of EB containing beating foci in the no-treatment and DMSO treatment groups, respectively. A gradual increase from d6 onwards led to 73% and 68% beating EB at d11 for the two groups, respectively. All numerical data are tabulated underneath the graph. Statistical significance was assessed with the non-parametric Mann Whitney test.

The contractile behaviour of differentiating E14 and ES-D3 cells were slightly different. ES-D3-derived EB initiated spontaneous contraction at d7 instead of d6 and gradually reached a maximum of 51% (untreated EB) and 46% (DMSO-treated EB) beating by d11, compared to 73% (untreated EB) and 68% (DMSO-treated EB) for E14-derived EB. These differences did not come as a surprise, since different cell lines are expected to show distinct behaviours and possibly divergent differentiation timing.

From the data presented above it becomes clear that DMSO did not positively or negatively influence any of the aspects of cell differentiation examined so far. Before concluding that DMSO can be used as an experimental control for all future experiments with BIO, it was essential to examine the gene expression profile of DMSO-treated E14-derived EB compared to untreated E14-derived EB.

6.*3.3. 0.1% DMSO treatment did not alter the gene profile of differentiating EB*

Next, the gene expression profile of differentiating E14 cells under no treatment and DMSO treatment was examined. Quantitative PCR analysis was performed on samples collected from three independent experiments. Typically, at least 30 d5 EB and 10 d11 EB were collected at the respective time point for gene expression analysis. All reactions were performed in triplicate. The ΔΔCt method was used for data analysis (Section 2.2.13.4, page 74, for more details on this method). Day 0 samples were used as the comparator, against which fold changes were measured. 14 genes of the following categories were analysed: pluripotency markers (*Oct4, Nanog, Sox2*), markers of the cardiac lineage (*Islet1, Nkx2.5, Gata-4, Tbx5, Mlc2v, Mlc2a, cTroponinI*), markers of other lineages and Wnt targets (*Brachyury, Goosecoid, Flk1, Hex* and *Lef-1*). Details about what each one of those genes represents and why we used it in this study are given in Sections 1.3.5 (page 14), 5.1.3 (page 174) and 6.1.1 (page 223). Expression of *Flk1*, *Brachyury, Mlc2a*, *Mlc2v, Hex* and *Lef-1* after DMSO treatment in differentiating E14 cells was similar to that of differentiating ES-D3 cells and is shown in the appendix. The expression of the rest of the genes is presented below.

6.3.3.1. Pluripotency genes

As expected, the *Oct4* stemness marker was highly expressed when cells were still pluripotent (d0) and then its expression quickly dropped by approximately 5 fold, reaching minimal levels by days 5 and 11, when most of the cells were fully differentiated. The expression patterns of *Sox2* and *Nanog* were similar with 2.5-5 fold and 1-5 fold changes, respectively, in their expression at days 5 and 11 compared to d0 (Figure 5.4). No significant differences were observed between untreated and DMSO-treated EB.

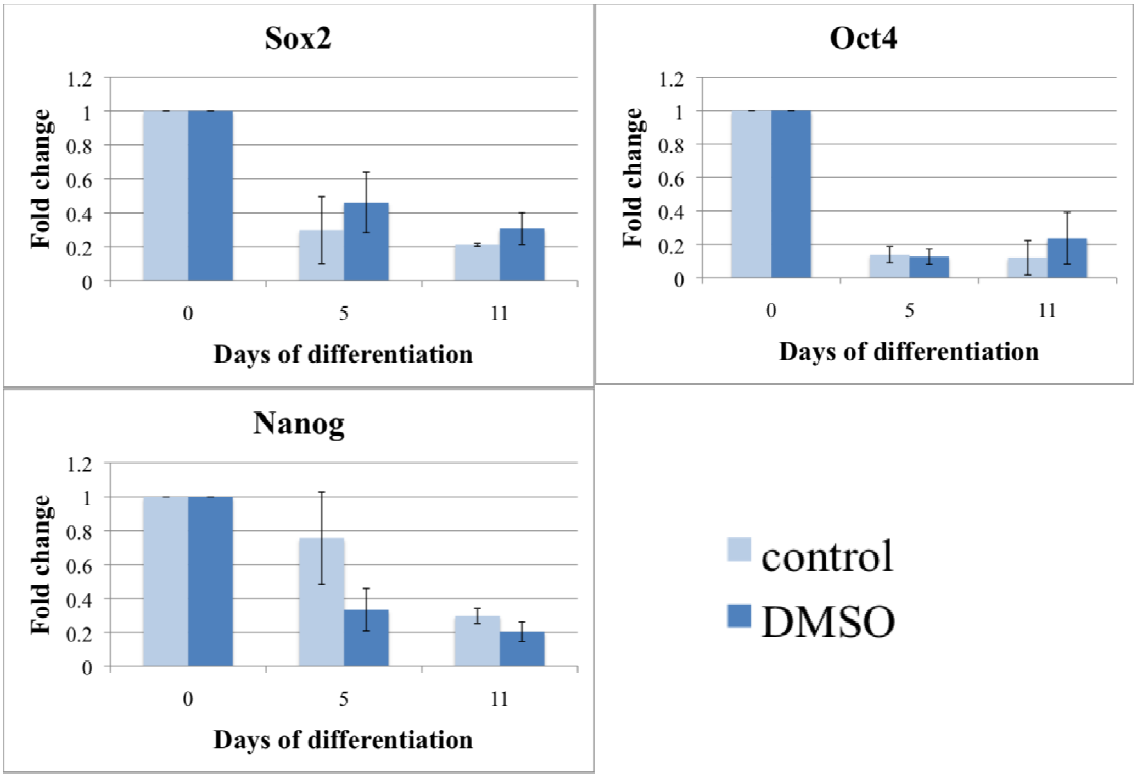

Figure 6. 4: Pluripotency gene expression analysis after 0.1% DMSO treatment. Treatment of differentiating ES cells with DMSO did not markedly alter their expression profile. The expression of pluripotency markers dropped by about 5 fold from d0 to d11 with small variations between control (media only) and DMSO treatment. No statistical significance was observed between any of the groups, as assessed by the one-way Anova test.

6.3.3.2. Mesodermal and cardiac genes

Markers of the mesodermal and cardiac cell lineages were of major interest in this study. *Gsc,* a mesodermal marker, followed a similar expression pattern to that of *Brachyury* (another mesodermal marker shown in the appendix), with increased levels at d5 (1.8 fold increase from d0 for both groups) and decreased levels at d11 (back to d0 levels for both groups) (Figure 6.5).

The early cardiac marker *Gata-4* was only minimally expressed at d0, reached high levels of expression by d5, when cardiac cells had been specified (20 fold and 10 fold higher than d0 in media and DMSO control, respectively), and remained fairly unchanged between days 5 and 11, after cardiac differentiation had occurred (insignificant 2 fold and 1.2 fold decrease in media and DMSO controls compared to d5, respectively) (Figure 6.5).

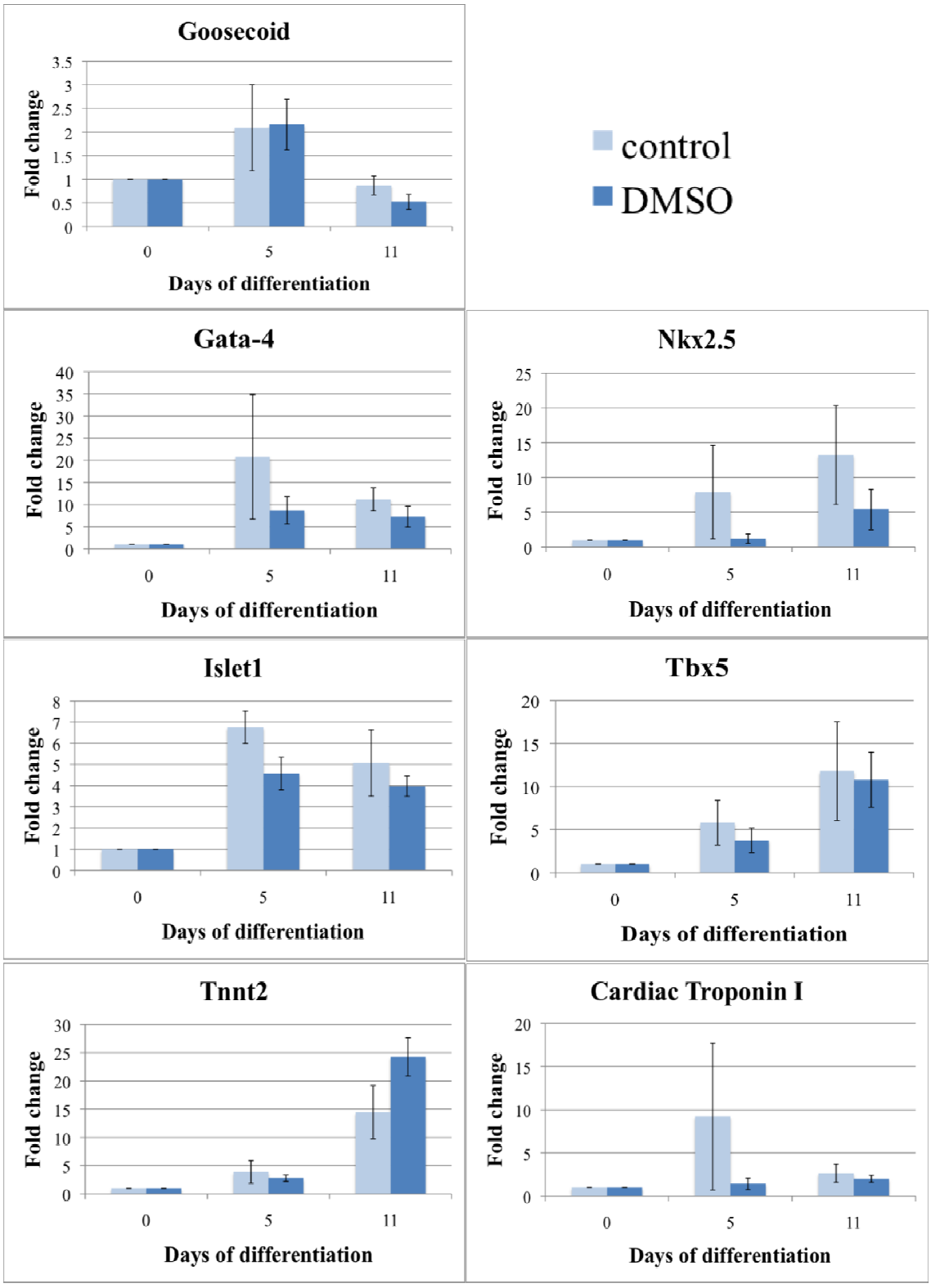

Figure 6. 5: Gene expression analysis of mesodermal and cardiac markers after DMSO treatment. Treatment of differentiating ES E14 cells with DMSO did not markedly alter their gene expression profile. The expression levels of *Gsc* were practically unchanged in the absence and presence of DMSO at days 5 and 11. The pattern of cardiac gene expression remained unaffected after DMSO treatment: *Gata-4, Isl1* and *cTroponinI* showed similar levels of expression at days 5 and 11, while *Nkx2.5, Tbx5* and *Tnnt2* showed a marked increase in their expression levels at d11 in both groups. Statistical significance was assessed by one-way Anova testing.

Isl1, an important early regulator of cardiogenesis, followed a similar expression pattern to that of *Gata-4*: the media control showed a 6.5 fold increase in *Isl1* expression at d5 compared to d0 and a small and insignificant 1.2 fold decrease at d11 compared to d5, while DMSO showed a 4.5 fold increase and a 1.1 fold decrease at days 5 and 11 compared to days 0 and 5, respectively. *Nkx2.5* and *Tbx5* followed a different expression pattern: they were low at d0 and gradually increased at days 5 and 11. Specifically, the expression of *Nkx2.5* in the media control increased 7.5 fold from d0 to d5 and 1.7 fold from d5 to d11, while in the DMSO control it did not increase between days 0 and 5 and showed a 5 fold increase at d11. The expression of *Tbx5* increased 5 and 4 fold from d0 to d5 and 2.2 and 2.8 fold from d5 to d11 in media and DMSO controls, respectively (Figure 6.5). No significant differences were observed between the untreated and DMSO-treated EB in the expression levels of early cardiac markers.

Late cardiac markers, such as *Mlc2a* and *Mlc2v* (shown in the appendix), were expressed at high levels only after cell plating (d5) and especially at d11. Another late cardiac gene, *Tnnt2*, which is a component of the contractile apparatus, was present most notably d5 onwards: at d5 both media and DMSO controls showed increased expression compared to d0 (3 and 2.5 fold, respectively) and at d11 the expression was even higher (5 and 9.6 fold compared to d5, respectively). Another component of the contractile apparatus of beating cells is carciac Troponin I (*cTnI*): its expression at d5 was 9 fold higher than d0 and at d11 3 fold lower than d5 in the media control, while it was 1.5 fold higher at d5 compared to d0 and 1.3 fold higher at d11 compared to d11 in the DMSO control. Any observed differences between the two control groups examined here were not found to be statistically significant (Figure 6.5).

Although some of the differences in gene expression levels between media and DMSO may seem considerable, it is important to note that the pattern of expression was, in most cases, the same in both categories and that large differences were usually accompanied by large error bars, indicating high variability at that specific time point and sample. No statistically significant difference ($p>0.1$ for all) was observed between media and DMSO in any of the genes studied here, as assessed with one-way Anova testing.

The expression profile of the genes presented above under control conditions (media only and DMSO) was as expected. Markers of stemness are expected to decrease after d0 as cells lose their pluripotency and cardiac markers are expected to increase after d0: early cardiac cells come on approximately at d5 and either remain

high or disappear at d11, while late cardiac genes come on later and remain present. Markers of mesoderm are expected to come on at d5 or before and then decrease as mesodermal cells acquire their subsequent fates and lose their transient mesodermal signature. Finally, *Hex* and *Flk1* are expected, as markers of endoderm and hemangioblast cells and their derivatives, respectively, to come on at d5 or earlier and either remain constant or increase at d11. Therefore, it seems reasonable to use the DMSO qPCR data as a baseline comparator for the following data analysis.

Taken together, the data presented so far illustrate that DMSO can reliably be used as a control for further experiments with BIO, as it did not significantly affect any of the aspects of ES cell differentiation that we examined. Therefore, in all data presented below only the DMSO control will be presented, alongside the experimental data. Also, the fact that no major differences in the patterns of gene expression were observed between the two cell lines (E14 and ES-D3), suggests that both the qPCR method and the stem cell differentiation assay are reliable and reproducible and that the two cell lines are comparable to each other.

6.4. The morphology and general properties of differentiating E14 ES cells after treatment with BIO

Preliminary work that was performed on differentiating E14 stem cells, presented in a previous report (MSc report, submitted in August 2007), showed that 1μM BIO was the most appropriate concentration to be used. It was initially used throughout the assay and showed reproducible results, with no signs of toxicity, against higher (5μM) and lower (0.2μM) dosages also tested. Therefore, it was decided that BIO would be used at a concentration of 1μM, diluted in DMSO. Five time points were used for the treatment with BIO: day 0 – day 2 (d0-d2), when cells in hanging drops start forming EBs, day 2 – day 5 (d2-d5), when EBs are in suspension and have started differentiating, day 5 – day 7 (d5-d7), when beating cardiomyocytes first appear and most of the lineages are already defined, day 7 – day 9 (d7-d9), when most of the cells that are destined to become cardiac cells have initiated spontaneous contraction and day 9 – day 11 (d9-d11), when cardiomyocytes and cells of other lineages are considered to be differentiated.

The use of fetal calf serum (FCS), an essential yet confounding factor in ES cell culture, has also been assessed in a previous report (MSc report, submitted in August 2007). It was shown that withdrawal of FCS before d5 of differentiation had adverse

effects on the differentiation potential of the cells, while serum starvation after d5 enhanced the beating potential of differentiating EB, without affecting their general morphology and size. It was, thus, concluded that FCS would be used from d0-d5 and removed from the media between d5-d11 (or d5-d15).

6.4.1. The morphology and size of differentiating EB after BIO treatment

No major differences were observed either in the appearance of BIO-treated and DMSO-treated EB while in suspension or in their spreading capacity after plating. Two important observations were, however, made. Firstly, EB that were treated with BIO between days 2 and 5 appeared larger than DMSO-treated EB (Figure 6.6) in three independent experiments. This implies either that the cells in the EB were larger than DMSO-treated EB or that there were more cells within each treated EB compared to untreated ones. This issue is addressed below with the cell counting data. Secondly, treatment of cells with BIO before d5 caused a decrease in the attachment ability of the cells. This became obvious during media changing, when most of the d0-d2 and d2-d5 BIO-treated EB were lost during pipetting, something that rarely happened for DMSO-treated EB. Looking more closely at the cells it became evident that they were loosely attached to the bottom of the wells and, therefore, even minor disturbances would make them detach.

The morphology and viability of the cells within each EB under different treatment conditions were also assessed, as described below. Cells from 5 days old d0-d2 and d2-d5 BIO-treated EB were measured, right before plating. Twelve EB were pooled together for each measurement and each condition. All measurements were repeated on samples from three independent experiments.

6.4.2. d0-d2 and d2-d5 BIO treatment did not affect the viability of the cells

Initially, the viability of the cells after d0-d2 BIO treatment was analyzed. Viability was not altered under the conditions examined, although a small but not significant decrease was observed between d0-d2 BIO-treated (71%, se=7) and DMSO-treated (71%, se=3) EB (p=0.171). Similarly, the viability after d2-d5 BIO treatment was not significantly altered (75%, se=8, p=0.136 compared to DMSO) (Figure 6.7). We can therefore conclude that the viability of the cells at d5 was not affected by treatment with BIO.

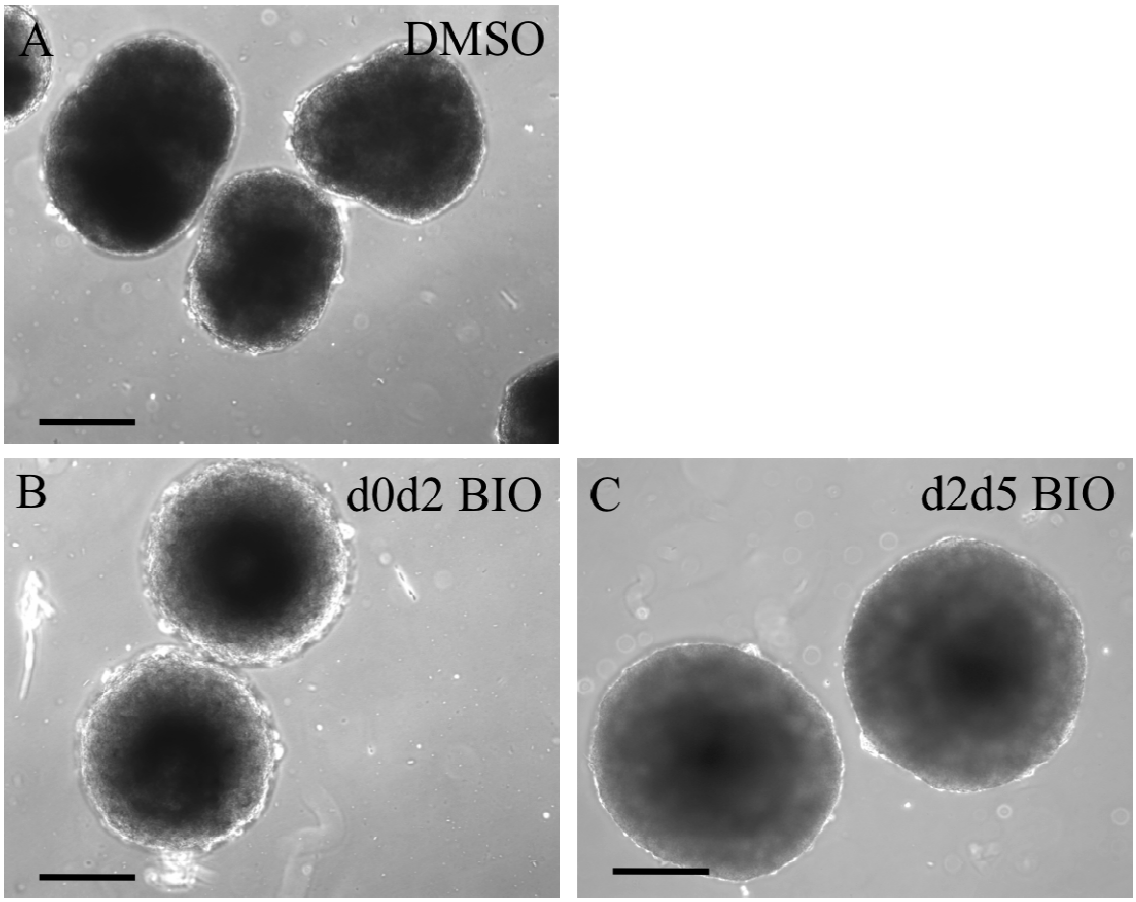

Figure 6. 6: Morphology of EB after BIO treatment. Addition of BIO between days 0 and 2 did not affect the size of EB, while treatment between days 2 and 5 increased it. Shown are bright-field microscopy images of 0.1% DMSO-treated, d0-d2 BIO-treated and d2-d5 BIO-treated EB. Scale bars represent 200 µm.

6.4.3. d0-d2 BIO treatment did not affect while the d2-d5 treatment increased the total cell count per EB

The total number of cells (including dead and alive cells) per EB at d5 was of interest, in order to assess proliferation and cell death levels. The total cell count seemed to be affected by BIO, only when this was added between days 2 and 5, in three independent experiments. Each EB consisted of 51500 cells (se=4991) after DMSO treatment, 44300 cells (se=15817) after d0-d2 BIO treatment and 79900 cells (se=3510) after d2-d5 BIO treatment (Figure 6.7). The difference between the latter group and the DMSO group was found statistically significant, with a p value lower than 0.05 (p=0.023 compared DMSO-treated EB), as calculated with one-way Anova followed by 2-sided Dunnett test (shown by the asterisk in Figure 6.7). The significance between the other groups was p>0.748. As the starting number of cells for each EB was always the same (450 cells in each 30µl hanging drop), changes in the proliferation and death levels of cells

are responsible for any observed differences in the number of cells that constitute each EB at d5. From the data presented above, it seems possible that the d2-d5 BIO-treated EB appeared (microscopically) larger because they contained more cells. The size of the cells within the EB was, however, also examined, as this could be another reason for the increased size of BIO-treated EB.

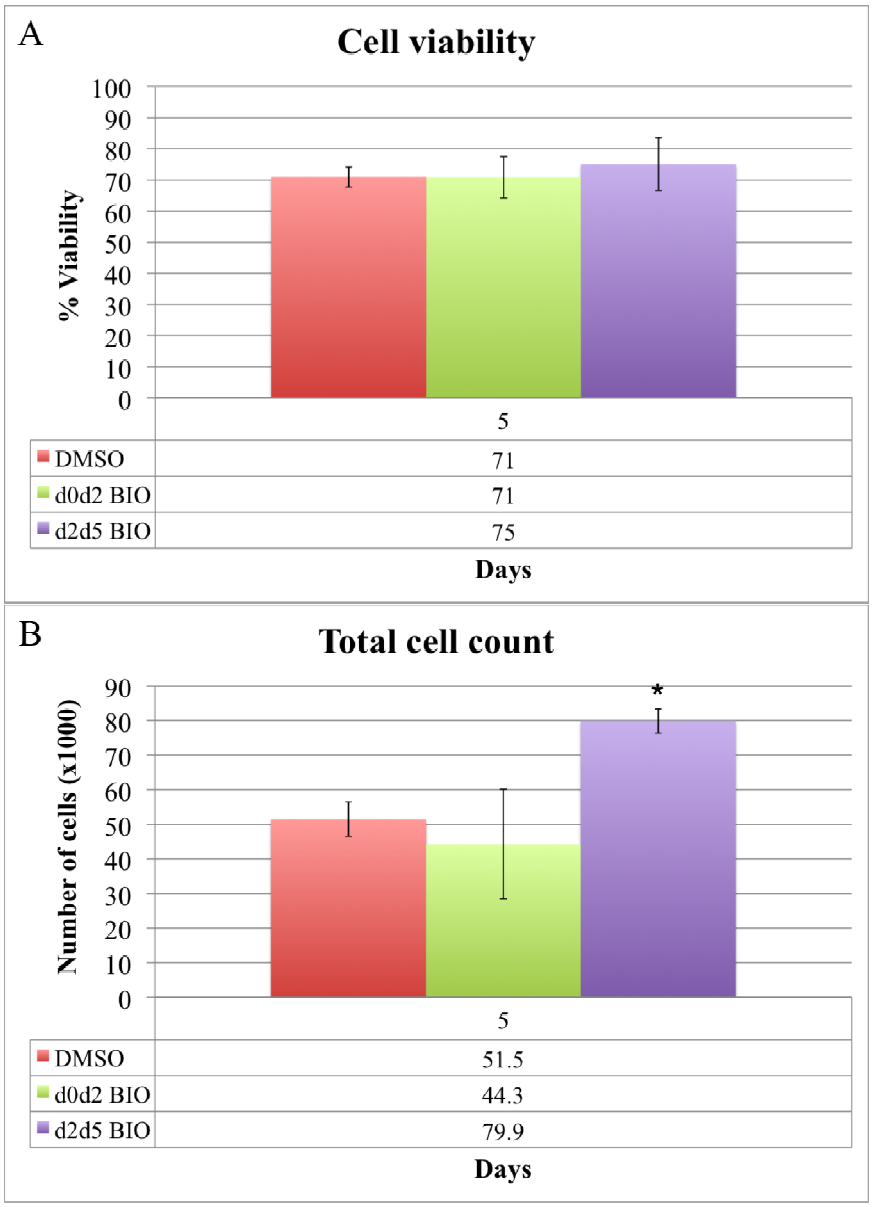

Figure 6. 7: Viability and cell count of BIO-treated EB. (A) The viability of DMSO-treated, d0-d2 BIO-treated and d2-d5 BIO-treated EB was not different at d5. No statistical significance was observed between all groups and the DMSO. (B) D0-d2 BIO treatment did not affect the total cell count of EB at d5, while d2-d5 BIO treatment significantly increased it (0.023). *p<0.05, as assessed by one-way Anova test. Mean values of 3 experiments are shown. Error bars represent standard errors of the mean.

6.4.4. d0-d2 and d2-d5 BIO treatment did not affect the size and shape of the cells

Concomitantly, we analyzed the size and shape of the cells, by looking at their diameter and circularity (Figure 6.8). No statistically significant differences were observed in any of the treatment groups examined (p=0.447 for the diameter and p=0.163 for the circularity for all groups against DMSO). The average cell diameter was 8.7μm (se=0.5) for the DMSO-treated, 8.5μm (se=1.1) for the d0-d2 BIO-treated and 9.5μm (se=1.1) for the d2-d5 BIO-treated cells. The average circularity, measured in units with 1 showing a perfectly circular cell, was 0.79 (se=0.01) for the DMSO-treated, 0.83 (se=0.01) for the d0-d2 BIO-treated and 0.78 (se=0.01) for the d2-d5 BIO-treated cells (Figure 6.8). These values indicate that the cells within the EB are not different in size and shape after treatment with BIO.

6.5. Investigation of the beating behaviour of differentiating E14 ES cells after treatment with BIO

One of the main focuses of the current study was the investigation of the effect of canonical Wnt pathway activation on the process of cardiogenesis. Therefore, examination of the beating behaviour of BIO-treated EB was of interest. Spontaneous contraction was initiated after EB were plated in 96-well plates at d5. The number of EB with beating foci increased gradually from d6 to d11 (or d15). The data presented below represent the mean values of at least three independent experiments and are shown in % percentages. For each experiment at least one 96-well plate, with one EB per well, was used for each condition. Scoring of beating areas was conducted under a brightfield microscope; each EB with at least one beating area was scored as a beating EB. One-way anova testing, followed when necessary by a 2-sided Dunnett test (see Section 2.6, page 81 for more details) was used for assessing statistical significance.

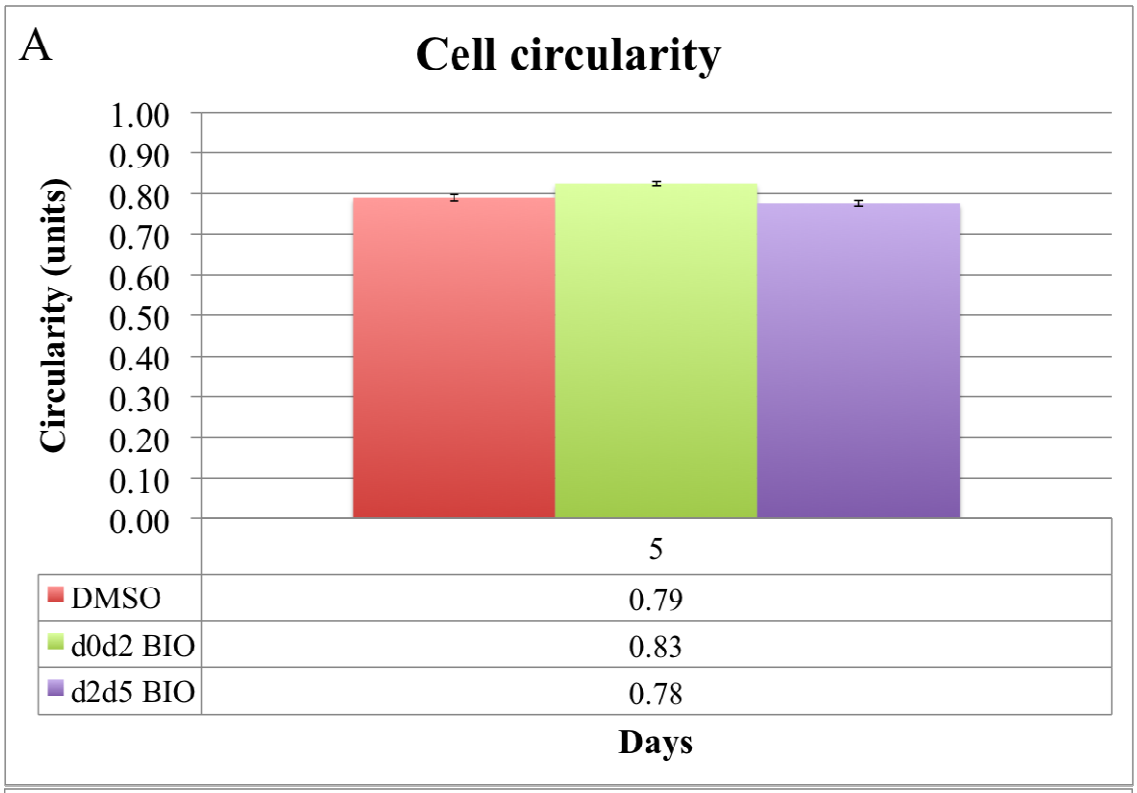

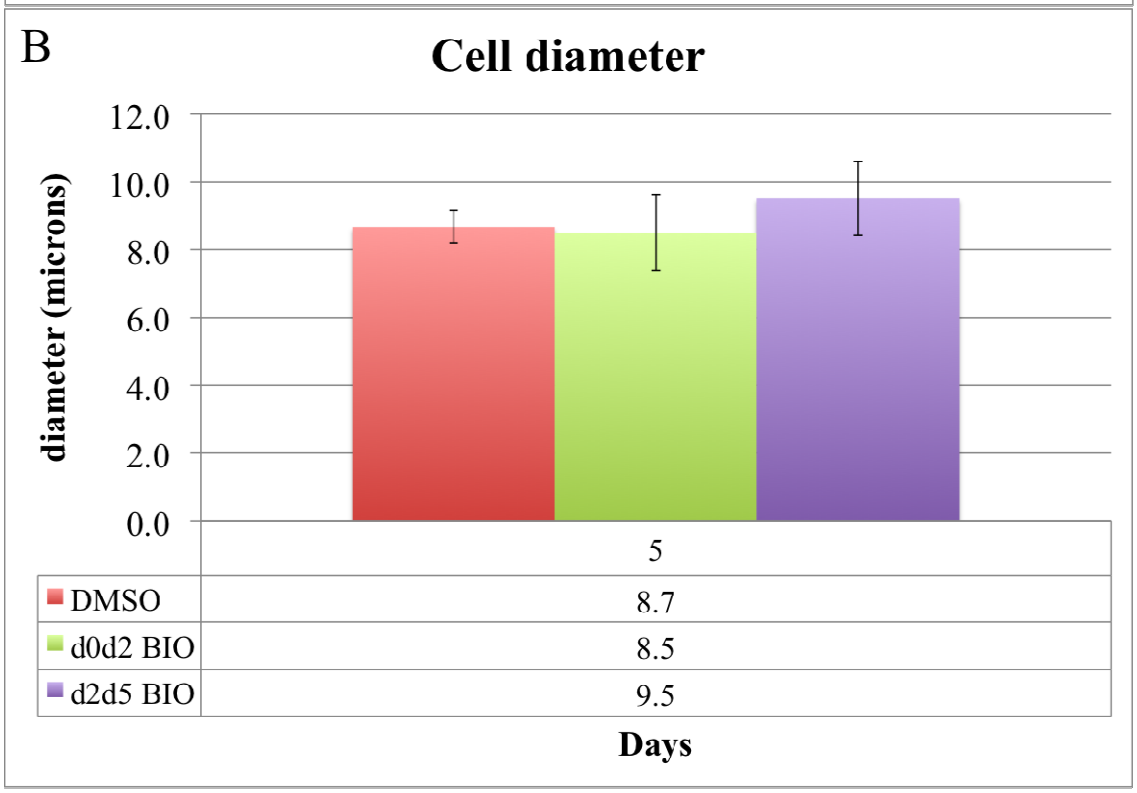

Figure 6. 8: Cell size and shape of BIO-treated EB. The circularity (A) and the diameter (B) of the cells are shown in this graph. (A) The average circularity was 0.79 (se=0.01), 0.83 (se=0.01) and 0.78 (se=0.01) for the DMSO-treated, d0-d2 BIO-treated and d2-d5 BIO-treated cells, respectively. (B) The average diameter was 9.8µm (se=0.5), 8.7µm (se=0.5), 8.5µm (se=1.1) and 9.5µm (se=1.1) for the DMSO-treated, d0-d2 BIO-treated and d2-d5 BIO-treated cells, respectively. No statistical significance was observed between any of these groups and the control groups (p=0.447 and p=0.163 for diameter and circularity against DMSO), as assessed by one-way Anova testing, followed by a 2-sided Dunnett test.

6.5.1. BIO treatment at d0–d2 decreased the occurrence of beating

Initially, we looked at the beating behaviour of differentiating E14 ES cells and assessed how this changed after BIO treatment. We were interested in the onset of spontaneous contraction and the number of EB that attain a cardiac fate at d11 and d15. Addition of 1μM BIO to E14 ES cells between d0 and d2 caused a significant suppression of cardiogenesis after d6 (Figure 6.9). Only approximately 11% (se=6) of the differentiating EB developed contracting foci until d11 and they only started doing so after d8 in all experiments, while DMSO-treated EB were already beating at d6 (p=0.014, 0.006, 0.006, 0.007, 0.007 and 0.007 for days 5 to 11, respectively, compared to DMSO). The observed decrease in the beating potential of the cells could be due to developmental delay caused by extended pluripotency or to differentiation towards other lineages. However, extending the experimental period to 15 days did not alter the behaviour and differentiation status of the cells; it seems that the cells were not able to become beating cardiomyocytes regardless of how long they stayed in culture (Figure 6.9).

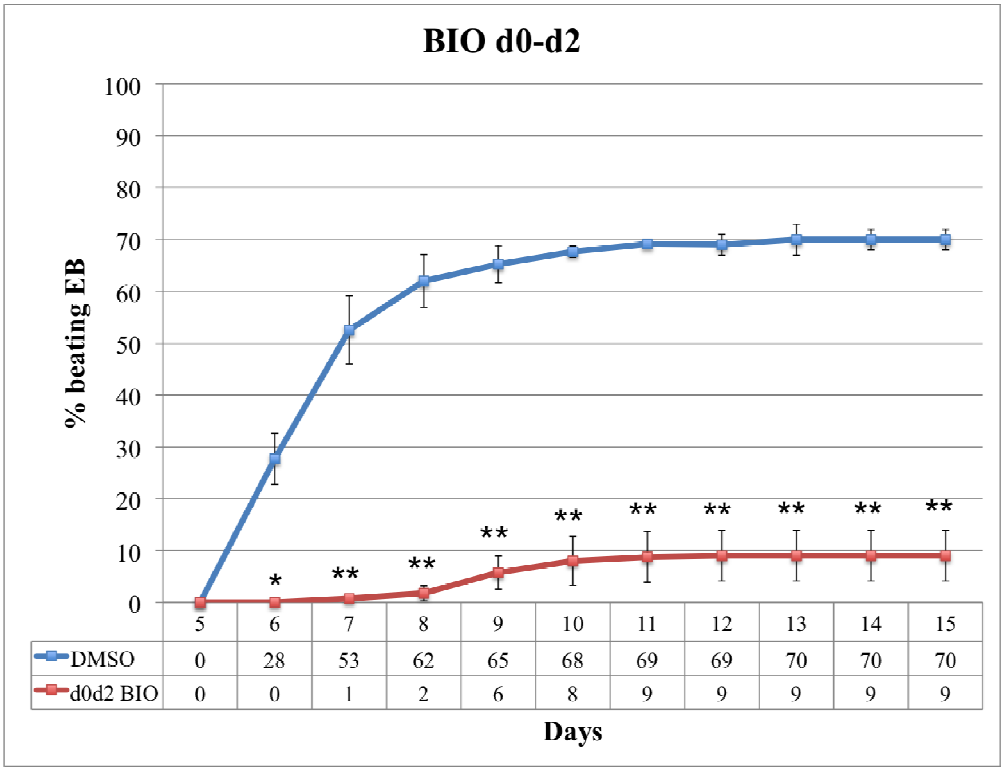

Figure 6. 9: Beating graphs after d0-d2 BIO treatment. Treatment between d0 and d2 caused a detrimental decrease in the ability of differentiating ES cells to initiate spontaneous contraction. The average percentages of beating cells are shown in the table. The onset of contraction was also affected: it occurred at d8 after d0-d2 BIO treatment compared to d6 for controls. The graphs show the mean values of four independent experiments and error bars represent standard errors of the mean. Statistical significance is indicated with asterisks: *p<0.05, **p<0.01, as calculated by the Mann Whitney test.

6.5.2. BIO treatment at d2–d5 suppressed in vitro cardiogenesis

Addition of BIO between days 2 and 5 had a dramatic effect on the occurrence of beating (Figure 6.10). Only 4% (se=0.9) and 5% (se=1.7) of the EB at d11 and d15, respectively, were found to contain contracting areas and the onset of contraction was considerably later (d9) than in the DMSO group (d6) ($p=0.007$, 0.003, 0.003, 0.003, 0.003 and 0.003 for days 5 to 11, respectively, compared to DMSO). It is, therefore, apparent that activation of the canonical Wnt pathway during this interval is detrimental for heart cell differentiation.

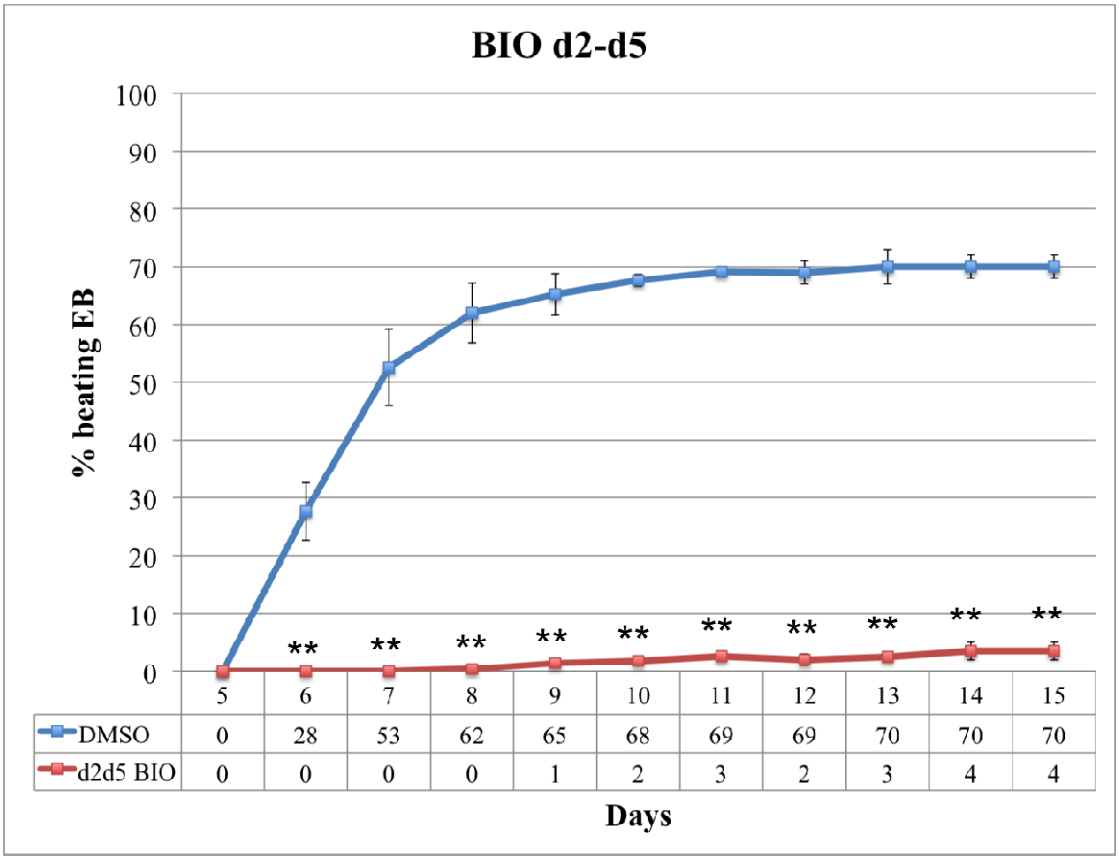

	5	6	7	8	9	10	11	12	13	14	15
DMSO	0	28	53	62	65	68	69	69	70	70	70
d2d5 BIO	0	0	0	0	1	2	3	2	3	4	4

Figure 6. 10: Beating graphs after d2-d5 BIO treatment. Treatment between d2 and d5 caused a detrimental decrease in the ability of differentiating cells to initiate spontaneous contraction. The average percentages of beating cells are shown in the table, below the graph. Spontaneous contraction initiated at d9 after d2-d5 BIO treatment compared to d6 for DMSO. The graphs show the mean values of five independent experiments and error bars represent standard errors of the mean. Statistical significance is indicated with asterisks: **p<0.01, as calculated by the Mann Whitney non-parametric test.

6.5.3. BIO treatment between days 5 and 11 repressed spontaneous contraction

Treatment with BIO at any time between d5 and d11 inhibited beating (Figures 6.11 and 6.12). When BIO was added at d5 (until d7) no contractile foci appeared until d11, indicating a significant decrease in the beating ability of EB (p=0.02 for d5 and p=0.01 for d6-d11 compared with DMSO). Extension of the observation period to 15 days did not reveal a late onset of spontaneous contraction; only on average 1% of EB contained beating foci at d11, compared to 70% of DMSO-treated EB (Figure 6.11). Most interestingly, when BIO was added after beating areas had already appeared, either at d7 (until d9) or at d9 (until d11), most of the beating activity halted and it only partially recovered after removal of the drug (Figure 6.12). Specifically, at d7, just before the d7-d9 BIO treatment, approximately 71% of cells were beating (no difference from DMSO, p=728) and this number was reduced to 18% at d8 after d7-d9 BIO treatment (significantly different with p=0.003 compared to DMSO).

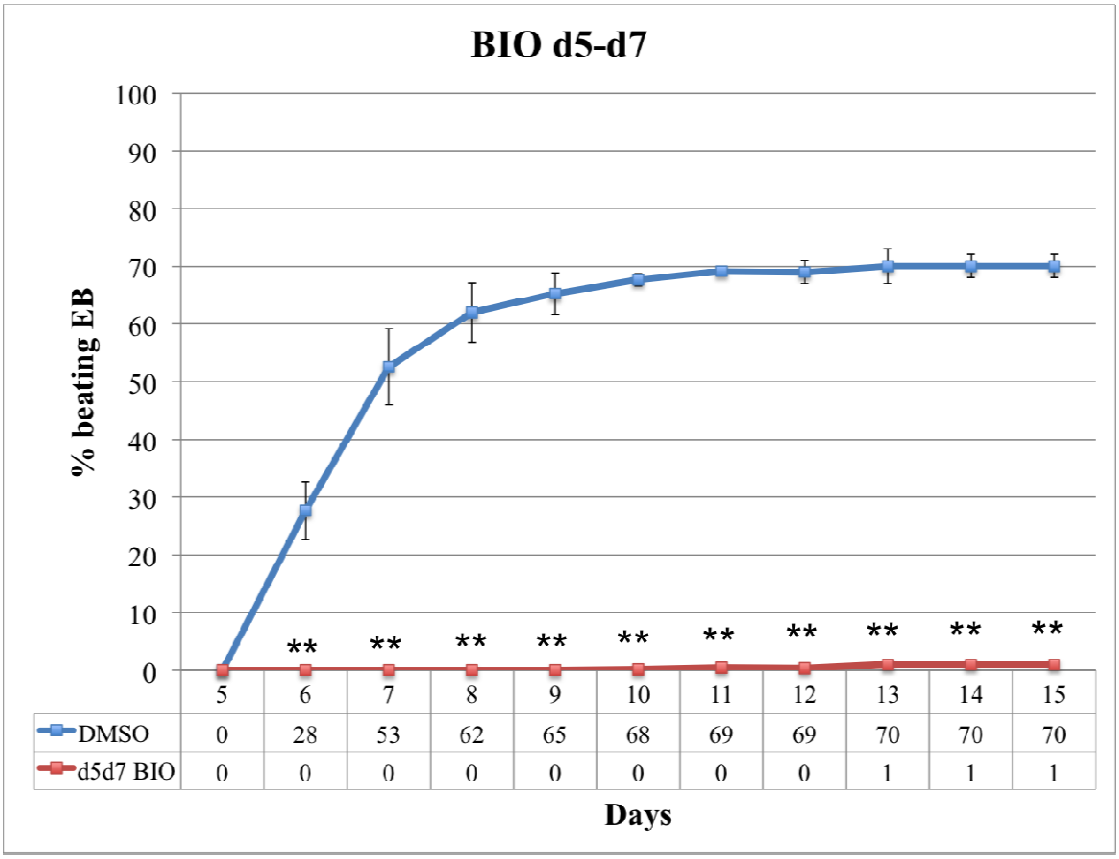

Figure 6. 11: Beating graph after d5-d7 BIO treatment. BIO treatment between d5 and d7 caused a detrimental decrease in the ability of differentiating cells to initiate spontaneous contraction. In fact, no beating was observed after d5-d7 BIO treatment until d13, when a mere 1% of EB contained beating foci, compared to 70% of DMSO-treated EB. The graph shows the mean values of seven independent experiments and error bars represent standard errors of the mean. Statistical significance is indicated with asterisks: **p<0.01, as calculated by the Mann Whitney non-parametric test.

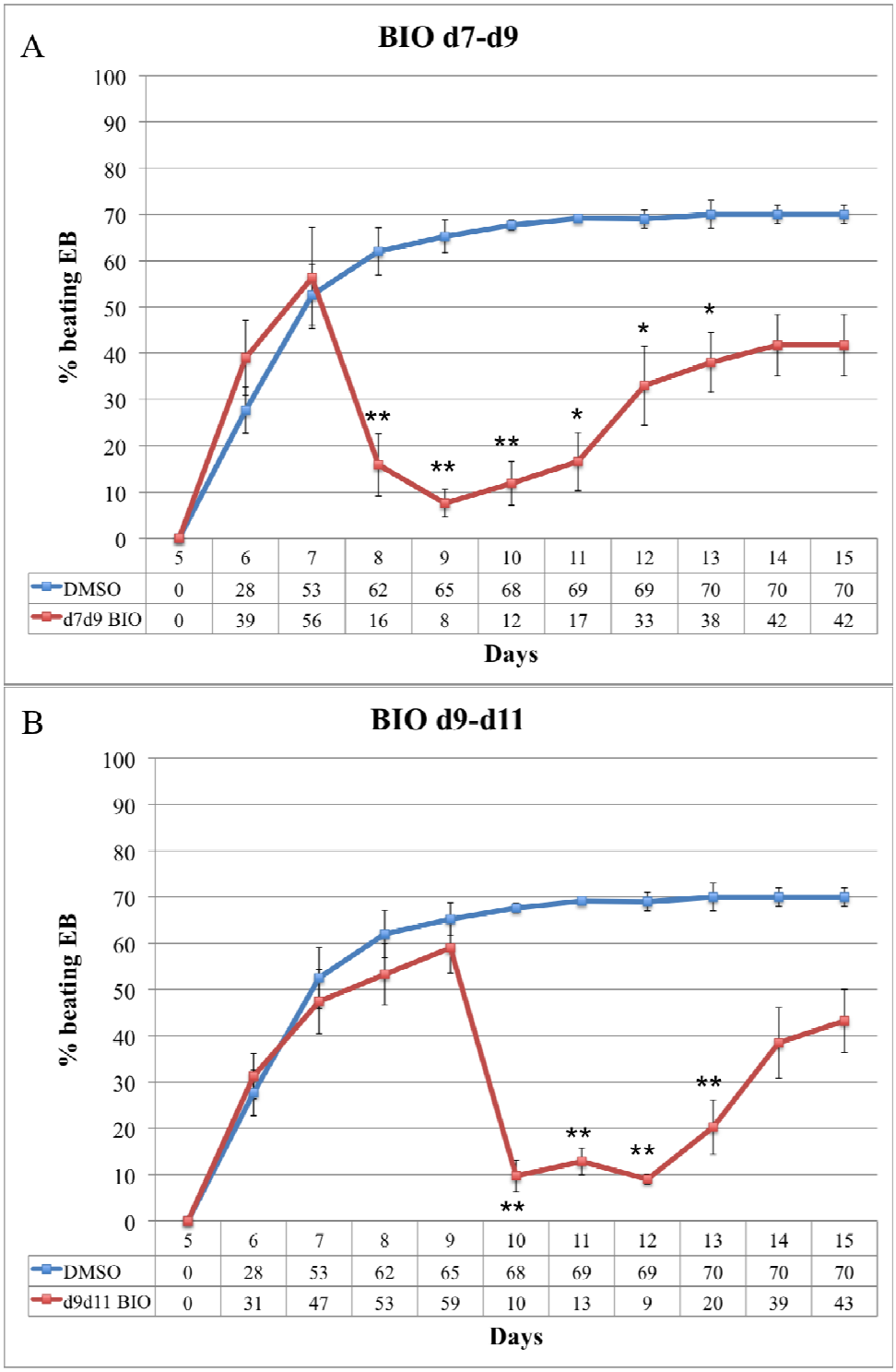

Figure 6. 12: Beating graphs after d7-d9 and d9-d11 BIO treatments. Addition of BIO after initiation of beating had taken place caused a halt in beating, which only partially recovered after removal of the drug. One day after addition of the drug, a significant 4 fold (p=0.003) and 5 fold (p=0.002) decrease in the occurrence of beating was observed after d7-d9 and d9-d11 BIO treatments, respectively. The rescue after removal of the drug was only partial until d15. The graphs show the mean values of seven independent experiments and error bars represent standard errors of the mean. Statistical significance is indicated with asterisks: *p<0.05, **p<0.01, as calculated by the Mann Whitney non-parametric test.

At d11, only 22% (se=9.2) of d7-d9 BIO-treated cells were beating, significantly less than DMSO-treated EB (p=0.023 compared to DMSO). Similarly, at d9, just before d9-d11 BIO treatment, on average 94% (se=2) of cells were beating (no difference with p=0.302 compared to DMSO), while at d10 and d11 after d9-d11 BIO treatment only 20% (se=9) and 25% (se=9) of EB were beating, respectively (both significantly different from DMSO with p=0.002 and p=0.008, respectively). The recovery of the beating activity was never complete even if the assay was extended to d15, when the number of beating EB seemed to have reached a plateau phase (Figure 6.12). However, the differences between d7-d9 and d9-d11 BIO-treated cells and DMSO-treated cells were not found to be significant after d13. The percentages of beating EB at d15 were 51% (se=11.5) and 62% (se=8) for the d7-d9 and d9-d11 BIO treatments, accounting for an approximately 50% and 60% recovery, respectively (p=0.083 and p=0.110, respectively).

6.6. Treatment with BIO had similar, albeit less severe effects on ES-D3 cells

It was also of importance to assess whether the two cell lines used in this thesis (ES-D3 in Chapter 5 and E14 in the current chapter) behaved in a similar way after the same treatment. Comparison of the two cell lines in Section 5.6.3 showed that both E14 and ES-D3 cells respond similarly to treatment with SP600125. The effect of BIO, administered between d0-d5 and d5-d11, was also examined on ES-D3 cells. As shown in Figure 6.13, addition of DMSO alone did not affect the beating behaviour of differentiating cells compared to the media control, as expected from the data presented in Chapter 5. Treatment with BIO, however, was shown to significantly ($p<0.05$ at d8-d11 for both treatments compared to DMSO) reduce contraction: only 7% (se=4) and 8% (se=4) of EB contained beating foci at d11 after d0-d5 and d5-d11 BIO treatment, compared to 51% (se=11) and 46% (se=13) after no treatment and DMSO treatment, respectively.

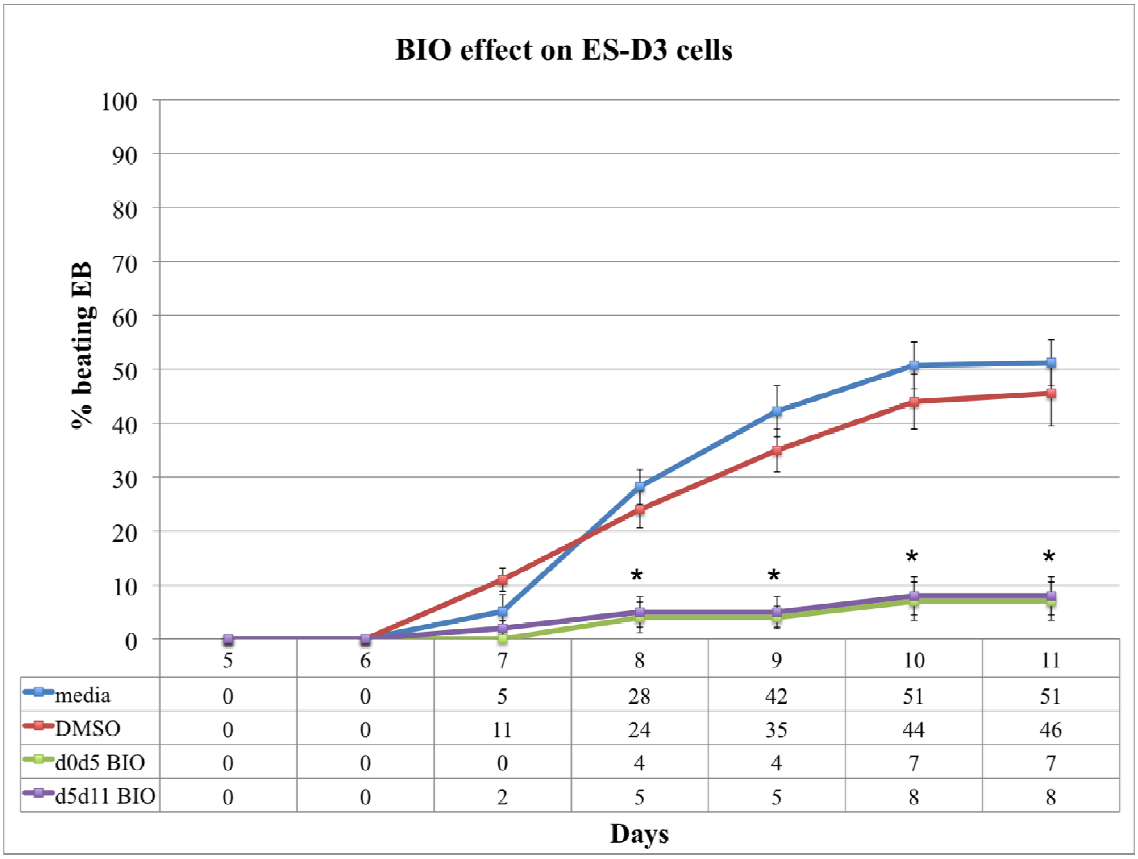

	5	6	7	8	9	10	11
media	0	0	5	28	42	51	51
DMSO	0	0	11	24	35	44	46
d0d5 BIO	0	0	0	4	4	7	7
d5d11 BIO	0	0	2	5	5	8	8

Figure 6. 13: Treatment with BIO had similar effects on ES-D3 and E14 cells. Addition of BIO between d0-d5 and d5-d11 significantly reduced the beating capacity of EB at d8 onwards. Initiation of beating occurred at d8 and at d7 after d0-d5 and d5-d11 BIO treatment, respectively. At the end of the experimental period, only 7% and 8% of EB contained beating foci after d0-d5 and d5-d11 BIO treatments, respectively, exhibiting a significant reduction compared to 51% and 46% beating EB in the control and DMSO groups. Statistical significance was assessed using the non-parametric Mann Whitney test. Asterisks indicate significance with $p<0.05$.

The data presented here alongside the results shown in Chapter 5 (Section 5.6.3, page 201) reiterate the notion that the two cell lines used in this study behave in a very similar way and respond similarly to various treatments. This will be of particular importance when the data from the two chapters (Chapters 5 and 6) are examined together in order to establish a common role for the Wnt network in ES cell differentiation and cardiac development (in Chapter 7).

6.7. Gene expression analysis of differentiating cells after BIO treatment

After analyzing the qPCR data from untreated and DMSO-treated differentiating E14 ES cells (Section 6.3.3, page 232) and assessing that their profiles fit in with the generally accepted physiological role that these genes play during development, the changes in the expression profiles of these genes were examined after activation of the canonical Wnt pathway by treatment with BIO. The DMSO data are included in all graphs and are used as controls. All time points represent the mean values of three independent experiments, with error bars showing standard errors of the mean. Asterisks indicate statistical significance, with p values lower than 0.05 shown with one asterisk. The ΔΔCt method was used for analysis of the qPCR data, as described in Section 2.2.13.4 (page 74). All values are expressed as fold changes compared to the calibrator (d0, set as 1). The results from d0-d2 and d2-d5 BIO treatments are presented first, followed by the results from the d5-d7, d7-d9 and d9-d11 BIO treatments.

Activation of the canonical Wnt pathway was confirmed by increased *Lef-1* expression, a direct downstream target of β-catenin (Behrens et al. 1996, Huber et al. 1996, Tutter et al. 2001). After d0-d2 BIO treatment the expression of *Lef-1* at d5 was slightly but not significantly (p=0.103) upregulated (Figure 6.14). However, after d2-d5 BIO treatment its expression at d5 was 2.5 fold higher than that of the DMSO control, indicating a considerable increase (p=0.030 compared to DMSO). The fact that the effect of the drug is reversible explains the discrepancy: at d5 the effect of the d0-d2 BIO treatment had already worn off because the drug had been removed since d2, whereas the effect of the d2-d5 BIO treatment was still ongoing. At d11 expression of *Lef-1* has regressed back to normal levels, comparable to the DMSO treatment.

6.7.1. After d0-d2, but not after d2-d5, BIO treatment pluripotency markers were severely affected

Initially, the expression of pluripotency genes (*Sox2, Nanog, Oct4*) after d0-d2 and d2-d5 BIO treatment was examined. D0-d2 BIO treatment caused an increase in the expression levels of these three genes compared to controls at d5, suggesting that BIO-treated cells maintained their undifferentiated status for longer than control cells (Figure 6.15). Expression of *Sox2, Oct4* and *Nanog* at d5 was 4.5, 30 and 40 fold higher, respectively, compared to the DMSO values. The difference was statistically significant between DMSO-treated and BIO-treated samples at d5 for *Sox2* and *Nanog* but not for

Oct4 (p=0.002, p=0.280 and p=0.034 for *Sox2*, *Oct4* and *Nanog*, respectively). However, at d11 the levels of expression of all three genes were indistinguishable from controls (0.1, 0.9 and 1.9 fold changes for *Sox2*, *Oct4* and *Nanog*, respectively), with p values higher than 0.1 (p=0.263, p=0.562 and p=0.113 for *Sox2*, *Oct4* and *Nanog*, respectively, compared to DMSO), which means that by that time cells have differentiated and have stopped expressing stemness markers.

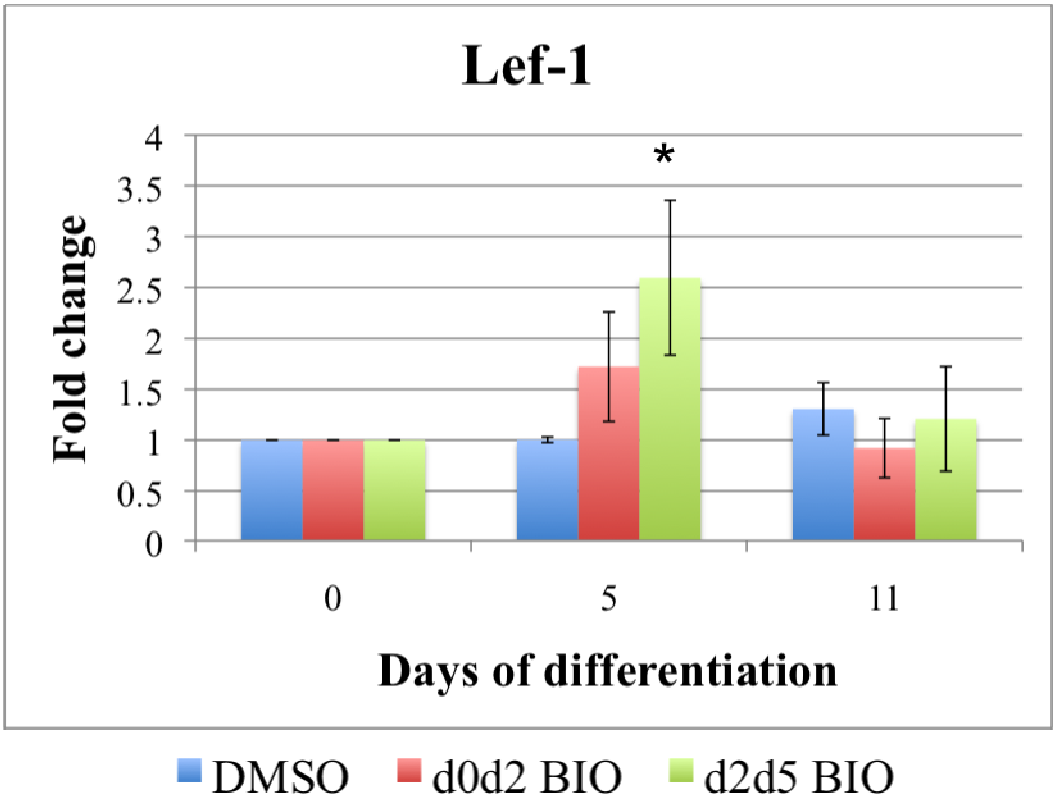

Figure 6. 14: Expression analysis of *Lef-1* after d0-d2 and d2-d5 BIO treatments. BIO treatment between d0-d2 and d2-d5 affected the expression levels of this downstream target of β-catenin at d5 but not at d11. At d5 the levels of *Lef-1* were slightly but not significantly upregulated after BIO treatment between days 0 and 2, while they were statistically significantly (p=0.030) increased after d2-d5 BIO treatment, compared to DMSO-treated EB. Its levels regressed to normal levels at d11. Statistical significance was assessed with the one-way Anova test and is shown with an asterisk: *p<0.05.

In contrast, d2-d5 addition of BIO did not affect the expression levels of *Sox2, Nanog* and *Oct4* at days 5 and 11. Expression of *Sox2, Oct4* and *Nanog* in d2-d5 BIO-treated EB was 10, 3 and 3 fold lower than controls at d5 and 6, 5 and 2 fold lower than controls at d11 (Figure 6.15). No statistical significance was observed between BIO-treated and DMSO-treated EB for most samples, with p values higher than 0.06. D11 *Sox2* expression was, however, significantly lower in d2-d5 BIO-treated EB compared

to DMSO-treated EB, a finding with probably little physiological significance (p=0.068, p=0.219 and p=0.137 at d5 and p=0.033, p=0.265 and p=0.212 at d11 for *Sox2, Oct4* and *Nanog*, respectively, compared to DMSO).

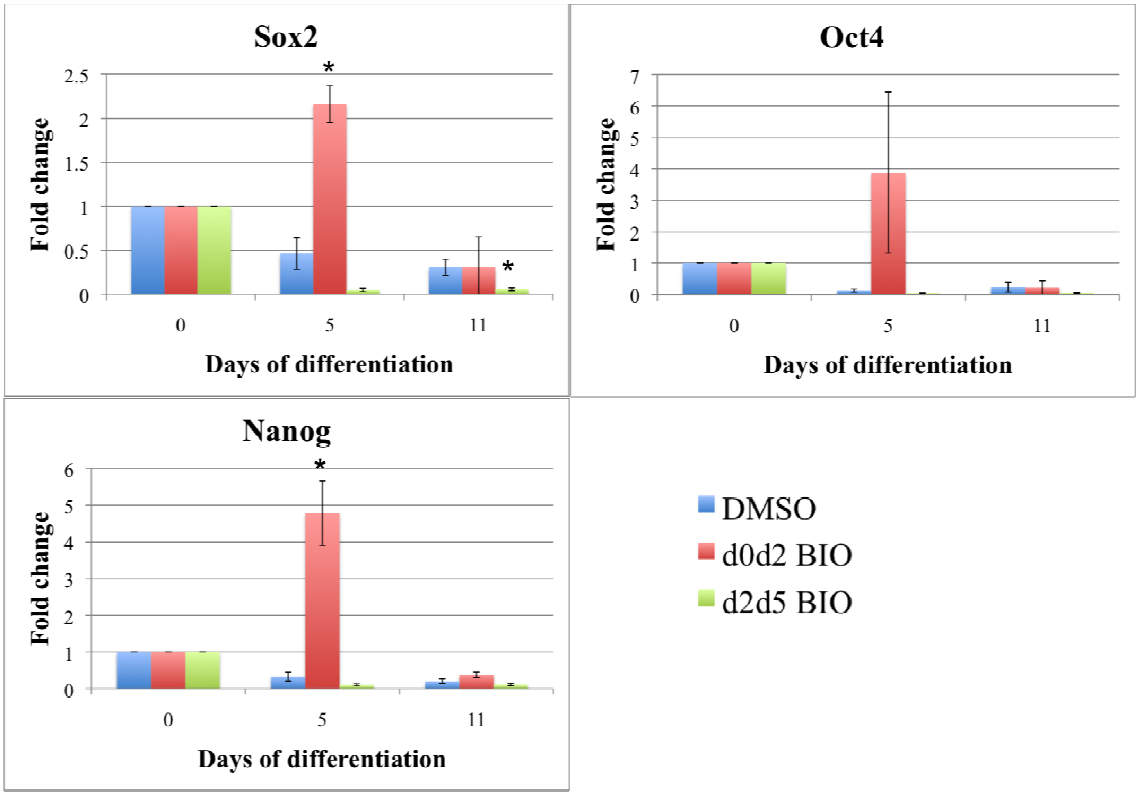

Figure 6. 15: Pluripotency gene expression analysis after d0-d2 and d2-d5 BIO treatments at days 0, 5 and 11. BIO treatment between days 0 and 2 affected the differentiation status of EB, while d2-d5 BIO treatment did not. Pluripotency markers (*Sox2, Oct4* and *Nanog*) were upregulated at d5 after d0-d2 BIO treatment (4.2, 39 and 16 fold, respectively) compared to the DMSO control. At d11 the expression levels of the three genes were indistinguishable from controls. Asterisks show significant differences compared to the DMSO control, with *p<0.05, as calculated by one-way Anova, followed by a 2-sided Dunnett test.

6.7.2. After d0-d2 and d2-d5 BIO treatments markers of various lineages were affected

Next, the expression levels of various lineage markers were assessed (Figure 6.16). The expression pattern of *Bry* and *Gsc* remained unchanged after d2-d5 BIO treatment at both d5 and d11: *Bry* expression was 1.3 fold lower at d5 and 1.2 fold higher at d11 (insignificant changes with p=0.0612 and p=0.989, respectively) than DMSO values,

while *Gsc* was 1.1 fold lower at d5 and 1.4 fold higher at d11 (p=0.189 and p=0.731, respectively) compared to DMSO values. However, the expression levels of these genes were significantly upregulated after d0-d2 BIO treatment, particularly at d5. *Bry* expression was 6 fold and *Gsc* 3.3 fold higher after d0-d2 BIO treatment compared to DMSO at d5, with respective p values p=0.0002 and p=0.02945. At d11, *Bry* was similar to the control (p=0.943), while *Gsc* was 4 fold higher than the control (p=0.002).

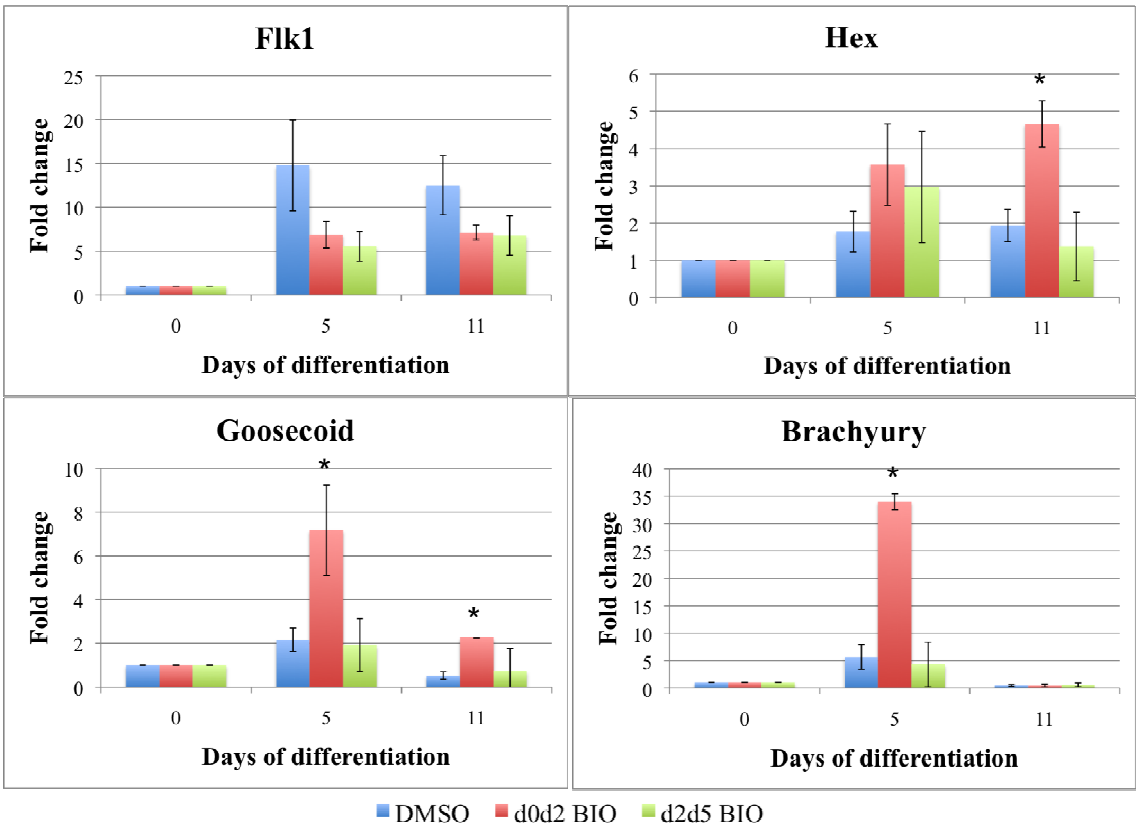

Figure 6. 16: Expression levels of markers of various cell lineages after BIO treatment. *Flk1* showed a decrease in its expression levels at days 5 and 11 after both d0-d2 and d2-d5 treatments, but none was found to be significant, compared to DMSO. The expression of *Hex* was unaltered at d5 but showed a significant (p=0.011) 2.2 fold increase at d11, compared to the DMSO control. *Gsc* and *Bry* showed significant increase (p=0.0002 and p=0.02945, respectively) in their expression levels at d5 (3.5 and 6.6 fold, respectively), while at d11 only *Gsc* showed a significant increase (p=0.002) compared to DMSO. Statistical significance was assessed with one-way Anova testing, followed by a 2-sided Dunnett test and is shown with asterisks in the graph: *p<0.05.

Flk1 (insignificantly 2 fold lower after d0-d2 BIO treatment compared to DMSO, p=0.332) and *Hex* (insignificantly 2 fold higher after d0-d2 BIO treatment compared to DMSO, p=0.346) expression levels at d5 were practically unaltered after d0-d2 BIO addition compared to the DMSO values. Similarly, at d11 *Flk1* (1.7 fold lower, p=0.924) expression was unaltered between d0-d2 BIO-treated and DMSO-treated EB. However, expression of *Hex* was found to be significantly higher (2.4 fold higher, p=0.011) after d0-d2 BIO treatment than DMSO at d11 (Figure 6.16). After d2-d5 BIO treatment, *Flk1* and *Hex* at both days 5 and 11 were not considerably different to controls. *Flk1* was 2.7 (p=0.305) and 1.8 (p=0.241) fold lower than DMSO at d5 and d11, respectively, and *Hex* was 1.7 fold higher (p=0.671) and 1.5 fold lower (p=0.606) than controls at d5 and d11, respectively.

6.7.3. After d0-d2 and d2-d5 BIO treatments cardiac genes were severely affected

Clearly, the genes of most relevance to our study were the early and late cardiac genes. At d5 *Tbx5*, *Nkx2.5* and *Gata-4* showed biphasic, although not statistically different from controls, responses to BIO treatment: after d0-d2 BIO treatment expression of *Tbx5* was 1.5 fold higher (p=0.621), of *Nkx2.5* 2.2 fold lower (p=0.249) and of *Gata-4* 2 fold lower (p=0.139) compared to DMSO, while after d2-d5 BIO treatment their respective expressions were 2.5 fold lower (p=0.212), 1.3 fold higher (p=0.953) and 3.2 fold higher (p=0.315) than controls (Figure 6.17). The expression of *Isl1* was significantly decreased at d5 compared to DMSO after d0-d2 (p=0.047) and d2-d5 BIO treatments (p=0.038). At day 11 after d0-d2 treatment, the expression of *Gata-4* dropped 1.3 fold (p=0.495), of *Nkx2.5* 5.8 fold (p=0.196), of *Tbx5* 1.4 fold (significant, p=0.049) and of *Islet1* 1.5 fold (significant, p=0.046), compared to DMSO. At d11 after d2-d5 BIO treatment, the fold changes were 2.1 (p=0.128) for *Gata-4*, 9.7 (p=0.148) for *Nkx2.5*, 2.7 (p=0.125) for *Tbx5* and 2.2 (significant, p=0.018) for *Islet1* compared to DMSO. The late cardiac genes examined here showed no changes in their expression levels at d5 but severe changes at d11 after either one or both treatments (Figure 6.17). Specifically, expression of *MLC2v* dropped 2.4 fold (significant, p=0.029), *Tnnt2* 1.8 fold (p=0.069) and *MLC2a* 1.3 fold (significant, p=0.047) after d0-d2 BIO treatment, while after d2-d5 BIO treatment the significant fold changes were 18 fold (p=0.001) for *MLC2v,* 3.4 (p=0.047) for *Tnnt2* and 13 (p=0.001) for *MLC2a,* compared to DMSO. Expression of *cTnI* at d11 was biphasic: 1.1 fold increase (p=0.367) after d0-d2 and 4.5 fold decrease (significant, p=0.047) after d2-d5 BIO treatments.

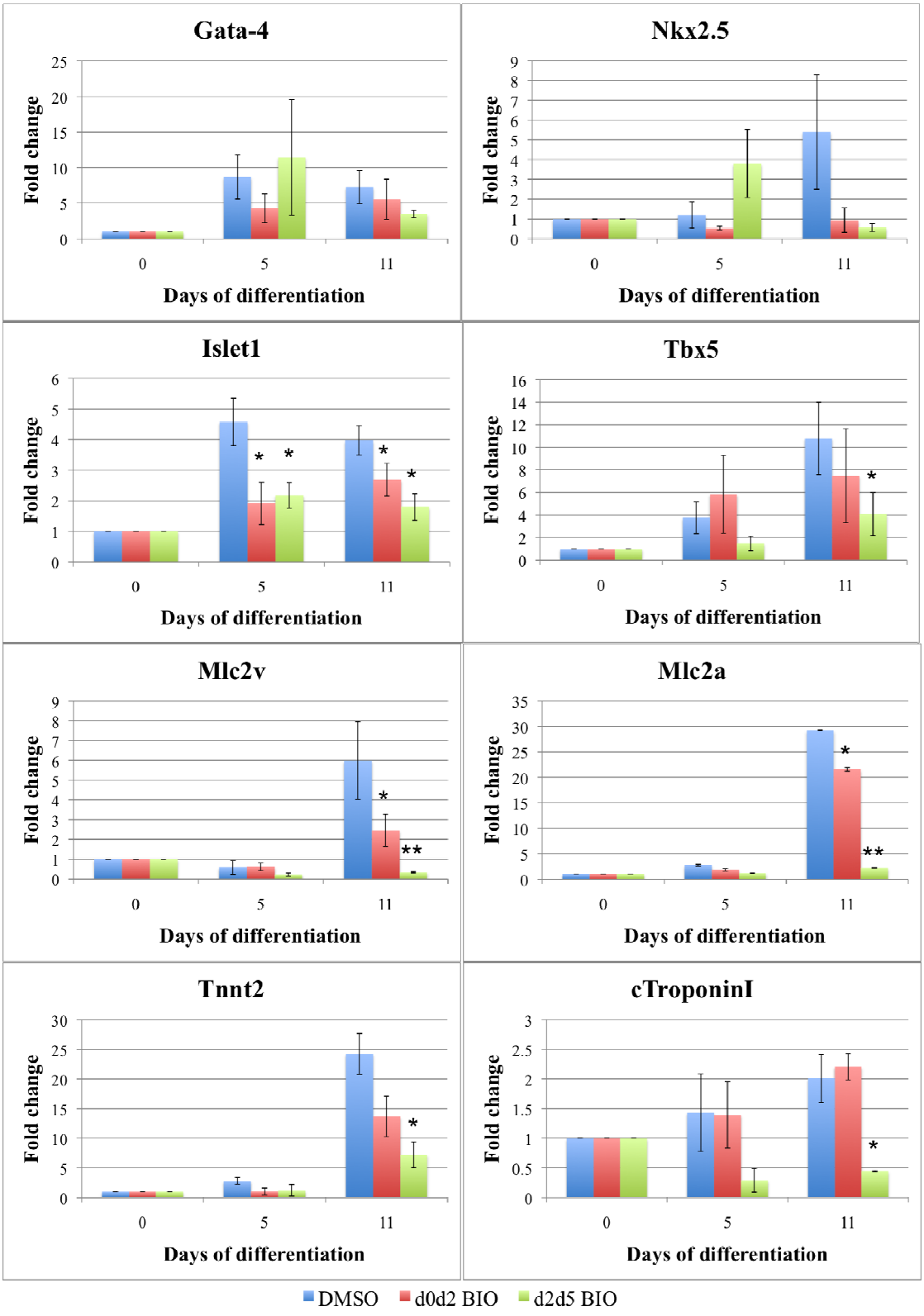

Figure 6. 17: Expression profile of cardiac genes after BIO treatments. *Gata-4* and *Nkx2.5* were shown not to be significantly affected by d0-d2 and d2-d5 BIO treatments. *Isl1* was significantly decreased at d5 and d11 after both treatments. *Tbx5* was significantly downregulated only after d2-d5 BIO treatment at d11. *Mlc2a* and *Mlc2v* were significantly affected at d11 by both BIO treatments. Similarly, *Tnnt2* was downregulated at d11 only after d2-d5 BIO treatment. D2-d5 BIO treatment had a more severe effect on *cTnI* at d11 than the d0-d2 BIO treatment. Statistical significance was assessed with one-way Anova testing, followed, where necessary, by a 2-sided Dunnett test.

6.7.4. BIO treatment between days 5 and 11 reduced expression of cardiac genes but did not alter other lineage markers

In the BIO treatments between days 5 and 11, we only looked at a subset of the genes analyzed earlier, as many of them were only of relevance during the very early stages of the differentiation process, before BIO was added to the cell media. For example, the pluripotency genes were not of relevance or interest in the late treatment groups, as they were only highly expressed at d0. Specifically, the expression levels of *Bry*, *Hex*, *Flk1*, *cTnI*, *Tbx5*, *Isl1* and *MLC2v* were analyzed (Figures 6.18 and 6.19).

Gene expression data from days 0 and 5 were identical to the respective DMSO controls, as no treatment was applied until that point. At d11 the expression of *Bry* was identical to that of the DMSO control for all late (d5-d7, d7-d9 and d9-d11) BIO treatments. The expression of *Flk1* and *Hex*, albeit slightly altered after late BIO treatments compared to controls, was not found to be significantly different, with $p>0.06$ in all cases (Figure 6.18).

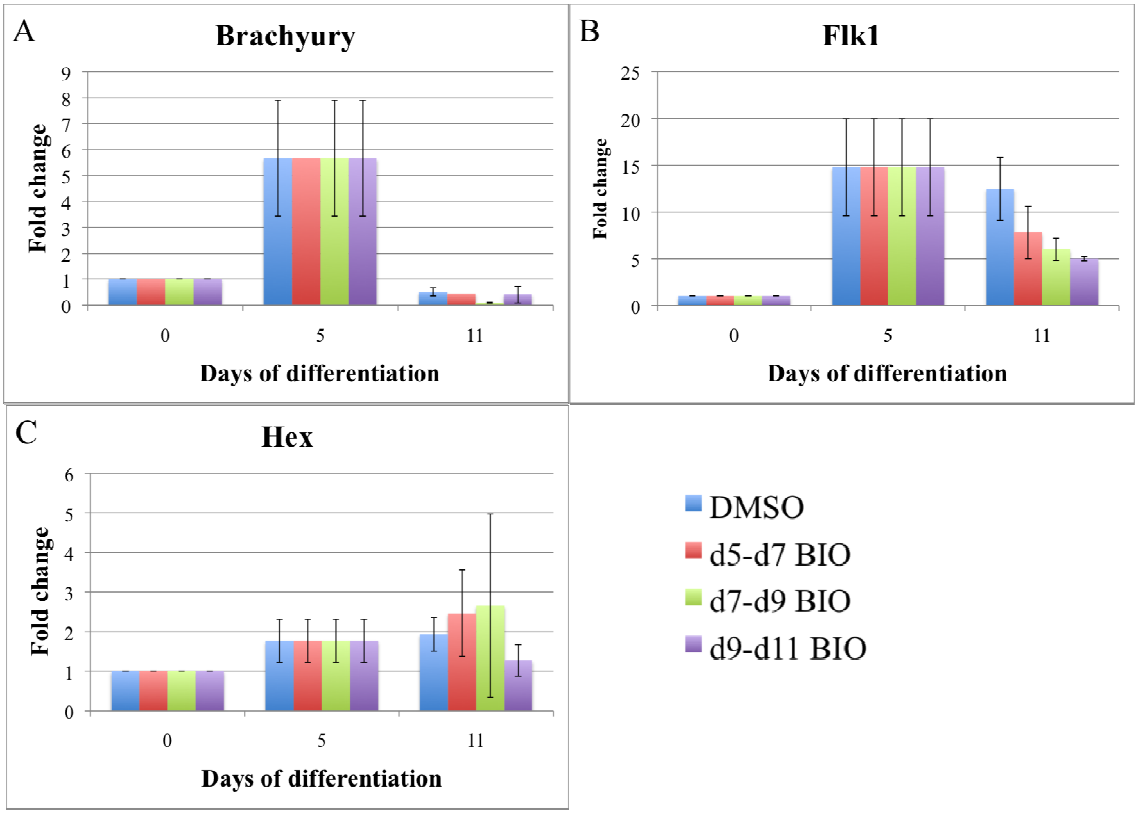

Figure 6. 18: Gene expression analysis of *Bry*, *Flk1* and *Hex* after late (d5-d7, d7-d9 and d9-d11) BIO treatments. D0 and d5 data are identical to the DMSO control because no treatment has been applied yet until that time point. Expression of *Bry*, *Flk1* and *Hex* was unaltered in all treatment groups at d11 compared to controls. Statistical significance was assessed with one-way Anova testing.

Isl1 showed significantly decreased expression at d11 after d5-d7 (3.3 fold decrease, p=0.046) and d9-d11 (3.8 fold decrease, p=0.043) BIO treatments, while it remained unaltered (1.2 fold decrease, p=0.137) after d7-d9 BIO treatment, compared to DMSO (Figure 6.19). Expression of *cTnI* followed a similar pattern: significant 30 fold (p=0.037), insignificant 1.2 fold (p=0.146) and significant 2.5 fold (p=0.047) reduction after d5-d7, d7-d9 and d9-d11 BIO treatments, respectively, compared to DMSO. Expression of *Tbx5* was significantly decreased after all three treatments: 9.5 fold (p=0.026), 3.2 fold (p=0.037) and 3.3 fold (p=0.047) fall after d5-d7, d7-d9 and d9-d11 BIO treatments, respectively, compared to DMSO (Figure 6.19). The expression of *Mlc2v* was differentially but not significantly affected by each of the BIO treatment: d5-d7 addition of BIO caused a 30 fold drop in its expression levels (p=0.137) compared to DMSO, d7-d9 BIO treatment caused a 1.2 fold increase (p=0.224), while d9-d11 treatment caused a 2 fold increase in its expression levels (p=0.067).

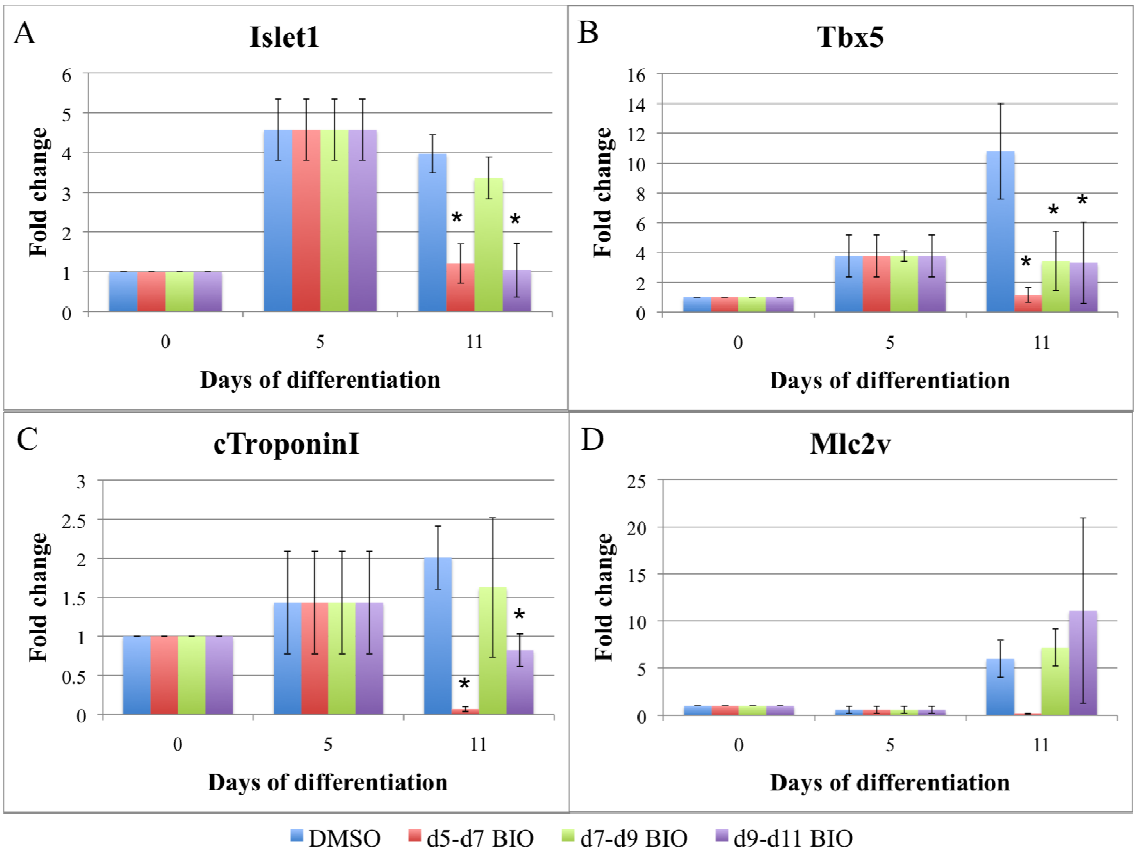

Figure 6. 19: Gene expression analysis of cardiac genes after late (d5-d7, d7-d9 and d9-d11) BIO treatments. D0 and d5 data were identical to the DMSO control because no treatment has been applied yet until that time point. *Isl1*, *Tbx5* and *cTroponinI* were significantly decreased at d11 after d5-d7 BIO treatment (p<0.05) compared to DMSO. In contrast, after d7-d9 BIO treatment, only *Tbx5* was significantly affected (p=0.037) while other genes remained unaltered. Treatment with BIO between days 9 and 11 caused a significant decrease in the expression of *Isl1* (p=0.043), *Tbx5* (p=0.047) and *cTroponinI* (p=0.047). Expression of *Mlc2v*, although increased after d9-d11 BIO treatment and decreased after d5-d7 BIO treatment, did not exhibit significance. Statistical significance was assessed using one-way Anova testing, followed by a 2-sided Dunnett test.

6.8. Discussion

A number of studies have shown that manipulation of the Wnt cascade during formation of EB *in vitro* greatly influences cell differentiation (Aubert et al., 2002, Gadue et al., 2006, Lindsley et al., 2006, ten Berge et al., 2008). β-catenin is a major regulator of gene transcription and even small or transient alterations in its stability and/or activity can cause significant changes in the expression of downstream genes (Barker et al., 2001, Hecht and Kemler, 2000, Tutter et al., 2001, Vleminckx et al., 1999). In this assay, activation of the canonical Wnt signalling throughout mouse ES cell differentiation, prevented induction of cardiac transcriptional regulators and blocked spontaneous contraction.

One of the genes that appeared to be reproducibly and reliably affected by all treatments was *Tbx5*. This gene has been suggested to be the beating gene (Takeuchi and Bruneau, 2009), that is a gene in the absence of which beating is unlikely to occur, or at least an essential gene for generation of beating cardiomyocytes (Ieda et al., 2010). Specifically, Takeuchi and Bruneau (2009) found that *Gata-4, Tbx5* and *Baf60c* (a subunit of the Swi/Snf-like BAF chromatin remodelling complex) were sufficient for differentiation of non-cardiogenic mesoderm to cardiomyocytes. *Nxk2.5*, although not part of the minimal set of factors that were required for cardiac differentiation in the work by Takeuchi and Bruneau (2009), was subsequently induced by the combinatorial activity of *Gata-4* and *Baf60c* (Takeuchi and Bruneau, 2009). Absence of *Tbx5* in this context did not allow beating foci to appear (Takeuchi and Bruneau, 2009). More recently, trans-differentiation of postnatal mouse cardiac and dermal fibroblasts into functional, beating cardiomyocytes was achieved by the combined activation of *Gata-4*, *Mef2c* and *Tbx5*, selected among 14 cardiomyocyte-inducing candidates (Ieda et al., 2010). There is an obvious discrepancy between the two studies: the former suggests *Gata-4, Tbx5* and *Baf60c* (Takeuchi and Bruneau, 2009) and the latter *Gata-4, Tbx5* and *Mef2c* (Ieda et al., 2010) as the minimal requirement for the cardiogenic program to occur. The main difference between the two systems is the differentiation status of the target cells: unspecified mesodermal cells (transient identity) in the former and fully differentiated fibroblasts (cardiac and dermal) in the latter. This difference may account for the distinct transcriptional requirements of the two systems, as it is not surprising that diverse starting material will respond differently to induction even by the same factors. Although a single master regulator of beating probably does not exist, and despite the fact that universal consensus on the minimal transcriptional requirement for

cardiac induction has not been reached, *Tbx5* has been shown to be an interesting candidate (Bruneau et al., 2001, Horb and Thomsen, 1999, Ieda et al., 2010, Liberatore et al., 2000, Takeuchi and Bruneau, 2009).

Another important early regulator of cardiogenesis, majorly affected in the current study, was *Islet1*. This gene was initially introduced as a marker of the secondary heart field (SHF) (Cai et al., 2003) but is nowadays considered an early cardiac transcription factor that controls, in a spatially and temporally specific way, the activation and activity of downstream cardiac genes in both PHF and SHF cells (Meilhac et al., 2004, Moretti et al., 2006). Its inhibition in most of the BIO-treated EB (d0-d2, d2-d5, d5-d7 and d9-d11 treatment groups) in this study indicates a severe compromise in the cardiogenic potential of the cells. Downregulation of *Isl1* after BIO treatment did not come as a surprise: β-catenin, which is stabilized after BIO treatment, has been shown to inhibit *Isl1* both *in vivo* and *in vitro* (Kwon et al., 2009). This downregulation has been associated with expansion of cardiac progenitor populations, which has however not been accompanied by increased presence of terminally differentiated cardiac cells; later on in the differentiation process the appearance of beating foci was severely compromised and so was the expression of cardiac sarcomeric genes, such as *Myh6, Myh7, Mlc2a, Mlc2v* (Kwon et al., 2009), similar to what is seen here. Interestingly, the two early BIO treatments (d0-d2 and d2-d5) did not affect atrial and ventricular cell fates differentially; they both significantly decreased the expression of *Mlc2v* and *Mlc2a*, markers of the two lineages respectively, at d11. The fact that early cardiac markers, such as *Gata-4* and *Nkx2.5*, were not severely affected by any of the BIO treatments indicates that initial specification of cardiac progenitors probably took place properly.

An indirect effect of BIO could also be related to the role that β-catenin plays in the cell membrane. There, it is found associated with adherens junctions in complexes with E-Cadherin and α-catenin, connecting the cytoskeleton of neighbouring cells (Drees et al., 2005, Yamada et al., 2005). The control of the dual functions of β-catenin in either cellular adhesion or in transcriptional regulation is of paramount importance for normal cellular function and is controlled by an array of factors (reviewed by Brembeck et al., 2006). Its regulation and stabilization by the Wnt pathway is one of them. Activated canonical Wnt signalling has been suggested to favour the nuclear function of β-catenin as a transcriptional co-activator in the expense of its membrane function (Gottardi and Gumbiner, 2004, Munemitsu et al., 1995). Therefore, hyper-activation of the canonical Wnt pathway by BIO in our system may have reinforced the

nuclear localization of β-catenin and have exhausted it from the cell membrane, affecting adhesion and communication between adjacent cells. Impaired communication between cardiomyocytes could affect spontaneous contraction, as it may inhibit signal transduction and cell coupling.

Currently, the canonical Wnt pathway is thought to have bi-phasic, stage-specific and antagonistic roles during cardiogenesis: early differentiation requires β-catenin signalling for the commitment of mesodermal cells into the cardiac lineage (Gadue et al., 2006, Lindsley et al., 2006, Wawrzak et al., 2007), while later in differentiation, proliferation and maturation of committed cardiomyocytes is inhibited by β-catenin (Naito et al., 2006). Similarly, fine-tuned regulation of canonical Wnt signals is required for hematopoietic stem cell self-renewal and differentiation (Naito et al., 2006). Activation of the canonical Wnt pathway in this assay did not produce a similar bi-phasic response: both early and late activation caused severe reduction in the cardiogenic potential of differentiating cells. The use of different cell culture systems and inhibitors/activators (general upstream ligands or inhibitors, downstream effectors) and the use or avoidance of serum may be the main reasons for the observed discrepancy. The timing of differentiation depends on the properties and growth requirements of each type of cells and is distinct for different cell lines. Of paramount importance is, also, the specific assay used for formation of EB: hanging drops, methylcellulose medium and low attachment dishes are only a few of the available methods (Dang et al., 2002, Mogi et al., 2009). The starting amount of cells that will form the EB is another essential determinant of the progression of cell differentiation. It has been suggested that the greater the initial amount of cells the more uniform and the more reliable the downstream processes are (Dang et al., 2002). In this study, 450 cells were set into each hanging drop for the formation of individual EB, similar to what Naito et al. (2006) used (Naito et al., 2006).

Importantly, in the current study, two different mouse cell lines were used: E14 ES cells and ES-D3 cells. They both responded similarly to BIO treatment at the time intervals examined, reinforcing the reliability and reproducibility of my findings. Moreover, in previous studies Wnt ligands (Wnt3a) and upstream inhibitors (Dkk-1, Fz8/Fc) of the canonical Wnt pathway were used, which may have a broad effect on the Wnt pathway, not only instructing canonical Wnt but also potentially non-canonical Wnt signalling (Caneparo et al., 2007). BIO, as an inhibitor of a downstream component of the canonical Wnt pathway (GSK3), is expected to act more selectively on the

canonical versus the non-canonical Wnt pathway, although as mentioned before, the Hedgehog pathway is likely to be affected as well.

In this study, upregulation of the canonical Wnt pathway when cells are still in hanging drops, greatly increased the presence of mesodermal cells but decreased the occurrence of beating, while in another study (Naito et al., 2006) early inhibition of β-catenin signalling did not affect mesoderm formation but abrogated cardiac differentiation. The canonical Wnt pathway has well-established and widely known roles in promoting mesodermal specification in many contexts (Gadue et al., 2006, Lekven et al., 2001, Lindsley et al., 2006, Wawrzak et al., 2007), reinforcing the reliability of our findings. The suggested late role of the canonical Wnt pathway agrees between the two studies with the presence of β-catenin being inhibitory for proliferation, maturation and expansion of cardiac cells. It is important to note at this point that although a bi-phasic response was not observed in the beating behaviour of the cells, a stage-specific response in the expression of some genes was noticed. Although not all differences were statistically significant it is worth mentioning the general trend of the gene expression profile of important genes. *Nkx2.5* and *Gata-4* showed decreased expression after d0-d2 treatment and increased expression after d2-d5 treatment, while *Tbx5* showed an increase and a decrease, respectively. Other key transcriptional regulators, though, did not share this response, possibly explaining the lack of enhanced cardiogenesis after the early activation of the canonical Wnt pathway. As explained before, *Isl1* may be an important factor affecting the expression of downstream cardiac genes.

Another interesting finding was the fact the d2-d5 BIO-treated EB contained significantly more cells at d5 than controls. The viability of the cells was not altered though, which suggests that the increased cell count arose from an increase in both dead and alive cells within each EB and that the cell death levels at that time were not severely affected. Such an effect is, therefore, possibly due to increased proliferation the first days of *in vitro* differentiation. This finding fits in with the current knowledge about β-catenin: downstream targets of the canonical Wnt cascade, such as *c-Myc*, *Lef-1* and *Tcf*, have been implicated with regulation of proliferation (Bernard and Eilers, 2006, Demeterco et al., 2002, Desbarats et al., 1996, Quasnichka et al., 2006) and activation of β-catenin itself has been shown to affect cellular proliferation (Adachi et al., 2007, Shang et al., 2004).

Additionally, activation of the canonical Wnt pathway has been shown to have the ability to prolong pluripotency and prevent differentiation (Anton et al., 2007, Sato et

al., 2004). Treatment with BIO in the current study had a similar effect: the three genes of the SON network (*Sox2, Oct-4* and *Nanog*) showed a considerable increase in their expression levels at d5 after the d0-d2 BIO treatment. This finding suggests that some of the cells within the EB still retain their stem cell identity at d5, a time when most, if not all, of the cells within the EB should have committed and started differentiating towards other cell lineages.

In vivo work carried out by Dr. Nicholas Child in our laboratory (unpulished) using BIO and Dkk-1 in zebrafish embryos, reinforced the findings of the current study. He found that addition of BIO at different time points during development of zebrafish embryos (during and around gastrulation) always caused a reduction in the total number of cardiomyocytes and considerable abnormalities in the morphology of the heart. He, just like in the work presented here, could not find a bi-phasic response similar to the one reported in the literature (Naito et al., 2006, Ueno et al., 2007).

Given the agreements and discrepancies described so far, it becomes clear that different cell assay systems that employ distinct experimental methods and varying analysis tools are difficult to amalgamate and directly compare. The current study highlights this issue and reinforces the notion that complementary *in vivo* models can prove invaluable in promoting and extending our knowledge from *in vitro* studies. Also, the use of more than one cell lines for confirmation of the obtained data is shown here to be beneficial.

6.9. Advantages and disadvantages of this study

Some important aspects of this study make it comprehensive, reliable and powerful. Two of its main advantages are its power and reproducibility. All of the beating experiments were repeated at least four independent times (some reaching even seven repetitions), with all showing the same pattern. There was no experiment throughout this study that did not agree with the data presented here.

Additionally, systematic statistical analysis was performed. Normality of the data was assessed individually at each occasion and statistical significance was examined using the appropriate parametric or non-parametric tests as required. This approach allowed for a thorough statistical analysis that did not rely on crude and often mistaken assumptions. Interpretation of the statistical differences, however, depends on the biological context, which should always be taken into account.

Another important and powerful asset of the current study was the assay itself. The hanging drop method that was used in the current work has been shown to be reliable, reproducible and consistent (Dang et al., 2002, Kurosawa, 2007), as discussed extensively in Section 5.11 (page 218). Additionally, the absence of serum in the cell differentiation culture system after d5 reinforced the establishment of a controlled environment, free of unknown confounding effects that may hinder unambiguous characterization of the differentiation process.

However, some aspects of the assay could be improved. The first is associated with the accurate measurement of the levels of β-catenin before and after activation of the canonical Wnt pathway by the pharmacological agent BIO. Although BIO has been extensively used as an upregulator of β-catenin in many different contexts (Manisastry et al., 2006, Martin et al., 2010, Meijer et al., 2003, Ueno et al., 2007), it is always advisable to assess the efficacy of the treatment. In this assay, the expression levels of *Lef-1* were used as an indication of the stabilization and increased transcriptional activity of β-catenin. This has been shown to be a reliable measure (Filali et al., 2002, Hovanes et al., 2001, Hovanes et al., 2000, Vadlamudi et al., 2005). Nevertheless, *Lef-1* is only one of the targets of β-catenin and although its activation is essential for further activation of downstream β-catenin targets through the β-catenin/TCF/Lef complex (Behrens et al., 1996, Huber et al., 1996, Roel et al., 2002, Seidensticker and Behrens, 2000), it is a relatively partial measure, possibly not accurately reflecting the fine fluctuations in the activity levels of β-catenin. A more direct method, like a lucipherase assay (TOPFlash, β-catenin-Fluc, β-catenin-CBG) that measures the transcriptional activity of β-catenin (Naik and Piwnica-Worms, 2007), could have been employed. The difficulty with the latter technique is the requirement for time-consuming transfections of various constructs, which is not always straightforward in stem cell culture. Analysis of the levels of β-catenin by western blotting, as performed in Chapter 5 for the levels of phospho-Jnk, would not have been useful. This is due to the fact that the levels of the protein are not necessarily affected by BIO; what is affected is its association with the APC/Axin/GSK3 inhibitory complex and its localization within the cell. Translocation of stabilized β-catenin from the cytoplasm to the nucleus has been used in the past as a measure of increased β-catenin signalling (Westfall et al., 2003). Immunohistochemistry experiments to identify this translocation were performed by other research group members with poor success, as it was difficult to assess the differences in staining between BIO-treated (increased nuclear staining) and untreated (mainly cytoplasmic staining) samples. Further optimization of the technique and improvement of the

imaging would probably meet the standards of previously published work (Westfall et al., 2003) and would reliably reveal activation of β-catenin signalling.

Another aspect of the assay that could be improved is associated with accurate counting of cardiomyocytes, involving FACS. Analysis of the suggested technique has been carried out in Section 5.10. With this approach, it would be possible to further elucidate how the process of cardiac specification, differentiation and expansion is affected by treatment with BIO and subsequent activation of the canonical Wnt pathway.

Additionally, as mentioned before, BIO, by inhibiting GSK3, not only activates the canonical Wnt pathway but also affects, to a lesser degree, the Hedgehog pathway (Li et al., 2007). Alternative or additional Wnt activators could have been used in this assay to confer more specificity to the pathway in question. However, most of the alternative options would be upstream activators of the pathway, which, due to their position, could potentially influence the non-canonical Wnt pathway as well. Overall, although other options were available, the most widely used and well-accepted downstream canonical Wnt activator remains BIO (Meijer et al., 2003).

Lastly, a multitude of other genes could have been used in the qPCR analysis, in order to identify possible changes in the expression profile and signature of BIO-treated cells. For example, neuronal markers (such as *Nestin* or *Otx1*) could have been used for characterization of ES-derived neuronal cells, which have been shown in the past to be antagonistic with cardiomyocytes in some contexts (Notarianni and Evans, 2006). Earlier and more global cardiac markers than the ones used, could have also been employed, such as *Mesp1* and *Mef2c*. *Mesp1*, as described in Section 1.3.2 (page 11), is considered the first pan-cardiac marker that is transiently expressed in mesodermal cells of cardiogenic potential (Bondue et al., 2008, Saga et al., 1999, Wu, 2008). Additional Wnt targets, of both the canonical and non-canonical Wnt pathway, could have, also, been studied. For example, Dkk-1, which is a known inhibitor of the canonical Wnt pathway (Bafico et al., 2001, Kawano and Kypta, 2003, Mao et al., 2001) is also a target of both the canonical Wnt (Gonzalez-Sancho et al., 2005) and the non-canonical Wnt/Jnk branches (Grotewold and Ruther, 2002b). Interestingly, Dkk-1 was, recently, found to activate the PCP pathway and regulate CE movements (Caneparo et al., 2007). It would have, thus, been an interesting candidate to look at, in order to elucidate the cross talk between the canonical and non-canonical Wnt pathway. Moreover, cell death and proliferation markers (such as c-Myc and cyclin-D2) could have been used in order to study the effect of activated β-catenin signalling in the survival of ES-derived cells.

Canonical Wnt signalling has been shown, in the past, to affect proliferation (Tseng et al., 2006).

6.10. Future work

In order to extend this work further a number of issues could be addressed and some experiments could be pursued. Firstly, it would be interesting to rescue the phenotype. This could be achieved by inhibiting the canonical Wnt pathway in parallel to its activation by BIO, in order to assess how specific the effect of the drug is; if complete rescue was observed then there would be good evidence to suggest that BIO acts solely or primarily through activation of the canonical Wnt pathway, while if the rescue was not complete or clear it would suggest that BIO may act, as discussed before, through other pathways as well. A caveat with this approach is the fact that GSK3 is downstream in the Wnt pathway and therefore, inhibition of the pathway by upstream molecules, such as Dkk-1 or Frizzled8/Fc (soluble Wnt antagonists) that are commonly used for this purpose, would possibly not completely counteract the effects of BIO. A good alternative candidate would be a dominant negative form of TCF4 that blocks transcription through β-catenin. This has, however, been shown to also affect Hedgehog signalling (Li et al., 2007).

Secondly, as described before, counting of the cardiomyocytes using FACS would further extend our understanding of how BIO and activation of the canonical Wnt pathway affect the formation of fully differentiated cardiac cells. It would also be of interest to study the morphology of individual cells within the EB in order to evaluate and analyse why they cannot initiate spontaneous contraction and how far in the cardiac differentiation lineage they have gone.

6.11. Summary and conclusion

Overall, in the work presented in this chapter I have shown that specific activation of the canonical Wnt pathway severely compromised the beating behaviour of differentiating ES cells. It is suggested that *Tbx5* and *Islet1*, important early cardiac regulators, are mediators of this effect as they were shown to be significantly and consistently inhibited under all conditions examined here. It is, also, important to note that in the current study there was no evidence of a positive effect of the canonical Wnt

signalling pathway on cardiogenesis, contradicting the current notion in the literature that suggests a bi-phasic and stage-specific role for this pathway during cardiac differentiation. My findings are in keeping with previous *in vivo* work carried out by other members of our research group, which showed that increase in Wnt/β-catenin signalling reduced the production of beating tissue in developing zebrafish embryo (Dr. Nicholas Child, unpublished).

In the next chapter, the findings from this chapter, studying the canonical Wnt pathway in differentiating mouse ES cells, will be discussed alongside the findings from previous chapters that focused on Jnk signalling, both in developing zebrafish embryos and in differentiating mouse ES cells. This will give us an insight into the role that the Wnt signalling network, as a whole, plays in cardiogenesis in different systems.

Chapter 7. Final discussion

7.1. Introduction

This thesis aimed at studying Jnk and canonical Wnt signalling in cardiogenesis. Jnk is a downstream effector of the non-canonical Wnt/PCP pathway, but it is also an important regulator of MAPK signalling. As both the Wnt and the MAPK pathways have been shown in the past to regulate heart development, it was hypothesized that Jnk might be an important mediator of cardiac differentiation, receiving input from Wnt and MAPK signals. Similarly, the canonical Wnt/β-catenin cascade has been shown to have essential roles during early and late cardiogenesis. Its role, however, has not been fully elucidated because of recent controversial reports. One of the goals of this study was to shed light on the controversy. The cross talk between Jnk and β-catenin was, also, of interest, as it has been suggested that the Wnt pathways (canonical and non-canonical) in fact work together, synergistically and/or antagonistically, and form a complex network that coordinates varied and even seemingly contradictory procedures.

Two models were used in this study: mouse embryonic stem (ES) cells and zebrafish embryos. Mouse ES cells, due to their pluripotency and their ability to differentiate into many cell types, provide a useful tool for the study of *in vitro* cardiogenesis. The events that lead from an undifferentiated naïve ES cell to a mesodermal cell, which will then further differentiate to a cardiac precursor and will finally form a cardiomyocyte, are thought to recapitulate at least some of the events that take place during induction, specification and differentiation of cardiomyocytes *in vivo*. ES cell-derived cardiomyocytes have been shown in the past to share many electrophysiological, morphological and genetic features with embryonic and postnatal cardiomyocytes (Boheler et al., 2002, Fijnvandraat et al., 2003, Hescheler et al., 1997, Hidaka et al., 2003, Sachinidis et al., 2003). *In vivo* zebrafish experimentation allowed for a comprehensive analysis of cardiogenesis-associated events at an organismal level, reflecting, not only cell-restricted processes, but also multifaceted tissue interactions. As cardiac development is not an isolated event, but depends upon movement of other tissues, responds to signalling cues from surrounding tissues and interacts with them, it is evident why its investigation in an animal is beneficial.

7.2. Summary of findings

The Jnk signalling pathway was investigated both *in vitro* and *in vivo* while the canonical Wnt pathway was examined *in vitro*. In summary, it was shown that in zebrafish there are four instead of the three *Jnk* genes that have been identified in mammals. Alternative splicing is expected to give rise to approximately 17 different protein-coding variants. Expression analysis of some of these variants showed differential timing and distribution, which possibly reflects distinct areas of activity (not further investigated here). Global inhibition of the kinase activity of jnk (inhibition of all isoforms in the whole embryo) at distinct time intervals during zebrafish embryonic development caused a range of defects. The formation of the ears and the eyes, as well as the patterning of the tail, were affected, but the most severely, reproducibly and frequently affected structure was the heart. The hearts of a significant percentage of gastrulation-inhibited (5.25-10 hpf) embryos were reversely looped (leftwards) and surrounded by pericardial oedema, while the hearts of a large number of segmentation-inhibited (10-22 hpf) embryos were unlooped, surrounded by oedema and had disturbed atrial-ventricular proportions. The proportions of the body (length and width) were also altered after jnk inhibition, causing a convergence extension (CE)-like phenotype.

Inhibition of the activity of Jnk in differentiating mouse ES cells also caused a cardiac-related phenotype: it significantly increased beating. It is still unclear whether the observed increase was due to enhanced cardiogenesis (more cells attaining a cardiac fate) or to improved communication and coordination between the cells resulting in enhanced signal propagation, although the evidence so far point to the latter. Temporal specific alterations of canonical Wnt targets after Jnk inhibition emphasized the need for investigation of the Wnt pathway as a network, examining both canonical and non-canonical contributions. For this reason, the effect of timely canonical Wnt activation in differentiating mouse ES cells was also examined. It was shown to delay differentiation, to inhibit the beating ability of cells and to reduce the expression of two essential cardiac regulators, *Tbx5* and *Islet1*. No positive effect of canonical Wnt activation on cardiogenesis was observed. All of these findings are further discussed below.

7.3. Manipulation of canonical Wnt and Jnk signalling

In the current study the canonical Wnt pathway and the Jnk signalling cascade were manipulated (activated and inhibited, respectively) in developing zebrafish embryos and

differentiating mouse ES cells, in order to establish their roles during cardiogenesis. Chemical inhibitors were used in order to achieve this purpose; BIO, was used as an activator of the canonical Wnt pathway and SP600125 as an inhibitor of Jnk signalling. The main advantage of chemical inhibition is the fact that it can be administered at specific intervals and for the required length of time during development, therefore, targeting specific processes. This important attribute is commonly counteracted by lack of specificity since closely related and similar proteins are likely to be targeted by the same chemicals. This more global effect can, however, also be a benefit for studies like the one presented here (the zebrafish study), whereby not all isoforms to be targeted are known and, therefore, design of specific inhibitors would be difficult if not impossible. Another disadvantage of chemical inhibitors is that since the activity of the protein is targeted (which makes the effects of the drug reversible) and not the producing gene, inefficiency (not achievement of the full effect) is more likely to be observed. In fact, such a phenomenon was observed to some extent in the ES cell work in the present study, whereby western blot analysis showed significant but not complete inhibition of phospho-Jnk. Knockout and knockdown technologies are expected to be more specific and efficient than chemical inhibition since they target specific genes, but in turn lack the ability for timely administration, temporal control and reversibility. Taken together, although alternatives were available for achieving the goals set in this study, the use of chemical inhibition was preferred because of its temporal amenability, which was of great interest here. Ideally, all experiments should be repeated and confirmed by using morpholino injections against specific genes or by establishing gene knockout strains.

7.4. Jnk signalling

Jnk signalling was the main focus of this thesis. In this section, the involvement of Jnk in the non-canonical Wnt and the MAPK cascade is discussed, along with potential cross talk with the canonical Wnt pathway.

7.4.1. Jnk acts in the Wnt network and in the MAPK pathway

Jnk is a kinase that belongs to the MAPK family and exerts its effects through signals relayed from the MAPK cascade and from the non-canonical Wnt pathway. Distinguishing the involvement of Jnk in either pathway is not straightforward in most

contexts, as overlapping domains of activity have been observed between the two pathways.

The *in vivo* work, presented in this study, revealed general body and specific heart abnormalities in developing zebrafish embryos after inhibition of jnk. These included low occurrence of eye and otic vesicle defects, alongside high prevalence body ratio disturbances and cardiac specification and morphogenesis defects. Gastrulation defects that may lead to a CE-like phenotype have been reported in both PCP and MAPK zebrafish mutants and morphants (Anastasaki et al., 2009, Hammerschmidt et al., 1996, Heisenberg et al., 2000, Jessen et al., 2002, Krens et al., 2008, Krens et al., 2006, Matsui et al., 2005, Park and Moon, 2002, Rauch et al., 1997, Schwarz-Romond et al., 2002, Seo et al., 2010, Solnica-Krezel et al., 1996, Topczewski et al., 2001, Zhu et al., 2008, Zhu et al., 2006). Also, abnormalities in the eyes and the otic vesicles have been previously observed in PCP mutants (Hammerschmidt et al., 1996, Heisenberg et al., 2000, Jessen et al., 2002, Park and Moon, 2002, Solnica-Krezel et al., 1996, Topczewski et al., 2001). Similar defects have not been reported in MAPK mutants and morphants but members of the MAPK family are known to be involved in head-associated morphogenesis (Acharya et al., 2011, Anastasaki et al., 2009, Furthauer et al., 2002, Rodriguez-Viciana et al., 2006, Snaar-Jagalska et al., 2003, Tidyman and Rauen, 2008, Tsang et al., 2004).

The heart defects observed in this study after Jnk inhibition were mainly associated with left-right patterning (of the body and subsequently of the heart), cardiac looping and atrial/ventricular fate specification and/or expansion. Members of the PCP pathway have been, recently, associated with establishment of the body left-right axis identities (Borovina et al., 2010, Guirao et al., 2010, Nonaka et al., 2005, Okada et al., 2005, Song et al., 2010). Members of the MAPK family have, in turn, been associated with regulation of the Nodal/Smad signalling cascade (Dennler et al., 2000, Hagemann and Blank, 2001), which is a major determinant of left-right patterning, both at the node and at the lateral plate mesoderm (LPM) (Ahmad et al., 2004, Baker et al., 2008, Brennan et al., 2002, Duboc et al., 2005, Kawasumi et al., 2011). Abnormalities in the initial left-right patterning are known to cause cardiac looping anomalies, including reverse looping and absence of looping (Bisgrove et al., 2000, Chen and Fishman, 2000a, Chen and Fishman, 2000b, Chen et al., 1997, Glickman and Yelon, 2002, Kathiriya and Srivastava, 2000, Yan et al., 1999), defects reminiscent of the jnk-inhibited phenotype observed here.

Since both pathways (Wnt and MAPK) have been shown to be active and to participate in zebrafish development and since inhibition of either has been individually shown to cause defects similar to the ones observed in this study, it is not possible to distinguish which pathway Jnk is mainly acting through in this context. It would not be surprising if Jnk responded to signals from both cascades during development, with each one potentially playing more important specific roles at discrete time intervals.

The *in vitro* work on Jnk (presented in Chapter 5) revealed increased beating, transient decrease in cell proliferation and late (at d11) loss of atrial gene expression. Jnk deficiency has been shown to cause severe defects in mesodermal and ectodermal development *in vitro* (Xu and Davis, 2010). P38 MAPK, another member of the MAPK family, has been shown to act as a switch between the neuronal and cardiac cell fate (inhibiting neurogenesis and promoting cardiomyogenesis) and to regulate the levels of apoptosis during ES cell culture (Aouadi et al., 2006). Erk/MAPK in turn, has been shown to promote differentiation of ES cells and to transiently induce proliferation (Marshall, 1995, Rose et al., 2010). Interestingly, in previous work (MSc report, submitted in August 2007) inhibition of other components of the non-canonical Wnt/PCP pathway (Rac and ROCK) on mouse E14 ES cells showed a similar increase in the contractile behaviour of differentiating ES cells, compared to what was observed after Jnk inhibition.

The findings and observations presented above highlight how interconnected the Wnt and MAPK pathways may be in the context of ES cell differentiation, causing similar and sometimes overlapping defects when disturbed. Although intriguing similarities were observed between the Jnk-, Rac- and ROCK-inhibited experiments, which would suggest a major contribution of the PCP pathway in the process of *in vitro* cardiogenesis, the involvement of MAPK cannot be excluded.

Taken together, with the tools used in the current study and with the information that is currently available in the literature, it has not been possible to distinguish the roles that Jnk plays in the context of the Wnt/PCP and the MAPK pathways. If this was required, additional work would have to be carried out, involving the use of inhibitors of other PCP and MAPK components, rescue experiments with effectors of both pathways and detection of the mRNA and protein levels as well as post-translational modifications (for example phosphorylation) of the molecules-targets involved.

7.4.2. Canonical and non-canonical Wnt/Jnk interplay

The interplay between canonical and non-canonical Wnt pathways was of interest in this study. It has been shown before that components of one pathway may affect signal relay through the other pathway and vice versa. Upstream in the two pathways, Wnt ligands, Frizzled receptors and Dishevelled proteins, although thought to participate in the canonical and non-canonical Wnt branches through different members of their families or through different domains of their proteins, have been shown to have a broader area of action than initially thought, at least in some contexts (Bryja et al., 2009, Caneparo et al., 2007, Davidson et al., 2005, Kestler and Kuhl, 2008, Maye et al., 2004, Mikels and Nusse, 2006, Tahinci et al., 2007, Tamai et al., 2000). Similarly, downstream effectors of the two pathways have been shown to participate, in some contexts, in both pathways (Esufali and Bapat, 2004, Kestler and Kuhl, 2008, Liao et al., 2006, Wu et al., 2008). In particular, Jnk has been shown in many publications to act in both the canonical and non-canonical Wnt pathways. Rac-1 and Jnk, PCP components, have been suggested to be important regulators of the translocation of β-catenin into the nucleus and activation of gene transcription through TCF (Esufali and Bapat, 2004, Wu et al., 2008). Activated by a canonical Wnt ligand (Wnt3a), Rac-1 in turn activates Jnk, which then acts on β-catenin (Wu et al., 2008). Inhibition of Jnk in this context had dramatic effects on Lef-1 luciferase exression (marker of canonical Wnt activation) (Wu et al., 2008). Another study showed that activation of c-Jun by Jnk, in response to signals from a Wnt-LRP5/6 complex in zebrafish, enhanced the formation of a Dishevelled/c-Jun/β-catenin/TCF complex in the nucleus that activated Wnt target gene transcription (Gan et al., 2008). In contrast, in mammalian cells, Jnk was shown to inhibit β-catenin-mediated gene transcription, while its inhibition in Xenopus embryos induced β-catenin target gene expression (Liao et al., 2006).

Initially, it was believed that the relation between the canonical and non-canonical Wnt pathways was antagonistic and thus, activation of one of them dictated inhibition of the other (Bryja et al., 2009, Caneparo et al., 2007, Davidson et al., 2005, Liao et al., 2006, Maye et al., 2004, Tahinci et al., 2007, Tamai et al., 2000, Zeng et al., 2005). However, nowadays with a multitude of studies having shown synergistic rather than antagonistic interactions between the two pathways (Esufali and Bapat, 2004, Gan et al., 2008, Upadhyay et al., 2008, Wu et al., 2008), it is believed that the outcome from the activation of one or the other pathway depends on the context and cannot be predicted (reviewed by Kestler and Kuhl, 2008).

In this study, severe disturbances in the canonical Wnt pathway were observed after Jnk inhibition but only late in differentiation, at d11, when the induction and specification of cardiac cells had already taken place. It is, therefore, unlikely that the detected alterations in the canonical Wnt pathway in this context had direct effects on the observed outcome. Nevertheless, it is noteworthy that subtle fluctuations in the activity of β-catenin signalling might not have been detected by the qPCR analysis performed here, because this did not include all days of differentiation and it did not look at other targets of the pathway. Given the studies published to date (some of which are presented above), Jnk could have undetected effects on the canonical Wnt pathway.

Taken together, although no major alterations in canonical Wnt-associated gene transcription (*Lef-1, Dkk-1*) were detected in this study during the early (and critical) stages of differentiation, it is possible, as suggested by numerous studies to date, that the Wnt/β-catenin pathway or at least some of its downstream targets are affected by SP600125 treatment. Although the published work so far points potentially to both activation and/or inhibition of canonical Wnt-mediated transcription after inhibition of Jnk, in the present study it is more likely that Jnk inhibition after SP600125 treatment caused a decrease in β-catenin signalling. This observation is based on the data from the BIO treatment (activation of canonical Wnt, Chapter 6) that showed decrease or even halt of beating.

7.5. Jnk signalling in cardiogenesis

Most of the cardiac defects observed in jnk-inhibited zebrafish embryos seem to be associated indirectly with the cardiogenic process. Looping defects are possibly associated with defective left-right patterning of the body that in turn disturbs the directionality of the jogging and looping processes and causes cardiac defects. Similarly, alterations in atrial and ventricular cell fates occurred when the drug (SP600125) was administered long after the specification events had taken place and had been completed. It was suggested that the observed changes in ventricular cell numbers were due to disturbances in proliferation levels rather than to defects in the specification process.

However, these indirect effects of SP600125 administration seem to have specific effects on the heart, although other organs were not investigated in much detail. The overall morphology of the developing embryos, though, was not severely affected so the

disturbances described above had, not exclusive, but probably more severe, effects on proper formation and morphogenesis of the heart.

In vitro, increased contractile behaviour of differentiating ES cells was observed after Jnk inhibition but this was not accompanied by a concomitant increase in the expression of cardiac genes. Also, the fact that this increase was observed even after late (d5-d11) SP600125 administration, when cells have already been irreversibly specified towards a cardiogenic fate, and the fact that cardiac Troponin-I staining showed a more clustered organization of beating cells after Jnk inhibition, support the idea that the observed enhancement in the beating ability of the cells is probably correlated not with enhanced cardiac specification but with alterations in the cellular conformation and organization of the beating cells.

Overall, both the *in vitro* and the *in vivo* data point to an extra-cardiac role of Jnk in heart differentiation. Further analysis of the cardiac phenotype of jnk-inhibited zebrafish embryos (looking at cell migration, cardiac function and cardiac cell specification) and of Jnk-inhibited differentiating mouse ES cells, would reveal the mechanism(s) through which Jnk exerts its effects in both contexts.

7.6. Canonical Wnt signalling in cardiogenesis

Canonical Wnt signalling has been shown to be an important determinant of cardiogenesis during early (Marvin et al., 2001, Schneider and Mercola, 2001) and late (Cohen et al. 2007) stages. In contrast to recently published studies (Naito et al., 2006, Ueno et al., 2007), *in vitro* data obtained in this study showed that activation of the canonical Wnt pathway, both at pre-beating and post-beating stages, had a consistently negative effect on ES-derived cardiogenesis, as identified by the reduction, or even absence, of the beating ability of the cells.

These findings are supported by previous work conducted in our research group by Dr. Nicholas Child on developing zebrafish embryos. Wnt/β-catenin was shown to negatively influence heart development throughout gastrulation. Specifically, abnormal cardiac morphology, reduced cardiomyocyte numbers and altered cell fates (more atrial cells and less ventricular cells) were observed. An extension of the *dhand* expression field rostrally and of the *nkx2.5* field caudally resulted in increased overlap of the cardiac field with the notochord, which has been shown in the past to be inhibitory for induction of cardiogenic mesoderm (Goldstein and Fishman, 1998, Serbedzija et al., 1998, Tzahor and Lassar, 2001).

Of note, in both studies no positive effect of activated canonical Wnt signalling was observed, at any time interval examined. Prevailing studies have suggested a bi-phasic and stage-specific role for canonical Wnt in cardiogenesis, promoting it at early stages and inhibiting it later in development (Naito et al., 2006, Ueno et al., 2007). The data obtained from this study contradict this idea. Interestingly, two more recent publications (Afouda et al., 2008, Wang et al., 2011) reinforce the traditional notion that β-catenin is inhibitory for cardiogenesis (Marvin et al., 2001, Schneider and Mercola, 2001). Afouda and colleagues (2008) showed that in Xenopus explants the canonical Wnt pathway causes suppression of cardiogenesis, at least in part, through inhibition of *Gata-4* (Afouda et al., 2008). In turn, Wang and colleagues (2010) used two mouse ES cell lines to show that timely inhibition of the canonical Wnt pathway (with Dkk-1 and XAV939) induced cardiomyogenesis (Wang et al., 2011). The work presented by Afouda and co-workers (2008) and Wang and colleagues (2010) emphasizes the fact that the conflict in the literature about the role that the canonical Wnt pathway plays during cardiogenesis remains unresolved (Afouda et al., 2008, Wang et al., 2011).

7.7. Conclusions

In summary, the aims of the current thesis were to establish the role of Jnk signalling during *in vivo* and *in vitro* cardiogenesis and to elucidate the temporal specific contribution of the canonical Wnt pathway during *in vitro* cardiac differentiation. It was hypothesized that inhibition of Jnk in developing zebrafish embryos and differentiating mouse ES cells would cause severe defects in cardiac induction and progression, as both non-canonical Wnt and MAPK pathways are known players in the cardiogenic process. Severe defects were, indeed, observed in zebrafish embryos after jnk inhibition during gastrulation and segmentation, including looping anomalies and ventricular cell expansion defects. However, in mouse ES cells inhibition of Jnk caused an increase in the occurrence of beating. Although more work needs to be carried out in order to fully elucidate the mechanism through which Jnk enhances beating in this context, there is evidence to suggest that this is not due to enhanced cardiogenesis (more cells attaining the cardiac fate) but to reorganization and clustering of the existing beating cells. The questions that have arisen from the differences between the *in vivo* and the *in vitro* models are where does the Jnk signal originate from, in which cells or tissues is its expression essential for induction of cardiogenesis and how does its inhibition produce

the observed phenotype. Answering these questions, which is not possible with the data obtained in this study, will probably shed more light in the underlying mechanism.

It was also hypothesized that manipulation of the canonical Wnt pathway would reveal stage-specific roles in cardiac development, both inhibiting or enhancing it, depending on the timing of the manipulation. Analysis of the beating pattern and the cardiac gene expression of differentiating mouse ES cells disproved this hypothesis and showed that activation of the Wnt/β-catenin pathway, irrespective of the timing of the treatment, severely and consistently decreased the beating occurrence of differentiating cells and the expression of major cardiac gene regulators. Further investigation is needed in order to fully elucidate the contradictory roles that have been suggested for the canonical Wnt pathway and to understand the differences observed between different systems and methods.

Chapter 8. Appendix

Genes	Forward sequence	Reverse Sequence
β-actin	GCTGGTCGTCGACAACGGCTC	CAAACATGATCTGGGTCATCTTTTC
Rps9	TGTTGACGCTAGACGAGAAGG	AATGAAGGATGGGATGTTCACC
Oct4	CACCATCTGTCGCTTCGAG	ACTCCACCTCACACGGTTCT
Nanog	AAGGCAGCCCTGATTCTTCT	GTGCTGAGCCCTTCTGAATC
Sox2	GCGGAGTGGAAACTTTTGTCC	CGGGAAGCGTGTACTTATCCTT
Brachyury	TGCTGCAGTCCCATGATAAC	TGTGCGTCAGTGGTGTGTAA
Goosecoid	ACCATCTTCACCGATGAGCAGC	CTTGGCTCGGCGGTTCTTAAAC
Hex	ACTACACGCACGCCCTACTC	ACTTGACCGCCTTTCCTTTT
Flk1	TTTGGCAAATACAACCCTTCAGA	GCAGAAGATACTGTCACCACC
CD31	GAGAGTGACAGCGGGGAGTA	GTGGTAAGTGATGGGTGCAG
Gata-4	TCAAACCAGAAAACGGAAGC	GTGGCATTGCTGGAGTTACC
Nkx2.5	CCACTCTCTGCTACCCACCT	CCAGGTTCAGGATGTCTTTGA
Tbx5	GGAGCCTGATTCCAAAGACA	TTCAGCCACAGTTCACGTTC
Islet-1	GTTTGTACGGGATCAAATGC	ATGCTGCGTTTCTTGTCCTT
MLC-2a	TCAGCTGCATTGACCAGAAC	AAGACGGTGAAGTTGATGGG
MLC-2v	AAAGAGGCTCCAGGTCCAAT	CCTCTCTGCTTGTGTGGTCA
cTroponin-T	GAGGAGGTGGTGGAGGAGTA	GGCTTCTTCATCAGGACCAA
Tnnt2	CAACATGATGCACTTTGGAGGGTAC	TCGCAGAACGTTGATTTCGTATTTC
Dkk-1	TCTGTCTGGCTTGCCGAAAG	TGTGGTCATTACCAAGGTTTTCA
Connexin-43	GAACACGGCAAGGTGAAGAT	GACGTGAGAGGAAGCAGTCC
Lef-1	TGTTTATCCCATCACGGGTGG	CATGGAAGTGTCGCCTGACAG
Jnk	AGCAGAAGCAAACGTGACAAC	CGCTTAGCATGGGTCTGATTC
c-Myc	CTGGATTTCCTTTGGGCGTT	TGGTGAAGTTCACGTTGAGGG
Cyclin-D2	TGGGCTTCAGCAGGATGATG	ACGGAACTGCTGCAGGCTGT

Table 8. 1: Sequences of mouse qPCR primer sequences. All primer sets were retrieved from previously published work. They were selected to span exon-exon boundaries, when possible, in order to avoid genomic DNA contamination.

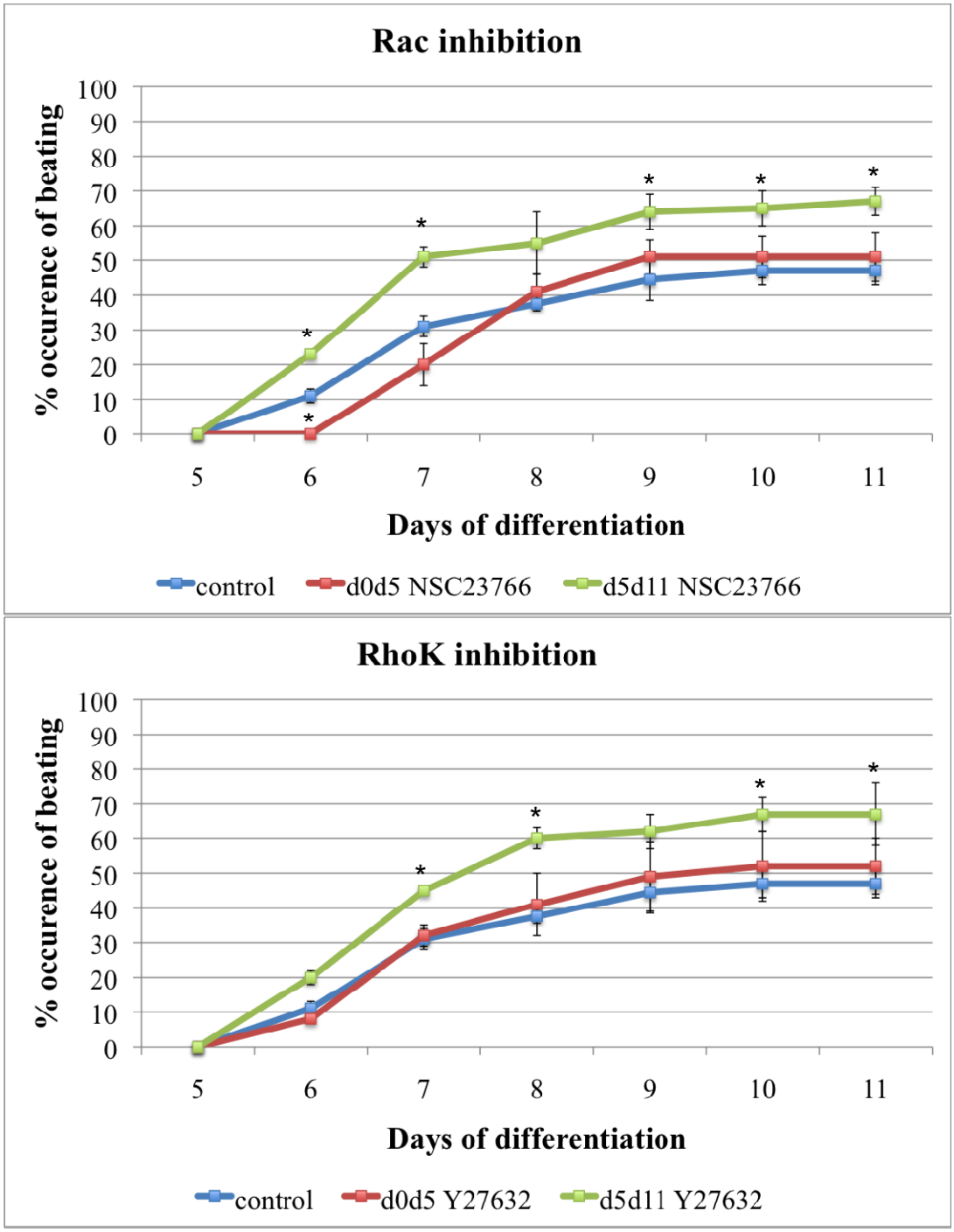

Figure 8. 1: Inhibition of Rac (with NSC23766) and ROCK (with Y27632) in differentiating E14 ES cells. In both cases late addition of the drug (d5-d11) caused significant activation of beating, while early drug administration (d0-d5) did not alter the beating behaviour of the cells. This work has been previously presented in my MSc report (submitted in August 2007). Statistical significance, shown with asterisks (*p<0.05) in the graph, was assessed using the non-parametric Mann Whitney test.

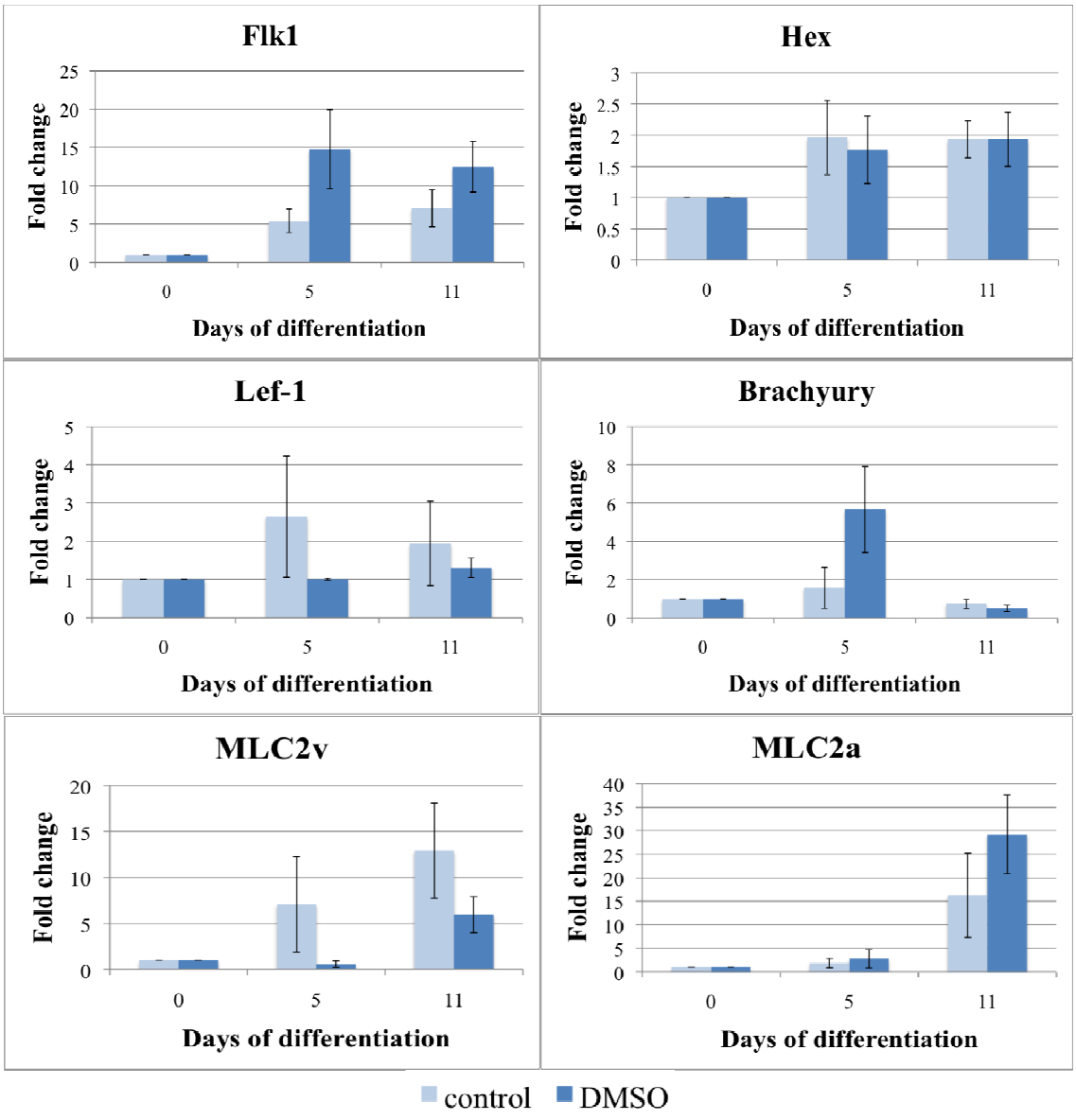

Figure 8. 2: qPCR analysis of differentiating E14 ES cells after DMSO treatment. The expression pattern of *Flk1, Hex, Lef-1, Brachyury, MLC2v* and *MLC2a* at days 0, 5 and 11 are shown here. The rest of the genes that were used as markers in this study are shown in Chapter 6, as their expression profile was slightly altered to that of DMSO-treated ES-D3 cells, presented in Chapter 5, and had to be discussed thoroughly. Statistical significance was assessed using one-way Anova testing, followed, when necessary by a 2-sided Dunnett test

9. References

Abu-Issa, R., Smyth, G., Smoak, I., Yamamura, K. and Meyers, E. N. (2002) 'Fgf8 is required for pharyngeal arch and cardiovascular development in the mouse', *Development,* 129, (19), pp. 4613-25.

Abu-Issa, R., Waldo, K. and Kirby, M. L. (2004) 'Heart fields: one, two or more?', *Dev Biol,* 272, (2), pp. 281-5.

Acharya, M., Huang, L., Fleisch, V. C., Allison, W. T. and Walter, M. A. (2011) 'A complex regulatory network of transcription factors critical for ocular development and disease', *Hum Mol Genet,* 20, (8), pp. 1610-24.

Ackermann, G. E. and Paw, B. H. (2003) 'Zebrafish: a genetic model for vertebrate organogenesis and human disorders', *Front Biosci,* 8, pp. d1227-53.

Adachi, K., Mirzadeh, Z., Sakaguchi, M., Yamashita, T., Nikolcheva, T., Gotoh, Y., Peltz, G., Gong, L., Kawase, T., Alvarez-Buylla, A., Okano, H. and Sawamoto, K. (2007) 'Beta-catenin signaling promotes proliferation of progenitor cells in the adult mouse subventricular zone', *Stem Cells,* 25, (11), pp. 2827-36.

Afouda, B. A., Martin, J., Liu, F., Ciau-Uitz, A., Patient, R. and Hoppler, S. (2008) 'GATA transcription factors integrate Wnt signalling during heart development', *Development,* 135, (19), pp. 3185-90.

Ahlgren, U., Pfaff, S. L., Jessell, T. M., Edlund, T. and Edlund, H. (1997) 'Independent requirement for ISL1 in formation of pancreatic mesenchyme and islet cells', *Nature,* 385, (6613), pp. 257-60.

Ahmad, F., Banerjee, S. K., Lage, M. L., Huang, X. N., Smith, S. H., Saba, S., Rager, J., Conner, D. A., Janczewski, A. M., Tobita, K., Tinney, J. P., Moskowitz, I. P., Perez-Atayde, A. R., Keller, B. B., Mathier, M. A., Shroff, S. G., Seidman, C. E. and Seidman, J. G. (2008) 'The role of cardiac troponin T quantity and function in cardiac development and dilated cardiomyopathy', *PLoS One,* 3, (7), pp. e2642.

Ahmad, N., Long, S. and Rebagliati, M. (2004) 'A southpaw joins the roster: the role of the zebrafish nodal-related gene southpaw in cardiac LR asymmetry', *Trends Cardiovasc Med,* 14, (2), pp. 43-9.

Ahn, D. and Ho, R. K. (2008) 'Tri-phasic expression of posterior Hox genes during development of pectoral fins in zebrafish: implications for the evolution of vertebrate paired appendages', *Dev Biol,* 322, (1), pp. 220-33.

Ai, D., Fu, X., Wang, J., Lu, M. F., Chen, L., Baldini, A., Klein, W. H. and Martin, J. F. (2007) 'Canonical Wnt signaling functions in second heart field to promote right ventricular growth', *Proc Natl Acad Sci U S A,* 104, (22), pp. 9319-24.

Akazawa, H. and Komuro, I. (2005) 'Cardiac transcription factor Csx/Nkx2-5: Its role in cardiac development and diseases', *Pharmacol Ther,* 107, (2), pp. 252-68.

Albalat, R., Baquero, M. and Minguillon, C. (2010) 'Identification and characterisation of the developmental expression pattern of tbx5b, a novel tbx5 gene in zebrafish', *Gene Expr Patterns,* 10, (1), pp. 24-30.

Albelda, S. M., Muller, W. A., Buck, C. A. and Newman, P. J. (1991) 'Molecular and cellular properties of PECAM-1 (endoCAM/CD31): a novel vascular cell-cell adhesion molecule', *J Cell Biol,* 114, (5), pp. 1059-68.

Amack, J. D. and Yost, H. J. (2004) 'The T box transcription factor no tail in ciliated cells controls zebrafish left-right asymmetry', *Curr Biol,* 14, (8), pp. 685-90.

Amati, B., Frank, S. R., Donjerkovic, D. and Taubert, S. (2001) 'Function of the c-Myc oncoprotein in chromatin remodeling and transcription', *Biochim Biophys Acta,* 1471, (3), pp. M135-45.

Amores, A., Force, A., Yan, Y. L., Joly, L., Amemiya, C., Fritz, A., Ho, R. K., Langeland, J., Prince, V., Wang, Y. L., Westerfield, M., Ekker, M. and Postlethwait, J. H. (1998) 'Zebrafish hox clusters and vertebrate genome evolution', *Science,* 282, (5394), pp. 1711-4.

Amura, C. R., Marek, L., Winn, R. A. and Heasley, L. E. (2005) 'Inhibited neurogenesis in JNK1-deficient embryonic stem cells', *Mol Cell Biol,* 25, (24), pp. 10791-802.

Anastasaki, C., Estep, A. L., Marais, R., Rauen, K. A. and Patton, E. E. (2009) 'Kinase-activating and kinase-impaired cardio-facio-cutaneous syndrome alleles have activity during zebrafish development and are sensitive to small molecule inhibitors', *Hum Mol Genet,* 18, (14), pp. 2543-54.

Andreka, P., Zang, J., Dougherty, C., Slepak, T. I., Webster, K. A. and Bishopric, N. H. (2001) 'Cytoprotection by Jun kinase during nitric oxide-induced cardiac myocyte apoptosis', *Circ Res,* 88, (3), pp. 305-12.

Antic, D., Stubbs, J. L., Suyama, K., Kintner, C., Scott, M. P. and Axelrod, J. D. (2010) 'Planar cell polarity enables posterior localization of nodal cilia and left-right axis determination during mouse and Xenopus embryogenesis', *PLoS One,* 5, (2), pp. e8999.

Anton, R., Kestler, H. A. and Kuhl, M. (2007) 'Beta-catenin signaling contributes to stemness and regulates early differentiation in murine embryonic stem cells', *FEBS Lett,* 581, (27), pp. 5247-54.

Aoki, Y., Niihori, T., Kawame, H., Kurosawa, K., Ohashi, H., Tanaka, Y., Filocamo, M., Kato, K., Suzuki, Y., Kure, S. and Matsubara, Y. (2005) 'Germline mutations in HRAS proto-oncogene cause Costello syndrome', *Nat Genet,* 37, (10), pp. 1038-40.

Aouadi, M., Binetruy, B., Caron, L., Le Marchand-Brustel, Y. and Bost, F. (2006) 'Role of MAPKs in development and differentiation: lessons from knockout mice', *Biochimie,* 88, (9), pp. 1091-8.

Arai, A., Yamamoto, K. and Toyama, J. (1997) 'Murine cardiac progenitor cells require visceral embryonic endoderm and primitive streak for terminal differentiation', *Dev Dyn,* 210, (3), pp. 344-53.

Arce, L., Yokoyama, N. N. and Waterman, M. L. (2006) 'Diversity of LEF/TCF action in development and disease', *Oncogene,* 25, (57), pp. 7492-504.

Arnold, S. J., Stappert, J., Bauer, A., Kispert, A., Herrmann, B. G. and Kemler, R. (2000) 'Brachyury is a target gene of the Wnt/beta-catenin signaling pathway', *Mech Dev,* 91, (1-2), pp. 249-58.

Asaoka, Y. and Nishina, H. (2010) 'Diverse physiological functions of MKK4 and MKK7 during early embryogenesis', *J Biochem,* 148, (4), pp. 393-401.

Aubert, J., Dunstan, H., Chambers, I. and Smith, A. (2002) 'Functional gene screening in embryonic stem cells implicates Wnt antagonism in neural differentiation', *Nat Biotechnol,* 20, (12), pp. 1240-5.

Augello, A., Kurth, T. B. and De Bari, C. (2010) 'Mesenchymal stem cells: a perspective from in vitro cultures to in vivo migration and niches', *Eur Cell Mater,* 20, pp. 121-33.

Aw, S. and Levin, M. (2008) 'What's left in asymmetry?', *Dev Dyn,* 237, (12), pp. 3453-63.

Bachiller, D., Klingensmith, J., Kemp, C., Belo, J. A., Anderson, R. M., May, S. R., McMahon, J. A., McMahon, A. P., Harland, R. M., Rossant, J. and De Robertis, E. M. (2000) 'The organizer factors Chordin and Noggin are required for mouse forebrain development', *Nature,* 403, (6770), pp. 658-61.

Baena-Lopez, L. A., Baonza, A. and Garcia-Bellido, A. (2005) 'The orientation of cell divisions determines the shape of Drosophila organs', *Curr Biol,* 15, (18), pp. 1640-4.

Bafico, A., Liu, G., Yaniv, A., Gazit, A. and Aaronson, S. A. (2001) 'Novel mechanism of Wnt signalling inhibition mediated by Dickkopf-1 interaction with LRP6/Arrow', *Nat Cell Biol,* 3, (7), pp. 683-6.

Bai, V. U., Cifuentes, E., Menon, M., Barrack, E. R. and Reddy, G. P. (2005) 'Androgen receptor regulates Cdc6 in synchronized LNCaP cells progressing from G1 to S phase', *J Cell Physiol,* 204, (2), pp. 381-7.

Bain, J., McLauchlan, H., Elliott, M. and Cohen, P. (2003) 'The specificities of protein kinase inhibitors: an update', *Biochem J,* 371, (Pt 1), pp. 199-204.

Baker, K., Holtzman, N. G. and Burdine, R. D. (2008) 'Direct and indirect roles for Nodal signaling in two axis conversions during asymmetric morphogenesis of the zebrafish heart', *Proc Natl Acad Sci U S A,* 105, (37), pp. 13924-9.

Bakkers, J., Kramer, C., Pothof, J., Quaedvlieg, N. E., Spaink, H. P. and Hammerschmidt, M. (2004) 'Has2 is required upstream of Rac1 to govern dorsal migration of lateral cells during zebrafish gastrulation', *Development,* 131, (3), pp. 525-37.

Balakirev, E. S. and Ayala, F. J. (2003) 'Pseudogenes: are they "junk" or functional DNA?', *Annu Rev Genet,* 37, pp. 123-51.

Bamforth, S. D., Braganca, J., Farthing, C. R., Schneider, J. E., Broadbent, C., Michell, A. C., Clarke, K., Neubauer, S., Norris, D., Brown, N. A., Anderson, R. H. and Bhattacharya, S. (2004) 'Cited2 controls left-right patterning and heart development through a Nodal-Pitx2c pathway', *Nat Genet,* 36, (11), pp. 1189-96.

Bao, Z. Z., Bruneau, B. G., Seidman, J. G., Seidman, C. E. and Cepko, C. L. (1999) 'Regulation of chamber-specific gene expression in the developing heart by Irx4', *Science,* 283, (5405), pp. 1161-4.

Bardwell, L. and Shah, K. (2006) 'Analysis of mitogen-activated protein kinase activation and interactions with regulators and substrates', *Methods,* 40, (3), pp. 213-23.

Barker, N. and Clevers, H. (2006) 'Mining the Wnt pathway for cancer therapeutics', *Nat Rev Drug Discov,* 5, (12), pp. 997-1014.

Barolo, S. (2006) 'Transgenic Wnt/TCF pathway reporters: all you need is Lef?', *Oncogene,* 25, (57), pp. 7505-11.

Barr, R. K., Kendrick, T. S. and Bogoyevitch, M. A. (2002) 'Identification of the critical features of a small peptide inhibitor of JNK activity', *J Biol Chem,* 277, (13), pp. 10987-97.

Barrow, J. R. (2006) 'Wnt/PCP signaling: a veritable polar star in establishing patterns of polarity in embryonic tissues', *Semin Cell Dev Biol,* 17, (2), pp. 185-93.

Basson, C. T., Bachinsky, D. R., Lin, R. C., Levi, T., Elkins, J. A., Soults, J., Grayzel, D., Kroumpouzou, E., Traill, T. A., Leblanc-Straceski, J., Renault, B., Kucherlapati, R., Seidman, J. G. and Seidman, C. E. (1997) 'Mutations in human TBX5 [corrected] cause limb and cardiac malformation in Holt-Oram syndrome', *Nat Genet,* 15, (1), pp. 30-5.

Bedford, F. K., Ashworth, A., Enver, T. and Wiedemann, L. M. (1993) 'HEX: a novel homeobox gene expressed during haematopoiesis and conserved between mouse and human', *Nucleic Acids Res,* 21, (5), pp. 1245-9.

Begemann, G. and Ingham, P. W. (2000) 'Developmental regulation of Tbx5 in zebrafish embryogenesis', *Mech Dev,* 90, (2), pp. 299-304.

Behrens, J., von Kries, J. P., Kuhl, M., Bruhn, L., Wedlich, D., Grosschedl, R. and Birchmeier, W. (1996) 'Functional interaction of beta-catenin with the transcription factor LEF-1', *Nature,* 382, (6592), pp. 638-42.

Belema Bedada, F., Technau, A., Ebelt, H., Schulze, M. and Braun, T. (2005) 'Activation of myogenic differentiation pathways in adult bone marrow-derived stem cells', *Mol Cell Biol,* 25, (21), pp. 9509-19.

Bennett, B. L., Sasaki, D. T., Murray, B. W., O'Leary, E. C., Sakata, S. T., Xu, W., Leisten, J. C., Motiwala, A., Pierce, S., Satoh, Y., Bhagwat, S. S., Manning, A. M. and Anderson, D. W. (2001) 'SP600125, an anthrapyrazolone inhibitor of Jun N-terminal kinase', *Proc Natl Acad Sci U S A,* 98, (24), pp. 13681-6.

Berger, I. R., Buschbeck, M., Bange, J. and Ullrich, A. (2005) 'Identification of a transcriptionally active hVH-5 pseudogene on 10q22.2', *Cancer Genet Cytogenet,* 159, (2), pp. 155-9.

Bernard, S. and Eilers, M. (2006) 'Control of cell proliferation and growth by Myc proteins', *Results Probl Cell Differ,* 42, pp. 329-42.

Binetruy, B., Heasley, L., Bost, F., Caron, L. and Aouadi, M. (2007) 'Concise review: regulation of embryonic stem cell lineage commitment by mitogen-activated protein kinases', *Stem Cells,* 25, (5), pp. 1090-5.

Biondi, R. M. and Nebreda, A. R. (2003) 'Signalling specificity of Ser/Thr protein kinases through docking-site-mediated interactions', *Biochem J,* 372, (Pt 1), pp. 1-13.

Bisgrove, B. W., Essner, J. J. and Yost, H. J. (2000) 'Multiple pathways in the midline regulate concordant brain, heart and gut left-right asymmetry', *Development,* 127, (16), pp. 3567-79.

Bockman, D. E. and Kirby, M. L. (1984) 'Dependence of thymus development on derivatives of the neural crest', *Science,* 223, (4635), pp. 498-500.

Bode, A. M. and Dong, Z. (2007) 'The functional contrariety of JNK', *Mol Carcinog,* 46, (8), pp. 591-8.

Bodor, G. S., Porterfield, D., Voss, E. M., Smith, S. and Apple, F. S. (1995) 'Cardiac troponin-I is not expressed in fetal and healthy or diseased adult human skeletal muscle tissue', *Clin Chem,* 41, (12 Pt 1), pp. 1710-5.

Boeuf, H., Hauss, C., Graeve, F. D., Baran, N. and Kedinger, C. (1997) 'Leukemia inhibitory factor-dependent transcriptional activation in embryonic stem cells', *J Cell Biol,* 138, (6), pp. 1207-17.

Bogoyevitch, M. A. (2006) 'The isoform-specific functions of the c-Jun N-terminal Kinases (JNKs): differences revealed by gene targeting', *Bioessays,* 28, (9), pp. 923-34.

Bogoyevitch, M. A. and Arthur, P. G. (2008) 'Inhibitors of c-Jun N-terminal kinases: JuNK no more?', *Biochim Biophys Acta,* 1784, (1), pp. 76-93.

Bogoyevitch, M. A., Boehm, I., Oakley, A., Ketterman, A. J. and Barr, R. K. (2004) 'Targeting the JNK MAPK cascade for inhibition: basic science and therapeutic potential', *Biochim Biophys Acta,* 1697, (1-2), pp. 89-101.

Bogoyevitch, M. A. and Kobe, B. (2006) 'Uses for JNK: the many and varied substrates of the c-Jun N-terminal kinases', *Microbiol Mol Biol Rev,* 70, (4), pp. 1061-95.

Boheler, K. R., Czyz, J., Tweedie, D., Yang, H. T., Anisimov, S. V. and Wobus, A. M. (2002) 'Differentiation of pluripotent embryonic stem cells into cardiomyocytes', *Circ Res,* 91, (3), pp. 189-201.

Boncinelli, E. and Mallamaci, A. (1995) 'Homeobox genes in vertebrate gastrulation', *Curr Opin Genet Dev,* 5, (5), pp. 619-27.

Bondue, A., Lapouge, G., Paulissen, C., Semeraro, C., Iacovino, M., Kyba, M. and Blanpain, C. (2008) 'Mesp1 acts as a master regulator of multipotent cardiovascular progenitor specification', *Cell Stem Cell,* 3, (1), pp. 69-84.

Borovina, A., Superina, S., Voskas, D. and Ciruna, B. (2010) 'Vangl2 directs the posterior tilting and asymmetric localization of motile primary cilia', *Nat Cell Biol,* 12, (4), pp. 407-12.

Bouchard, C., Thieke, K., Maier, A., Saffrich, R., Hanley-Hyde, J., Ansorge, W., Reed, S., Sicinski, P., Bartek, J. and Eilers, M. (1999) 'Direct induction of cyclin D2 by Myc contributes to cell cycle progression and sequestration of p27', *EMBO J,* 18, (19), pp. 5321-33.

Boureux, A., Vignal, E., Faure, S. and Fort, P. (2007) 'Evolution of the Rho family of ras-like GTPases in eukaryotes', *Mol Biol Evol,* 24, (1), pp. 203-16.

Boutros, M., Paricio, N., Strutt, D. I. and Mlodzik, M. (1998) 'Dishevelled activates JNK and discriminates between JNK pathways in planar polarity and wingless signaling', *Cell,* 94, (1), pp. 109-18.

Brade, T., Gessert, S., Kuhl, M. and Pandur, P. (2007) 'The amphibian second heart field: Xenopus islet-1 is required for cardiovascular development', *Dev Biol,* 311, (2), pp. 297-310.

Brembeck, F. H., Rosario, M. and Birchmeier, W. (2006) 'Balancing cell adhesion and Wnt signaling, the key role of beta-catenin', *Curr Opin Genet Dev,* 16, (1), pp. 51-9.

Brennan, J., Lu, C. C., Norris, D. P., Rodriguez, T. A., Beddington, R. S. and Robertson, E. J. (2001) 'Nodal signalling in the epiblast patterns the early mouse embryo', *Nature,* 411, (6840), pp. 965-9.

Brennan, J., Norris, D. P. and Robertson, E. J. (2002) 'Nodal activity in the node governs left-right asymmetry', *Genes Dev,* 16, (18), pp. 2339-44.

Brennan, J. and Skarnes, W. C. (1999) 'Gene trapping in mouse embryonic stem cells', *Methods Mol Biol,* 97, pp. 123-38.

Brenner, C., Deplus, R., Didelot, C., Loriot, A., Vire, E., De Smet, C., Gutierrez, A., Danovi, D., Bernard, D., Boon, T., Pelicci, P. G., Amati, B., Kouzarides, T., de Launoit, Y., Di Croce, L. and Fuks, F. (2005) 'Myc represses transcription through recruitment of DNA methyltransferase corepressor', *EMBO J,* 24, (2), pp. 336-46.

Bromham, L. and Penny, D. (2003) 'The modern molecular clock', *Nat Rev Genet,* 4, (3), pp. 216-24.

Bruce, S. J., Gardiner, B. B., Burke, L. J., Gongora, M. M., Grimmond, S. M. and Perkins, A. C. (2007) 'Dynamic transcription programs during ES cell differentiation towards mesoderm in serum versus serum-freeBMP4 culture', *BMC Genomics,* 8, pp. 365.

Bruneau, B. G. (2005) 'Developmental biology: tiny brakes for a growing heart', *Nature,* 436, (7048), pp. 181-2.

Bruneau, B. G., Bao, Z. Z., Tanaka, M., Schott, J. J., Izumo, S., Cepko, C. L., Seidman, J. G. and Seidman, C. E. (2000) 'Cardiac expression of the ventricle-specific homeobox gene Irx4 is modulated by Nkx2-5 and dHand', *Dev Biol,* 217, (2), pp. 266-77.

Bruneau, B. G., Nemer, G., Schmitt, J. P., Charron, F., Robitaille, L., Caron, S., Conner, D. A., Gessler, M., Nemer, M., Seidman, C. E. and Seidman, J. G. (2001) 'A murine model of Holt-Oram syndrome defines roles of the T-box transcription factor Tbx5 in cardiogenesis and disease', *Cell,* 106, (6), pp. 709-21.

Bruno, W. J., Socci, N. D. and Halpern, A. L. (2000) 'Weighted neighbor joining: a likelihood-based approach to distance-based phylogeny reconstruction', *Mol Biol Evol,* 17, (1), pp. 189-97.

Bryja, V., Andersson, E. R., Schambony, A., Esner, M., Bryjova, L., Biris, K. K., Hall, A. C., Kraft, B., Cajanek, L., Yamaguchi, T. P., Buckingham, M. and Arenas, E. (2009) 'The extracellular domain of Lrp5/6 inhibits noncanonical Wnt signaling in vivo', *Mol Biol Cell,* 20, (3), pp. 924-36.

Buckingham, M., Meilhac, S. and Zaffran, S. (2005) 'Building the mammalian heart from two sources of myocardial cells', *Nat Rev Genet,* 6, (11), pp. 826-35.

Burch, J. B. (2005) 'Regulation of GATA gene expression during vertebrate development', *Semin Cell Dev Biol,* 16, (1), pp. 71-81.
Cai, C. L., Liang, X., Shi, Y., Chu, P. H., Pfaff, S. L., Chen, J. and Evans, S. (2003) 'Isl1 identifies a cardiac progenitor population that proliferates prior to differentiation and contributes a majority of cells to the heart', *Dev Cell,* 5, (6), pp. 877-89.
Cameron, S. J., Malik, S., Akaike, M., Lerner-Marmarosh, N., Yan, C., Lee, J. D., Abe, J. and Yang, J. (2003) 'Regulation of epidermal growth factor-induced connexin 43 gap junction communication by big mitogen-activated protein kinase1/ERK5 but not ERK1/2 kinase activation', *J Biol Chem,* 278, (20), pp. 18682-8.
Caneparo, L., Huang, Y. L., Staudt, N., Tada, M., Ahrendt, R., Kazanskaya, O., Niehrs, C. and Houart, C. (2007) 'Dickkopf-1 regulates gastrulation movements by coordinated modulation of Wnt/beta catenin and Wnt/PCP activities, through interaction with the Dally-like homolog Knypek', *Genes Dev,* 21, (4), pp. 465-80.
Capdevila, J., Vogan, K. J., Tabin, C. J. and Izpisua Belmonte, J. C. (2000) 'Mechanisms of left-right determination in vertebrates', *Cell,* 101, (1), pp. 9-21.
Carta, C., Pantaleoni, F., Bocchinfuso, G., Stella, L., Vasta, I., Sarkozy, A., Digilio, C., Palleschi, A., Pizzuti, A., Grammatico, P., Zampino, G., Dallapiccola, B., Gelb, B. D. and Tartaglia, M. (2006) 'Germline missense mutations affecting KRAS Isoform B are associated with a severe Noonan syndrome phenotype', *Am J Hum Genet,* 79, (1), pp. 129-35.
Cartwright, P., McLean, C., Sheppard, A., Rivett, D., Jones, K. and Dalton, S. (2005) 'LIF/STAT3 controls ES cell self-renewal and pluripotency by a Myc-dependent mechanism', *Development,* 132, (5), pp. 885-96.
Casal, J., Lawrence, P. A. and Struhl, G. (2006) 'Two separate molecular systems, Dachsous/Fat and Starry night/Frizzled, act independently to confer planar cell polarity', *Development,* 133, (22), pp. 4561-72.
Cavodeassi, F., Carreira-Barbosa, F., Young, R. M., Concha, M. L., Allende, M. L., Houart, C., Tada, M. and Wilson, S. W. (2005) 'Early stages of zebrafish eye formation require the coordinated activity of Wnt11, Fz5, and the Wnt/beta-catenin pathway', *Neuron,* 47, (1), pp. 43-56.
Chang, L., Jones, Y., Ellisman, M. H., Goldstein, L. S. and Karin, M. (2003) 'JNK1 is required for maintenance of neuronal microtubules and controls phosphorylation of microtubule-associated proteins', *Dev Cell,* 4, (4), pp. 521-33.
Chapman, S. C., Brown, R., Lees, L., Schoenwolf, G. C. and Lumsden, A. (2004) 'Expression analysis of chick Wnt and frizzled genes and selected inhibitors in early chick patterning', *Dev Dyn,* 229, (3), pp. 668-76.
Charron, F. and Nemer, M. (1999) 'GATA transcription factors and cardiac development', *Semin Cell Dev Biol,* 10, (1), pp. 85-91.
Charron, F., Paradis, P., Bronchain, O., Nemer, G. and Nemer, M. (1999) 'Cooperative interaction between GATA-4 and GATA-6 regulates myocardial gene expression', *Mol Cell Biol,* 19, (6), pp. 4355-65.
Chazaud, C. and Rossant, J. (2006) 'Disruption of early proximodistal patterning and AVE formation in Apc mutants', *Development,* 133, (17), pp. 3379-87.
Chen, J. N. and Fishman, M. C. (2000a) 'Genetic dissection of heart development', *Ernst Schering Res Found Workshop*, (29), pp. 107-22.
Chen, J. N. and Fishman, M. C. (2000b) 'Genetics of heart development', *Trends Genet,* 16, (9), pp. 383-8.
Chen, S. and Kimelman, D. (2000) 'The role of the yolk syncytial layer in germ layer patterning in zebrafish', *Development,* 127, (21), pp. 4681-9.

Chen, J. N., van Eeden, F. J., Warren, K. S., Chin, A., Nusslein-Volhard, C., Haffter, P. and Fishman, M. C. (1997) 'Left-right pattern of cardiac BMP4 may drive asymmetry of the heart in zebrafish', *Development,* 124, (21), pp. 4373-82.

Chien, K. R., Knowlton, K. U., Zhu, H. and Chien, S. (1991) 'Regulation of cardiac gene expression during myocardial growth and hypertrophy: molecular studies of an adaptive physiologic response', *FASEB J,* 5, (15), pp. 3037-46.

Chin, A. J., Tsang, M. and Weinberg, E. S. (2000) 'Heart and gut chiralities are controlled independently from initial heart position in the developing zebrafish', *Dev Biol,* 227, (2), pp. 403-21.

Choukroun, G., Hajjar, R., Fry, S., del Monte, F., Haq, S., Guerrero, J. L., Picard, M., Rosenzweig, A. and Force, T. (1999) 'Regulation of cardiac hypertrophy in vivo by the stress-activated protein kinases/c-Jun NH(2)-terminal kinases', *J Clin Invest,* 104, (4), pp. 391-8.

Chow, C. W., Rincon, M., Cavanagh, J., Dickens, M. and Davis, R. J. (1997) 'Nuclear accumulation of NFAT4 opposed by the JNK signal transduction pathway', *Science,* 278, (5343), pp. 1638-41.

Christoffels, V. M., Habets, P. E., Franco, D., Campione, M., de Jong, F., Lamers, W. H., Bao, Z. Z., Palmer, S., Biben, C., Harvey, R. P. and Moorman, A. F. (2000) 'Chamber formation and morphogenesis in the developing mammalian heart', *Dev Biol,* 223, (2), pp. 266-78.

Chu, W. M., Ostertag, D., Li, Z. W., Chang, L., Chen, Y., Hu, Y., Williams, B., Perrault, J. and Karin, M. (1999) 'JNK2 and IKKbeta are required for activating the innate response to viral infection', *Immunity,* 11, (6), pp. 721-31.

Ciruna, B., Jenny, A., Lee, D., Mlodzik, M. and Schier, A. F. (2006) 'Planar cell polarity signalling couples cell division and morphogenesis during neurulation', *Nature,* 439, (7073), pp. 220-4.

Cohen, E. D., Wang, Z., Lepore, J. J., Lu, M. M., Taketo, M. M., Epstein, D. J. and Morrisey, E. E. (2007) 'Wnt/beta-catenin signaling promotes expansion of Isl-1-positive cardiac progenitor cells through regulation of FGF signaling', *J Clin Invest,* 117, (7), pp. 1794-804.

Collignon, J., Varlet, I. and Robertson, E. J. (1996) 'Relationship between asymmetric nodal expression and the direction of embryonic turning', *Nature,* 381, (6578), pp. 155-8.

Collodi, P., Kamei, Y., Sharps, A., Weber, D. and Barnes, D. (1992) 'Fish embryo cell cultures for derivation of stem cells and transgenic chimeras', *Mol Mar Biol Biotechnol,* 1, (4-5), pp. 257-65.

Cordray, P. and Satterwhite, D. J. (2005) 'TGF-beta induces novel Lef-1 splice variants through a Smad-independent signaling pathway', *Dev Dyn,* 232, (4), pp. 969-78.

Cowling, V. H. and Cole, M. D. (2007) 'Turning the tables: Myc activates Wnt in breast cancer', *Cell Cycle,* 6, (21), pp. 2625-7.

Cowling, V. H., D'Cruz, C. M., Chodosh, L. A. and Cole, M. D. (2007) 'c-Myc transforms human mammary epithelial cells through repression of the Wnt inhibitors DKK1 and SFRP1', *Mol Cell Biol,* 27, (14), pp. 5135-46.

Curtin, J. A., Quint, E., Tsipouri, V., Arkell, R. M., Cattanach, B., Copp, A. J., Henderson, D. J., Spurr, N., Stanier, P., Fisher, E. M., Nolan, P. M., Steel, K. P., Brown, S. D., Gray, I. C. and Murdoch, J. N. (2003) 'Mutation of Celsr1 disrupts planar polarity of inner ear hair cells and causes severe neural tube defects in the mouse', *Curr Biol,* 13, (13), pp. 1129-33.

Dang, S. M., Kyba, M., Perlingeiro, R., Daley, G. Q. and Zandstra, P. W. (2002) 'Efficiency of embryoid body formation and hematopoietic development from embryonic stem cells in different culture systems', *Biotechnol Bioeng,* 78, (4), pp. 442-53.

Dani, C., Smith, A. G., Dessolin, S., Leroy, P., Staccini, L., Villageois, P., Darimont, C. and Ailhaud, G. (1997) 'Differentiation of embryonic stem cells into adipocytes in vitro', *J Cell Sci,* 110 (Pt 11), pp. 1279-85.

Das, M., Jiang, F., Sluss, H. K., Zhang, C., Shokat, K. M., Flavell, R. A. and Davis, R. J. (2007) 'Suppression of p53-dependent senescence by the JNK signal transduction pathway', *Proc Natl Acad Sci U S A,* 104, (40), pp. 15759-64.

Davidson, G., Wu, W., Shen, J., Bilic, J., Fenger, U., Stannek, P., Glinka, A. and Niehrs, C. (2005) 'Casein kinase 1 gamma couples Wnt receptor activation to cytoplasmic signal transduction', *Nature,* 438, (7069), pp. 867-72.

Davidson, S. M. and Morange, M. (2000) 'Hsp25 and the p38 MAPK pathway are involved in differentiation of cardiomyocytes', *Dev Biol,* 218, (2), pp. 146-60.

Davis, R. J. (2000) 'Signal transduction by the JNK group of MAP kinases', *Cell,* 103, (2), pp. 239-52.

de Alboran, I. M., O'Hagan, R. C., Gartner, F., Malynn, B., Davidson, L., Rickert, R., Rajewsky, K., DePinho, R. A. and Alt, F. W. (2001) 'Analysis of C-MYC function in normal cells via conditional gene-targeted mutation', *Immunity,* 14, (1), pp. 45-55.

de Pater, E., Clijsters, L., Marques, S. R., Lin, Y. F., Garavito-Aguilar, Z. V., Yelon, D. and Bakkers, J. (2009) 'Distinct phases of cardiomyocyte differentiation regulate growth of the zebrafish heart', *Development,* 136, (10), pp. 1633-41.

De, S. K., Chen, L. H., Stebbins, J. L., Machleidt, T., Riel-Mehan, M., Dahl, R., Chen, V., Yuan, H., Barile, E., Emdadi, A., Murphy, R. and Pellecchia, M. (2009a) 'Discovery of 2-(5-nitrothiazol-2-ylthio)benzo[d]thiazoles as novel c-Jun N-terminal kinase inhibitors', *Bioorg Med Chem,* 17, (7), pp. 2712-7.

De, S. K., Stebbins, J. L., Chen, L. H., Riel-Mehan, M., Machleidt, T., Dahl, R., Yuan, H., Emdadi, A., Barile, E., Chen, V., Murphy, R. and Pellecchia, M. (2009b) 'Design, synthesis, and structure-activity relationship of substrate competitive, selective, and in vivo active triazole and thiadiazole inhibitors of the c-Jun N-terminal kinase', *J Med Chem,* 52, (7), pp. 1943-52.

Deacon, T., Dinsmore, J., Costantini, L. C., Ratliff, J. and Isacson, O. (1998) 'Blastula-stage stem cells can differentiate into dopaminergic and serotonergic neurons after transplantation', *Exp Neurol,* 149, (1), pp. 28-41.

Dell'Era, P., Ronca, R., Coco, L., Nicoli, S., Metra, M. and Presta, M. (2003) 'Fibroblast growth factor receptor-1 is essential for in vitro cardiomyocyte development', *Circ Res,* 93, (5), pp. 414-20.

Demeterco, C., Itkin-Ansari, P., Tyrberg, B., Ford, L. P., Jarvis, R. A. and Levine, F. (2002) 'c-Myc controls proliferation versus differentiation in human pancreatic endocrine cells', *J Clin Endocrinol Metab,* 87, (7), pp. 3475-85.

Denicourt, C., Legault, P., McNabb, F. A. and Rassart, E. (2008) 'Human and mouse cyclin D2 splice variants: transforming activity and subcellular localization', *Oncogene,* 27, (9), pp. 1253-62.

Dennler, S., Andre, J., Alexaki, I., Li, A., Magnaldo, T., ten Dijke, P., Wang, X. J., Verrecchia, F. and Mauviel, A. (2007) 'Induction of sonic hedgehog mediators by transforming growth factor-beta: Smad3-dependent activation of Gli2 and Gli1 expression in vitro and in vivo', *Cancer Res,* 67, (14), pp. 6981-6.

Dennler, S., Prunier, C., Ferrand, N., Gauthier, J. M. and Atfi, A. (2000) 'c-Jun inhibits transforming growth factor beta-mediated transcription by repressing Smad3 transcriptional activity', *J Biol Chem,* 275, (37), pp. 28858-65.

Derijard, B., Hibi, M., Wu, I. H., Barrett, T., Su, B., Deng, T., Karin, M. and Davis, R. J. (1994) 'JNK1: a protein kinase stimulated by UV light and Ha-Ras that binds and phosphorylates the c-Jun activation domain', *Cell,* 76, (6), pp. 1025-37.

Desbarats, L., Schneider, A., Muller, D., Burgin, A. and Eilers, M. (1996) 'Myc: a single gene controls both proliferation and apoptosis in mammalian cells', *Experientia,* 52, (12), pp. 1123-9.

Ding, L., Liang, X. G., Hu, Y., Zhu, D. Y. and Lou, Y. J. (2008) 'Involvement of p38MAPK and reactive oxygen species in icariin-induced cardiomyocyte differentiation of murine embryonic stem cells in vitro', *Stem Cells Dev,* 17, (4), pp. 751-60.

Doetschman, T. C., Eistetter, H., Katz, M., Schmidt, W. and Kemler, R. (1985) 'The in vitro development of blastocyst-derived embryonic stem cell lines: formation of visceral yolk sac, blood islands and myocardium', *J Embryol Exp Morphol,* 87, pp. 27-45.

Dong, C., Yang, D. D., Wysk, M., Whitmarsh, A. J., Davis, R. J. and Flavell, R. A. (1998) 'Defective T cell differentiation in the absence of Jnk1', *Science,* 282, (5396), pp. 2092-5.

Dorin, D., Alano, P., Boccaccio, I., Ciceron, L., Doerig, C., Sulpice, R. and Parzy, D. (1999) 'An atypical mitogen-activated protein kinase (MAPK) homologue expressed in gametocytes of the human malaria parasite Plasmodium falciparum. Identification of a MAPK signature', *J Biol Chem,* 274, (42), pp. 29912-20.

Dougherty, C. J., Kubasiak, L. A., Prentice, H., Andreka, P., Bishopric, N. H. and Webster, K. A. (2002) 'Activation of c-Jun N-terminal kinase promotes survival of cardiac myocytes after oxidative stress', *Biochem J,* 362, (Pt 3), pp. 561-71.

Drab, M., Haller, H., Bychkov, R., Erdmann, B., Lindschau, C., Haase, H., Morano, I., Luft, F. C. and Wobus, A. M. (1997) 'From totipotent embryonic stem cells to spontaneously contracting smooth muscle cells: a retinoic acid and db-cAMP in vitro differentiation model', *FASEB J,* 11, (11), pp. 905-15.

Dravid, G., Ye, Z., Hammond, H., Chen, G., Pyle, A., Donovan, P., Yu, X. and Cheng, L. (2005) 'Defining the role of Wnt/beta-catenin signaling in the survival, proliferation, and self-renewal of human embryonic stem cells', *Stem Cells,* 23, (10), pp. 1489-501.

Drees, F., Pokutta, S., Yamada, S., Nelson, W. J. and Weis, W. I. (2005) 'Alpha-catenin is a molecular switch that binds E-cadherin-beta-catenin and regulates actin-filament assembly', *Cell,* 123, (5), pp. 903-15.

Duboc, V., Rottinger, E., Lapraz, F., Besnardeau, L. and Lepage, T. (2005) 'Left-right asymmetry in the sea urchin embryo is regulated by nodal signaling on the right side', *Dev Cell,* 9, (1), pp. 147-58.

Edgar, A. J. (2002) 'The human L-threonine 3-dehydrogenase gene is an expressed pseudogene', *BMC Genet,* 3, pp. 18.

Eferl, R., Sibilia, M., Hilberg, F., Fuchsbichler, A., Kufferath, I., Guertl, B., Zenz, R., Wagner, E. F. and Zatloukal, K. (1999) 'Functions of c-Jun in liver and heart development', *J Cell Biol,* 145, (5), pp. 1049-61.

Efron, B., Halloran, E. and Holmes, S. (1996) 'Bootstrap confidence levels for phylogenetic trees', *Proc Natl Acad Sci U S A,* 93, (23), pp. 13429-34.

Eilers, M. (1999) 'Control of cell proliferation by Myc family genes', *Mol Cells,* 9, (1), pp. 1-6.

Eisen, J. S. and Smith, J. C. (2008) 'Controlling morpholino experiments: don't stop making antisense', *Development,* 135, (10), pp. 1735-43.

Eisenberg, C. A. and Eisenberg, L. M. (1999) 'WNT11 promotes cardiac tissue formation of early mesoderm', *Dev Dyn,* 216, (1), pp. 45-58.

Eisenberg, C. A., Gourdie, R. G. and Eisenberg, L. M. (1997) 'Wnt-11 is expressed in early avian mesoderm and required for the differentiation of the quail mesoderm cell line QCE-6', *Development,* 124, (2), pp. 525-36.

Eisenberg, L. M. (2002) 'Belief vs. scientific observation: the curious story of the precardiac mesoderm', *Anat Rec,* 266, (4), pp. 194-7.
Eisenberg, L. M. and Eisenberg, C. A. (2006) 'Wnt signal transduction and the formation of the myocardium', *Dev Biol,* 293, (2), pp. 305-15.
Ekker, S. C., McGrew, L. L., Lai, C. J., Lee, J. J., von Kessler, D. P., Moon, R. T. and Beachy, P. A. (1995) 'Distinct expression and shared activities of members of the hedgehog gene family of Xenopus laevis', *Development,* 121, (8), pp. 2337-47.
Ellies, D. L., Stock, D. W., Hatch, G., Giroux, G., Weiss, K. M. and Ekker, M. (1997) 'Relationship between the genomic organization and the overlapping embryonic expression patterns of the zebrafish dlx genes', *Genomics,* 45, (3), pp. 580-90.
Ema, M., Takahashi, S. and Rossant, J. (2006) 'Deletion of the selection cassette, but not cis-acting elements, in targeted Flk1-lacZ allele reveals Flk1 expression in multipotent mesodermal progenitors', *Blood,* 107, (1), pp. 111-7.
Ennos, A. R. (2006) *Statistical and data handling skills in biology.* Pearson: New York.
Episkopou, V., Arkell, R., Timmons, P. M., Walsh, J. J., Andrew, R. L. and Swan, D. (2001) 'Induction of the mammalian node requires Arkadia function in the extraembryonic lineages', *Nature,* 410, (6830), pp. 825-30.
Eriksson, M. and Leppa, S. (2002) 'Mitogen-activated protein kinases and activator protein 1 are required for proliferation and cardiomyocyte differentiation of P19 embryonal carcinoma cells', *J Biol Chem,* 277, (18), pp. 15992-6001.
Erter, C. E., Solnica-Krezel, L. and Wright, C. V. (1998) 'Zebrafish nodal-related 2 encodes an early mesendodermal inducer signaling from the extraembryonic yolk syncytial layer', *Dev Biol,* 204, (2), pp. 361-72.
Essner, J. J., Amack, J. D., Nyholm, M. K., Harris, E. B. and Yost, H. J. (2005) 'Kupffer's vesicle is a ciliated organ of asymmetry in the zebrafish embryo that initiates left-right development of the brain, heart and gut', *Development,* 132, (6), pp. 1247-60.
Essner, J. J., Vogan, K. J., Wagner, M. K., Tabin, C. J., Yost, H. J. and Brueckner, M. (2002) 'Conserved function for embryonic nodal cilia', *Nature,* 418, (6893), pp. 37-8.
Esufali, S. and Bapat, B. (2004) 'Cross-talk between Rac1 GTPase and dysregulated Wnt signaling pathway leads to cellular redistribution of beta-catenin and TCF/LEF-mediated transcriptional activation', *Oncogene,* 23, (50), pp. 8260-71.
Evans, M. J. and Kaufman, M. H. (1981) 'Establishment in culture of pluripotential cells from mouse embryos', *Nature,* 292, (5819), pp. 154-6.
Evans, S. M., Yan, W., Murillo, M. P., Ponce, J. and Papalopulu, N. (1995) 'tinman, a Drosophila homeobox gene required for heart and visceral mesoderm specification, may be represented by a family of genes in vertebrates: XNkx-2.3, a second vertebrate homologue of tinman', *Development,* 121, (11), pp. 3889-99.
Evans, T. (2009) 'Fishing for a WNT-PGE2 link: beta-catenin is caught in the stem cell net-work', *Cell Stem Cell,* 4, (4), pp. 280-2.
Fagotto, F., Jho, E., Zeng, L., Kurth, T., Joos, T., Kaufmann, C. and Costantini, F. (1999) 'Domains of axin involved in protein-protein interactions, Wnt pathway inhibition, and intracellular localization', *J Cell Biol,* 145, (4), pp. 741-56.
Fan, C., Liu, M. and Wang, Q. (2003) 'Functional analysis of TBX5 missense mutations associated with Holt-Oram syndrome', *J Biol Chem,* 278, (10), pp. 8780-5.
Fan, L., Crodian, J., Liu, X., Alestrom, A., Alestrom, P. and Collodi, P. (2004) 'Zebrafish embryo cells remain pluripotent and germ-line competent for multiple passages in culture', *Zebrafish,* 1, (1), pp. 21-6.

Fanto, M., Weber, U., Strutt, D. I. and Mlodzik, M. (2000) 'Nuclear signaling by Rac and Rho GTPases is required in the establishment of epithelial planar polarity in the Drosophila eye', *Curr Biol,* 10, (16), pp. 979-88.
Feijoo, C. G., Onate, M. G., Milla, L. A. and Palma, V. A. (2011) 'Sonic hedgehog (Shh)-Gli signaling controls neural progenitor cell division in the developing tectum in zebrafish', *Eur J Neurosci,* 33, (4), pp. 589-98.
Feldman, B., Gates, M. A., Egan, E. S., Dougan, S. T., Rennebeck, G., Sirotkin, H. I., Schier, A. F. and Talbot, W. S. (1998) 'Zebrafish organizer development and germ-layer formation require nodal-related signals', *Nature,* 395, (6698), pp. 181-5.
Felsenstein, J. (1981) 'Evolutionary trees from DNA sequences: a maximum likelihood approach', *J Mol Evol,* 17, (6), pp. 368-76.
Felsenstein, J. (1996) 'Inferring phylogenies from protein sequences by parsimony, distance, and likelihood methods', *Methods Enzymol,* 266, pp. 418-27.
Felsenstein, J. (2001) 'Taking variation of evolutionary rates between sites into account in inferring phylogenies', *J Mol Evol,* 53, (4-5), pp. 447-55.
Ferrandi, C., Ballerio, R., Gaillard, P., Giachetti, C., Carboni, S., Vitte, P. A., Gotteland, J. P. and Cirillo, R. (2004) 'Inhibition of c-Jun N-terminal kinase decreases cardiomyocyte apoptosis and infarct size after myocardial ischemia and reperfusion in anaesthetized rats', *Br J Pharmacol,* 142, (6), pp. 953-60.
Fijnvandraat, A. C., van Ginneken, A. C., de Boer, P. A., Ruijter, J. M., Christoffels, V. M., Moorman, A. F. and Lekanne Deprez, R. H. (2003) 'Cardiomyocytes derived from embryonic stem cells resemble cardiomyocytes of the embryonic heart tube', *Cardiovasc Res,* 58, (2), pp. 399-409.
Filali, M., Cheng, N., Abbott, D., Leontiev, V. and Engelhardt, J. F. (2002) 'Wnt-3A/beta-catenin signaling induces transcription from the LEF-1 promoter', *J Biol Chem,* 277, (36), pp. 33398-410.
Firulli, A. B., McFadden, D. G., Lin, Q., Srivastava, D. and Olson, E. N. (1998) 'Heart and extra-embryonic mesodermal defects in mouse embryos lacking the bHLH transcription factor Hand1', *Nat Genet,* 18, (3), pp. 266-70.
Fleming, T. P., Pratt, H. P. and Braude, P. R. (1987) 'The use of mouse preimplantation embryos for quality control of culture reagents in human in vitro fertilization programs: a cautionary note', *Fertil Steril,* 47, (5), pp. 858-60.
Foley, A. C., Gupta, R. W., Guzzo, R. M., Korol, O. and Mercola, M. (2006) 'Embryonic heart induction', *Ann N Y Acad Sci,* 1080, pp. 85-96.
Foley, A. C. and Mercola, M. (2005) 'Heart induction by Wnt antagonists depends on the homeodomain transcription factor Hex', *Genes Dev,* 19, (3), pp. 387-96.
Frank, D. U., Fotheringham, L. K., Brewer, J. A., Muglia, L. J., Tristani-Firouzi, M., Capecchi, M. R. and Moon, A. M. (2002) 'An Fgf8 mouse mutant phenocopies human 22q11 deletion syndrome', *Development,* 129, (19), pp. 4591-603.
Fujii, R., Yamashita, S., Hibi, M. and Hirano, T. (2000) 'Asymmetric p38 activation in zebrafish: its possible role in symmetric and synchronous cleavage', *J Cell Biol,* 150, (6), pp. 1335-48.
Funke, B., Edelmann, L., McCain, N., Pandita, R. K., Ferreira, J., Merscher, S., Zohouri, M., Cannizzaro, L., Shanske, A. and Morrow, B. E. (1999) 'Der(22) syndrome and velo-cardio-facial syndrome/DiGeorge syndrome share a 1.5-Mb region of overlap on chromosome 22q11', *Am J Hum Genet,* 64, (3), pp. 747-58.
Furthauer, M., Lin, W., Ang, S. L., Thisse, B. and Thisse, C. (2002) 'Sef is a feedback-induced antagonist of Ras/MAPK-mediated FGF signalling', *Nat Cell Biol,* 4, (2), pp. 170-4.
Gadue, P., Huber, T. L., Paddison, P. J. and Keller, G. M. (2006) 'Wnt and TGF-beta signaling are required for the induction of an in vitro model of primitive streak

formation using embryonic stem cells', *Proc Natl Acad Sci U S A,* 103, (45), pp. 16806-11.
Gage, P. J., Suh, H. and Camper, S. A. (1999) 'Dosage requirement of Pitx2 for development of multiple organs', *Development,* 126, (20), pp. 4643-51.
Galceran, J., Farinas, I., Depew, M. J., Clevers, H. and Grosschedl, R. (1999) 'Wnt3a-/--like phenotype and limb deficiency in Lef1(-/-)Tcf1(-/-) mice', *Genes Dev,* 13, (6), pp. 709-17.
Gan, X. Q., Wang, J. Y., Xi, Y., Wu, Z. L., Li, Y. P. and Li, L. (2008) 'Nuclear Dvl, c-Jun, beta-catenin, and TCF form a complex leading to stabilization of beta-catenin-TCF interaction', *J Cell Biol,* 180, (6), pp. 1087-100.
Gao, C. and Chen, Y. G. (2010) 'Dishevelled: The hub of Wnt signaling', *Cell Signal,* 22, (5), pp. 717-27.
Gao, M., Labuda, T., Xia, Y., Gallagher, E., Fang, D., Liu, Y. C. and Karin, M. (2004) 'Jun turnover is controlled through JNK-dependent phosphorylation of the E3 ligase Itch', *Science,* 306, (5694), pp. 271-5.
Garg, V., Kathiriya, I. S., Barnes, R., Schluterman, M. K., King, I. N., Butler, C. A., Rothrock, C. R., Eapen, R. S., Hirayama-Yamada, K., Joo, K., Matsuoka, R., Cohen, J. C. and Srivastava, D. (2003) 'GATA4 mutations cause human congenital heart defects and reveal an interaction with TBX5', *Nature,* 424, (6947), pp. 443-7.
Garriock, R. J., D'Agostino, S. L., Pilcher, K. C. and Krieg, P. A. (2005) 'Wnt11-R, a protein closely related to mammalian Wnt11, is required for heart morphogenesis in Xenopus', *Dev Biol,* 279, (1), pp. 179-92.
Garrity, D. M., Childs, S. and Fishman, M. C. (2002) 'The heartstrings mutation in zebrafish causes heart/fin Tbx5 deficiency syndrome', *Development,* 129, (19), pp. 4635-45.
Garry, D. J. and Olson, E. N. (2006) 'A common progenitor at the heart of development', *Cell,* 127, (6), pp. 1101-4.
Gaspard, N., Bouschet, T., Herpoel, A., Naeije, G., van den Ameele, J. and Vanderhaeghen, P. (2009) 'Generation of cortical neurons from mouse embryonic stem cells', *Nat Protoc,* 4, (10), pp. 1454-63.
Gaunt, S. J., Blum, M. and De Robertis, E. M. (1993) 'Expression of the mouse goosecoid gene during mid-embryogenesis may mark mesenchymal cell lineages in the developing head, limbs and body wall', *Development,* 117, (2), pp. 769-78.
Gerits, N., Kostenko, S. and Moens, U. (2007) 'In vivo functions of mitogen-activated protein kinases: conclusions from knock-in and knock-out mice', *Transgenic Res,* 16, (3), pp. 281-314.
Gettings, M., Serman, F., Rousset, R., Bagnerini, P., Almeida, L. and Noselli, S. (2010) 'JNK signalling controls remodelling of the segment boundary through cell reprogramming during Drosophila morphogenesis', *PLoS Biol,* 8, (6), pp. e1000390.
Gianakopoulos, P. J. and Skerjanc, I. S. (2005) 'Hedgehog signaling induces cardiomyogenesis in P19 cells', *J Biol Chem,* 280, (22), pp. 21022-8.
Gilbert, S. F. (2003) *Developmental biology.* Sinauer Associates: Sunderland, Mass.
Gissel, C., Doss, M. X., Hippler-Altenburg, R., Hescheler, J. and Sachinidis, A. (2006) 'Generation and characterization of cardiomyocytes under serum-free conditions', *Methods Mol Biol,* 330, pp. 191-219.
Glickman, N. S. and Yelon, D. (2002) 'Cardiac development in zebrafish: coordination of form and function', *Semin Cell Dev Biol,* 13, (6), pp. 507-13.

Glinka, A., Wu, W., Delius, H., Monaghan, A. P., Blumenstock, C. and Niehrs, C. (1998) 'Dickkopf-1 is a member of a new family of secreted proteins and functions in head induction', *Nature,* 391, (6665), pp. 357-62.

Goldman, B. I. and Wurzel, J. (1992) 'Effects of subcultivation and culture medium on differentiation of human fetal cardiac myocytes', *In Vitro Cell Dev Biol,* 28A, (2), pp. 109-19.

Goldmuntz, E., Bamford, R., Karkera, J. D., dela Cruz, J., Roessler, E. and Muenke, M. (2002) 'CFC1 mutations in patients with transposition of the great arteries and double-outlet right ventricle', *Am J Hum Genet,* 70, (3), pp. 776-80.

Goldstein, A. M. and Fishman, M. C. (1998) 'Notochord regulates cardiac lineage in zebrafish embryos', *Dev Biol,* 201, (2), pp. 247-52.

Gonzalez-Sancho, J. M., Aguilera, O., Garcia, J. M., Pendas-Franco, N., Pena, C., Cal, S., Garcia de Herreros, A., Bonilla, F. and Munoz, A. (2005) 'The Wnt antagonist DICKKOPF-1 gene is a downstream target of beta-catenin/TCF and is downregulated in human colon cancer', *Oncogene,* 24, (6), pp. 1098-103.

Goode, D. K., Callaway, H. A., Cerda, G. A., Lewis, K. E. and Elgar, G. (2011) 'Minor change, major difference: divergent functions of highly conserved cis-regulatory elements subsequent to whole genome duplication events', *Development,* 138, (5), pp. 879-84.

Goodrich, L. V. and Strutt, D. (2011) 'Principles of planar polarity in animal development', *Development,* 138, (10), pp. 1877-92.

Gottardi, C. J. and Gumbiner, B. M. (2004) 'Distinct molecular forms of beta-catenin are targeted to adhesive or transcriptional complexes', *J Cell Biol,* 167, (2), pp. 339-49.

Graichen, R., Xu, X., Braam, S. R., Balakrishnan, T., Norfiza, S., Sieh, S., Soo, S. Y., Tham, S. C., Mummery, C., Colman, A., Zweigerdt, R. and Davidson, B. P. (2008) 'Enhanced cardiomyogenesis of human embryonic stem cells by a small molecular inhibitor of p38 MAPK', *Differentiation,* 76, (4), pp. 357-70.

Grandori, C., Cowley, S. M., James, L. P. and Eisenman, R. N. (2000) 'The Myc/Max/Mad network and the transcriptional control of cell behavior', *Annu Rev Cell Dev Biol,* 16, pp. 653-99.

Granot, I., Bechor, E., Barash, A. and Dekel, N. (2002) 'Connexin43 in rat oocytes: developmental modulation of its phosphorylation', *Biol Reprod,* 66, (3), pp. 568-73.

Grimes, A. C. and Kirby, M. L. (2009) 'The outflow tract of the heart in fishes: anatomy, genes and evolution', *J Fish Biol,* 74, (5), pp. 983-1036.

Grotewold, L. and Ruther, U. (2002a) 'Bmp, Fgf and Wnt signalling in programmed cell death and chondrogenesis during vertebrate limb development: the role of Dickkopf-1', *Int J Dev Biol,* 46, (7), pp. 943-7.

Grotewold, L. and Ruther, U. (2002b) 'The Wnt antagonist Dickkopf-1 is regulated by Bmp signaling and c-Jun and modulates programmed cell death', *EMBO J,* 21, (5), pp. 966-75.

Grunwald, D. J. and Eisen, J. S. (2002) 'Headwaters of the zebrafish -- emergence of a new model vertebrate', *Nat Rev Genet,* 3, (9), pp. 717-24.

Guindon, S. and Gascuel, O. (2003) 'A simple, fast, and accurate algorithm to estimate large phylogenies by maximum likelihood', *Syst Biol,* 52, (5), pp. 696-704.

Guirao, B., Meunier, A., Mortaud, S., Aguilar, A., Corsi, J. M., Strehl, L., Hirota, Y., Desoeuvre, A., Boutin, C., Han, Y. G., Mirzadeh, Z., Cremer, H., Montcouquiol, M., Sawamoto, K. and Spassky, N. (2010) 'Coupling between hydrodynamic forces and planar cell polarity orients mammalian motile cilia', *Nat Cell Biol,* 12, (4), pp. 341-50.

Guo, N., Hawkins, C. and Nathans, J. (2004) 'Frizzled6 controls hair patterning in mice', *Proc Natl Acad Sci U S A,* 101, (25), pp. 9277-81.
Guo, N., Mogues, T., Weremowicz, S., Morton, C. C. and Sastry, K. N. (1998) 'The human ortholog of rhesus mannose-binding protein-A gene is an expressed pseudogene that localizes to chromosome 10', *Mamm Genome,* 9, (3), pp. 246-9.
Gupta, S., Barrett, T., Whitmarsh, A. J., Cavanagh, J., Sluss, H. K., Derijard, B. and Davis, R. J. (1996) 'Selective interaction of JNK protein kinase isoforms with transcription factors', *EMBO J,* 15, (11), pp. 2760-70.
Gupta, S., Campbell, D., Derijard, B. and Davis, R. J. (1995) 'Transcription factor ATF2 regulation by the JNK signal transduction pathway', *Science,* 267, (5196), pp. 389-93.
Gupta, S. and Davis, R. J. (1994) 'MAP kinase binds to the NH2-terminal activation domain of c-Myc', *FEBS Lett,* 353, (3), pp. 281-5.
Habas, R., Dawid, I. B. and He, X. (2003) 'Coactivation of Rac and Rho by Wnt/Frizzled signaling is required for vertebrate gastrulation', *Genes Dev,* 17, (2), pp. 295-309.
Hagemann, C. and Blank, J. L. (2001) 'The ups and downs of MEK kinase interactions', *Cell Signal,* 13, (12), pp. 863-75.
Hallaq, H., Pinter, E., Enciso, J., McGrath, J., Zeiss, C., Brueckner, M., Madri, J., Jacobs, H. C., Wilson, C. M., Vasavada, H., Jiang, X. and Bogue, C. W. (2004) 'A null mutation of Hhex results in abnormal cardiac development, defective vasculogenesis and elevated Vegfa levels', *Development,* 131, (20), pp. 5197-209.
Hamada, H., Meno, C., Watanabe, D. and Saijoh, Y. (2002) 'Establishment of vertebrate left-right asymmetry', *Nat Rev Genet,* 3, (2), pp. 103-13.
Hamblet, N. S., Lijam, N., Ruiz-Lozano, P., Wang, J., Yang, Y., Luo, Z., Mei, L., Chien, K. R., Sussman, D. J. and Wynshaw-Boris, A. (2002) 'Dishevelled 2 is essential for cardiac outflow tract development, somite segmentation and neural tube closure', *Development,* 129, (24), pp. 5827-38.
Hammerlein, A., Weiske, J. and Huber, O. (2005) 'A second protein kinase CK1-mediated step negatively regulates Wnt signalling by disrupting the lymphocyte enhancer factor-1/beta-catenin complex', *Cell Mol Life Sci,* 62, (5), pp. 606-18.
Hammerschmidt, M., Pelegri, F., Mullins, M. C., Kane, D. A., Brand, M., van Eeden, F. J., Furutani-Seiki, M., Granato, M., Haffter, P., Heisenberg, C. P., Jiang, Y. J., Kelsh, R. N., Odenthal, J., Warga, R. M. and Nusslein-Volhard, C. (1996) 'Mutations affecting morphogenesis during gastrulation and tail formation in the zebrafish, Danio rerio', *Development,* 123, pp. 143-51.
Han, Z., Chang, L., Yamanishi, Y., Karin, M. and Firestein, G. S. (2002) 'Joint damage and inflammation in c-Jun N-terminal kinase 2 knockout mice with passive murine collagen-induced arthritis', *Arthritis Rheum,* 46, (3), pp. 818-23.
Harvey, R. P. (1999) 'Seeking a regulatory roadmap for heart morphogenesis', *Semin Cell Dev Biol,* 10, (1), pp. 99-107.
Hayashi, M. and Lee, J. D. (2004) 'Role of the BMK1/ERK5 signaling pathway: lessons from knockout mice', *J Mol Med,* 82, (12), pp. 800-8.
He, T. C., Sparks, A. B., Rago, C., Hermeking, H., Zawel, L., da Costa, L. T., Morin, P. J., Vogelstein, B. and Kinzler, K. W. (1998) 'Identification of c-MYC as a target of the APC pathway', *Science,* 281, (5382), pp. 1509-12.
He, X., Saint-Jeannet, J. P., Wang, Y., Nathans, J., Dawid, I. and Varmus, H. (1997) 'A member of the Frizzled protein family mediating axis induction by Wnt-5A', *Science,* 275, (5306), pp. 1652-4.

He, Z., Li, J. J., Zhen, C. H., Feng, L. Y. and Ding, X. Y. (2006) 'Effect of leukemia inhibitory factor on embryonic stem cell differentiation: implications for supporting neuronal differentiation', *Acta Pharmacol Sin,* 27, (1), pp. 80-90.

Hecht, A. and Kemler, R. (2000) 'Curbing the nuclear activities of beta-catenin. Control over Wnt target gene expression', *EMBO Rep,* 1, (1), pp. 24-8.

Heikkila, R., Schwab, G., Wickstrom, E., Loke, S. L., Pluznik, D. H., Watt, R. and Neckers, L. M. (1987) 'A c-myc antisense oligodeoxynucleotide inhibits entry into S phase but not progress from G0 to G1', *Nature,* 328, (6129), pp. 445-9.

Heisenberg, C. P. and Nusslein-Volhard, C. (1997) 'The function of silberblick in the positioning of the eye anlage in the zebrafish embryo', *Dev Biol,* 184, (1), pp. 85-94.

Heisenberg, C. P., Tada, M., Rauch, G. J., Saude, L., Concha, M. L., Geisler, R., Stemple, D. L., Smith, J. C. and Wilson, S. W. (2000) 'Silberblick/Wnt11 mediates convergent extension movements during zebrafish gastrulation', *Nature,* 405, (6782), pp. 76-81.

Henderson, D. J. and Chaudhry, B. (2011) 'Getting to the heart of planar cell polarity signaling', *Birth Defects Res A Clin Mol Teratol,* 91, (6), pp. 460-7.

Henderson, D. J., Conway, S. J., Greene, N. D., Gerrelli, D., Murdoch, J. N., Anderson, R. H. and Copp, A. J. (2001) 'Cardiovascular defects associated with abnormalities in midline development in the Loop-tail mouse mutant', *Circ Res,* 89, (1), pp. 6-12.

Heo, Y. S., Kim, S. K., Seo, C. I., Kim, Y. K., Sung, B. J., Lee, H. S., Lee, J. I., Park, S. Y., Kim, J. H., Hwang, K. Y., Hyun, Y. L., Jeon, Y. H., Ro, S., Cho, J. M., Lee, T. G. and Yang, C. H. (2004) 'Structural basis for the selective inhibition of JNK1 by the scaffolding protein JIP1 and SP600125', *EMBO J,* 23, (11), pp. 2185-95.

Hernandez-Garcia, D., Castro-Obregon, S., Gomez-Lopez, S., Valencia, C. and Covarrubias, L. (2008) 'Cell death activation during cavitation of embryoid bodies is mediated by hydrogen peroxide', *Exp Cell Res,* 314, (10), pp. 2090-9.

Herrmann, B. G. and Kispert, A. (1994) 'The T genes in embryogenesis', *Trends Genet,* 10, (8), pp. 280-6.

Hescheler, J., Fleischmann, B. K., Lentini, S., Maltsev, V. A., Rohwedel, J., Wobus, A. M. and Addicks, K. (1997) 'Embryonic stem cells: a model to study structural and functional properties in cardiomyogenesis', *Cardiovasc Res,* 36, (2), pp. 149-62.

Hidaka, K., Lee, J. K., Kim, H. S., Ihm, C. H., Iio, A., Ogawa, M., Nishikawa, S., Kodama, I. and Morisaki, T. (2003) 'Chamber-specific differentiation of Nkx2.5-positive cardiac precursor cells from murine embryonic stem cells', *FASEB J,* 17, (6), pp. 740-2.

Hilfiker-Kleiner, D., Hilfiker, A., Castellazzi, M., Wollert, K. C., Trautwein, C., Schunkert, H. and Drexler, H. (2006) 'JunD attenuates phenylephrine-mediated cardiomyocyte hypertrophy by negatively regulating AP-1 transcriptional activity', *Cardiovasc Res,* 71, (1), pp. 108-17.

Hirosumi, J., Tuncman, G., Chang, L., Gorgun, C. Z., Uysal, K. T., Maeda, K., Karin, M. and Hotamisligil, G. S. (2002) 'A central role for JNK in obesity and insulin resistance', *Nature,* 420, (6913), pp. 333-6.

Hirotsune, S., Yoshida, N., Chen, A., Garrett, L., Sugiyama, F., Takahashi, S., Yagami, K., Wynshaw-Boris, A. and Yoshiki, A. (2003) 'An expressed pseudogene regulates the messenger-RNA stability of its homologous coding gene', *Nature,* 423, (6935), pp. 91-6.

Hochedlinger, K., Wagner, E. F. and Sabapathy, K. (2002) 'Differential effects of JNK1 and JNK2 on signal specific induction of apoptosis', *Oncogene,* 21, (15), pp. 2441-5.
Hoffman, J. I. and Kaplan, S. (2002) 'The incidence of congenital heart disease', *J Am Coll Cardiol,* 39, (12), pp. 1890-900.
Holmes, I. (2003) 'Using guide trees to construct multiple-sequence evolutionary HMMs', *Bioinformatics,* 19 Suppl 1, pp. i147-57.
Holtzinger, A. and Evans, T. (2005) 'Gata4 regulates the formation of multiple organs', *Development,* 132, (17), pp. 4005-14.
Hong, N., Li, Z. and Hong, Y. (2011) 'Fish stem cell cultures', *Int J Biol Sci,* 7, (4), pp. 392-402.
Hooper, M., Hardy, K., Handyside, A., Hunter, S. and Monk, M. (1987) 'HPRT-deficient (Lesch-Nyhan) mouse embryos derived from germline colonization by cultured cells', *Nature,* 326, (6110), pp. 292-5.
Horb, M. E. and Thomsen, G. H. (1999) 'Tbx5 is essential for heart development', *Development,* 126, (8), pp. 1739-51.
Houart, C., Caneparo, L., Heisenberg, C., Barth, K., Take-Uchi, M. and Wilson, S. (2002) 'Establishment of the telencephalon during gastrulation by local antagonism of Wnt signaling', *Neuron,* 35, (2), pp. 255-65.
Hovanes, K., Li, T. W., Munguia, J. E., Truong, T., Milovanovic, T., Lawrence Marsh, J., Holcombe, R. F. and Waterman, M. L. (2001) 'Beta-catenin-sensitive isoforms of lymphoid enhancer factor-1 are selectively expressed in colon cancer', *Nat Genet,* 28, (1), pp. 53-7.
Hovanes, K., Li, T. W. and Waterman, M. L. (2000) 'The human LEF-1 gene contains a promoter preferentially active in lymphocytes and encodes multiple isoforms derived from alternative splicing', *Nucleic Acids Res,* 28, (9), pp. 1994-2003.
Hreniuk, D., Garay, M., Gaarde, W., Monia, B. P., McKay, R. A. and Cioffi, C. L. (2001) 'Inhibition of c-Jun N-terminal kinase 1, but not c-Jun N-terminal kinase 2, suppresses apoptosis induced by ischemia/reoxygenation in rat cardiac myocytes', *Mol Pharmacol,* 59, (4), pp. 867-74.
Hu, N., Sedmera, D., Yost, H. J. and Clark, E. B. (2000) 'Structure and function of the developing zebrafish heart', *Anat Rec,* 260, (2), pp. 148-57.
Hu, N., Yost, H. J. and Clark, E. B. (2001) 'Cardiac morphology and blood pressure in the adult zebrafish', *Anat Rec,* 264, (1), pp. 1-12.
Huang, C., Sheikh, F., Hollander, M., Cai, C., Becker, D., Chu, P. H., Evans, S. and Chen, J. (2003a) 'Embryonic atrial function is essential for mouse embryogenesis, cardiac morphogenesis and angiogenesis', *Development,* 130, (24), pp. 6111-9.
Huang, C. J., Tu, C. T., Hsiao, C. D., Hsieh, F. J. and Tsai, H. J. (2003b) 'Germ-line transmission of a myocardium-specific GFP transgene reveals critical regulatory elements in the cardiac myosin light chain 2 promoter of zebrafish', *Dev Dyn,* 228, (1), pp. 30-40.
Huang, S. M., Mishina, Y. M., Liu, S., Cheung, A., Stegmeier, F., Michaud, G. A., Charlat, O., Wiellette, E., Zhang, Y., Wiessner, S., Hild, M., Shi, X., Wilson, C. J., Mickanin, C., Myer, V., Fazal, A., Tomlinson, R., Serluca, F., Shao, W., Cheng, H., Shultz, M., Rau, C., Schirle, M., Schlegl, J., Ghidelli, S., Fawell, S., Lu, C., Curtis, D., Kirschner, M. W., Lengauer, C., Finan, P. M., Tallarico, J. A., Bouwmeester, T., Porter, J. A., Bauer, A. and Cong, F. (2009) 'Tankyrase inhibition stabilizes axin and antagonizes Wnt signalling', *Nature,* 461, (7264), pp. 614-20.

Huber, O., Korn, R., McLaughlin, J., Ohsugi, M., Herrmann, B. G. and Kemler, R. (1996) 'Nuclear localization of beta-catenin by interaction with transcription factor LEF-1', *Mech Dev,* 59, (1), pp. 3-10.

Huber, T. L., Kouskoff, V., Fehling, H. J., Palis, J. and Keller, G. (2004) 'Haemangioblast commitment is initiated in the primitive streak of the mouse embryo', *Nature,* 432, (7017), pp. 625-30.

Huelsken, J., Vogel, R., Brinkmann, V., Erdmann, B., Birchmeier, C. and Birchmeier, W. (2000) 'Requirement for beta-catenin in anterior-posterior axis formation in mice', *J Cell Biol,* 148, (3), pp. 567-78.

Ibanes, M. and Izpisua Belmonte, J. C. (2009) 'Left-right axis determination', *Wiley Interdiscip Rev Syst Biol Med,* 1, (2), pp. 210-9.

Ieda, M., Fu, J. D., Delgado-Olguin, P., Vedantham, V., Hayashi, Y., Bruneau, B. G. and Srivastava, D. (2010) 'Direct reprogramming of fibroblasts into functional cardiomyocytes by defined factors', *Cell,* 142, (3), pp. 375-86.

Ingham, P. W. (1997) 'Zebrafish genetics and its implications for understanding vertebrate development', *Hum Mol Genet,* 6, (10), pp. 1755-60.

Ishizaki, T., Naito, M., Fujisawa, K., Maekawa, M., Watanabe, N., Saito, Y. and Narumiya, S. (1997) 'p160ROCK, a Rho-associated coiled-coil forming protein kinase, works downstream of Rho and induces focal adhesions', *FEBS Lett,* 404, (2-3), pp. 118-24.

Jackman, W. R., Yoo, J. J. and Stock, D. W. (2010) 'Hedgehog signaling is required at multiple stages of zebrafish tooth development', *BMC Dev Biol,* 10, pp. 119.

Jacq, C., Miller, J. R. and Brownlee, G. G. (1977) 'A pseudogene structure in 5S DNA of Xenopus laevis', *Cell,* 12, (1), pp. 109-20.

Jaeschke, A., Karasarides, M., Ventura, J. J., Ehrhardt, A., Zhang, C., Flavell, R. A., Shokat, K. M. and Davis, R. J. (2006) 'JNK2 is a positive regulator of the cJun transcription factor', *Mol Cell,* 23, (6), pp. 899-911.

Jaeschke, A., Rincon, M., Doran, B., Reilly, J., Neuberg, D., Greiner, D. L., Shultz, L. D., Rossini, A. A., Flavell, R. A. and Davis, R. J. (2005) 'Disruption of the Jnk2 (Mapk9) gene reduces destructive insulitis and diabetes in a mouse model of type I diabetes', *Proc Natl Acad Sci U S A,* 102, (19), pp. 6931-5.

Jamali, M., Karamboulas, C., Rogerson, P. J. and Skerjanc, I. S. (2001) 'BMP signaling regulates Nkx2-5 activity during cardiomyogenesis', *FEBS Lett,* 509, (1), pp. 126-30.

Jenkins, K. J., Correa, A., Feinstein, J. A., Botto, L., Britt, A. E., Daniels, S. R., Elixson, M., Warnes, C. A. and Webb, C. L. (2007) 'Noninherited risk factors and congenital cardiovascular defects: current knowledge: a scientific statement from the American Heart Association Council on Cardiovascular Disease in the Young: endorsed by the American Academy of Pediatrics', *Circulation,* 115, (23), pp. 2995-3014.

Jessen, J. R., Topczewski, J., Bingham, S., Sepich, D. S., Marlow, F., Chandrasekhar, A. and Solnica-Krezel, L. (2002) 'Zebrafish trilobite identifies new roles for Strabismus in gastrulation and neuronal movements', *Nat Cell Biol,* 4, (8), pp. 610-5.

Jimenez, B., Volpert, O. V., Reiher, F., Chang, L., Munoz, A., Karin, M. and Bouck, N. (2001) 'c-Jun N-terminal kinase activation is required for the inhibition of neovascularization by thrombospondin-1', *Oncogene,* 20, (26), pp. 3443-8.

Jones, D. T., Taylor, W. R. and Thornton, J. M. (1992) 'The rapid generation of mutation data matrices from protein sequences', *Comput Appl Biosci,* 8, (3), pp. 275-82.

Juntilla, M. M. and Koretzky, G. A. (2008) 'Critical roles of the PI3K/Akt signaling pathway in T cell development', *Immunol Lett,* 116, (2), pp. 104-10.

Kadoya, T., Khurana, A., Tcherpakov, M., Bromberg, K. D., Didier, C., Broday, L., Asahara, T., Bhoumik, A. and Ronai, Z. (2005) 'JAMP, a Jun N-terminal kinase 1 (JNK1)-associated membrane protein, regulates duration of JNK activity', *Mol Cell Biol,* 25, (19), pp. 8619-30.

Kalderon, D. (2002) 'Similarities between the Hedgehog and Wnt signaling pathways', *Trends Cell Biol,* 12, (11), pp. 523-31.

Kallunki, T., Deng, T., Hibi, M. and Karin, M. (1996) 'c-Jun can recruit JNK to phosphorylate dimerization partners via specific docking interactions', *Cell,* 87, (5), pp. 929-39.

Kalmar, T., Lim, C., Hayward, P., Munoz-Descalzo, S., Nichols, J., Garcia-Ojalvo, J. and Martinez Arias, A. (2009) 'Regulated fluctuations in nanog expression mediate cell fate decisions in embryonic stem cells', *PLoS Biol,* 7, (7), pp. e1000149.

Kanazawa, S., Soucek, L., Evan, G., Okamoto, T. and Peterlin, B. M. (2003) 'c-Myc recruits P-TEFb for transcription, cellular proliferation and apoptosis', *Oncogene,* 22, (36), pp. 5707-11.

Kane, D. A. and Kimmel, C. B. (1993) 'The zebrafish midblastula transition', *Development,* 119, (2), pp. 447-56.

Kathiriya, I. S. and Srivastava, D. (2000) 'Left-right asymmetry and cardiac looping: implications for cardiac development and congenital heart disease', *Am J Med Genet,* 97, (4), pp. 271-9.

Kattman, S. J., Huber, T. L. and Keller, G. M. (2006) 'Multipotent flk-1+ cardiovascular progenitor cells give rise to the cardiomyocyte, endothelial, and vascular smooth muscle lineages', *Dev Cell,* 11, (5), pp. 723-32.

Kattman, S. J., Koonce, C. H., Swanson, B. J. and Anson, B. D. (2011a) 'Stem cells and their derivatives: a renaissance in cardiovascular translational research', *J Cardiovasc Transl Res,* 4, (1), pp. 66-72.

Kattman, S. J., Witty, A. D., Gagliardi, M., Dubois, N. C., Niapour, M., Hotta, A., Ellis, J. and Keller, G. (2011b) 'Stage-specific optimization of activin/nodal and BMP signaling promotes cardiac differentiation of mouse and human pluripotent stem cell lines', *Cell Stem Cell,* 8, (2), pp. 228-40.

Kawano, Y. and Kypta, R. (2003) 'Secreted antagonists of the Wnt signalling pathway', *J Cell Sci,* 116, (Pt 13), pp. 2627-34.

Kawasumi, A., Nakamura, T., Iwai, N., Yashiro, K., Saijoh, Y., Belo, J. A., Shiratori, H. and Hamada, H. (2011) 'Left-right asymmetry in the level of active Nodal protein produced in the node is translated into left-right asymmetry in the lateral plate of mouse embryos', *Dev Biol*.

Kay, B. K. and Kehoe, J. W. (2004) 'PDZ domains and their ligands', *Chem Biol,* 11, (4), pp. 423-5.

Keegan, B. R., Meyer, D. and Yelon, D. (2004) 'Organization of cardiac chamber progenitors in the zebrafish blastula', *Development,* 131, (13), pp. 3081-91.

Keller, G. (2005) 'Embryonic stem cell differentiation: emergence of a new era in biology and medicine', *Genes Dev,* 19, (10), pp. 1129-55.

Keller, G., Kennedy, M., Papayannopoulou, T. and Wiles, M. V. (1993) 'Hematopoietic commitment during embryonic stem cell differentiation in culture', *Mol Cell Biol,* 13, (1), pp. 473-86.

Keller, I., Bensasson, D. and Nichols, R. A. (2007) 'Transition-transversion bias is not universal: a counter example from grasshopper pseudogenes', *PLoS Genet,* 3, (2), pp. e22.

Kelly, R. G., Brown, N. A. and Buckingham, M. E. (2001) 'The arterial pole of the mouse heart forms from Fgf10-expressing cells in pharyngeal mesoderm', *Dev Cell,* 1, (3), pp. 435-40.

Kemler, R., Hierholzer, A., Kanzler, B., Kuppig, S., Hansen, K., Taketo, M. M., de Vries, W. N., Knowles, B. B. and Solter, D. (2004) 'Stabilization of beta-catenin in the mouse zygote leads to premature epithelial-mesenchymal transition in the epiblast', *Development,* 131, (23), pp. 5817-24.

Kemp, C., Willems, E., Abdo, S., Lambiv, L. and Leyns, L. (2005) 'Expression of all Wnt genes and their secreted antagonists during mouse blastocyst and postimplantation development', *Dev Dyn,* 233, (3), pp. 1064-75.

Kemp, C. R., Willems, E., Wawrzak, D., Hendrickx, M., Agbor Agbor, T. and Leyns, L. (2007) 'Expression of Frizzled5, Frizzled7, and Frizzled10 during early mouse development and interactions with canonical Wnt signaling', *Dev Dyn,* 236, (7), pp. 2011-9.

Kengaku, M., Capdevila, J., Rodriguez-Esteban, C., De La Pena, J., Johnson, R. L., Izpisua Belmonte, J. C. and Tabin, C. J. (1998) 'Distinct WNT pathways regulating AER formation and dorsoventral polarity in the chick limb bud', *Science,* 280, (5367), pp. 1274-7.

Kerkela, R. and Force, T. (2006) 'p38 mitogen-activated protein kinase: a future target for heart failure therapy?', *J Am Coll Cardiol,* 48, (3), pp. 556-8.

Kestler, H. A. and Kuhl, M. (2008) 'From individual Wnt pathways towards a Wnt signalling network', *Philos Trans R Soc Lond B Biol Sci,* 363, (1495), pp. 1333-47.

Kibar, Z., Vogan, K. J., Groulx, N., Justice, M. J., Underhill, D. A. and Gros, P. (2001) 'Ltap, a mammalian homolog of Drosophila Strabismus/Van Gogh, is altered in the mouse neural tube mutant Loop-tail', *Nat Genet,* 28, (3), pp. 251-5.

Kilian, B., Mansukoski, H., Barbosa, F. C., Ulrich, F., Tada, M. and Heisenberg, C. P. (2003) 'The role of Ppt/Wnt5 in regulating cell shape and movement during zebrafish gastrulation', *Mech Dev,* 120, (4), pp. 467-76.

Kim, S. H., Shin, J., Park, H. C., Yeo, S. Y., Hong, S. K., Han, S., Rhee, M., Kim, C. H., Chitnis, A. B. and Huh, T. L. (2002) 'Specification of an anterior neuroectoderm patterning by Frizzled8a-mediated Wnt8b signalling during late gastrulation in zebrafish', *Development,* 129, (19), pp. 4443-55.

Kimmel, C. B. and Law, R. D. (1985a) 'Cell lineage of zebrafish blastomeres. I. Cleavage pattern and cytoplasmic bridges between cells', *Dev Biol,* 108, (1), pp. 78-85.

Kimmel, C. B. and Law, R. D. (1985b) 'Cell lineage of zebrafish blastomeres. II. Formation of the yolk syncytial layer', *Dev Biol,* 108, (1), pp. 86-93.

Kimura, M. (1968) 'Evolutionary rate at the molecular level', *Nature,* 217, (5129), pp. 624-6.

Kimura-Yoshida, C., Nakano, H., Okamura, D., Nakao, K., Yonemura, S., Belo, J. A., Aizawa, S., Matsui, Y. and Matsuo, I. (2005) 'Canonical Wnt signaling and its antagonist regulate anterior-posterior axis polarization by guiding cell migration in mouse visceral endoderm', *Dev Cell,* 9, (5), pp. 639-50.

Kirby, M. L., Gale, T. F. and Stewart, D. E. (1983) 'Neural crest cells contribute to normal aorticopulmonary septation', *Science,* 220, (4601), pp. 1059-61.

Kirkpatrick, J. A., Jr. and DiGeorge, A. M. (1968) 'Congenital absence of the thymus', *Am J Roentgenol Radium Ther Nucl Med,* 103, (1), pp. 32-7.

Kishimoto, Y., Lee, K. H., Zon, L., Hammerschmidt, M. and Schulte-Merker, S. (1997) 'The molecular nature of zebrafish swirl: BMP2 function is essential during early dorsoventral patterning', *Development,* 124, (22), pp. 4457-66.

Kishino, H. and Hasegawa, M. (1990) 'Converting distance to time: application to human evolution', *Methods Enzymol,* 183, pp. 550-70.

Kitamura, K., Miura, H., Miyagawa-Tomita, S., Yanazawa, M., Katoh-Fukui, Y., Suzuki, R., Ohuchi, H., Suehiro, A., Motegi, Y., Nakahara, Y., Kondo, S. and

Yokoyama, M. (1999) 'Mouse Pitx2 deficiency leads to anomalies of the ventral body wall, heart, extra- and periocular mesoderm and right pulmonary isomerism', *Development,* 126, (24), pp. 5749-58.
Klaus, A., Saga, Y., Taketo, M. M., Tzahor, E. and Birchmeier, W. (2007) 'Distinct roles of Wnt/beta-catenin and Bmp signaling during early cardiogenesis', *Proc Natl Acad Sci U S A,* 104, (47), pp. 18531-6.
Knighton, D. R., Zheng, J. H., Ten Eyck, L. F., Ashford, V. A., Xuong, N. H., Taylor, S. S. and Sowadski, J. M. (1991) 'Crystal structure of the catalytic subunit of cyclic adenosine monophosphate-dependent protein kinase', *Science,* 253, (5018), pp. 407-14.
Koshida, S., Shinya, M., Mizuno, T., Kuroiwa, A. and Takeda, H. (1998) 'Initial anteroposterior pattern of the zebrafish central nervous system is determined by differential competence of the epiblast', *Development,* 125, (10), pp. 1957-66.
Krens, S. F., Corredor-Adamez, M., He, S., Snaar-Jagalska, B. E. and Spaink, H. P. (2008) 'ERK1 and ERK2 MAPK are key regulators of distinct gene sets in zebrafish embryogenesis', *BMC Genomics,* 9, pp. 196.
Krens, S. F., Spaink, H. P. and Snaar-Jagalska, B. E. (2006) 'Functions of the MAPK family in vertebrate-development', *FEBS Lett,* 580, (21), pp. 4984-90.
Kubalak, S. W., Miller-Hance, W. C., O'Brien, T. X., Dyson, E. and Chien, K. R. (1994) 'Chamber specification of atrial myosin light chain-2 expression precedes septation during murine cardiogenesis', *J Biol Chem,* 269, (24), pp. 16961-70.
Kuhl, M., Sheldahl, L. C., Malbon, C. C. and Moon, R. T. (2000) 'Ca(2+)/calmodulin-dependent protein kinase II is stimulated by Wnt and Frizzled homologs and promotes ventral cell fates in Xenopus', *J Biol Chem,* 275, (17), pp. 12701-11.
Kumar, S. (2005) 'Molecular clocks: four decades of evolution', *Nat Rev Genet,* 6, (8), pp. 654-62.
Kurosawa, H. (2007) 'Methods for inducing embryoid body formation: in vitro differentiation system of embryonic stem cells', *J Biosci Bioeng,* 103, (5), pp. 389-98.
Kurosawa, H., Imamura, T., Koike, M., Sasaki, K. and Amano, Y. (2003) 'A simple method for forming embryoid body from mouse embryonic stem cells', *J Biosci Bioeng,* 96, (4), pp. 409-11.
Kwee, L., Baldwin, H. S., Shen, H. M., Stewart, C. L., Buck, C., Buck, C. A. and Labow, M. A. (1995) 'Defective development of the embryonic and extraembryonic circulatory systems in vascular cell adhesion molecule (VCAM-1) deficient mice', *Development,* 121, (2), pp. 489-503.
Kuan, C. Y., Yang, D. D., Samanta Roy, D. R., Davis, R. J., Rakic, P. and Flavell, R. A. (1999) 'The Jnk1 and Jnk2 protein kinases are required for regional specific apoptosis during early brain development', *Neuron,* 22, (4), pp. 667-76.
Kuhl, M., Sheldahl, L. C., Malbon, C. C. and Moon, R. T. (2000) 'Ca(2+)/calmodulin-dependent protein kinase II is stimulated by Wnt and Frizzled homologs and promotes ventral cell fates in Xenopus', *J Biol Chem,* 275, (17), pp. 12701-11.
Kuo, C. T., Morrisey, E. E., Anandappa, R., Sigrist, K., Lu, M. M., Parmacek, M. S., Soudais, C. and Leiden, J. M. (1997) 'GATA4 transcription factor is required for ventral morphogenesis and heart tube formation', *Genes Dev,* 11, (8), pp. 1048-60.
Kurosawa, H. (2007) 'Methods for inducing embryoid body formation: in vitro differentiation system of embryonic stem cells', *J Biosci Bioeng,* 103, (5), pp. 389-98.
Kurosawa, H., Imamura, T., Koike, M., Sasaki, K. and Amano, Y. (2003) 'A simple method for forming embryoid body from mouse embryonic stem cells', *J Biosci Bioeng,* 96, (4), pp. 409-11.

Kwon, C., Arnold, J., Hsiao, E. C., Taketo, M. M., Conklin, B. R. and Srivastava, D. (2007) 'Canonical Wnt signaling is a positive regulator of mammalian cardiac progenitors', *Proc Natl Acad Sci U S A,* 104, (26), pp. 10894-9.
Kwon, C., Qian, L., Cheng, P., Nigam, V., Arnold, J. and Srivastava, D. (2009) 'A regulatory pathway involving Notch1/beta-catenin/Isl1 determines cardiac progenitor cell fate', *Nat Cell Biol,* 11, (8), pp. 951-7.
Kyoi, S., Otani, H., Matsuhisa, S., Akita, Y., Tatsumi, K., Enoki, C., Fujiwara, H., Imamura, H., Kamihata, H. and Iwasaka, T. (2006) 'Opposing effect of p38 MAP kinase and JNK inhibitors on the development of heart failure in the cardiomyopathic hamster', *Cardiovasc Res,* 69, (4), pp. 888-98.
Labbe, E., Letamendia, A. and Attisano, L. (2000) 'Association of Smads with lymphoid enhancer binding factor 1/T cell-specific factor mediates cooperative signaling by the transforming growth factor-beta and wnt pathways', *Proc Natl Acad Sci U S A,* 97, (15), pp. 8358-63.
Ladd, A. N., Yatskievych, T. A. and Antin, P. B. (1998) 'Regulation of avian cardiac myogenesis by activin/TGFbeta and bone morphogenetic proteins', *Dev Biol,* 204, (2), pp. 407-19.
Lafontant, P. J. and Field, L. J. (2006) 'The cardiomyocyte cell cycle', *Novartis Found Symp,* 274, pp. 196-207; discussion 208-13, 272-6.
Lampe, P. D. and Lau, A. F. (2004) 'The effects of connexin phosphorylation on gap junctional communication', *Int J Biochem Cell Biol,* 36, (7), pp. 1171-86.
Laugwitz, K. L., Moretti, A., Caron, L., Nakano, A. and Chien, K. R. (2008) 'Islet1 cardiovascular progenitors: a single source for heart lineages?', *Development,* 135, (2), pp. 193-205.
Lawrence, P. A., Struhl, G. and Casal, J. (2007) 'Planar cell polarity: one or two pathways?', *Nat Rev Genet,* 8, (7), pp. 555-63.
Lazic, S. and Scott, I. C. (2011) 'Mef2cb regulates late myocardial cell addition from a second heart field-like population of progenitors in zebrafish', *Dev Biol,* 354, (1), pp. 123-33.
Leahy, A., Xiong, J. W., Kuhnert, F. and Stuhlmann, H. (1999) 'Use of developmental marker genes to define temporal and spatial patterns of differentiation during embryoid body formation', *J Exp Zool,* 284, (1), pp. 67-81.
Lee, H. H., Chang, S. F., Lo, F. S., Chao, H. T. and Lin, C. Y. (2003) 'Duplication of 111 bases in exon 1 of the CYP21 gene is combined with deletion of CYP21P-C4B genes in steroid 21-hydroxylase deficiency', *Mol Genet Metab,* 79, (3), pp. 214-20.
Lei, K. and Davis, R. J. (2003) 'JNK phosphorylation of Bim-related members of the Bcl2 family induces Bax-dependent apoptosis', *Proc Natl Acad Sci U S A,* 100, (5), pp. 2432-7.
Lekven, A. C., Thorpe, C. J., Waxman, J. S. and Moon, R. T. (2001) 'Zebrafish wnt8 encodes two wnt8 proteins on a bicistronic transcript and is required for mesoderm and neurectoderm patterning', *Dev Cell,* 1, (1), pp. 103-14.
Leung, T., Chen, X. Q., Manser, E. and Lim, L. (1996) 'The p160 RhoA-binding kinase ROK alpha is a member of a kinase family and is involved in the reorganization of the cytoskeleton', *Mol Cell Biol,* 16, (10), pp. 5313-27.
Li, X., Deng, W., Lobo-Ruppert, S. M. and Ruppert, J. M. (2007) 'Gli1 acts through Snail and E-cadherin to promote nuclear signaling by beta-catenin', *Oncogene,* 26, (31), pp. 4489-98.
Liang, Q. and Molkentin, J. D. (2003) 'Redefining the roles of p38 and JNK signaling in cardiac hypertrophy: dichotomy between cultured myocytes and animal models', *J Mol Cell Cardiol,* 35, (12), pp. 1385-94.

Liao, C. J., Chen, C. P., Wang, M. K., Chiang, P. N. and Pai, C. W. (2006) 'Sorption of chlorophenoxy propionic acids by organoclay complexes', *Environ Toxicol,* 21, (1), pp. 71-9.

Liao, P., Wang, S. Q., Wang, S., Zheng, M., Zhang, S. J., Cheng, H., Wang, Y. and Xiao, R. P. (2002) 'p38 Mitogen-activated protein kinase mediates a negative inotropic effect in cardiac myocytes', *Circ Res,* 90, (2), pp. 190-6.

Liberatore, C. M., Searcy-Schrick, R. D. and Yutzey, K. E. (2000) 'Ventricular expression of tbx5 inhibits normal heart chamber development', *Dev Biol,* 223, (1), pp. 169-80.

Lickert, H., Takeuchi, J. K., Von Both, I., Walls, J. R., McAuliffe, F., Adamson, S. L., Henkelman, R. M., Wrana, J. L., Rossant, J. and Bruneau, B. G. (2004) 'Baf60c is essential for function of BAF chromatin remodelling complexes in heart development', *Nature,* 432, (7013), pp. 107-12.

Liersch, R., Nay, F., Lu, L. and Detmar, M. (2006) 'Induction of lymphatic endothelial cell differentiation in embryoid bodies', *Blood,* 107, (3), pp. 1214-6.

Lin, A., Minden, A., Martinetto, H., Claret, F. X., Lange-Carter, C., Mercurio, F., Johnson, G. L. and Karin, M. (1995) 'Identification of a dual specificity kinase that activates the Jun kinases and p38-Mpk2', *Science,* 268, (5208), pp. 286-90.

Lin, X. and Xu, X. (2009) 'Distinct functions of Wnt/beta-catenin signaling in KV development and cardiac asymmetry', *Development,* 136, (2), pp. 207-17.

Lincoln, J., Alfieri, C. M. and Yutzey, K. E. (2006) 'BMP and FGF regulatory pathways control cell lineage diversification of heart valve precursor cells', *Dev Biol,* 292, (2), pp. 292-302.

Lindeman, R. E. and Pelegri, F. (2010) 'Vertebrate maternal-effect genes: Insights into fertilization, early cleavage divisions, and germ cell determinant localization from studies in the zebrafish', *Mol Reprod Dev,* 77, (4), pp. 299-313.

Lindsley, R. C., Gill, J. G., Kyba, M., Murphy, T. L. and Murphy, K. M. (2006) 'Canonical Wnt signaling is required for development of embryonic stem cell-derived mesoderm', *Development,* 133, (19), pp. 3787-96.

Liu, C., Liu, W., Lu, M. F., Brown, N. A. and Martin, J. F. (2001) 'Regulation of left-right asymmetry by thresholds of Pitx2c activity', *Development,* 128, (11), pp. 2039-48.

Lloyd, S., Fleming, T. P. and Collins, J. E. (2003) 'Expression of Wnt genes during mouse preimplantation development', *Gene Expr Patterns,* 3, (3), pp. 309-12.

Long, S., Ahmad, N. and Rebagliati, M. (2003) 'The zebrafish nodal-related gene southpaw is required for visceral and diencephalic left-right asymmetry', *Development,* 130, (11), pp. 2303-16.

Long, M. and Langley, C. H. (1993) 'Natural selection and the origin of jingwei, a chimeric processed functional gene in Drosophila', *Science,* 260, (5104), pp. 91-5.

Lopez-Sanchez, C., Garcia-Martinez, V. and Schoenwolf, G. C. (2001) 'Localization of cells of the prospective neural plate, heart and somites within the primitive streak and epiblast of avian embryos at intermediate primitive-streak stages', *Cells Tissues Organs,* 169, (4), pp. 334-46.

Lu, D. Q., Bei, J. X., Feng, L. N., Zhang, Y., Liu, X. C., Wang, L., Chen, J. L. and Lin, H. R. (2008) 'Interleukin-1beta gene in orange-spotted grouper, Epinephelus coioides: molecular cloning, expression, biological activities and signal transduction', *Mol Immunol,* 45, (4), pp. 857-67.

Luu, N. T., Rainger, G. E., Buckley, C. D. and Nash, G. B. (2003) 'CD31 regulates direction and rate of neutrophil migration over and under endothelial cells', *J Vasc Res,* 40, (5), pp. 467-79.

Lyons, I., Parsons, L. M., Hartley, L., Li, R., Andrews, J. E., Robb, L. and Harvey, R. P. (1995) 'Myogenic and morphogenetic defects in the heart tubes of murine embryos lacking the homeo box gene Nkx2-5', *Genes Dev,* 9, (13), pp. 1654-66.
Ma, C., Fan, L., Ganassin, R., Bols, N. and Collodi, P. (2001) 'Production of zebrafish germ-line chimeras from embryo cell cultures', *Proc Natl Acad Sci U S A,* 98, (5), pp. 2461-6.
Ma, D., Yang, C. H., McNeill, H., Simon, M. A. and Axelrod, J. D. (2003) 'Fidelity in planar cell polarity signalling', *Nature,* 421, (6922), pp. 543-7.
Ma, X. L., Kumar, S., Gao, F., Louden, C. S., Lopez, B. L., Christopher, T. A., Wang, C., Lee, J. C., Feuerstein, G. Z. and Yue, T. L. (1999) 'Inhibition of p38 mitogen-activated protein kinase decreases cardiomyocyte apoptosis and improves cardiac function after myocardial ischemia and reperfusion', *Circulation,* 99, (13), pp. 1685-91.
Mably, J. D., Mohideen, M. A., Burns, C. G., Chen, J. N. and Fishman, M. C. (2003) 'heart of glass regulates the concentric growth of the heart in zebrafish', *Curr Biol,* 13, (24), pp. 2138-47.
Mackay, K. and Mochly-Rosen, D. (1999) 'An inhibitor of p38 mitogen-activated protein kinase protects neonatal cardiac myocytes from ischemia', *J Biol Chem,* 274, (10), pp. 6272-9.
Magin, T. M., McWhir, J. and Melton, D. W. (1992) 'A new mouse embryonic stem cell line with good germ line contribution and gene targeting frequency', *Nucleic Acids Res,* 20, (14), pp. 3795-6.
Manisastry, S. M., Han, M. and Linask, K. K. (2006) 'Early temporal-specific responses and differential sensitivity to lithium and Wnt-3A exposure during heart development', *Dev Dyn,* 235, (8), pp. 2160-74.
Mao, B., Wu, W., Li, Y., Hoppe, D., Stannek, P., Glinka, A. and Niehrs, C. (2001) 'LDL-receptor-related protein 6 is a receptor for Dickkopf proteins', *Nature,* 411, (6835), pp. 321-5.
Marlow, F., Topczewski, J., Sepich, D. and Solnica-Krezel, L. (2002) 'Zebrafish Rho kinase 2 acts downstream of Wnt11 to mediate cell polarity and effective convergence and extension movements', *Curr Biol,* 12, (11), pp. 876-84.
Marlow, F., Zwartkruis, F., Malicki, J., Neuhauss, S. C., Abbas, L., Weaver, M., Driever, W. and Solnica-Krezel, L. (1998) 'Functional interactions of genes mediating convergent extension, knypek and trilobite, during the partitioning of the eye primordium in zebrafish', *Dev Biol,* 203, (2), pp. 382-99.
Marques, S. R., Lee, Y., Poss, K. D. and Yelon, D. (2008) 'Reiterative roles for FGF signaling in the establishment of size and proportion of the zebrafish heart', *Dev Biol,* 321, (2), pp. 397-406.
Marshall, C. J. (1995) 'Specificity of receptor tyrosine kinase signaling: transient versus sustained extracellular signal-regulated kinase activation', *Cell,* 80, (2), pp. 179-85.
Martin, B. L. and Kimelman, D. (2008) 'Regulation of canonical Wnt signaling by Brachyury is essential for posterior mesoderm formation', *Dev Cell,* 15, (1), pp. 121-33.
Martin, G. R. (1981) 'Isolation of a pluripotent cell line from early mouse embryos cultured in medium conditioned by teratocarcinoma stem cells', *Proc Natl Acad Sci U S A,* 78, (12), pp. 7634-8.
Martin, H., Flandez, M., Nombela, C. and Molina, M. (2005) 'Protein phosphatases in MAPK signalling: we keep learning from yeast', *Mol Microbiol,* 58, (1), pp. 6-16.
Martin, J., Afouda, B. A. and Hoppler, S. (2010) 'Wnt/beta-catenin signalling regulates cardiomyogenesis via GATA transcription factors', *J Anat,* 216, (1), pp. 92-107.

Martin, J. H., Mohit, A. A. and Miller, C. A. (1996) 'Developmental expression in the mouse nervous system of the p493F12 SAP kinase', *Brain Res Mol Brain Res,* 35, (1-2), pp. 47-57.
Martinez, A., Castro, A., Dorronsoro, I. and Alonso, M. (2002) 'Glycogen synthase kinase 3 (GSK-3) inhibitors as new promising drugs for diabetes, neurodegeneration, cancer, and inflammation', *Med Res Rev,* 22, (4), pp. 373-84.
Marvin, M. J., Di Rocco, G., Gardiner, A., Bush, S. M. and Lassar, A. B. (2001) 'Inhibition of Wnt activity induces heart formation from posterior mesoderm', *Genes Dev,* 15, (3), pp. 316-27.
Matakatsu, H. and Blair, S. S. (2004) 'Interactions between Fat and Dachsous and the regulation of planar cell polarity in the Drosophila wing', *Development,* 131, (15), pp. 3785-94.
Matsuda, T., Nakamura, T., Nakao, K., Arai, T., Katsuki, M., Heike, T. and Yokota, T. (1999) 'STAT3 activation is sufficient to maintain an undifferentiated state of mouse embryonic stem cells', *EMBO J,* 18, (15), pp. 4261-9.
Matsui, T., Raya, A., Kawakami, Y., Callol-Massot, C., Capdevila, J., Rodriguez-Esteban, C. and Izpisua Belmonte, J. C. (2005) 'Noncanonical Wnt signaling regulates midline convergence of organ primordia during zebrafish development', *Genes Dev,* 19, (1), pp. 164-75.
Maulik, N., Sato, M., Price, B. D. and Das, D. K. (1998) 'An essential role of NFkappaB in tyrosine kinase signaling of p38 MAP kinase regulation of myocardial adaptation to ischemia', *FEBS Lett,* 429, (3), pp. 365-9.
Maye, P., Zheng, J., Li, L. and Wu, D. (2004) 'Multiple mechanisms for Wnt11-mediated repression of the canonical Wnt signaling pathway', *J Biol Chem,* 279, (23), pp. 24659-65.
McCurley, A. T. and Callard, G. V. (2008) 'Characterization of housekeeping genes in zebrafish: male-female differences and effects of tissue type, developmental stage and chemical treatment', *BMC Mol Biol,* 9, pp. 102.
McDonald, P. H., Chow, C. W., Miller, W. E., Laporte, S. A., Field, M. E., Lin, F. T., Davis, R. J. and Lefkowitz, R. J. (2000) 'Beta-arrestin 2: a receptor-regulated MAPK scaffold for the activation of JNK3', *Science,* 290, (5496), pp. 1574-7.
McFadden, D. G. and Olson, E. N. (2002) 'Heart development: learning from mistakes', *Curr Opin Genet Dev,* 12, (3), pp. 328-35.
McGrath, J. and Brueckner, M. (2003) 'Cilia are at the heart of vertebrate left-right asymmetry', *Curr Opin Genet Dev,* 13, (4), pp. 385-92.
McKenna, D. H. and Brunstein, C. G. (2011) 'Umbilical cord blood: current status and future directions', *Vox Sang,* 100, (1), pp. 150-62.
Medvinsky, A., Rybtsov, S. and Taoudi, S. (2011) 'Embryonic origin of the adult hematopoietic system: advances and questions', *Development,* 138, (6), pp. 1017-31.
Meijer, L., Skaltsounis, A. L., Magiatis, P., Polychronopoulos, P., Knockaert, M., Leost, M., Ryan, X. P., Vonica, C. A., Brivanlou, A., Dajani, R., Crovace, C., Tarricone, C., Musacchio, A., Roe, S. M., Pearl, L. and Greengard, P. (2003) 'GSK-3-selective inhibitors derived from Tyrian purple indirubins', *Chem Biol,* 10, (12), pp. 1255-66.
Meilhac, S. M., Esner, M., Kelly, R. G., Nicolas, J. F. and Buckingham, M. E. (2004) 'The clonal origin of myocardial cells in different regions of the embryonic mouse heart', *Dev Cell,* 6, (5), pp. 685-98.
Menard, C., Grey, C., Mery, A., Zeineddine, D., Aimond, F. and Puceat, M. (2004) 'Cardiac specification of embryonic stem cells', *J Cell Biochem,* 93, (4), pp. 681-7.

Merrill, B. J., Pasolli, H. A., Polak, L., Rendl, M., Garcia-Garcia, M. J., Anderson, K. V. and Fuchs, E. (2004) 'Tcf3: a transcriptional regulator of axis induction in the early embryo', *Development,* 131, (2), pp. 263-74.
Metzger, J. M., Lin, W. I. and Samuelson, L. C. (1994) 'Transition in cardiac contractile sensitivity to calcium during the in vitro differentiation of mouse embryonic stem cells', *J Cell Biol,* 126, (3), pp. 701-11.
Meyer, A. and Van de Peer, Y. (2005) 'From 2R to 3R: evidence for a fish-specific genome duplication (FSGD)', *Bioessays,* 27, (9), pp. 937-45.
Mighell, A. J., Smith, N. R., Robinson, P. A. and Markham, A. F. (2000) 'Vertebrate pseudogenes', *FEBS Lett,* 468, (2-3), pp. 109-14.
Mikels, A. J. and Nusse, R. (2006) 'Purified Wnt5a protein activates or inhibits beta-catenin-TCF signaling depending on receptor context', *PLoS Biol,* 4, (4), pp. e115.
Minamino, T., Yujiri, T., Terada, N., Taffet, G. E., Michael, L. H., Johnson, G. L. and Schneider, M. D. (2002) 'MEKK1 is essential for cardiac hypertrophy and dysfunction induced by Gq', *Proc Natl Acad Sci U S A,* 99, (6), pp. 3866-71.
Miyabayashi, T., Teo, J. L., Yamamoto, M., McMillan, M., Nguyen, C. and Kahn, M. (2007) 'Wnt/beta-catenin/CBP signaling maintains long-term murine embryonic stem cell pluripotency', *Proc Natl Acad Sci U S A,* 104, (13), pp. 5668-73.
Mjaatvedt, C. H., Nakaoka, T., Moreno-Rodriguez, R., Norris, R. A., Kern, M. J., Eisenberg, C. A., Turner, D. and Markwald, R. R. (2001) 'The outflow tract of the heart is recruited from a novel heart-forming field', *Dev Biol,* 238, (1), pp. 97-109.
Mocanu, M. M., Baxter, G. F., Yue, Y., Critz, S. D. and Yellon, D. M. (2000) 'The p38 MAPK inhibitor, SB203580, abrogates ischaemic preconditioning in rat heart but timing of administration is critical', *Basic Res Cardiol,* 95, (6), pp. 472-8.
Mogi, A., Ichikawa, H., Matsumoto, C., Hieda, T., Tomotsune, D., Sakaki, S., Yamada, S. and Sasaki, K. (2009) 'The method of mouse embryoid body establishment affects structure and developmental gene expression', *Tissue Cell,* 41, (1), pp. 79-84.
Mohit, A. A., Martin, J. H. and Miller, C. A. (1995) 'p493F12 kinase: a novel MAP kinase expressed in a subset of neurons in the human nervous system', *Neuron,* 14, (1), pp. 67-78.
Molkentin, J. D., Antos, C., Mercer, B., Taigen, T., Miano, J. M. and Olson, E. N. (2000) 'Direct activation of a GATA6 cardiac enhancer by Nkx2.5: evidence for a reinforcing regulatory network of Nkx2.5 and GATA transcription factors in the developing heart', *Dev Biol,* 217, (2), pp. 301-9.
Molkentin, J. D., Lin, Q., Duncan, S. A. and Olson, E. N. (1997) 'Requirement of the transcription factor GATA4 for heart tube formation and ventral morphogenesis', *Genes Dev,* 11, (8), pp. 1061-72.
Montcouquiol, M., Rachel, R. A., Lanford, P. J., Copeland, N. G., Jenkins, N. A. and Kelley, M. W. (2003) 'Identification of Vangl2 and Scrb1 as planar polarity genes in mammals', *Nature,* 423, (6936), pp. 173-7.
Moon, D. O., Kim, M. O., Choi, Y. H., Kim, N. D., Chang, J. H. and Kim, G. Y. (2008) 'Bcl-2 overexpression attenuates SP600125-induced apoptosis in human leukemia U937 cells', *Cancer Lett,* 264, (2), pp. 316-25.
Moore, A. W., McInnes, L., Kreidberg, J., Hastie, N. D. and Schedl, A. (1999) 'YAC complementation shows a requirement for Wt1 in the development of epicardium, adrenal gland and throughout nephrogenesis', *Development,* 126, (9), pp. 1845-57.
Moorman, A. F. and Christoffels, V. M. (2003) 'Cardiac chamber formation: development, genes, and evolution', *Physiol Rev,* 83, (4), pp. 1223-67.

Moorman, A. F., Christoffels, V. M., Anderson, R. H. and van den Hoff, M. J. (2007) 'The heart-forming fields: one or multiple?', *Philos Trans R Soc Lond B Biol Sci,* 362, (1484), pp. 1257-65.

Moretti, A., Caron, L., Nakano, A., Lam, J. T., Bernshausen, A., Chen, Y., Qyang, Y., Bu, L., Sasaki, M., Martin-Puig, S., Sun, Y., Evans, S. M., Laugwitz, K. L. and Chien, K. R. (2006) 'Multipotent embryonic isl1+ progenitor cells lead to cardiac, smooth muscle, and endothelial cell diversification', *Cell,* 127, (6), pp. 1151-65.

Morin, S., Charron, F., Robitaille, L. and Nemer, M. (2000) 'GATA-dependent recruitment of MEF2 proteins to target promoters', *EMBO J,* 19, (9), pp. 2046-55.

Mukhopadhyay, M., Shtrom, S., Rodriguez-Esteban, C., Chen, L., Tsukui, T., Gomer, L., Dorward, D. W., Glinka, A., Grinberg, A., Huang, S. P., Niehrs, C., Izpisua Belmonte, J. C. and Westphal, H. (2001) 'Dickkopf1 is required for embryonic head induction and limb morphogenesis in the mouse', *Dev Cell,* 1, (3), pp. 423-34.

Muller, B. and Grossniklaus, U. (2010) 'Model organisms--A historical perspective', *J Proteomics,* 73, (11), pp. 2054-63.

Mummery, C., Ward-van Oostwaard, D., Doevendans, P., Spijker, R., van den Brink, S., Hassink, R., van der Heyden, M., Opthof, T., Pera, M., de la Riviere, A. B., Passier, R. and Tertoolen, L. (2003) 'Differentiation of human embryonic stem cells to cardiomyocytes: role of coculture with visceral endoderm-like cells', *Circulation,* 107, (21), pp. 2733-40.

Munemitsu, S., Albert, I., Souza, B., Rubinfeld, B. and Polakis, P. (1995) 'Regulation of intracellular beta-catenin levels by the adenomatous polyposis coli (APC) tumor-suppressor protein', *Proc Natl Acad Sci U S A,* 92, (7), pp. 3046-50.

Munoz-Sanjuan, I. and Brivanlou, A. H. (2002) 'Neural induction, the default model and embryonic stem cells', *Nat Rev Neurosci,* 3, (4), pp. 271-80.

Murdoch, J. N., Henderson, D. J., Doudney, K., Gaston-Massuet, C., Phillips, H. M., Paternotte, C., Arkell, R., Stanier, P. and Copp, A. J. (2003) 'Disruption of scribble (Scrb1) causes severe neural tube defects in the circletail mouse', *Hum Mol Genet,* 12, (2), pp. 87-98.

Muslin, A. J. (2008) 'MAPK signalling in cardiovascular health and disease: molecular mechanisms and therapeutic targets', *Clin Sci (Lond),* 115, (7), pp. 203-18.

Myant, K. and Sansom, O. (2011) 'Efficient Wnt mediated intestinal hyperproliferation requires the cyclin D2-CDK4/6 complex', *Cell Div,* 6, (1), pp. 3.

Naik, S. and Piwnica-Worms, D. (2007) 'Real-time imaging of beta-catenin dynamics in cells and living mice', *Proc Natl Acad Sci U S A,* 104, (44), pp. 17465-70.

Naito, A. T., Shiojima, I., Akazawa, H., Hidaka, K., Morisaki, T., Kikuchi, A. and Komuro, I. (2006) 'Developmental stage-specific biphasic roles of Wnt/beta-catenin signaling in cardiomyogenesis and hematopoiesis', *Proc Natl Acad Sci U S A,* 103, (52), pp. 19812-7.

Nakamura, T., Sano, M., Songyang, Z. and Schneider, M. D. (2003) 'A Wnt- and beta -catenin-dependent pathway for mammalian cardiac myogenesis', *Proc Natl Acad Sci U S A,* 100, (10), pp. 5834-9.

Nakaya, K., Murakami, M. and Funaba, M. (2008) 'Regulatory expression of Brachyury and Goosecoid in P19 embryonal carcinoma cells', *J Cell Biochem,* 105, (3), pp. 801-13.

Nakaya, K., Ooishi, R., Funaba, M. and Murakami, M. (2009) 'A JNK inhibitor SP600125 induces defective cytokinesis and enlargement in P19 embryonal carcinoma cells', *Cell Biochem Funct,* 27, (7), pp. 468-72.

Narita, N., Heikinheimo, M., Bielinska, M., White, R. A. and Wilson, D. B. (1996) 'The gene for transcription factor GATA-6 resides on mouse chromosome 18 and is expressed in myocardium and vascular smooth muscle', *Genomics,* 36, (2), pp. 345-8.

Naruishi, K., Nishimura, F., Yamada-Naruishi, H., Omori, K., Yamaguchi, M. and Takashiba, S. (2003) 'C-jun N-terminal kinase (JNK) inhibitor, SP600125, blocks interleukin (IL)-6-induced vascular endothelial growth factor (VEGF) production: cyclosporine A partially mimics this inhibitory effect', *Transplantation,* 76, (9), pp. 1380-2.

Nei, M. and Kumar, S. (2000) *Molecular evolution and phylogenetics.* Oxford University Press: Oxford ; New York.

Ng, E. S., Davis, R. P., Azzola, L., Stanley, E. G. and Elefanty, A. G. (2005) 'Forced aggregation of defined numbers of human embryonic stem cells into embryoid bodies fosters robust, reproducible hematopoietic differentiation', *Blood,* 106, (5), pp. 1601-3.

Nguyen, V. H., Schmid, B., Trout, J., Connors, S. A., Ekker, M. and Mullins, M. C. (1998) 'Ventral and lateral regions of the zebrafish gastrula, including the neural crest progenitors, are established by a bmp2b/swirl pathway of genes', *Dev Biol,* 199, (1), pp. 93-110.

Niihori, T., Aoki, Y., Narumi, Y., Neri, G., Cave, H., Verloes, A., Okamoto, N., Hennekam, R. C., Gillessen-Kaesbach, G., Wieczorek, D., Kavamura, M. I., Kurosawa, K., Ohashi, H., Wilson, L., Heron, D., Bonneau, D., Corona, G., Kaname, T., Naritomi, K., Baumann, C., Matsumoto, N., Kato, K., Kure, S. and Matsubara, Y. (2006) 'Germline KRAS and BRAF mutations in cardio-facio-cutaneous syndrome', *Nat Genet,* 38, (3), pp. 294-6.

Nijmeijer, R. M., Leeuwis, J. W., DeLisio, A., Mummery, C. L. and Chuva de Sousa Lopes, S. M. (2009) 'Visceral endoderm induces specification of cardiomyocytes in mice', *Stem Cell Res,* 3, (2-3), pp. 170-8.

Nishii, K., Morimoto, S., Minakami, R., Miyano, Y., Hashizume, K., Ohta, M., Zhan, D. Y., Lu, Q. W. and Shibata, Y. (2008) 'Targeted disruption of the cardiac troponin T gene causes sarcomere disassembly and defects in heartbeat within the early mouse embryo', *Dev Biol,* 322, (1), pp. 65-73.

Niwa, H. (2007) 'How is pluripotency determined and maintained?', *Development,* 134, (4), pp. 635-46.

Niwa, H., Burdon, T., Chambers, I. and Smith, A. (1998) 'Self-renewal of pluripotent embryonic stem cells is mediated via activation of STAT3', *Genes Dev,* 12, (13), pp. 2048-60.

Noguchi, K., Kitanaka, C., Yamana, H., Kokubu, A., Mochizuki, T. and Kuchino, Y. (1999) 'Regulation of c-Myc through phosphorylation at Ser-62 and Ser-71 by c-Jun N-terminal kinase', *J Biol Chem,* 274, (46), pp. 32580-7.

Nolan, T., Hands, R. E. and Bustin, S. A. (2006) 'Quantification of mRNA using real-time RT-PCR', *Nat Protoc,* 1, (3), pp. 1559-82.

Nonaka, S., Tanaka, Y., Okada, Y., Takeda, S., Harada, A., Kanai, Y., Kido, M. and Hirokawa, N. (1998) 'Randomization of left-right asymmetry due to loss of nodal cilia generating leftward flow of extraembryonic fluid in mice lacking KIF3B motor protein', *Cell,* 95, (6), pp. 829-37.

Nonaka, S., Yoshiba, S., Watanabe, D., Ikeuchi, S., Goto, T., Marshall, W. F. and Hamada, H. (2005) 'De novo formation of left-right asymmetry by posterior tilt of nodal cilia', *PLoS Biol,* 3, (8), pp. e268.

Noonan, J. A., Wilson, C. B., Spencer, F. C. and Talbert, W. M., Jr. (1968) 'Cerebral and cardiac complications from bacterial endocarditis. A successfully managed case with unusual complications', *Am J Dis Child,* 116, (6), pp. 666-74.

Nora, J. J. (1968) 'Multifactorial inheritance hypothesis for the etiology of congenital heart diseases. The genetic-environmental interaction', *Circulation,* 38, (3), pp. 604-17.
Notarianni, E. and Evans, M. (2006) *Embryonic Stem Cells: a practical approach.* Oxford University Press: Oxford New York.
Nusse, R. (2003) 'Wnts and Hedgehogs: lipid-modified proteins and similarities in signaling mechanisms at the cell surface', *Development,* 130, (22), pp. 5297-305.
O'Brien, T. X., Lee, K. J. and Chien, K. R. (1993) 'Positional specification of ventricular myosin light chain 2 expression in the primitive murine heart tube', *Proc Natl Acad Sci U S A,* 90, (11), pp. 5157-61.
Ogawa, K., Nishinakamura, R., Iwamatsu, Y., Shimosato, D. and Niwa, H. (2006) 'Synergistic action of Wnt and LIF in maintaining pluripotency of mouse ES cells', *Biochem Biophys Res Commun,* 343, (1), pp. 159-66.
Okada, Y., Takeda, S., Tanaka, Y., Belmonte, J. C. and Hirokawa, N. (2005) 'Mechanism of nodal flow: a conserved symmetry breaking event in left-right axis determination', *Cell,* 121, (4), pp. 633-44.
Olson, E. N. (2006) 'Gene regulatory networks in the evolution and development of the heart', *Science,* 313, (5795), pp. 1922-7.
Orsborn, A. M., Li, W., McEwen, T. J., Mizuno, T., Kuzmin, E., Matsumoto, K. and Bennett, K. L. (2007) 'GLH-1, the C. elegans P granule protein, is controlled by the JNK KGB-1 and by the COP9 subunit CSN-5', *Development,* 134, (18), pp. 3383-92.
Pagon, R. A., Graham, J. M., Jr., Zonana, J. and Yong, S. L. (1981) 'Coloboma, congenital heart disease, and choanal atresia with multiple anomalies: CHARGE association', *J Pediatr,* 99, (2), pp. 223-7.
Pandur, P., Lasche, M., Eisenberg, L. M. and Kuhl, M. (2002) 'Wnt-11 activation of a non-canonical Wnt signalling pathway is required for cardiogenesis', *Nature,* 418, (6898), pp. 636-41.
Park, M. and Moon, R. T. (2002) 'The planar cell-polarity gene stbm regulates cell behaviour and cell fate in vertebrate embryos', *Nat Cell Biol,* 4, (1), pp. 20-5.
Park, M., Wu, X., Golden, K., Axelrod, J. D. and Bodmer, R. (1996) 'The wingless signaling pathway is directly involved in Drosophila heart development', *Dev Biol,* 177, (1), pp. 104-16.
Parr, B. A., Cornish, V. A., Cybulsky, M. I. and McMahon, A. P. (2001) 'Wnt7b regulates placental development in mice', *Dev Biol,* 237, (2), pp. 324-32.
Pasumarthi, K. B., Nakajima, H., Nakajima, H. O., Soonpaa, M. H. and Field, L. J. (2005) 'Targeted expression of cyclin D2 results in cardiomyocyte DNA synthesis and infarct regression in transgenic mice', *Circ Res,* 96, (1), pp. 110-8.
Patel, S., Yenush, L., Rodriguez, P. L., Serrano, R. and Blundell, T. L. (2002) 'Crystal structure of an enzyme displaying both inositol-polyphosphate-1-phosphatase and 3'-phosphoadenosine-5'-phosphate phosphatase activities: a novel target of lithium therapy', *J Mol Biol,* 315, (4), pp. 677-85.
Patient, R. K. and McGhee, J. D. (2002) 'The GATA family (vertebrates and invertebrates)', *Curr Opin Genet Dev,* 12, (4), pp. 416-22.
Pearson, L. L., Castle, B. E. and Kehry, M. R. (2001) 'CD40-mediated signaling in monocytic cells: up-regulation of tumor necrosis factor receptor-associated factor mRNAs and activation of mitogen-activated protein kinase signaling pathways', *Int Immunol,* 13, (3), pp. 273-83.
Pease, S., Braghetta, P., Gearing, D., Grail, D. and Williams, R. L. (1990) 'Isolation of embryonic stem (ES) cells in media supplemented with recombinant leukemia inhibitory factor (LIF)', *Dev Biol,* 141, (2), pp. 344-52.

Pedersen, R. A., Wu, K. and Balakier, H. (1986) 'Origin of the inner cell mass in mouse embryos: cell lineage analysis by microinjection', *Dev Biol,* 117, (2), pp. 581-95.
Pelengaris, S., Khan, M. and Evan, G. (2002) 'c-MYC: more than just a matter of life and death', *Nat Rev Cancer,* 2, (10), pp. 764-76.
Pellizzari, L., D'Elia, A., Rustighi, A., Manfioletti, G., Tell, G. and Damante, G. (2000) 'Expression and function of the homeodomain-containing protein Hex in thyroid cells', *Nucleic Acids Res,* 28, (13), pp. 2503-11.
Pera, M. F., Reubinoff, B. and Trounson, A. (2000) 'Human embryonic stem cells', *J Cell Sci,* 113 (Pt 1), pp. 5-10.
Perez-Pomares, J. M., Phelps, A., Sedmerova, M. and Wessels, A. (2003) 'Epicardial-like cells on the distal arterial end of the cardiac outflow tract do not derive from the proepicardium but are derivatives of the cephalic pericardium', *Dev Dyn,* 227, (1), pp. 56-68.
Peterkin, T., Gibson, A., Loose, M. and Patient, R. (2005) 'The roles of GATA-4, -5 and -6 in vertebrate heart development', *Semin Cell Dev Biol,* 16, (1), pp. 83-94.
Peterkin, T., Gibson, A. and Patient, R. (2007) 'Redundancy and evolution of GATA factor requirements in development of the myocardium', *Dev Biol,* 311, (2), pp. 623-35.
Peterkin, T., Gibson, A. and Patient, R. (2009) 'Common genetic control of haemangioblast and cardiac development in zebrafish', *Development,* 136, (9), pp. 1465-74.
Petrich, B. G., Eloff, B. C., Lerner, D. L., Kovacs, A., Saffitz, J. E., Rosenbaum, D. S. and Wang, Y. (2004) 'Targeted activation of c-Jun N-terminal kinase in vivo induces restrictive cardiomyopathy and conduction defects', *J Biol Chem,* 279, (15), pp. 15330-8.
Petrich, B. G., Gong, X., Lerner, D. L., Wang, X., Brown, J. H., Saffitz, J. E. and Wang, Y. (2002) 'c-Jun N-terminal kinase activation mediates downregulation of connexin43 in cardiomyocytes', *Circ Res,* 91, (7), pp. 640-7.
Pfaff, S. L., Mendelsohn, M., Stewart, C. L., Edlund, T. and Jessell, T. M. (1996) 'Requirement for LIM homeobox gene Isl1 in motor neuron generation reveals a motor neuron-dependent step in interneuron differentiation', *Cell,* 84, (2), pp. 309-20.
Pfaffl, M. W. (2001) 'A new mathematical model for relative quantification in real-time RT-PCR', *Nucleic Acids Res,* 29, (9), pp. e45.
Pfeifer, I., Anderson, C., Werner, R. and Oltra, E. (2004) 'Redefining the structure of the mouse connexin43 gene: selective promoter usage and alternative splicing mechanisms yield transcripts with different translational efficiencies', *Nucleic Acids Res,* 32, (15), pp. 4550-62.
Phillips, H. M., Hildreth, V., Peat, J. D., Murdoch, J. N., Kobayashi, K., Chaudhry, B. and Henderson, D. J. (2008) 'Non-cell-autonomous roles for the planar cell polarity gene Vangl2 in development of the coronary circulation', *Circ Res,* 102, (5), pp. 615-23.
Phillips, H. M., Rhee, H. J., Murdoch, J. N., Hildreth, V., Peat, J. D., Anderson, R. H., Copp, A. J., Chaudhry, B. and Henderson, D. J. (2007) 'Disruption of planar cell polarity signaling results in congenital heart defects and cardiomyopathy attributable to early cardiomyocyte disorganization', *Circ Res,* 101, (2), pp. 137-45.
Pikkarainen, S., Tokola, H., Kerkela, R. and Ruskoaho, H. (2004) 'GATA transcription factors in the developing and adult heart', *Cardiovasc Res,* 63, (2), pp. 196-207.
Polychronopoulos, P., Magiatis, P., Skaltsounis, A. L., Myrianthopoulos, V., Mikros, E., Tarricone, A., Musacchio, A., Roe, S. M., Pearl, L., Leost, M., Greengard, P. and Meijer, L. (2004) 'Structural basis for the synthesis of indirubins as potent

and selective inhibitors of glycogen synthase kinase-3 and cyclin-dependent kinases', *J Med Chem,* 47, (4), pp. 935-46.
Ponchel, F., Toomes, C., Bransfield, K., Leong, F. T., Douglas, S. H., Field, S. L., Bell, S. M., Combaret, V., Puisieux, A., Mighell, A. J., Robinson, P. A., Inglehearn, C. F., Isaacs, J. D. and Markham, A. F. (2003) 'Real-time PCR based on SYBR-Green I fluorescence: an alternative to the TaqMan assay for a relative quantification of gene rearrangements, gene amplifications and micro gene deletions', *BMC Biotechnol,* 3, pp. 18.
Poole, C. A., Flint, M. H. and Beaumont, B. W. (1985) 'Analysis of the morphology and function of primary cilia in connective tissues: a cellular cybernetic probe?', *Cell Motil,* 5, (3), pp. 175-93.
Postlethwait, J. H., Woods, I. G., Ngo-Hazelett, P., Yan, Y. L., Kelly, P. D., Chu, F., Huang, H., Hill-Force, A. and Talbot, W. S. (2000) 'Zebrafish comparative genomics and the origins of vertebrate chromosomes', *Genome Res,* 10, (12), pp. 1890-902.
Prall, O. W., Menon, M. K., Solloway, M. J., Watanabe, Y., Zaffran, S., Bajolle, F., Biben, C., McBride, J. J., Robertson, B. R., Chaulet, H., Stennard, F. A., Wise, N., Schaft, D., Wolstein, O., Furtado, M. B., Shiratori, H., Chien, K. R., Hamada, H., Black, B. L., Saga, Y., Robertson, E. J., Buckingham, M. E. and Harvey, R. P. (2007) 'An Nkx2-5/Bmp2/Smad1 negative feedback loop controls heart progenitor specification and proliferation', *Cell,* 128, (5), pp. 947-59.
Privratsky, J. R., Newman, D. K. and Newman, P. J. (2010) 'PECAM-1: conflicts of interest in inflammation', *Life Sci,* 87, (3-4), pp. 69-82.
Prochnow, N. and Dermietzel, R. (2008) 'Connexons and cell adhesion: a romantic phase', *Histochem Cell Biol,* 130, (1), pp. 71-7.
Qi, M. and Elion, E. A. (2005) 'MAP kinase pathways', *J Cell Sci,* 118, (Pt 16), pp. 3569-72.
Quasnichka, H., Slater, S. C., Beeching, C. A., Boehm, M., Sala-Newby, G. B. and George, S. J. (2006) 'Regulation of smooth muscle cell proliferation by beta-catenin/T-cell factor signaling involves modulation of cyclin D1 and p21 expression', *Circ Res,* 99, (12), pp. 1329-37.
Raman, M., Chen, W. and Cobb, M. H. (2007) 'Differential regulation and properties of MAPKs', *Oncogene,* 26, (22), pp. 3100-12.
Rao, G., Pedone, C. A., Coffin, C. M., Holland, E. C. and Fults, D. W. (2003) 'c-Myc enhances sonic hedgehog-induced medulloblastoma formation from nestin-expressing neural progenitors in mice', *Neoplasia,* 5, (3), pp. 198-204.
Rauch, G. J., Hammerschmidt, M., Blader, P., Schauerte, H. E., Strahle, U., Ingham, P. W., McMahon, A. P. and Haffter, P. (1997) 'Wnt5 is required for tail formation in the zebrafish embryo', *Cold Spring Harb Symp Quant Biol,* 62, pp. 227-34.
Regan, C. P., Li, W., Boucher, D. M., Spatz, S., Su, M. S. and Kuida, K. (2002) 'Erk5 null mice display multiple extraembryonic vascular and embryonic cardiovascular defects', *Proc Natl Acad Sci U S A,* 99, (14), pp. 9248-53.
Reifers, F., Walsh, E. C., Leger, S., Stainier, D. Y. and Brand, M. (2000) 'Induction and differentiation of the zebrafish heart requires fibroblast growth factor 8 (fgf8/acerebellar)', *Development,* 127, (2), pp. 225-35.
Reiter, J. F., Alexander, J., Rodaway, A., Yelon, D., Patient, R., Holder, N. and Stainier, D. Y. (1999) 'Gata5 is required for the development of the heart and endoderm in zebrafish', *Genes Dev,* 13, (22), pp. 2983-95.
Reiter, J. F., Verkade, H. and Stainier, D. Y. (2001) 'Bmp2b and Oep promote early myocardial differentiation through their regulation of gata5', *Dev Biol,* 234, (2), pp. 330-8.

Renlund, N., Pieretti-Vanmarcke, R., O'Neill, F. H., Zhang, L., Donahoe, P. K. and Teixeira, J. (2008) 'c-Jun N-terminal kinase inhibitor II (SP600125) activates Mullerian inhibiting substance type II receptor-mediated signal transduction', *Endocrinology,* 149, (1), pp. 108-15.

Resnick, L. and Fennell, M. (2004) 'Targeting JNK3 for the treatment of neurodegenerative disorders', *Drug Discov Today,* 9, (21), pp. 932-9.

Ribeiro, I., Kawakami, Y., Buscher, D., Raya, A., Rodriguez-Leon, J., Morita, M., Rodriguez Esteban, C. and Izpisua Belmonte, J. C. (2007) 'Tbx2 and Tbx3 regulate the dynamics of cell proliferation during heart remodeling', *PLoS One,* 2, (4), pp. e398.

Ribes, V., Balaskas, N., Sasai, N., Cruz, C., Dessaud, E., Cayuso, J., Tozer, S., Yang, L. L., Novitch, B., Marti, E. and Briscoe, J. (2010) 'Distinct Sonic Hedgehog signaling dynamics specify floor plate and ventral neuronal progenitors in the vertebrate neural tube', *Genes Dev,* 24, (11), pp. 1186-200.

Riesgo-Escovar, J. R., Jenni, M., Fritz, A. and Hafen, E. (1996) 'The Drosophila Jun-N-terminal kinase is required for cell morphogenesis but not for DJun-dependent cell fate specification in the eye', *Genes Dev,* 10, (21), pp. 2759-68.

Riley, P. R., Gertsenstein, M., Dawson, K. and Cross, J. C. (2000) 'Early exclusion of hand1-deficient cells from distinct regions of the left ventricular myocardium in chimeric mouse embryos', *Dev Biol,* 227, (1), pp. 156-68.

Risau, W., Sariola, H., Zerwes, H. G., Sasse, J., Ekblom, P., Kemler, R. and Doetschman, T. (1988) 'Vasculogenesis and angiogenesis in embryonic-stem-cell-derived embryoid bodies', *Development,* 102, (3), pp. 471-8.

Rivera-Feliciano, J., Lee, K. H., Kong, S. W., Rajagopal, S., Ma, Q., Springer, Z., Izumo, S., Tabin, C. J. and Pu, W. T. (2006) 'Development of heart valves requires Gata4 expression in endothelial-derived cells', *Development,* 133, (18), pp. 3607-18.

Roberts, A. E., Araki, T., Swanson, K. D., Montgomery, K. T., Schiripo, T. A., Joshi, V. A., Li, L., Yassin, Y., Tamburino, A. M., Neel, B. G. and Kucherlapati, R. S. (2007) 'Germline gain-of-function mutations in SOS1 cause Noonan syndrome', *Nat Genet,* 39, (1), pp. 70-4.

Rocke, J., Lees, J., Packham, I. and Chico, T. (2009) 'The zebrafish as a novel tool for cardiovascular drug discovery', *Recent Pat Cardiovasc Drug Discov,* 4, (1), pp. 1-5.

Rodriguez-Viciana, P., Tetsu, O., Tidyman, W. E., Estep, A. L., Conger, B. A., Cruz, M. S., McCormick, F. and Rauen, K. A. (2006) 'Germline mutations in genes within the MAPK pathway cause cardio-facio-cutaneous syndrome', *Science,* 311, (5765), pp. 1287-90.

Roel, G., Hamilton, F. S., Gent, Y., Bain, A. A., Destree, O. and Hoppler, S. (2002) 'Lef-1 and Tcf-3 transcription factors mediate tissue-specific Wnt signaling during Xenopus development', *Curr Biol,* 12, (22), pp. 1941-5.

Rogers, J. S. (1997) 'On the consistency of maximum likelihood estimation of phylogenetic trees from nucleotide sequences', *Syst Biol,* 46, (2), pp. 354-7.

Rohr, S., Otten, C. and Abdelilah-Seyfried, S. (2008) 'Asymmetric involution of the myocardial field drives heart tube formation in zebrafish', *Circ Res,* 102, (2), pp. e12-9.

Rones, M. S., McLaughlin, K. A., Raffin, M. and Mercola, M. (2000) 'Serrate and Notch specify cell fates in the heart field by suppressing cardiomyogenesis', *Development,* 127, (17), pp. 3865-76.

Rose, B. A., Force, T. and Wang, Y. (2010) 'Mitogen-activated protein kinase signaling in the heart: angels versus demons in a heart-breaking tale', *Physiol Rev,* 90, (4), pp. 1507-46.

Ross, A. J., May-Simera, H., Eichers, E. R., Kai, M., Hill, J., Jagger, D. J., Leitch, C. C., Chapple, J. P., Munro, P. M., Fisher, S., Tan, P. L., Phillips, H. M., Leroux, M. R., Henderson, D. J., Murdoch, J. N., Copp, A. J., Eliot, M. M., Lupski, J. R., Kemp, D. T., Dollfus, H., Tada, M., Katsanis, N., Forge, A. and Beales, P. L. (2005) 'Disruption of Bardet-Biedl syndrome ciliary proteins perturbs planar cell polarity in vertebrates', *Nat Genet,* 37, (10), pp. 1135-40.

Roszko, I., Sawada, A. and Solnica-Krezel, L. (2009) 'Regulation of convergence and extension movements during vertebrate gastrulation by the Wnt/PCP pathway', *Semin Cell Dev Biol,* 20, (8), pp. 986-97.

Roux, P. P. and Blenis, J. (2004) 'ERK and p38 MAPK-activated protein kinases: a family of protein kinases with diverse biological functions', *Microbiol Mol Biol Rev,* 68, (2), pp. 320-44.

Rudy-Reil, D. and Lough, J. (2004) 'Avian precardiac endoderm/mesoderm induces cardiac myocyte differentiation in murine embryonic stem cells', *Circ Res,* 94, (12), pp. e107-16.

Rui, Y., Xu, Z., Xiong, B., Cao, Y., Lin, S., Zhang, M., Chan, S. C., Luo, W., Han, Y., Lu, Z., Ye, Z., Zhou, H. M., Han, J., Meng, A. and Lin, S. C. (2007) 'A beta-catenin-independent dorsalization pathway activated by Axin/JNK signaling and antagonized by aida', *Dev Cell,* 13, (2), pp. 268-82.

Sabapathy, K., Hochedlinger, K., Nam, S. Y., Bauer, A., Karin, M. and Wagner, E. F. (2004) 'Distinct roles for JNK1 and JNK2 in regulating JNK activity and c-Jun-dependent cell proliferation', *Mol Cell,* 15, (5), pp. 713-25.

Sabapathy, K., Hu, Y., Kallunki, T., Schreiber, M., David, J. P., Jochum, W., Wagner, E. F. and Karin, M. (1999) 'JNK2 is required for efficient T-cell activation and apoptosis but not for normal lymphocyte development', *Curr Biol,* 9, (3), pp. 116-25.

Sabapathy, K., Kallunki, T., David, J. P., Graef, I., Karin, M. and Wagner, E. F. (2001) 'c-Jun NH2-terminal kinase (JNK)1 and JNK2 have similar and stage-dependent roles in regulating T cell apoptosis and proliferation', *J Exp Med,* 193, (3), pp. 317-28.

Sachinidis, A., Fleischmann, B. K., Kolossov, E., Wartenberg, M., Sauer, H. and Hescheler, J. (2003) 'Cardiac specific differentiation of mouse embryonic stem cells', *Cardiovasc Res,* 58, (2), pp. 278-91.

Sadoshima, J., Montagne, O., Wang, Q., Yang, G., Warden, J., Liu, J., Takagi, G., Karoor, V., Hong, C., Johnson, G. L., Vatner, D. E. and Vatner, S. F. (2002) 'The MEKK1-JNK pathway plays a protective role in pressure overload but does not mediate cardiac hypertrophy', *J Clin Invest,* 110, (2), pp. 271-9.

Saga, Y., Miyagawa-Tomita, S., Takagi, A., Kitajima, S., Miyazaki, J. and Inoue, T. (1999) 'MesP1 is expressed in the heart precursor cells and required for the formation of a single heart tube', *Development,* 126, (15), pp. 3437-47.

Saijoh, Y., Oki, S., Ohishi, S. and Hamada, H. (2003) 'Left-right patterning of the mouse lateral plate requires nodal produced in the node', *Dev Biol,* 256, (1), pp. 160-72.

Sakaguchi, T., Kikuchi, Y., Kuroiwa, A., Takeda, H. and Stainier, D. Y. (2006) 'The yolk syncytial layer regulates myocardial migration by influencing extracellular matrix assembly in zebrafish', *Development,* 133, (20), pp. 4063-72.

Sakaguchi, T., Mizuno, T. and Takeda, H. (2002) 'Formation and patterning roles of the yolk syncytial layer', *Results Probl Cell Differ,* 40, pp. 1-14.

Saneyoshi, T., Kume, S., Amasaki, Y. and Mikoshiba, K. (2002) 'The Wnt/calcium pathway activates NF-AT and promotes ventral cell fate in Xenopus embryos', *Nature,* 417, (6886), pp. 295-9.

Sansom, O. J., Meniel, V. S., Muncan, V., Phesse, T. J., Wilkins, J. A., Reed, K. R., Vass, J. K., Athineos, D., Clevers, H. and Clarke, A. R. (2007) 'Myc deletion rescues Apc deficiency in the small intestine', *Nature,* 446, (7136), pp. 676-9.

Sato, M. and Yost, H. J. (2003) 'Cardiac neural crest contributes to cardiomyogenesis in zebrafish', *Dev Biol,* 257, (1), pp. 127-39.

Sato, N., Meijer, L., Skaltsounis, L., Greengard, P. and Brivanlou, A. H. (2004) 'Maintenance of pluripotency in human and mouse embryonic stem cells through activation of Wnt signaling by a pharmacological GSK-3-specific inhibitor', *Nat Med,* 10, (1), pp. 55-63.

Satoh, W., Matsuyama, M., Takemura, H., Aizawa, S. and Shimono, A. (2008) 'Sfrp1, Sfrp2, and Sfrp5 regulate the Wnt/beta-catenin and the planar cell polarity pathways during early trunk formation in mouse', *Genesis,* 46, (2), pp. 92-103.

Satyanarayana, A. and Kaldis, P. (2009) 'Mammalian cell-cycle regulation: several Cdks, numerous cyclins and diverse compensatory mechanisms', *Oncogene,* 28, (33), pp. 2925-39.

Scapin, G., Patel, S. B., Lisnock, J., Becker, J. W. and LoGrasso, P. V. (2003) 'The structure of JNK3 in complex with small molecule inhibitors: structural basis for potency and selectivity', *Chem Biol,* 10, (8), pp. 705-12.

Schang, L. M. (2003) 'The cell cycle, cyclin-dependent kinases, and viral infections: new horizons and unexpected connections', *Prog Cell Cycle Res,* 5, pp. 103-24.

Schier, A. F. (2001) 'Axis formation and patterning in zebrafish', *Curr Opin Genet Dev,* 11, (4), pp. 393-404.

Schier, A. F. (2009) 'Nodal morphogens', *Cold Spring Harb Perspect Biol,* 1, (5), pp. a003459.

Schlange, T., Andree, B., Arnold, H. H. and Brand, T. (2000) 'BMP2 is required for early heart development during a distinct time period', *Mech Dev,* 91, (1-2), pp. 259-70.

Schneider, V. A. and Mercola, M. (2001) 'Wnt antagonism initiates cardiogenesis in Xenopus laevis', *Genes Dev,* 15, (3), pp. 304-15.

Schonwasser, D. C., Marais, R. M., Marshall, C. J. and Parker, P. J. (1998) 'Activation of the mitogen-activated protein kinase/extracellular signal-regulated kinase pathway by conventional, novel, and atypical protein kinase C isotypes', *Mol Cell Biol,* 18, (2), pp. 790-8.

Schott, J. J., Benson, D. W., Basson, C. T., Pease, W., Silberbach, G. M., Moak, J. P., Maron, B. J., Seidman, C. E. and Seidman, J. G. (1998) 'Congenital heart disease caused by mutations in the transcription factor NKX2-5', *Science,* 281, (5373), pp. 108-11.

Schubbert, S., Bollag, G. and Shannon, K. (2007) 'Deregulated Ras signaling in developmental disorders: new tricks for an old dog', *Curr Opin Genet Dev,* 17, (1), pp. 15-22.

Schubbert, S., Zenker, M., Rowe, S. L., Boll, S., Klein, C., Bollag, G., van der Burgt, I., Musante, L., Kalscheuer, V., Wehner, L. E., Nguyen, H., West, B., Zhang, K. Y., Sistermans, E., Rauch, A., Niemeyer, C. M., Shannon, K. and Kratz, C. P. (2006) 'Germline KRAS mutations cause Noonan syndrome', *Nat Genet,* 38, (3), pp. 331-6.

Schultheiss, T. M., Xydas, S. and Lassar, A. B. (1995) 'Induction of avian cardiac myogenesis by anterior endoderm', *Development,* 121, (12), pp. 4203-14.

Schulze, M., Belema-Bedada, F., Technau, A. and Braun, T. (2005) 'Mesenchymal stem cells are recruited to striated muscle by NFAT/IL-4-mediated cell fusion', *Genes Dev,* 19, (15), pp. 1787-98.

Schwartz, R. S. and Mueller, R. L. (2010) 'Variation in DNA substitution rates among lineages erroneously inferred from simulated clock-like data', *PLoS One,* 5, (3), pp. e9649.
Schwarz-Romond, T., Asbrand, C., Bakkers, J., Kuhl, M., Schaeffer, H. J., Huelsken, J., Behrens, J., Hammerschmidt, M. and Birchmeier, W. (2002) 'The ankyrin repeat protein Diversin recruits Casein kinase Iepsilon to the beta-catenin degradation complex and acts in both canonical Wnt and Wnt/JNK signaling', *Genes Dev,* 16, (16), pp. 2073-84.
Schwarz-Romond, T., Fiedler, M., Shibata, N., Butler, P. J., Kikuchi, A., Higuchi, Y. and Bienz, M. (2007a) 'The DIX domain of Dishevelled confers Wnt signaling by dynamic polymerization', *Nat Struct Mol Biol,* 14, (6), pp. 484-92.
Schwarz-Romond, T., Metcalfe, C. and Bienz, M. (2007b) 'Dynamic recruitment of axin by Dishevelled protein assemblies', *J Cell Sci,* 120, (Pt 14), pp. 2402-12.
Sedletcaia, A. and Evans, T. (2011) 'Heart chamber size in zebrafish is regulated redundantly by duplicated tbx2 genes', *Dev Dyn*.
Seidensticker, M. J. and Behrens, J. (2000) 'Biochemical interactions in the wnt pathway', *Biochim Biophys Acta,* 1495, (2), pp. 168-82.
Seifert, J. R. and Mlodzik, M. (2007) 'Frizzled/PCP signalling: a conserved mechanism regulating cell polarity and directed motility', *Nat Rev Genet,* 8, (2), pp. 126-38.
Seo, J., Asaoka, Y., Nagai, Y., Hirayama, J., Yamasaki, T., Namae, M., Ohata, S., Shimizu, N., Negishi, T., Kitagawa, D., Kondoh, H., Furutani-Seiki, M., Penninger, J. M., Katada, T. and Nishina, H. (2010) 'Negative regulation of wnt11 expression by Jnk signaling during zebrafish gastrulation', *J Cell Biochem,* 110, (4), pp. 1022-37.
Serbedzija, G. N., Chen, J. N. and Fishman, M. C. (1998) 'Regulation in the heart field of zebrafish', *Development,* 125, (6), pp. 1095-101.
Serluca, F. C. (2008) 'Development of the proepicardial organ in the zebrafish', *Dev Biol,* 315, (1), pp. 18-27.
Shalaby, F., Ho, J., Stanford, W. L., Fischer, K. D., Schuh, A. C., Schwartz, L., Bernstein, A. and Rossant, J. (1997) 'A requirement for Flk1 in primitive and definitive hematopoiesis and vasculogenesis', *Cell,* 89, (6), pp. 981-90.
Shang, X. Z., Zhu, H., Lin, K., Tu, Z., Chen, J., Nelson, D. R. and Liu, C. (2004) 'Stabilized beta-catenin promotes hepatocyte proliferation and inhibits TNFalpha-induced apoptosis', *Lab Invest,* 84, (3), pp. 332-41.
Shao, Z., Bhattacharya, K., Hsich, E., Park, L., Walters, B., Germann, U., Wang, Y. M., Kyriakis, J., Mohanlal, R., Kuida, K., Namchuk, M., Salituro, F., Yao, Y. M., Hou, W. M., Chen, X., Aronovitz, M., Tsichlis, P. N., Bhattacharya, S., Force, T. and Kilter, H. (2006) 'c-Jun N-terminal kinases mediate reactivation of Akt and cardiomyocyte survival after hypoxic injury in vitro and in vivo', *Circ Res,* 98, (1), pp. 111-8.
Sharma, S., Jackson, P. G. and Makan, J. (2004) 'Cardiac troponins', *J Clin Pathol,* 57, (10), pp. 1025-6.
Sherr, C. J. and Roberts, J. M. (1995) 'Inhibitors of mammalian G1 cyclin-dependent kinases', *Genes Dev,* 9, (10), pp. 1149-63.
Silva, J., Barrandon, O., Nichols, J., Kawaguchi, J., Theunissen, T. W. and Smith, A. (2008) 'Promotion of reprogramming to ground state pluripotency by signal inhibition', *PLoS Biol,* 6, (10), pp. e253.
Simons, M. and Mlodzik, M. (2008) 'Planar cell polarity signaling: from fly development to human disease', *Annu Rev Genet,* 42, pp. 517-40.
Singla, D. K., Schneider, D. J., LeWinter, M. M. and Sobel, B. E. (2006) 'wnt3a but not wnt11 supports self-renewal of embryonic stem cells', *Biochem Biophys Res Commun,* 345, (2), pp. 789-95.

Sinha, D., Wang, Z., Ruchalski, K. L., Levine, J. S., Krishnan, S., Lieberthal, W., Schwartz, J. H. and Borkan, S. C. (2005) 'Lithium activates the Wnt and phosphatidylinositol 3-kinase Akt signaling pathways to promote cell survival in the absence of soluble survival factors', *Am J Physiol Renal Physiol,* 288, (4), pp. F703-13.

Skromne, I. and Stern, C. D. (2001) 'Interactions between Wnt and Vg1 signalling pathways initiate primitive streak formation in the chick embryo', *Development,* 128, (15), pp. 2915-27.

Slusarski, D. C. and Pelegri, F. (2007) 'Calcium signaling in vertebrate embryonic patterning and morphogenesis', *Dev Biol,* 307, (1), pp. 1-13.

Small, E. M. and Krieg, P. A. (2003) 'Transgenic analysis of the atrialnatriuretic factor (ANF) promoter: Nkx2-5 and GATA-4 binding sites are required for atrial specific expression of ANF', *Dev Biol,* 261, (1), pp. 116-31.

Small, E. M. and Krieg, P. A. (2004) 'Molecular regulation of cardiac chamber-specific gene expression', *Trends Cardiovasc Med,* 14, (1), pp. 13-8.

Smith, A. (2005) 'The battlefield of pluripotency', *Cell,* 123, (5), pp. 757-60.

Smith, A. G. (2001) 'Embryo-derived stem cells: of mice and men', *Annu Rev Cell Dev Biol,* 17, pp. 435-62.

Smith, A. G., Heath, J. K., Donaldson, D. D., Wong, G. G., Moreau, J., Stahl, M. and Rogers, D. (1988) 'Inhibition of pluripotential embryonic stem cell differentiation by purified polypeptides', *Nature,* 336, (6200), pp. 688-90.

Smith, D. W., Lemli, L. and Opitz, J. M. (1964) 'A Newly Recognized Syndrome of Multiple Congenital Anomalies', *J Pediatr,* 64, pp. 210-7.

Smith, K. and Dalton, S. (2010) 'Myc transcription factors: key regulators behind establishment and maintenance of pluripotency', *Regen Med,* 5, (6), pp. 947-59.

Snaar-Jagalska, B. E., Krens, S. F., Robina, I., Wang, L. X. and Spaink, H. P. (2003) 'Specific activation of ERK pathways by chitin oligosaccharides in embryonic zebrafish cell lines', *Glycobiology,* 13, (10), pp. 725-32.

Sohl, G. and Willecke, K. (2003) 'An update on connexin genes and their nomenclature in mouse and man', *Cell Commun Adhes,* 10, (4-6), pp. 173-80.

Solan, J. L. and Lampe, P. D. (2005) 'Connexin phosphorylation as a regulatory event linked to gap junction channel assembly', *Biochim Biophys Acta,* 1711, (2), pp. 154-63.

Solan, J. L. and Lampe, P. D. (2008) 'Connexin 43 in LA-25 cells with active v-src is phosphorylated on Y247, Y265, S262, S279/282, and S368 via multiple signaling pathways', *Cell Commun Adhes,* 15, (1), pp. 75-84.

Solan, J. L. and Lampe, P. D. (2009) 'Connexin43 phosphorylation: structural changes and biological effects', *Biochem J,* 419, (2), pp. 261-72.

Solnica-Krezel, L., Stemple, D. L., Mountcastle-Shah, E., Rangini, Z., Neuhauss, S. C., Malicki, J., Schier, A. F., Stainier, D. Y., Zwartkruis, F., Abdelilah, S. and Driever, W. (1996) 'Mutations affecting cell fates and cellular rearrangements during gastrulation in zebrafish', *Development,* 123, pp. 67-80.

Song, H., Hu, J., Chen, W., Elliott, G., Andre, P., Gao, B. and Yang, Y. (2010) 'Planar cell polarity breaks bilateral symmetry by controlling ciliary positioning', *Nature,* 466, (7304), pp. 378-82.

Soonpaa, M. H., Koh, G. Y., Pajak, L., Jing, S., Wang, H., Franklin, M. T., Kim, K. K. and Field, L. J. (1997) 'Cyclin D1 overexpression promotes cardiomyocyte DNA synthesis and multinucleation in transgenic mice', *J Clin Invest,* 99, (11), pp. 2644-54.

Srivastava, D. (2006) 'Making or breaking the heart: from lineage determination to morphogenesis', *Cell,* 126, (6), pp. 1037-48.

Srivastava, D., Thomas, T., Lin, Q., Kirby, M. L., Brown, D. and Olson, E. N. (1997) 'Regulation of cardiac mesodermal and neural crest development by the bHLH transcription factor, dHAND', *Nat Genet,* 16, (2), pp. 154-60.
Stainier, D. Y. (2001) 'Zebrafish genetics and vertebrate heart formation', *Nat Rev Genet,* 2, (1), pp. 39-48.
Stainier, D. Y. and Fishman, M. C. (1992) 'Patterning the zebrafish heart tube: acquisition of anteroposterior polarity', *Dev Biol,* 153, (1), pp. 91-101.
Stainier, D. Y., Lee, R. K. and Fishman, M. C. (1993) 'Cardiovascular development in the zebrafish. I. Myocardial fate map and heart tube formation', *Development,* 119, (1), pp. 31-40.
Stark, K., Vainio, S., Vassileva, G. and McMahon, A. P. (1994) 'Epithelial transformation of metanephric mesenchyme in the developing kidney regulated by Wnt-4', *Nature,* 372, (6507), pp. 679-83.
Steel, M. and Penny, D. (2000) 'Parsimony, likelihood, and the role of models in molecular phylogenetics', *Mol Biol Evol,* 17, (6), pp. 839-50.
Strahle, U., Blader, P. and Ingham, P. W. (1996) 'Expression of axial and sonic hedgehog in wildtype and midline defective zebrafish embryos', *Int J Dev Biol,* 40, (5), pp. 929-40.
Stronach, B. E. and Perrimon, N. (1999) 'Stress signaling in Drosophila', *Oncogene,* 18, (45), pp. 6172-82.
Strutt, D. I. (2001) 'Asymmetric localization of frizzled and the establishment of cell polarity in the Drosophila wing', *Mol Cell,* 7, (2), pp. 367-75.
Strutt, H. and Strutt, D. (2009) 'Asymmetric localisation of planar polarity proteins: Mechanisms and consequences', *Semin Cell Dev Biol,* 20, (8), pp. 957-63.
Sumanas, S. and Larson, J. D. (2002) 'Morpholino phosphorodiamidate oligonucleotides in zebrafish: a recipe for functional genomics?', *Brief Funct Genomic Proteomic,* 1, (3), pp. 239-56.
Sumandea, M. P., Vahebi, S., Sumandea, C. A., Garcia-Cazarin, M. L., Staidle, J. and Homsher, E. (2009) 'Impact of cardiac troponin T N-terminal deletion and phosphorylation on myofilament function', *Biochemistry,* 48, (32), pp. 7722-31.
Sun, L., Bradford, C. S. and Barnes, D. W. (1995) 'Feeder cell cultures for zebrafish embryonal cells in vitro', *Mol Mar Biol Biotechnol,* 4, (1), pp. 43-50.
Tabin, C. J. and Vogan, K. J. (2003) 'A two-cilia model for vertebrate left-right axis specification', *Genes Dev,* 17, (1), pp. 1-6.
Tachibana, H., Perrino, C., Takaoka, H., Davis, R. J., Naga Prasad, S. V. and Rockman, H. A. (2006) 'JNK1 is required to preserve cardiac function in the early response to pressure overload', *Biochem Biophys Res Commun,* 343, (4), pp. 1060-6.
Tahinci, E., Thorne, C. A., Franklin, J. L., Salic, A., Christian, K. M., Lee, L. A., Coffey, R. J. and Lee, E. (2007) 'Lrp6 is required for convergent extension during Xenopus gastrulation', *Development,* 134, (22), pp. 4095-106.
Takada, S., Stark, K. L., Shea, M. J., Vassileva, G., McMahon, J. A. and McMahon, A. P. (1994) 'Wnt-3a regulates somite and tailbud formation in the mouse embryo', *Genes Dev,* 8, (2), pp. 174-89.
Takahashi, T., Lord, B., Schulze, P. C., Fryer, R. M., Sarang, S. S., Gullans, S. R. and Lee, R. T. (2003) 'Ascorbic acid enhances differentiation of embryonic stem cells into cardiac myocytes', *Circulation,* 107, (14), pp. 1912-6.
Takao, Y., Yokota, T. and Koide, H. (2007) 'Beta-catenin up-regulates Nanog expression through interaction with Oct-3/4 in embryonic stem cells', *Biochem Biophys Res Commun,* 353, (3), pp. 699-705.
Takeuchi, J. K. and Bruneau, B. G. (2009) 'Directed transdifferentiation of mouse mesoderm to heart tissue by defined factors', *Nature,* 459, (7247), pp. 708-11.

Tam, P. P., Parameswaran, M., Kinder, S. J. and Weinberger, R. P. (1997) 'The allocation of epiblast cells to the embryonic heart and other mesodermal lineages: the role of ingression and tissue movement during gastrulation', *Development,* 124, (9), pp. 1631-42.

Tam, P. P. and Steiner, K. A. (1999) 'Anterior patterning by synergistic activity of the early gastrula organizer and the anterior germ layer tissues of the mouse embryo', *Development,* 126, (22), pp. 5171-9.

Tamai, K., Semenov, M., Kato, Y., Spokony, R., Liu, C., Katsuyama, Y., Hess, F., Saint-Jeannet, J. P. and He, X. (2000) 'LDL-receptor-related proteins in Wnt signal transduction', *Nature,* 407, (6803), pp. 530-5.

Tamimi, Y., Skarie, J. M., Footz, T., Berry, F. B., Link, B. A. and Walter, M. A. (2006) 'FGF19 is a target for FOXC1 regulation in ciliary body-derived cells', *Hum Mol Genet,* 15, (21), pp. 3229-40.

Tamura, K. and Nei, M. (1993) 'Estimation of the number of nucleotide substitutions in the control region of mitochondrial DNA in humans and chimpanzees', *Mol Biol Evol,* 10, (3), pp. 512-26.

Tamura, K., Peterson, D., Peterson, N., Stecher, G., Nei, M. and Kumar, S. (2011) 'MEGA5: Molecular Evolutionary Genetics Analysis using Maximum Likelihood, Evolutionary Distance, and Maximum Parsimony Methods', *Mol Biol Evol*.

Tanemura, S., Momose, H., Shimizu, N., Kitagawa, D., Seo, J., Yamasaki, T., Nakagawa, K., Kajiho, H., Penninger, J. M., Katada, T. and Nishina, H. (2009) 'Blockage by SP600125 of Fcepsilon receptor-induced degranulation and cytokine gene expression in mast cells is mediated through inhibition of phosphatidylinositol 3-kinase signalling pathway', *J Biochem,* 145, (3), pp. 345-54.

Tang, D. G., Chen, Y. Q., Newman, P. J., Shi, L., Gao, X., Diglio, C. A. and Honn, K. V. (1993) 'Identification of PECAM-1 in solid tumor cells and its potential involvement in tumor cell adhesion to endothelium', *J Biol Chem,* 268, (30), pp. 22883-94.

Tanoue, T., Adachi, M., Moriguchi, T. and Nishida, E. (2000) 'A conserved docking motif in MAP kinases common to substrates, activators and regulators', *Nat Cell Biol,* 2, (2), pp. 110-6.

Tanoue, T. and Nishida, E. (2003) 'Molecular recognitions in the MAP kinase cascades', *Cell Signal,* 15, (5), pp. 455-62.

Targoff, K. L., Schell, T. and Yelon, D. (2008) 'Nkx genes regulate heart tube extension and exert differential effects on ventricular and atrial cell number', *Dev Biol,* 322, (2), pp. 314-21.

Tartaglia, M., Cordeddu, V., Chang, H., Shaw, A., Kalidas, K., Crosby, A., Patton, M. A., Sorcini, M., van der Burgt, I., Jeffery, S. and Gelb, B. D. (2004) 'Paternal germline origin and sex-ratio distortion in transmission of PTPN11 mutations in Noonan syndrome', *Am J Hum Genet,* 75, (3), pp. 492-7.

Technau, U. (2001) 'Brachyury, the blastopore and the evolution of the mesoderm', *Bioessays,* 23, (9), pp. 788-94.

ten Berge, D., Koole, W., Fuerer, C., Fish, M., Eroglu, E. and Nusse, R. (2008) 'Wnt signaling mediates self-organization and axis formation in embryoid bodies', *Cell Stem Cell,* 3, (5), pp. 508-18.

Terada, R., Warren, S., Lu, J. T., Chien, K. R., Wessels, A. and Kasahara, H. (2011) 'Ablation of Nkx2-5 at mid-embryonic stage results in premature lethality and cardiac malformation', *Cardiovasc Res,* 91, (2), pp. 289-99.

Terami, H., Hidaka, K., Katsumata, T., Iio, A. and Morisaki, T. (2004) 'Wnt11 facilitates embryonic stem cell differentiation to Nkx2.5-positive cardiomyocytes', *Biochem Biophys Res Commun,* 325, (3), pp. 968-75.

Terrett, J. A., Newbury-Ecob, R., Cross, G. S., Fenton, I., Raeburn, J. A., Young, I. D. and Brook, J. D. (1994) 'Holt-Oram syndrome is a genetically heterogeneous disease with one locus mapping to human chromosome 12q', *Nat Genet,* 6, (4), pp. 401-4.

Thaler, J. P., Koo, S. J., Kania, A., Lettieri, K., Andrews, S., Cox, C., Jessell, T. M. and Pfaff, S. L. (2004) 'A postmitotic role for Isl-class LIM homeodomain proteins in the assignment of visceral spinal motor neuron identity', *Neuron,* 41, (3), pp. 337-50.

Thisse, B., Heyer, V., Lux, A., Alunni, V., Degrave, A., Seiliez, I., Kirchner, J., Parkhill, J. P. and Thisse, C. (2004) 'Spatial and temporal expression of the zebrafish genome by large-scale in situ hybridization screening', *Methods Cell Biol,* 77, pp. 505-19.

Thisse, C. and Thisse, B. (2008) 'High-resolution in situ hybridization to whole-mount zebrafish embryos', *Nat Protoc,* 3, (1), pp. 59-69.

Thisse, C., Thisse, B., Schilling, T. F. and Postlethwait, J. H. (1993) 'Structure of the zebrafish snail1 gene and its expression in wild-type, spadetail and no tail mutant embryos', *Development,* 119, (4), pp. 1203-15.

Thomas, P. Q., Brown, A. and Beddington, R. S. (1998) 'Hex: a homeobox gene revealing peri-implantation asymmetry in the mouse embryo and an early transient marker of endothelial cell precursors', *Development,* 125, (1), pp. 85-94.

Thomson, J. A. and Marshall, V. S. (1998) 'Primate embryonic stem cells', *Curr Top Dev Biol,* 38, pp. 133-65.

Thor, S., Andersson, S. G., Tomlinson, A. and Thomas, J. B. (1999) 'A LIM-homeodomain combinatorial code for motor-neuron pathway selection', *Nature,* 397, (6714), pp. 76-80.

Tidyman, W. E. and Rauen, K. A. (2008) 'Noonan, Costello and cardio-facio-cutaneous syndromes: dysregulation of the Ras-MAPK pathway', *Expert Rev Mol Med,* 10, pp. e37.

Tong, C., Yin, Z., Song, Z., Dockendorff, A., Huang, C., Mariadason, J., Flavell, R. A., Davis, R. J., Augenlicht, L. H. and Yang, W. (2007) 'c-Jun NH2-terminal kinase 1 plays a critical role in intestinal homeostasis and tumor suppression', *Am J Pathol,* 171, (1), pp. 297-303.

Topczewski, J., Sepich, D. S., Myers, D. C., Walker, C., Amores, A., Lele, Z., Hammerschmidt, M., Postlethwait, J. and Solnica-Krezel, L. (2001) 'The zebrafish glypican knypek controls cell polarity during gastrulation movements of convergent extension', *Dev Cell,* 1, (2), pp. 251-64.

Torban, E., Kor, C. and Gros, P. (2004) 'Van Gogh-like2 (Strabismus) and its role in planar cell polarity and convergent extension in vertebrates', *Trends Genet,* 20, (11), pp. 570-7.

Toumadje, A., Kusumoto, K., Parton, A., Mericko, P., Dowell, L., Ma, G., Chen, L., Barnes, D. W. and Sato, J. D. (2003) 'Pluripotent differentiation in vitro of murine ES-D3 embryonic stem cells', *In Vitro Cell Dev Biol Anim,* 39, (10), pp. 449-53.

Trinh, L. A. and Stainier, D. Y. (2004) 'Cardiac development', *Methods Cell Biol,* 76, pp. 455-73.

Tsang, M., Maegawa, S., Kiang, A., Habas, R., Weinberg, E. and Dawid, I. B. (2004) 'A role for MKP3 in axial patterning of the zebrafish embryo', *Development,* 131, (12), pp. 2769-79.

Tseng, A. S., Engel, F. B. and Keating, M. T. (2006) 'The GSK-3 inhibitor BIO promotes proliferation in mammalian cardiomyocytes', *Chem Biol,* 13, (9), pp. 957-63.

Tuncman, G., Hirosumi, J., Solinas, G., Chang, L., Karin, M. and Hotamisligil, G. S. (2006) 'Functional in vivo interactions between JNK1 and JNK2 isoforms in obesity and insulin resistance', *Proc Natl Acad Sci U S A,* 103, (28), pp. 10741-6.

Turjanski, A. G., Vaque, J. P. and Gutkind, J. S. (2007) 'MAP kinases and the control of nuclear events', *Oncogene,* 26, (22), pp. 3240-53.

Tutter, A. V., Fryer, C. J. and Jones, K. A. (2001) 'Chromatin-specific regulation of LEF-1-beta-catenin transcription activation and inhibition in vitro', *Genes Dev,* 15, (24), pp. 3342-54.

Tzahor, E. and Lassar, A. B. (2001) 'Wnt signals from the neural tube block ectopic cardiogenesis', *Genes Dev,* 15, (3), pp. 255-60.

Ueno, S., Weidinger, G., Osugi, T., Kohn, A. D., Golob, J. L., Pabon, L., Reinecke, H., Moon, R. T. and Murry, C. E. (2007) 'Biphasic role for Wnt/beta-catenin signaling in cardiac specification in zebrafish and embryonic stem cells', *Proc Natl Acad Sci U S A,* 104, (23), pp. 9685-90.

Upadhyay, G., Goessling, W., North, T. E., Xavier, R., Zon, L. I. and Yajnik, V. (2008) 'Molecular association between beta-catenin degradation complex and Rac guanine exchange factor DOCK4 is essential for Wnt/beta-catenin signaling', *Oncogene,* 27, (44), pp. 5845-55.

Ursitti, J. A., Petrich, B. G., Lee, P. C., Resneck, W. G., Ye, X., Yang, J., Randall, W. R., Bloch, R. J. and Wang, Y. (2007) 'Role of an alternatively spliced form of alphaII-spectrin in localization of connexin 43 in cardiomyocytes and regulation by stress-activated protein kinase', *J Mol Cell Cardiol,* 42, (3), pp. 572-81.

Vadlamudi, U., Espinoza, H. M., Ganga, M., Martin, D. M., Liu, X., Engelhardt, J. F. and Amendt, B. A. (2005) 'PITX2, beta-catenin and LEF-1 interact to synergistically regulate the LEF-1 promoter', *J Cell Sci,* 118, (Pt 6), pp. 1129-37.

Vallier, L., Mancip, J., Markossian, S., Lukaszewicz, A., Dehay, C., Metzger, D., Chambon, P., Samarut, J. and Savatier, P. (2001) 'An efficient system for conditional gene expression in embryonic stem cells and in their in vitro and in vivo differentiated derivatives', *Proc Natl Acad Sci U S A,* 98, (5), pp. 2467-72.

Vanin, E. F. (1985) 'Processed pseudogenes: characteristics and evolution', *Annu Rev Genet,* 19, pp. 253-72.

Veeman, M. T., Axelrod, J. D. and Moon, R. T. (2003) 'A second canon. Functions and mechanisms of beta-catenin-independent Wnt signaling', *Dev Cell,* 5, (3), pp. 367-77.

Vleminckx, K., Kemler, R. and Hecht, A. (1999) 'The C-terminal transactivation domain of beta-catenin is necessary and sufficient for signaling by the LEF-1/beta-catenin complex in Xenopus laevis', *Mech Dev,* 81, (1-2), pp. 65-74.

Vogeli, K. M., Jin, S. W., Martin, G. R. and Stainier, D. Y. (2006) 'A common progenitor for haematopoietic and endothelial lineages in the zebrafish gastrula', *Nature,* 443, (7109), pp. 337-9.

Vonica, A. and Gumbiner, B. M. (2002) 'Zygotic Wnt activity is required for Brachyury expression in the early Xenopus laevis embryo', *Dev Biol,* 250, (1), pp. 112-27.

Wada, H. and Okamoto, H. (2009) 'Roles of noncanonical Wnt/PCP pathway genes in neuronal migration and neurulation in zebrafish', *Zebrafish,* 6, (1), pp. 3-8.

Waetzig, V. and Herdegen, T. (2005) 'Context-specific inhibition of JNKs: overcoming the dilemma of protection and damage', *Trends Pharmacol Sci,* 26, (9), pp. 455-61.

Waldo, K. L., Kumiski, D. and Kirby, M. L. (1996) 'Cardiac neural crest is essential for the persistence rather than the formation of an arch artery', *Dev Dyn,* 205, (3), pp. 281-92.
Waldo, K. L., Kumiski, D. H., Wallis, K. T., Stadt, H. A., Hutson, M. R., Platt, D. H. and Kirby, M. L. (2001) 'Conotruncal myocardium arises from a secondary heart field', *Development,* 128, (16), pp. 3179-88.
Walkley, C. R. (2011) 'Erythropoiesis, anemia and the bone marrow microenvironment', *Int J Hematol,* 93, (1), pp. 10-3.
Wallingford, J. B., Goto, T., Keller, R. and Harland, R. M. (2002) 'Cloning and expression of Xenopus Prickle, an orthologue of a Drosophila planar cell polarity gene', *Mech Dev,* 116, (1-2), pp. 183-6.
Wang, H., Hao, J. and Hong, C. C. (2011) 'Cardiac induction of embryonic stem cells by a small molecule inhibitor of Wnt/beta-catenin signaling', *ACS Chem Biol,* 6, (2), pp. 192-7.
Wang, Y., Guo, N. and Nathans, J. (2006) 'The role of Frizzled3 and Frizzled6 in neural tube closure and in the planar polarity of inner-ear sensory hair cells', *J Neurosci,* 26, (8), pp. 2147-56.
Wang, Y. and Nathans, J. (2007) 'Tissue/planar cell polarity in vertebrates: new insights and new questions', *Development,* 134, (4), pp. 647-58.
Wang, Y. X., Qian, L. X., Liu, D., Yao, L. L., Jiang, Q., Yu, Z., Gui, Y. H., Zhong, T. P. and Song, H. Y. (2007) 'Bone morphogenetic protein-2 acts upstream of myocyte-specific enhancer factor 2a to control embryonic cardiac contractility', *Cardiovasc Res,* 74, (2), pp. 290-303.
Wang, Y., Su, B., Sah, V. P., Brown, J. H., Han, J. and Chien, K. R. (1998) 'Cardiac hypertrophy induced by mitogen-activated protein kinase kinase 7, a specific activator for c-Jun NH2-terminal kinase in ventricular muscle cells', *J Biol Chem,* 273, (10), pp. 5423-6.
Warga, R. M. and Kimmel, C. B. (1990) 'Cell movements during epiboly and gastrulation in zebrafish', *Development,* 108, (4), pp. 569-80.
Warga, R. M. and Nusslein-Volhard, C. (1999) 'Origin and development of the zebrafish endoderm', *Development,* 126, (4), pp. 827-38.
Watterson, G. A. (1983) 'On the time for gene silencing at duplicate Loci', *Genetics,* 105, (3), pp. 745-66.
Wawrzak, D., Metioui, M., Willems, E., Hendrickx, M., de Genst, E. and Leyns, L. (2007) 'Wnt3a binds to several sFRPs in the nanomolar range', *Biochem Biophys Res Commun,* 357, (4), pp. 1119-23.
Webb, S. E. and Miller, A. L. (2007) 'Ca2+ signalling and early embryonic patterning during zebrafish development', *Clin Exp Pharmacol Physiol,* 34, (9), pp. 897-904.
Weber, U., Paricio, N. and Mlodzik, M. (2000) 'Jun mediates Frizzled-induced R3/R4 cell fate distinction and planar polarity determination in the Drosophila eye', *Development,* 127, (16), pp. 3619-29.
Wei, L., Roberts, W., Wang, L., Yamada, M., Zhang, S., Zhao, Z., Rivkees, S. A., Schwartz, R. J. and Imanaka-Yoshida, K. (2001) 'Rho kinases play an obligatory role in vertebrate embryonic organogenesis', *Development,* 128, (15), pp. 2953-62.
Weinbrenner, C., Liu, G. S., Cohen, M. V. and Downey, J. M. (1997) 'Phosphorylation of tyrosine 182 of p38 mitogen-activated protein kinase correlates with the protection of preconditioning in the rabbit heart', *J Mol Cell Cardiol,* 29, (9), pp. 2383-91.
Weir, J. T. and Schluter, D. (2008) 'Calibrating the avian molecular clock', *Mol Ecol,* 17, (10), pp. 2321-8.

Westerfield, M. (1993) *The zebrafish book : a guide for the laboratory use of zebrafish (Brachydanio rerio).* M. Westerfield: Eugene, OR.
Westfall, T. A., Hjertos, B. and Slusarski, D. C. (2003) 'Requirement for intracellular calcium modulation in zebrafish dorsal-ventral patterning', *Dev Biol,* 259, (2), pp. 380-91.
Weston, C. R., Wong, A., Hall, J. P., Goad, M. E., Flavell, R. A. and Davis, R. J. (2003) 'JNK initiates a cytokine cascade that causes Pax2 expression and closure of the optic fissure', *Genes Dev,* 17, (10), pp. 1271-80.
Whelan, S., Lio, P. and Goldman, N. (2001) 'Molecular phylogenetics: state-of-the-art methods for looking into the past', *Trends Genet,* 17, (5), pp. 262-72.
Wiens, J. J. (2006) 'Missing data and the design of phylogenetic analyses', *J Biomed Inform,* 39, (1), pp. 34-42.
Wiley, L. M. (1984) 'Cavitation in the mouse preimplantation embryo: Na/K-ATPase and the origin of nascent blastocoele fluid', *Dev Biol,* 105, (2), pp. 330-42.
Wilson, S. W. and Houart, C. (2004) 'Early steps in the development of the forebrain', *Dev Cell,* 6, (2), pp. 167-81.
Winter, C. G., Wang, B., Ballew, A., Royou, A., Karess, R., Axelrod, J. D. and Luo, L. (2001) 'Drosophila Rho-associated kinase (Drok) links Frizzled-mediated planar cell polarity signaling to the actin cytoskeleton', *Cell,* 105, (1), pp. 81-91.
Wo, Y. B., Zhu, D. Y., Hu, Y., Wang, Z. Q., Liu, J. and Lou, Y. J. (2008) 'Reactive oxygen species involved in prenylflavonoids, icariin and icaritin, initiating cardiac differentiation of mouse embryonic stem cells', *J Cell Biochem,* 103, (5), pp. 1536-50.
Wobus, A. M., Wallukat, G. and Hescheler, J. (1991) 'Pluripotent mouse embryonic stem cells are able to differentiate into cardiomyocytes expressing chronotropic responses to adrenergic and cholinergic agents and Ca2+ channel blockers', *Differentiation,* 48, (3), pp. 173-82.
Wong, H. C., Mao, J., Nguyen, J. T., Srinivas, S., Zhang, W., Liu, B., Li, L., Wu, D. and Zheng, J. (2000) 'Structural basis of the recognition of the dishevelled DEP domain in the Wnt signaling pathway', *Nat Struct Biol,* 7, (12), pp. 1178-84.
Wu, S. M. (2008) 'Mesp1 at the heart of mesoderm lineage specification', *Cell Stem Cell,* 3, (1), pp. 1-2.
Wu, S. M., Fujiwara, Y., Cibulsky, S. M., Clapham, D. E., Lien, C. L., Schultheiss, T. M. and Orkin, S. H. (2006) 'Developmental origin of a bipotential myocardial and smooth muscle cell precursor in the mammalian heart', *Cell,* 127, (6), pp. 1137-50.
Xi, J., Khalil, M., Shishechian, N., Hannes, T., Pfannkuche, K., Liang, H., Fatima, A., Haustein, M., Suhr, F., Bloch, W., Reppel, M., Saric, T., Wernig, M., Janisch, R., Brockmeier, K., Hescheler, J. and Pillekamp, F. (2010) 'Comparison of contractile behavior of native murine ventricular tissue and cardiomyocytes derived from embryonic or induced pluripotent stem cells', *FASEB J,* 24, (8), pp. 2739-51.
Xie, Y., Puscheck, E. E. and Rappolee, D. A. (2006) 'Effects of SAPK/JNK inhibitors on preimplantation mouse embryo development are influenced greatly by the amount of stress induced by the media', *Mol Hum Reprod,* 12, (4), pp. 217-24.
Xiong, J. W., Battaglino, R., Leahy, A. and Stuhlmann, H. (1998) 'Large-scale screening for developmental genes in embryonic stem cells and embryoid bodies using retroviral entrapment vectors', *Dev Dyn,* 212, (2), pp. 181-97.
Xu, P. and Davis, R. J. (2010) 'c-Jun NH2-terminal kinase is required for lineage-specific differentiation but not stem cell self-renewal', *Mol Cell Biol,* 30, (6), pp. 1329-40.

Yagi, H., Furutani, Y., Hamada, H., Sasaki, T., Asakawa, S., Minoshima, S., Ichida, F., Joo, K., Kimura, M., Imamura, S., Kamatani, N., Momma, K., Takao, A., Nakazawa, M., Shimizu, N. and Matsuoka, R. (2003) 'Role of TBX1 in human del22q11.2 syndrome', *Lancet,* 362, (9393), pp. 1366-73.

Yamada, G., Mansouri, A., Torres, M., Stuart, E. T., Blum, M., Schultz, M., De Robertis, E. M. and Gruss, P. (1995) 'Targeted mutation of the murine goosecoid gene results in craniofacial defects and neonatal death', *Development,* 121, (9), pp. 2917-22.

Yamada, S., Pokutta, S., Drees, F., Weis, W. I. and Nelson, W. J. (2005) 'Deconstructing the cadherin-catenin-actin complex', *Cell,* 123, (5), pp. 889-901.

Yamada, T., Yoshikawa, M., Kanda, S., Kato, Y., Nakajima, Y., Ishizaka, S. and Tsunoda, Y. (2002) 'In vitro differentiation of embryonic stem cells into hepatocyte-like cells identified by cellular uptake of indocyanine green', *Stem Cells,* 20, (2), pp. 146-54.

Yamaguchi, T. P., Takada, S., Yoshikawa, Y., Wu, N. and McMahon, A. P. (1999) 'T (Brachyury) is a direct target of Wnt3a during paraxial mesoderm specification', *Genes Dev,* 13, (24), pp. 3185-90.

Yamanaka, H., Moriguchi, T., Masuyama, N., Kusakabe, M., Hanafusa, H., Takada, R., Takada, S. and Nishida, E. (2002) 'JNK functions in the non-canonical Wnt pathway to regulate convergent extension movements in vertebrates', *EMBO Rep,* 3, (1), pp. 69-75.

Yamashita, J., Itoh, H., Hirashima, M., Ogawa, M., Nishikawa, S., Yurugi, T., Naito, M. and Nakao, K. (2000) 'Flk1-positive cells derived from embryonic stem cells serve as vascular progenitors', *Nature,* 408, (6808), pp. 92-6.

Yamashita, J. K., Takano, M., Hiraoka-Kanie, M., Shimazu, C., Peishi, Y., Yanagi, K., Nakano, A., Inoue, E., Kita, F. and Nishikawa, S. (2005) 'Prospective identification of cardiac progenitors by a novel single cell-based cardiomyocyte induction', *FASEB J,* 19, (11), pp. 1534-6.

Yan, Y. T., Gritsman, K., Ding, J., Burdine, R. D., Corrales, J. D., Price, S. M., Talbot, W. S., Schier, A. F. and Shen, M. M. (1999) 'Conserved requirement for EGF-CFC genes in vertebrate left-right axis formation', *Genes Dev,* 13, (19), pp. 2527-37.

Yang, C. H., Axelrod, J. D. and Simon, M. A. (2002) 'Regulation of Frizzled by fat-like cadherins during planar polarity signaling in the Drosophila compound eye', *Cell,* 108, (5), pp. 675-88.

Yang, D., Tournier, C., Wysk, M., Lu, H. T., Xu, J., Davis, R. J. and Flavell, R. A. (1997) 'Targeted disruption of the MKK4 gene causes embryonic death, inhibition of c-Jun NH2-terminal kinase activation, and defects in AP-1 transcriptional activity', *Proc Natl Acad Sci U S A,* 94, (7), pp. 3004-9.

Yang, S. H., Whitmarsh, A. J., Davis, R. J. and Sharrocks, A. D. (1998) 'Differential targeting of MAP kinases to the ETS-domain transcription factor Elk-1', *EMBO J,* 17, (6), pp. 1740-9.

Yao, A., Charlab, R. and Li, P. (2006) 'Systematic identification of pseudogenes through whole genome expression evidence profiling', *Nucleic Acids Res,* 34, (16), pp. 4477-85.

Yatskievych, T. A., Pascoe, S. and Antin, P. B. (1999) 'Expression of the homebox gene Hex during early stages of chick embryo development', *Mech Dev,* 80, (1), pp. 107-9.

Yelon, D. and Stainier, D. Y. (1999) 'Patterning during organogenesis: genetic analysis of cardiac chamber formation', *Semin Cell Dev Biol,* 10, (1), pp. 93-8.

Yoshida, H., Hastie, C. J., McLauchlan, H., Cohen, P. and Goedert, M. (2004) 'Phosphorylation of microtubule-associated protein tau by isoforms of c-Jun N-terminal kinase (JNK)', *J Neurochem,* 90, (2), pp. 352-8.

Yost, H. J. (2003) 'Left-right asymmetry: nodal cilia make and catch a wave', *Curr Biol,* 13, (20), pp. R808-9.

You, Z., Saims, D., Chen, S., Zhang, Z., Guttridge, D. C., Guan, K. L., MacDougald, O. A., Brown, A. M., Evan, G., Kitajewski, J. and Wang, C. Y. (2002) 'Wnt signaling promotes oncogenic transformation by inhibiting c-Myc-induced apoptosis', *J Cell Biol,* 157, (3), pp. 429-40.

Zaffran, S., Kelly, R. G., Meilhac, S. M., Buckingham, M. E. and Brown, N. A. (2004) 'Right ventricular myocardium derives from the anterior heart field', *Circ Res,* 95, (3), pp. 261-8.

Zamparini, A. L., Watts, T., Gardner, C. E., Tomlinson, S. R., Johnston, G. I. and Brickman, J. M. (2006) 'Hex acts with beta-catenin to regulate anteroposterior patterning via a Groucho-related co-repressor and Nodal', *Development,* 133, (18), pp. 3709-22.

Zehnder, J. L., Hirai, K., Shatsky, M., McGregor, J. L., Levitt, L. J. and Leung, L. L. (1992) 'The cell adhesion molecule CD31 is phosphorylated after cell activation. Down-regulation of CD31 in activated T lymphocytes', *J Biol Chem,* 267, (8), pp. 5243-9.

Zeisberg, E. M., Ma, Q., Juraszek, A. L., Moses, K., Schwartz, R. J., Izumo, S. and Pu, W. T. (2005) 'Morphogenesis of the right ventricle requires myocardial expression of Gata4', *J Clin Invest,* 115, (6), pp. 1522-31.

Zeng, X., Tamai, K., Doble, B., Li, S., Huang, H., Habas, R., Okamura, H., Woodgett, J. and He, X. (2005) 'A dual-kinase mechanism for Wnt co-receptor phosphorylation and activation', *Nature,* 438, (7069), pp. 873-7.

Zhang, Y., Bai, X. T., Zhu, K. Y., Jin, Y., Deng, M., Le, H. Y., Fu, Y. F., Chen, Y., Zhu, J., Look, A. T., Kanki, J., Chen, Z., Chen, S. J. and Liu, T. X. (2008) 'In vivo interstitial migration of primitive macrophages mediated by JNK-matrix metalloproteinase 13 signaling in response to acute injury', *J Immunol,* 181, (3), pp. 2155-64.

Zhao, B., Etter, L., Hinton, R. B., Jr. and Benson, D. W. (2007) 'BMP and FGF regulatory pathways in semilunar valve precursor cells', *Dev Dyn,* 236, (4), pp. 971-80.

Zhao, Y., Samal, E. and Srivastava, D. (2005) 'Serum response factor regulates a muscle-specific microRNA that targets Hand2 during cardiogenesis', *Nature,* 436, (7048), pp. 214-20.

Zhong, J. and Kyriakis, J. M. (2007) 'Dissection of a signaling pathway by which pathogen-associated molecular patterns recruit the JNK and p38 MAPKs and trigger cytokine release', *J Biol Chem,* 282, (33), pp. 24246-54.

Zhong, W., Xie, Y., Wang, Y., Lewis, J., Trostinskaia, A., Wang, F., Puscheck, E. E. and Rappolee, D. A. (2007) 'Use of hyperosmolar stress to measure stress-activated protein kinase activation and function in human HTR cells and mouse trophoblast stem cells', *Reprod Sci,* 14, (6), pp. 534-47.

Zhou, J., Qu, J., Yi, X. P., Graber, K., Huber, L., Wang, X., Gerdes, A. M. and Li, F. (2007) 'Upregulation of gamma-catenin compensates for the loss of beta-catenin in adult cardiomyocytes', *Am J Physiol Heart Circ Physiol,* 292, (1), pp. H270-6.

Zhu, S., Korzh, V., Gong, Z. and Low, B. C. (2008) 'RhoA prevents apoptosis during zebrafish embryogenesis through activation of Mek/Erk pathway', *Oncogene,* 27, (11), pp. 1580-9.

Zhu, S., Liu, L., Korzh, V., Gong, Z. and Low, B. C. (2006) 'RhoA acts downstream of Wnt5 and Wnt11 to regulate convergence and extension movements by

involving effectors Rho kinase and Diaphanous: use of zebrafish as an in vivo model for GTPase signaling', *Cell Signal,* 18, (3), pp. 359-72.